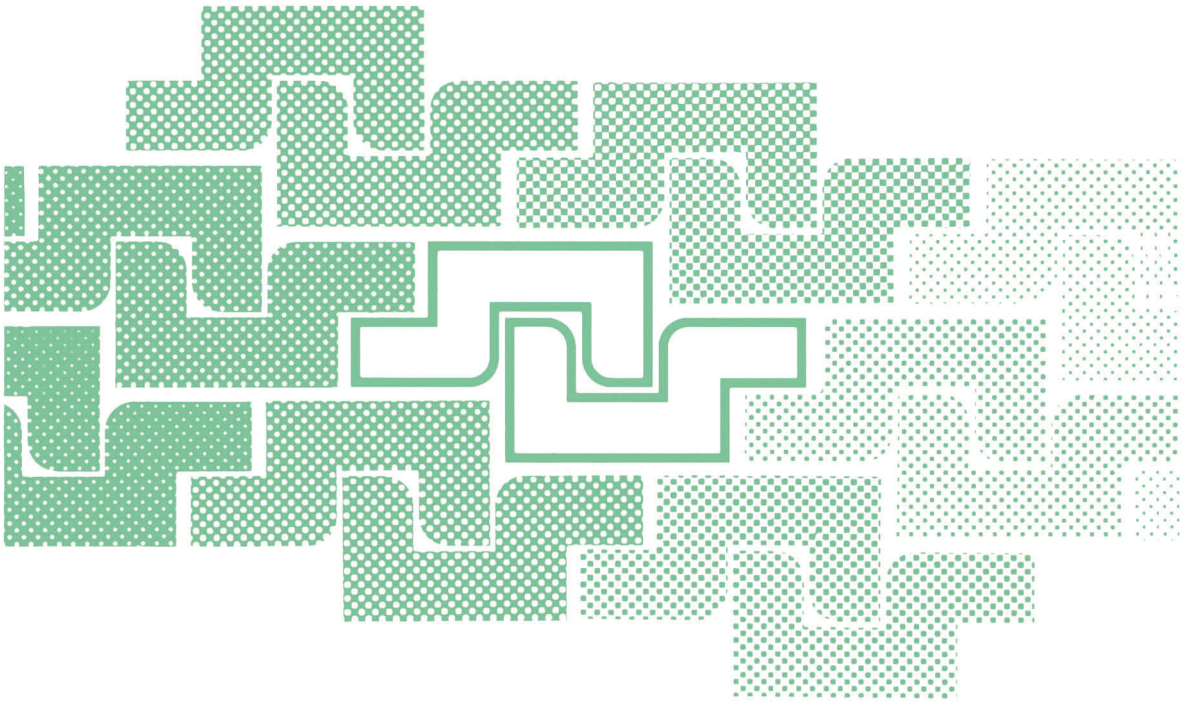

The Adria Microplate: GPS Geodesy, Tectonics and Hazards

Edited by

Nicholas Pinter, Gyula Grenerczy,
John Weber, Seth Stein and Damir Medak

NATO Science Series

IV. Earth and Environmental Sciences – Vol. 61

The Adria Microplate: GPS Geodesy, Tectonics and Hazards

NATO Science Series

A Series presenting the results of scientific meetings supported under the NATO Science Programme.

The Series is published by IOS Press, Amsterdam, and Springer (formerly Kluwer Academic Publishers) in conjunction with the NATO Public Diplomacy Division

Sub-Series

I. Life and Behavioural Sciences	IOS Press
II. Mathematics, Physics and Chemistry	Springer (formerly Kluwer Academic Publishers)
III. Computer and Systems Science	IOS Press
IV. Earth and Environmental Sciences	Springer (formerly Kluwer Academic Publishers)

The NATO Science Series continues the series of books published formerly as the NATO ASI Series.

The NATO Science Programme offers support for collaboration in civil science between scientists of countries of the Euro-Atlantic Partnership Council. The types of scientific meeting generally supported are "Advanced Study Institutes" and "Advanced Research Workshops", and the NATO Science Series collects together the results of these meetings. The meetings are co-organized by scientists from NATO countries and scientists from NATO's Partner countries – countries of the CIS and Central and Eastern Europe.

Advanced Study Institutes are high-level tutorial courses offering in-depth study of latest advances in a field.
Advanced Research Workshops are expert meetings aimed at critical assessment of a field, and identification of directions for future action.

As a consequence of the restructuring of the NATO Science Programme in 1999, the NATO Science Series was re-organized to the four sub-series noted above. Please consult the following web sites for information on previous volumes published in the Series.

http://www.nato.int/science
http://www.springeronline.com
http://www.iospress.nl

Series IV: Earth and Environmental Sciences – Vol. 61

The Adria Microplate: GPS Geodesy, Tectonics and Hazards

edited by

Nicholas Pinter
Southern Illinois University,
Carbondale, IL, U.S.A.

Grenerczy Gyula
Satellite Geodetic Observatory,
Penc, Hungary

John Weber
Grand Valley State University ,
Allendale, MI, U .S.A.

Seth Stein
Northwestern University,
Evanston, IL, U.S.A.

and

Damir Medak
University of Zagreb, Croatia

Published in cooperation with NATO Public Diplomacy Division

Proceedings of the NATO Advanced Research Workshop on
The Adria Microplate: GPS Geodesy, Tectonics and Hazards
Veszprém, Hungary
April 4–7, 2004

A C.I.P. Catalogue record for this book is available from the Library of Congress.

ISBN-10 1-4020-4234-5 (PB)
ISBN-13 978-1-4020-4234-8 (PB)
ISBN-10 1-4020-4233-7 (HB)
ISBN-13 978-1-4020-4233-1 (HB)
ISBN-10 1-4020-4235-3 (e-book)
ISBN-13 978-1-4020-4235-5 (e-book)

Published by Springer,
P.O. Box 17, 3300 AA Dordrecht, The Netherlands.

www.springeronline.com

Printed on acid-free paper

Table of Contents

Geodetic Measurement and Geodynamics

Seismology, Seismic Hazard, and Societal Impacts of Adria Tectonics

Preface

Since its first application to geodynamical problems, GPS geodesy has gradually revealed the nature of motion and deformation for most active areas of deformation across the Earth. One of the last remaining regional-scale problems is the motion and associated deformation in the peri-Adriatic region. Selected local-scale studies have examined aspects of this motion, but to date no regional team has systematically attacked the full regional scope of this problem. This NATO Advanced Research Workshop (ARW) was designed to bring together an international group of scientists working in the peri-Adriatic region to: (1) review research activities and results completed to date, (2) share technical expertise, and (3) provide a springboard for future collaborative research on Adria geodynamics.

This NATO ARW was held from April 4-7, 2004 in Veszprém, Hungary. The meeting venue was the Veszprém center of the Hungarian Academy of Sciences (VEAB), located on the ramparts of the city's castle district. Workshop participants included 32 participants from 15 different countries. Most participants arrived in Budapest on April 3, staying at the Hotel Peregrinus, just off the Vaci Utca pedestrian zone in central Pest (access to the Peregrinus courtesy of the Geophysics Department, Eötvös Loránd Technical University). This unofficial "staging" day facilitated assembly of participants from different locations, allowed opportunity to explore the historic center of Budapest, and allowed overseas participants to recover from their jet-lag. Early on the morning of April 4, additional participants arrived at the Peregrinus to join the group on the chartered bus trip to Veszprém. With Budapest traffic (uncharacteristically) light on a Sunday morning, the bus delivered the group to Veszprém. Additional workshop participants also arrived independently in Veszprém during the morning of April 4. Formal activities of the ARW began with lunch on April 4 and continued through dinner on April 6. After a formal welcome and convocation speech on the first day, four half-day plenary sessions were held, each consisting of 7-9 presentations. Themes of each of these sessions were: (1) Regional Tectonics of South-Central Europe, (2) Geologic Evidence and Recent Research on Adria Motion, (3) Geodetic Infrastructure and Research in the Peri-Adriatic Region, and (4) Adria Plate Motion and Societal Impacts. A particularly popular element of the workshop took place during the fifth half-day session. This summative review consisted of four "break-out" sessions, reports of break-out session chairs, a panel discussion, and a final summative review or the workshop and future milestones. Areas of agreement were identified, as well as remaining areas of debate. In addition, attention focused on important scientific questions and the potential for international and interdisciplinary research in the future.

Records of the workshop included a volume of extended abstracts that was distributed at the time of the meeting as well as a compilation of Powerpoint presentations. Regarding the latter, we solicited all participants whether they would be willing to share their Powerpoint presentations with the group as a while; we then produced a CD that was distributed to all workshop participants who contributed their presentations. The final record of the workshop is this volume. A total of 26 papers were contributed, and each one was peer reviewed by at least two reviewers, one of the Associate Editors, as well as both of the two lead editors. We thank all of the authors and all of the reviewers for their tremendous efforts, and we believe that those efforts are reflected here in an outstanding and timely contribution to the science of geodesy, tectonics, and the understanding of the peri-Adriatic region.

Finally, the editors would like to thank the NATO Science Commission for its support for the Veszprém workshop and for this volume, the Geophysics Department of Eötvös Lórand University for its co-sponsorship and logistical support of the meeting, and the Hungarian Academy of Science for the use of its meeting, lodging, and dining facilities in Veszprém. Special thanks are due to our Workshop Coordinator, Dr. Sandor Frey of the Satellite Geodetic Observatory. Dr. Frey's tremendous efforts in advance of and during the meeting were critical to its successful outcome. We would also like to thank Mr. Endre Dómbradi and Ms. Anita Horváth for their capable and good-natured assistance during the running of the workshop.

The editors

RECENT ADVANCES IN PERI-ADRIATIC GEODYNAMICS AND FUTURE RESEARCH DIRECTIONS

Nicholas Pinter
Dept. of Geology, Southern Illinois University, Carbondale IL 62901-4324, USA
npinter@geo.siu.edu

Gyula Grenerczy
Satellite Geodetic Observatory, Institute of Geodesy, Cartography, and Remote Sensing, Penc, Hungary
grener@elte.hu

ABSTRACT

This volume presents the current status of research into the geodynamics of the Adriatic region and the surrounding areas of Italy, the Alps, the Pannonian basin, and the eastern margin of the Adriatic as far south as Greece. Contributions here come from the fields of technical and applied geodesy, tectonics, structural geology, paleomagnetism, seismology, and other fields. Papers are grouped together into five major themes: (1) Introduction and regional tectonic framework; (2) Geologic evidence of Adria motion; (3) Geodetic infrastructure and technology; (4) Geodetic measurements and geodynamics; and (5) Seismology, seismic hazard, and societal impacts of Adria tectonics.

Several areas of consensus and several unresolved questions have emerged in this field. First, recent GPS surveys almost universally conclude that Adria currently is moving independent of both Eurasia and Africa/Nubia. However, Nubia motion remains imperfectly constrained, and a better distribution and density of GPS measurements across Africa is desirable. The precise boundaries of Adria also remain open to a variety of different interpretations. To the northeast, current deformation appears to be distributed over a broad zone, with "Adria push" penetrating through the Dinarides and Pannonian basin. This on-going motion of Adria appears to be driving active lateral extrusion to the northeast, and similar processes may be active at the northwestern corner of Adria, in and around the Western Alps. Within the Adriatic region itself, seismicity and variations in GPS vectors across the region have been interpreted by some as internal fragmentation of Adria, and several geometries have been proposed.

In the future, expanded research focused on regional peri-Adriatic geodynamics would have both theoretical scientific benefits as well as tangible applications. The motion of Adria and Adria-driven deformation exert first-order controls on earthquake hazard and other natural hazards such as slope failure and soil erosion. In addition, the geodynamic pattern and tectonic history

N. Pinter et al. (eds.), The Adria Microplate: GPS Geodesy, Tectonics and Hazards, 1–20.

also control the distribution of minerals and other economic resources; in particular Adria-related tectonics have controlled hydrocarbon accumulation in locations such as the Pannonian basin. Potential for future research includes cross-disciplinary work, for example linking GPS geodetic measurements with geological or perhaps paleoseismic techniques to identify specific structures and their history of deformation integrated through several full seismic cycles. In addition, future geodetic research should be international, fully spanning the Adriatic block and its boundary zones, with the goal of producing a dense, methodologically homogenous velocity field.

Keywords: Adria, Eastern Mediterranean, south-central Europe, geodynamics, GPS geodesy

INTRODUCTION

This volume presents the results of a NATO Advanced Research Workshop (ARW) entitled "The Adria Microplate: GPS Geodesy, Tectonics, and Hazards" that was held April 4-7, 2004 at the Veszprém center of the Hungarian Academy of Sciences (VEAB) in Veszprém, Hungary. The purpose of the workshop was to bring together geodetic and earth scientists in order to focus on the geodynamics of the peri-Adriatic region, an area which encompasses the Adriatic Sea itself, portions of the Eastern Mediterranean, and a broad swath of south-central Europe. The geodynamics of this region appear to be dominated by the motion of "Adria" (Seuss, 1883), a lithospheric unit (microplate, plate promontory, block, or series of blocks) centered on the Adriatic Sea. Effects of Adria motion are manifested within the Adria block, at its boundaries (the locations and nature of which are discussed later in this paper), and over long distances into the surrounding areas of south-central Europe and the Mediterranean.

The goals of this workshop were to bring together a broadly interdisciplinary group of scientists working on or in the peri-Adriatic region to: 1) review research activities and results completed to date, 2) identify areas of consensus as well as unresolved questions surrounding the geodynamics of Adria, and 3) provide a springboard for future collaborative research. Disciplines represented at the workshop included technical geodesy, applied geodesy, tectonics, seismology, paleomagnetics, and geology. It was a central premise of the workshop that such a broadly cross-disciplinary approach was necessary in order to characterize the full range of impacts of Adria motion as well as to utilize all available tools for answering the remaining questions related to Adria motion and Adria-related deformation. A conclusion of the workshop was that there are indeed a number of unresolved questions and that future

research utilizing a more unified approach – both interdisciplinary and international – would have the best chance of resolving these questions.

SUMMARY OF CONTRIBUTIONS TO THIS VOLUME

This paper summarizes and synthesizes some of the major findings of the Veszprém ARW on Adria. The large majority of the participants in the workshop contributed papers to this volume, with the result that the major technical background and results are presented in full detail in the subsequent pages. As a general introduction to the book, we will begin with a brief summary of the papers here and follow with a synthesis of the major themes and findings. Contributions to this volume have been organized into the following groups:

- Introduction and regional tectonic framework
- Geologic evidence of Adria motion
- Geodetic infrastructure and technology
- Geodetic measurements and geodynamics
- Seismology, seismic hazard, and societal impacts of Adria tectonics

Introduction and Regional Tectonic Framework

In the first section of this book, three sets of authors synthesize regional tectonic models of the Eastern Mediterranean and south-central Europe. In the first paper, Stein and Sella review the Cenozoic tectonic history of the peri-Adriatic region, with particular emphasis on previous studies that have determined a rotation pole and/or GPS vector fields for the Adria microplate. Stein and Sella suggest that slowing of the Tyrrhenian subduction since the Pliocene, and the possible cessation of that subduction today, altered the geometry and motion of Adria, with the Italian peninsula west of the Apennine axis now moving with Europe. Stein and Sella conclude by highlighting several open problems for future work, noting that the Eurasia-Africa convergence zone is complex and has evolved rapidly over the geologically recent past.

Hollenstein et al. review the setting and tectonic history of Adria and summarize their own GPS geodetic results across the Eurasia-Africa boundary zone. They note that GPS shows that the Eurasian Plate, including Corsica and Sardinia and extending to the southern margin of the Tyrrhenian Sea, is highly

rigid and that Adria forms a kinematically distinct domain. They determine strain and strain-rate fields in several areas, including through Sicily and Calabria and in the Aegean region, and conclude that these patterns represent preliminary steps towards fully understanding the detailed geodynamics of the broader region.

Mantovani et al. present a detailed model of the Neogene-to-Quaternary evolution and interactions of the Adriatic block. They address the contentious question of whether Adria represents a rigid promontory linked to Africa or whether it represents a truly independent microplate. The authors suggest that Adria moved with Africa from the Permian until the middle Pliocene, at which time it decoupled as a result of the westward push of the Anatolian system. In support of this model, Mantovani and his coauthors assert that: 1) Adria underwent a period of clockwise rotation during the Late Pliocene, and 2) the Nubian Plate moves NNE-ward in the central Mediterranean (in contrast to the northwesterly motion previously inferred by Dewey et al., 1989; DeMets et al., 1990; Sella et al., 2002; and others). At the Veszprém workshop, the two suggestions above generated substantial discussion.

Geologic Evidence on Adria Motion

The second group of papers in this volume present a range of geologic data that constrain the past and present motion of Adria and Adria-related deformation in the broader region. The first two papers in this group, by Márton and Sagnotti, review paleomagnetic research from several locations around the Adriatic region. Márton presents new results from three sets of peri-Adriatic field areas: 1) the Adriatic foreland (Istria Peninsula, Colli Eugenei), 2) the imbricated Adria margin (Venetian Alps, Mura depression, central Dalmatia), and 3) the broader circum-Adriatic area (eastern Alps, Mura Depression, northern Croatia). Tertiary-age counterclockwise rotations were identified in all three of these field areas, leading Márton to conclude that this entire region lies on a coherent Adria block, which has rotated counterclockwise during the Cenozoic, and perhaps beginning in the latest Miocene to early Pliocene. Sagnotti notes the same counterclockwise rotation throughout most of Italy, including 20° of CCW rotation during the Plio-Pleistocene in the southern Apennines. In contrast, Sagnotti notes clockwise rotation of Calabria and Sicily, which he integrates into a “saloon door” model (see Fig. 4; Sagnotti, this volume) in response to southeastward migration of Tyrrhenian subduction.

Two subsequent papers, by Piccardi et al. and Ferranti and Oldow, explore neotectonic processes and geology in Italy. Piccardi et al. focus on

recent fault activity in two sets of field areas: 1) along the axis of the Apennines (Norcia, Fucino, Vallo di Diano, Val d'Agri), and 2) through the Gargano peninsula. The authors document late Quaternary activity in all of the Apennine study areas, generally consisting of normal and/or transtensional slip. In the Gargano area, several distinct fault structures show Quaternary to even Holocene activity, with cumulative slip of 0.8-0.9 mm/yr, although the authors note that the system appears to terminate offshore to the east of the peninsula. The paper by Ferranti and Oldow present a regional synthesis of Neogene to Quaternary deformation through Italy based on locations of foredeep deposits (horizontal displacements) and uplifted coastal terraces and other erosional surfaces (vertical displacements). The horizontal deformation pattern through the Apennines is dominated by the southeastward migration of paired belts of foreland contraction and hinterland extension, which represents the inferred rollback of the subducting Tyrrhenian slab previously noted, at an average rate of about 16 mm/yr (6.3-1.3 Ma). Ferranti and Oldow interpret the vertical-deformation pattern as showing late-stage uplift caused by a transition from thin-skinned to thick-skinned deformation due to impingement of the thrust belt onto thicker Apulian lithosphere of the Adria interior.

The remaining two papers in this section also focus on neotectonics, but located in Albania (Aliaj) and Slovenia (Vrabec and Fodor). Aliaj notes that Albania coincides with the transition from the Dinarides in the north to the Hellenides in the south. Neotectonic activity within Albania varies markedly from its "internal zone," characterized by Pliocene-to-recent extensional faulting, to its "external zone," characterized by NE-SW-oriented compression on folds and reverse and transpressional faults. Other distinct tectonic regions of Albania include the peri-Adriatic foredeep and the largely undeformed offshore foreland. Vrabec and Fodor explore the tectonic setting and Neogene to Quaternary activity in Slovenia, at the northeast margin of Adria. Much of Slovenia is dominated by transpressional to strike-slip tectonics. The so-called Dinaric faults, which are NW-SE structures located in the northern Dinarides, document recent to active dextral slip of up to several kilometres of cumulative motion. The Periadriatic Fault Zone (PAF) is a regional dextral structure that accommodated large-scale differential block motion during the Miocene extrusion of the Eastern Alps (see discussion later in this paper), and this structure appears to be active and regionally significant today, extending eastward into Croatia along the Drava fault or others. Other areas with geologically recent and/or on-going activity in Slovenia include the Sava Folds and what Vrabec and Fodor dub the "shear lens" located between the PAF and the Sava fault to the south.

Geodetic Infrastructure and Technology

The third group of papers in this volume outline some of the geodetic activities and infrastructure in several countries surrounding the Adriatic and in the broader south-central European region. Stangl and Bruyninx review the principles of determining site velocities using permanent GPS time series and note several of the sources of error that may degrade the precision of site determinations. Focusing on the needs of peri-Adriatic geodynamics, they note that a key limitation is station distribution, which currently is insufficiently dense and sub-optimally distributed for determining the detailed deformation pattern in the region. The next paper, by Fejes, reviews the history, composition, and operations of the Central European Geodynamical Reference Network (CEGRN). The consortium which operates and supports CEGRN currently consists of 14 partner institutions in 13 countries, and the network consists (at the time of publication) of over 30 permanent GPS stations and over 30 additional regularly measured campaign sites arrayed from Italy eastward to Bulgaria and northward to Poland and Germany. The paper by Mulic et al. (her institution itself a member of the CEGRN Consortium) accomplishes two goals: (1) it outlines the geologic and tectonic setting of Bosnia and Herzegovina (one of the first such papers in English), and (2) the paper reviews the history and status of geodynamical GPS in that country. Bosnia and Herzegovina straddles the central Dinarides, with its geology and tectonics ranging from the imbricate Adria margin in the southwest to the Inner Dinarides in the northeast, which have a Neogene history more strongly linked to events in the Pannonian basin. The country began systematic geodetic measurements for geodynamical purposes in 1998.

The next paper in this group, by Marjanovic-Kavanagh, reviews a range of ground-based geodetic techniques that are used for measurement of position change. In addition, several sources of error and/or variability in these measurements are discussed, including temperature change, changes in atmospheric pressure and humidity, water-table variations, Earth tides, and the effects of heterogeneities in local geology. Koler also discusses the use of ground-based geodetic measurements. Specifically, he reviews historical levelling surveys that date back in Slovenia to the late 19th century as well as modern, high-precision levelling techniques. Results of dense measurements of vertical motion around Ljubljana and around the Slovenian nuclear power plant at Krsko are highlighted. In the following paper, Odalovic reviews geodetic activities in Serbia, focusing on a regional gravimetric survey used to construct a national geoid map, accurate to about 10 cm. In the final paper of this section,

Medak and Pribicevic describe 1997 and 2001 campaign surveys of a network of 43 stabilized sites surrounding Zagreb, Croatia. These GPS measurements were processed using GAMIT software and revealed velocities that exceeded the measurement uncertainties, suggesting possible near-field strain.

Geodetic Measurements and Geodynamics

The fourth group of papers are loosely grouped together based on their focus on determining regional patterns and rates of deformation and/or plate motion. Altiner et al. present the results of the CRODYN experiment, including processed results from the experiment's final campaign survey in 1998. The CRODYN network consisted of 20 stations in 1994 located in Croatia, Italy, and Slovenia, with 14 additional stations located in Albania and Bosnia and Herzegovina for two subsequent campaigns in 1996 and 1998. Horizonatal velocities are show relative to station GRAZ, a proxy for stable Europe. Vertical velocities are also estimated, with all but 2 sites showing apparent uplift (see Fig. 4; Altiner et al., this volume). The combined horizontal velocities, including the 1998 CRODYN campaign, show a very consistent pattern of northeastward motion relative to GRAZ, with velocities in the Dinarides generally decreasing with distance away from the coast and a general trend of increasing velocities to the south relative to the northern Adriatic.

Oldow and Ferranti also present geodynamical results of multiple campaign GPS surveys. Their Peri-Tyrrhenian Geodetic Array (PTGA) consists of 49 campaign sites in southern Italy, Sicily, and Sardinia. They combine the results of the 1995, 1997, and 2000 PTGA campaigns with other publicly available GPS results and with earthquake slip vectors to reiterate the model presented in Oldow, 2002, in which Adria is subdivided into a northwestern and a separate southeastern velocity domains separated at the Gargano-Dubrovnik line. Regionally, Oldow and Ferranti identify a broadly arcuate contractional domain which runs from the northwestern Adria block through the Calabrian arc and then through parts of Sicily and the southernmost Tyrrhenian Sea, separating extensional domains across the central Tyrrhenian basin and western Italy and another such extensional domain in the southern Adriatic and Ionian Seas. Locally, Oldow and Ferranti observe that their GPS velocities in Sicily, Calabria, and elsewhere are highly variable, which they interpret as highly heterogeneous deformation of the upper crust, separated from the lower lithosphere across a regional basal decollement system.

To the southeast, Delikaraoglou et al. discuss the tectonic setting and results of their AEGEANET network through the Aegean and elsewhere in

Greece. New GPS measurements also were combined with older triangulation/trilateration measurements yielding velocities measured over times spans of 40 years or more. The Aegean is extremely active relative to most other areas reviewed in this volume, with high levels of seismicity and over 1 m of north-south extension measured across the AEGEANET network.

Weber et al. present results from the Periadriatic-Istria Velocity Observations (PIVO) experiment. The PIVO network included 35 campaign sites located in northern Croatia and the Istria peninsula and elsewhere in Slovenia, as well as a broader-aperture array of permanent GPS stations in the surrounding region. The Istria peninsula was considered a particularly promising target for geodynamical measurements because it represents the largest available onshore promontory extending into the interior of the presumably stable Adria microplate. Results presented here, based on campaigns in 2001 and 2003, confirm the counterclockwise rotation observed by previous workers, with a rotation pole shifted significantly from that inferred by Ward (1994) and others, but relatively close to that of Anderson and Jackson (1987). Weber et al. argue that these results confirm that Adria is not fragmented at the latitude of the Gargano peninsula.

In the last paper of this group presenting the results of regional geodynamical analyses, Grenerczy and Kenyeres present velocities derived from the CEGRN network with particular emphasis on the motion of Adria and propagation of this motion northeastward through the Dinarides and into the Pannonian basin and the Carpathians. Grenerczy and Kenyeres document a systematic rotation of Adria at a rate of –0.35 °/Myr, with velocities of 3.5-5 mm/yr in the south, 3-4 mm/yr in the central Adriatic, and 2.5-3.5 mm/yr in the north. This motion is distinct from that of Nubia, tending to confirm Adria's status as a distinct microplate. Regionally, Grenerczy and Kenyeres document 2.3±0.3 mm/yr of convergence in the Eastern Alps across a narrow deformation zone; in contrast, the 2 mm/yr of shortening observed across the Dinarides appears to span a diffuse deformation zone at least 360 km wide. An additional 1-1.5 mm/yr of Adria-related deformation "leaks" into the Pannonian basin, although no active motion or deformation of the Carpathians can be resolved.

Seismology, Seismic Hazard, and Societal Impacts of Adria Tectonics

The final group of papers in this volume include contributions focusing on seismicity of the peri-Adriatic region, the related seismic hazard, and other

implications of Adria motion for humans and human society. Thouvenot and Fréchet present the results of 14 years of dense seismic monitoring in the Western Alps and in the surrounding areas at the northwestern corner of the Adria microplate. Extension oriented radial to the trend of the Western Alps is widespread, including along the Briançonnais and Piedmont seismic trends. This extension is interpreted as gravitational collapse or possibly buoyancy forces operating within the range. To the west, focal mechanisms suggest predominantly dextral slip on faults oriented parallel to the axis of the Western Alps. This strike-slip activity is interpreted as a subtle form of tectonic extrusion (see discussion below) in response to Adria motion and rotation. Compressional seismicity is noted in the Padan arc, south of Turin, and in the northern Ligurian Sea. The Padan arc is a zone of anomalously deep hypocenters – down to 112 km – that remains enigmatic; the Ligurian Sea earthquakes are more typically shallow, and Thouvenant and Fréchet relate this E-W to NW-SE compression to Adria-driven "lateral expulsion" of the southwestern Alps.

Muço examines two seismic catalogues: ADRIA-1, a 500-year record of felt earthquake, and ADRIA-2 a 40-year record of instrumental seismicity of earthquakes down to about M2, both for the circum-Adriatic region. These time-series of earthquake occurrence are analysed for spatial and temporal patterns, in particular cross-correlation between events that may imply triggering. Tóth et al. also look at long-duration records of seismicity, in their case using a database that includes events back to 456 A.D. recorded from the northernmost Adriatic Sea eastward across the Pannonian basin and the Carpathian chain. Historical earthquakes as well as instrumentally measured events document that the highest levels of seismicity in the region are in the Vrancea zone, in which three events greater than M6.5 have occurred since 1977. The Pannonian basin is less active, with an average recurrence time for events $M \geq 6$ of about 100 years. Tóth et al. present a seismic-hazard map for the greater Pannonian-Carpathian region, with contours of peak ground acceleration calculated for a 10% exceedance probability and a 475-year return time, and they note additional site-specific hazards such as liquefaction.

In the final paper of this volume, Bada et al. provide an important overview of some of the applications and implications of Adria geodynamics on human society, using specific example from the Pannonian region. They note that on-going "Adria push" is most clearly manifested in the attenuated crust of the Pannonian basin as differential vertical motion. This vertical deformation has concrete applications for a broad range of issues, including slope stability, soil erosion, flood hazard, earthquake hazard, water resources management, and

hydrocarbon occurrence. Bada et al. provide detailed analyses of the impacts of Adria-driven geodynamics on Pannonian fluvial systems and flooding, seismic hazard in the region, and petroleum resources. In terms of flooding, tectonically driven subsidence creates areas of low relief and elevated flood hazard. Looking at earthquake activity, Bada et al. note that the Pannonian region is characterized by "low- to medium-level seismicity," but that special threats exist for the several large cities in the region (e.g., Vienna, Bratislava, Budapest, Trieste, Ljubljana, and Zagreb) that are situated on or adjacent to active or potentially active faults. Seven nuclear power plants (Fig. 7, Table 1, Bada et al., this volume) also are located across this region. Lastly, Bada et al. enumerate the processes by which Adria-driven tectonics – in this case, Plio-Pleistocene uplift and inversion of Pannonian basin structures – have driven hydrocarbon maturation and migration and constructed most of the traps, thus generating and explaining the occurrence of hydrocarbon resources exploited within the Pannonian basin region today.

SYNTHESIS OF RECENT ADRIA RESEARCH

After reviewing the contributions to this volume in the previous section, we will presume to synthesize the results presented in this volume as well as the previous literature on Adria motion and the geodynamics of the peri-Adriatic region. This section includes the conclusions of a series of "breakout" sessions convened on the last day of the Veszprém ARW. Although not every attendee may agree with every point presented here, a consensus emerged regarding several aspects of Adria research. In contrast, several other questions clearly remain unresolved and represent promising avenues for future research.

Adria as a Promontory of Africa or Independent Microplate?

Perhaps the oldest tectonic debate in the Adriatic arena is whether the Adria "lithospheric unit" represents a rigid promontory of Africa or whether it is moving independently as a separate microplate (e.g., Argand, 1924; Zijderveld et al., 1970; McKenzie, 1972; Hsü, 1977; Channel and Horváth, 1976; Anderson, 1987; Anderson and Jackson, 1987; Mantovani et al., 1990; Channel, 1996; Nocquet et al., 2001; Muttoni et al., 2001). Although a range of opinions can still be found on this question, one area of increasingly clear agreement emerges from the recent literature (Anderson and Jackson, 1987; Westaway,

1990; Ward, 1994; Calais et al., 2002; Oldow et al., 2002; Battaglia et al., 2004) and from the Veszprém meeting and this volume (Oldow and Ferranti, Weber et al., Grenerczy and Kenyeres, this volume) – virtually all of the new regional GPS measurements on Adria have concluded that parts or all of the Adria unit are moving distinctly from both Nubia and Eurasia.

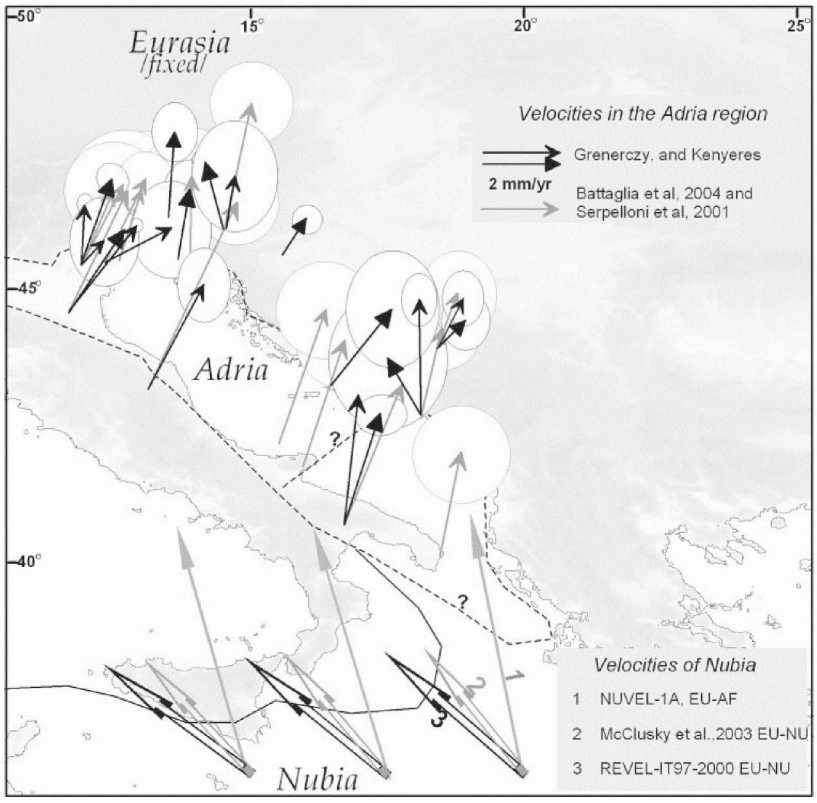

Figure 1. GPS velocities in the Adria region with reference to stable Eurasia and their 95% confidence level together with the velocities of Nubia with reference to Eurasia inferred from global plate motion models NUVEL-1A after De Mets et al., 1994 and REVEL after Sella et al., 2002.

In Fig. 1, crustal velocities obtained from the European Reference Network, Central European GPS Geodynamic Reference Network and local

GPS networks are shown with reference to fixed Eurasia together with their confidence limits (after Serpelloni et al., 2003; Battaglia et al., 2004; Grenerczy and Kenyeres, this volume). A first observation is that all of the stations in the represented parts of the Adria region show significant velocities relative to stable Eurasia. Without exception, each of the velocities is oriented to the NNE. The significant 2.5-4.5 mm/yr, NNE-oriented velocities with reference to fixed Eurasia are largely uniform throughout the Adria region, supporting the kinematic independence of the Adria region from Eurasia. The velocities of Nubia relative to fixed Eurasia near Adria compared to the GPS velocities in the Adria region also show significant differences in both orientation and magnitude. If Adria itself or any part belonged to Nubia, the velocities would be larger and oriented to the NW; instead there is a ~60-70° difference in orientation and 1-3 mm/yr difference in magnitude between the velocities observed in the Adria region and the predicted velocities of Nubia from the GPS-based global plate motion models relative to Eurasia.

One caveat to the conclusion above, however, is voiced by Mantovani et al. (this volume) – that defining Adria kinematically and distinguishing it from Nubia by pointing to the statistically significant difference in velocities assumes that the motion of each unit has been fully and accurately quantified. A broad body of data have been used to characterize Africa/Nubia motion (e.g., Dewey, 1989; DeMets et al., 1990; Sella et al., 2002), but it is true that GPS sites – particularly permanent GPS stations – are relatively sparse and sub-optimally distributed across the African continent. In the case of Adria, independent geologic evidence points to a long-term pattern of motion separate from Africa (e.g., Márton et al., 2003; Márton, this volume, and references therein), but a better constrained GPS solution for the motion of Nubia and the other areas of Africa would certainly be a desirable goal for a broad range of applications.

Boundaries and Fragmentation of Adria

Closely related to the debate above is the question of identifying the boundaries of Adria, including any internal boundaries that would define whether Adria is fragmented or rather whether acts as a larger coherent unit. Although there appears to be convergence regarding the existence and nature of the Adria microplate, there is wide divergence of opinion on how exactly this microplate should be drawn on a map. As a starting point, Adria can be generally delineated using the distribution of earthquake epicentres (see for example McKenzie, 1972; Anderson and Jackson, 1987). North of the Adriatic Sea, earthquakes and geologic structures define a general trend running through

the Central Alps and parallel with the northern margin of the Po plain. Compressional focal mechanisms, and compressional geological structures, in this area are consistent with continued impingement of Adria into the southern margin of stable Europe at a rate that has been geodetically estimated at 2.3±0.3 mm/yr (Grenerczy and Kenyeres, this volume), and there seems to be the greatest degree of agreement regarding the nature and location of this northern boundary.

The western boundary of Adria, running southeastward through the Italian peninsula, is less clear. Earthquake epicentres are concentrated along the axis of the northern and southern Apennines (e.g., Chiarabba et al., 2005), and several workers have drawn their western boundary of Adria along the axis of the range (e.g., Anderson and Jackson, 1987). Other authors appear to favor a boundary coincident with the easternmost position of the Appeninic frontal thrust (e.g., Rosenbaum and Lister, 2004). In support of either one or the other of these interpretations, Stein and Sella (this volume) see Italy west of the Apennines moving with Eurasia. In contrast, Oldow et al. (2002) suggest that the northern Apennines may be wholly embedded within a coherent Northwestern Adria-Tyrrhenian lithospheric unit (also see the discussion of Adria fragmentation below). Weber et al. (this volume) note a related issue, questioning whether or not extensional faults along the Apennines are lithospheric in scale, and whether this extension is consistent with relative plate motion or merely with gravitational collapse. Similar questions could also be raised in the Western Alps, where the Penninic Front thrust boundary now is marked by dominantly extensional earthquakes (Thouvenant and Fréchet, this volume).

The eastern boundary of Adria also remains somewhat enigmatic. Although the regional state of stress along the western margin of the Adriatic Sea clearly is transpressional, consistent with GPS-measured and geologically determined motion of Adria relative to the Dinarides and the European Platform, drawing a discrete line on a map is a difficult task. Aliaj (this volume) notes a well defined foredeep and a discrete frontal thrust interpreted in seismic-reflection profiles off the coast of Albania, but an alternative viewpoint is that these features may date partially or entirely to ancestral convergence along the eastern margin of Adria and may not fully characterize the motion now active or active in geologically recent time. To the north, in Slovenia, the detailed neotectonic mapping and analyses of Vrabec and Fodor (this volume) shows that none of the faults near the Adriatic coast nor into the Dinarides accommodates all of the relative motion between Adria and the European Platform. The Periadriatic fault zone, which may have accommodated as much as 550 km of

dextral slip since the Oligocene (Tari, 1994; Fodor et al., 1998; see discussion of extrusion below), appears to be active (Weber et al., this volume) but does not appear to take up more than a portion of the total motion. Analyzing regional GPS data from Adria across the Dinarides to the European Platform, Grenerczy and Kenyeres (this volume) see roughly 2 mm/yr of shortening distributed over a deformation zone approximately 360 km wide, with an additional 1.0-1.5 mm/yr of slip transferred farther in-board and through the Pannonian basin. This model is consistent with the pattern of seismicity, with high levels along the Adriatic coast and the Dinarides, but with activity that broadly diminishes to the northeast (Bada et al., Tóth et al, this volume).

As previously noted, there is the least degree of agreement regarding the nature and location of the southern margin of Adria. The range of opinions on this question begins with the authors who maintain that Adria is promontory of Africa and therefore has no southern boundary. Among the other papers that do infer motion between Adria and Africa, boundaries that have been suggested include: the Kefallinia fault zone and/or the Apulia escarpment (e.g., Battaglia et al., 2004; Mantovani et al., 2002), the Straits of Otranto (e.g., Anderson, 1987; Ward, 1994), the Gargano-Dubrovnik line (e.g., Stein and Sella, this volume), and along the Ortona-Roccamonfina and Anzio-Ancona lines (Oldow et al., 2002). The location of this boundary, the slip rate across it, and the absolute motions of the blocks separated by such a boundary are the issues upon which turn the question of the fragmentation of Adria, with explicitly differing views outlined by Weber (this volume) and Oldow et al. (2002) and Oldow and Ferranti (this volume). An extreme view of the fragmentation of Adria was presented by Nocquet et al. (2001), who found GPS velocity residuals consistent with pervasive internal deformation of Adria. Ferranti and Oldow (this volume) and Oldow and Ferranti (this volume) suggest a similar explanation to explain the high degree of variability in GPS and earthquake slip vectors across Italy.

Adria Push and Tectonic Extrusion

One of the themes discussed extensively during the Veszprém workshop was Adria-driven extrusion, including well documented lateral extrusion during the Tertiary and possible on-going extrusion in one or more areas of the peri-Adriatic region. Lateral extrusion of the Eastern Alps in response to progressive northward motion of Adria (or “Apulia”) was proposed by Ratchbacher (1991a; 1991b), who used the term roughly synonymously with “tectonic escape” (Burke and Sengör, 1986) and “tectonic extrusion” (Tapponnier et al., 1986). Ratchbacher proposed that extrusion of the Eastern Alps probably began in the

Oligocene and culminated in the Miocene and was manifested by a transition from continuing compression in the central portions of the range, to extensional deformation on the eastern flanks of the Alps, to long-travelled strike-slip faulting into what is now the Pannonian basin and the Carpathians (Ratshbacher, 1991b). In this model, conditions that favored this episode of extrusion included: the northward motion of Adria during this time, a strong foreland buttress (the European Platform), an unconstrained eastern boundary, and overthickened crust that was subsequently thermally weakened and became gravitationally unstable (Ratchbacher, 1991a). Subsequent models have emphasized the third point above, that the most rapid extrusion in the Eastern Alps may have coincided with slab roll-back in the Carpathians and rapid foundering of the Pannonian basin (Horváth and Cloetingh, 1996). According to this model, Carpathian subduction-hinge retreat created accommodation space that allowed the lateral escape of the Eastern Alps. Along these lines, the end of Carpathian subduction at 5-6 Ma (Horváth and Cloetingh, 1996; Fodor et al., 1998) ended the generation of this accommodation space and thus blocked further escape to the northeast of the Adria indentor (Horváth and Cloetingh, 1996; Vrabec and Fodor, this volume; F. Horváth, oral presentation at the Veszprém ARW).

Another major question regarding Adria-driven lateral extrusion is to what extent this process is continuing today. In the areas to the northeast of the Adria block, which were most strongly affected by past episode(s) of tectonic extrusion, several authors interpret the patterns of recent and active faulting and GPS measurements of deformation as evidence that modest lateral escape has continued up to and including the present (Bada et al., Grenerczy and Kenyeres, Vrabec and Fodor, Weber et al., this volume; F. Horváth, oral presentation at the Veszprém ARW). Although extrusion-related rates of fault slip and regional deformation clearly are much slower today than during periods of peak activity in the Tertiary, the pattern of deformation appears roughly similar. In explaining this sharp contrast in rates, it may be important to note that large-scale tectonic extrusion is often seen as the combined effects of horizontal translation in front of a rigid indentor as well as the result of gravitational instability of the overthickened core of the orogen (e.g., Ratchbacher, 1991a). It is plausible that the on-going northward motion of Adria continues to act as an indentor, but rates of strike-slip faulting and other deformation have been reduced both by the lack of accommodation space to the east as well as by reduced gravitational potential in the Eastern Alps. In possible contrast to the Eastern Alps, however, Thouvenant and Fréchet (this volume) favor active gravitational collapse as explanation for the modern state of stress

the Western Alps. Thouvenant and Fréchet present a regionally consistent model of active extrusion at the northwest corner of Adria, with gravitational collapse documented by active extension radial to the range – a pattern of deformation corroborated by GPS (Nocquet et al., 2001) – and active indentor-driven escape suggested by strike-slip and transpressional deformation in the West Alpine foreland into the northern Ligurian Sea.

CONCLUSIONS

This volume brings together contributions from a group of researchers that is both international – including every nationality in the peri-Adriatic rim – and broadly interdisciplinary. Disciplines represented here include GPS geodesy, tectonics, structural geology, paleomagnetism, seismology, and tectonic geomorphology. Papers are grouped together into five major themes: (1) Introduction and regional tectonic framework; (2) Geologic evidence of Adria motion; (3) Geodetic infrastructure and technology; (4) Geodetic measurements and geodynamics; and (5) Seismology, seismic hazard, and societal impacts of Adria tectonics. Together this volume represents the first major scientific compilation focused entirely on Adriatic regional tectonics and the geological and broader implications of Adria motion.

From the papers in this volume, from the discussion in break-out sessions at the conclusion of the Veszprém ARW, and from the broader body of literature and research in the tectonics of south-central Europe, several areas of consensus seem to be emerging along with several unresolved questions that should be addressed in future research. First among the areas of consensus is the observation that recent geodetic studies almost universally conclude that the Adriatic lithospheric unit currently is moving independent of both Eurasia and Africa/Nubia. An important caveat to this statement is that the motion of Nubia remains imperfectly constrained, and a better distribution and density of GPS measurements across Africa in the future would serve a broad range of applications. Far less agreement can be found regarding the precise locations of the boundaries of Adria. Although the Adriatic Sea is generally surrounded by compressional faults and earthquake focal mechanisms to the north, extension along the axis of the Apennines, and transpressional deformation in the Dinarides, regional maps drawn by different workers document a surprisingly wide range of different opinions delineating the margins of Adria. To the northeast, for example, several faults and fault systems may have acted as discrete plate boundaries in the geological past, but current deformation appears

to be distributed over a broad microplate-boundary zone up to several hundred kilometers wide.

The region to the northeast of Adria, encompassing the Eastern Alps, the northern Dinarides, the Pannonian basin, experienced one or more episodes of lateral extrusion during the Tertiary. The continuing motion of Adria appears to be driving active, albeit slower extrusional processes today. Similar sets of processes also may be active around the northwestern corner of Adria, in the Western Alps, Western Alpine foreland, and the northern Ligurian Sea. In addition to the questions regarding the locations and nature of the boundaries of Adria, there is heated debate regarding internal boundaries and deformation within the Adriatic region. Although Adria was originally defined as a core of low seismicity relative to its external boundaries, a fair number of earthquakes do occur across the interior of the Adriatic. This internal seismicity, along with variations in GPS vectors across the region have led to several different – generally mutually exclusive – models in which Adria is internally fragmented across one or more proposed internal boundaries or perhaps even pervasively deforming.

This overview of the current status of Adria-related research shows that there is tremendous potential for future research, in particular work involving international and cross-disciplinary cooperation. In the peri-Adriatic region, a large quantity of GPS and other geodetic measurements have been made over past years, but a dense regional solution has not yet been produced. This can be explained at least partly by the fragmentation of previous geodetic efforts, which have been conducted without the regionally coordinated measurements focused on the Adriatic or the internationally coordinated analysis which would be required to fuse independent campaign networks into a seamless velocity solution at the plate-boundary scale. Such a dense, regional geodynamical picture of south-central Europe and the Eastern Mediterranean would have both theoretical scientific benefits as well as applications to a number of socially significant issues. As outlined by Bada et al. and others (this volume), Adria motion controls the pattern and level of seismic and other geological hazards as well as the occurrence and nature of a range of natural resources such as hydrocarbons. Break-out sessions and a panel discussion that concluded the Veszprém ARW suggested that future research activities should include both specific bi-lateral projects (e.g., Italian-Albanian) that cross national boundaries as well as perhaps one or more truly multi-national cooperative research projects that fully span the peri-Adriatic region.

ACKNOWLEDGEMENTS

The authors would again like to thank the NATO Science Commission for providing support for the Veszprém workshop and this volume, the Geophysics Dept. of Eötvös Lórand University for its co-sponsorship of the meeting, and the Hungarian Academy of Science for the use of its facilities in Veszprém. Special thanks are due to Dr. Sandor Frey of the Satellite Geodetic Observatory who served as Workshop Coordinator and whose organizational skills and commitment to detail guaranteed the smooth and successful outcome of the meeting. We also thank Endre Dómbradi and Anita Horváth for their assistance during the workshop.

REFERENCES

Anderson H. Is the Adriatic an African promontory? Geology 1987; 15: 212-215.

Anderson H., Jackson J. Active tectonics of the Adriatic region. Geophys. J. R. Astr. Soc. 1987; 91: 937-983.

Argand E. La tectonique de L'Asie. Proc. Int. Geol. Congr. 1924; XIII: 171.

Battaglia M., Murray M.H., Serpelloni E., Burgmann R. The Adriatic region: an independent microplate within the Africa-Eurasia collision zone. Geophys. Res. Lett. 2004; 31:10.1029/2004GL019723.

Burke K., Sengör A.M.C. Tectonic escape in the evolution of the continental crust. In *Reflection Seismology: The Continental Crust*, M. Barazangi and L. Brown, eds. Geodynamics Series, 14: 41-53. Washington, DC: American Geophysical Union, 1986.

Calais E., Nocquet J.-M., Jouanne F., Tardy M. Current strain regime in the western Alps from continuous Global Positioning System measurements, 1996-2001. Geology 2002; 30: 651-654

Channell J.E.T. Paleomagnetism and paleogeography of Adria. In: *Paleomagnetism and tectonics of the Mediterranean region*, A. Morris and D.H. Tarling, eds. Geological Society Special Publication, 1996, 105: 119-132.

Channel J.E.T., Horváth, P. The African/Adriatic promontory as a palaeogeographic premise for Alpine orogeny and plate movements in Carpatho-Balkan region. Tectonophysics 1976; 35: 71-101.

Chiarabba C., Jovane L., DiStefano R. A new view of Italian seismicity using 20 years of instrumental recordings. Tectonophysics 2005; 395: 251-268.

DeMets C., Gordon R.G., Argus D.F., Stein S. Current plate motions. Geophys. J. Int. 1990; 101: 425-478.

Dewey J.F., Helman M.L., Turco E., Hutton D.H.W., Knott. S. Kinematics of the western Mediterranean. In *Alpine Tectonics*, M.P. Coward, D. Dietrich, R.G. Park, eds., London: Geol. Soc. London Spec. Publ. 1989; 45: 265–283.

Fodor L., Jelen B., Márton E., Skaberne D., Car J., Vrabec M. Miocene-Pliocene tectonic evolution of the Slovenian Periadriatic Line and surrounding area: implications for Alpine-Carpathian extrusion models. Tectonics 1998; 17: 690-709.

Herak D., Herak M., Prelogovic E., Markusic S., Markulin Z. Jabuka island (Central Adriatic Sea) earthquakes of 2003. Tectonophysics 2005; 398: 167-180.

Horváth F., Cloething S. Stress-induced late-stage subsidence anomalies in the Pannonian Basin. Tectonophysics 1996; 266: 287-300.

Hsü K.J. Tectonic extrusion of the Mediterranean Sea basins. In *The Ocean Basins and Margins, 4A: The Eastern Mediterranean*, A.E.M. Nairn, W.H. Kanes, F.G. Stehli, eds., p. 29-75, New York: Plenum Press, 1977.

Jolivet L., Faccenna C. Mediterranean extension and the Africa-Eurasia collision. Tectonics 2000; 19:1095-1106.

Laubscher H.P. Plate boundaries and microplates in Alpine history. Am. J. Science 1975; 275: 865-876.

Mantovani E., Albarello D., Babbucci D., Tamburelli C., Viti M. Trench-Arc-BackArc Systems in the Mediterranean area: Examples of Extrusion Tectonics. In *Reconstruction of the evolution of the Alpine-Himalayan Orogen*, G. Rosenbaum, G.S. Lister, eds. J. of the Virtual Explorer 2002; 8: 131-147.

Mantovani E., Babbucci D., Albarello D., Mucciarelli M. Deformation pattern in the central Mediterranean and behavior of the African/Adriatic promontory. Tectonophysics 1990; 179: 63-79.

Márton E., Drobne K., Cosovic V., Moro A. Palaeomagnetic evidence for Tertiary counterclockwise rotation of Adria. Tectonophysics 2003; 377: 143-156.

McClusky, S., Reilinger R., Mahmoud S., Ben Sari D., Tealeb A. GPS constraints on Africa (Nubia) and Arabia plate motions. Geophys. J. Int. 2003; 155, 126-138.

McKenzie D. Active tectonics of the Mediterranean Region, Geophys J. R. Astr. Soc. 1972; 30: 109-185.

Muttoni G., Garzanti E., Alfonsi L., Cirilli S., Germani D., Lowrie W. Motion of Africa and Adria since the Permian: paleomagnetic and paleoclimatic constraints from northern Libya. Earth and Planetary Science Letters 2001; 192:159-74.

Nocquet J-M., Calais E., Altamimi Z., Sillard P., Boucher C. Intraplate deformation in western Europe deduced from an analysis of the International Terrestrial Reference Frame 1997 (ITRF97) velocity field. J. Geophys. Res. 2001; 106:11,239-11,257.

Oldow J.S., Ferranti L., Lewis D.S., Campbell J. K., D'Argenio B, Catalano R., Pappone G., Carmignani L., Conti P., Aiken C. Active fragmentation of Adria, the north Africa promontory, central Mediterranean orogen. Geology 2002; 30: 779-782.

Ratschbacher L., Dingeldey C., Miller C., Hacker B.R., McWilliams M.O. Formation, subduction, and exhumation of Penninic oceanic crust in the Eastern Alps: time constraints from $^{40}AR/^{39}Ar$ geochronology. Tectonophysics 2004; 394: 155-170.

Ratschbacher L., Merle O. Lateral extrusion in the Eastern Alps, part 1: boundary conditions and experiments scaled for gravity. Tectonics 1991, 10: 245-256.

Ratschbacher L., Frisch W., Linzer H. G., Merle O. Lateral extrusion in the Eastern Alps, part 2: structural analysis. Tectonics 1991; 10: 257-271.

Rosenbaum G., Lister G.S. Neogene and Quaternary rollback evolution of the Tyrrhenian sea, the Apennines, and the Sicilian Maghrebides. Tectonics 2004, 23:10.1029/2003TC001518.

Sella G.F., Dixon T.H., Mao A. REVEL: A model for Recent plate velocities from space geodesy. Journal of Geophysical Research 2002; 107: B4, 10.1029/2000JB000033.

Suess E. *Das Antlitz der Erde*. Prague: Tempsky, 1883.

Tapponnier P., Peltzer G., Armijo R. On the mechanics of the collision between India and Asia. In *Collision Tectonics*, M.P. Coward, A.C. Ries, eds. London: Geol. Soc. Spec. Publ. 1986; 19: 115-157.

Tari G. *Alpine tectonics of the Pannonian basin*, Ph.D. diss., 501 pp., Houston: Rice University, 1994.

Ward S. Constraints on the seismotectonics of the central Mediterranean from Very Long Baseline Interferometry. Geophys. J. Int. 1994; 11:441-452.

Westaway R. Present-day kinematics of the plate boundary zone between Africa and Europe, from the Azores to the Aegean. Earth. Planet. Sci. Lett. 1990; 96: 393-406.

Wortmann U.G., Weissert H., Funk H., Hauck J. Alpine plate kinematics revisited; the Adrian problem. Tectonics 2001; 20:134-147.

Zijderveld J.D.A., Hazeu G.J.A., Nardin M., Van der Voo R. Shear in the Tethys and the Permian paleomagnetism in the Southern Alps, including new results. Tectonophysics 1970; 10: 639.

PLEISTOCENE CHANGE FROM CONVERGENCE TO EXTENSION IN THE APENNINES AS A CONSEQUENCE OF ADRIA MICROPLATE MOTION

Seth Stein and Giovanni F. Sella
Department of Geological Sciences, Northwestern University, Evanston IL 60208 USA
seth@earth.nwu.edu

"Deciphering the sequence of tectonic events in this region can be likened to attempting to reconstruct the pictures in a stack of jigsaw puzzles when 90% of the pieces are missing and the remaining 10% are no longer in their original shape."

Morris and Tarling, 1996

ABSTRACT

Discussions about the Adria microplate offer differing views depending on the timescale and data considered. Neotectonic studies using earthquake mechanisms and GPS site velocities find Adria moving northeastward away from Italy, bounded by an extensional boundary in the Apennines and convergent boundaries in the Dinarides and Venetian Alps. However, geologic data show that Adria was subducting southwestward beneath Italy during Mio-Pliocene time. We suggest that these views are consistent and reflect the recent spatio-temporal evolution of a multiplate system. We assume that during Mio-Pliocene time, Adria was no longer part of Africa and had become an independent microplate. Convergence occurred as Adria moved northeastward with respect to Eurasia as at present, because the faster back-arc spreading in the Tyrrhenian Sea caused Adria to move southwestward with respect to Italy. The transition from convergence to extension in the Apennines during the past 2 My resulted from the cessation of subduction in the Apennines accompanied by breakoff of the subducting Adria slab, and the associated cessation of back-arc spreading in the Tyrrhenian Sea. As a result, western Italy became part of Eurasia, and Adria's northeastward motion produced a new extensional boundary along the Apennines.

INTRODUCTION

Considerable attention, illustrated by the papers in this volume, has been directed over the years to assessing the present and past tectonics of the circum-Adriatic region (Figure 1). Essentially the question is how crustal blocks in the area have moved during the complex and on-going collision of the African and Eurasian plates, which is thought to have begun in Cretaceous

N. Pinter et al. (eds.), The Adria Microplate: GPS Geodesy, Tectonics and Hazards, 21–34.

time and has built the present Alpine mountain belt (Dewey et al., 1989). The boundary zone between the two major plates appears to have involved a number of distinct blocks that have moved – and still do – as coherent entities distinct from the two major plates. One important question is whether the Adria region behaves at present and in the past as part of Eurasia, a distinct microplate, or as a promontory of Africa. At present, the latter possibility is posed in terms of Adria being distinct from Nubia (Africa west of the East African Rift, along which Africa began splitting 15-35 Ma). Views on this issue depend on the assumed extent of the region defined as Adria, and the time and data types considered.

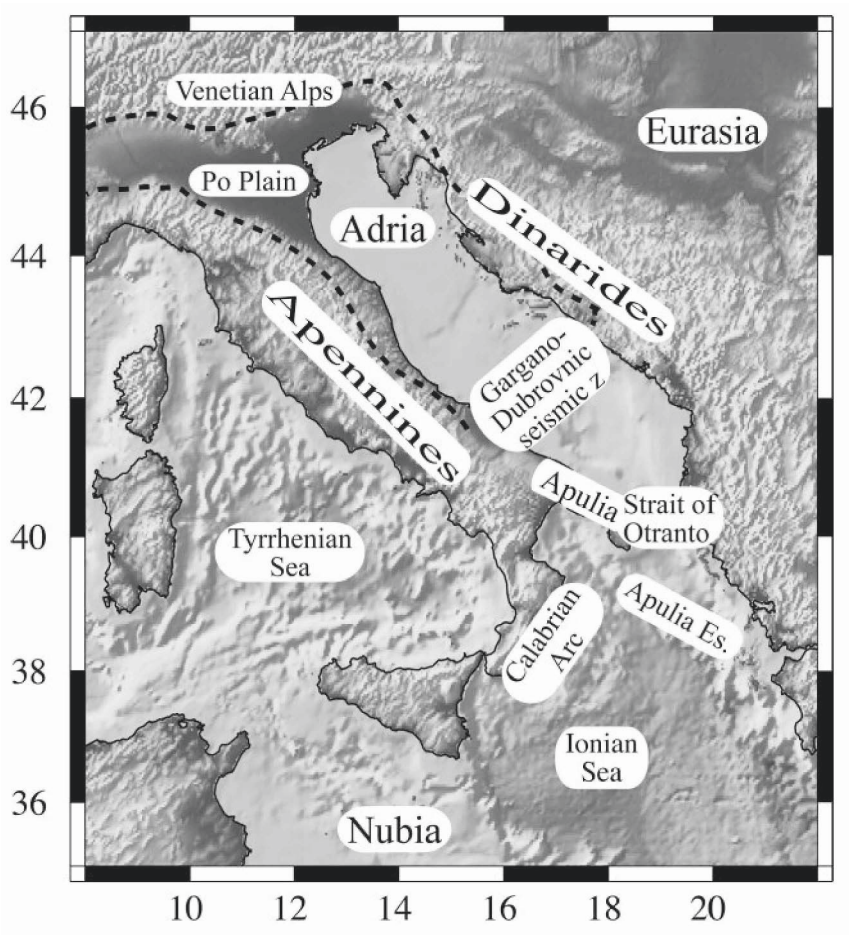

Figure 1. Geography of the circum-Adriatic region. Dashed line denotes approximate boundary of present Adria microplate.

NEOTECTONIC VIEW

Not surprisingly, the issue is most directly addressed for the present, where crustal motions are directly observed (Figure 2). Anderson and Jackson (1987a) and Anderson (1987) noted lower levels of seismicity in the Adriatic Sea and eastern Italy relative to their surroundings, and proposed that this region acted as an Adria microplate. In their model Adria rotates with respect to Eurasia about a pole in the northern Po plain. Hence earthquakes in the Apennines, which show dominantly but not exclusively normal faulting, reflect extension between western Italy south of the Po plain (presently considered to be part of Eurasia) and Adria, whereas the thrust faulting mechanisms in the Dinarides and Venetian Alps reflect Adria-Eurasia convergence. The pole's proximity to the microplate illustrates a common pattern for microplates in the boundary zone between major plates, in which the pole for the relative motion between the major plates is far away, so motion between them varies slowly along the boundary, whereas those for the microplate's motion with respect to the major plates are nearby and so describe rapidly varying motion (Engeln et al., 1988).

This basic picture has been confirmed by GPS data (Calais et al., 2002; Battaglia et al., 2004; Weber et al., this volume). Continuous GPS (CGPS) sites MATE and MEDI show eastern Italy moving northeast relative to stable Eurasia. This motion is essentially perpendicular to the direction of Nubia's motion with respect to Eurasia shown by global plate motion models (DeMets et al., 1994) or space geodetic data (Sella et al., 2002; Grenerczy and Kenyeres, this volume; Kahle, this volume), as illustrated by the motion of site LAMP. Interestingly, the space geodetic data show slower motion than predicted by the NUVEL-1A model. Although the difference may reflect weaknesses in NUVEL-1A, which averages motion over the past 3 Ma, it may also represent real slowing.

Statistical tests (Battaglia et al., 2004) show that the improved fit to the GPS data, resulting from the assumption of an Adria microplate distinct from Nubia, exceeds that expected purely by chance due to the introduction of the three additional parameters associated with an additional Euler vector (Stein and Gordon, 1984), so the microplate and its general motion are kinematically resolved. However, its boundary geometry remains under investigation. Due to the presence of extensional earthquakes in the southern Apennines, Anderson (1987) and Ward (1994) draw the southern boundary with Nubia at the Strait of Otranto, although there is little seismicity along this presumed boundary. In contrast, Calais et al. (2002) favor a similar geometry but suggest that the southern boundary is further north and extends seaward from the Gargano peninsula to Dubrovnik, as implied by a zone of seismicity (Console et al., 1993). Battaglia et al. (2004) favor a similar geometry but add a second microplate to the south separated from Nubia

along the Apulia escarpment and Kefallinia fault. In contrast, Oldow et al. (2002) favor two Adria microplates, with northern and central Italy and the Tyrrhenian Sea on the northern one, such that the northern Apennines are not a plate boundary.

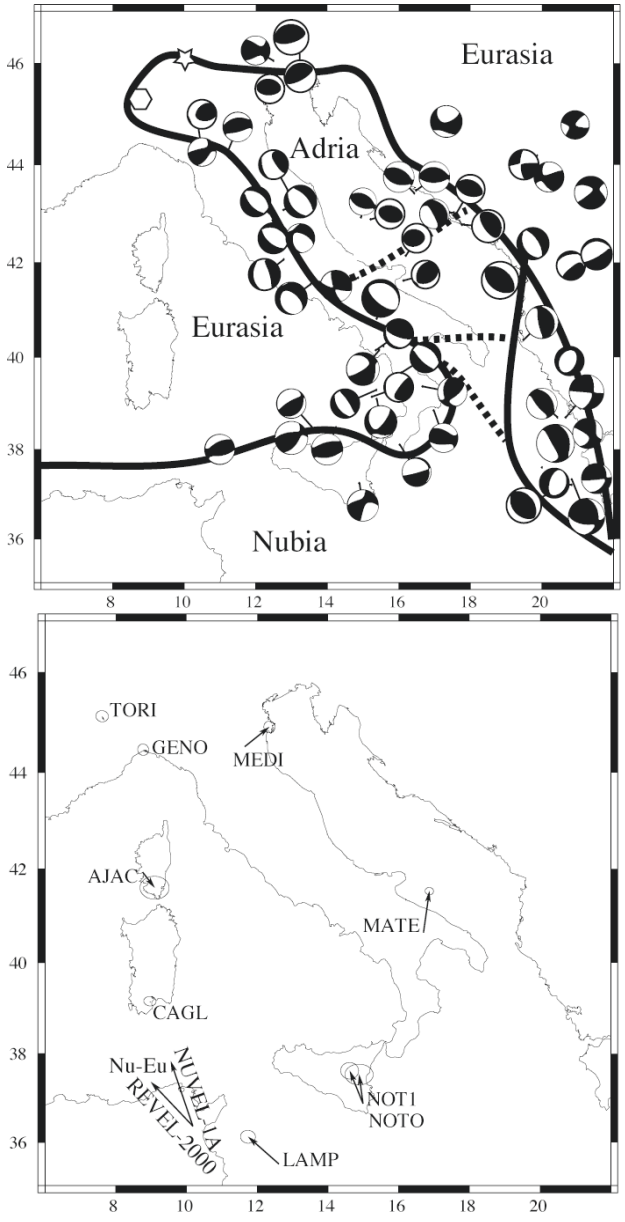

Figure 2. Neotectonics of the circum-Adriatic region. Top: selected earthquake mechanisms from Harvard CMT catalog. Plate boundaries are illustrative, because the precise geometry remains unresolved. Dashed lines indicate some of the proposed southern boundaries of the Adria microplate. Star and hexagon are Adria-Eurasia pole locations from Anderson and Jackson (1987a) and Calais et al. (2002). Bottom: motion of CGPS sites with respect to Eurasia. Error ellipses are 2 σ.

As the papers in this volume illustrate, the steady accumulation of GPS data at more sites spanning longer time series (and hence yielding more precise velocities) is likely to significantly advance understanding of the motion and boundary geometry of Adria. For example, the fact that sites TORI, GENO, AJAC, and CAGL have no significant motion with respect to Eurasia suggests that they are not part of a distinct Adria. The discrepancy between NOTO/NOT1 and LAMP suggests that Sicily may not be part of Nubia.

GEOLOGIC VIEW

Geologic studies offer a seemingly different view (Figures 3, 4). Beginning in Miocene time, Adria subducted westward beneath Italy, forming the Apennines as the northwestern-trending segment of an arcuate thrust belt that extends through Calabria to Sicily (Royden et al., 1987). The arc evolved in association with the opening of the Tyrrhenian Sea beginning about 15 Ma, which is interpreted as back-arc spreading associated with retrograde (rollback) motion of the Adria slab (Malinverno and Ryan, 1986; Rosenbaum and Lister, 2004). As subduction migrated eastward, Italy rotated counterclockwise with respect to Eurasia, as shown by paleomagnetic data. Hence, during this time, a western Italy microplate moved independently from Eurasia.

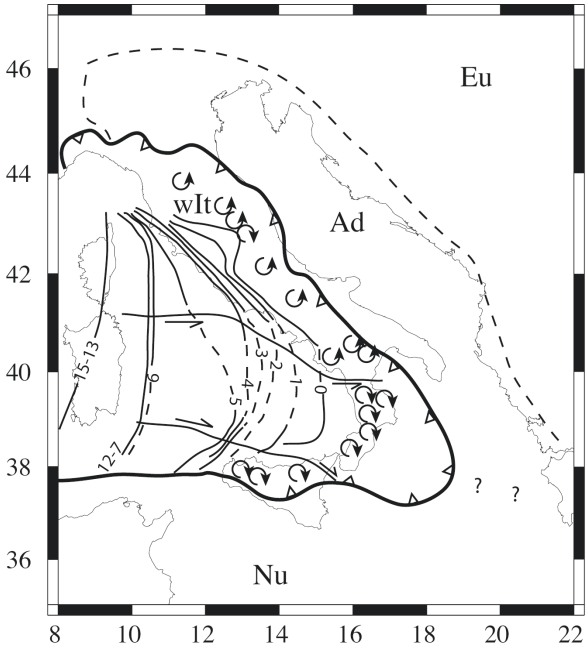

Figure 3. Inferred post-15 Ma evolution of the magmatic arc, shown by isochrones in Ma, associated with opening of the Tyrrhenian Sea and rollback motion of the Adria slab. As subduction migrated eastward, western Italy (wIt) rotated counterclockwise with respect to Eurasia, as shown by paleomagnetic data north of the 41 parallel strike-slip fault zone. (After Rosenbaum and Lister, 2004)

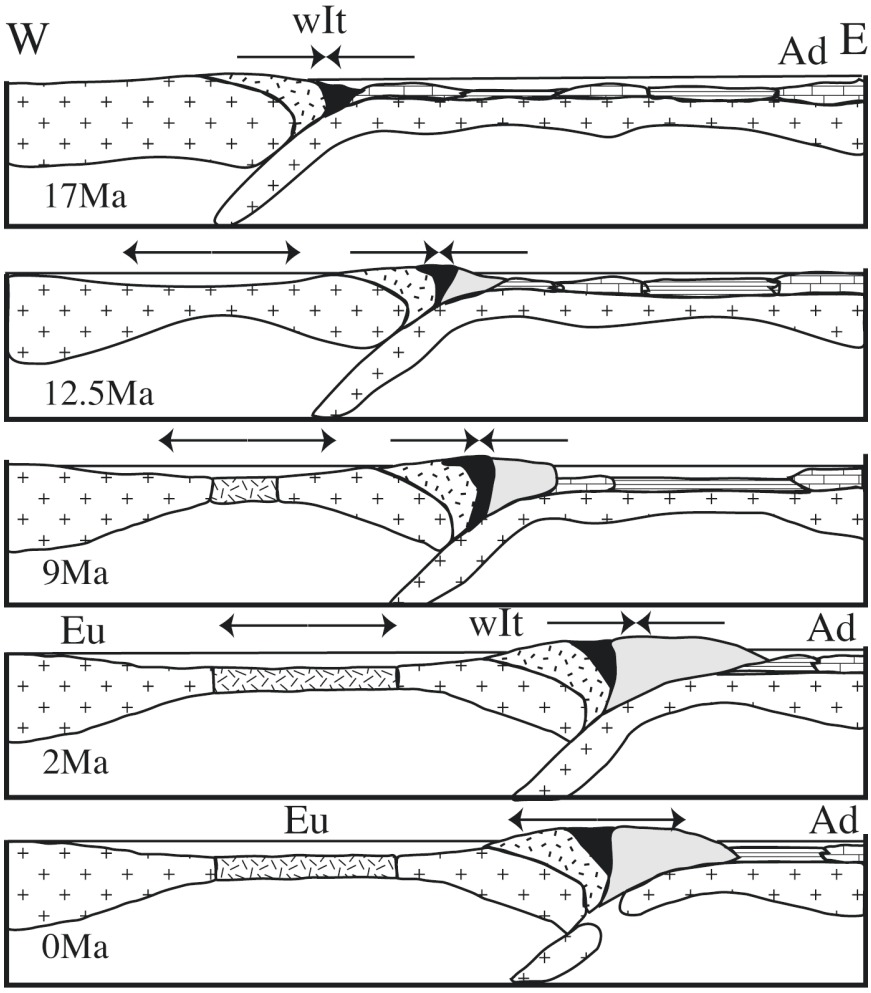

Figure 4. Schematic evolution of the Tyrrhenian Sea and Apennine arc. In this modification of Malinverno's and Ryan's (1986) scenario, subduction and back-arc spreading ceased within the past 2 My, making Italy west of the Apennines part of Eurasia (Eu). Adria (Ad) motion then caused a shift from convergence to extension in the Apennines.

This subduction, however, has been slowing since Pliocene time. At present, earthquakes deeper than about 200 km below the Tyrrhenian Sea occur only in the Sicily-Calabria portion of the arc, suggesting that active subduction beneath the Apennines has ceased (Anderson and Jackson, 1987b). Convergence is indicated by the thrust-fault mechanisms north of Sicily, and by GPS data (Figure 2) showing Sicily moving northwestward with respect to Eurasia (Grenerczy and Kenyeres, this volume; Kahle, this volume). A similar view emerges from seismic tomography that shows a high-velocity slab

extending to the surface only below Calabria (Wortel and Spakman, 2000). Wortel and Spakman (2000) interpret the slab geometry as a consequence of progressive slab detachment, beginning about 8 Ma in the northern Apennines, which has by now detached the slab except in Calabria (Figure 5). The slab detachment hypothesis remains under discussion, largely owing to differences between the results of tomographic studies (Lucente et al., 1999). However, there is general agreement that subduction along the Apennines has either stopped or is near its end, whether because of slab detachment or because oceanic crust in the Adriatic has been subducted, leaving only unsubductable continental crust (Lucente et al., 1999). Similarly, the extension in the northern Tyrrhenian Sea is thought to have stopped, although it may continue in the south (Rosenbaum and Lister, 2004).

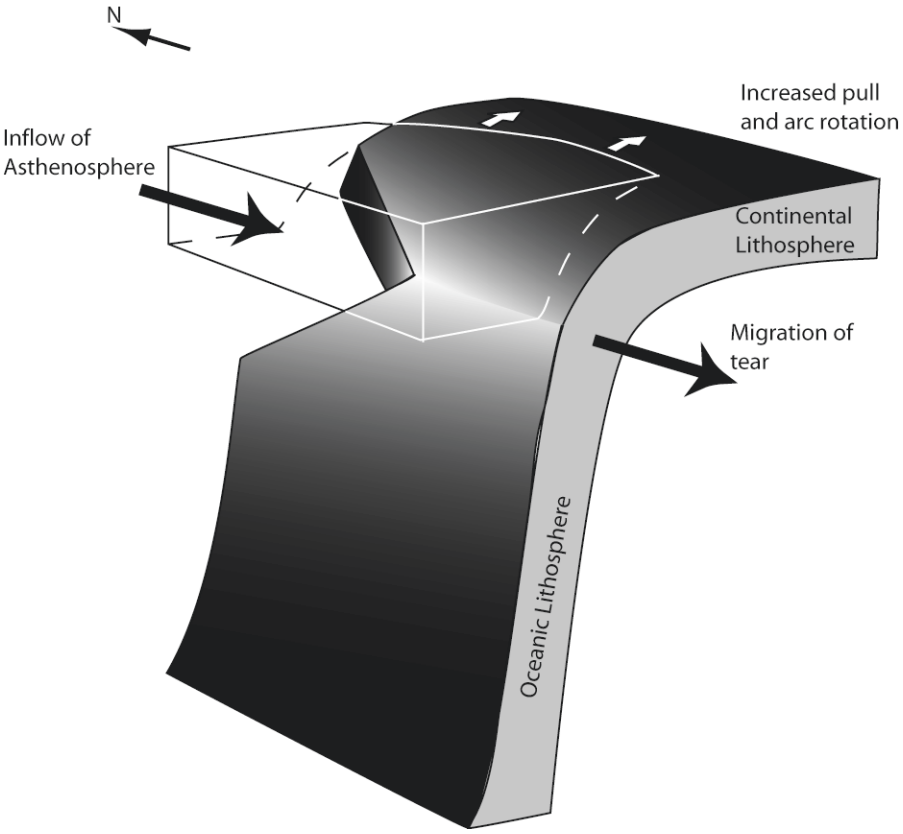

Figure 5. Slab detachment model of Wortel and Spakman (2000), shown for the case where detachment of the Adria slab begins in the north and propagates southward.

TRANSITION IN PLATE MOTIONS

We suggest that the ending of subduction, slab detachment, and spreading in the northern Tyrrhenian Sea gave rise to a change in regional plate motions that explains the Pleistocene shift from convergence to extension in the Apennines. This scenario is summarized in Figure 4, which modifies the sequence proposed by Malinverno and Ryan (1986). We regard their "present" geometry as somewhat older, perhaps 2 Ma, and assume that subduction and back-arc spreading are no longer occurring. Hence Italy west of the Apennines now moves as part of Eurasia rather than as a distinct block. Adria now moves northeastward with respect to Eurasia, making the Apennines an extensional boundary between Adria and western Italy, now Eurasia. Initiation of this boundary is indicated by the 0.8 Ma change from compression to extension in the Apennines (Bertotti et al., 1997; Piccardi et al., 1999), and its present nature is indicated by active faulting and extensional earthquake mechanisms. (Although our interpretation is that the extensional events illustrate a divergent plate boundary, they can also be interpreted as back-arc extension above on-going subduction (Frepoli and Amato, 1997).)

How this transition might have taken place depends on the relative plate motions at the time, which are essentially unknown. Figure 6 illustrates hypothetical linear velocities with respect to Eurasia at a point in the Apennines located at 43°N, 13°E. Africa-Eurasia motion (7.5 mm/yr at N27°W) is illustrated by that predicted by NUVEL-1A (DeMets et al., 1994), which gives an average over the past 3 My. Adria-Eurasia motion (3.5 mm/yr at N36°E) is illustrated by the present motion derived from GPS site velocities by Calais et al. (2002). Absent magnetic anomaly data in the Tyrrhenian Sea, we crudely estimate a western Italy-Eurasia motion of 13 mm/yr at N40°E from the motion of the northern Apennine magmatic arc over the past 3 My (Rosenbaum and Lister, 2004).

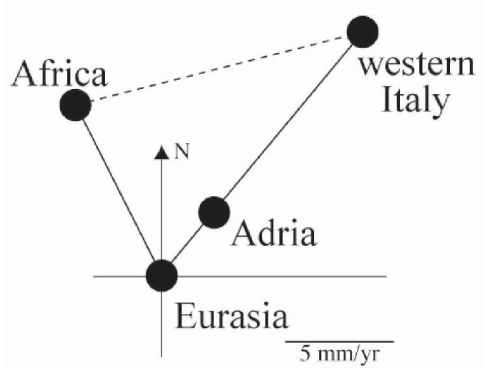

Figure 6. Linear velocity vectors for possible Adria, western Italy, and Africa plate motions with respect to Eurasia prior to the change in plate motions within the past 2 My.

Comparing these velocities is at best schematic, given both their individual uncertainties and the fact that they span different time periods. Even so, the velocities allow us to explore how the transition in plate motion may have occurred.

For simplicity, we assume that Adria already existed as an independent microplate, whose motion with respect to Eurasia was similar to the present motion. In this case, as a result of the difference in northeastward motion rates, Adria moved southwestward at about 10 mm/yr with respect to western Italy, causing convergence beneath the Apennines. Once subduction and back-arc opening ceased, western Italy moved as part of Eurasia, and the Apennines became an extensional Adria-Eurasia boundary.

DISCUSSION

The transition in plate geometry we suggest is a simple approach to reconciling two different views of Adria's behavior each emerging from different data over different times. This transition is a plausible consequence of a widely assumed change in the geometry of subduction and back-arc spreading. How the transition occurred depends on the nature of Adria and its surroundings before the transition.

For this issue, the past plate geometry on Adria's eastern boundary is crucial. The Dinarides are thought to have formed by eastward subduction of Adria prior to the Late Eocene (Pamic et al., 2002ab), after which convergence slowed as a consequence of slab break-off. Possible evidence for slab break-off comes from the absence of deep- or intermediate-depth earthquakes beneath the Dinarides, which argues against a continuous subducting Adriatic slab. Resolving the presence or absence of a high-velocity slab has been a challenge for tomographic studies. Initial studies showed a high-velocity anomaly ringing the Adriatic on both sides at about 250 km depth that did not extend to the surface, as shown in de Boorder et al. (1998). Subsequent studies find this anomaly smaller, as shown in Carminati et al. (1998) or absent (Marone et al., 2004). Post-Eocene deformation included right-lateral motion (Picha, 2002).

Figure 7 shows a schematic scenario for how Adria and its surroundings may have evolved over the past 30 My. Initially, we assume that Adria was part of Africa (soon to be Nubia), consistent with paleomagnetic (Channell, 1996) and paleontologic (Bosellini, 2002) data that are interpreted as showing that in the Cretaceous Adria was not distinct from Africa, whereas it clearly is today. (A contrary view is that Adria has been independent since the Cretaceous (Platt et al., 1989).)

Adria (perhaps part of Africa/Nubia) subducting beneath the Dinarides. Slab begins tearing. Open triangles indicate detached slab. Velocities (thick arrows) are shown with respect to Eurasia.

Subduction of Adria beneath western Italy (wIt) begins, forming the Apennines. Extension results from back arc spreading in the Tyrrhenian sea. Slab beneath the Dinarides keeps tearing.

Nubia changes direction to NNW. Adria moves NE yielding a zone of deformation on its southern boundary. Extension in the Tyrrhenian sea increases in the south, wIT rotates CCW, and the subducting slab beneath the Apennines begins to tear.

Slab beneath Apennines torn all the way to Calabria. Extension in the Tyrrhenian sea slows.

Tyrrhenian sea extension stopped, making western Italy part of Eurasia. Adria moves as a rigid plate north of the Gargano-Dubrovnic seismic zone (GDSZ). Extension occurs along the Apennines and slow convergence continues on the eastern boundary

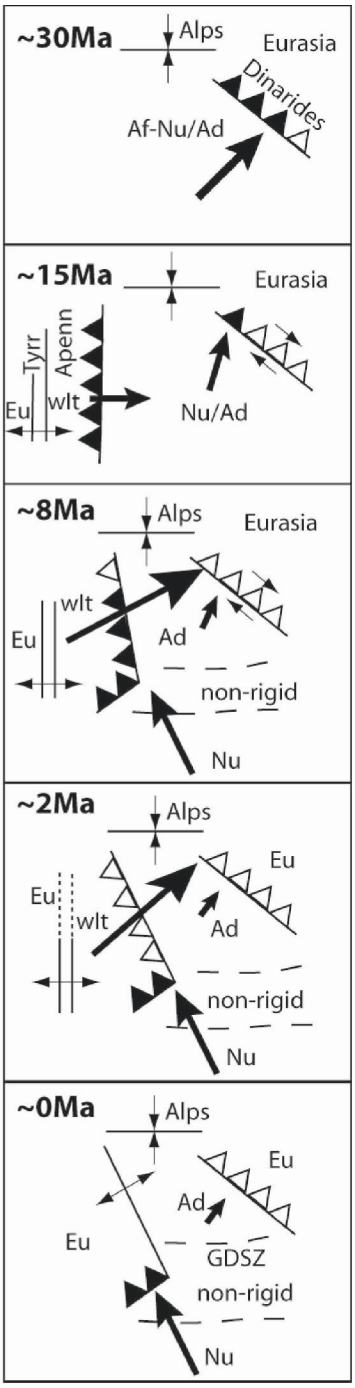

Figure 7: Schematic scenario for how Adria and its surroundings may have evolved over the past 30 My.

Hence, at some point during the complex history of Africa-Eurasia convergence, Adria began to move independently. In the Miocene, subduction began beneath the Apennines, causing back arc extension in the Tyrrhenian Sea. A combination of the effects of the new western boundary and slab detachment in the east (beginning at the southern end) slowed Adria-Eurasia convergence and changed its direction, causing strike-slip motion along Adria's eastern boundary. Although Adria may have become distinct from Nubia at this time, we suspect that it occurred later. At about 8 Ma, Adria separated as a consequence of Nubia's change to its present northwestward motion with respect to Eurasia (Dewey et al., 1989). Hence Adria preserved northeastward motion even though Africa's motion changed. A broad deformation zone, coinciding with the already-thinned crust of the Ionian Sea (Catalano et al., 2001), marked the new Nubia-Adria boundary zone, which remains ill-defined today. At about the same time, progressive slab detachment began in the northern Apennines. Eventually, detachment extended south to Calabria, ending back-arc spreading in the Tyrrhenian Sea and making western Italy part of Eurasia.

This scenario is, of course, speculative. However, we think it offers useful insights into the evolution of Adria and its eastern and western boundaries, which need to be considered simultaneously. Testing these ideas and moving beyond them involves several possible lines of research. First, it is crucial to understand how motion varied around Adria as a function of time. At present, because of the nearby Adria-Eurasia pole, these motions change rapidly along strike. Hence it would be important to understand these motions at least for the past 15 My. For example, the focal mechanisms show present convergence in the Dinarides, and the pole position implies strike slip further to the north. Geologic evidence could help test whether the past motions were similar. There has also been extensive discussion in the paleomagnetic literature about rotations in the circum-Adriatic area, including both regions considered to be part of present Adria and regions surrounding it (Channell, 1996; Marton et al., 2002). As noted by the paper's epigram, these data can help establish at what time Adria became an independent entity, and how its motion both before and after this time affected its surroundings.

A particularly crucial issue is to understand the geometry of Adria's boundaries and the relation of Adria both at present and in the past to the African (now Nubian) Plate. At present, as noted earlier, it is unclear where Adria ends to the south and Nubia begins. For example, the motions of MEDI and MATE are discordant. It seems likely that Calabria, Apulia, and eastern Sicily are not part of Adria, but instead are blocks distinct from both Adria and Nubia. Although present convergence is often assumed to occur south of Sicily, the thrust fault mechanisms north of Sicily imply that some convergence occurs there at present. However, GPS data show that the motion of site NOTO in southern Sicily is somewhat discrepant from that of LAMP,

on the Nubian Plate. How and when this geometry developed is a crucial question, and presumably reflects the complex history of both the subduction geometry and the larger-scale complex history of Africa-Eurasia motion. Understanding these kinematic issues would give important insight into the complex dynamics of this multi-plate system's evolution.

In summary, Adria and its surroundings illustrate that, although Africa-Eurasia convergence has been going for a very long time, the boundary zone between these two major plates remains complex and rapidly evolving.

ACKNOWLEDGEMENTS

We thank Nicholas Pinter and Gyula Grenerczy for inviting us to this conference and hence forcing us to confront and learn a little about the tectonics of this fascinating region, and the conference participants for their valuable presentations. We also thank Rob Govers, Luigi Piccardi, Suzan van der Lee, John Weber, and Rinus Wortel for stimulating discussions.

REFERENCES

Anderson H.A. Is the Adriatic an African promontory? Geology 1987; 15: 212-215.

Anderson H.A., Jackson J.A. Active tectonics of the Adriatic region. Geophys. J. R. Astron. Soc. 1987a; 91: 937-983.

Anderson H.A., Jackson J.A. The deep seismicity of the Tyrrhenian Sea. Geophys. J. R. Astron. Soc. 1987b; 91: 613-637.

Battaglia M., Murray M.H., Serpelloni E., Burgmann R. The Adriatic region: an independent microplate within the Africa-Eurasia collision zone. Geophys. Res. Lett. 2004; 31:10.1029/2004GL019723.

Bertotti G., Capozzi R., Picotti V. Extensional controls on Quaternary tectonics, geomorphology, and sedimentation of the N-Apennines foothills and adjacent Po plain (Italy). Tectonophysics 1997; 282: 291-301.

Bosellini A. Dinosaurs "rewrite" the geodynamics of the eastern Mediterranean and the paleogeography of the Apulia platform. Earth Sci. Rev. 2002; 59: 211-234.

Calais E., Nocqet J.-M., Jouanne F., Tardy M. Current strain regime in the western Alps from continuous Global Positioning System measurements. 1996-2001. Geology 2002; 30: 651-654.

Carminati E., Wortel M.J.R., Spakman W., Sabadini R. The role of slab detachment processes in the opening of the western-central Mediterranean basins: some geological and geophysical evidence. Tectonophysics 1998; 160: 651-665.

Catalano R., Doglioni C., Merlini, S. On the Mesozoic Ionian Basin. Geophys. J. Int. 2001; 144: 49-64.

Channell J.E.T. “Paleomagnetism and paleogeography of Adria.” In *Paleomagnetism and tectonics of the Mediterranean region,* A. Morris and D. H. Tarling, eds., Geol. Soc. Spec. Publ. 1996; 105: 119-132.

Console R., Di Giovambattista R., Favali P., Presgrave B., Smriglio G. Seismicity of the Adria microplate. Tectonophysics 1993; 218: 343-354.

de Boorder H., Spakman W., White S.H., Wortel M.J.R. Late Cenozoic mineralization, orogenic collapse, and slab detachment in the European Alpine Belt. Earth Planet Sci. Lett. 1998; 164: 569-575.

DeMets C., Gordon R.G., Argus D.F., Stein S. Effect of recent revisions to the geomagnetic reversal time scale on estimates of current plate motion. Geophys. Res. Lett. 1994; 21: 2191-2194.

Dewey J.F., Helman M.L., Turco E., Hutton D.H.W., Knott S.D. "Kinematics of the western Mediterranean." In *Alpine Tectonics*, M. P. Coward, D. Dietrich, R. G. Park, eds., London: Geol. Soc. London Spec. Publ. 1989; 45: 265-284.

Engeln J.F., Stein S., Werner J., Gordon R. Microplate and shear zone models for oceanic spreading center reorganizations. J. Geophys. Res. 1988; 93:2839-2856.

Frepoli A., Amato A. Contemporaneous extension and compression in the northern Apennines from earthquake fault planes. Geophys. J. Int. 1997; 129: 368-388.

Lucente F., Chiarabba C., Cimini G., Giardini D. Tomographic constraints on the geodynamic evolution of the Italian region. J. Geophys. Res. 1999; 104:20,307-20,327.

Malinverno A., Ryan W.B.F. Extension in the Tyrrhenian sea and shortening in the Apennines as a result of arc migration driven by sinking of the lithosphere. Tectonics 1986; 5: 227-245.

Marone F., van der Lee S., Giardini D. Three-dimensional upper-mantle S-velocity model for the Eurasia-Africa plate boundary region. Geophys. J. Int. 2004; 158: 109-130.

Marton E., Pavelic D., Tomljenovic B., Avanic R., Pamic J., Marton P. In the wake of a counterclockwise rotating Adriatic microplate: Neogene Paleomagnetic results from northern Croatia. Int. J. Earth Sci. 2002; 91: 514-523.

Morris A., Tarling D. H. eds., *Paleomagnetism and tectonics of the Mediterranean region*, Geol. Soc. Spec. Publ. 1996; 105.

Oldow J.S., Ferranti L., Lewis D.S., Campbell J. K., D'Argenio B., Catalano R., Pappone G., Carmignani L., Conti P., Aiken C. Active fragmentation of Adria, the north Africa promontory, central Mediterranean orogen. Geology 2002; 30: 779-782.

Piccardi L., Gaudemer Y., Tapponier P., Boccaletti M. Active oblique extension in the central Apennines (Italy): evidence from the Fucino region. Geophys. J. Int. 1999; 139: 499-530.

Pamic J., Tomljenovic B., Balen D. Geodynamic and petrologic evolution of Alpine ophiolites from the central and NW Dinarides: an overview. Lithos. 2002a; 65: 113-142.

Pamic J., Balen D., Herak M. Origin and geodynamic evolution of Late Paleogene magmatic associations along the Periadriatic-Sava-Vardar magmatic belt. Geodinamica Acta. 2002b; 15: 209-213.

Picha F. Late orogenic strike-slip faulting and escape tectonics in frontal Dinarides-Hellenides, Croatia, Yugoslavia, Albania, and Greece. Bull. Amer. Assoc. Petrol. Geol. 2002; 86: 1659-1671.

Platt J. P., Behrmann J.H., Cunningham P.C., Dewey J.F., Helman M., Parish M., Wallis S., Weston P.J. Kinematics of the Alpine arc and the motion history of Adria. Nature 1989; 337: 158-161.

Rosenbaum G., Lister G.S. Neogene and Quaternary rollback evolution of the Tyrrhenian sea, the Apennines, and the Sicilian Maghrebides. Tectonics 2004; 23:10.1029/2003TC001518.

Royden L.H., Patacca E., Scandone P. Segmentation and configuration of subducted lithosphere in Italy: an important control on thrust-belt and foredeep basin evolution. Geology 1987; 15:714-717.

Sella G.F., Dixon T.H., Mao A. REVEL: A model for recent plate velocities from space geodesy. J. Geophys. Res. 2002; 107:10.1029/2000JB000033.

Stein S., Gordon R.G. Statistical tests of additional plate boundaries from plate motion inversions. Earth Planet Sci. Lett. 1984; 69: 401-412.

Ward S.N. Constraints on the seismotectonics of the central Mediterranean from Very Long Baseline Interferometry. Geophys. J. Int. 1994; 117: 441-452.

Wortel M.J.R., Spakman W. Subduction and slab detachment in the Mediterranean-Carpathian region. Science 2000; 290: 1910-1919.

PLATE TECTONIC FRAMEWORK AND GPS-DERIVED STRAIN-RATE FIELD WITHIN THE BOUNDARY ZONES OF THE EURASIAN AND AFRICAN PLATES

Christine Hollenstein, Hans-Gert Kahle, Alain Geiger
Geodesy and Geodynamics Lab, ETH Zürich, Switzerland
hollenstein@geod.baug.ethz.ch

ABSTRACT

The Adriatic microplate forms the central part of the Alpine-Mediterranean plate boundary area located between the African and Eurasian Plates. The Eurasia/Africa collision is closely related to continental subduction. Superimposed on the relatively slow counterclockwise rotation of the African Plate, complex dynamic processes affect lithospheric blocks between the two major plates. Seismic results indicate the presence of subducted lithosphere below the Alpine-Mediterranean collision belt. The belt displays pronounced differences in structural style. Compressional deformation and mountain building can be traced around the Adriatic block including the Calabrian and Hellenic arcs. Recent GPS results reveal large motion for the Anatolian/Aegean microplates directed towards west-southwest, relative to the Eurasian Plate. In the Calabrian Arc and Ionian Sea area, there is a complex distribution of compressional and tensional stress regimes. Most recent GPS results indicate a relatively strong compressional strain regime to the north of Sicily, which is concordant with fault-plane solutions of recent earthquakes and which is indicative of the position of the actual kinematic boundary of the African Plate. The Tyrrhenian Sea and its surroundings move like the Eurasian Plate. The boundaries of the Anatolian/Aegean Plates are characterized by large strain rates due to rapid W-SW oriented movement that reaches 35 mm/y.

INTRODUCTION

New geodetic instrumentation and improved spaceborne measuring techniques permit a more accurate interpretation of recent crustal movements. At the same time, synthesis of multidisciplinary quantities and inversion of observations for geodynamically relevant parameters form part of current and future international activities, such as pursued by the Working Group of European Geoscientists for the Establishment of Networks for Earth-Science Research (WEGENER; Plag et al., 1998). In hazardous areas, either continuous GPS or repetitive measuring campaigns at shorter time intervals have been continued and strengthened. This allows for the determination of space and time variations in the regional strain tensors.

N. Pinter et al. (eds.), The Adria Microplate: GPS Geodesy, Tectonics and Hazards, 35–50.

The results achieved so far can be considered as a first important step towards a better understanding of the geologic evolution, geophysical structure and present-day dynamics of the Alpine-Mediterranean region (Kahle and Mueller, 1998). However, most of the deformation processes are not yet fully understood. Mapping the kinematic pattern (horizontal and vertical motions) in specific areas where lithospheric detachment seems to be active or may have faded out will yield important kinematic data as boundary conditions for modeling arc evolution and back-arc basin development. The current height components of deformations are, to date, almost completely unknown, but as time passes the signals of vertical motions will become recognizable in long-term time series of GPS observations. With modern space-geodetic techniques, it will become possible to provide data which ultimately will enable us to shed light on the plate tectonic processes of the Alpine-Mediterranean region and better assess the pattern of current crustal deformation around the Adriatic microplate.

The purpose of this paper is to summarize the present-day crustal movements and geodetic strain field for the wider European area, and to focus on the southern and southeastern boundary of the Adriatic microplate, in particular.

PLATE TECTONIC FRAMEWORK

In a simplistic picture, the recent major tectonic processes in the Mediterranean-Alpine region can be understood as a consequence of sea-floor spreading in the Atlantic Ocean, the Red Sea and the Gulf of Aden. Higher spreading rates in the South Atlantic as compared to the rates in the North Atlantic cause a gradual counterclockwise rotation of the African Plate resulting in a northwestward directed push against Eurasia.

Seismic activity in the Mediterranean-Alpine regions (Figure 1) impressively illustrates the existence and dimensions of the so-called "Adriatic promontory" of the African Plate proposed by Channell and Horvath (1976). Figure 1 also clearly demonstrates the existence of the Aegean-Anatolian microplate.

The Mediterranean-Alpine region has been shaped by numerous episodes of destruction and creation of oceanic lithosphere. From Ocean Drilling Program data across the Tyrrhenian Sea, Kastens et al. (1988) inferred that tilting, subsidence and rifting had occurred on the margin near Sardinia. Emplacement of basaltic crust in the central Tyrrhenian Sea started in the Tortonian. In contrast, the formation of basaltic crust in the southeastern part of the Tyrrhenian Sea began not earlier than Late Pliocene. This later date of initiation of basaltic crust formation is in agreement with suggestions that the Tyrrhenian Sea has grown southeastward towards the

Calabrian arc. A key issue in the assessment of recent crustal movements around the Tyrrhenian Sea is the analysis of GPS observations. Recent results will be shown below.

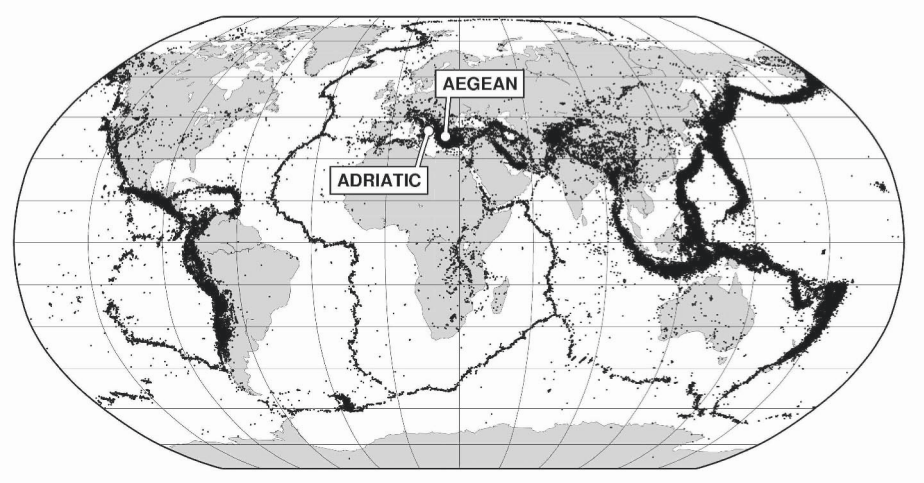

Figure 1. World seismicity 1973-2001 (M>4) after USGS-NEIC (http://gldss7.cr.usgs.gov/neis/epic/epic.html).

Subduction of the African Plate is still going on today beneath the Hellenic, Calabrian and Gibraltar arcs, resulting in the extension and subsidence of the Aegean, Tyrrhenian and Alboran basins (see Figure 2). Mapping of the Mohorovicic discontinuity (the "Moho"), which separates the crust from the upper mantle, has been carried out by many investigators based on seismic refraction and reflection surveys. Deep crustal roots have been found under the Betics, Pyrenees, Alps, Dinarides, Hellenides, and Caucasus mountain ranges. The regions with the smallest crustal thickness correlate with episodes of recent subsidence, such as in the Pannonian basin. A third feature are the "oceanized" basins, including the Alboran Sea, the Tyrrhenian Sea, the Ionian Sea, the southern Aegean Sea, and the Black Sea. The Ionian Sea is underlain by an oceanic type of crust. The Mediterranean Ridge, extending from the Apulian plateau to the island of Rhodes and the southern part of the Antalya basin, has an intermediate-type crust. The margins of the Eastern Mediterranean Sea are bound by normal continental crust. While the southern and eastern coastal regions of the Eastern Mediterranean are typical passive continental margins, the northern boundaries are active continental margins comprising the Calabrian, Hellenic and Tauric arcs associated with compressional processes.

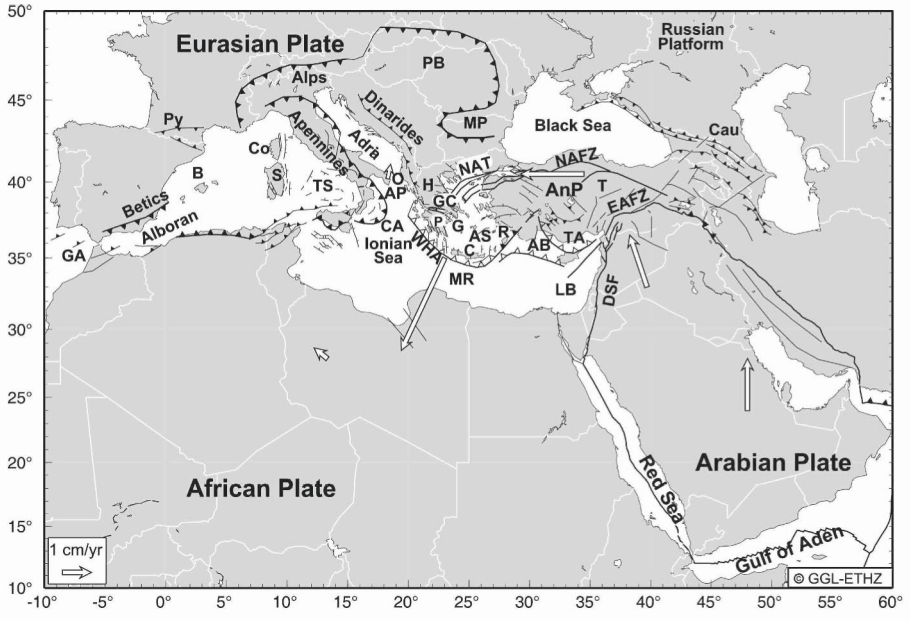

Figure 2. Geotectonic framework of the Mediterranean region and surrounding areas. The arrows represent plate motions relative to Eurasia (Kahle et al., 1998; Africa (Nubia) motion after Sella et al., 2002). AB: Antalya basin, AnP: Anatolian microplate, AP: Apulian plateau, AS: Aegean Sea, B: Balearic islands, C: Crete, CA: Calabrian arc, Cau: Caucasus, Co: Corsica, DSF: Dead Sea Fault, EAFZ: East Anatolian Fault Zone, G: Greece, GA: Gibraltar arc, GC: Gulf of Corinthos, H: Hellenides, LB: Levant basin, MP: Moesian Platform, MR: Mediterranean ridge, NAFZ: North Anatolian Fault Zone, NAT: North Aegean Trough, O: Otranto, P: Peloponnesus, Py: Pyrenees, PB: Pannonian basin, R: Rhodes, S: Sardinia, T: Turkey, TA: Tauric arc, TS: Tyrrhenian Sea, WHA: West Hellenic arc.

To map the gross features of the lithosphere-asthenosphere system, dispersion of surface waves has been analyzed (Panza et al., 1980). Significant deviations from the average European thickness value of 90 to 100 km were found in the Balearic and Tyrrhenian basins (each with a thickness of about 30 km). The considerable increase in lithospheric thickness (up to 130 km) beneath the central and eastern part of the Southern Alps suggests subduction of the Eurasian Plate under the Adriatic microplate. Due to the plate collision south of the Alps, the lithosphere reacts by a pronounced thickening, producing high-velocity, high-density, cold and slowly subsiding "lithospheric roots". The actual plate boundary between Africa and Eurasia is characterized by deep structural features in the Alpine area and in the northernmost part of Africa.

In eastern and northern Turkey, seismic activity is primarily associated with the East and North Anatolian Transform fault zones. The East Anatolian and Dead Sea Transform fault zones exhibit predominant left-lateral motion, while the North Anatolian fault motion is governed by right-lateral strike slip. Horizontal displacement on these faults is determined by the relative motion between the Eurasian and Arabian Plates, with the Anatolian plate moving to the west (McClusky et al., 2000). In the western part of Turkey as well as in central and southern Greece, tensional earthquake mechanisms dominate, due to normal faulting in the Aegean graben system.

An Alpine orogenic belt can be traced from the Dinarides and Hellenides in the west through the Hellenic island arc and the Aegean archipelago to the Taurides in Turkey. The geological framework of the Aegean Sea is characterized by thrusting of the Hellenic nappes over the stable pre-Apulian zone along a NW-SE-trending front. The outward growth of the Mediterranean Ridge complex as a function of time has been elucidated by Kastens (1991). She concluded that the seaward migration of the Mediterranean Ridge has accelerated since its initiation from about 6 mm/y to 22 mm/y.

Under the southern Aegean Sea, the slab seems to be uninterrupted, with a clear outline of the Wadati-Benioff zone. Detailed neotectonic studies on the Ionian islands, the Gulf of Corinthos and the Peloponnesus have revealed a complex strain pattern for the Quaternary (Spakman, 1990). Compression dominates in the external part of the Hellenic arc, north-south extension is observed around the Gulf of Corinthos, while east-west extension has been found in the southern Peloponnesus and in western Crete. In the internal part of the Hellenic, arc-normal faulting is observed from the Gulf of Corinthos to Crete. The strain-rate field in the Hellenic-Aegean region is most likely due to the superposition of back-arc spreading in the Aegean Sea and the collision with the Apulian microplate. Recent GPS results are displayed and discussed below.

Lowrie (1980) suggested that the Apennine peninsula, the island chain of Corsica and Sardinia as well as the Iberian peninsula have all undergone counterclockwise rotations to a varying degree. Whether this slow rotation is still in progress will have to be tested in the future by dedicated GPS measurements. The first complete repetition of GPS measurements at stations in the western Hellenic Arc tied across the Strait of Otranto to an additional station in southern Apulia was carried out in 1991. The results – if compared to the 1989 GPS measurements, a high-class triangulation in the 1970´s and distance measurements in the 1930's – suggest a shortening of the distance between Othoni island in northwestern Greece and Specchia Cristi in southern Apulia of 9 mm per year over the past 60 years (Kahle et al., 1993). Repeated GPS measurements have been carried out to reveal whether this trend can be confirmed (see below).

Along the southeastern margin of the Tyrrhenian Sea bordering the Apennine peninsula and Sicily, there is a chain of elongated peripheral basins filled with thick sediments. Based on combined seismic-refraction and -reflection experiments carried out in the central Tyrrhenian Sea, a depth of 12 km to the crust-mantle transition zone was found, corresponding to a total crustal thickness of 8 to 9 km (Finetti and Morelli, 1972) which points towards an intermediate (rifted) to oceanic type of crust.

RECENT CRUSTAL MOVEMENTS AND STRAIN RATE FIELDS

Based on 6 years of continuous GPS data of the European IGS (International GPS Service), EUREF (European Reference Frame) and Greek stations, a kinematic field has been derived and plotted relative to the rotation of the North American Plate (Figure 3). It is remarkable that almost all of the resulting velocity vectors of crustal motion follow small circles about a pole that had been deduced from geophysical information (DeMets et al., 1990).

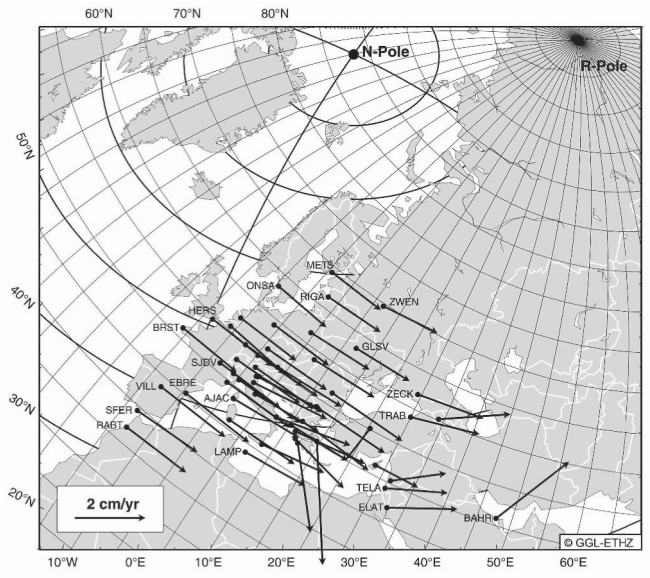

Figure 3. GPS-rates of crustal motion relative to the North-American Plate. The rotation of the North-American Plate was subtracted, using a rotation rate of 0.195°/My around a pole located at 2.3°N and 79.7°W (Heflin and Argus, pers. commun., 1998). N-Pole is the geographical North Pole, while R-Pole (63.2°N, 134.5°E) and the corresponding gridlines represent a geophysical pole of rotation of the Eurasian Plate (DeMets et al., 1990).

In order to visualize the rates of crustal motion relative to Eurasia, the rotational part of the Eurasian Plate (relative to ITRF97) was subtracted using a rotation rate of 0.262°/My around a pole located at 59.0°N and 97.1°W (Heflin and Argus, pers. commun., 1998; Figure 4).

As a result, it can be seen that the Eurasian stations (except those in Greece, Turkey and bordering regions) have only small motions (on the order of 1 mm/yr). So there is almost no internal deformation within the Eurasian plate. The African Plate motion is visible in the southwest, as documented by stations in southwest Spain, Morocco, Sicily and the island of Lampedusa. The Arabia Plate motion is seen in the southeast for the station Bahrain. Most striking are the large westward and southwestward velocities of the Anatolian and Aegean microplates, respectively. But the Adriatic microplate also clearly shows a different kinematic behavior compared to the Eurasian Plate.

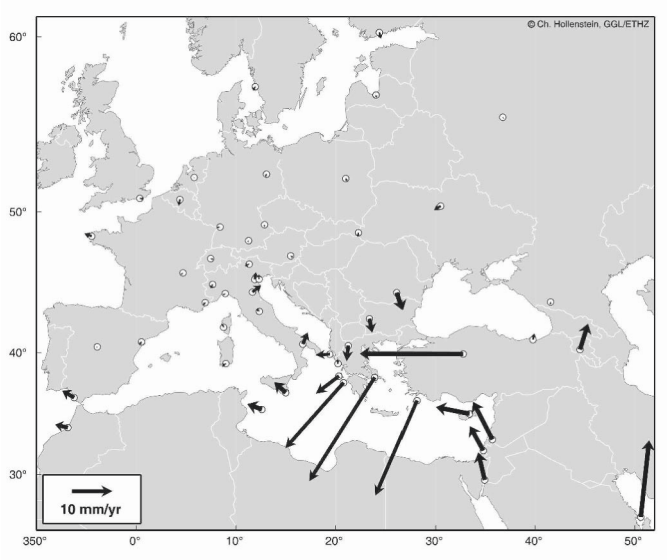

Figure 4. Rates of crustal motion relative to Eurasia, derived from continuous GPS data of IGS, EUREF and Greek sites between 1995 and 2001.

In the following discussion, more detailed GPS velocity and strain-rate results are presented for the central and eastern Mediterranean. The strain-rate field is calculated from the velocities at GPS sites by least-squares collocation. Collocation is a general method of least-squares adjustment which includes parameter estimation, filtering and prediction/interpolation. The displacements, the signal-to-noise ratio of the displacements, and a covariance function are used as input. Details are given in Kahle et al. (2000). Since the velocities and the strain rates are directly interrelated by a

differential equation, the strain-rate field (Figure 6) can be determined without explicitly gridding the velocity field.

To visualize the deformation attributed to seismotectonic processes active on major fault systems, the normal and shear strain rates associated with the major faults in the eastern Mediterranean were calculated (Figs. 7 and 8). Details of this calculation can be found in Straub (1996). The locations of faults do not influence the strain-rate results, they only defines the points at which we calculate and show the strain rates. Removing a fault or introducing a new one, does not change the results along the other faults. No fault does not mean that there is no strain; we simply do not show it.

In Figure 5a, the velocity results from continuous and repeated GPS measurements in southern Italy between 1994 and 2001 after Hollenstein et al. (2003) are shown. The velocities in Figure 5b show the integration of recent GPS data from a number of GPS campaigns in the eastern Mediterranean. Fig 6 represents the collocated strain-rate fields for the two areas overlain with fault plane solution of major earthquakes. The strain-rate field for the central Mediterranean (Figure 6a) is based on the velocities of Figure 5a. Due to the lack of GPS data on the African side of the Hellenic arc, the strain-rate field along this trench is only weakly constrained. To obtain realistic strain rates in the eastern Mediterranean (Figure 6b), the velocities of Figure 5b therefore were supplemented by velocities representing the motion of the African Plate. The corresponding points were introduced to the south of the seismic belt, and we used rates calculated from a rigid Africa (Nubia) rotation (Sella et al., 2002).

Seismicity and fault-plane solutions for southern Italy show active deformation, which varies between N-S shortening and NE-SW extension on normal faults along the Apennine Chain (Anderson and Jackson, 1987). The Dinaric coast region is deforming on strike-slip and thrust faults. A belt of NE-SW shortening continues into northwestern Greece along numerous transcurrent fault systems (Mantovani et al., 1992). NE-SW-oriented compression is also seen in the GPS-based strain rates in northwestern Greece (Figure 7). There are too few GPS stations in this region and to the north for one to go into further detail.

The GPS velocities and the strain rates in the region of southern Italy support the following results of previous work. Compression between Apulia and northwestern Greece (5 mm/y), extension across the southern Apennines (Amato and Montone, 1997; Hunstad et al., 2003) right-lateral movement between Vulcano and Lipari (Bonaccorso, 2002), as well as extension and dextral strike slip in the Sicily Rift Zone (Cello, 1987).

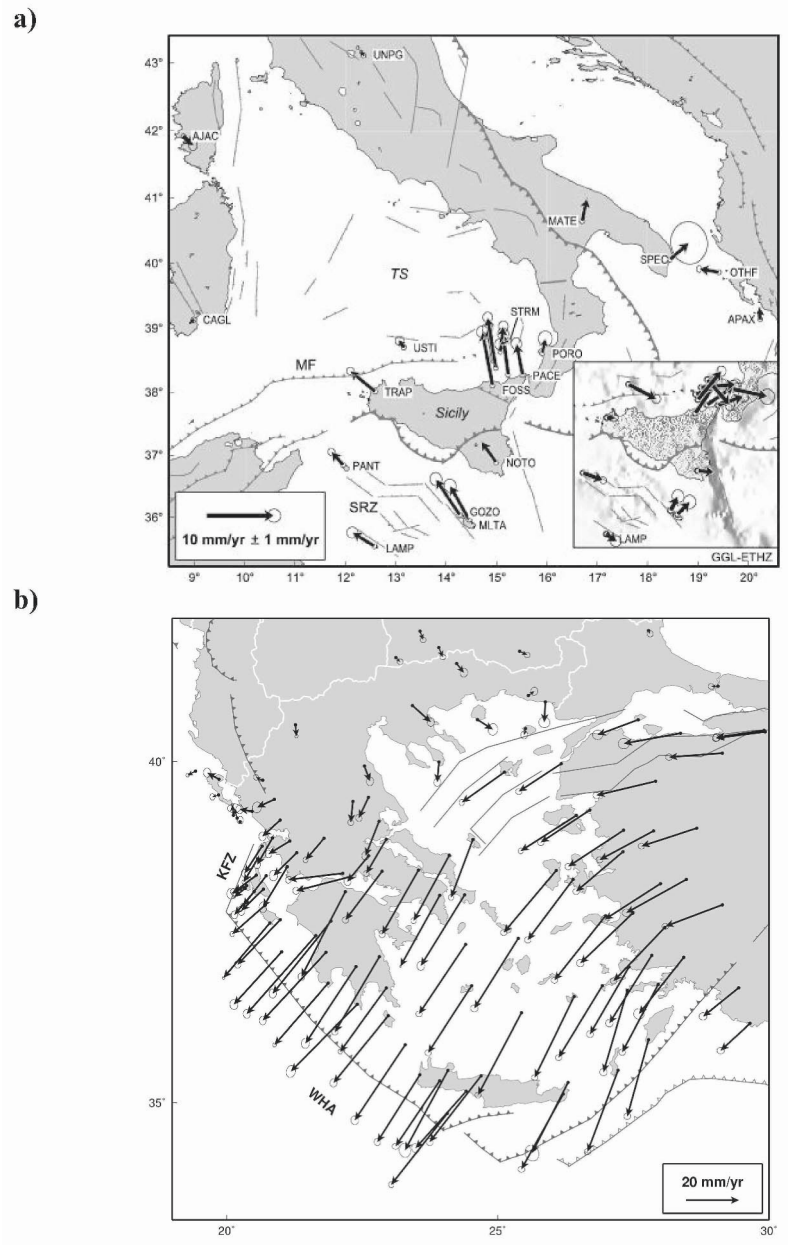

Figure 5. GPS velocity fields relative to Eurasia. The error ellipses represent the 1-sigma confidence region. a) For southern Italy, based on results from Hollenstein et al. (2003). Inset: velocities relative to Africa. b) For the eastern Mediterranean, combined velocity field based on GPS results from McClusky et al. (2000), Kotzev et al. (2001), and Cocard et al. (1999). Notice the different scales in a) and b). KFZ: Kephalonia Fault Zone, MF: Maghrebian front, SRZ: Sicily Rift Zone, TS: Tyrrhenian Sea, WHA: West Hellenic Arc.

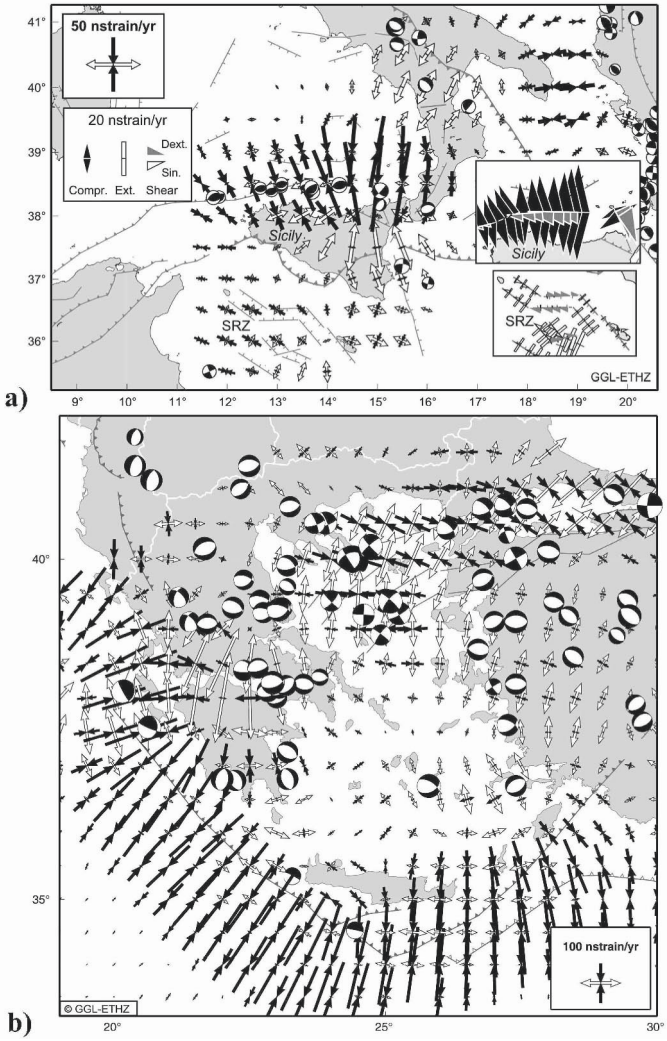

Figure 6. Principal values and axes of strain rates calculated from the velocities shown in Figure 5 and – for 6b – some additional virtual rates representing the motion of the African Plate. The scales are given in nanostrain/yr; they equal a relative motion of 1 mm/yr over a distance of 1000 km normal to the fault. If the width of the deformation zone is multiplied by the strain rates, the total relative motion is obtained. The focal mechanisms of larger earthquakes are from Harvard CMT solutions (http://www.seismology.harvard.edu), Jackson et al. (1992) and Pondrelli et al. (2002; http://www.ingv.it/seismoglo/RCMT/). a) For southern Italy (Hollenstein et al., 2003). Insets: Normal and shear strain rates associated with selected faults. b) For eastern Mediterranean. Notice the different scales in a) and b). There is large compression to the north of Sicily. The regions around the Gulf of Corinthos are characterized by large extensional strain rates. The SW Aegean Sea is nearly strain free. Along the West Hellenic Arc, significant compression is observed. The focal mechanisms correspond quite well to the type of deformation identified by GPS observations. Especially remarkable is the relatively quiet of the central Aegean.

In addition, new kinematic constraints have been obtained. The Eurasian Plate extends beyond Corsica and Sardinia to the Tyrrhenian Sea. Statistically insignificant displacement for Corsica and Sardinia were also found by Oldow et al. (2002). Whether these new, short-term GPS results are indicative of a tectonic reorganization in the Tyrrhenian/Calabrian area is under discussion and will remain an open interesting question (Faccenna et al., 2004; Pondrelli et al., 2004; Goes et al., 2004; Rosenbaum et al., 2004). The island of Lampedusa is situated on the African shelf and moves like the African Plate. Also, the Sicily Rift Zone and the southwestern coast of Sicily are dominated by the African Plate motion. The compression between the African and Eurasian Plates seems to be concentrated along the Maghrebian front to the northwest and north of Sicily, which is consistent with compressional focal mechanisms of earthquakes which have occurred along this belt. Large north components of the velocities in northeastern Sicily (up to 8 mm/y) enhance compression to the north and cause extension in the interior of Sicily.

The velocity field in the eastern Mediterranean is separated into two main parts by the North Anatolian Fault Zone (NAFZ), North Aegean Trough (NAT) and the Kephalonia Fault Zone (KFZ). To the north and northwest, relatively small and Eurasia-like motions are observed. Northern Greece and southern Bulgaria move to the south and southwest with rates between 2 and 5 mm/y, while the area to the northeast of the KFZ shows westward to northwestward motion. To the south of the above mentioned line, Anatolian-Aegean block is moving rapidly, turning from westward direction along the NAFZ to southwestward direction in the Aegean Sea. The rates reach 40 mm/yr. A large increase of velocities is found along the KFZ, from less than 10 mm/yr in the north up to more than 30 mm/yr in the south within a distance of 200 km.

Our results indicate a relatively strain-free region in the central southern Aegean, between the volcanic and the non-volcanic Hellenic arc (37° to 38°N and 35° to 36°N, respectively). High extensional strain rates are confined to the northern Aegean Sea and to western Anatolia. Maps of in-situ stress measurements compiled by Rebai et al. (1992) show mainly N-S extensional horizontal stress in central Greece, which is also seen in the GPS results.

The seismic cluster in the south-eastern Aegean Sea, coincides with NW-SE-oriented extension, also accompanied by recent active volcanism. Comparison with the seismic strain-rate fields derived from an inversion of moment tensors of seismic events show that this area is characterized by a pronounced seismic strain deficit (Jenny et al., 2004).

Normal deformation rate components on the major fault zones reveal large extension in central Greece, centered around the Gulf of Corinthos (Figure 7). The West Hellenic arc is associated with strong compression. The

relatively small compression to the southwest of Crete is caused by a measurement point which is located very close to the arc. It shifted the large compression more to the south, which is not shown on this map.

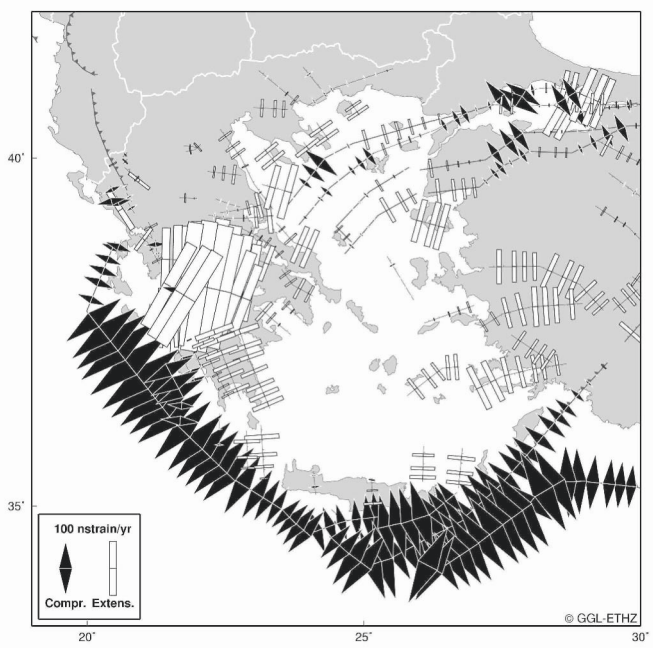

Figure 7. Normal deformation rates associated with major faults.

Northwest Anatolia is dominated by the both extension and compression. The SW-trending portions of the NAFZ are associated with compression, whereas the NW-oriented segments show mostly extensional activity. This can be related to the restraining and releasing stress behavior along the NAFZ which changes its strike on several well-defined fault segments. The western part of Anatolia is characterized by N-S-oriented extensional strain rates, coincident with W-E-trending graben structures, that are also associated with large normal earthquakes.

The southwestern margin of Greece is dominated mainly by the subduction of the African Plate along the Hellenic trench. The most important fault zone taking up this motion is the KFZ (Kahle et al., 2000). The dextral nature of the KFZ is clearly illustrated by the shear strain rates shown in Figure 8. This area shows intense seismicity as well. Devastating earthquakes with magnitudes of M>7, associated with dextral fault-plane solutions (FPS), occurred on the central Ionian islands in 1945 and 1953 (Stiros et al., 1994), in 1972 (Anderson and Jackson, 1987), and in 1983 (Kiratzi and Langston, 1991).

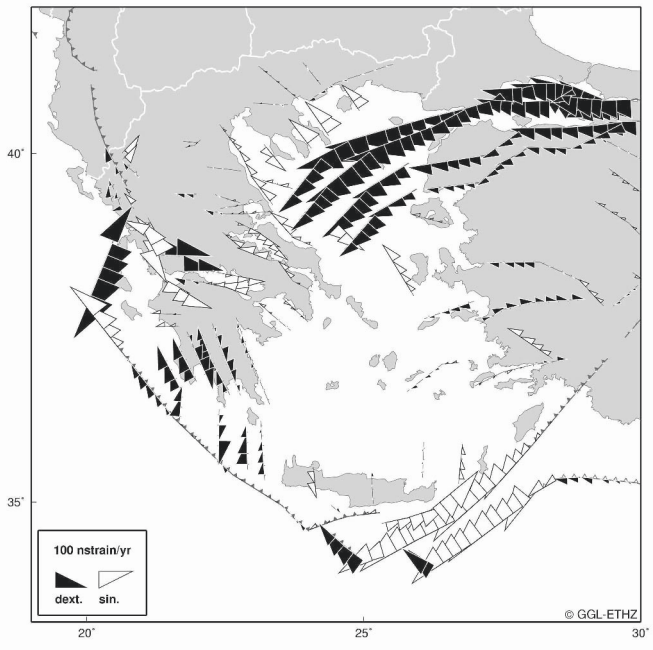

Figure 8. Shear strain rates associated with major faults.

The northern and central Aegean area is governed by distributed right-lateral strike-slip faulting (Taymaz et al., 1991). The GPS strain-rate analysis reveals that these features are dominated by right-lateral components of shear (Figure 8) accompanied by extension, ranging between NNE-SSW to NNW-SSE directions. The dextral sense of motion along the NAFZ, clearly visible in the GPS results, is also documented on the FPS (Figure 6). Sinistral shear strain is dominant in the area beginning east of the island of Crete, running along the island of Rhodes and into southwest Turkey, identifying the Strabo and Pliny troughs, which act as transcurrent faults, separating the moving Aegean Plate from the eastern Mediterranean basins.

CONCLUSIONS

- The kinematic field in the Eastern Mediterranean is characterized by W-WSW-SW motion of 20-40 mm/yr for Anatolia-Aegean, relative to Eurasia. A distinct right-lateral strike-slip boundary is aligned with the zone following the Black Sea–Marmara–Epirus–central Ionian Islands. The Tyrrhenian Sea block moves like Eurasia, and the Sicily rift zone

like Africa. The KFZ right-lateral strike-slip delineates the end of the West Hellenic subduction.

- Results of the strain-rate field calculation reveal pronounced extension in western Anatolia, the Aegean region and in central northern Greece, where normal faulting earthquakes are predominant. Significant compression is found perpendicular to the West Hellenic arc, between Apulia and northwestern Greece, and to the north of the coastline of Sicily. Maximum dextral shear has been found along the NAFZ-NAT-KFZ line. N-S-oriented extensional strain rates dominate in central Greece, accompanied by normal faulting earthquake mechanisms.
- The calculation of normal and shear components of the deformation rates on major fault systems show that three main types of strain distribution dominate: extension in the Aegean region and central northern Greece, compression perpendicular to the Hellenic arc, and shear along the NAFZ-NAT-KFZ line . In the southern Ionian islands, compression occurs in a N34°E direction across the Hellenic arc. The Central Southern Aegean is strain-free.
- Deficits in seismically-released strain are apparent in the Eastern Mediterranean (Kahle et al., 1999, 2000; Jenny et al., 2004).
- In summary, we conclude that the strain-rate field in the central and eastern Mediterranean is further constrained by GPS data. The results are considered as a first preliminary step towards a better understanding of the complex present-day dynamics of the eastern Mediterranean-Alpine region, with a focus on the southeastern boundary of the Adriatic microplate, in particular.

ACKNOWLEDGEMENTS

This study benefited greatly from discussions and cooperation with M. Cocard, now University of Laval Quebec, Canada, and D. Giardini, S. Goes and S. Jenny, Institute of Geophysics, ETH Zürich. We thank G. Grenerczy and O. Odalovic for critically reviewing the manuscript and helpful suggestions for its improvement. This work was financed by ETH research grant 41-2647.5 and EU grant ENV4-CT97-0519. The GPS measurements in Italy were supported by ETH Zürich and Centro Spaziale di Matera, Italy.

REFERENCES

Amato A., Montone P. Present-day stress field and active tectonics in southern peninsular Italy. Geophys. J. Int. 1997; 130: 519-534.

Anderson H.A., Jackson J.A. The deep seismicity of the Tyrrhenian sea. Geophys. J.R. Astr. Soc. 1987; 9: 613-638.

Bonaccorso A. Ground deformation of the southern sector of the Aeolian islands volcanic arc from geodetic data. Tectonophysics 2002; 350(3): 181-192.

Cello G. Structure and deformation processes in the Strait of Sicily Rift Zone. Tectonophysics 1987; 141: 237-247.

Channell J.E.T., Horváth F. The African - Adriatic promontory as a paleogeographic premise for Alpine orogeny and plate movements in the Carpatho - Balkan region. Tectonophysics 1976; 35: 71-101.

Cocard M., Kahle H.-G., Peter Y., Geiger A., Veis G., Felekis S., Billiris H., Paradissis D. New constraints on the rapid crustal motion of the Aegean region: recent results inferred from GPS measurements (1993-1998) acrosss the West Hellenic Arc, Greece. Earth and Planetary Science Letters 1999; 172: 39-47.

DeMets C., Gordon R. G., Argus D. F. and Stein S. Current Plate Motions. Geophys. J. Int. 1990; 101(2): 425-478.

Faccenna C., Piromallo C., Crespo-Planc A., Jolivet L., Rossetti F. Lateral slab deformation and the origin of the western Mediterranean arcs. Tectonics 2004; 23: TC 1012.

Finetti I., Morelli C. Wide-scale digital seismic exploration of the Mediterranean Sea, Boll. Geofis. Teor. Appl. 1972; 14: 291-342.

Goes S., Giardini D., Jenny S., Hollenstein C., Kahle H.-G., Geiger A. A recent tectonic reorganisation in the South-Central Mediterranean. Earth and Planetary Science Letters 2004. In press.

Hollenstein C., Kahle H.-G., Geiger A., Jenny S., Goes S., Giardini D. New GPS constraints on the Africa-Eurasia plate boundary zone in southern Italy. Geophys. Res. Lett. 2003; 30(18): 1935, doi:10.1029/2003GL017554.

Hunstad I., Selvaggi G., D'Agostino N., England P., Clarke P., Pierozzi M. Geodetic strain in peninsular Italy between 1875 and 2001. Geophys. Res. Lett. 2003; 30(4): 1181, doi:10.1029/2002GL016447.

Jackson J., Haines J. Holt W. The horizontal velocity field in the deforming Aegean Sea region determined from the Moment Tensors of earthquakes. J. Geophys. R. 1992; 97(B12): 17,657-17,684.

Jenny S., Goes S., Giardini, D., Kahle H.-G. Earthquake recurrence parameters from seismic and geodetic strain rates in the eastern Mediterranean. Geophys. J. Int. 2004. In press.

Kahle H.-G., Müller M.V., Mueller St., Veis G., Billiris H., Paradissis D., Drewes H., Kaniuth K., Stuber K., Tremel H., Zerbini S., Corrado G., Verrone G. Monitoring West Hellenic Arc Tectonics and Calabrian Arc Tectonics ("WHAT A CAT") Using the Global Positioning System. In *Contribution of Space Geodesy to Geodynamics*, D. Smith and D. Turcotten eds., AGU Geodynamics Series, 1993; 23: 417-429.

Kahle H.-G., St. Mueller. Structure and dynamics of the Eurasian-African plate boundary system. J. Geodynamics 1998; 25(3-4): 303-325.

Kahle H.-G., Straub C., Reilinger R., McClusky S., King R., Hurst K., Veis G., Kastens K., Cross P. The strain rate field in the eastern Mediterranean region, estimated by repeated GPS measurements. Tectonophysics 1998; 294: 237-252.

Kahle H.-G., Cocard M., Peter Y., Geiger A., Reilinger R., McClusky S., King R., Barka A., Veis G. The GPS strain rate field in the Aegean Sea and western Anatolia. Geophys. Res. Lett. 1999; 26: 2513-2516.

Kahle H.-G., Cocard M., Peter Y., Geiger A., Reilinger R. S., Barka A., Veis G. GPS-derived strain rate field within the boundary zones of the Eurasian, African, and Arabian plates. J. Geophys. Res. 2000; 105(B10): 23,353-23,370.

Kastens K. Rate of outward growth of the Mediterranean Ridge accretionary complex. Tectonophysics 1991; 199: 25-50.

Kastens K., Mascle J. et al. ODP Leg 107 in the Tyrrhenian Sea: Insights into passive margin and back-arc basin evolution. Geol. Soc. Amer. Bull. 1988; 100: 1140-1156.

Kiratzi A., Langston C.A. Moment tensor inversion of the 1983 Jan. Keffalinia event of Ionian islands (Greece). Geophys. J. Int. 1991; 105: 529-535.

Kotzev et al. GPS study of active tectonics in Bulgaria: results from 1996 to 1998. J. Geodynamics 2001; 31: 189-200.

Lowrie W. A paleomagnetic overview of the Alpine system, Mémoire du B.R.G.M., Orléans, France 1980; 115: 316-330.

Mantovani E., Albarello D., Babbucci D., Tamburelli C. Recent geodynamic evolution of the Central Mediterranean region. Dept. Earth Sciences-University of Siena 1992; 88 pp.

McClusky S., Balassanian S., Barka A., Demir C., Georgiev I., Hamburger M., Hurst K., Kahle H.-G., Kastens K., Kekelidze G., King R., Kotzev V., Lenk O., Mahmoud S., Mishin A., Nadariya M., Ouzounis A., Paradissis D., Peter Y., Prilepin M., Reilinger R., Sanli I., Seeger H., Tealeb A., Tokzoz M., Veis G. GPS constraints on plate kinematics and dynamics in the eastern Mediterranean and Caucasus. J. Geophys. Res. 2000; 105(B3): 5695-5719.

Oldow J.S., Ferranti L., Lewis D., Campbell L., B.D'Argenio B., Catalano R., Pappone G., Carmignani L., Conti P., Aiken C. Active fragmentation of Adria, the north African promontory, central Mediterranean orogen. Geol. Soc. Amer. Bull. 2002; 30: 779-782.

Panza G., Mueller St., Calcagnile G. The gross features of the lithosphere-asthenosphere system in Europe from seismic surface waves and body waves. Pure and Applied Geophys. 1980; 118:1209-1213.

Plag H.-P., Ambrosius B., Baker T., Beutler G., Bianco G., Blewitt G., Boucher C., Davis J., Degnan J., Johansson J., Kahle H.-G., Kumkova I., Marson I., Mueller St., Pavlis E., Pearlman M., Richter B., Spakman W., Tatevian S., Tomasi P., Wilson P.., Zerbini S. Scientific objectives of current and future WEGENER activities. Tectonophysics 1998; 294: 177-223.

Pondrelli S., Morelli A., Ekström G., Mazza S., Boschi E., Dziewonski A. M. European-Mediterranean regional centroid-moment tensors: 1997-2000. Phys. Earth Planet. Int. 2002; 130: 71-101.

Pondrelli S., Piromallo C., Serpelloni E. Convergence vs. retreat in southern Tyrrhenian Sea: Insights from kinematics. Geophys. Res. Lett. 2004; 31: L06611.

Rebai S., Philip H., Tabouda A. Modern tectonic stress field in the Mediterranean region: Evidence for variation in stress directions at different scales. Geophys. J. Int. 1992; 110: 106-140.

Rosenbaum G., Lister G. Neogene and Quaternary rollback evolution of the Tyrrhenian Sea, the Apennines, and the Sicilian Maghrebides. Tectonics 2004; 23: TC 1013.

Sella G.F., Dixon T.H., Mao A. REVEL: A model for recent plate velocities from space geodesy. J. Geophys. Res. 2002; 107(B4), doi:10.1029/2000JB000033.

Spakman W. Tomographic images of the upper mantle below central Europe and the Mediterranean. Terra Nova 1990; 2: 542-553.

Stiros S., Pirazzoli P., Laborel J., Laborel-Deguen F. The 1953 earthquake Cephalonia (western Hellenic Arc): Coastal uplift and halotectonic faulting. Geophys. J. Int. 1994; 117(3): 834-849.

Straub C. *Recent crustal deformation and strain accumulation in the Marmara Sea region, N.W. Anatolia, inferred from GPS measurements*, Ph.D. diss., ETH Zurich, 1996.

Taymaz T., Jackson J., McKenzie D. Active tectonics of the north and central Aegean Sea. Geophys. J. Int. 1991; 106: 433-490.

POST-LATE MIOCENE KINEMATICS OF THE ADRIA MICROPLATE: INFERENCES FROM GEOLOGICAL, GEOPHYSICAL AND GEODETIC DATA

Enzo Mantovani [1], Daniele Babbucci [1], Marcello Viti [1], Dario Albarello [1], Enrico Mugnaioli [1], Nicola Cenni [2], Giuseppe Casula [3]
1: University of Siena, Siena, Italy
mantovani@unisi.it
2: University of Bologna, Bologna, Italy
3: INGV of Bologna, Bologna, Italy

ABSTRACT

The space-time distribution of deformation in the central Mediterranean area suggests that the Adriatic domain (Adria) has moved coherently with Africa up until the late Miocene and that, subsequently, it decoupled from Africa (Nubia) and underwent a clockwise (CW) rotation with respect to Eurasia. This event was determined by the westward push of the Anatolian-Aegean-Balkan system, after its collision with the southern Adriatic continental domain. The CW rotation of the Adria microplate induced a strong compressional regime in the central Mediterranean region, which can account for the major tectonic events that occurred in this zone since the late Miocene. These include the renewal of accretionary activity in the Apenninic belt, the opening of the central Tyrrhenian basin, the detachment of the Iblean microplate from mainland Africa and the development of a major fracture in the northern Adriatic foreland. The CW rotation of the Adria plate came to an end around the late Pliocene-early Pleistocene due to the collision of the Adria continental domain with the Southern Apennines. After this event, Adria has undergone a slow CCW rotation with respect to Eurasia. This kinematic pattern during the last evolutionary phase is suggested by the distribution of Quaternary deformation in the peri-Adriatic zones, in particular the shortening recognized at the eastern (Dinarides-Hellenides) and northern (southern Eastern Alps) boundaries of Adria, and is consistent with the seismological and geodetic evidence in the Adriatic and peri-Adriatic regions. No significant recent deformation can be recognized between Adria and Africa, at the Pliocene decoupling zone or at any other possible decoupling tectonic belt. This suggests no, or at most very little, relative motion between these two domains during the Quaternary. The possible implications of this last evidence on Nubia-Eurasia kinematics are discussed.

N. Pinter et al. (eds.), The Adria Microplate: GPS Geodesy, Tectonics and Hazards, 51–69.

INTRODUCTION

The past and present kinematic behaviour of the Adriatic region (Adria; Figure 1) with respect to the stable part of Africa (Nubia) is still a matter of debate.

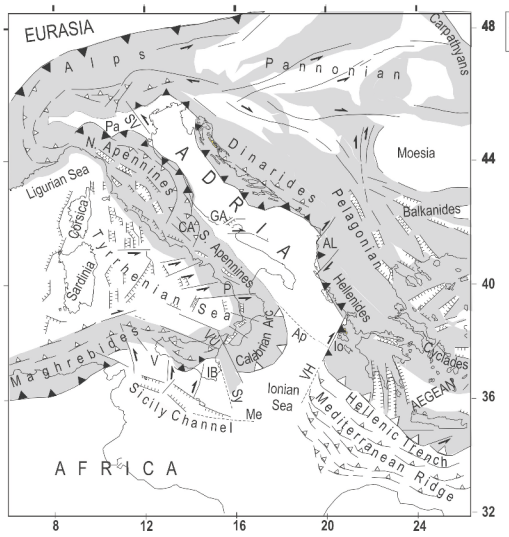

Figure 1. Sketch of major tectonic features in the central Mediterranean. 1) thrusting; 2) subduction zones; 3, 4, 5) compressional, tensional and strike-slip deformations. Grey area identifies the orogenic belts. Ap=Apulian escarpment; AL=Albania; CA=Central Apennines; GA=Gargano zone; IB=Iblean block; Io=Ionian islands; Me=Medina fault; P=Palinuro fault; Pa=Padanian region; SV= Schio-Vicenza fault system; Sy=Syracuse escarpment; VH=Victor Hensen fault system; V=Ventura block; VU=Vulcano fault.

Some authors have argued, on the basis of geological and paleomagnetic evidence, that this domain has moved as an African promontory since the Permian (Muttoni et al., 2001) or, at least, since the early Miocene (e.g., Channell and Horvath, 1976; Dewey et al., 1989), whereas other authors suggest that a distinct Adriatic microplate, composing at least part of the area, presently moves independent of Nubia (Anderson and Jackson, 1987; Westaway, 1990; Favali et al., 1993; Oldow et al., 2002; Nocquet and Calais, 2003). This last hypothesis has been suggested mainly by the fact that the Adriatic-Eurasia kinematics, deduced by earthquake slip vectors and geodetic data, is not compatible with the Nubia-Eurasia relative motion predicted by present-day global kinematic models like NUVEL-1 (DeMets et al., 1990). This work describes an alternative kinematic history of Adria which can coherently account for the time-space distribution of major deformations observed in the central Mediterranean area (Mantovani et al., 1997a, 2002; Mantovani, 2004). It is then

pointed out that no significant decoupling can actually be recognized between Adria and Nubia since the early Pleistocene. Some remarks are also made about the possible implications of the above evidence on the recent/present Nubia-Eurasia relative motion.

LATE CENOZOIC EVOLUTION OF ADRIA AND THE SURROUNDING REGIONS

Around the late Miocene, the tectonic setting in the central Mediterranean region (Figure 2) underwent a drastic change indicated by several coeval tectonic events:

- A major sinistral shear zone, the Schio-Vicenza fault system, developed in the northern Adriatic foreland and southern Alps (e.g., Castellarin and Cantelli, 2000).
- Following a period of relative orogenic quiescence, a violent pulse of accretionary activity occurred in the Apenninic belt, particularly in the Southern Apennines and the Calabrian Arc (Castellarin and Vai, 1986; Ortolani and Pagliuca, 1988; Patacca et al., 1993).
- Extensional tectonics ceased in the northern Tyrrhenian basin and began in the central Tyrrhenian (Magnaghi-Vavilov basin), with the lengthening axis oriented roughly E-W (Finetti and Del Ben, 1986; Sartori, 1990; Sartori and Capozzi, 1998).
- Renewal of vertical movement occurred along the Syracuse and Apulian escarpments, which mark the transition from the Ionian oceanic domain to the adjacent continental lithosphere of the Iblean and Adriatic domains respectively (e.g., Sartori, 1990).
- A major transtensional decoupling zone that included the Victor-Hensen and Medina faults developed in the central Ionian region from the Ionian islands to eastern Sicily (Hieke and Wanninger, 1985; Reuther, 1987; Cello, 1987; Della Vedova and Pellis, 1989; Hieke and Dehghani, 1999). This shear zone was active from the late Miocene to the Pleistocene.
- The Iblean-Ventura crustal wedge decoupled from mainland Africa by the activation of a system of transtensional faults in the Sicily Channel (Finetti and Del Ben, 1986; Reuther, 1987).

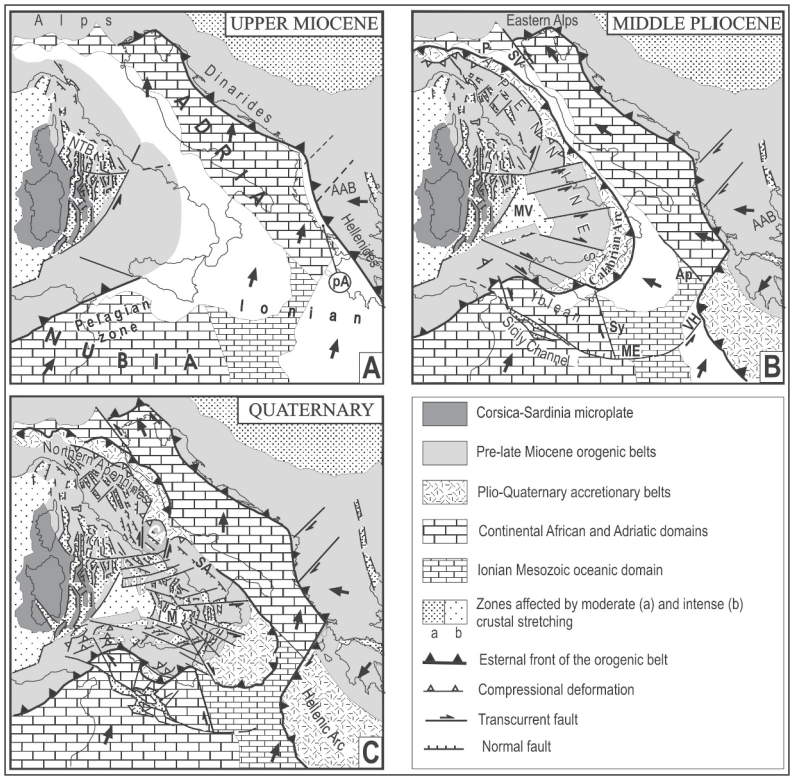

Figure 2. Proposed evolutionary reconstruction of the central Mediterranean region (Mantovani et al., 2002). Upper Miocene: the Adria domain still moves in connection with Nubia. White areas identify the parts of the Adriatic-African domain which will be consumed during the successive evolution. Middle Pliocene: since the Late Miocene, the Adria microplate, driven by the westward push of the Anatolian-Aegean-Balkan system (AAB), decouples from Nubia and rotates CW. Quaternary: the collision of the Southern Apennines (SA) with the continental Adriatic domain causes the cessation of subduction and consequently of accretionary activity at this consuming boundary and a new change in the kinematics of Adria. Black arrows show the kinematics of Adria, Nubia and AAB system with respect to Eurasia. Present coastlines are shown for reference. Ap=Apulian escarpment; M=Marsili basin, MV=Magnaghi-Vavilov basin, NTB=northern Tyrrhenian basin, P=Padanian region, pA=preApulian zone, SV=Schio-Vicenza fault system, VH-ME = Victor-Hensen and Medina fault systems, Sy = Syracuse escarpment.

Any attempt at reconstructing the Pliocene geodynamics and plate kinematic pattern in the central Mediterranean should provide a coherent explanation for those coeval tectonic events. We propose a possible solution of

this problem (Figure 2). The first paleogeographic map (Figure 2a) shows the tectonic setting in the central Mediterranean region around the Upper Miocene, when the Adriatic was still connected with the African Plate as documented by geological evidence in the Ionian and Pelagian regions (e.g., Illies, 1981; Reuther, 1987). The Africa-Adria domain and the westward extruding Anatolian-Aegean-Balkan (AAB) system (Figure 2a) were converging at the expense of the intervening low-buoyancy oceanic lithosphere, the pre-Apulian zone (Mercier et al., 1987).

Around the late Miocene, the collision between the continental Adriatic domain and the AAB system caused the end of subduction, leading to suturing of that convergent boundary. After the collision (Figure 2b), the push of the AAB system forced Adria to decouple from its Padanian protuberance and from Nubia and to rotate CW (Mantovani et al., 1997a, 2002; Mantovani, 2004). This interpretation can provide plausible explanations for the tectonic events mentioned above. The decoupling from the Padanian protuberance is consistent with the activation of the Schio-Vicenza shear zone (e.g., Castellarin and Cantelli, 2000), while the presumed decoupling of Adria from Nubia may explain the development of the transtensional Victor Hensen-Medina-Sicily Channel fault system.

The hypothesis that, after its decoupling from Africa, the Adria microplate rotated CW can explain the observed deformation pattern in the Tyrrhenian-Apennines region. Under the roughly E-W compression induced by the convergence between southernmost Adria and the African continental domain (Tunisia), a fragment of Africa – i.e., the Iblean microplate – decoupled from the mainland and extruded roughly northward. This can account for the initiation or renewal of tectonic activity at the zones surrounding this crustal wedge as the Syracuse escarpment, the Sicily Channel and the Maghrebian belt (e.g., Sartori, 1990 and references therein). The extrusion of the Iblean wedge and the simultaneous CW rotation of Adria induced a strongly contractional regime in the Alpine/Apenninic orogenic system which lay between these blocks and the Corsica-Sardinia microplate. The shortening was accommodated by the roughly eastward escape of crustal wedges from the Alpine-Apenninic belt, at the expense of low-buoyancy lithosphere lying to the west of Adria and in the Ionian area (Figure 2b). This interpretation (Mantovani et al., 1997a, 2002) can explain the reactivation of accretionary activity in the Apenninic belt around the late Miocene (e.g., Castellarin and Vai, 1986; Ortolani and Pagliuca, 1988; Patacca et al., 1993) and the contemporaneous development of crustal stretching in the wake of the extruding wedges, which led to the formation of the Magnaghi-Vavilov basin (Sartori, 1990).

A new drastic change in the deformation pattern occurred in the central Mediterranean region around the late Pliocene-early Pleistocene:

- Accretionary activity came to an end in the Southern Apennines (e.g., Patacca et al., 1993; Cinque et al., 1993) leading to suturing of this covergent boundary.

- Crustal stretching ceased in the Magnaghi-Vavilov basin and began more to the south, leading to the opening of the Marsili basin (e.g., Finetti and Del Ben, 1986; Sartori, 1990).

- Accretionary activity along the external (Ionian) front of the Calabrian Arc accelerated (Rossi and Sartori, 1981; Sartori, 1990; Patacca et al., 1993).

- Tectonic activity and extension accelerated in the Calabrian wedge, as indicated by the formation of several troughs, sphenocasms and transverse faults (e.g., Finetti and Del Ben, 1986; Van Dijk and Okkes, 1991).

- Uplift accelerated in the zone involved in the convergence between Adria and the Africa-Iblean domain, that is, the Calabrian Arc and the Southern Apennines (e.g., Westaway, 1993).

- Accretionary activity reactivated along the southeastern boundary of Adria, the southern Dinarides-Hellenides, after a relatively long period of quiescence, since the late Miocene (e.g., Mercier et al., 1987).

In our opinion, the key event which may help clarify the geodynamic context and which can coherently explain all the tectonic events listed above is the suturing of the Apenninic trench zone. This event testifies that the extruding Apennines crustal wedges collided with the Adriatic continental foreland. This collision determined the end of the CW rotation of Adria. After this event, Nubia-Adria convergence was no longer accommodated by the consuming process under the Southern Apennines (e.g., Patacca et al., 1993). This accelerated the lateral expulsion of the Calabrian wedge at the expense of the Ionian low-buoyancy zone. This kinematic interpretation (Figure 2c) can coherently account for the above-mentioned compressional, tensional and transcurrent deformation of Quaternary age along the borders of the Calabrian wedge and inside it (Mantovani et al., 1997a, 2002; Mantovani, 2004).

The shortening observed along the eastern (e.g., Mercier et al., 1987) and northern (e.g., Del Ben et al., 1991; Castellarin et al., 1992) boundaries of Adria since the late Pliocene suggests that, in the last evolutionary phase, Adria has undergone a slow CCW rotation with respect to Eurasia, with N- to NNE-ward motion in the southern part and NNW- to N-ward motion in the northern part (Figure2c). These kinematics are also suggested by the analysis of seismological and geodetic data (e.g., Anderson and Jackson, 1987; Nocquet and Calais, 2003).

The fact that this motion is not compatible with the NW-ward motion of Nubia predicted by the NUVEL-1 model in the central Mediterranean has led some authors to suggest that the two plates are moving independently, which implies the presence of a decoupling zone accommodating their relative motion. Since this problem appears to be crucial for understanding the tectonic setting in the central Mediterranean region and the relative motion between Nubia and Eurasia, we discuss it in detail in the next section.

EVIDENCE AND SPECULATIONS ABOUT THE ADRIA-NUBIA DECOUPLING

Various hypotheses have been advanced about the presumed decoupling zone between Nubia and Adria. Anderson and Jackson (1987) tentatively suggested that such a decoupling zone could be located in the southernmost Adriatic. However, this location is not supported by clear evidence, neither in terms of seismicity (only few earthquakes have occurred in historical times along a short segment of this zone, CPTI Working Group, 1999) nor by the presence of tectonic features, as pointed out by some authors (e.g., Westaway, 1990; Argnani et al., 2001).

Meletti et al. (2000) suggested that the Syracuse escarpment (Figure1) is the Nubia-Adria boundary zone. This hypothesis appears to be unfounded, since the escarpment does not interrupt the structural continuity between Adria and the Ionian/African domain.

Westaway (1990) proposed a SW-NE-oriented decoupling zone running from the northern Gargano zone to the central Dinarides. Favali et al. (1993) suggested that the decoupling zone consists of a roughly E-W-trending fault system running from the southern Gargano zone to Albania. Oldow et al. (2002) proposed a more complex boundary between Nubia and the Adria, involving a transverse fault in the central Adriatic Sea lying north of the decoupling zone proposed by Westaway (1990).

All these proposed central Adriatic decoupling zones are based on the hypothesis that the faults recognized in the Gargano zone and offshore of it cut through the Adria microplate to its eastern border. However, this is not consistent with the available evidence. While the Gargano structural high and the adjacent offshore area is recognized as an active tectonic zone based on geological and geophysical data, the faults in that zone have only a limited seaward extension (e.g., De Alteriis, 1995; Argnani et al., 1993).

Also, the distribution of earthquake epicentres in the Adriatic area since the year 1600 A.D. does not show any clear evidence in support of the central Adriatic decoupling zones (e.g., Slejko et al., 1999; Mantovani, 2004 and references therein). The only seismicity map showing a concentration of earthquakes along the presumed decoupling in the central Adriatic is presented by Oldow et al. (2002), but this map is based only on the preliminary USGS catalogue.

The viability of the proposed decoupling zones should also be evaluated by analysing their compatibility with the strain regimes implied by the respective Adria-Nubia kinematic models. We present, for instance, such an analysis for the plate configuration and kinematics (Figure 3) proposed by Oldow et al. (2002).

Since no significant changes in the tectonic setting have occurred in the central Mediterranean area during the Quaternary (e.g., Dercourt et al., 1986; Finetti et al., 1987; Mantovani et al. 2002), one can reasonably assume that the recent kinematic pattern, such as shown in Figure 3, matches the pattern for at least the last 2 My. Under this assumption, a significant shortening (on the order of 10 km) is expected along the presumed central Adriatic boundary zone (sector CD in Figure 3) as an effect of the presumed Adria-Nubia convergence. However, geological and geophysical evidence (e.g., Finetti et al., 1987; Slejko et al., 1999; De Alteriis, 1995) does not show such deformations in the central Adriatic. It is also very difficult to reconcile the shear deformation implied by the presumed kinematic pattern in the sectors BC and DE of the presumed Adria-Nubia boundary (Figure 3), with the seismicity and neotectonic deformation observed in the Southern Apennines (e.g., Cinque et al., 1993; Viti et al., 2001) and the northern Dinarides (e.g., Renner and Slejko, 1994).

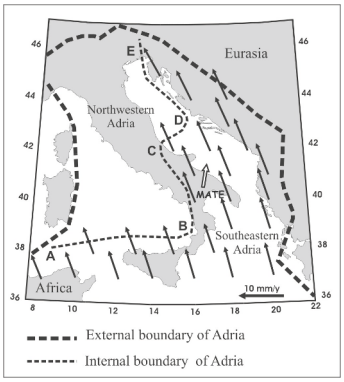

Figure 3. Geometry of the Adria and Africa (Nubia) domains and their velocity fields proposed by Oldow et al. (2002). The velocity vectors in Nubia are compatible with the NUVEL-1 pole (DeMets et al., 1990). The motion of the NW Adria block with respect to Eurasia is negligible. The Nubia-Adria plate boundary suggested by Oldow et al. (2002) is divided in sectors, identified by letters, in order to facilitate the discussion in the text. The open arrow in southern Italy indicates the geodetic velocity of the Matera (MATE) station (Anzidei et al., 2001).

RECENT ADRIA KINEMATICS AND THE NUBIA-EURASIA RELATIVE MOTION

The evidence of negligible recent relative motion between Adria and Nubia could allow using the motion of Adria as a constraint on the kinematics of Nubia. In particular, this would suggest that Nubia moves roughly NNE-ward in the central Mediterranean region. This conclusion is corroborated by the NNE-oriented velocity vector of the Matera station (Figure 3) that is the most stable and reliable geodetic information in the area, due to a long observation period and the coherent results from different (VLBI, SLR and GPS) geodetic techniques (Devoti et al., 2002).

The same Nubia kinematics are suggested by the morphology of the Hellenic and Cyprus Arcs, which are both characterized by SE-NW-oriented trench zones and perpendicular strike-slip faults. The morphology of this plate boundary indicates that the convergence between Nubia and the Anatolian-Aegean system is NE-ward. This evidence is generally attributed to the fact that the Aegean zone is moving SW-ward with a velocity much higher than that of Nubia. However, this high velocity is only supported by geodetic observations (e.g., McClusky et al., 2003), which indicate motion rates ranging between 20 and 40 mm/y. Geological data and long-term seismicity features along the North Anatolian fault system (Barka, 1992) suggest that the recent rate of motion of the Anatolian-Aegean system has been in the range of 8-10 mm/y. This evidence is consistent with the estimated seismic convergence rate at the Hellenic trench (e.g., Jackson and McKenzie, 1988). Numerical experiments, carried out with elastic-viscous models (Mantovani et al., 2001a) have shown that the difference between the middle- to long-term (geological) and short-term (geodetically determined) kinematics of the Anatolian-Aegean system can be explained as an effect of post-seismic relaxation induced by the last sequence of strong earthquakes along the North Anatolian fault system beginning in 1939 (e.g., Barka, 1992).

In our opinion, any discussion about the implications of the morphology of the Hellenic Arc should take into account the long-term rather than the short-term kinematics of the Anatolian-Aegean system. If the slow long-term motion rate of the Anatolian-Aegean system is considered, the morphology of the Hellenic Arc is compatible with a NE-ward motion of Nubia oriented more-or-less coincident with the motion suggested by the kinematics of the Adriatic plate.

The evidence and arguments above suggest that the predictions of global kinematic models for Nubia-Eurasia motion should be reconsidered, as suggested for instance, by Albarello et al. (1995). One major reason for reconsideration is that this motion has been derived based on the assumption that Eurasia moves as a rigid plate, which does not take into account the occurrence of significant seismotectonic activity in several zones of Western Europe, from Portugal to the Rhine graben system. This activity could imply that some parts of Western Europe do not move with the stable part of Eurasia lying east of the Rhine graben system. In that case, kinematic data along the Mid-Atlantic ridge bordering Western Europe and those along the Azores-Gibraltar belt would not be representative of North America-Eurasia and Nubia-Eurasia relative motions, respectively. In order to explore the possible effects of this alternative plate configuration, Albarello et al. (1995) computed Nubia-Stable Eurasia Euler poles using the procedure adopted by DeMets et al. (1990), but considering a data set without the North Atlantic data bordering Western Europe and along the Azores-Gibraltar tectonic belt. This investigation has shown that a number of the acceptable Nubia-stable Eurasia poles that reproduce data within their errors predict a roughly NNE-ward motion of Nubia in the central Mediterranean region, which is compatible with the Nubia kinematics suggested by the kinematics of Adria and the morphology of the Hellenic and Cyprus Arcs.

The kinematics of the Atlantic-Iberian block obtained by considering the kinematic indicators in the Mid-Atlantic ridges facing Western Europe and those along the Azores-Gibraltar seismic belt imply a roughly SE-NW convergence with Nubia, which is compatible with the deformation pattern recognized in the collision zone between Nubia and Iberia (Albarello et al., 1995; Mantovani, 2004 and references therein).

Nubia-Eurasia Euler poles have been tentatively deduced from GPS data (e.g., Sella et al., 2002; McClusky et al., 2003; Nocquet and Calais, 2003). However, the reliability of these preliminary attempts can hardly be evaluated, mainly because the geodetic stations presently available in the Nubian Plate are few and are mostly located along the deforming margins of the plate (Sella et al. 2002; Mantovani, 2004). Furthermore, the analysis of these data has shown that the location of the Nubia-Eurasia Euler poles is strongly dependent on the selection of stations used in data inversion (Mantovani, 2004).

NUMERICAL MODELING

Numerical modelling provides quantitative insights into the recent/present kinematic pattern in the central Mediterranean region and into the

reliability of the Nubia-Eurasia kinematic models discussed above (Mantovani et al., 2001b). The aim of these experiments was to reproduce the strain field in the central-eastern Mediterranean area deduced from neotectonic and seismological constraints. This has been achieved by imposing kinematic boundary conditions to an elastic model where major tectonic decoupling zones, such as strike-slip faults, under-thrusting fronts and extensional belts, are simulated by narrow zones with values of elastic parameters much lower than those adopted for blocks. Since all decoupling zones in the model act simultaneously, the results obtained are thought to be representative of the long-term tectonic behavior, during which it can reasonably be assumed that all tectonic zones have experienced seismic or aseismic movement.

The results of this investigation have shown that a satisfactory fit of the observed strain field, in spite of its considerable lateral heterogeneity, can be obtained by imposing kinematic boundary conditions consistent with the Nubia motion suggested by Albarello et al. (1995) and with the westward motion of the Anatolian wedge (e.g., McKenzie, 1978). Details about the model parameterization adopted in computations, the observed strain field and the level of agreement between observed and computed strain fields for the preferred solution are given by Mantovani et al. (2001b).

The preferred displacement field obtained by modeling (Figure4a) implies that Adria moves roughly NNE-ward in the southern part, consistently with geodetic (Anzidei et al., 2001; Nocquet and Calais, 2003) and geological (e.g., Mantovani, 2004) data and moves roughly NNW-ward in the northern part, in accord with earthquake slip vectors in the southern Alps (Anderson and Jackson, 1987).

Some uncertainty might surround the motion predicted for the northernmost part of Adria, due to the vicinity of this zone to the border of the model, which could imply some boundary effect. Some geodetic measurements in Slovenia and the northern Dinarides (e.g., Weber et al., 2004) suggest a prevalent N-ward motion, while other geodetic data (Altiner, 2001) indicated NNW-ward motion. Considering the highly fractured nature of this zone, lwhich is located at the margin of the Adria microplate, Eastern Alps and Dinaric structures (e.g., Vrabec and Fodor, 2004), it is not easy to understand if these geodetic data are representative of the kinematics of the Adria microplate with respect to Eurasia.

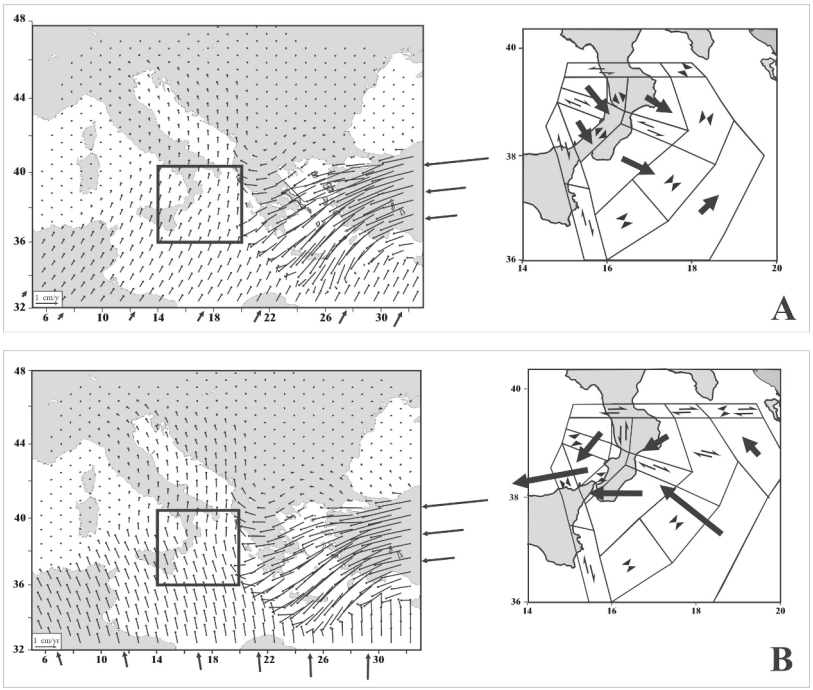

Figure 4. A) The left figure shows the displacement field (thin arrows) with respect to stable Eurasia in the central Mediterranean area, obtained by finite element modeling, which is compatible with the strain pattern deduced from neotectonic and seismological evidence (Mantovani et al., 2001b). Kinematic boundary conditions (arrows along the external borders) have been imposed to the model to simulate the Nubia-Eurasia convergence suggested by Albarello et al. (1995), Euler pole at 41.6 Nord and 11.8 West with angular velocity of 0.12°/My and the westward motion of the Anatolian-Aegean system. The smaller figure on the right (inset in the left picture) shows the displacement field (thick black arrows) of the Calabrian wedges with respect to the adjacent Adriatic foreland. Converging and diverging black triangles respectively indicate a dominance of shortening and extension in the decoupling belts; little half arrows show the sense of shear. B) As in (A), but imposing the Nubia-Eurasia convergence predicted by the NUVEL-1 model. The main purpose of this figure is to point out that very different kinematic patterns of the Calabrian Arc (right) are predicted by adopting the two alternative Nubia-Eurasia kinematic models here considered and that, in particular, the pattern shown in B is not consistent with the widely recognized SE- to E-ward extrusion of the Calabrian wedge. See text for comments.

Modeling can also provide quantitative insights into the compatibility of different Nubia-Eurasia kinematic models with the observed features in the

study area. An aspect of the computed displacement field which may be very useful for discriminating between the two alternative Nubia-Eurasia kinematic models discussed above is the behaviour of the Calabrian wedge lying between Nubia and Adria (Figure 4, inset). Our numerical model suggests that in the compressional regime induced by the convergence of Nubia, Anatolia and Eurasia, the Calabrian wedge is being extruded roughly ESE-ward, with respect to Adria at the expense of the Ionian lithosphere. This prediction is compatible with the pattern of deformations recognized in the zones surrounding the Calabrian Arc since the late Pliocene. In particular, it can account for the opening of the Marsili basin (e.g., Sartori, 1990), in the wake of the Calabrian extruding wedges, for shortening in the external Calabrian Arc, along the front of the escaping wedges (e.g., Rossi and Sartori, 1981; Sartori, 1990) and for the strike-slip movements recognized along the sinistral Palinuro and dextral Vulcano fault systems, which acted as the lateral boundaries of the extruding Calabrian wedges (e.g., Finetti and Del Ben, 1986).

In addition, the SW-NE-oriented compression which has driven the extrusion of the Calabrian wedges can account for the fast uplift and lateral bowing of that arc (Westaway, 1993; Scheepers et al., 1994; Meloni et al., 1997) and for the considerable acceleration of tectonic activity which affected it, as documented by the formation or reactivation of a number of major transverse discontinuities and longitudinal troughs (e.g., Finetti and Del Ben, 1986; VanDijk and Okkes, 1991). The distribution of seismicity and the pattern of recent deformation indicate that Calabrian Arc deformation is still going on (Mantovani et al. 1997b).

Figure 4b illustrates the displacement field obtained by keeping the same boundary conditions as used in the previous experiment, except for the motion of Nubia, for which the NUVEL-1 solution is adopted. The most evident feature of this displacement field is the partial divergence of Nubia from Adria. This divergence is accommodated by the dextral activation of a shear zone in the northern Calabrian Arc (Palinuro fault) and southern Adriatic. However, this contradicts the sinistral shear observed at the Palinuro fault (e.g., Finetti and Del Ben, 1986). More generally, the model predicts WSW-ward motion of the Calabrian wedge with respect to the Adriatic domain, which disagrees with the well recognized E- to SE-ward migration of this wedge (e.g., Finetti and Del Ben, 1986; Dercourt et al., 1986; Dewey et al., 1989). Furthermore, the kinematic pattern shown in Figure 4b can not explain the uplift, bowing, outward escape and tectonic disruption that the Calabrian Arc has undergone since the late Pliocene.

The kinematic pattern shown in Figure 4b represents only one of the possible ways to accommodate the imposed boundary conditions. Other solutions can be achieved by adopting different parameterizations of the model, particularly by changing the location of the decoupling fault between Nubia and Adria. However, in any case, the divergence between Adria and Nubia implied by the NUVEL-1 model should be accommodated by one or more major dextral shear zones, which are not recognized in the study area.

CONCLUSIONS AND DISCUSSION

Our analysis of the space-time distribution of deformation in the central Mediterranean region suggests that:

1) Adria moved in close connection with Nubia until the late Miocene

2) During the Pliocene, Adria underwent a CW rotation at the expense of the low buoyancy domain which lay west of it. This drastic change of kinematics was driven by the westward push of the Anatolian-Aegean-Balkan system after its collision with the southern continental Adriatic domain

3) This kinematic pattern lasted until the late Pliocene or early Pleistocene, when the Adriatic continental margin collided with the Southern Apennines. After this collision, Adria has undergone a slow CCW rotation with respect to Eurasia at the expense of its eastern and northern margins. On-going CCW rotation of Adria is suggested by seismological and geodetic data (e.g., Anderson and Jackson, 1987; Nocquet and Calais, 2003) and can also account, in a quantitative way, for the recent strain pattern in the central Mediterranean region deduced from neotectonic and seismological data (Mantovani et al., 2001b).

The fact that the motion of Nubia in the central Mediterranean area predicted by the NUVEL-1 model is not compatible with the inferred Adria kinematics led a number of authors to look for a decoupling zone between Nubia and Adria. However, the solutions so far proposed for this problem are rather ambiguous, as suggested by the considerable spread (from the central Adriatic zone to eastern Sicily) in the proposed location of the presumed decoupling zone. An accurate analysis of the available evidence, in particular seismic and neotectonic activity, does not indicate any significant Quaternary deformation between Adria and Nubia.

This evidence would suggest that Nubia in the central Mediterranean region moves roughly NNE-ward, compatible with the kinematics of Adria.

These kinematics of Nubia are compatible with the morphology of the Hellenic and Cyprus Arcs and with Nubia kinematics proposed by Albarello et al. (1995).

Of course, the hypotheses we advance about the evolutionary history and present kinematic/tectonic setting of the Adriatic reflect our point of view and can be critically analysed and then accepted or abandoned in favour of other interpretations reported in literature. However, in order to make this comparison significant, the consistency of the alternative interpretations with the major tectonic events described in this and other papers (Mantovani et al., 1997b; 2001b, 2002; Mantovani, 2004) should be analysed. Some kinematic or tectonic models proposed in the recent literature are based on very limited data sets, often confined to one field of Earth sciences (e.g., paleomagnetism, geology, geodesy, etc) or to very small zones with respect to the dimensions of the geodynamic or kinematic model proposed. For instance, the hypothesis that Adria has undergone a CCW rotation around the end of Miocene has been advanced on the basis of paleomagnetic data in the northern Adriatic and peri-Adriatic zones (Marton, 2004) which does not agree with the kinematics proposed in this work. This evidence could indicate that our reconstruction is not reliable or that, at least, it must be reconsidered since it cannot account for significant evidence in a part of the system which is taken into account. However, on the other hand, one should consider that our kinematic model can coherently account for the time-space distribution of major tectonic events in the central Mediterranean area since the late Miocene. To support the reliability of the CCW rotation of Adria proposed by Marton et al. (2004), one should explore the difficulties that this kinematics may encounter in providing a coherent explanation of the observed deformation pattern. An accurate analysis of this last problem has led us to believe that such difficulties are very high, as also suggested by the fact that no alternative geodynamic interpretations have been so far proposed in literature able to coherently account for the complex post-late Miocene deformation pattern in the central Mediterranean region. In this regard, one could point out that the northern part of Adria is flanked by shear zones oriented roughly SSE-NNW: the Schio-Vicenza sinistral fault on the left and the system of parallel transcurrent dextral faults recognized in the northern Dinarides (e.g., Vrabec and Fodor, 2004) on the right, which could have behaved as lateral guides for the roughly NNW-ward drift of Adria in the Pliocene. This evidence cannot easily be reconciled with the CCW rotation of Adria suggested by Marton et al. (2004).

In order to explore all possible ways out from this problem, it may also be useful taking into account the possible uncertainty in the paleomagnetic data given by Marton et al. (2004). As pointed out in that paper, the exact time of rotation is not constrained directly. Moreover, it cannot be excluded that the

kinematics of Adria in the period involved were more complex than a single rotation or that the sites of paleomagnetic measurements did not move in connection with Adria. Other uncertainty could affect the determination of the Africa paleo-poles from which the relative rotation of Adria with respect to Nubia are deduced. Different kinematics of Adria have been proposed by other authors on the basis of paleomagnetic data. For instance, Channell (1996) and Muttoni et al. (1997) suggest that no significant rotation has occurred between Africa and Adria since the Jurassic. A review of paleomagnetic studies in the southern Adriatic area (Meloni et al., 1997) suggests that paleomagnetic data in this region do not allow recognition of its Tertiary kinematics.

A final remark may be devoted to the interpretation of geodetic observations. This kind of data provides the most important, and possibly the most unique, information on the short-term kinematics of plates and microplates. However, one should take into account the possibility that such kinematics do not coincide with the mid to long-term kinematic pattern derived from geological and geophysical evidence, particularly in zones where post-seismic relaxation could produce significant effects (e.g., Mantovani et al., 2001a; Viti et al., 2003). Furthermore, one should be aware that the plausibility of the plate kinematic models deduced by geodetic data crucially depends on whether the assumed configuration of plates and their boundaries are reliable.

ACKNOWLEDGEMENTS

We are grateful to Prof. Hans Kahle, Prof. Seth Stein and Dr. Marko Vrabec for their very useful suggestions. This research has been financed by the Ministry of Research (MIUR), the National Space Agency (ASI) and Regione Toscana.

REFERENCES

Albarello D., Mantovani E., Babbucci D., Tamburelli C. Africa-Eurasia kinematics: main constraints and uncertainties. Tectonophysics 1995; 243: 25-36.

Altiner Y. The contribution of GPS data to the detection of the Earth crust deformations illustrated by GPS campaigns in the Adria region. Geophys. J. Int. 2001; 145: 550-559.

Anderson H.A., Jackson J.A. Active tectonics of the Adriatic region. Geophys. J.R. Astr.Soc. 1987; 91: 937-983.

Anzidei M., Baldi P., Casula G., Galvani A., Mantovani E., Pesci A., Riguzzi F., Serpelloni F. Insights on the present day crustal motion in the central Mediterranean area from GPS surveys. Geophys. J. Int. 2001; 146: 98-110.

Argnani A., Favali P., Frugoni F., Gasperini M., Ligi M., Marani M., Mattietti G. and Mele G. Foreland deformational pattern in the Southern Adriatic Sea. Annali di Geofisica 1993; 36: 229-247.

Argnani A., Frugoni F., Cosi R., Ligi M., Favali P. Tectonics and seismicity of the Apulian ridge south of Salento peninsula (Southern Italy). Annali di Geofisica 2001; 44: 527-540.

Barka A. The North Anatolian fault zone. Annales Tectonicae 1992; 6:164-195.

Castellarin A., Cantelli L. Neo-Alpine evolution of the Southern Eastern Alps. J. Geody. 2000; 30: 251-274.

Castellarin A., Vai G.B. "Southalpine versus Po Plain Apenninic Arcs." In *The origin of arcs*, F.C Wezel, eds., Elsevier, Amsterdam. 1986.

Castellarin A., Cantelli L., Fesce A.M., Mercier J.L., Ricotti V., Pini G.A., Prosser G., Selli L. Alpine compressional tectonics in the Southern Alps. Relationships with the N-Apennines. Annales Tectonicae 1992; 6: 62-94.

Cello G. Structure and deformation processes in the Strait of Sicily "rift zone". Tectonophysics 1987; 141: 237-247.

Channell J.E.T., Horvath F. The Africa-Adriatic promontory as a paleogeographical premise for Alpine orogeny and plate movements in the Carpatho-Balkan region. Tectonophysics 1976; 35: 71-101.

Channell J.E.T. "Palaeomagnetism and palaeogeography of Adria." In *Palaeomagnetism and Tectonics of the Mediterranean region*, A. Morris, D.H. Tarling, eds., London: Geol. Soc. London Spec. Publ. 1996;105.

Cinque A., Patacca E., Scandone P., Tozzi M. Quaternary kinematic evolution of the southern Apennines. Relationships between surface geological features and deep lithospheric structures. Annali di Geofisica 1993; 36: 249-260.

CPTI Working Group, *Catalogo Parametrico dei Terremoti Italiani,* GNDT – ING – SGA – SSN, eds., Tipografia Compositori, Bologna (I), 1999.

De Alteriis B. Different foreland basins in Italy: examples from the central and southern Adriatic Sea. Tectonophysics 1995; 252: 349-373.

Del Ben A., Finetti I., Rebez A., Slejko D. Seismicity and seismotectonics at the Alps - Dinarides contact. Boll. Geof. Teor. Appl. 1991; 33: 166-176.

Della Vedova, B., Pellis G. New heat flow density measurements in the Ionian sea' Proceedings 8th Meeting GNGTS, Roma November 7-9, 1989.

DeMets C., Gordon R.G., Argus D.F., Stein S. Current Plate Motions. Geophys. J. 1990; 101: 425-478.

Dercourt J., Zonenshain L.P., Ricou L.E., Kazmin V.G., Le Pichon X, Knipper A.L., Grandjacquet C., Sbortshikov I.M., Geyssant J., Lepvrirer C., Pechersky D.H., Boulin J., Sibuet J.C., Savostin L.A., Sorokhtin O., Westphal M., Bazchenov M.L., Lauer J.P., Biju-Duval B. Geological evolution of the Tethys belt from Atlantic to the Pamirs since the Lias. Tectonophysics 1986; 123-315.

Devoti R., Ferraro C., Gueguen E., Lanotte R., Luceri V., Nardi A., Pacione R., Rutigliano P., Sciarretta C., Vespe F. Geodetic control on recent tectonic movements in the central Mediterranean area. Tectonophysics 2002; 346: 151-167.

Dewey J.F., Helman M.L., Turco E., Hutton D.H.W., Knott S.D. "Kinematics of the western Mediterranean." In *Alpine Tectonics*, M.P. Coward, D. Dietrich, R.G. Park, eds., London: Geol. Soc. London Spec. Publ. 1989; 45: 265-283.

Favali P., Funiciello R., Mattietti G., Mele G., Salvini F. An active margin across the Adriatic sea (central Mediterranean sea). Tectonophysics 1993; 219: 109-117.

Finetti I., Del Ben A. Geophysical study of the Tyrrhenian opening. Boll. Geof. Teor. Appl. 1986; 110: 75-156.

Finetti I., Bricchi G., Del Ben A., Pipan M., Xuan Z. Geophysical study of the Adria plate. Mem. Soc. Geol. Int. 1987; 40: 335-344.

Hieke W., Wanninger A. The Victor Hensen Seahill (central Ionian sea). Morphology and structural aspect. Mar. Geol. 1985; 64: 343-350.

Hieke W., Dehghani G.A. The Victor Hensen structure in the central Ionian Sea and its relation to the Medina Ridge (Eastern Mediterranean). Z. Dt. Geol. Ges. 1999; 149: 487-505.

Illies J. Graben formation in the Maltese Islands: a case history. Tectonophysics 1981; 73: 151-168.

Jackson J., McKenzie D. The relationship between plate motions and seismic moment tensors, and the rates of active deformation in the Mediterranean and Middle East. Geophys. J. 1988; 93: 45-73.

Mantovani E. "Evolutionary reconstruction of the Mediterranean region: extrusion tectonics driven by plate convergence." In *Deep seismic exploration of the Mediterranean region,* I.R. Finetti, eds., CROP: Elsevier, 2004. In press.

Mantovani E., Albarello D., Tamburelli C., Babbucci D., Viti M. Plate convergence, crustal delamination, extrusion tectonics and minimization of shortening work as main controlling factors of the recent Mediterranean deformation pattern. Annali di Geofisica 1997a; 40: 611-643.

Mantovani E., Albarello D., Babbucci D., Tamburelli C. Recent/present tectonic processes in the italian region and their relation with seismic and volcanic activity. Annales Tectonicae 1997b; 11: 27-57.

Mantovani E., Viti M., Cenni N., Albarello D., Babbucci D. Short and long term deformation patterns in the Aegean-Anatolian system: insights from space geodetic data (GPS). Geophys. Res. Lett. 2001a; 28: 2325-2328.

Mantovani E., Cenni N., Albarello D., Viti M., Babbucci D., Tamburelli C., D'Onza F. Numerical simulation of the observed strain field in the central-eastern Mediterranean region. J. Geody. 2001b; 31: 519-556.

Mantovani E., Albarello D., Babbucci D., Tamburelli C., Viti M. Trench-Arc-BackArc systems in the Mediterranean area: examples of extrusion tectonics. J. of the Virtual Explorer 2002; 8: 125-141.

McClusky S., Reilinger R., Mahmoud S., Ben Sari D., Tealeb A. GPS constraints on Africa (Nubia) and Arabia plate motion. Geophys. J. Int. 2003; 155: 126-138.

McKenzie D. Active tectonics of the Alpine - Himalayan belt: the Aegean Sea and sorrounding region. Geophys. J.R. Astr. Soc. 1978; 55: 217-254.

Meletti C. Patacca E., Scandone P. Construction of a seismotectonic model: the case of Italy. Pure Appl. Geophys. 2000; 157: 11-35.

Meloni A., Alfonsi L., Florindo F., Sagnotti L., Speranza F., Winkler A. Neogene and Quaternary geodynamic evolution of the Italian peninsula: the contribution of Paleomagnetic data. Annali di Geofisica 1997; 40: 705-727.

Mercier J., Sorel D., Simeakis K. Changes in the state of stress in the overriding plate of a subduction zone: the Aegean Arc from the Pliocene to the Present. Annales Tectonicae 1987; 1: 20-39.

Muttoni G., Garzanti E., Alfonsi L., Birilli S., Germani D., Lowrie W. Motion of Africa and Adria since the Permian: paleomagnetic and paleoclimatic constraints from northern Libya. Earth Planet Sci. Lett. 2001; 192: 159-174.

Nocquet J.M., Calais E. Crustal velocity field of western Europe from permanent GPS array solutions, 1996-2001. Geophy. J. Int. 2003; 154: 72-88.

Oldow J.S., Ferranti L., Lewis D.S., Campbell J.K., D'Argenio B., Catalano R., Pappone G., Carmignani L., Conti P., Aiken C.L.V. Active fragmentation of Adria, the north African promontory, central Mediterranean Orogen. Geology 2002; 930: 779-782.

Ortolani F., Pagliuca S. Evidenze strutturali e geomorfologiche di tettonica compressiva quaternaria al margine orientale della catena sudappenninica. Mem. Soc. Geol. It. 1988; 41: 1219-1227.

Patacca E., Sartori R., Scandone P. "Tyrrhenian basin and Apennines. Kinematic evolution and related dynamic constraints." In *Recent evolution and seismicity of the Mediterranean Region*, E. Boschi, E. Mantovani, A. Morelli, eds., Kluwer Academic Publishers: Dordrecht, 1993.

Reuther C.D. Extensional tectonic within central Mediterranean segment of the Afro-European zone of convergence. Mem. Soc. Geol. It. 1987; 38: 69-80.

Rossi S., Sartori R. A seismic reflection study of the External Calabrian Arc in the Northern Ionian Sea (Eastern Mediterranean). Mar. Geophys. Res. 1981; 4: 403-426.

Sartori R. "The main results of ODP LEG 107 in the frame of neogene to recent geology of perityrrhenian areas". In *Proceedings of the Ocean drilling program, scientific results*, K.A. Kastens, J. Mascle et al. eds., 1990.

Sartori R., Capozzi R. "Patterns of Neogene to Recent rift-related subsidence in the Tyrrhenian domain." In *Sedimentary basins: models and constraints,* S. Cloeting, G. Ranalli, C.A. Ricci, eds., International School "Earth and Planetary Sciences", Certosa di Pontignano, Siena, 1998.

Scheepers P.J.J., Langereis C.G., Zijderveld J.D.A., Hilgen F.J. Paleomagnetic evidence for a Pleistocene clockwise rotation of the Calabro-Peloritan block (southern Italy). Tectonophysics 1994; 230: 19-48.

Sella G.F., Dixon T.H., Mao A. REVEL: a model for recent plate velocities from space geodesy. J. Geophys. Res. 2002; 107: ETG 1-32.

Slejko D., Camassi R., Cecic L., Herak D., Herak M., Kociu S., Kouskona V., Lapajne J., Makropoulos K., Meletti C., Muco B., Papaioannoiu C., Peruzza L., Rebez A., Scandone P., Sulstarova E., Voulgaris N., Zivcic M., Zupancic P. Seismic hazard assessement for Adria. Annali di Geofisica 1999; 42: 1085-1107.

Van Dijk J.P., Okkes M. Neogene tectonostratigraphy and kinematics of Calabrian basins; implications for the geodynamics of the Central Mediterranean. Tectonophysics 1991; 196: 23-60.

Viti M., Albarello D., Mantovani E. Classification of seismic strain estimates in the Mediterranean region from a 'bootstrap' approach. Geophys. J. Int. 2001; 146: 399-415.

Viti M., D'Onza F., Mantovani E., Albarello D., Cenni N. Post-seismic relaxation and earthquake triggering in the southern Adriatic region. Geophys. J. Int. 2003; 153: 645-657.

Westaway R. Present-day kinematics of the plate boundary zone between Africa and Europe, from the Azores to the Aegean. Earth Planet Sci. Lett. 1990; 96: 393-406.

Westaway R. Quaternary uplift in Southern Italy. J. Geophys. Res. 1993; 98: 21741-21772.

PALEOMAGNETIC EVIDENCE FOR TERTIARY COUNTERCLOCKWISE ROTATION OF ADRIA WITH RESPECT TO AFRICA

Emő Márton
Eötvös Loránd Geophysical Institute, Palaeomagnetic Laboratory, Budapest, Hungary
paleo@elgi.hu

ABSTRACT

Paleomagnetic observations are presented from: (1) the Adriatic foreland, (2) the imbricated margin of Adria and (3) the circum-Adriatic region, including from north of the Periadriatic line and from the Dinaric nappe system. Results from the Adriatic foreland call for the separation of Adria from Africa during the Tertiary, based upon significant counterclockwise rotation with respect to Africa observed on Eocene rocks. The rotation timing is constrained more precisely by paleomagnetic results from the imbricated Adria margin and from areas surrounding Adria. Results from these regions suggest that the most likely time for the rotation is the end of Miocene to the earliest Pliocene.

Keywords: Adria, Paleomagnetism, Tertiary, counterclockwise rotation

INTRODUCTION

Adria has played an important role in the geodynamic history of the central Alpine-Mediterranean belt. Since the 1970s, paleomagnetists have attempted to test if the Adriatic promontory model suggested by Argand (1924) was valid and if Adria remained a promontory, rigidly connected to Africa, or if Adria decoupled from Africa to form an independent microplate. Based on pre-Tertiary paleomagnetic results, some authors supported the first model (e.g., Channell et.al., 1996; VanderVoo, 1993; Muttoni et al., 2001), whereas other authors supported the second model (Márton and Veljović, 1983; Vandenberg, 1983; Márton and Nardi, 1994).

In theory, paleomagnetic research is suitable to supply a definite answer to questions like those above. In practice, there are difficulties and uncertainties which resulted in persistent disagreement among paleomagnetists working on Adriatic questions. The most important limitation has been the scarcity of suitable outcrops in the autochthonous core of Adria, which caused some authors to "transport" paleomagnetic data from heavily tectonized and/or allochthonous areas to represent rigid Adria (e.g.; Channell,

N. Pinter et al. (eds.), The Adria Microplate: GPS Geodesy, Tectonics and Hazards, 71–80.

1996; Muttoni, et al. 2001; Thöny et al., 2003). Another problem in the Adriatic region has been uncertainty regarding the pre-Tertiary part of the African apparent polar wander path (for details, see Márton, 1993).

The Tertiary segment of the African apparent polar wander path, however, seems to be fairly stable (Besse and Courtillot, 1991, 2002-2003). From this reference system, relative movements (or the lack thereof) with respect to Africa can be more reliably traced than in earlier times. This is one reason why the present paper focuses upon the Tertiary. A second important advantage of the young age is that paleomagnetic declinations reflect a less complicated pattern of rotations than do older paleomagnetic declinations from the same area (since a declination characterizing a rock unit is the cumulative result of all the rotations affecting the unit after the acquisition of the paleomagnetic signal).

In recent years, Tertiary paleomagnetic results were obtained from Adria, including from the core and from the imbricated margin. The former were from stable Istria (Márton et al., 2003) and from Colli Euganei (Márton et al., in prep), both considered unequivocally as belonging to autochthonous Adria; the latter results were from the imbricated margin of the Adriatic foreland (Dalmatia, Kissel et al., 1995; Márton et al., 2003) and from the Southern Alps (Márton et al., in prep.). The data from these areas also will be discussed in the context of Tertiary paleomagnetic data representing the circum-Adriatic region, where young rotations have been induced by the motion of Adria.

TERTIARY COUNTERCLOCKWISE ROTATION OF ADRIA

Adriatic Foreland

The youngest Tertiary sediments both in Istria and in the Colli Euganei (Figure 1.) are of Eocene age. In Istria, Eocene platform carbonates post-date Cretaceous rocks of the same type, above a large stratigraphic gap (late Senonian-earliest Eocene). The platform persisted till the Lutetian, when the sedimentary basin started to deepen and flysch was deposited. In the Colli Euganei, upper Cretaceous-Paleocene pelagic Scaglia limestones were covered, following a short hiatus in the lower Eocene, by middle and upper Eocene marls.

Tightly clustered and primary paleomagnetic directions were obtained from the subhorizontal Eocene sediments of Istria (Márton et al., 2003). Eocene sediments from the Colli Euganei yielded similar paleomagnetic directions (Márton et al., in prep.). The mean directions of the two areas are statistically identical (Figure 1, areas 1 and 2), which justifies the definition of

a single paleomagnetic direction for the two areas of the Adriatic foreland (Figure 1, direction 1, 2). These results suggest that Adria rotated about 25° counterclockwise (CCW) with respect to the present north.

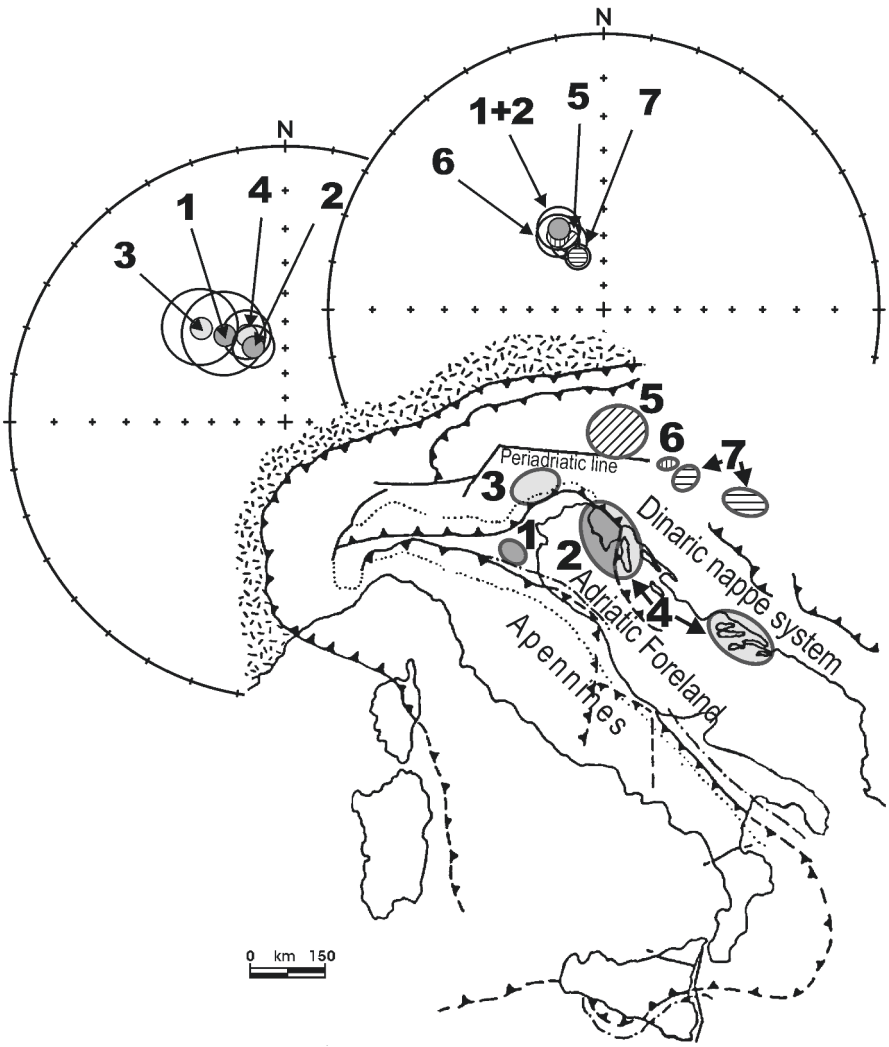

Figure 1. Study area, including the Adriatic foreland (1: Colli Euganei, 2: Stable Istria); the imbricated margin (3: Venetian Alps, 4: para-autochthonous Istria and Dalmatia); and the circum-Adriatic region (5: intramontane basins of the Eastern Alps, 6: Mura depression, 7: Medvednica-Hrvatsko Zagorje Mts. and Slavonian Mts., respectively), together with mean palaeomagnetic directions with confidence circles for the respective areas. Note that mean paleomagnetic directions for all areas exhibit similar angles of CCW deviation from the north, suggesting co-ordinated movement in latest Miocene to early Pliocene times.

Imbricated Adria

The gently deformed Adriatic foreland is surrounded by folded and thrusted belts. From the north-northeastern imbricated margin (situated between the Adriatic foreland and the Periadriatic line and the Dinaric nappe system, Figure1.), paleomagnetic data relevant to Tertiary movements are distributed from the Venetian Alps through para-authochthonous Istria down to central Dalmatia (Márton et al., 2003, in prep).

In the Venetian Alps, Eocene flysch is overlain by Chattian to Messinian, dominantly clastic deposits. The whole sequence was intensively folded and faulted in the middle and late Miocene (Castellarin and Cantelli, 2000). On-going deformation is suggested by destructive earthquakes in the Friuli corner and in the frontal part of the Venetian Alps.

In the northern, para-autochthonous part of Istria and in central Dalmatia, the Eocene stratigraphy is similar to that of autochthonous Istria, and like in that area, post-Eocene marine sediments are lacking. Two main tectonic events are recognized: one in the latest Eocene and another in the Pliocene (e.g., Tari, 2002).

In contrast to the Adriatic foreland, the paleomagnetic directions from the imbricated margin of Adria are younger (of post-folding age) than the stratigraphic ages of the Eocene and Miocene rocks studied in the Venetian Alps and the latest Cretaceous-Eocene rocks in the imbricated part of Istria and in Dalmatia. One notable exception is the Eocene flysch in central Dalmatia, which seems to have preserved primary magnetization (Kissel et al., 1995), despite the strong deformation due to the position of the flysch (underlain by imbricated platform carbonates and overlain by Dinaric thrust sheets). The paleomagnetic direction in area 4 (Figure 1) combines results obtained by Márton et al. (2003) and Kissel et al. (1995). In the former case, the mean paleomagnetic directions are without tilt corrections; in the latter case, tilt corrections have been applied (but without the problematic oroclinal corrections; for details read Márton et al., 2003). Despite the age differences of magnetization within area 4, the paleomagnetic directions cluster tightly. In area 3, the paleomagnetic direction is similar (Figure 1). At the same time, directions in both areas are consistent with the Eocene paleomagnetic directions (Figure1, areas 1 and 2) that characterize the foreland. The implication is that the Adriatic foreland and its imbricated margin must have behaved as a single unit when the CCW rotation took place. The most likely time for this rotation is latest Miocene or early Pliocene. Such timing is based upon observations from the Venetian Alps, where the age of the deformation is mid-late Miocene and the CCW-rotated paleomagnetic declination is of post-deformational age (i.e., deformation was followed by the acquisition of the remanence and even later by the rotation).

Circum-Adriatic region

Motion of Adria is thought to account for a number of young tectonic features in the surrounding regions (e.g., Bada et al., 1999; Tomljenović and Csontos, 2001). There are certain areas in these regions where paleomagnetic studies were carried out on Tertiary rocks. As a result, significant Tertiary CCW rotations were revealed in the Eastern Alps, (Márton et al., 2000; Figure 1, area 5), in the Mura depression (Márton et al., 2002a; Figure 1, area 6), and in northern Croatia (Márton et al., 2002b; Figure 1, area 7).

The Tertiary sediments of the Eastern Alps occur in a number of intramontane basins that were formed in connection with Miocene lateral tectonic extrusion (Ratschbacher et al., 1991). The basins are filled with clastic material deposited in fluviatile, lacustrine and marine environments, between 18 and 10 Ma. The paleomagnetic results obtained from the

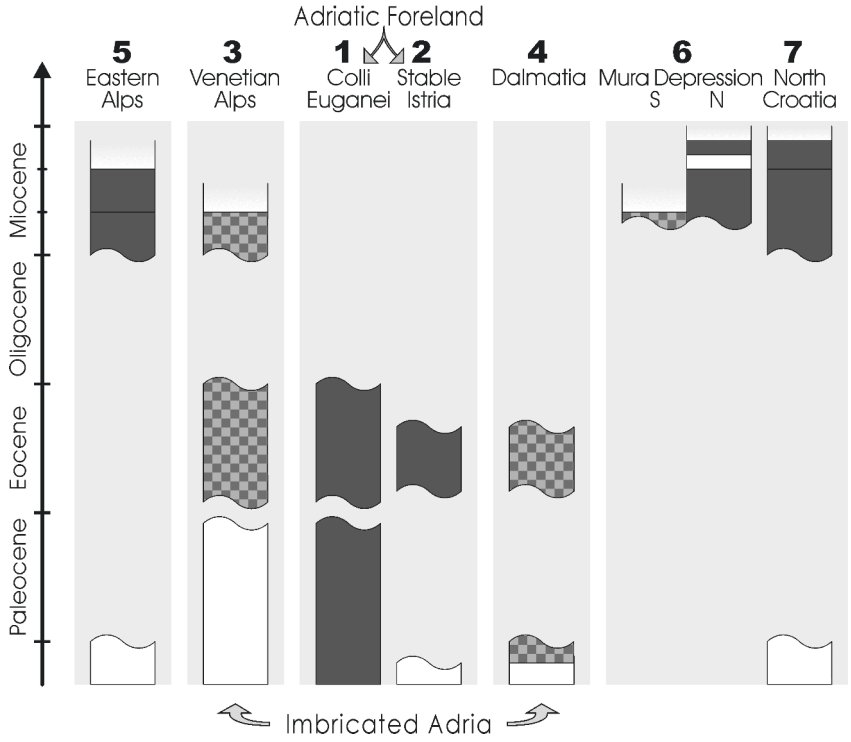

Figure 2. Simplified stratigraphic columns for the different areas (numbers refer to Figure 1) of Adria and the circum-Adriatic region. Note the absence of sediments younger than Eocene in the Adriatic foreland and in Dalmatia and the large stratigraphic gaps elsewhere. Sediments with primary remanences are shown in black; the checked parts indicate remanences of post-tectonic age.

intramontane basins suggest that the area east of the Tauern window rotated CCW during the Miocene. Two phases of rotation were distinguished. The older, mid-Miocene phase was connected to lateral tectonic escape and was interpreted in a model of domino-shaped blocks rotating between the Ennstal fault and the Periadriatic shear zone; the younger phase (Figure1, area 5) was interpreted as "microplate-like" rotation (Márton at al., 2000) which must have taken place some time after 12 Ma (the lower age limit is constrained by the age of the youngest sediment studied, which still exhibited westerly declination).

In the Mura depression, the complex basement is covered by lower to mid-Miocene marine clastic sediments that are overlain by brackish to freshwater deposits of Lake Pannon. The Miocene fill of the basin was folded and faulted at the end of Miocene or in the early Pliocene (Fodor et al., 1998; Márton et al., 2002). Both pre- and post-folding paleomagnetic signals were obtained from the basin (Figure 1, area 6; Figure 2, column 6). The first type of paleomagnetic signal characterizes the northern part; the second, the southern margin. Both signals exhibit the same moderate CCW rotation, suggesting that the rotation post-dates not only the deposition of the youngest sediment (about 8 Ma), but also the deformation (around 5 Ma)

In northern Croatia, the Paleozoic and Mesozoic basement is covered by Neogene sediments, which were first deposited in separate basins (Medvednica-Hrvatsko Zagorje and Slavonian Mts areas) and were unified during a later marine transgression around 17.5 Ma. From 13.5 Ma onwards, northern Croatia became part of Lake Pannon. The Neogene sediments of northern Croatia have primary remanences with westerly declinations (Figure1, area 7; Figure2, column 7). The age of the youngest sediments studied (about 6 Ma) constrains the lower limit to the time of the rotation.

In summary, the Tertiary paleomagnetic results from the circum-Adriatic region suggest that the last rotation in the region was CCW and was of the same angle as in the Adriatic foreland (Figure1, areas 1, 2, and 5-7). The lower time limit of the rotations is constrained by the age of the youngest sediments yielding paleomagnetic result from the respective areas, which is about 12 Ma (area 5), 8 Ma (area 6) and 6 Ma (area 7), and the age of the last deformation in area 6, which took place around 5 Ma. The upper age limit is open to speculation. It stands to reason, however, to assume that the last rotations in the circum-Adriatic region are synchronous.

ROTATION OF ADRIA WITH RESPECT TO AFRICA

As we have seen, the Adriatic foreland experienced significant CCW rotation with respect to north (Figure 1). The question is if this is also a significant rotation with respect to Africa. In order to answer this question,

coeval African and Adriatic results are compared through the respective paleomagnetic poles (Figure 3).

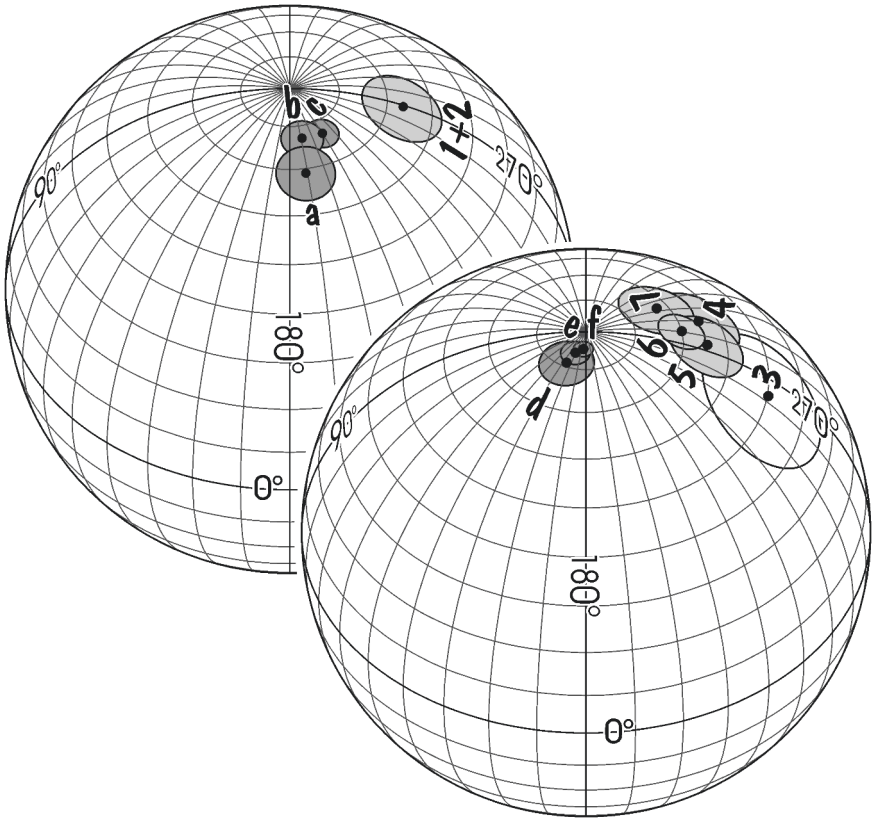

Figure 3. Comparison of coeval paleo-poles for Africa (a-f) and for Adria and the circum-Adriatic region (1-7). Numbers 1-7 refer to Figs 1 and 2 and are used throughout the text. Key to the African poles: a: 45 Ma (Muttoni et al., 2001), b: 50 Ma (Besse and Courtillot, 1991), c: 50 Ma (Besse and Courtillot, 2002, 2003), d: 14 Ma (Muttoni et al., 2001), e: 10 Ma (Besse and Courtillot, 1991), f: 10 Ma (Besse and Courtillot, 2002, 2003).

The Eocene paleomagnetic pole for Adria is situated at lon. 270°, lat. 66°N. Eocene African poles plot close to lon. 190°, lat. 75°N. As Figure 3 illustrates, the positions are significantly different, with no overlap between the Adriatic and African poles, including the confidence circles. Alternatively, by comparing paleomagnetic declinations, we calculate expected declination for Adria from the African pole(s) on the assumption that the relative position of the two has not changed since the Eocene. The obtained declination is practically aligned with the present north. Obviously, the measured

declination for the Adriatic foreland is different (Figure 1), and the difference is due to a Tertiary CCW rotation of Adria with respect to Africa. Incidentally, the rotation with respect to north and with respect to Africa is practically of the same angle.

Similar relationship exists between African reference poles and the poles calculated from the paleomagnetic directions for areas 3 and 4 and 5-7 since the rotations in these areas are linked to the rotation of the core of Adria, we can estimate the timing of the Tertiary decoupling of Adria from Africa as latest Miocene-early Pliocene.

CONCLUSIONS

As demonstrated, there is a striking similarity between the youngest known paleomagnetic declinations from the Adriatic foreland, from the imbricated margin of Adria and from the circum-Adriatic region, indicating 25° CCW rotation with respect to north and with respect to Africa. The Eocene paleomagnetic data from the Adriatic foreland can be interpreted in a flexible way, permitting the rotation any time after the Eocene. In contrast, the timing of the rotations is constrained for the circum-Adriatic area by the age of the youngest source rocks and/or the youngest deformation events, as occurring around 5 Ma. A link between the foreland and the circum-Adriatic region is provided by the paleomagnetic results from the imbricated margin of Adria, especially by those from the Miocene sediments of the Venetian Alps. The results are best interpreted in terms of the rotation of a microplate comprising the Adriatic foreland, its imbricated margin and the circum-Adriatic region north of Adria during an end-of-Miocene to early Pliocene CCW rotation with respect to Africa.

ACKNOWLEDGEMENT

The work was financially supported by the Hungarian Scientific Research Found (OTKA) project no. T034364. Reviews by Nicholas Pinter and Leonardo Sagnotti helped to improve the manuscript. Technical assistance by Gábor Imre is gratefully acknowledged.

REFERENCES

Argand E. La tectonique de l'Asie. Congr. Géol. Int., C. R., 13th Sess., 1924; 171-172.

Bada G., Horváth F., Gerner P., Fejes I. Review of the present day geodynamics of the Pannonian basIn progress and problems. J. Geodynamics 1999; 27: 501-527.

Besse J., Courtillot V. Revised and synthetic apparent polar wander path of the African, Eurasian, North American and Indian plates, and true polar wander since 200 Ma. J. Geophys. Res. 1991; 96(B3): 4029-4050.

Besse J., Courtillot V. Apparent and true polar wander and the geometry of the geomagnetic field over the last 200 Myr. J. Geophys. Res. 2002; 107(B11): EPM6-1-31.

Besse J., Courtillot V. Correction to "Apparent and true polar wander and the geometry of the geomagnetic field over the last 200 Myr". J. Geophys. Res. 2003; 108(B10): EPM3-1-2.

Castellarin A., Cantelli L. Neo-Alpine evolution of the Southern Eastern Alps. J. Geodynamics 2000; 30: 251-274.

Channell J.E.T. "Palaeomagnetism and paleogeography of Adria." In *Palaeomagnetism and tectonics of the Mediterranean Region*, A. Morris, D.H. Tarling, eds., Geol. Soc. Spec. Publ. 1996; 105:119-132.

Fodor L., Jelen B., Márton E., Skaberne D., Čar J., Vrabec M. Miocene-Pliocene tectonic evolution of the Slovenian Periadriatic Line and surrounding area - Implications for Alpine-Carpathian extrusion models. Tectonics 1998; 17: 690-709.

Kissel C., Speranza F., Miličević V. Paleomagnetism of external southern and central Dinarides and northern Albanides: implications for the Cenozoic activity of the Scutari-Peć traverse zone. J. Geophys. Res. 1995; 100: 14,999-15,007.

Márton E. "Paleomagnetism in the Mediterraneum from Spain to the Aegean: a review of data relevant to Cenozoic movements." In *Recent Evolution and Seismicity of the Mediterranean Region*, E. Boschi, E. Mantovani, A. Morelli, eds., Kluwer Academic Publishers, 1993.

Márton E., Nardi G. Cretaceous palaeomagnetic results from Murge (Apulia, Southern Italy): tectonic implications. Geo. J. Int. 1994; 119: 842-856.

Márton E., Veljović D. Paleomagnetism of the Istria peninsula, Yugoslavia. Tectonophysics 1983; 91: 73-87.

Márton E., Kuhlemann J., Frisch W., Dunkl I. Miocene rotations in the Eastern Alps - Paleomagnetic results from intramontane basin sediments. Tectonophysics 2000; 323: 163-182.

Márton E., Fodor L., Jelen B., Márton P., Rifelj H., Kevrić R. Miocene to Quaternary deformation in NE Slovenia: complex paleomagnetic and structural study. J. Geodynamics 2002a; 34: 627-651.

Márton E., Pavelić D., Tomljenović B., Avanić R., Pamić J., Márton P. In the wake of a counterclockwise rotating Adriatic microplate: Neogene paleomagnetic results from Northern Croatia. Int. J. Earth Sciences 2002b; 91: 514-523.

Márton E., Ćosović V., Drobne K., Moro A. Palaeomagnetic evidence for Tertiary counterclockwise rotation of Adria. Tectonophysics 2003; 377: 143-156.

Márton E., Zampieri D., Dunkl I., Frisch W., Grandesso P., Kázmér M., Braga G. Tertiary rotations of the Venetian Alps and their foreland-tectonic implications of new paleomagnetic data. In prep.

Muttoni G., Garzanti E., Alfonsi L., Cirilli S., Germani D., Lowrie W. Motion of Africa and Adria since the Permian: paleomagnetic and paleoclimatic constraints from northern Libya. Earth and Planetary Science Letters 2001; 192: 159-174.

Ratschbacher L., Frisch W., Linzer H.G., Merle O. Lateral extrusion in the Eastern Alps, part 2: Structural analysis. Tectonics 1991; 10: 257-271.

Tari V. Evolution of the northern and western Dinarides: a tectonostratigraphic approach. EGS Stephan Mueller Special Publication Series 2002; 1: 1-21.

Thöny W., Ortner H., Scholger R. An APWP (Apparent Polar Wanderpath) for the Alpine-Adria microplate. Annales Universitatis Scientiarum Budapestinensis, Sectio Geologica 2003; 35: 123-124.

Tomljenocić B., Csontos L. Neogene–Quaternary structures in the border zone between Alps, Dinarides and Pannonian Basin (Hrvatsko zagorje and Karlovac Basins, Croatia). Int. J. Earth Sciences 2001; 90: 560-578.

Van der Voo R. *Paleomagnetism of the Atlantic, Tethys and Iapetus oceans*. Cambridge: Cambridge University Press, 1993.

VandenBerd J. Reappraisal of paleomagnetic data from Gargano (south Italy). Tectonophysics 1983; 98: 29-41.

PALEOMAGNETIC CONSTRAINTS FOR THE RECONSTRUCTION OF THE GEODYNAMIC EVOLUTION OF THE APENNINES DURING THE MIDDLE MIOCENE - PLEISTOCENE

Leonardo Sagnotti
Istituto Nazionale di Geofisica e Vulcanologia, Roma, Italy
sagnotti@ingv.it

ABSTRACT

The Apennines are a mountain belt developed during the Neogene along the western margin of the Adria microplate. This paper presents an updated review of paleomagnetic research aimed at the reconstruction of the geodynamic evolution of the Italian Peninsula and Sicily. Paleomagnetic data collected in the Apennines since the 1970s support the view that the Italian peninsula consists of an articulated system, with vertical-axis rotations distributed over distinct geodynamical provinces and geological times. Vertical-axis rotations are generally counterclockwise in the Apennines and clockwise in the Sicilian Maghrebides. These rotations were mostly linked to the transport and bending of allochthonous units along multiple thrusts. The most recent paleomagnetic data indicate that large and variable vertical-axis rotations characterized the development of various individual arcuate thrust fronts. Some of these rotations may have occurred at very rapid rates. The detailed understanding of these local rotations and the refinement of high-resolution age models for the various phases of vertical-axis rotations are the new frontier and challenge for future paleomagnetic studies in Italy.

Keywords: Apennines, Italy, paleomagnetism, vertical axis rotations

INTRODUCTION

The Apennines, together with the Calabrian block and the Sicilian Maghrebides, constitute a continuous mountain belt encircling the Tyrrhenian Sea (Figure 1). According to current geodynamic models, the evolution of the Central Mediterranean geodynamic system during the Neogene was driven by the progression of subduction rollback in the area of relative convergence between the African and Eurasian plates (i.e., Malinverno and Ryan, 1986; Lucente et al., 1999; Faccenna et al., 2001a, 2001b, 2004; Rosenbaum and Lister 2004). The interaction and evolution of the individual sectors of this complex geodynamic system resulted in the formation of narrow arcs composed of allochthonous tectono-stratigraphic units stacked in accretionary wedges verging toward the Adriatic-African foreland.

N. Pinter et al. (eds.), The Adria Microplate: GPS Geodesy, Tectonics and Hazards, 81–94.

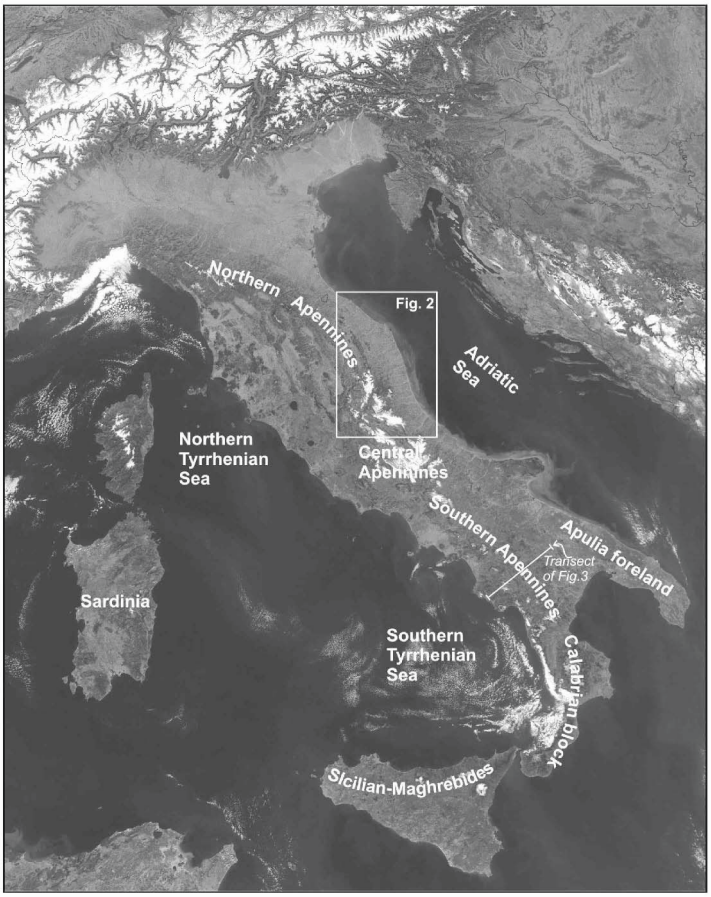

Figure 1. Satellite image of the Italian peninsula, showing the main geodynamic provinces discussed in the text. The location of the area reported in Figure 2 and of the cross section reported in Figure 3 are also shown.

In such a tectonic context, vertical-axis rotations are likely and such rotations have been documented by paleomagnetic studies conducted in the Italian Peninsula since the 1970's. Paleomagnetic data represent a key tool to quantify displacements of the individual tectono-stratigraphic units and to assist reconstructions of the pre-orogenic paleogeography. This paper presents a review of the contribution given by paleomagnetism to the reconstruction of the geodynamic evolution of the Apennines during the Middle Miocene to Pleistocene, coeval with the main tectonic phases that were responsible for the present structural setting (i.e., Patacca et al., 1990).

TECTONIC AND GEODYNAMIC SETTING OF THE APENNINES

The Apennines constitute an imbricate fold-and-thrust belt which includes the Italian peninsula and extendsover a length of about 1500 km (Figure 1). This belt developed since the Middle Miocene, largely in response to the east-southeastward retreat of a regional subduction zone involving passive sinking of a west-northwestward-dipping Ionian oceanic lithosphere in the south and possibly Adriatic continental lithosphere in the north (i.e., Malinverno and Ryan, 1986; Selvaggi and Amato, 1992; Selvaggi and Chiarabba, 1995; Lucente et al., 1999; Faccenna et al., 2001a; 2001b). The tectono-stratigraphic units composing the present-day Apennines originally formed in distinct paleogeographic domains along the western margin of the Adria microplate. These tectonostratigraphic units are now piled up in an imbricated thrust system that verges toward the Adriatic foreland.

Northern-Central Apennines and Northern Tyrrhenian Sea

The northern Apennines are composed of several folds and thrust sheets which describe a major arc. The structural axes parallel the external (Adriatic) margin of the belt and turn from approximately N-S in the south to almost WNW-ESE in the north. Within this broad arcuate structure, several minor arcs developed in response to multiple compressional phases that induced both out-of-sequence nappe stacking and in-sequence external frontal accretion of the belt toward the Adriatic foreland. According to recent studies, the regional basement of the northern Apennines nappes is also involved in the deformation and is cut by high-angle thrust ramps inverting pre-existing normal faults (Coward et al., 1999; Speranza and Chiappini, 2002). Crustal shortening in the external northern Apennines is estimated at ca. 10-20%, with an average shortening rate of 1.5-2.5 mm/yr for the last 4 Myr (Coward et al., 1999).

During the same period, extension progressively dissected the internal sector of the belt, inducing its collapse. This extension migrated eastward following the compressional front and was accompanied by diffused magmatism (Elter et al., 1975; Patacca et al., 1990; Jolivet et al., 1998). This extension produced several syn-rift basins along the Tyrrhenian margin, filled by Upper Miocene to Pleistocene “neoautochthonous” marine, brackish and continental sedimentary sequences (Martini and Sagri, 1993).

There is little evidence of compressional deformation along the Adriatic front after the Early Pleistocene; nevertheless, ongoing

compressional activity is suggested by moderate compressional seismicity along the Adriatic coast (Frepoli and Amato, 1997) and reconstruction of the present stress field by borehole breakout analysis north of 43°N (Mariucci et al., 1999; Sagnotti et al., 1999).

Southern Apennines and the Arc surrounding the Southern Tyrrhenian Sea

The southern Apennines are the result of progressive polyphase non-coaxial deformation characterized by a succession in time of different stress regimes (Menardi Noguera and Rea, 2000). The present structure developed from a thrust belt built during the Late Miocene by imbrication of various tectono-stratigraphic units subjected to large differential displacement. This original belt underwent a major translation event during the Pliocene, related to the involvement of the basement in the thrust tectonics (Cello and Mazzoli, 1999; Menardi Noguera and Rea, 2000; Speranza and Chiappini, 2002). The occurrence of Early Pliocene sediments underneath thrust units indicate a total horizontal displacement of ca. 50 km during the last 3.5 Myr (Catalano et al., 2004), confirming the significance of translation toward the foreland of the allochthonous nappes and their thrust-top basins during the Plio-Pleistocene. Differences in the structural styles of the various tectono-stratigraphic units of the southern Apennines induced disharmonic deformation between the deep Inner Apulian Platform and the overlying allochthonous units (Menardi Noguera and Rea, 2000). In the external zone of the southern Apennines, the buried thrust front was active at least until the Plio-Pleistocene transition (*Globorotalia inflata* zone) in the northern part, whereas in the southern part it was active until the middle Early Pleistocene (Emiliano). The distribution and facies of the Plio-Pleistocene sediments in the southern Apennines also indicate that most of the vertical displacement along the thrust ridges developed during the Late Pliocene (Catalano et al., 2004).

Beginning in the Tortonian, extension dissected the Appenines and progressively migrated from the internal to the external parts of the orogen. The age for this extension and accompanying uplift is Calabrian in the internal sector of the belt and Sicilian in the axial zone. In the southern Tyrrhenian Sea, extensional tectonics produced crustal thinning and ocean-floor spreading during the Pliocene and Pleistocene (Kastens and Mascle, 1990; Sartori, 1990). In the Middle Pleistocene, left-lateral strike-slip tectonics induced by the south-eastward migration of the Calabrian Arc become the predominant mode of deformation within the belt (Cinque et al., 1993; Cello and Mazzoli, 1999; Menardi Noguera and Rea, 2000; Catalano et al., 2004).

The present-day stress field, as indicated by seismicity and borehole breakout analysis, is characterized by a prevailing NE-oriented extension (Amato and Montone, 1997; Montone and Amato, 1999). Geological evidence suggest that normal faults in the southern Apennines developed after ca. 0.7 Ma (Pantosti et al, 1993; Westaway, 1993).

PALEOMAGNETIC RESEARCH AND IMPLICATIONS FOR GEODYNAMICS

Paleomagnetic data have been collected in the Apennines with the purpose to develop geodynamical reconstruction since the 1970's. The first studies focused on the Jurassic to Oligocene carbonate sequences of the Umbria-Marche basin, thought to be autochthonous or semi-autochthonous. These studies suggested a counterclockwise (CCW) rotation of Italy as a single block (Lowrie and Alvarez, 1974, 1975; Channell and Tarling, 1975; Klootwijk and VandenBerg, 1975), developed more or less continuously since Late Cretaceous (i.e., VandenBerg et al., 1978).

Progressive increases in the distribution and density of paleomagnetic data drastically changed the interpretation above. A review of the paleomagnetic contribution to the reconstruction of the geodynamical evolution of the Italian Peninsula and main islands was provided by Meloni et al. (1997) with special emphasis on the first 20 years of paleomagnetic research applied to geodynamic reconstructions in Italy (early 1970's - early 1990's). Paleomagnetic results gradually pointed out a complex geodynamic history with multiple tectonic phases and vertical-axis rotations distributed over space and geological time. Together with a better understanding of the complexity of the rotational patterns, the ages assigned to the rotation phases were also progressively revised (see Table III in Meloni et al., 1997).

In the early 1990's, collection of extensive new paleomagnetic data from Plio-Pleistocene sequences, previously neglected, brought the next major step in the geodynamic interpretation, showing that even the most recent tectonic phases involved significant vertical-axis rotations and clearly demonstrating that a composite differential evolution of the various tectonic settings characterized the last few million years (i.e., Sagnotti, 1992; Scheepers, 1992; Scheepers et al., 1993; Scheepers and Langereis, 1994).

During the last decade, refinement of the paleomagnetic analysis (both in terms of analytical protocols and the spatial and temporal distribution of the collected data) contributed significantly to improving the detailed understanding of the vertical-axis rotations accompanying the evolution of the system. An updated review of the paleomagnetic contribution to the geodynamic studies in the Apennines is outlined below.

Northern - Central Apennines and Northern Tyrrhenian Sea

The present fold-and-thrust belt of the northern and central Apennines consists of arcuate structures characterized by widespread vertical-axis rotations. Extension along the Tyrrhenian margin since the Late Miocene produced the collapse of the western area of the orogenic belt but did not induce vertical-axis rotation (Sagnotti et al., 1994; Mattei et al, 1996a, 1996b). This clearly pointed out that the extension and rifting in the northern Tyrrhenian Sea did not induce the paleomagnetic rotations observed in the belt. These rotations instead were produced by broad translation and bending of the allochthonous tectono-stratigraphic units along multiple thrusts. A post-Messinian oroclinal bending of the main northern Apennine arc is indicated by paleomagnetic data collected all along the Adriatic margin and Po Plain (Speranza et al., 1997; Muttoni et al, 1998). The analysis of paleomagnetic data collected all along the external front the main northern Apennine arc, integrated with magnetic anisotropy data from the same paleomagnetic sites, indicate that the present shape of this arc derives from post-Messinian bending of an originally straight belt oriented approximately N40°W (Speranza et al., 1997; Sagnotti et al., 1998). Tomographic images of the upper mantle beneath the northern Apennines suggest that the genesis of the arc may have been controlled by a deep process of bending of subducting Adriatic plate (Lucente and Speranza, 2001). The timing of this process, however, is still poorly defined. Paleomagnetic data from the Plio-Pleistocene sequences deposited in front of the belt suggest that CCW rotations in the northern part may be younger than 3 Ma and that differential motions of individual thrust sheets occurred even after the Early Pleistocene (Sagnotti et al., 2000). This conclusion is consistent with recent paleomagnetic investigations of some second-order arcs (i.e., the Gran Sasso range) that indicate that complex rotational patterns are a key feature of the Apenninic arcuate thrust fronts (Speranza et al., 2003a; Satolli, 2003; Satolli et al., in review).

The integration of available paleomagnetic, magnetic anisotropy, stress field and various geophysical data indicates that a lithosphere-scale, NNE-SSW-oriented discontinuity bisects the Adriatic coast at a longitude of about 14°E. This discontinuity was likely active since the late Tortonian (Figure 2) and may be associated with a different evolution of the subduction processes in the north versus in the south (Sagnotti et al., 1999).

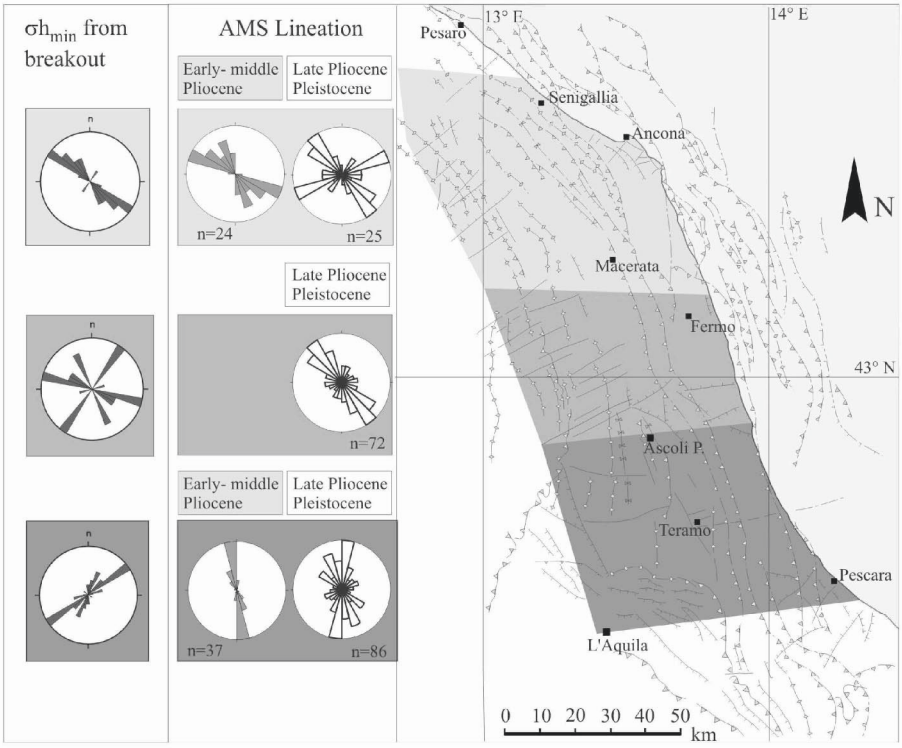

Figure 2. Rose diagrams show the mean directions for the minimum horizontal stress (σhmin, estimated from breakout analysis) and magnetic lineation (estimated from anisotropy of magnetic susceptibility, AMS, analysis), grouped as a function of areal distribution and age of deep wells and sampling sites. The integration of σhmin and magnetic lineation directions indicate a transition in the Plio-Pleistocene and present stress field along the Adriatic margin of the north-central Apennines that can be associated to a lithospheric discontinuity between the northern and the southern Apennines (see Sagnotti et al., 1999).

Southern Apennines and the Arc surrounding the Southern Tyrrhenian Sea

Extension and rifting in the southern Tyrrhenian Sea were also synchronous with development and eastward migration of compression in the southern Apennine belt toward the Apulia foreland. Paleomagnetic data demonstrate that the southern Apennine allochthonous structures underwent a large and rather uniform CCW rotation (mean of 80°) after the middle Miocene (Gattacceca and Speranza, 2002). Most of this rotation (ca. 60°) occurred during the Late Miocene, earlier than the main spreading phases in the southern Tyrrhenian Sea. However this rotation was coeval with the first

extensional and rifting episodes which developed to the east of the Sardinia block after that it completed its CCW rotation (now estimated at 16 Ma-early Langhian; Speranza et al., 2002). Present knowledge of regional geology indicates that this rotational phase was likely limited to the detached nappes that constitute the upper part of the tectonic pile and were subjected to large transport and internal imbrication.

A further 20° of CCW rotation, on average, was measured in different Plio-Pleistocene sedimentary sequences of the southern Apennines, deposited in piggy-back basins on top of the eastward-translating tectonic nappes (Sagnotti, 1992; Scheepers et al., 1993; Scheepers 1994; Scheepers and Langereis, 1994). This rotational phase, developed since the Late Pliocene, can be linked to the deep structural development of the Inner Apulian Carbonate Platform (Figure 3), which is dissected by high-angle low-displacement reverse faults. Therefore, the Plio-Pleistocene phase of CCW rotation may have a deeper control than the previous, larger CCW rotational episode (Gattacceca and Speranza, 2002). Regional geological data indicate that the buried thrust front of the southern Apennines was no longer active after the end of the Early Pleistocene, which is in agreement with new paleomagnetic data indicating that Plio-Pleistocene 20° CCW rotation was completed before the Jaramillo sub-chron and occurred at a surprisingly rapid rate over less than 0.5 million years (Mattei et al., in press).

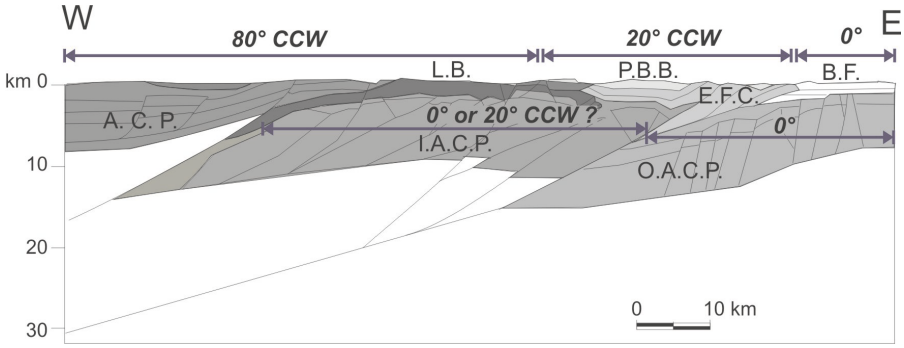

Figure 3. Structural cross section across the southern Apennines (redrawn from Menardi Noguera and Rea, 2000), illustrating the various \ vertical-axis rotations affecting the main structural units. A.C.P.: Apennine Carbonate Platform; L.B.: Lagonegro Basin; I.A.C.P.: Inner Apulian Carbonate Platform; P.B.B.: Piggy-back Basins; E.F.C.: External Flysch Complex; O.A.C.P.: Outer Apulian Carbonate Platform; B.F.: Bradanic Foredeep.

In conclusion, the available paleomagnetic data and their related time constraints, when considered in the framework of the overall knowledge on the geodynamic structure and evolution of the southern Apennines, indicate that the vertical-axis CCW rotations of the allochthonous structures and their

sedimentary covers were largely a result of the emplacement and translation of the accretionary wedge complex.

Extensional and strike-slip tectonics, which developed mostly after the Early Pleistocene, do not appear to contribute significantly to the vertical-axis rotation pattern. Moreover, Plio-Pleistocene rotations were synchronous with main spreading and formation of oceanic crust in the southern Tyrrhenian Sea and with south-eastward drift of the Calabrian block, in response to the retreating passive sinking of the Ionian lithospheric slab (Figure 4). In contrast to the northern Tyrrhenian Sea, where the extensional basins developed by collapse of the inner belt and were not subjected to vertical-axis rotations, the extensional basins developed in the southern Tyrrhenian Sea on top of the drifting Calabrian block were subjected to CW rotations of about 15°-20° (Speranza et al., 2000a). These basins developed as syn-rift structures to the east of the present eastern Sardinia shelf (Mattei et al., 2002) and drifted together with the Calabria block during opening and spreading of the southern Tyrrhenian Sea.

Furthermore, large CW rotations are known for the allochthounous structures of the Sicilian Maghrebides (Channell et al., 1980; 1990; Oldow et al., 1990; Scheepers and Langereis, 1993; Speranza et al, 1999, 2000b, 2003b). Such rotations were almost synchronous and symmetric (i.e., they sum up to a total of ca. 100° CW) with those measured in the Southern Apennines (Figure 4). They occurred mostly (i.e., ca. 70°) during the Middle-Late Miocene, whereas the remaining ~30° of CW rotation occurred during the Plio-Pleistocene.

All the available paleomagnetic data place specific timing constraints that can be considered in the context of recently proposed mechanisms for the formation of the Calabrian Arc. Such mechanisms associate the formation of the arc with (1) fragmentation of the slab, inducing a large component of lateral mantle flow which in turn accelerated retreat of the subduction hinge (Faccenna et al., 2004); or with (2) the arrival of light carbonate platform at the subduction zone, initiating slab tear and activity of major strike-slip faults (Rosenbaum and Lister, 2004). Paleomagnetic data indicate that the largest rotations occurred before oceanic spreading in the southern Tyrrhenian Sea. Shaping of the southern Apennines-Calabria block-Sicilian Maghrebides Arc occurred mostly during the initial Middle-Late Miocene Tyrrhenian rifting episodes, whereas the subsequent Plio-Pleistocene oceanic break-up and sea-floor spreading in the southern Tyrrhenian basins (Vavilov and Marsili basins dated at 5-2 Ma and 2-0 Ma, respectively) drove the south-eastward drift of the belt system but caused little additional curvature (Gattacceca and Speranza, in press).

Data from Plio-Pleistocene sediments in the Apulian foreland show that no vertical-axis rotation occurred since the Late Pliocene or earlier

(Scheepers, 1992), indicating that the outer Apulian platform behaved as an independent structure with respect to the Apennine chain.

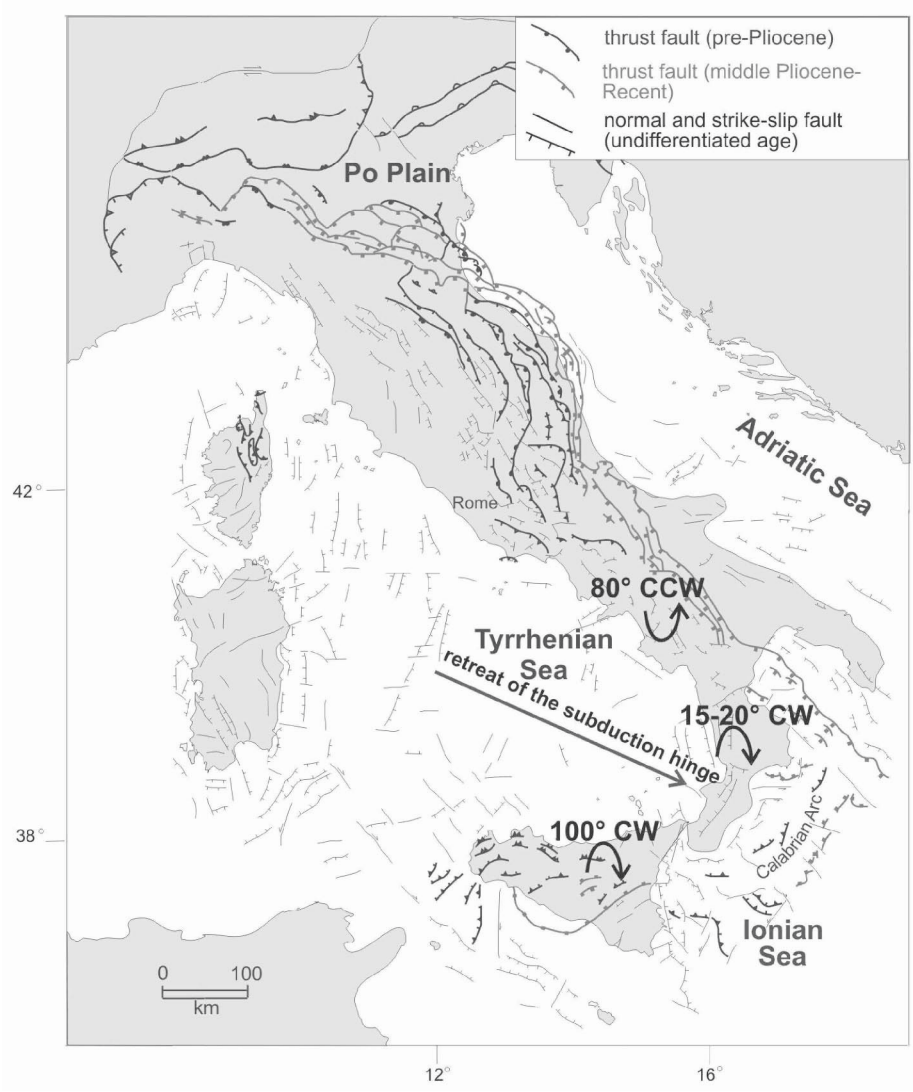

Figure 4. Schematic structural map of the Italian Peninsula, showing the mean vertical-axis rotation pattern around the southern Tyrrhenian Sea. This pattern supports a "saloon door" opening dynamics and implies a genetic link between southeastward retreat of the subduction hinge, opening of the southern Tyrrhenian Sea and vertical-axis rotation in the southern Apennines and the Sicilian Maghebides (see text for further discussion).

CONCLUSIONS

The first thirty years of paleomagnetic research in the Italian Apennines, focused on regional geodynamical problems and reconstructions and defined broad patterns of vertical-axis rotations in the main geodynamic provinces of the Italian peninsula. Paleomagnetic data contributed significantly to a better understanding of the geodynamic evolution of the system, providing quantitative constraints for the development of regional geodynamic models (i.e., Rosenbaum and Lister, 2004). Paleomagnetic data revealed a complex geodynamic history, with production of various arcuate structures during emplacement of allochthonous structures. The general trend of paleomagnetic rotation appears to have been driven mainly by complex subduction-related processes which affected the Ionian lithosphere and the western margin of Adria, processes that controlled the geodynamic evolution of the whole central Mediterranean.

At present, paleomagnetism still represents a powerful tool to investigate the detailed evolution of individual geological structures within the Apennine belt. This opportunity is clearly demonstrated by the most recent paleomagnetic data, which indicate that large and complex vertical-axis rotations characterized the development of second-order arcuate thrust fronts in the Apennines. The new frontier and challenges for future paleomagnetic studies in the Apennines therefore seems to be understanding the details of local rotations in single structural units and the refinement of high-resolution age models to reconstruct the temporal evolution of the various phases of vertical-axis rotations. This can be achieved by integration of paleomagnetic studies focused on the definition of vertical-axis rotation with multidisciplinary (magneto)stratigraphic studies in suitable sedimentary sequences for high-resolution dating of tectonic events and calculation of the rates of various geologic and geodynamic processes.

ACKNOWLEDGEMENTS

Reviews by Nicholas Pinter and Luigi Piccardi improved the manuscript.

REFERENCES

Amato A., Montone P. Present-day stress field and active tectonics in southern peninsular Italy. Geophys. J. Int. 1997; 130: 519-534.

Catalano S., Monaco C., Tortorici L., Paltrinieri W., Steel N. Neogene-Quaternary evolution of the southern Apennines. Tectonics 2004; 23, doi: 10.1029/2003TC001512.

Cello G., Mazzoli S. Apennine tectonics in Southern Italy: a review. J. Geodynamics 1999; 27: 191-211.

Channell J.E.T., Tarling D.H. Paleomagnetism and rotation of Italy. Earth Plan. Sci. Lett. 1975; 25: 177-188.

Channell J.E.T., Catalano R., D'Argenio B. Palaeomagnetism and deformation of the Mesozoic continental margin in Sicily. Tectonophysics 1980; 61: 391-407.

Channell J.E.T., Oldow J.S., Catalano R. D'Argenio B. Palaeomagnetically determined rotations in the western Sicilian fold and thrust belt. Tectonics 1990; 9:641-660.

Cinque A., Patacca E., Scandone P., Tozzi M. Quaternary kinematic evolution of the southern Apennines: Relationships between surface geological features and deep lithospheric structures. Ann. Geofis.1993; 36: 249–259.

Coward M.P., De Donatis M., Mazzoli S., Paltrinieri W., Wezel F.C. Frontal part of the northern Apennines fold and thrust belt in the Romagna-Marche area (Italy): Shallow and deep structural styles. Tectonics 1999; 18: 559–574.

Elter P., Giglia G., Tongiorgi M., Trevisan L. Tensional and compressional areas in recent (Tortonian to Present) evolution of north Apennines. Boll. Geofis. Teor. Appl. 1975; 17: 3–18.

Faccenna C., Funiciello F., Giardini D., Lucente F.P. Episodic back-arc extension during restricted mantle convection in the central Mediterranean. Earth Planet. Sci. Lett. 2001a; 187: 105–116.

Faccenna C., Becker T.W., Lucente F.P., Jolivet L., Rossetti F. History of subduction and back-arc extension in the central Mediterranean. Geophys. J. Int. 2001b; 145: 809–820.

Faccenna C., Piromallo C., Crespo-Blanc A., Jolivet L., Rossetti F. Lateral slab deformation and the origin of western Mediterranean arcs. Tectonics 2004; 23, doi: 10.1029/2002TC001488

Frepoli A., Amato A. Contemporaneous extension and compression in the northern Apennines from earthquake fault-plane solutions. Geophys. J. Int. 1997; 129: 368-388.

Gattacceca J., Speranza F. Paleomagnetism of Jurassic to Miocene sediments from the Apenninic carbonate platform (southern Apennines, Italy): evidence for a 60° counterclockwise Miocene rotation. Earth and Planet. Sci. Lett. 2002; 201:19-34.

Gattacceca J., Speranza F.. Paleomagnetic constraints for the tectonic evolution of the southern Apennines belt (Italy). Boll. Soc. Geol. It. In press.

Jolivet L. et al. Midcrustal shear zones in postorogenic extension: Example from the northern Tyrrhenian Sea. J. Geophys. Res. 1998; 103: 12,123–12,160.

Kastens K. A., Mascle J. The geological evolution of the Tyrrhenian Sea: An introduction to the scientific results of ODP Leg 107. Proc. Ocean Drill. Program Sci. Results 1990; 107: 3–26.

Klootwijk C.T., VandenBerg J. The rotation of Italy: preliminary paleomagnetic data from the Umbrian sequence, northern Apennines. Earth Planet. Sci. Lett. 1975; 25: 263-273.

Lowrie W., Alvarez W. Rotation of Italian peninsula. Nature 1974; 251: 285-288.

Lowrie W., Alvarez W. Paleomagnetic evidence for rotation of the Italian peninsula. J. Geophys. Res. 1975; 80: 1579-1592.

Lucente F.P., Chiarabba C., Cimini G.B., Giardini D. Tomographic constraints on the geodynamic evolution of the Italian region. J. Geophys. Res. 1999; 104: 20,307–20,327.

Lucente F.P., Speranza F. Belt bending driven by lateral bending of subducting lithospheric slab: geophysical evidences from the northern Apennines (Italy). Tectonophysics 2001; 337: 53-64.

Malinverno A., Ryan W.B.F. Extension in the Tyrrhenian sea and shortening in the Apennines as results of arc migration driven by sinking of the lithosphere. Tectonics 1986; 5: 227-245.

Mariucci M.T., Amato A., Montone P. Recent tectonic evolution and present stress in the Northern Apennines (Italy). Tectonics 1999; 18: 108-118.

Martini I.P., Sagri M. Tectono-sedimentary characteristics of late Miocene-Quaternary extensional basins of the northern Apennines, Italy. Earth Sci. Rev. 1993; 34: 197–233.

Mattei M., Kissel C., Funiciello R. No tectonic rotation of the Tuscan margin (Italy) since Upper Messinian: structural and geodynamical implications. J. Geophys. Res. 1996a; 101: 2835-2845.

Mattei M., Kissel C., Sagnotti L., Funiciello R., Faccenna C. "Lack of Late Miocene to Present rotation in the northern Tyrrhenian margin (Italy): a constraint on geodynamic evolution" In *Palaeomagnetism and Tectonics of the Mediterranean region*, A. Morris, D.H. Tarling, eds., Geol. Soc. Spec. Publ. 1996 b; 105: 141-146.

Mattei M., Cipollari P., Cosentino D., Argentieri A., Rossetti F., Speranza F., Di Bella L. The Miocene tectono-sedimentary evolution of the southern Tyrrhenian Sea: stratigraphy, structural and palaeomagnetic data from the on-shore Amantea basin (Calabrian Arc, Italy). Basin Res. 2002; 14: 147-168.

Mattei M., Petrocelli V., Lacava D., Schiattarella M. Paleomagnetic evidence for Pleistocene ultra-rapid vertical-axis rotations in the Southern Apennine (Italy). Geology. In press.

Meloni A., Alfonsi L., Florindo F., Sagnotti L., Speranza F., Winkler A. Neogene and Quaternary geodynamic evolution of the Italian peninsula: the contribution of paleomagnetic data. Ann. Geofis. 1997, XL: 705-727.

Menardi N.A., Rea G. Deep structure of the Campanian-Lucanian Arc (southern Apennine, Italy). Tectonophysics 2000; 324: 239– 266.

Montone P., Amato A. Active stress map of Italy. J. Geophys. Res. 1999; 104: 25,595–25,610.

Muttoni G., Argnani A., Kent D.V., Abrahamsen N., Cibin U. Paleomagnetic evidence for Neogene tectonic rotations in the northern Apennines, Italy. Earth Planet. Sci. Lett. 1998; 154: 25-40.

Oldow J.S., Channell J.E.T, Catalano R., D'Argenio B. Contemporaneous thrusting and large-scale rotations in the western Sicilian fold and thrust belt. Tectonics, 1990; 9: 661-681.

Pantosti D., Schwarz D.P., Valensise G. Paleoseismology along the 1980 Irpinia earthquake fault and implications for earthquake recurrence in the spouthern Apennines. J. Geophys. Res. 1993; 98: 6561-6577.

Patacca E., Sartori R., Scandone P. Tyrrhenian Basin and Apenninic Arcs: kinematic relations since late Tortonian times. Mem. Soc. Geol. Int. 1990; 45: 425-451.

Rosenbaum G., Lister G.S. Neogene and Quaternary rollback evolution of the Tyrrhenian Sea, the Apennines and the Sicilian Maghrebides. Tectonics 2004; 23, doi: 10.1029/2003TC001518

Sagnotti L. Paleomagnetic evidence for a Pleistocene counterclockwise rotation of the Sant'Arcangelo basin. Geophys. Res. Lett. 1992; 19: 135-138.

Sagnotti L., Mattei M., Faccenna C., Funiciello R. Paleomagnetic Evidence for No Tectonic Rotation of the Central Italy Tyrrhenian Margin Since Upper Pliocene. Geophys. Res. Lett. 1994; 21: 481-484.

Sagnotti L., Speranza F., Winkler A., Mattei M., Funiciello R. Magnetic fabric of clay sediments from the external northern Apennines (Italy). Phys. Earth Planet. Int. 1998; 105: 73-93.

Sagnotti L., Winkler A., Montone P., Di Bella L., Florindo F., Mariucci M.T., Marra F., Alfonsi L., Frepoli A. Magnetic Anisotropy of Plio-Pleistocene Sediments From the Adriatic Margin of the Northern Apennines (Italy): Implications for the Time-Space Evolution of the Stress-Field. Tectonophysics 1999; 311: 139-153.

Sagnotti L., Winkler A., Alfonsi L., Florindo F., Marra F. Paleomagnetic constraints on the Plio-Pleistocene geodynamic evolution of the external central-northern Apennines (Italy). Earth Planet. Sci. Lett. 2000; 180: 243-257.

Sartori R. The main results of ODP Leg 107 in the frame of Neogene to recent geology of peri-Tyrrhenian areas. Proc. Ocean Drill. Program Sci. Results 1990; 107: 715 – 730.

Satolli S. *Formazione della catena arcuate del Gran Sasso: nuove analisi paleomagnetiche e vincoli geologico-strutturali*, Univ. Degree Thesis, 178 pp., Università di Chieti, 2003.

Satolli S., Speranza F., Calamita F. Paleomagnetism of the Gran Sasso range salient (central Apennines, Italy): pattern of orogenic rotations related to nonrotational hinterland indentation. Tectonics, in review.

Scheepers P.J.J. No tectonic rotation for the Apulia-Gargano foreland in the Pleistocene. Geophys. Res. Lett. 1992; 19: 2275-2278.

Scheepers, P.J.J. Tectonic rotations in the Tyrrhenian arc system during the Quaternary and late Tertiary. Geol. Ultraj. 1994; 112: 1-352.

Scheepers P.J.J., Langereis C.G. Analysis of NRM directions from the Rossello composite: implications for the tectonic rotation of the Caltanissetta basin, Sicily. Earth Planet. Sci. Lett. 1993; 119: 243-258.

Scheepers P.J.J., Langereis C.G., Hilgen F.J. Counterclockwise rotations in the southern Apennines during the Pleistocene: paleomagnetic evidence from the Matera area. Tectonophysics 1993; 225: 379-410.

Scheepers P.J.J., Langereis C.G. Paleomagnetic evidence for counter-clockwise rotations in the southern Apennines fold-and-thrust belt during the Late Pliocene and middle Pleistocene. Tectonophysics 1994; 239: 43-59.

Selvaggi G., Amato A. Subcrustal earthquakes in the northern Appennines (Italy): Evidence for a still active subduction? Geophys. Res. Lett. 1992; 19: 2127 – 2130.

Selvaggi G., Chiarabba C. Seismicity and P-wave velocity image of the southern Tyrrhenian subduction zone. Geophys. J. Int. 1995; 122: 818 – 826.

Speranza F., Sagnotti L., Mattei M. Tectonics of the Umbria-Marche-Romagna arc (central northern Apennines, Italy): new paleomagnetic constraints. J. Geophys. Res. 1997; 102: 3153-3166.

Speranza F., Maniscalco R., Mattei M., Di Stefano A., Butler R.W.H., Funiciello R. Timing and magnitude of rotations in the frontal thrust system of southwestern Sicily. Tectonics 1999; 18: 1178-1197.

Speranza F., Mattei M., Sagnotti L., Grasso F. Rotational differences between the northern and southern Tyrrhenian domains: paleomagnetic constraints from the Amantea basin (Calabria, Italy). J. Geol. Soc. London 2000; 157: 327-334.

Speranza F., Maniscalco R., Mattei M., Funiciello R. Paleomagnetism in the Sicilian Maghrebides: review of the data and implications for the tectonic styles and shortening estimates. Mem. Soc. Geol. It. 2000b; 55: 95-102.

Speranza F., Chiappini M. Thick-skinned tectonics in the external Apennines: New evidence from magnetic anomaly analysis. J. Geophys. Res. 2002; 107, 10. 1029/2000JB000027

Speranza F., Villa I.M., Sagnotti L., Florindo F., Cosentino D., Cipollari P., Mattei M. Age of the Corsica-Sardinia rotation and Liguro-Provençal Basin spreading: New paleomagnetic and Ar/Ar evidences. Tectonophysics 2002; 347: 231-251.

Speranza F., Adamoli L., Maniscalco R., Florindo F. Genesis and evolution of an arcuate mountain front: paleomagnetic and geological evidence from the Gran Sasso range (central Apennines, Italy). Tectonophysics 2003; 362: 183-197.

Speranza F., Maniscalco R., Grasso M. Pattern of orogenic rotations in central-eastern Sicily: Implications for the chronology of the Tyrrhenian Sea spreading. J. Geol. Soc. London 2003b; 160: 183-195.

VandenBerg J., Klootwijk C.T., Wonders A.A.H. Late Mesozoic and Cenozoic movements of the Italian peninsula: further paleomagnetic data from the Umbrian sequence. Geol. Soc. Am. Bull. 1978; 89: 133-150.

Westaway R. Quaternary uplift of southern Italy. J. Geophys. Res. 1993; 98: 21741-21772.

GEO-STRUCTURAL EVIDENCE FOR ACTIVE OBLIQUE EXTENSION IN SOUTH-CENTRAL ITALY

Luigi Piccardi[1], Emanuele Tondi[2], Giuseppe Cello[2]
1: C.N.R. - Institute of Geosciences and Earth Resources, Via G. La Pira 4, 50121 Firenze, Italy. piccardi@geo.unifi.it
2: Department of Earth Science, University of Camerino, Via Gentile III da Varano, 62032 Camerino (MC), Italy

ABSTRACT

Active tectonic processes in south-central Italy have been analyzed by means of spatial and kinematic analysis of fault zones In (i) the axial zones of the Apenninic mountain chain, where most of the seismic strain is released within intramontane basin areas (i.e., Norcia, Fucino, Vallo di Diano, high Agri Valley, etc.); and (ii) in the Gargano promontory, where earthquakes with magnitudes up to 6 and 7 have occurred. Our work focuses on a better understanding of the most recent deformation processes acting in these areas, and the relative motion between the Adriatic and Tyrrhenian crustal units. In order to derive the information above, we integrated structural and seismological data from the Apennines and the Gargano area. The results of our analysis show that the style of active deformation in both of these areas is broadly consistent with the current stress field. Kinematic data from slip indicators on active fault planes are, in fact, consistent with the geometric proprieties and spatial arrangement of the various fault segments and indicate that most of the active structures are characterized by oblique motion. The overall direction of extension appears to be at fairly high angle to the trend of the Apennines, with a component of horizontal left-lateral motion between Tyrrhenia and Adria.
Keywords: Structural geology, active faults, earthquakes, Apennines.

INTRODUCTION

Structural analysis of active faults provides spatial and kinematic data which may be used for determining the present-day deformation pattern of a region, and hence for assessing the currently active tectonic regime. Here, we present data collected in key areas in the Apennines (Figure 1), along the western margin of the Adria microplate, and in the Gargano promontory in order to better understand the most recent deformation processes occurring in these areas and to assess slip vector patterns and relative motion between the Adriatic and Tyrrhenian regions.

N. Pinter et al. (eds.), The Adria Microplate: GPS Geodesy, Tectonics and Hazards, 95–108.

Along the axial zones of the Apennines, the main active structures consist mostly of a few NW-SE-oriented faults (often bounding intramontane basins; Calamita et al., 1994; Cello et al., 1997; Piccardi et al., 1999; Cello et al., 2003) which are thought to be responsible for most of the seismicity of the area (Barchi et al., 2000 and references therein; Tondi and Cello, 2003). We focused our investigations in the Norcia and Fucino basins in the central Apennines, in the Vallo di Diano-high Agri Valley area in the southern Apennines, and on the Gargano promontory (along the Mattinata fault zone; Figure 1). In historical times, all these areas have been affected by strong earthquakes, with magnitudes up to M7 (Gruppo di lavoro CPTI, 1999).

In order to obtain constraints for evaluating fault-zone characteristics and slip-vector data from which to derive the currently active stress field, our study was mostly based on: (i) remote sensing imagery (LANDSAT and SPOT satellite images and 1:33,000- and 1:13,000-scale aerial photographs); and (ii) field observations at outcropping fault zones, both in bedrock units and in Quaternary continental deposits.

TECTONIC FRAMEWORK

The Apennine fold-and-thrust belt of mainland Italy (Figure 1) is an Africa-verging mountain chain belonging to the peri-Adriatic orogenic system. The overall structure of the belt is the result of the convergence between the African and Eurasian plates since the Late Cretaceous (e.g., Dewey et al., 1989 and references therein).

The late collision between orogenic segments of the system (i.e., Tyrrhenia and Adria) is responsible for the emplacement of Apenninic units during Miocene to Pleistocene times. Apenninic units include various thrust-sheets and slices made of Mesozoic carbonates and Neogene deposits emplaced onto the Apulian platform (Parotto & Praturlon, 1981; Bally et al., 1986; Malinverno & Ryan, 1986; Patacca & Scandone, 1989; Cello et al., 1989; Cello & Mazzoli, 1999). Available geophysical data also show that crustal thickness below the mountain range is about 30-40 km (Bally et al., 1986; Nicolich, 1989), whereas lithospheric thickness is up to 90 km (Müller & Panza 1986).

Several authors suggest that thrust accretion against the Adriatic continental margin and subduction-related back-arc extension were driven by gravity-induced sinking of the Adriatic and Ionian lithosphere beneath the Tyrrhenian active margin (e.g., Malinverno & Ryan, 1986; Royden et al., 1987; Doglioni et al., 1994). E- to NE-directed thrusting and associated foredeep/thrust-top basin sedimentation record a forward progression towards

the Adriatic foreland up to the Middle Pleistocene (e.g., Ricci Lucchi, 1986; Cipollari & Cosentino, 1995).

The fold-and-thrust-belt structure, mainly resulting from the latest stages of accretion (i.e., since the Miocene), is dissected by newly-formed faults and by inherited structural features re-activated as normal and strike-slip faults. In the internal sectors of the chain (e.g., in Tuscany), these faults control the development and evolution of Mio-Pliocene basins (e.g., Decandia et al., 1998) and are therefore coeval with thrust structures that are still active further to the east.

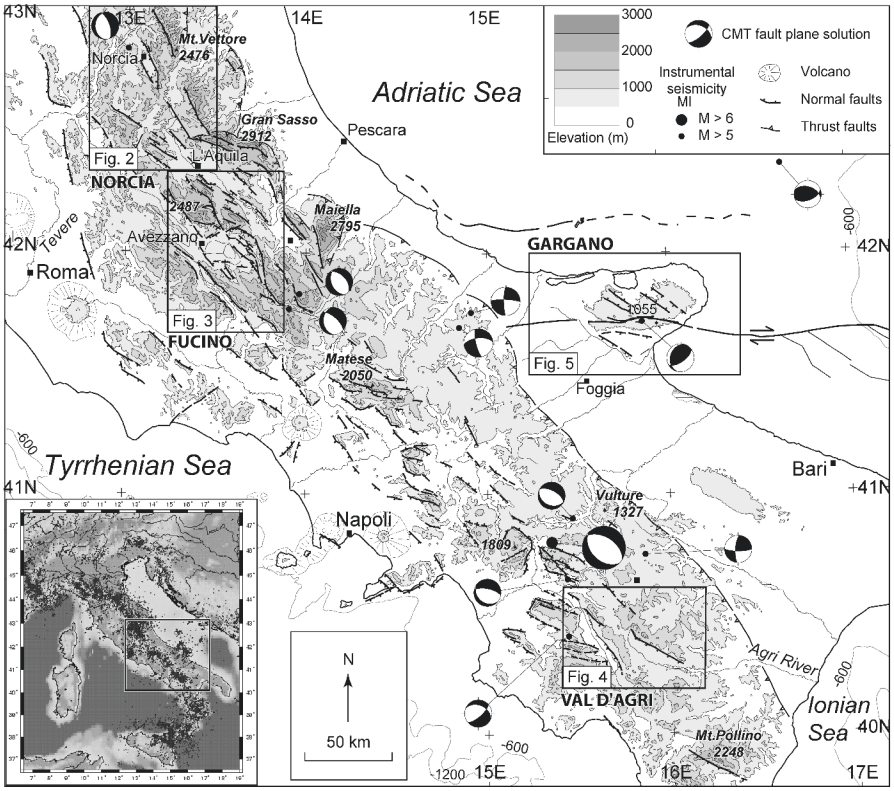

Figure 1. Locations discussed in the text, including major active faults and focal mechanisms (from Gasparini et al., 1985; Harvard Seismology: Centroid-Moment Tensor Project, 2004; Catalogue of Swiss Seismological Service, 2001; INGV-Harvard European-Mediterranean Regional Centroid-Moment Tensors Project, 2004) of earthquakes are shown (modified from Piccardi et al., 1999). Inset: crustal seismicity of Italy (from http://www.ingv.it/~roma/).

During the Middle Pleistocene (at about 700 ky b.p; Dramis, 1992 and references therein; Cinque et al., 1993; Hyppolite et al., 1994; Mantovani et al., 1996; Cello et al., 1997; Piccardi, 1997; Di Bucci and Mazzoli, 2002), a major geodynamic change is recorded both in the Apennines and adjacent foothill areas. According to some authors (McKenzie, 1972; Channell et al., 1979; Anderson, 1987; Anderson and Jackson, 1987; Platt et al. 1989), this change was mostly driven by the N-NW motion of Adria with respect to stable Europe.

The Norcia area

The Norcia fault zone (Figure 2a) belongs to the Late Quaternary (post-700 ka) central Apennines fault system (CAFS in Cello et al., 1997 and Tondi, 2000). Structures of the CAFS overprint and/or invert older structures of the Apennines fold-and-thrust belt (Calamita et al., 1994 and references therein) and represent a kinematically coherent fault network that developed in response to the stress field that has been acting in the region since the Middle Pleistocene.

The CAFS includes active faults that extend from Colfiorito to L'Aquila, over a total length of about 100 km. Several faults within the CAFS bound small tectonic depressions (e.g., the Norcia basin; Figure 2b) which are filled with Pleistocene to Holocene, coarse-grained continental deposits. These deposits are cut by faults with recent activity suggested by remarkably fresh scarps. In the Norcia area, the historical seismic record shows that earthquakes are mostly characterized by moderate magnitudes (M6-7), but a few major events reached intensities of about X-XI MCS and equivalent magnitudes around M6.5-7.0 (Gruppo di Lavoro CPTI, 1999).

Structural data from the CAFS (Cello et al., 1997) show that roughly N-S-trending left-lateral strike-slip and transtensional/normal faults (from NNW-SSE- to WNW-ESE-trending) are kinematically consistent with a Late-Quaternary regional stress field characterized by a NE-SW-oriented minimum horizontal compressive stress (σ_h) and by a NW-SE-trending maximum horizontal compressive stress (σ_H). Slip rates on active faults are in the range of 0.9-1.5 mm/yr for normal and 0.4-0.6 mm/yr for strike-slip components, respectively. The analysis of spatial and temporal characteristics of fault development and related earthquake activity of the CAFS shows that the displacement rate of the whole system in the last 700 ka is about 1.6 cm/yr (Tondi & Cello, 2003).

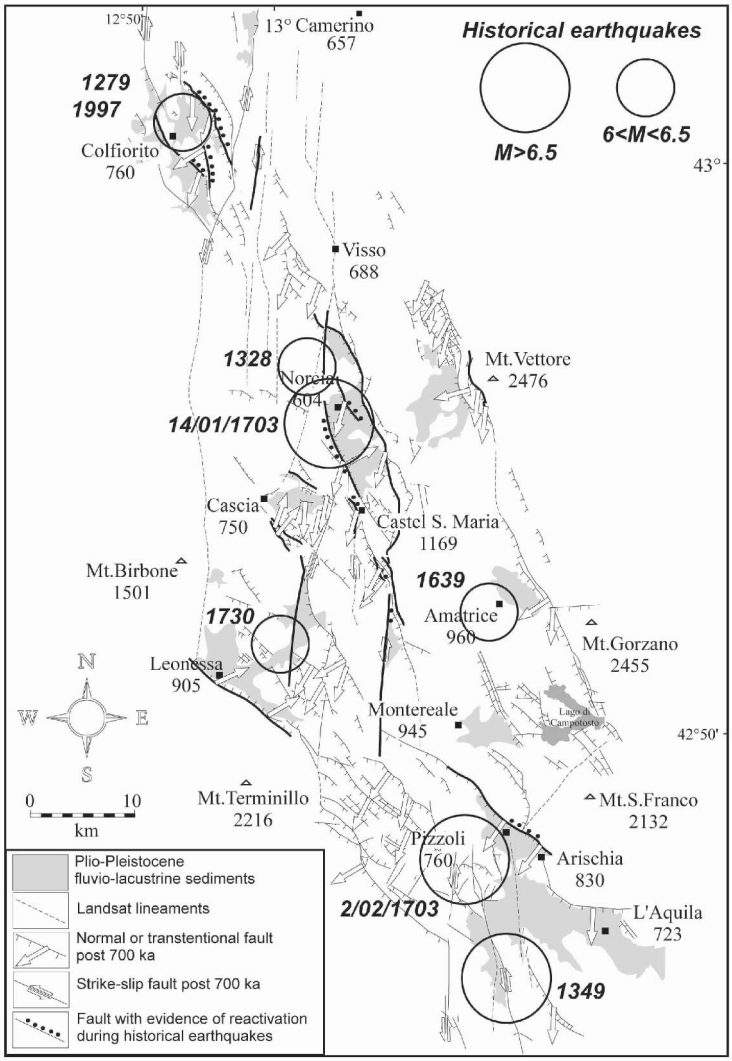

Figure 2. The Central Apennines Fault System (CAFS; modified from Cello et al., 1997).

The Fucino area

The Fucino basin (Figure 3) is the most conspicuous intramontane Quaternary basin of the central Apennines, south and west of the highest summits. The basin is floored by a flat plain, ~30 km wide and with an elevation of ~650 m, and it is completely land-locked. The surrounding

mountains rise above 1500 m, exposing Mesozoic to Cenozoic carbonate shelf units and Miocene terrigenous deposits. The tectonic depression is filled by fluvio-lacustrine sediments, from Late Pliocene to Early Pleistocene to Holocene in age (Mostardini & Merlini, 1986). The basin is surrounded by long-recognized Quaternary normal-transtensional faults (e.g., Bosi, 1975).

The Fucino area was hit by the Avezzano earthquake on January 15, 1915 (Intensity XI MCS, M_s=7.0, Grupppo di Lavoro CPTI, 1999) which caused more than 30,000 deaths. Surface faulting occurred along the east side of the basin, with open cracks 0.3-1 m wide and average vertical throws of 30-90 cm up to a maximum of 3 m (e.g., Serva et al., 1986).

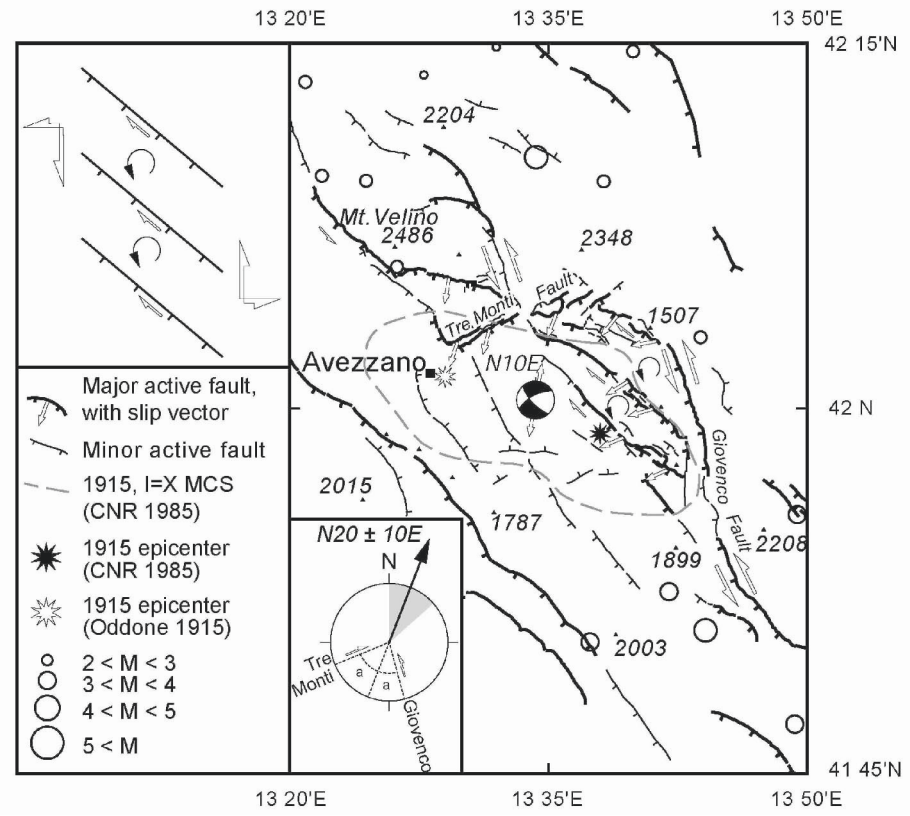

Figure 3. Active faults in the Fucino intramontane basin (modified from Piccardi et al., 1999).

Slip indicators along the NW-striking SW-dipping active faults along the east side of the basin show that most of the faults exhibit oblique motion. Vertical slip rates computed from active normal-transtensional faults affecting the Fucino area are in the range of 0.5-1 mm/yr (Piccardi *et al*., 1999). The

parallel strikes and dextral overlaps of these faults imply counterclockwise rotation of the blocks they separate (Piccardi, 1995, Piccardi & Cello, 2003). At a larger scale, such rotations are consistent with a left-lateral component of motion between the Fucino basin and the ranges east of it. In addition to regional extension, our results suggest that a component of sinistral motion occurs along the Abruzzi segment of the NW-SE-trending Apenninic belt.

The Vallo di Diano-high Agri Valley area

The Vallo di Diano and the High Agri Valley (Figure 4) represent two intramontane basins filled by Quaternary fluvio-lacustrine sediments and colluvium (Giano et al., 2000 and references therein). These basins are oriented NNW-SSE and WNW-ESE, respectively. The epicenter of the 1857 Basilicata earthquake (maximum intensity X MCS; Mallet, 1862; Boschi et al., 1997)was located in this area, and extensive ground effects were recorded. In this sector of the southern Apennines, two distinct active fault systems are exposed: The Vallo di Diano Fault System (DIFS) and the Val d'Agri Fault System (VAFS; Cello et al., 2003).

In the Vallo di Diano area (Figure 4) recent activity is concentrated along NW-SE-trending normal to transtensional faults. These faults are exposed at the surface along a length of about 15 km, locally cutting Upper Pleistocene-Holocene slope deposits. Kinematic indicators (striae and shear fibers on slickensided surfaces) show mainly dip-slip motion. The geometry of the stress field, obtained by fault inversion (Delvaux, 1993), reveals an extensional regime with an R value of 0.67. Since R values between 0.66 and 1.00 indicate that $\sigma_1 \approx \sigma_2 >> \sigma_3$, we suggest that changes in stress axes may have occurred repeatedly in the area.

In the northern portion of the High Agri Valley (Figure 4), a Quaternary fault system consisting of roughly N120-trending, left-lateral strike-slip faults (Benedetti *et al.*, 1998; Cello *et al.*, 2003) is exposed for a total length of about 15 km. Secondary structures associated with the main system include: (i) N20-N30-trending, right-lateral faults; (ii) N80-N100-trending, normal to left-lateral transtensional faults; and (iii) N130-N150 trending, left-lateral transpressional faults. Upper Pleistocene-Holocene slope deposits are locally displaced by ESE-oriented strike-slip faults. In particular, slope deposits dated at 30 ka (Giano *et al.*, 2000) are cut by a fault zone trending roughly N110°. This fault zone displaces the slope deposits with left-lateral transtensional kinematics. The occurrence of striae on the fault plane allowed us to quantify a minimum offset (post-30 ka) of about 15 m and to compute a time-averaged slip rate of 0.4-0.5 mm/year.

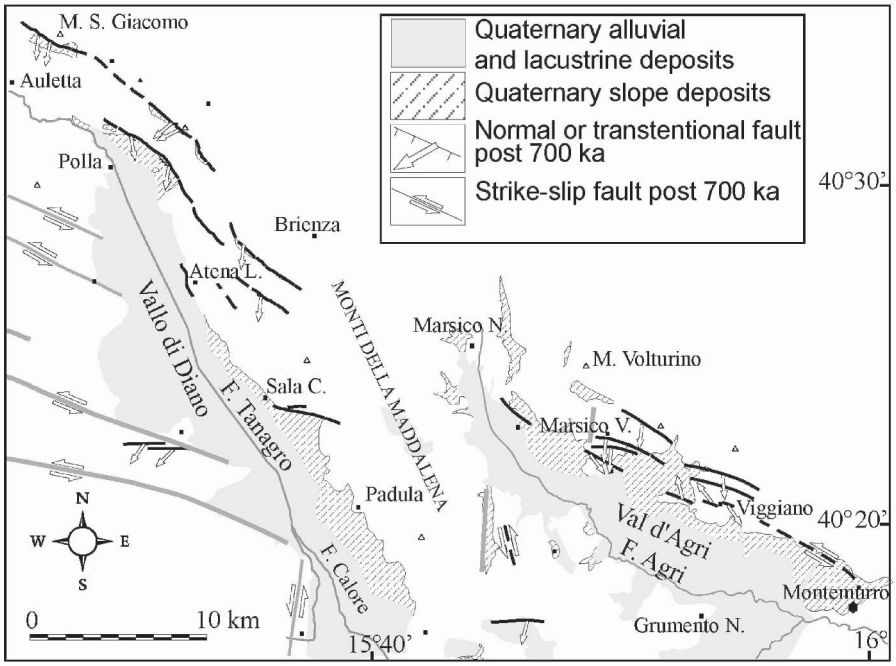

Figure 4. Active faults in the Vallo di Diano (DIFS) and in the Val d'Agri (VAFS; modified from Cello et al., 2003).

The geometry of the stress field derived by inversion of slip data collected from the Val d'Agri faults is characterized by a sub-horizontal σ_1 axis trending roughly E-W, and by a sub-vertical σ_3 axis oriented roughly N-S. This geometry defines a strike-slip regime with a R value of 0.69, suggesting that, as previously, changes in the principal axes of the stress ellipsoid may have occurred over time.

The Gargano area

The Gargano promontory (Figure 5) is a carbonate massif reaching elevations of more than 1000 m. It belongs to the Adria microplate, the foreland of both the Apenninic and the Dinaric mountain chains (Ciaranfi & Ricchetti, 1980; Mostardini & Merlini, 1986; Funiciello *et al.*, 1991). The carbonate platform sequence, over 4000 m thick and ranging in age from the Upper Jurassic to Middle Miocene, is discordantly overlain by thin, discontinuous, Late Pliocene-Pleistocene deposits. A Triassic evaporite unit

(Burano Anidrite) lies beneath the carbonate rocks and acts as a décollement surface (Bosellini *et al.*, 1993, and references therein).

The deformation pattern of this area appears to be quite simple, and regional tectonic structures are easily recognizable. The most prominent active tectonic feature in the area is the sub-vertical, strike-slip Mattinata fault (Funiciello *et al.,* 1988). The Mattinata fault is a spectacular E-W-trending fault, running over 60 km through the southern portion of the Gargano massif. The fault is the on-land expression of a regional fault system, and seismic-reflection data clearly show that the system extends both the the west (until the main frontal thrust of the Apennines; Borre et al., 2003; Piccardi, in press) and to the east (offshore into the Adriatic sea). This fault system forms an active crustal deformation belt called the South Gargano Line (Funiciello et al., 1991; Doglioni et al., 1994, 1996, and references therein). The fault system is interpreeted as a right-lateral, segmented structure, capable of repeated Holocene surface faulting and responsible for the most relevant historic seismic events of the area (the July 30,1627, M=6.7, San Severo earthquake; Piccardi, 1998; Boschi et al., 1997; Gruppo di Lavoro CPTI, 1999).

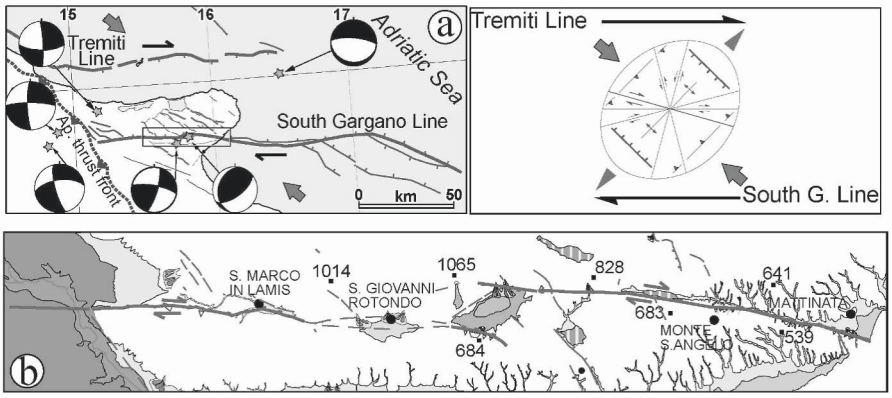

Figure 5. a) Active faults in the Gargano area, (modified from Piccardi, in press) and b) along the Mattinata fault system.

A right-lateral component of motion along the South Gargano Line is indicated by both geologic and geomorphic evidence along single fault segments and by the large-scale arrangement of normal faults at the offshore "horse-tail" termination of the system (Piccardi, 1998 and Piccardi, in press). Such dextral slip is consistent with available focal mechanisms (Gasparini et al., 1985; Harvard Seismology: Centroid-Moment Tensor Project, 2004; Catalogue of Swiss Seismological Service, 2001; Figure 5). The cumulative slip rate of strike-slip fault segments belonging to the Mattinata fault system

is in the range of 0.8-0.9 mm/yr (Piccardi, 1998; Borre et al., 2003). The right-lateral slip along the Mattinata fault is due to a stress state condition characterized by a σ_1 oriented roughly NW-SE and a σ_3 oriented about NE-SW (Figure 5).

DISCUSSION AND CONCLUSIONS

Most authors who have worked in south-central Italy agree that in the Late Miocene to Early Pleistocene, the Apennines were affected by extension in the axial zone of the belt. This extension probably resulted from the contraction occurring at that time on the foreland side of the orogen (e.g., Lavecchia, 1988; Decandia et al., 1998). On the other hand, the subsequent geodynamic evolution of the orogen, and especially the active tectonic processes operating in these areas, are still a matter of debate. According to Meletti et al. (2000) and Lavecchia et al. (2003), the NE-verging compressional front of the central Apennines, which is characterised by low to medium seismicity, is still active and is related to the flexure-hinge retreat of a lithospheric slab belonging to the Adria microplate and now sinking beneath the chain (e.g., Anderson, 1987). Alternatively, according to other authors (e.g., Bertotti et al., 1997; Carminati et al., 1999; Di Bucci and Mazzoli, 2002), thrusting and folding ended in the Early Pleistocene.

In fact, active fault systems exposed in the Apennines and in the Gargano area show overprinting of older structures, which suggests that they dissect pre-existing features of the orogenic belt along a well-constrained NNW-SSE trend. These later faults localize most of the strain accumulated in the area during the last 700 ky. This conclusion is consistent with the seismic-moment release of historical earthquakes in the region over the last 1000 years (Westaway, 1992) and with recent studies on the spatial and temporal properties of fault development and related earthquake activity, which show that the displacement rate of the system as a whole is 1.6 cm/yr over the same time window (Tondi & Cello, 2003).

Slip indicators, and the overlapping geometry of fault segments, also show that most of the faults in the axial zones of the Apennines exhibit oblique slip and that the overall direction of extension appears to be at a fairly high angle to the trend of the mountain belt. This, of course, implies a component of horizontal left-lateral displacement between Tyrrhenia and Adria.

A similar kinematic scenario also has been inferred from the pattern of active deformation and from available seismological data for other areas, for example the Matese Mts. (Galli & Galadini, 2003 and references therein) and Irpinia (Pantosti & Valensise, 1990). The fault-plane solution for the

M6.9 1980 Irpinia earthquake (Deschamps & King 1984; Westaway & Jackson 1984, 1987) as well as the right-stepping surface scarps and slickensides generated by that earthquake (Westaway & Jackson 1984, 1987; Pantosti & Valensise, 1990) are in full agreement with the occurrence of oblique extension in the Apennines.

Moreover, an oblique component of motion in this area is also needed in order to allow northwestward motion of Adria. Ongoing indentation of Adria into the Alpine edifice is particularly evident in the Venetian Alps, where growing anticlines and active thrusting may be observed at the front of the southern Alpine chain.

In conclusion, we suggest that active tectonics in the south-central Italian peninsula may be best interpreted as controlled by two principal processes. The first involves tectonic uplift, possibly related to slab detachment and associated unbending of the foreland plate. The second, responsible for oblique extension resulting in a component of left-lateral motion (Piccardi et al., 1997; Cello et al., 1997; Piccardi et al., 1999; Piccardi and Cello, in press), is due to the ongoing N-NW motion of Adria with respect to Europe.

REFERENCES

Anderson H.A. Is the Adriatic an African promontory? Geology 1987; 15: 212-215.

Anderson H.A., Jackson J.A. Active tectonics of the Adriatic region. Geophys. J. R. Astron. Soc. 1987; 91: 937-983.

Bally A.W., Burbi L., Cooper C., Ghelardoni R. Balanced sections and seismic reflection profiles across the Central Apennines. Mem. Soc. Geol. It. 1986; 35: 257-310.

Barchi M., Galadini F., Lavecchia G., Messina P., Michetti A.M., Peruzza L., Pizzi A., Tondi E., Vittori E. Sintesi delle conoscenze sulle faglie attive in Italia Centrale: parametrizzazione ai fini della caratterizzazione della pericolosità sismica. CNR-Gruppo Nazionale per la Difesa dai Terremoti - Roma, 2000.

Benedetti L., Tapponier P., King G. C. P., Piccardi L. Surface rupture of the 1857 Southern Italian earthquake. Terra Nova 1998; 10(4): 206-210.

Bertotti G., Capozzi R., Picotti V. Extension controls Quaternary tectonics, geomorphology and sedimentation of the N-Apennines foothills and adjacent Po Plain (Italy). Tectonophysics 1997; 282: 291-301.

Borre K., Cacon S., Cello G., Kontny B., Kostak B., Lykke-Andersen H., Moratti G., Piccardi L., Stemberk J., Tondi E., Vilimek V. The COST project in Italy: analysis and monitoring of seimogenic faults in the Gargano and Norcia areas (central-southern Apennines, Italy). J. Geodynamics 2003; 36: 3-18.

Boschi E., Guidoboni E., Ferrari G., Valensise G., Gasperini P. Catalogo dei forti terremoti in Italia del 461 a.C. al 1990, ING-SGA, Bologna, 1997.

Bosellini A., Neri C., Luciani V. Guida ai carbonati Cretaceo-Eocenici di scarpata e bacino del Gargano (Italia meridionale). Annali dell'Università di Ferrara (nuova serie), Sez. Scienze della Terra, suppl. to vol. 4, Bologna, 1993.

Bosi C. Osservazioni preliminari su faglie probabilmente attive nell'Appennino centrale. Bol. Soc. Geol. It. 1975; 94: 827-856.

Calamita F., Coltorti M., Farabollini P., Pizzi A. Le faglie normali quaternarie nella Dorsale appenninica umbro-marchigiana. Proposta di un modello di tettonica d'inversione. Studi Geol. Camerti. Vol. Spec. 1994; 211-225.

Carminati E., Giunchi C., Argnani A., Sabadini R., Fernandez M. Plio-Quaternary vertical motion of the Northern Apennines: Insights from dynamic modeling. Tectonics 1999; 18(4): 703-718.

Catalogue of Swiss Seismological Service, 2001. Catalogue of Moment Tensor Solutions in the European-Mediterranean region, years 2000-2001. http://www.seismo.ethz.ch/info/mt.html.

Cello G., Mazzoli S. Apennine tectonics in Southern Italy: a review. J. Geodynamics 1999; 27: 191-211.

Cello G., Martini N., Paltrinieri W., Tortorici L. Structural styles in the frontal zones of the southern Apennines, Italy: an example from the Molise district. Tectonics 1989; 8(4): 753-768.

Cello G., Mazzoli S., Tondi E., Turco E. Active tectonics in the central Apennines and possible implications for seismic hazard analysis in peninsular Italy. Tectonophysics 1997; 272: 43-68.

Cello G., Tondi E., Micarelli L., Mattioni L. Active tectonics and earthquake sources in the epicentral area of the 1857 Basilicata earthquake (Southern Italy). J. Geodynamics 2003; 36: 37-50.

Channell J. E. T., D'Argenio B., Horwath F. Adria, the African promontory, in Mesozoic Mediterranean paleogeography. Earth Sc. Rev. 1979; 15: 213-292.

Ciaranfi N., Ricchetti G. Considerazioni sulla neotettonica del Promontorio del Gargano (Foglio 157, M. S. Angelo; Foglio 156, S. Marco in Lamis). Prog. Final. Geod. Publ. 1980; 356.

Cinque A., Patacca E., Scandone P., Tozzi M. Quaternary kinematic evolution of the Southern Apennines. Relationships between surface geological features and deep lithospheric structures. Annali di Geofisica 1993; 36: 249-260.

Cipollari P., Cosentino D. Miocene unconformities in the Central Apennines: geodynamic significance and sedimentary basin evolution. Tectonophysics 1995; 252: 375-389.

Decandia F.A., Lazzarotto A., Liotta D., Cernobori L., Nicolich R. The CROP 03 traverse: insights on postcollisional evolution of the Northern Apennines. Mem. Soc. Geol. It. 1998; 52: 427-439.

Delvaux D. The TENSOR program for paleostress reconstruction: exaples fro the east African and Baikal rift zones. Terra Nova 1993; 5: 216, Abstracts supplement No. 1.

Deschamps A., King G.C.P. Aftershocks of the Campania-Lucania (Italy) earthquake of 23 november 1980. Bull. Seismol. Soc. Am. 1984; 74: 2483-2517.

Dewey J.F., Helman M.L., Turco E., Hutton D.H.W., Knott S.D. "Kinematics of the western Mediterranean". In *Alpine Tectonics*, M.P. Coward, D. Dietrich, R.G. Park, eds., London: Geol. Soc. London Spec. Publ. 1989; 45: 265-283.

Di Bucci D., Mazzoli S. Active tectonics of the Northern Apennines and Adria geodynamics: new data and a discussion. J. Geodynamics 2002; 34: 687-707.

Doglioni C., Mongelli F., Pieri P. The Puglia uplift (SE Italy): an anomaly in the foreland of the Apenninic subduction due to buckling of a thick continental lithosphere. Tectonics 1994; 13(5): 1309-1321.

Doglioni C., Tropeano M., Mongelli F., Pieri P. Middle-late Pleistocene uplift of Puglia: an anomaly in the Apenninic foreland. Mem. Soc. Geol. It. 1996; 51.

Dramis F. Il ruolo dei sollevementi tettonici a largo raggio nella genesi del rilievo appenninico. Studi Geologici Camerti, Special Issue 1992; 9-15.

Funiciello R., Montone P., Salvini F., Tozzi M. Caratteri strutturali del Promontorio del Gargano. Mem. Soc. Geol. It. 1988; 41: 1235-1243.

Funiciello R., Montone P., Parotto M., Salvini F., Tozzi M. Geodynamic evolution of an intra-orogenic foreland: the Apulia case history (Italy). Boll. Soc. Geol. It. 1991; 110: 419-425.

Galli P., Galadini F. Disruptive earthquakes revealed by faulted archaeological relics in Samnium (Molise, southern Italy). Geophy. Res. Let. 2003; 30(5): art. no. 1266.

Gasparini C., Iannaccone G., Scarpa R. Fault plane solutions and seismicity of the Italian peninsula. Tectonophysics 1985; 117: 59-78.

Giano S.I., Maschio L., Alessio M., Ferranti L., Improta S., Schiattarella M. Radiocarbon dating of active faulting in the Agri high valley, Southern Italy. J. Geodynamics 2000; 29: 371-386.

Gruppo di Lavoro C.P.T.I. Catalogo Parametrico dei Terremoti Italiani. ING, GNDT, SGA, SSN, Bologna, 1999.

Harvard Seismology: Centroid-Moment Tensor Project, 2004, http://www.seismology.harvard.edu/projects/CMT/

Hippolyte J.-Cl., Angelier J., Roure F. A major geodynamic change revealed by Quaternary stress patterns in the Southern Apennines (Italy). Tectonophysics 1994; 230: 199-210.

INGV-Harvard European-Mediterranean Regional Centroid-Moment Tensors Project 2004, http://www.ingv.it/seismoglo/RCMT/.

Lavecchia G. The Tyrrhenian-Apennine system: structural setting and seismotectogenesis. Tectonophysics 1988; 147: 263-296.

Lavecchia G., Boncio P., Creati N. A lithospheric-scale seismogenic thrust in central Italy. J. Geodynamics 2003; 36(1-2): 79-94.

Malinverno A., Ryan W.B.F. Extension in the Tyrrhenian Sea and shortening in the Apennines as a result of arc migration driven by sinking of the lithosphere. Tectonics 1986; 5(2): 227-245.

Mallet R. *The great Neapolitan earthquake of 1857. The first principles of observational seismology*. London, 1862.

Mantovani E., Albarello D., Tamburelli C., Babbucci D. Evolution of the Tyrrhenian basin and surrounding regions as a result of the Africa-Eurasia convergence. J. Geodynamics 1996; 21(1): 35-72.

McKenzie D. Active tectonics of the Mediterranean Region, Geophys. J. R. Astr. Soc. 1972; 30: 109-185.

Meletti C., Patacca E., Scandone P. Construction of a Seismotectonic model: the case of Italy. Pure Appl. Geophys. 2000; 157: 11-35.

Mostardini F., Merlini S. Appennino centro-meridionale. Sezioni Geologiche e proposta di modello strutturale. Mem. Soc. Geol. It. 1986; 35: 177-202.

Müller S., Panza G.F. Evidence of a deep-reaching lithospheric root under the Alpine arc. Developments in Geotectonics 1986; 21: 93-113.

Nicolich R. Crustal structures from seismic studies in the frame of the European Geotraverse (Southern segment) and CROP Project. In *The lithosphere in Italy*, CNR-Accademia Nazionale dei Lincei, Roma, 1989.

Pantosti D., Valensise G. Faulting mechanism and complexity of the 23 November 1980, Campania-Lucania earthquake, inferred from surface observations. J. Geophys. Res. 1990; 95: 15,319-15,341.

Parotto M., Praturlon A. Duecento anni di ricerche geologiche nell'Italia centrale. Volume Giubilare della Soc. Geol. Italiana 1981; 242-278.

Patacca E., Scandone P. Post-Tortonian mountain building in the Apennines: the role of the passive sinking of a relic lithospheric slab. In *The lithosphere in Italy*, CNR-Accademia Nazionale dei Lincei, Roma, 1989.

Piccardi L. Structural and morphological observations on the Ventrino active fault. Annales Tectonicae 1995; 9: 39-54.

Piccardi L. Cinematica attuale, comportamento sismico e sismologia storica della faglia attiva di Monte Sant'Angelo (Gargano): la possibile rottura superficiale del 'leggendario' terremoto del 493 d.C. Geografia Fisica e Dinamica Quaternaria 1998; 21: 155-166.

Piccardi L. Paleoseismic evidence of legendary earthquakes: the apparition of Archangel Michael at Monte Sant'Angelo (Gargano, Italy). Tectonophysics. In press.

Piccardi L., Sani F., Bonini M., Boccaletti M., Moratti G., Gualtierotti A. Deformazioni quaternarie nell'Appennino centro-settentrionale: evidenze ed implicazioni. Il Quaternario 1997; 10(2): 273-280.

Piccardi L., Gaudemer Y., Tapponnier P., Boccaletti M. Active oblique extension in the central Apennines (Italy): evidence from the Fucino basin. Geophisical J. Int. 1999; 139(2): 499-530.

Piccardi L., Cello G. Kinematic evolution of the active fault system of the Fucino basin (Central Apennines, Italy). Studi Geologici Camerti. 2003.

Platt J.P., Behrmann J.H., Cunningham P.C., Dewey J.F., Helman M., Parish M., Shepley M.G., Wallis S., Weston P.J. Kinematics of the Alpine arc and the motion history of Adria. Nature 1989; 337: 158-161.

Ricci L.F. The Oligocene to Recent foreland basins of the Northern Apennines. In *Foreland Basins,* P.A. Allen, P. Homewood, eds., Int. Association of Sedimentologists, Special Publication 1986; 8.

Royden L., Patacca E., Scandone P. Segmentation and configuration of the subducted lithosphere in Italy: an important control on thrust-belt and foredeep basin evolution. Geology 1987; 15: 714-717.

Serva L., Blumetti A.M., Michetti A.M. Gli effetti sul terreno del terremoto del Fucino (13 gennaio 1915); tentativo di interpretazione della evoluzione tettonica recente di alcune strutture. Mem. Soc. Geol. It. 1986; 35: 893-907.

Tondi E.. Geological analysis and seismic hazard in the Central Apennines. J. Geodynamics 2000; 29(3-5): 517-534.

Tondi E., Cello G. Spatiotemporal Evolution of the Central Apennines Fault System (Italy). J. Geodynamics 2003; 36: 113-128.

Westaway R.W.C. Seismic moment summation for historical earthquakes in Italy: tectonic implications. J. Geophys. Res. 1992; 97: 15,437-15,464.

Westaway R.W.C., Jackson J. Surface faulting in the southern Italian Campania-Basilicata earthquake of 23 November 1980. Nature 1984; 312: 436-438.

Westaway R.W.C., Jackson J. The earthquake of 1980 November 23 in Campania-Basilicata (southern Italy), Geophys. J. R. Astron. Soc. 1987; 90: 375-443.

RATES OF LATE NEOGENE DEFORMATION ALONG THE SOUTHWESTERN MARGIN OF ADRIA, SOUTHERN APENNINES OROGEN, ITALY

Luigi Ferranti[1] and John S. Oldow[2]
1: Dipartimento di Scienze della Terra, Universitá di Napoli Federico II, 80138 Napoli, Italy
lferrant@unina.it
2: Department of Geological Sciences, University of Idaho, Moscow 83844-3022, Idaho, USA

ABSTRACT

During latest Miocene to Early Pleistocene deformation of the southwestern margin of Adria, the frontal thrust of the Southern Apennines orogen migrated toward the foreland rapidly (~16 mm/yr) and was accompanied by subsidence with the frontal thrust belt and foredeep remaining at or below sea level. In contrast, the orogenic hinterland experienced extension, which was accompanied by uplift at ~0.3 mm/yr along the eastern transition to the contractional belt but net subsidence and formation of the Tyrrhenian basin farther west. Through time, the extensional belt progressively widened toward the northeast at the same rate as the encroachment of the thrust front on the Adriatic foreland. Following a mid-Pleistocene reduction in horizontal displacement rate associated with impingement of the thrust belt on thick crust of the Adriatic interior, the frontal thrust belt and foreland experienced uplift at ~0.5 mm/yr as contraction stepped to deeper structural levels. Uplift of the eastern margin of the extensional hinterland continued at ~0.3 mm/yr and is followed by tectonic subsidence along the Tyrrhenian coast of southern Italy. Today, the pattern of mid-Pleistocene displacements continues, as suggested by seismicity and GPS velocities.

The similarity in migration rates of contractional and extensional fronts across southern Italy over the last 6 million years supports models of crustal delamination and roll-back of the subducted Adriatic slab as a fundamental driving mechanism for deformation along the western margin of Adria. Temporal variations in the vertical and horizontal rates of deformation, however, probably reflect differences in crustal structure and are not directly related to lithospheric processes. The reduction in the horizontal displacement rate associated with the onset of rapid foreland and frontal thrust belt uplift during the Early Pleistocene corresponds to a change from thin- to thick-skinned contraction initiated with the involvement of thick continental crust in regional shortening. Thin continental crust promoted thin-skinned contraction accompanied by subsidence, whereas thicker continental crust resulted in thick-skinned shortening and uplift.

N. Pinter et al. (eds.), The Adria Microplate: GPS Geodesy, Tectonics and Hazards, 109–131.

INTRODUCTION

Assessment of vertical and horizontal displacements and displacement rates within the orogens rimming the deformed margins of Adria (Argand, 1927; Laubscher, 1975; Channell et al., 1979; Dercourt et al., 1986) in the central Mediterranean has the potential to supply vital insight into crustal and lithospheric processes operating during continental collision. Nevertheless, the application of kinematic constraints derived from these orogens to geodynamic models is hindered by two issues: (1) uncertainty in the relationship between orogenic displacement and the relative motion between lithospheric plates, and (2) to what degree present-day surface motions reflect orogenic displacements occurring over geologic time scales.

The central Mediterranean offers an unusual situation where the relative plate motion between Africa and Europe is well constrained (Dewey et al., 1989) and deformation rates in parts of the orogen surrounding Adria are high. Divergence between orogenic displacement and relative plate motion in the western and central Mediterranean has long been recognized (Malinverno and Ryan, 1986; Dewey et al., 1989) and led to orogenic models involving crustal delamination and slab roll-back driven only indirectly by plate convergence (Malinverno and Ryan, 1986; Royden et al., 1987; Channell and Mareschal, 1989; Doglioni, 1991; Gueguen et al., 1998; Faccenna et al., 2001). Lateral changes in the magnitude and style of deformation within the orogen surrounding Adria strongly suggest that the kinematic evolution of the deformed belts is intimately intertwined with pre-existing crustal architecture.

Today, the active deformation pattern within the Adria interior and in the deformed belts placed at its margins is illustrated by GPS velocities, strain indicators and seismicity (e.g., Anzidei et al., 2001; Oldow et al., 2002; Hollenstain et al., 2003; this volume). Integration of GPS geodesy and regional seismicity suggests that surface and upper crustal motions in the western margin of Adria mainly reflect orogenic displacement (Oldow and Ferranti, this volume). Thus, active deformation processes might give insight into the displacement history of deformed belts achieved during the so-called orogenic float (Oldow et al., 1990). However, extrapolation of the geodetic and seismicity record to geologic time-scales is notoriously difficult, and within most of the circum-Adriatic orogen it is hindered by the poor resolution of the geologic record.

In order to get insight into the relation between active crustal deformation, orogenic displacements and relative plate motion in the southwestern margin of Adria, where contractional and extensional deformation coexists since the Miocene in the Apenninic deformed belt (Malinverno and Ryan, 1986; Patacca et al., 1990), we have reconstructed the

spatial-temporal pattern of deformation rates over a time scale of several million years. Using the tight age control on contractional motion provided by synorogenic sequences preserved in outcrop and in petroleum exploration wells, the constraints on extensional displacement provided by the crustal structure of the extended hinterland, and the differential elevation of uplifted markers of ancient base level, we establish a regional pattern of vertical and horizontal motion from the latest Miocene to the Late Pleistocene. Systematic spatial displacement patterns are observed within tectonically defined domains across the Apenninic belt, and supports models of crustal delamination and slab roll-back. Temporal variations in displacement rates appear controlled by the inherited crustal structure, and the geological history of tectonism may be still recognized in the ongoing kinematics pattern.

TECTONIC SETTING

The orogens surrounding the central and western Mediterranean Sea are characterized by coeval belts of foreland contraction and hinterland extension that advanced toward the continental interiors (e.g., Channell et al., 1979; Gueguen et al., 1998; Faccenna et al., 2001). Activity in the orogens progressively decreases in age from west to east (Gueguen et al., 1998) and today is concentrated along the western Adriatic margin in the central Mediterranean. Here, the transport direction and migration of deformation fronts is at a high-angle to relative motion of Africa and Europe (Dewey et al., 1989) and typically are viewed as products of crustal delamination and roll-back of a slab composed of the Adriatic mantle and lower crust (Royden et al., 1987; Channell and Mareschal, 1989; Doglioni, 1991; Gueguen et al., 1998; Faccenna et al., 2001).

In southern Italy (Figure 1, 2), Neogene deformation propagated toward the Apulian sector of the Adriatic foreland as Mesozoic and Cenozoic rocks were stripped from the western margin of Adria, a continental block with African affinity (Argand, 1927; Channell et al., 1979), and incorporated as thrust imbricates within the Southern Apennine fold and thrust belt. Contraction was accompanied by extension, which from the Early Miocene resulted in hinterland stretching of continental crust and local emplacement of oceanic crust beneath the southern Tyrrhenian Sea (Figure 1). The age of Tyrrhenian Sea rifting progressively decreases from the center of the basin toward the southeast, where Pliocene-Quaternary sea floor is exposed (Malinverno and Ryan, 1986; Kastens et al., 1988)

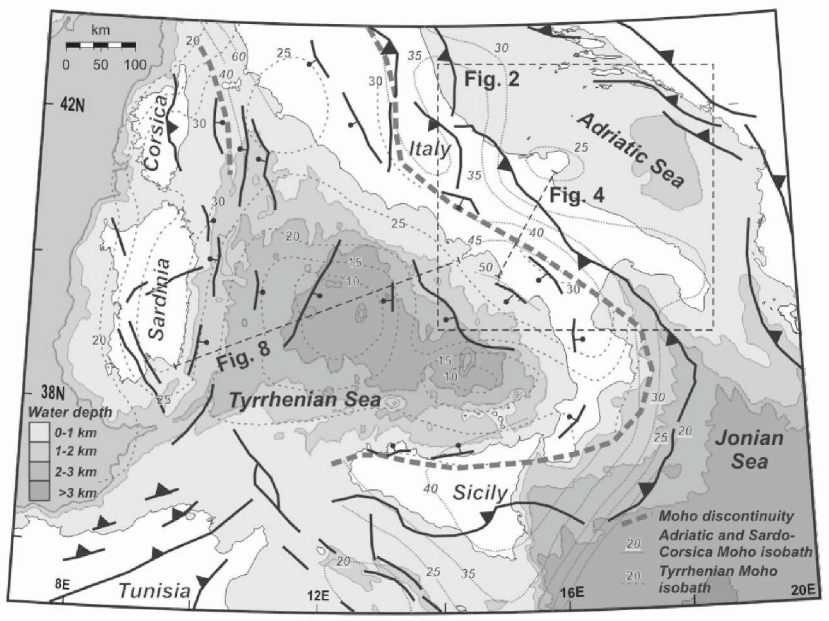

Figure 1. Tectonic map of the circum-Tyrrhenian region showing the crustal structure, the discontinuity between Adriatic/European and Tyrrhenian Moho (after Cassinis et al., 2003), bathymetry, and the main contractional and extensional structures.

Geophysical data show contrasting crustal structure between the Tyrrhenian and Apenninic domains of the orogen, and the transition is abrupt (Figure 1; Scarascia et al., 1994; Cassinis et al., 2003). The crust changes from up to 50 km thick in the east to less than 10 km beneath the southeastern Tyrrhenian Sea (Figure 1), which along the Calabrian margin is underlain by a well-defined Benioff zone dipping steeply to the northwest (Selvaggi and Chiarabba, 1995; Cimini, 1999).

Within the Southern Apennines, the progressive development of contractional and extensional structures is recorded within three tectonic sectors referred to here as the inner belt, frontal thrust belt, and the Apulia foreland (Figure 2). A profound lateral difference exists in facies and thickness of the Mesozoic-Tertiary sedimentary sections exposed in the foreland, frontal thrust belt and inner belt (Figure 3). The Apulia foreland is floored by ~6 km of Mesozoic-Tertiary platform to slope carbonate and evaporite which overlay upper Paleozoic weakly metamorphosed clastics (Ricchetti and Mongelli, 1980). The frontal thrust belt is largely floored by Mesozoic-Miocene rocks of the Lagonegro basin, which had an original ~1 km thickness (D'Argenio and Alvarez, 1980).

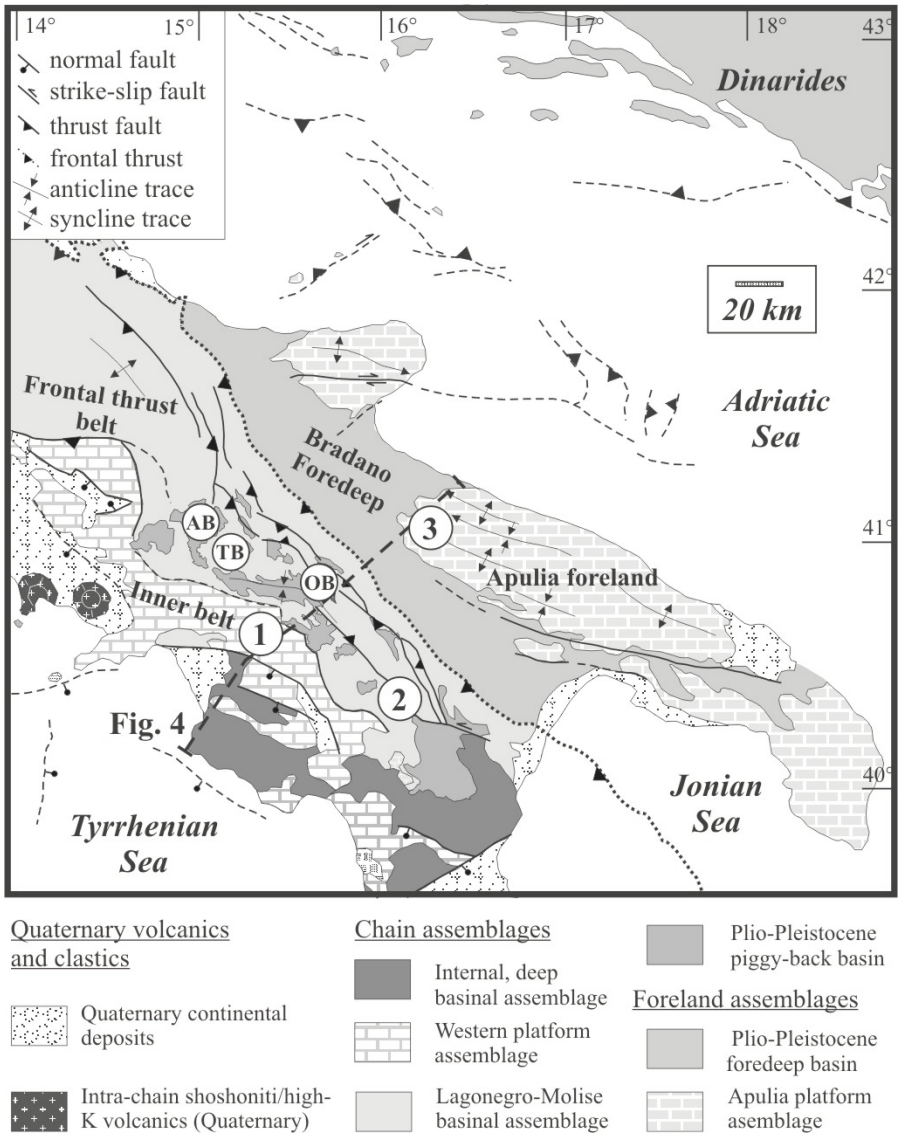

Figure 2. Generalized tectonic map of the Southern Apennines (location in Figure 1). Numbers 1,2,3, refer to thickness column in Figure 3. OB, AB, TB=Ofanto, Trevico, Ariano basin (cfr. Figure 7, 10).

The inner belt includes ~3.5 km of Mesozoic-Tertiary carbonates of the Western platform, structurally overlain by deep basinal, ophiolitic-bearing fragments of the subducted Tethyan oceanic crust, once intervening between

Adria and Europe (Figure 2). The different facies patterns were deposited in ancient sedimentary environments of the Adriatic margin before onset of shortening and growth of the fold and thrust belt, and reflect systematic lateral variability in crustal thickness (Figure 3; Channell et al., 1979; D'Argenio and Alvarez, 1980).

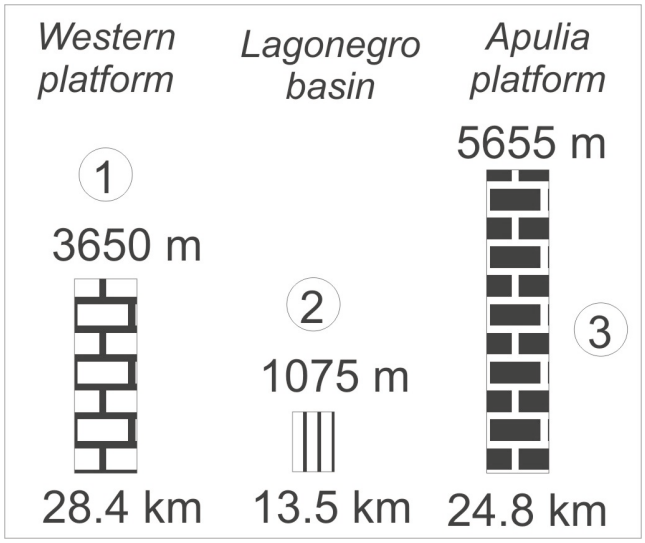

Figure 3. Generalized thickness of Mesozoic-Cenozoic rocks of the Apulia platform, Lagonegro basin and Western platform (location in Figure 2), including (bottom) the calculated crustal thickness (data after D'Argenio and Alvarez, 1980).

A different Neogene structural evolution is also recorded within the foreland, frontal and inner belts. The outcropping Apulia foreland is affected by large wavelength folds which strike west to northwest, and together with its offshore extension experienced Miocene through Quaternary folding and traspressional faulting (Figure 2; de Alteriis, 1995; Bertotti et al., 1999, 2001).

The westerly extension of the foreland buried beneath the Pliocene-Pleistocene foredeep basin and the fold and thrust belt is documented by synorogenic deposits hit by exploratory wells on top of pre-orogenic Apulia carbonates (Figure 4; Casero et al., 1988; Patacca and Scandone, 2001). Wells, gravimetric and seismic reflection data suggest that part of the buried foreland experienced contraction as well (Figure 4), but the timing and amount of shortening are poorly constrained (Casero et al., 1988; Mazzotti et al., 2000; Mazzoli et al., 2000). Apulian thrust imbricates include the sedimentary upper crust, but involvement of mid-crustal crystalline rocks is debated (Casero et al., 1988; Speranza and Chiappini, 2002).

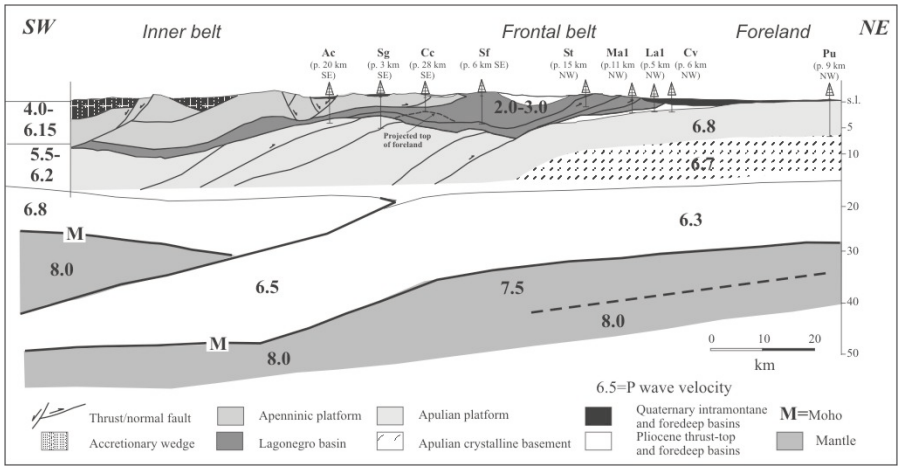

Figure 4. Crustal section across the Southern Apennines. Velocity structure after Cassinis et al., 2003 (location in Figure 1) and upper crustal geology modified after Mazzotti et al., 2000 (location in Figure 4).

Within the frontal thrust belt, rocks of the Lagonegro basin were imbricated during Late Miocene, and during Pliocene-Early Pleistocene were transported northeast over the western margin of the foreland (Patacca and Scandone, 2001).

Late Oligocene-Miocene contractional structures of the inner belt (Patacca et al, 1990; Cello and Mazzoli, 1999) were overprinted during Pliocene and Quaternary by normal faults (Figure 2; 4; Ferranti et al., 1996; Ferranti and Oldow, 1999) which during the Quaternary accompanied continental deposition in intermountain basins (Brancaccio et al., 1991) and shoshonitic, high-K volcanism on the eastern Tyrrhenian margin (Beccaluva et al., 1989).

The carbonate platform and basinal imbricates are unconformably covered by Miocene siliciclastic and evaporite rocks, which were deposited in migrating foredeep and piggyback basins and are now incorporated into the thrust belt (Patacca et al., 1990). Pliocene-Lower Pleistocene marine to continental sediments correlative to the Bradanic foredeep deposits are found in piggyback basins of the frontal thrust belt, but they are lacking in the inner belt (Figure 2; 4).

The present-day pattern of regional deformation is reflected in crustal seismicity and Global Positioning System (GPS) velocity fields (Figure 5).

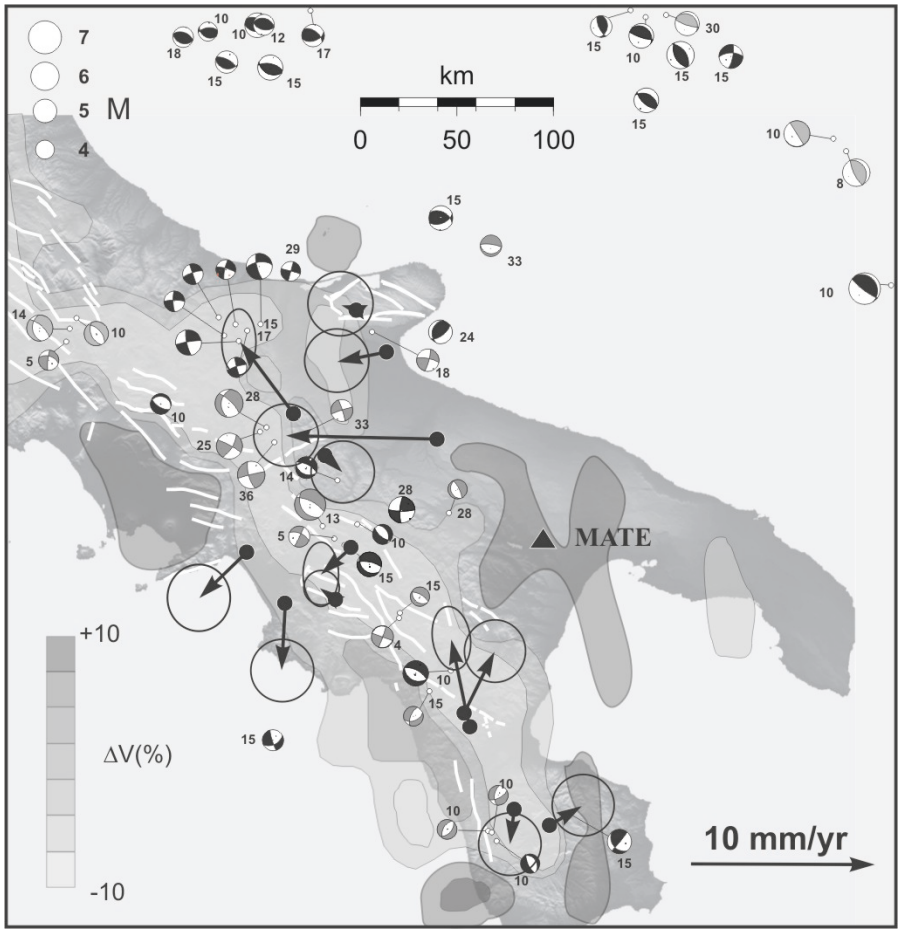

Figure 5. Active deformation in Southern Italy: focal depth and mechanisms of 4.0≤M≤6.9 crustal earthquakes (black: Harvard CMT, 1976-2004 and Mednet CMT, 1997-2004; grey: 1908-1980 focals from Gasparini et al., 1985; light grey:1908-1984 focals from Anderson and Jackson, 1987); active faults (white lines); the 22 km depth P-waves velocity anomaly (Di Stefano et al., 1999); and PTGA velocity field in MATE International GPS Service site (triangle) fixed frame (ellipses are 2-sigma uncertainties)

Earthquake focal mechanisms record northeast-southwest extension with a locus along the axis of the Apennine chain and northeast-southwest to north-south contraction offshore the Apulian foreland and along the Dalmatian coast (Figure 5). Across the orogen, GPS velocities record a complex pattern of surface displacement (Oldow et al., 2002; Oldow and Ferranti, this volume) consistent with simultaneous contraction to transpression and extension to transtension in the eastern and western parts of

Southern Italy, respectively. The belt of extensional focal mechanisms and the spatially associated array of seismogenic extensional faults reside in the mountain chain at the transition between the inner and frontal zones, and spatially coincide with the locus of maximum P-wave low-velocity anomalies at a depth of ~20 km (Figure 5; Di Stefano et al., 1999).

From east to west, the topography in the Southern Apennines shows a marked asymmetry (Figure 4). The Murge and Gargano blocks are uplifted up to 0.8 km, and the frontal thrust belt forms a gentle plateau with 1 km average elevation. In contrast, the inner belt has higher elevations of over 2 km, and to the west passes abruptly to depths of > 3 km below sea level in the Tyrrhenian basin (Figure 1).

HORIZONTAL DISPLACEMENTS

Timing constraints for the arrival of the thrust belt above specific locations on the foreland plate are provided by the spatial distribution of Latest Miocene-Latest Pliocene foredeep deposits in wells that penetrate the allochthon. The location of the thrust front at any specific stage is shown in Figure 6 as the initial position, so that the coeval depositional sequence drilled by wells is just being deposited within the foredeep basin. A northeast sense of regional displacement is defined by the averaged orientation of tectonic fabrics, particularly by large-trace folds in synorogenic rocks (Figure 2).

A number of potential errors in the restoration process arise from ambiguities in position and age of rocks drilled beneath the allochthon, from the unaccounted displacement suffered by their bedrock, and from the unknown degree of internal coherency of the allochthon. Fortunately, faunal ages from synorogenic rocks below the allochthon are resolved to within a few 100 kyrs (Patacca et al., 1990; Patacca and Scandone, 2001), and tectonic removal of synorogenic parautochthonous rocks of the buried foreland is not significant (e.g., Balduzzi et al., 1982). Both the spatial distribution of shortening within the buried foreland (Casero et al., 1988; Menardi-Noguera and Rea, 2001; Mazzoli et al., 2000; Mazzotti et al., 2000) and internal imbrication within the allochthon are not adequately constrained to be included in displacement estimates, but probably do not contribute substantially to the displacement budget. The smooth amplitude of folds and the high-angle dip of reverse faults affecting the buried foreland (Figure 4; Mazzoli et al., 2000; Menardi-Noguera and Rea, 2000) call for shortening limited to within few tens of km. In addition, wells that penetrate the allochthon never encounter Pliocene-Quaternary rocks interleaved between pre-Pliocene imbricates (e.g., Balduzzi et al., 1982), arguing against substantial internal imbrication of the allochthon. Based on the above

arguments, exploration wells southwest of the buried thrust front are shown at their present-day position (Figure 6).

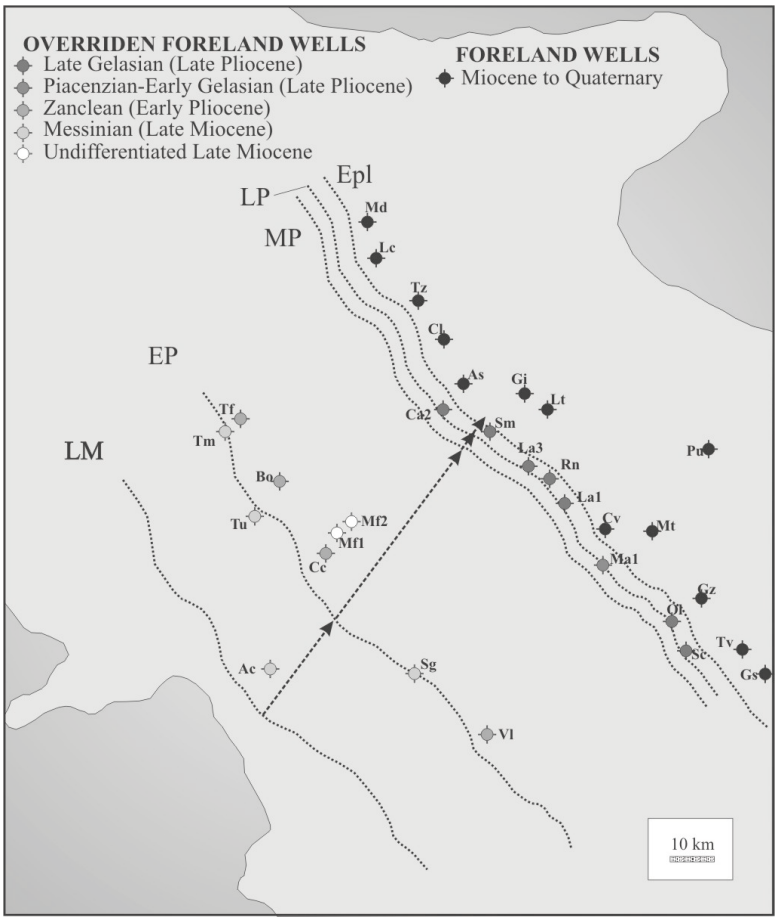

Figure 6. Position of the frontal thrust in the Southern Apennines during Latest Miocene (LM), Early Pliocene (EP), Middle Pliocene (MP), Early Pleistocene (EPl). Wells: Ac=Acerno; As=Ascoli Satriano; Bo=Bonito; Ca2=Candela 2; Cc=Ciccone; Cl=Calvello; Cv=Calvino; Gi=Giardinetto; Gs=Grassano; Gz=Genzano; La1=Lavello 1; La3=Lavello 3; Lc2=Lucera 2; Lt=La Torre; Ma=Maschito; Md=Montedoro; Mf1=M. Forcuso 1; Mf2=M. Forcuso 2; Ol=Oliveto Lucano; Pu=Puglia; Rn=Rendina; Sc=S. Chirico; Sg=San Gregorio Magno; Sm=Serra S. Mercurio; Tf= Tranfaglia; Tm=Trimonte; Tu=Taurasi; Tv=Tolve; Tz=Tavernazza; Vl=Vallauria.

The age of thrust belt displacement decreases regularly toward the foreland from Latest Miocene in the eastern part of the inner belt to Earliest Pliocene in the western frontal belt and to Early Pleistocene at the very front

(Figure 6). The thrust front moved nearly 80 km from Latest Miocene to Early Pleistocene, when motion of the allochthon vanished and the thrust front was buried by Middle Pleistocene ~0.8 Ma (Patacca and Scandone, 2001) foredeep deposits.

The latest Miocene to Early Pleistocene displacement rate history for the thrust front is shown by a series of stair-step boxes containing all possible displacement curves (Figure 7). The possibility that the front experienced large instantaneous jumps separated by intervals of no motion cannot be discounted. However, nearly continuous deposition in piggyback basins of the frontal thrust belt showing growth relations with evolving structures within the allochthon (Figure 2; Hippolyte et al., 1994a; Patacca and Scandone, 2001; Ferranti and Oldow, manuscript in prep.) better constrains the displacement trajectory of the thrust front (small boxes in Figure 7) and suggests a more steady-state displacement path. An average displacement of ~16 mm/yr (Figure 7) is determined from the thrust-front position for the latest Miocene (6.3 Ma) to Early Pleistocene (1.3 Ma).

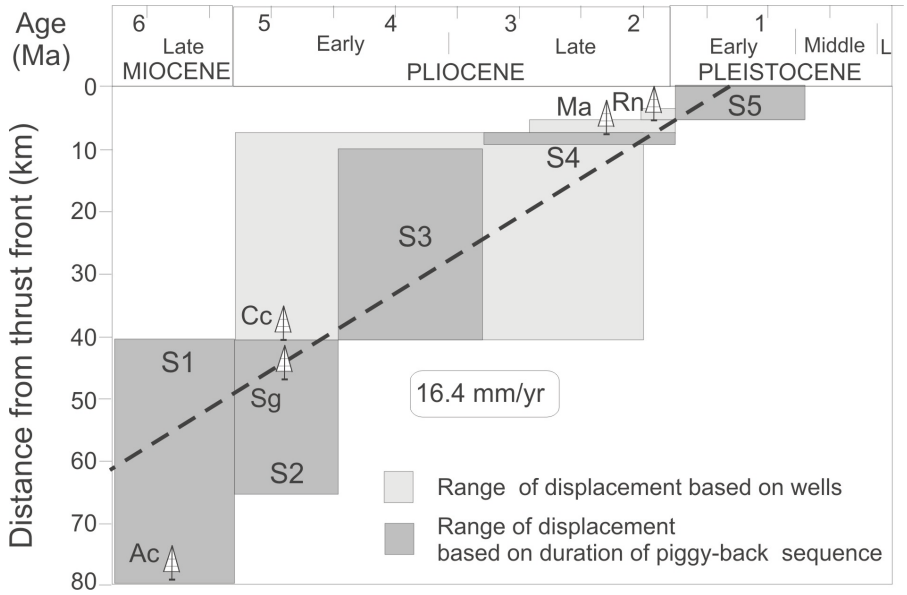

Figure 7. Latest Miocene to Quaternary horizontal displacement rate of thrust front in the Southern Apennines, wells labeled as in Figure 6, S1 to S5 are piggyback basin depositional sequences in the frontal thrust belt (Ofanto basin, location in Figure 2).

Contraction in southern Italy, however, did not cease with the Early Pleistocene demise of the thrust front. Rather, offshore seismic profiles (de Alteriis, 1995; Pieri et al., 1997) and onland mesostructural data from Middle Pleistocene to younger rocks (Hippolyte et al., 1994a; Pieri et al., 1997; Casciello et al., 2000) document distributed shortening across the frontal belt and foreland. The younger contractional structures formed locally at the surface and are probably related to deformation stepping to deeper levels. Seismicity documents that the northern part of the foreland is dominated by thrust and strike-slip earthquakes whose focal depths between 15-30 km indicate shortening of the deep crust (Figure 5). Similarly, GPS velocities show continued shortening at ~5 mm/yr between the foreland and frontal thrust belt (Figure 5; Oldow and Ferranti, this volume).

Estimates of the coeval extension front migration within the inner belt are less accurate. Pliocene subsidence in extensional basins of the Tyrrhenian continental margin (e.g., Sacchi et al., 1994), possibly related to motion on low-angle normal faults (Ferranti et al., 1996; Ferranti and Oldow, 1999), and activity of high-angle normal and transtensional faults broadly recorded by Early Pleistocene continental deposits (Hippolyte et al., 1994b) highlight the easterly propagation of the extensional front ahead of the migrating thrust belt. The Middle Pleistocene to modern position of the extensional front documented by the narrow belt of active extensional faults and seismicity (Figure 5) lies at the transition between inner and median zone.

The rate of propagation of the extensional front within the whole hinterland can be estimated by restoration of a regional crustal profile in the central Tyrrhenian Sea (Figure 8). Extension involving delamination to a 20 km thickness (Di Stefano et al., 1999) and subsequent stretching of an originally 30 km thick crust can sustain rates of between ~15-19 mm/yr since the ~9-13 My initiation of extension (Kastens et al., 1988; Patacca et al., 1990), which are consistent with a common migration rate for the contractional and extensional belts of deformation.

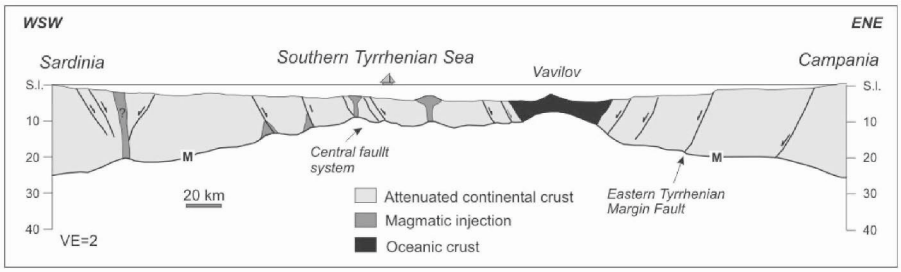

Figure 8. Crustal section across the Tyrrhenian Sea (location in Figure 1).

VERTICAL DISPLACEMENTS

Across southern Italy, vertical displacements are documented by the variable altitude of marine terraces and notches, basal unconformities and shallow-marine regression surfaces, and continental erosional surfaces (Figure 9). Building on the pioneering studies of Brancaccio et al. (1991), Amato and Cinque (1999), Ascione and Romano (1999) and Amato (2000), our regional compilation of latest Miocene through late Pleistocene paleohorizontal surfaces shows that marker altitudes increase as a function of age (Figure 10).

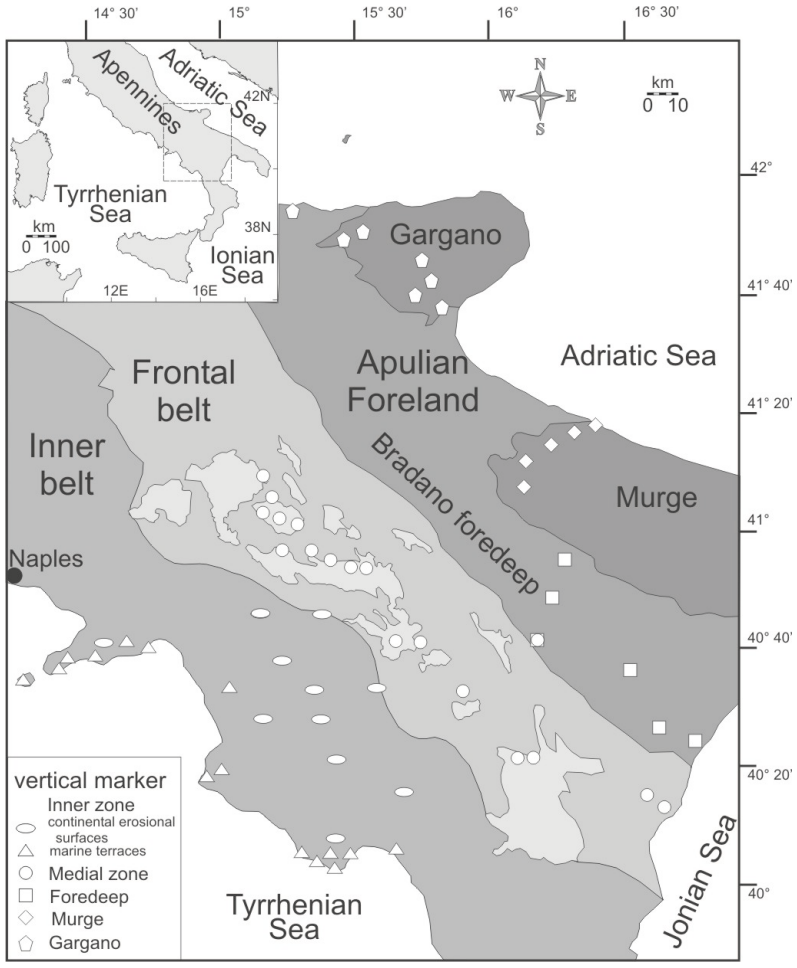

Figure 9. Spatial distribution of vertical markers in Southern Italy.

Variability in the altitude of individual surfaces also increases with age (e.g., Amato and Cinque, 1999) and is attributed to offset by extensional faults within the inner belt and by folds and thrust faults in the foreland and frontal thrust belt. For this analysis, we used the maximum elevation recorded for specific markers to estimate uplift rates, and, within the limits of uncertainty, the rates are linear over intervals of 10^6 years (Figure 10).

The rate uncertainty arises from imprecise age control, ambiguity in altitude measurement, lack of paleodepth or paleoelvation compensation, eustatic corrections to surface elevations, and crustal loading associated with eustatic change. Crustal loading during 120 m of eustatic sea level variation (Lambeck et al., 2004) and ambiguity in surface altitude measurement (Hare et al., 2001) are between 20-40 m and contribute little to rate uncertainty, considering the range of observed elevations being up to 1.7 km.

Concerning the continental erosional surfaces of the inner belt, rate estimation may be strongly affected by lack of compensation for their original elevation above sea level (a.s.l). For this analysis, we calculate separate regression lines through continental surfaces and younger marine terraces, respectively (Figure 10A). However, the lowest continental surface merges with the highest marine terrace and was probably close to sea level during formation (Amato and Cinque, 1999), and thus the two regression lines may be directly comparable. As regards the basal and top unconformities of Pliocene-Pleistocene marine sequences, in almost all the cases they bound shallow marine to coastal deposits, and errors deriving by lack of paleodepth compensation can be neglected.

The dominant contributor to the uncertainty budget is age ambiguity. Absolute ages exist only for a few markers (e.g., Amato, 2000). Biostratigraphic age control is good for the upper and lower surfaces of stratigraphic sequences (Hippolyte et al., 1994a; Patacca and Scandone, 2001) but dated geomorphic surfaces are rare and ages typically are relative. With few exceptions, the chronology of Pleistocene marine terraces is constructed relative to the radiometrically dated 130 ka marker (e.g., Ascione and Romano, 1999), and relative ages for latest Miocene to Pliocene marine and continental surfaces are controlled by dated sedimentary deposits and/or geomorphic features (Amato and Cinque, 1999).

The age ambiguity directly impacts rate determination but also contributes to altitude uncertainty through sea-level corrections, which are drawn from radiometrically controlled eustatic (Chappel et al., 1996) and less precise sequence stratigraphic curves (Haq et al., 1987) for markers younger and older than the Middle Pleistocene, respectively. Imprecise age control adds up to 100 m of elevation uncertainty (Figure 10).

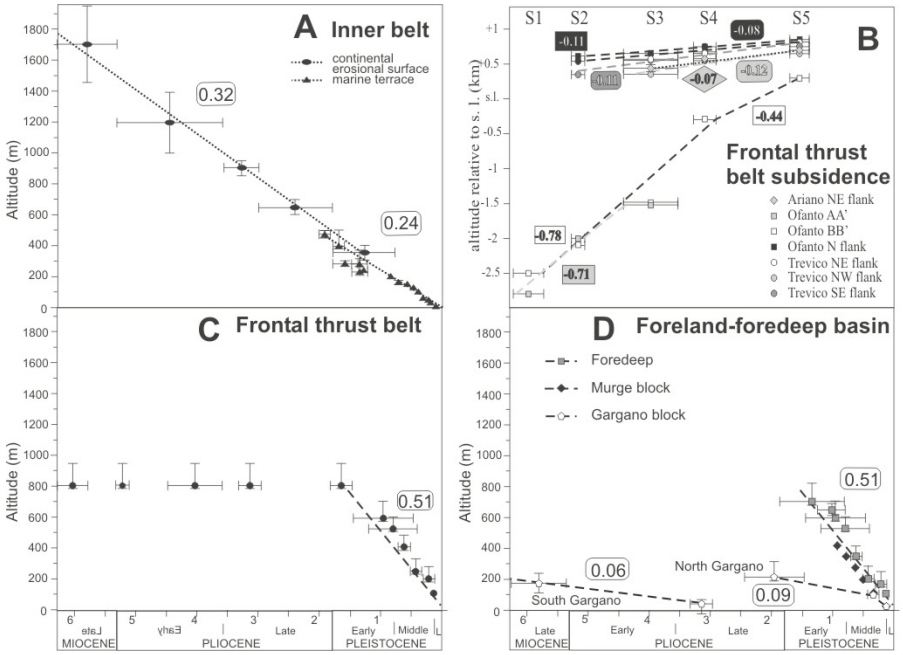

Figure 10. Latest Miocene to Quaternary vertical displacement rates (in mm/yr) in southern Italy. Piggyback basins of the frontal thrust belt located in Figure 2. Ofanto AA' and BB' refers to seismic sections from Hippolyte et al. (1994b).

The altitudes of Pleistocene marine terraces and deposits of the inner belt (Brancaccio et al., 1991; Ascione and Romano, 1999) systematically increase with age at a rate of 0.24 mm/yr (Figure 10A). Latest Miocene to Pliocene markers are relics of four orders of continental surfaces (Amato and Cinque, 1999), which are linearly distributed with age and define an uplift rate of 0.32 mm/yr (Figure 10A). Along the Tyrrhenian coastal region of the inner belt, uplift ceased in the Late Pleistocene and 130 ka marine terraces lie close to expected eustatic elevations (Brancaccio et al., 1991).

No significant uplift occurred in the frontal belt from the latest Miocene to Early Pleistocene. In this region, paleo-sea level is estimated from the basal unconformities of sedimentary sequences deposited in piggyback basins. Substantial difference in local subsidence rate related to structure growth affect these sequences according to position in the basin (Figure 10B) but shallow-marine conditions persisted as the basins subsided. Little average elevation existed in the frontal belt until the Earliest Pleistocene, and the maximum altitude of ~800 m for paleohorizontal markers reflects younger uplift at a rate of ~0.5 mm/y (Figure 10C).

The Pleistocene record of foreland uplift (Figure 10D) is similar to that of the frontal thrust belt, with a rate of ~0.5 mm/yr since the late Early Pleistocene (~1.3 Ma). In the foredeep basin, successively younger marine regression surfaces of the Lower to Middle Pleistocene fill of the foredeep basin decrease in elevation from 700 to 500 m. Toward the Ionian coast, the regression surfaces are incised by a flight of Middle to Upper Pleistocene marine terraces stepped in ten orders between 20 and 450 m a.s.l. (Amato, 2000). The elevation of the 130 ka and younger markers indicate that Late Pleistocene to recent uplift increased to ~1 mm/yr within the frontal thrust belt and western foredeep basin (ibid).

A different altitude distribution of vertical markers is recorded in the Gargano and Murge blocks of the Apulia foreland, respectively (Figure 9, 10D). Within the Murge to the south, 16 marine terraces locally associated to deposits are found between the coastline and 450 m a.s.l. close to the summit of the tectonic block, and are assigned to the uppermost Early Pleistocene-Holocene (Ciaranfi et al., 1996). Conversely, in the Gargano area to the north, only few marine terraces and associated deposits are found. Along the southern side of Gargano, Middle-Upper Pliocene and Uppermost Miocene (possibly Lower Pliocene) terraces and deposits occur at 50 to 220 m a.s.l. respectively (Bertotti et al., 1999). A morphologically higher marine terrace (550-600 m a.s.l.) and relics of erosional surfaces forming the summit envelope of the Gargano anticlinorium (800-880 m a.s.l.) represent older sea-level markers but their age is unknown. Much of the uplift in Gargano occurred between Middle-Late Miocene and Early Pliocene at ~0.06 mm/yr, and may be related to thrusting and ~ 30 % shortening (Bertotti et al., 1999). In contrast, uplift of Murge is younger and occurred steadily at ~0.5 mm/yr from 1.3 Ma to 130 ka. In spite of a long-term difference in the uplift history, between Gargano and Murge, the consistent 25-30 m a.s.l. elevation of the 130 ka marker (Bordoni and Valensise, 1998) suggests a coherent behavior of the two blocks during the Late Pleistocene, when uplift rate decreased to ~0.20 mm/yr.

DISCUSSION

The pattern of vertical and horizontal displacement in the Southern Apennines is complex and reflects different tectonic processes during the Late Neogene tectonic history of the orogen (Figure 11).

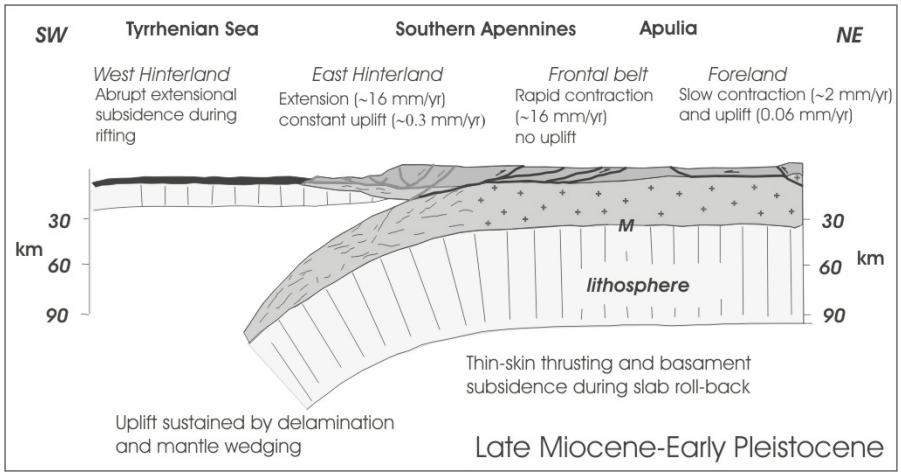

Figure 11A. Latest Miocene-Early Pleistocene tectonic setting and displacement rates.

From Latest Miocene to Early Pleistocene (Figure 11A), eastward transport of the thrust front at ~16 mm/yr occurred with the frontal thrust belt lying at or below sea level, and only a volumetrically insignificant portion of synorogenic sediments were stripped from the underlying foreland and incorporated into the advancing allochthon. Subsurface records suggest only a few kilometers of shortening within the buried foreland (Menardi-Noguera and Rea, 2000; Mazzoli et al., 2001), and deformation in the Southern Apennines was dominated by thin-skinned contraction. Maintenance of sea level conditions and transport of the allochthon with limited involvement of underlying rocks suggest significant basement subsidence and supports the slab roll-back hypothesis (e.g., Royden et al., 1987).

During Miocene and Pliocene advancement of the thrust belt, the foreland experienced minor contraction, which from Bertotti et al (1999) data can be estimated at between 1.5-2.1 mm/yr, and uplift at 0.06 mm/yr (Figure 10D). Foreland deformation probably reflect lithospheric scale-folding and involvement of the deep Adriatic crust in south-directed thrusting (Bertotti et al., 2001).

Through time, the extensional hinterland migrated easterly and kept pace with thrust front migration (Figure 11A). Larger magnitude stretching concentrated in the western portion of the hinterland where the Tyrrhenian basin was formed (Figure 1, 8). The passage from contractional to extensional belts, however, records uplift of the eastern margin of the hinterland at ~0.3 mm/yr over the last 6 Ma before ultimate subsidence into the Tyrrhenian basin (Figure 11A).

We infer that uplift of the eastern part of the hinterland is related to crustal delamination and mantle upwelling, that apparently contributed to the onset of regional extension (Channell and Mareschal, 1989; Doglioni, 1991). Mantle upwelling beneath the delaminated upper crust provides a dynamic (D'Agotino and McKenzie, 1999) or isostatic (Westaway, 1993) support to crustal uplift, and possibly control the extrusion of shoshonitic to K-alkali magmas (Figure 2; cf. Serri et al., 1993). Today, the eastern tip of crustal delamination coincides with the locus of active extension along the axis of the Apenninic chain, with a region of low crustal velocity (Figure 5; Di Stefano et al, 1999), and with the encroachment of the younger Tyrrhenian Moho above the flexed Adriatic Moho (Figure 1, 2).

The transition from uplift to tectonic subsidence beneath the Tyrrhenian Sea in the western hinterland occurs along the present-day shoreline where marine terraces dated to 130 ka and younger are found at predicted eustatic altitudes. The transition, however, is abrupt as reflected in the westerly topographic asymmetry of the Southern Apennines (Figure 4). Across this boundary, Mesozoic-Tertiary rocks record over 1.5 km of differential elevation between exposures in the Apennine chain and their position below the continental shelf to the southwest. The coastal region apparently lies at a state of near equilibrium between uplift and extensional subsidence. Notably, where subsidence is greatest, extensional earthquakes are rare, but GPS velocities directed away from the Apennine foreland and toward the Tyrrhenian basin are high (Figure 5).

During the Early Pleistocene a different pattern of displacement rates established in the region (Figure 11B). The frontal thrust belt and foreland record initiation of rapid regional uplift at ~0.5 mm/yr which coincides with cessation of horizontal displacement on the thin-skinned thrust front and onset of distributed shortening in the region. Broad uplift lies far to the northeast of the locus of delamination-induced uplift, and rather reflects thick-skin thrusting or growing lithospheric folds in the Adriatic block (Figure 2; Bertotti et al., 2001). The recent (<130 ka) decrease in Murge and Gargano uplift together with the increased uplift in the frontal belt and foredeep is consistent with differential growth in fold amplitude (Bertotti et al., 2001) or thrust fault propagation.

Post-Early Pleistocene shortening involving the whole eastern part of southern Italy is consistent with the present deformation pattern documented by contractional and traspressional earthquakes and GPS velocities (Figure 5; Oldow and Ferranti, this volume). The focal depths of thrust and strike-slip earthquakes near Gargano range between 15 and 30 km (Figure 5) and constrain the thrust detachments to root within the crystalline crust of the Adria interior. From the Middle Pleistocene onward, horizontal displacement rate estimates are poor, but present-day rates from GPS velocities (ibid) show

continued shortening between the foreland and frontal thrust belt and extension in the inner belt at ~5 mm/yr (Figure 11B).

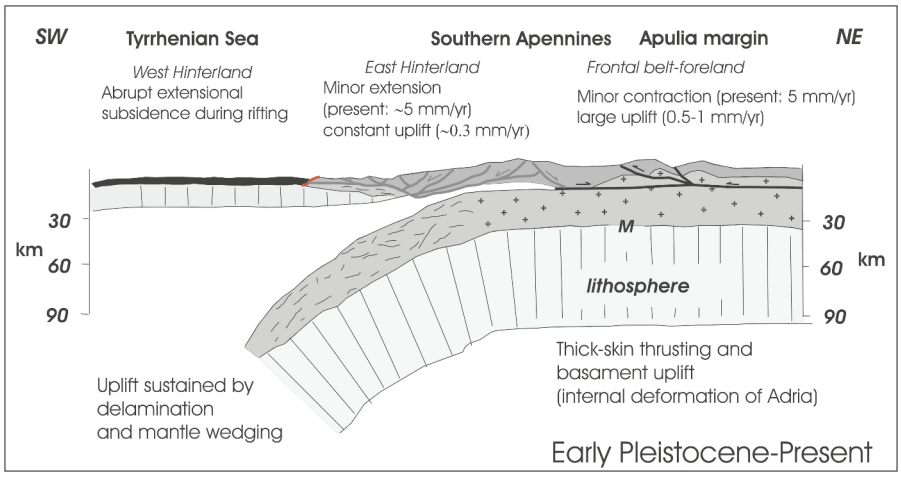

Figure 11B. Early Pleistocene-Present tectonic setting and displacement rates.

Differences in the pattern and rates between the Late Miocene-Early Pleistocene (Figure 11A) and the Early Pleistocene to the present (Figure 11B) displacement histories of the frontal thrust belt and foreland reflect transition from thin- to thick-skinned shortening, which stems from the crustal architecture inherited from Mesozoic rifting. During a large part of the Mesozoic, severe crustal thinning occurred on the western Adriatic margin and the deep marine Lagonegro basin (Figure 3) intervened between the Apulia and the Western platforms (Channell et al., 1979; D'Argenio and Alvarez, 1980). During Neogene contraction, the thin crust flooring the Lagonegro basin accommodated basement subsidence and rapid horizontal migration of thin thrust sheets over the foreland. We suspect that a similar situation occurred during the earlier contractional history of the inner belt, where the continental crust beneath the Western platform outboard the Tethyan ocean might have accommodated thin-skinned thrusting and basement subsidence, as suggested by the occurrence of deep Miocene piggyback basins (e.g., Patacca et al., 1990).

In a similar way, the mid-Pleistocene uplift of the frontal thrust belt and foreland during thick-skinned shortening at a reduced rate resulted from impingement of the thrust belt onto the thick Apulia lithosphere (Malinverno and Ryan, 1986; Doglioni et al., 1994).

The broad topographic expression of the Southern Apennines and Tyrrhenian Sea (Figure 4, 8) together with regional gravity suggest that

formation of the Apenninic mountain chain was controlled by uplift during the initial stages of extension associated with crustal delamination and mantle derived dynamic uplift of the region (D'Agostino and McKenzie, 1999). Only after sustained extensional faulting does subsidence dominate and the hinterland pass into the Tyrrhenian basin. Conversely, topography of the foreland and frontal thrust belt results from deep-seated contraction, whose onset in the foredeep basin and Murge block dates back to the late Early Pleistocene, but in Gargano might be significantly older (Bertotti et al., 1999).

CONCLUSIONS

In southern Italy, the consistent eastward migration of the contractional and extensional fronts during the last ~6 Ma supports progressive delamination of the Adriatic upper crust during roll-back of the underlying lower crust and lithospheric mantle. Mantle upwelling beneath the delaminated eastern hinterland might sustain long-term uplift before dramatic tectonic subsidence in the Tyrrhenian basin to the west. Conversely, thick-skin thrusting and folding rooted in the lower crust well in the interior of the Adriatic plate drives younger, rapid uplift of the frontal thrust belt and foreland.

The integrated geologic and geodetic record of deformation illustrates the progressive disintegration of the upper crustal layer of Adria and do not provide independent information on the kinematics of the Adria plate. The Pleistocene variation in rates and in the pattern of vertical motion can not be directly related to changes in the rate of propagation of the delamination front but rather reflect the control exercised by the inherited crustal architecture of the Adria margin.

ACKNOWLEDGEMENTS

This study benefited from discussions with W. McClelland. We thank S. Stein and D. Delikaraoglou for insightful reviews.

REFERENCES

Amato A. Estimating Pleistocene tectonic uplift rates in the South-Eastern Apennines (Italy) from erosional landsurfaces and marine terraces. In *Geomorphology, human activity and global environmental change*, O. Slaymaker, eds., London: John Wiley & Sons, 2000; 67-68.

Amato A., Cinque A. Erosional landsurfaces of the Campano-Lucano Apennines (S. Italy): Genesis, evolution, and tectonic implications. Tectonophysics 1999; 315: 251-267.

Anderson H.A., Jackson J.A. Active tectonics of the Adriatic region. Geophys. J. R. A. S. 1987; 91: 937-983.

Ascione A., Romano P. Vertical movements on the eastern margin of the Tyrrhenian extensional basin. New data from Mt. Bulgheria (Southern Apennines, Italy). Tectonophysics 1999; 315: 337-356.

Balduzzi A., Casnedi R., Crescenti U., Tonna M. Il Plio-Pleistocene del sottosuolo del bacino pugliese (avanfossa appenninica). Geologica Romana 1982; 21: 1-28.

Beccaluva L., Brotzu P., Macciotta G., Morbidelli L., Serri G., Traversa G. Cainozoic tectono-magmatic evolution and inferred mantle sources in the Sardo-Tyrrhenian area. In *The Lithosphere in Italy. Advances in Earth Science Research*, A. Boriani, M. Bonafede, G.B. Piccardo, G.B. Vai, eds., Roma: Atti Conv. Lincei 1989; 80: 229-248.

Bertotti G., Casolari E., Picotti V. The Gargano promontory: a Neogene contractional belt within the Adriatic plate. Terra Nova 1999; 11: 168-173.

Bertotti G., Picotti V., Chilovi C., Fantoni R., Merlini S., Mosconi A. Neogene to Quaternary sedimentary basins in the south Adriatic (Central Mediterranean): Foredeeps and lithospheric buckling. Tectonics 2001; 20: 771-787.

Bordoni P., Valensise G. Deformation of the 125 ka marine terraces in Italy: tectonic implications. In *Coastal Tectonics*, I. Stewart, C. Vita-Finzi, eds., London: Geol. Soc. London Spec. Publ. 1998; 146: 71-110.

Brancaccio L., Cinque A., Romano P., Rosskopf C., Russo F., Santangelo N., Santo A. Geomorphology and neotectonic evolution of a sector of the Tyrrhenian flank of the Southern Apennines (Region of Naples, Italy). Zeitschr fűr Geomorphologie, supplement band, 1991; 82: 47-58.

Casciello E., Cesarano M., Ferranti L., Oldow J. S., Pappone G. Pleistocene non-coaxial fold development in the northern portion of the S. Arcangelo Basin (Southern Apennines). Memorie Società Geologica Italiana 2000; 55: 133-140.

Casero P., Roure R., Endignoux L., Moretti I., Muller C., Sage L., Vially R. Neogene geodynamic evolution of Southern Apennines. Memorie Società Geologica Italiana 1988; 41: 109-120.

Cassinis R., Scarascia S., Lozej A. The deep crustal structure of Italy and surrounding areas from seismic refraction data. A new synthesis. Bollettino Società Geologica Italiana 2003; 122: 365-376.

Cello G., Mazzoli S. Apennine tectonics in southern Italy: a review. J. Geodynamics 1999; 27: 191-211.

Channell J.E.T., Mareschal J.C. Delamination and asymmetric lithospheric thickening in the development of the Tyrrhenian Rift. In *Alpine Tectonics*, M. P. Coward, D. Dietrich, R. G. Park, eds., London: Geol. Soc. London Spec. Publ. 1989; 45: 285-302.

Channell J.E.T., D'Argenio B., Horvath F. Adria, the African Promontory, in Mesozoic Mediterranean paleogeography. Earth Science Reviews 1979; 15: 213-292.

Chappel J., Omura A., Esat T., McCulloch M., Pandolfi J., Ota Y., Pillans B. Reconciliation of late Quaternary sea levels derived from coral terraces at Huon Peninsula with deep sea oxygen isotope records. Earth Plan. Scie. Lett. 1996; 141: 227-236.

Ciaranfi N., Pieri P., Ricchetti G. Note alla carta geologica delle Murge. Memorie Società Geologica Italiana 1996; 41: 449-460.

Cimini G.B. P-wave deep velocity structure of the SouthernTyrrhenian subduction zone from non-linear telesesmic traveltime tomography. Geophys. Res. Lett. 1999; 26: 3709-3712.

D'Agostino N., McKenzie D. Convective suppotrt of long-wavelength topography in the Apenniners (Italy). Terra Nova 1999; 11: 234-238.

D'Argenio B., Alvarez W. Stratigraphic evidence for crustal thickness changes on the southern Tethyan margin durino the Alpine cycle. Geol. Soc. Am. Bull. 1980; 91: 681-689.

deAlteriis G. Different foreland basins in Italy: examples from the central and western Adriatic sea. Tectonophysics 1995; 252: 349-373.

Dercourt J., Zonenshain L.P., Ricou L.E., Kazmin V.G., Le Pichon X., Knipper A.L., Grandjacquet C., Sbortshikov I.M., Geyssant J., Lepvrier C., Pechersky D.H., Boulin J., Sibuet J.C., Savostin L.A., Sorokhtin O. Westphal, M., Bazhenov, M.L., Lauer, J.P., Biju-Duval, B., Geological evolution of the Tethys Belt from the Atlantic to the Pamirs since the Liassic. Tectonophysics 1986; 123: 241-315.

Dewey J.F., Helman M.L., Turco E., Hutton D.H.W., Knott S. Kinematics of the Western Mediterranean. In *Alpine Tectonics*, M. P. Coward, D. Dietrich, R. G. Park, eds., London: Geol. Soc. London Spec. Publ. 1989; 45: 265–283.

Di Stefano R., Chiarabba C., Lucente F., Amato A. Crustal and uppermost mantle structure in Italy from the inversion of P-wave arrival times Geodynamic implications. Geophys. J. Int. 1999; 139: 483-498.

Doglioni C., Mongelli F., Pieri P. The Puglia uplift (SE Italy): An anomaly in the foreland of the Apenninic subduction due to buckling of a thick continental lithosphere. Tectonics 1994; 13: 1309-1321.

Doglioni C. A proposal of kinematic modelling for W-dipping subductions. Possible applications to the Tyrrhenian-Apennines system. Terra Nova 1991; 3: 423-434.

Faccenna C., Becker T.W., Lucente F.P., Jolivet L., Rossetti F. History of subduction and back-arc extension in the Central Mediterranean. Geophys. J. Int. 2001; 145: 809-820.

Ferranti L., Oldow J.S., Sacchi M. Pre-Quaternary extension in the Southern Apennine belt, Italy: Arcuation and orogen-parallel collapse. Tectonophysics 1996; 260: 325-347.

Ferranti L., Oldow J.S. History and tectonic implications of low-angle detachment faults and orogen-parallel extension, Picentini Mountains, Southern Apennines fold and thrust belt, Italy. Tectonics 1999; 18: 498-526.

Gasparini G., Iannaccone G., Scarpa R., Fault plane solutions and seismicity of the Italian peninsula. Tectonophysics 1985; 117: 59-78.

Gueguen E., Doglioni C., Fernandez M. On the post-25 Mageodynamic evolution of the western Mediterranean. Tectonophysics 1998; 298: 259–269.

Haq B.U., Hardenbol J., Vail P.R. Chronology of fluctuating sea level since the Triassic. Science 1987; 235: 1156-1167.

Hare J., Ferguson J.F., Aiken C.L.V., Oldow J.S. Quantitative characterization of paleo lake terrace features using high-resolution DEMs: Shoreline terraces of Pleistocene Lake Lahontan, Nevada. J. Geophys. Res. 2001; 106: 26,761-26,774.

Hippolyte J.C., Angelier J., Roure F., Casero P. Piggyback basin development and thrust belt evolution: Structural and palaeostress analyses of Plio-Quaternary basins in the Southern Apennines. J. Struct. Geol. 1994; 16: 159-173.

Hippolyte J.C., Angelier J., Roure F (b). A major geodynamic change revealed by Quaternary stress patterns in the Southern Apennines (Italy). Tectonophysics 1994; 230:199-210.

Kastens K., Mascle J. ODP 107 Scientific Staff, ODP leg 107 in the Tyrrhenian Sea: Insights into passive margin and back-arc basin evolution. Geol. Soc. Am. Bull. 1988; 100: 1140-1156.

Lambeck K., Antonioli F., Purcell A., Silenzi S. Sea-level change along the Italian coast for the past 10.000 yr. Quaternary Science Review 2004; 23: 1567-1598.

Laubscher H.P. Plate boundaries and microplates in Alpine history. Ame. J. Sci. 1975; 275: 865-876.

Malinverno A., Ryan W.B.F. Extension in the Tyrrhenian Sea and shortening in the Apennines as a result of arc migration driven by sinking of the lithosphere. Tectonics 1986; 5: 227-245.

Mazzoli S., Corrado S., De Donatis M., Scrocca D., Butler R. W. H., Di Bucci D., Naso G., Nicolai C., Zucconi V. Time and space variability of “thin-skinned” and “thick-skinned” thrust tectonics in the Apennines (Italy). Rendiconti Accademia Nazionale dei Lincei, 2000; 9: 5-39.

Mazzotti A., Stucchi E., Fradelizio G.L., Zanzi L., Scandone P. Seismic exploration in complex terrains: a processing experience in the Southern Apennines. Geophysics 2000; 65: 1402-1417.

Menardi-Noguera A., Rea G. Deep structure of the Campanian-Lucanian Arc (Southern Apennine, Italy). Tectonophysics 2000; 324: 239-265.

Oldow J.S., Ferranti L., Lewis D.S., Campbell J.K., D'Argenio B., Catalano R., Pappone G., Carmignani L., Conti P., Aiken C.L.V. Active fragmentation of Adria, the north African promontory, central Mediterranean orogen. Geology 2002; 30: 779-782.

Oldow J.S., Bally A., Avè Lallemant H. Transpression, orogenic float and lithospheric balance. Geology 1990; 18: 991-994.

Patacca E., Sartori R., Scandone P. Tyrrhenian Basin and Apenninic arcs: kinematic relations since late Tortonian times. Memorie della Società Geologica Italiana 1990; 45: 425-451.

Patacca E., Scandone P. Late thrust propagation and sedimentary response in the thrust belt-foredeep system of the Southern Apennines (Pliocene-Pleistocene). In *Anatomy of a mountain belt: the Apennines and adjacent Mediterranean basins*, G.B. Vai, I.P. Martini, eds., Dordecht: Kluwer Academic Publishers 2001; 401-440.

Pieri P., Vitale G., Benedice P., Dogliosi C., Gallicchio S., Giano S. I., Loizzo R., Moretti M., Prosser G., Sabato L., Schiattarella M., Tramutoli M., Tropeano M. Tettonica quaternaria nell'area Bradanico-Ionica. Il Quaternario 1997; 10: 535-542.

Ricchetti G., Monelli F. Flessione e campo gravimetrico della micropiastra apula. Bollettino Società Geologica Italiana 1980; 99: 431-436.

Royden L., Patacca E, Scandone P. Segmentation and configuration of subducted lithosphere in Italy: An important control on thrust-belt and foredeep-basin evolution. Geology 1987; 15: 714-717.

Sacchi M., Infuso S., Marsella E., Late Pliocene-Early Pleistocene compressional tectonics in the offshore of Campania. Bollettino Geofisica Teorica e Applicata 1994; 36: 141-144.

Scarascia S., Lozej A., Cassinis R. Crustal structures of the Ligurain, Tyrrhenian, and Ionian seas and adjacent onshore areas interpreted from wide-angle seismic profiles. Bollettino Geofisica Teorica Applicata 1994; 36: 5-19.

Selvaggi G., Chiarabba C. Seismicity and P-wave velocity image of the southern Tyrrhenian subduction zone. Geophys. J. Int. 1995; 121: 818-826.

Serri G., Innocenti F., Manetti P. Geochemical andpetrological evidence of the subduction of deliminated Adriaticcontinental lithosphere in the genesis of the Neogene-Quaternary magmatism of central Italy. Tectonophysics 1993; 223: 117–147.

Speranza F., Chiappini M. Thick-skinned tectonics in the external Apennies, Italy: New evdence from magnetic anomaly analysis. J. Geophys. Res. 2002; 107, doi:10.1029/2000JB000027.

Westaway R. Quaternary uplift of southern Italy. J. Geophys. Res. 1993; 87: 21,741-21,772.

THE ALBANIAN OROGEN: CONVERGENCE ZONE BETWEEN EURASIA AND THE ADRIA MICROPLATE

Shyqyri Aliaj
Seismological Institute, Academy of Sciences of Albania
aliaj@sizmo.edu.al

ABSTRACT

In Albania and Greece, along the southern convergent margin of the Eurasia Plate, we distinguish a northern segment of the margin, belonging to the Adriatic continental collision, and a southern one, belonging to the Aegean (Hellenic) Arc related to active oceanic subduction. The boundary between the Aegean Arc and the Adriatic collision is the Cephalonia Transform Fault. The Albanian orogen and surroundings are divided into two active tectonic domains: an external compressional domain, constituting the Adriatic collision zone, and an internal extensional domain. In Albania, Adria collides with Eurasia along a series of thrusts. The Albanian orogenic front is thrusting over the Adria microplate, partly over Apulian platform and partly over Albanian Basin (southern Adriatic basin). The Albanian orogenic thrust front is cut and displaced by the Othoni Island-Dhermi, the north Sazani Island, and the Gjiri i Drinit-Lezha strike-slip faults, which divide the orogen into separate segments with diachronous development: The NW-trending Lefkas-Corfu offshore segment, where the Ionian zone consists of the orogenic front; The NW-trending Karaburuni-Sazani Island offshore segment, where the Sazani Zone comprises the orogenic front; The ~N-trending Frakulla-Durresi mainly onshore segment, where Ionian zone makes up this orogenic front, and The W-NW-trending Lezha-Ulqini segment, where the orogenic front is composed of Kruja Zone. The Adriatic collision zone is the most seismically active region in Albania and makes up the Ionian-Adriatic coastal earthquake belt at the eastern margin of the Adria microplate.

Keywords*:* Adriatic collision, Adria microplate, Albania, neotectonics, thrust front

INTRODUCTION

From the geological standpoint, Albania belongs to the Dinarides (*sensu latu)*, which forms the southern branch of the Alpine fold-thrust belt. The Dinarides extend south from the Southern Alps, along the east coast of the Adriatic and Ionian Seas, and through the Aegean Sea to meet the Taurides and form the Dinaro-Tauric Arc. The Dinarides are separated by the Shkodra-Peja transverse fault zone (Figure 3) into two segments: the Dinarides (*sensu strictu)* and the Hellenides. The Dinaride-Hellenide

N. Pinter et al. (eds.), The Adria Microplate: GPS Geodesy, Tectonics and Hazards, 133–149.

transition occurs in Albania. The Aegean (Hellenic) Arc makes up the southern part of the Hellenides and, unlike the Albanian-eastern Adriatic collision zone in the northern Hellenides and southern Dinarides, has geological and geophysical features which resemble those of island arcs (Mercier et al., 1987). The Aegean Arc is situated between the Arabia-Africa/Eurasia collision to the east and the Adriatic collision to the west. The change from Aegean oceanic subduction to Adriatic continental subduction and collision is accomodated by a right-lateral transform fault along the western edge of the Cephalonia-Lefkas Islands (Monopolis and Bruneton, 1982).

The Mediterranean orogenic belt resulted from the movement of the African and Eurasian plates as well as a number of small independent micoplates. The tectonic evolution of the Central Mediterranean was profoundly influenced by Adria, a microplate or block of continental lithosphere underlying eastern Italy and the Po plain and the Adriatic Sea, west of the Dinarides that behaved as a tectonic indenter during convergence between Africa and Europe (Channel and Horvath, 1976).

The unusual loop shape of the Apennine, Alpine, Dinaric and Hellenic chain, which surrounds the undeformed Po plain, the Adriatic Sea and the Apulian platform, attracted the attention of a number of early systematic geological studies. This undeformed region, acted as a rigid element, extending 1300 km in length and 100 to 200 km in width. Mechanically, it contrasts sharply with the surrounding, strongly compressed and plastically deformed zones. Argand (1924) regarded Adria as a promontory of the African continent, and as a small continental plate with consuming margins besides those of the southeast. The Dinarides and Hellenides, in which the geological structure of Albania is developed, are located along the eastern margin of the Adria microplate (Giese and Reutter, 1978). Tectonic transport in the Dinarides and Hellenides is towards the Adria microplate and thus they are front-to-front with and convergence towards the Apennines. Folds, thrusts and nappes are the typical structures recording contraction in the orogenic (fold) belts encircling the Adria microplate. The loop shape of the circum-Adriatic orogens may be due to the irregularly shape of the Adria promontory that interacted with the European (pre-Alpine) Plate. There is as yet no clear delineation between the Adriatic microplate and the Nubian Plate.

The tectonic boundaries along the edges of Adria are seismically active and the present-day dimensions of the Adria foreland are delineated by crustal earthquakes (Anderson and Jackon, 1987; Oldow et al., 2002; Wortmann et al., 2001).

ADRIATIC-EURASIAN COLLISION

The Adriatic-Eurasian collision is taken up along the western coast of former Yugoslavia, Albania and central Greece. Along the Albania-Greece southern convergent margin of the Eurasia Plate, following others, we distinguish a northern segment belonging to the Adriatic-Eurasia continental collision, and a southern segment belonging to the Aegean Arc and its oceanic subduction zone. Results inferred from GPS measurements show that in NW Greece (north of the Gulf of Amvrakia), sites are more-or-less stationary, whereas the Aegean Arc in Ionian Islands and Peloponnesus undergo pronounced SW-oriented movements at an average rate of 2-3 cm/yr with reference to the station of Matera, Italy (Kahle et al., 1995). The edge of this domain is marked by the presence of an active right-lateral transform fault zone, termed the Cephalonia fault zone

The orogen in Albania and its surroundings are divided into two domains with different present-day tectonics: an external compressional domain, constituting the Adriatic collision zone, and the internal extensional domain. The external tectonic zones (Sazani, Ionian and Kruja zones), which make up the orogenic fronts in the Adriatic collision zone, constitute deformed sedimentary cover thrust towards the southwest (Aliaj, 1997). The rapidly subsiding Peri-Adriatic foredeep developed in front of these advancing external thrust sheets. The Adriatic collision zone is the most seismically active zone in Albania, which is represented by the Ionian-Adriatic coastal earthquake belt along the eastern margin of the Adria microplate (Sulstarova et al., 1980; Aliaj, 1998, 2003). Numerous focal-mechanism solutions of shallow earthquakes show that horizontal compression (thrust faulting) dominates along the Adriatic collision as well as along the SW-convex edge of the Hellenic Arc, while extension dominates behind them (Sulstarova, 1986; Muço, 1994; Papazachos and Papazachos, 1989; Figure 6).

NEOTECTONICS OF ALBANIA

Albania is one of the most seismically active countries in Europe. Most strong earthquakes occur in 3 well-defined seismic belts (Figure 1):

a) The Ionian-Adriatic coastal earthquake belt at the eastern margin of Adria, which trends northwest-southeast;

b) The Peshkopi-Korça earthquake belt, which trends north-south, and

c) The Elbasani-Dibra earthquake belt, which trends north-easterly (Sulstarova et al., 1980; Aliaj, 1988, 2000, 2003).

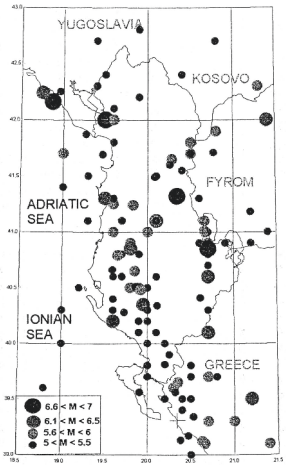

Figure 1. The epicenters of earthquakes in Albania with M=>5.0 for the 20th century (from Muço et al., 2002).

The neotectonic geomorphology of the interior of the country has a horst-graben arrangement due to Pliocene-Quaternary normal faulting, whereas in the external domain the topography is mountainous, except for the Peri-Adriatic Depression. The present-day tectonic stress field has been well studied via microtectonics (Aliaj, 1988) and earthquake focal-mechanism solutions (Sulstarova, 1986; Muço, 1994). In the external domain, the average axis of compression is oriented NE-SW (average azimuth 225^0), whereas in the internal domain the average axis of extension is NNW-SSE (average azimuth 340^0; Aliaj, 1988; Sulstarova, 1986).

Four large neotectonic units have been recognized in Albania based on the sense, intensity and chronology of vertical movements (Aliaj, 1998; Figure 2):

1. Internal Alpine unit affected by post-Pliocene extensional tectonics
2. External Alpine unit strongly affected by pre-Pliocene compression
3. Peri-Adriatic foredeep strongly affected by post-Pliocene compression
4. Foreland in Adriatic and Ionian offshore
5. The internal unit comprises terrains east of Kruja zone, while the external unit includes terrains of Kruja, Ionian and Sazani zones (Figure 3).

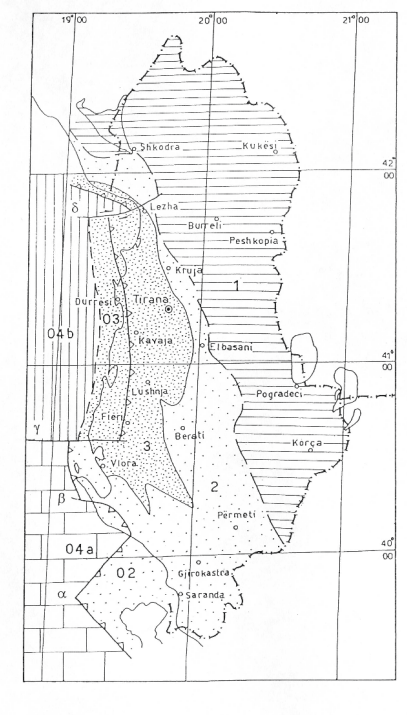

Figure 2. Map of neotectonic (Pliocene-Quaternary) zonation of Albania (from Aliaj, 2000). The four large neotectonic units are noted by numbers on the map: 1. Internal unit, 2. External unit (02 = its offshore sectors), 3. Peri-Adriatic Foredeep (03= its offshore sector), 04. Foreland in offshore (04a=Apulian platform, 04b=Albanian Basin). The Albanian orogenic front is cut and displaced by, from south to north, the Othoni Island-Dhermi (α), the Gjiri i Ariut-Dukat (β), the north Sazani Island (γ), and the Gjiri i Drinit-Lezha (δ) strike-slip faults.

Internal Alpine unit

The internal Alpine unit comprises terrains east of the Kruja zone (Figure 3). This unit was affected by strong extension during the Pliocene to Quaternary, which resulted in horst-graben structures and topography. As a consequence, new lake basins have been formed within the grabens and horsts and associated mountain blocks and continue forming today (Aliaj, 1998). The horst-graben morpho-structural ensemble arose as the horst mountain blocks underwent relative uplift; the highest peaks in this region now reach elevations between 2000 and 2800 m (Figure 5).

The internal unit is split into three sub-areas by the Shkodra-Peja and Elbasani-Dibra transverse fault zones (Figure 3). The principal oddity of the neotectonic structure south of the Shkodra-Peja fault is that the main pre-

Pliocene NW-trending structures are cut obliquely by the N-S-trending Peshkopi-Korça Pliocene to Quaternary graben and fault zones. Most of the new Pliocene to Quaternary depressions in the internal area underwent subsidence in the Pliocene or early Quaternary, while, in the Middle to Upper Pleistocene to Holocene, they were incised (and probably uplifted) and developed river terraces. The Korça and Pogradeci depressions and that of Shkodra continued subsiding during the Quaternary; this is shown by their flat surfaces and lack of river terraces. Due to subsidence, Lakes Ohrid, Prespa and Shkodra assumed their final shapes in the Quaternary. The faults bounding these Pliocene to Quaternary lake depressions are mainly normal faults, but also have strike-slip components.

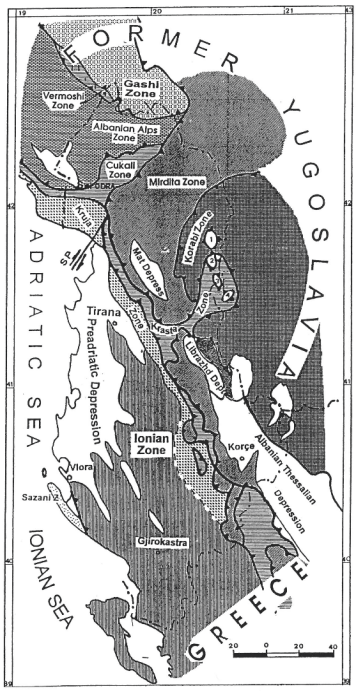

Figure 3. The tectonic zonation of Albania (from Meço et al., 2000). SP= Shkodra-Peja transverse fault dividing the Dinarides from the Hellenides. 1, 2, 3, 4: windows of the Kruja zone.

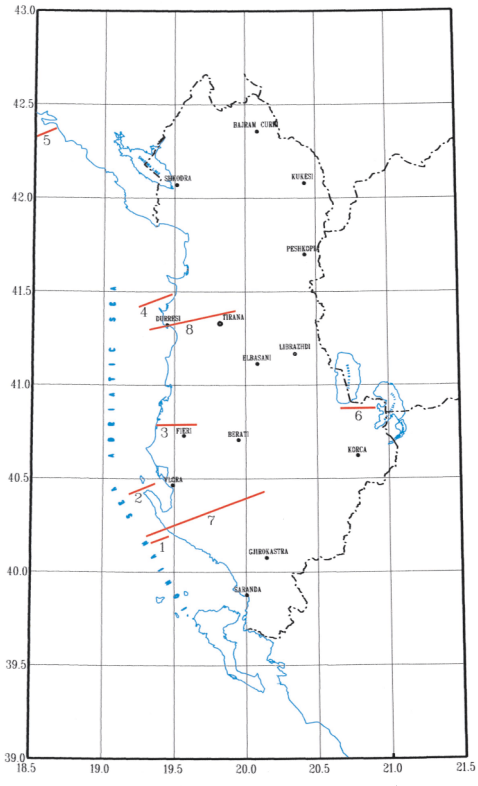

Figure 4. Map showing the locations of seismic lines and geological cross-sections, as follows: 1: Ionian offshore, 25 km south of town of Vlora (Figure 7), 2: slightly south of Sazani Island (Figure 9), 3: slightly north of town Fieri (Figure 10), 4: 15 km north of town Durresi (Figure 11), 5: area of Boka Kotorska (Figure 13), 6: slightly south of town Pogradeci (Figure 5), 7: Ionian offshore to Mt. Trebeshina (Figure 8), 8: Adriatic offshore to Mt. Dajti (Figure 12).

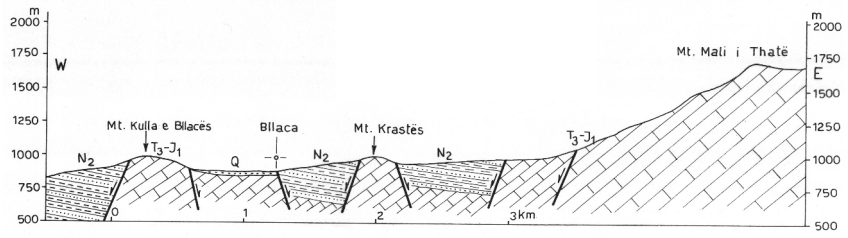

Figure 5. Geological cross-section, slightly south of the town of Pogradeci, through the Ohrid-Korça graben zone. Lithologies are as follows: T3-J1-Upper Triasic-Lower Jurassic limestones, N2-Pliocene molasse sediments, Q-Quaternary sediments.

External Alpine unit

The external unit includes the Kruja and the Ionian and Sazani zones to the offshore (Figure 3). The Kruja zone is made up of Cretaceous-Eocene platform carbonates and Oligocene flysch (Figure 12), the Ionian zone is made up of Mesozoic-Eocene basinal carbonates and Oligocene-Lower Miocene flysch (Figure 8, 12), and the Sazani zone is made up of Cretaceous-Paleogene platform carbonates (Figure 9). These regions have been strongly deformed by folds, reverse faults, including both thrusts and occasional back-thrusts, and strike-slip faults; all faults are inherited from the main Alpine compressive phases. Compressional deformation continues to the present. The shortening from cross-sections in Ionian zone of southern Albania is estimated from 45% (Aliaj et al., 1989) up to 100% (Bega et al., 2003). Active crustal shortening along the western coast of former Yugoslavia, Albania and Greece occurs at about 2 mm/yr (Papazachos et al., 1992).

The current structure of the external zone derives from the ancient one. It developed through progressive deformation from successive compressive phases, followed by strong Pliocene to Quaternary uplift.

The geomorphology in this unit is clearly related to the structure (Aliaj, 1988). The external zone is characterized by uplifting anticlinal mountains separated by synclinal valleys, all trending northwestward. At the Vlora-Tepelena flexure, the Ionian chains plunge towards the north along this trend, the Peri-Adriatic Depression formed over the top of the Ionian structures. Generally, the structures of the external unit trend SE. On their western flanks, the anticlinal ridges are bordered by low synclinal zones through which reverse faults or thrusts are generally expressed by a sharp break in topography (Figure 8). In addition, back-thrusts dipping toward the west are also present. These thrusts and back-thrusts were active during the Pliocene-Quaternary. The anticlinal ridges attain considerable elevations, exceeding 2000 m. A number of strike-slip faults cleave the external unit.

Peri-Adriatic foredeep

The Peri-Adriatic foredeep includes the hills and plains of the western lowlands of Albania and molasse sediments which accumulated from the Middle Miocene to the end of Pliocene. The Peri-Adriatic foredeep is located west of the external area, between the Shkodra-Peja fault and the Vlora-Tepelena transverse flexure. West of the Peri-Adriatic depression, the foreland extends into offshore. The Peri-Adriatic depression is regarded as a foredeep because it is located over the outer (western) margin of the Albanian orogen and records a rearrangement of structural styles and orientations. A

number of north- to northwest-trending Miocene-Pliocene narrow anticlines and wide synclines are present in the Peri-Adriatic foredeep. Generally, the positive structures are well expressed topographically (Aliaj, 1998). Seismic data show that the Mio-Pliocene anticlines are associated with thrusts or back-thrusts (Figure 10, 11). Some secondary strike-slip faults offset anticlinal axes. Compressional deformation in Peri-Adriatic depression persists up to the present day (Skrami and Aliaj, 1995).

Undeformed to weakly deformed foreland in the Adriatic and Ionian offshore

The offshore foreland is situated west of the Peri-Adriatic foredeep and Sazani zone, as well as west of the Ionian zone south of the Othoni Island-Dhermi transform fault (Figure 2). In the offshore foreland, two different carbonate facies have been distinguished (Aliaj, 1998):

a) The offshore foreland with basinal carbonates of pre-Oligocene age has been named the Albanian Basin or South Adriatic Basin and has not been affected by deformation (Figure 10-13), and

b) The foreland with platform carbonates of Upper Triassic-Oligocene age, termed the Apulian platform, has been weakly deformed by normal faulting (Figure 9).

THE ALBANIAN OROGENIC FRONT THRUST CONTACT WITH THE ADRIA MICROPLATE

Based on the oil and gas seismic explorations carried out during the last 15 years by foreign companies, the convergent boundary between the Albanian orogen and Adria is now well constrained to be located in the Ionian and Adriatic offshore. The Albanian orogenic thrust front is cut and displaced by the Othoni Island-Dhermi, the northern Sazani Island, and the Gjiri i Drinit-Lezha strike-slip faults, which divide the orogen into separate segments showing diachronous development (Aliaj, 1998, 2000). The following segments of the orogenic thrust front of the Albania orogen have been recognized (Figure 6):

1. The NW-trending Lefkas-Corfu segment
2. The NW-trending Karaburuni-Sazani Island segment
3. The ~N-trending Frakulla-Durresi segment
4. The W-NW-trending Lezha-Ulqini segment

The NW-trending Lefkas-Corfu segment

The NW-trending Lefkas-Corfu slope segment of the orogen front overthrusts the Apulian platform (Sorel, 1989). Further northwestwards, the orogenic front is cut by the NE-trending Othoni Island-Dhermi strike-slip fault, which coincides with the transition from the continental shelf to the Ionian offshore bathyal depths between the Island of Corfu and the town of Himara. Along this segment, a thin imbricate section of the Ionian Zone was displaced southwest for about 45 km, and was overthrust on the Apulian platform.

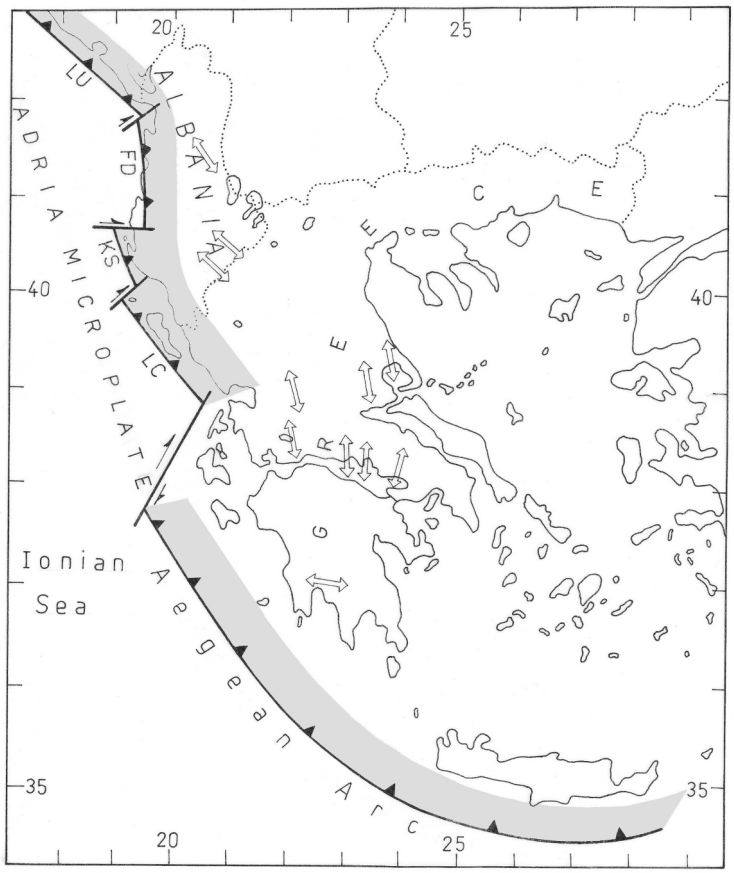

Figure 6. Southern convergent margin of Eurasia Plate: Adriatic collision and Aegean Arc. Segments of Adriatic collision frontal thrust are noted by capital letters, as follows: LC-Lefkas-Corfu, KS- Karaburuni- Sazani Island, FD-Frakulla-Durresi, and LU-Lezha-Ulqini. The strike-slip faults cutting the orogen front, from south to north, are as follows: the Othoni Island-Dhermi, the northern Sazani Island and the Gjiri i Drinit-Lezha faults.

The NW-trending Karaburuni-Sazani Island segment

The orogenic front of the Sazani zone is presently north of the Othoni Island-Dhermi strike-slip fault. The continental slope southwest of Mali i Kanalit Mountain is deformed and, as a result of minor thrusts, the transition from the Mali i Kanalit back-thrust monocline to the Apulian platform occurs along the Sazani zone orogenic front (Figure 7).

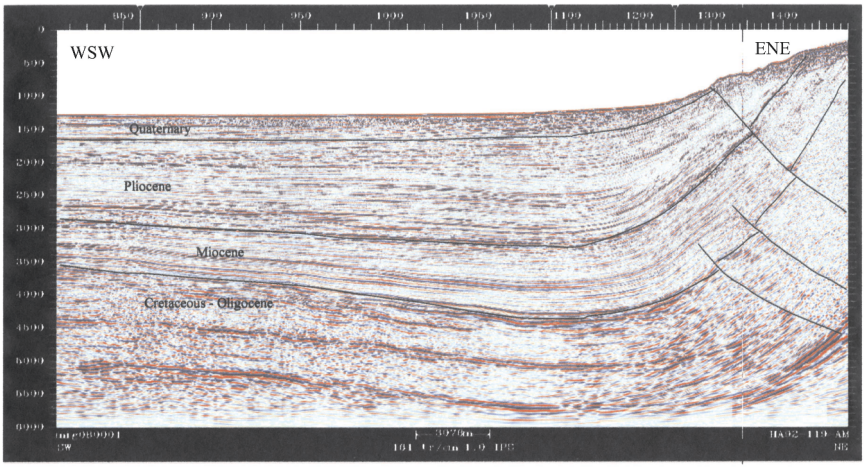

Figure 7. Seismic section through the Ionian offshore, 25 km south of the town of Vlora, showing the transition through some minor thrust faults from Apulian platform to the backthrust monocline of Sazani zone.

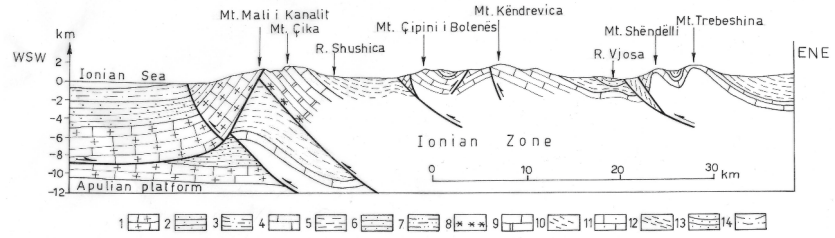

Figure 8. Geological cross-section from Ionian offshore, 25 km south of the town of Vlora, to Mt. Trebeshina, showing a triangular zone at the orogen thrust front as well as the Ionian Zone structures. Lithologies are as follows: Apulian platform and Sazani Zone: 1. Upper Triassic-Oligocene neritic carbonates, 2. Miocene terrigenous sediments, 3. Pliocene-Quaternary terrigenous sediments. **Albanian BasIn** 4. Pelagic carbonates, 5. Oligocene-Lower Miocene terrigenous sediments, 6. Middle-Upper Miocene terrigenous sediments, 7. Pliocene-Quaternary terrigenous sediments. **Ionian Zone**: 8. Upper Permian-Lower Triassic evaporites, 9. Upper Triassic-Eocene carbonates (pelagic ones from the Upper Liassic), 10. Oligocene-Lower Miocene flysch. **Kruja zone**: 11. Cretaceous-Eocene neritic carbonates, 12. Oligocene flysch. **Peri-Adriatic foredeep**: 13. Middle-Upper Miocene molasse, 14. Pliocene molasse.

Along this front, Cretaceous carbonates are backthrust over Upper Triassic dolomites of the Çika anticline of Ionian zone, forming a triangular zone at the depth (Figure 8). North of the Gjiri i Ariut-Dukat strike-slip fault, there is a NW-trending thrust that marks the contact of the Karaburuni-Sazani thrust front with the Apulian platform (Figure 9).

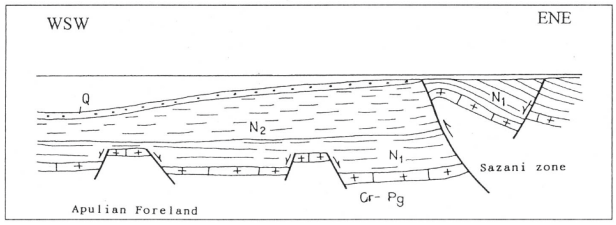

Figure 9. Schematic geological cross-section in the offshore, slightly south of Sazani Island (from seismic data; Aliaj, 1998), showing the thrusting of Sazani zone over Apulian platform. Lithologies are as follows: Cr-Pg-Cretaceous-Paleogene platform limestones, N1-Miocene clastics, N2-Pliocene clastics, Q-Quaternary marine sediments.

The ~N-trending Frakulla-Durresi segment

North of an E-W-trending transverse fault near Sazani Island, the transition from the Apulian platform to the Albanian Basin (South Adriatic Basin) occurs in the Adriatic offshore (Figure 2). The front of the orogen there is buried under molasses of Middle Miocene age exposed onshore on coastal terrains of the Peri-Adriatic depression and may pass along the Frakulla-Durresi anticlinal line of quasi-northern extension (Aliaj, 1998; Bega, 1995). Seismic data show that the Mio-Pliocene anticlines of Peri-Adriatic depression are associated with thrust or back-thrust faults (Aliaj, 1971, 1988; Biçoku, 1964). These have been termed over-fault anticlines (Aliaj, 1971) or determined by Biçoku (1964) as having been "placed in narrow zones of some big faults found under the Neogene cover". Some of these faults appear to be flower structures and "palm tree" structures associate with oblique thrusts (Aliaj, 2000).

The N-trending Frakulla-Durresi anticline (Figure 6) has been subjected to dextral transpressional associated with oblique northeast-southwest regional horizontal compression in post-Pliocene time. This is why flower and "palm tree" structures formed here at the same time that folding was occurring in the Peri-Adriatic depression. The Ardenica anticline is a "palm tree" type of flower-structure fault associated with a W-dipping oblique back-thrust (Figure 10). In the Durresi anticline, the main fault is a W-dipping

back-thrust that cuts marine Quaternary sediments that are still horizontal (Figure 11).

The orogenic front along the Frakulla-Durresi segment is marked at the surface by thrusting and back-thrusting. Along the Ardenica and Durresi anticlines, the thick Oligocene- to Quaternary-age clastic sediments of the South Adriatic Basin (Albanian Basin) have been detached from their carbonate substratum and have glided along a decollement at the level of the Oligocene clastics. The clastic sediments were largely back-thrust on frontal thrust structures of the Ionian zone, forming triangular zones at depth (Figures 10-12). In the Ardenica seismic section the clastic sediments of Albanian Basin were displaced eastwards by around 50 km and were strongly folded into trains of anticlines and synclines (Figure 10).

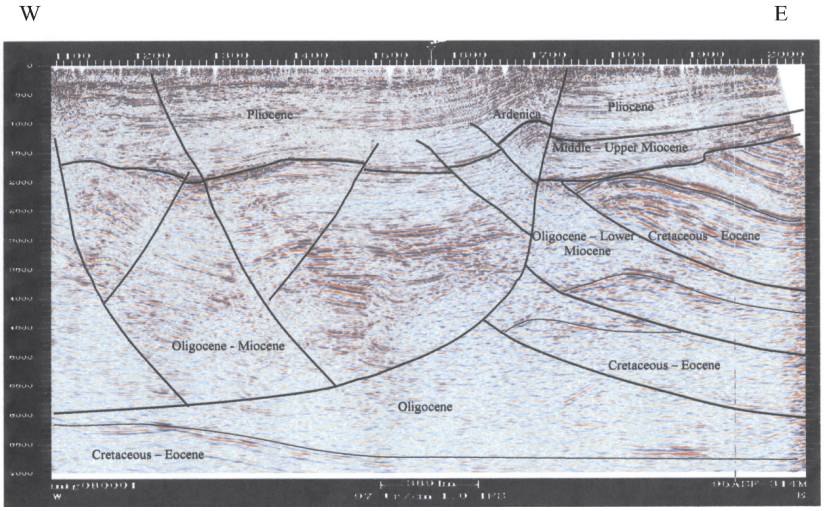

Figure 10. Seismic section from the Adriatic coastline eastwards, passing slightly north of the town of Fieri, showing a large backthrust of deformed clastic sediments of the Albanian Basin over the buried orogen thrust front.

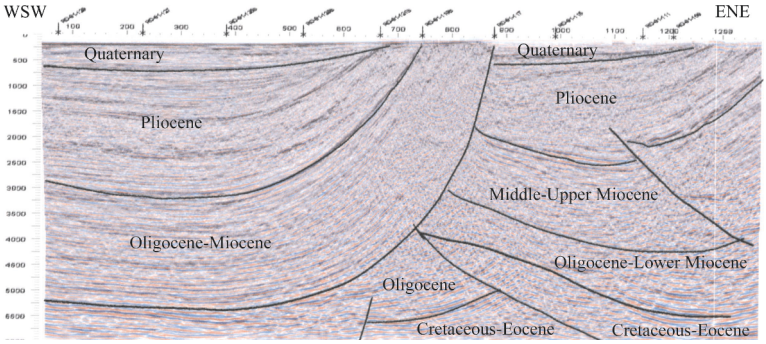

Figure 11. Seismic section through Adriatic offshore, 15 km north of the town of Durresi, showing a triangular zone at the buried orogen thrust front.

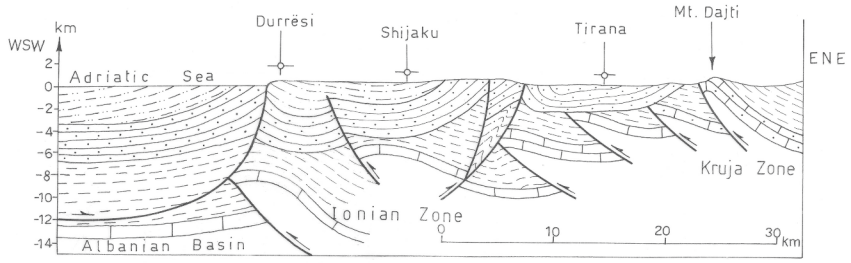

Figure 12. Geological cross-section from Adriatic offshore, 20 km WSW of the town of Durresi to Mt. Dajti, showing the buried orogen thrust front as well as Peri-Adriatic depression structures overlain on structures of the Ionian and Kruja zones. See Fig. 5 for description of lithologies.

The W-NW-trending Lezha-Ulqini segment

The orogenic front north of the Gjiri i Drinit-Lezha strike-slip fault, in the Adriatic offshore, belongs to the Kruja zone (Aliaj, 1998; Dragasevic, 1983). The buried orogenic front, northwest-trending here, is expressed by the Kruja zone thrusting over the Albanian Basin, (Figure 13).

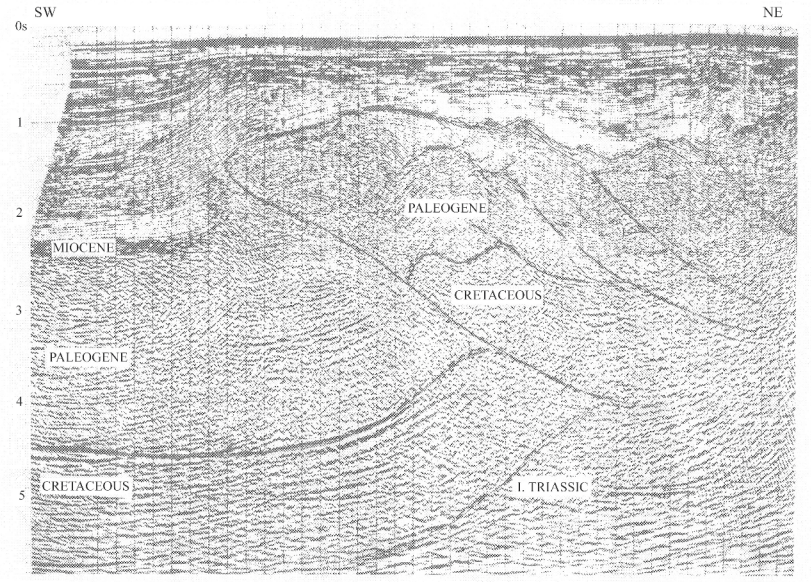

Figure 13. Seismic section through the area of Boka Kotorska perpendicular to the coastline (from Dragasevic, 1983), showing the overthrusting of the buried orogenic front over the South Adriatic Basin.

Local back-thrusting observed at Karaburuni-Sazani and Frakulla-Durresi segments of the frontal thrust of the Adriatic collision zone is quite different from the regional back-thrusting in Western Alps caused by Eo-Alpine and Apulian lithospheric wedging (Roure et al., 1990). In the Albanian case, the Adria microplate (Adriatic plate) is unaffected by such wedging; instead it was rigidly subducted during Alpine deformation beneath the Albanian orogen.

The external margin of the fold–and-thrust belt in Albania was thrust onto the Adria microplate, partly over the Apulian platform and partly over the Albanian Basin.

Segmentation along the orogenic thrust front

The previous discussion demonstrated that the convergent thrust boundary between the Albanian orogen and the undeformed Adria microplate is highly segmented (Figure 6). South of the Othoni Island-Dhermi strike-slip fault, the Ionian zone makes up the orogenic front, whereas to north of the Sazani Island strike-slip fault, the front consists of the Sazani zone. From the Peri-Adriatic depression to the Gjiri i Drinit-Lezha strike-slip fault, the front is buried under molasse but apparently comprised of the Ionian zone. North of the Gjiri i Drinit-Lezha strike-slip fault, the front is in the Kruja zone, and once again concealed under molasse. It is surmised that the segmentation results from cutting and displacement of the orogenic thrust front by these strike-slip faults (Aliaj, 1998, 2000).

The orogen front has been diachronously developed, as follows: at the end of Oligocene for the Kruja zone, at the beginning of Middle Miocene for the Ionian zone, and at the end of Miocene for the Sazani zone.

ACKNOWLEDGEMENTS

I would like to thank Eng. Agron Xhavo, Director of the National Hydrocarbon Agency, for allowing me to use some recent seismic sections that cross the boundary between Adria microplate and Albanian orogen. I also acknowledge fruitful discussions with Dr. Vilson Bare during the geologic interpretation of the seismic sections used in this paper, and with Dr. Zamir Bega for sharing his views on the geologic framework of the Albanian orogenic belt. I also would like to thank Prof. John Weber for a constructive and helpful review of my paper. Special thanks also to Prof. John Oldow for the useful comments in reviewing the manuscript.

REFERENCES

Aliaj Sh. Adriatic Depression and its structures in the light of geophysical data. Bul. USHT, Ser. Shk. Nat. 1971; 3: 25-41 (in Albanian).

Aliaj Sh. *Neotectonics and Seismicity of Albania*, D.Sc. Thesis, 265 pp., Archive of Seismological Institute, Albanian, 1988.

Aliaj Sh. Alpine geological evolution of Albania. Albanian J. of Natural & Technical Sciences 1997; 3: 68-81.

Aliaj Sh. Neotectonic structure of Albania. Albanian J. of Natural & Technical Sciences 1998; 4: 15-42.

Aliaj Sh. Neotectonics and seismicity of Albania. In book of Meço, S., Aliaj, Sh. and Turku, I: Geology of Albania 155-178. Gebruder Borntraeger. Berlin. Stuttgart, 2000.

Aliaj Sh. Seismic source zones in Albania. Albanian Seminar, Paris 26-28 June 2003. Archive of Seismological Institute, Tirana, 2003.

Anderson H., Jackson J. Active tectonics of Adriatic region. J. R. Astr. Soc. 1987, 91: 937-983.

Argand E. La Tectonique de l' Asie. Proc. Int. Geol. Congr. XIII 1924; 171.

Bega Z. *Thrust and backthrust systems of External Albanides*, D.Sc. Thesis, 155 pp., Archive of Faculty of Geology and Mining Tirana, Albanian, 1995.

Bega Z., Ballauri A., Meehan, P. Buttressing Role of the Apulian Platform on the Structural Style of Southern Albania. Albanian Seminar, Paris 26-28 June, 2003. Archive of OMV Albanien, Tirana, 2003.

Biçoku T. *Analysis and synthesis of seismic explorations in Periadriatic Depression*, D. Sc. Thesis, 271 pp., Central Archive of Geology Tirana, Albanian, 1964.

Channel J.E.T., Horvath P. The African/Adriatic Promontory as a Palaeogeographic Premise for Alpine Orogeny and Plate Movements in Carpatho-Balkan Region. Tectonophysics 1976; 35: 71-103

Dragasevic T. Oil geologic exploration in Montenegro offshore, Yugoslavia. Nafta, 1983; 34 (7-8): 397-404.

Giese P., Reutter K.J. Crustal and structural features of the Mediterranean Sea. Boll. Geof. Teor. Appl. 1978; XIV: 56.

Kahle H-G., Muller M.V., Geiger A., Danuser G., Mueller S., Veis G., Billiris H., Paradissis D. The strain field in northwestern Greece and the Ionian Islands: results inferred from GPS measurements. Tectonophysics 1995; 249.

Meço S., Aliaj Sh., Turku I. Geology of Albania, 246 pp., Gebruder Borntraeger. Berlin. Stuttgart, 2000.

Mercier J.L., Sorel D., Simeakis K. Changes in the state of stress in the overriding plate of a subduction zone: the Aegean Arc from the Pliocene to the present. Annales Tectonica 1987; I(1): 20-39.

Monopolis D., Bruneton A. Ionian Sea (Western Greece): its structural outline deduced from drilling and geophysical data. Tectonophysics 1982; 83.

Muço B., Focal mechanism solutions of Albanian earthquakes for the period 1964-1988. Tectonophysics 1994; 231: 311-323.

Muço B., Vaccari F., Panza G., Kuka N. Seismic zonation of Albania using a deterministic approach. Tectonophysics 2002; 344: 277-288.

Oldow J.S., Ferranti L., Lewis D.S., Campbell J.K., D'Argenio B., Catalano R., Pappone G., Carmignani L., Conti P., Aiken C.L.V. Active fragmentation of Adria, the north African promontory, central Mediterranean orogen. Geology 2002; 30(9): 779-782.

Papazachos B., Papazachos C. On Greek Earthquakes. Ziti Publications, Thessaloniki, 356 pp., 1989.

Roure F., Polino R., Nicolich R. Early Neogene deformation beneath the Po plaIn constraints on the post-collisional Alpine evolution. Mem. Soc. Geol. France, N.S. 1990; 156.

Skrami J., Aliaj Sh. Thrusts and back-thrusts on Preadriatic Depression (Albania) deduced from exploration seismics. Geol. Soc. Greece No 4 - Proc. of the XV Congress of the Carpatho-Balkan Geological Association, 1995; 1139-1143.

Sorel D., L'evolution structurale de la Grece Nordoccidentale depuis le Miocene dans le cadre geodynamique de l'Arc Egeen. These d'Etat, 306 pp, Universite de Paris- Sud, Orsay, 1989.

Sulstarova E., Koçiaj S., Aliaj Sh. Seismic Regionalization of Albania. Shtypshkronja "Mihal Duri" Tirana, 297 pp., (in Albanian and in English), 1980.

Sulstarova E., *Focal mechanism of earthquakes and present-day tectonic stress field in Albania,* D.Sc. Thesis, 230 pp., Archive of Seismological Institute Tirana, Albanian,

Wortmann U.G., Weissert H., Funk H., Hauck J. 2001. Alpine plate kinematics revisited: The Adria problem. Tectonics 1986; 20: 134-147.

LATE CENOZOIC TECTONICS OF SLOVENIA: STRUCTURAL STYLES AT THE NORTHEASTERN CORNER OF THE ADRIATIC MICROPLATE

Marko Vrabec[1] and László Fodor[2]
1: Department of Geology, University of Ljubljana, Ljubljana, Slovenia
markovrabec@netscape.net
2: Hungarian Geological Institute, Budapest, Hungary

ABSTRACT

We describe the structures and styles of deformation at the northeastern margin of the Adria microplate during Miocene to recent times. Throughout the Miocene, deformation induced by Adria-Europe convergence was partitioned between thrusting in the Dinaric and South-Alpine belts and eastward escape in front of the Adriatic indenter, north of the Periadriatic fault zone. At the Miocene-Pliocene transition, a temporary termination of tectonic escape and the onset of Adria counterclockwise rotation triggered a major change in regional tectonics. At that time, major strike-slip and contractional deformation started between rigid Adria and the Periadriatic fault, accompanied by uplift, folding, strike-slip basin formation, and, perhaps, rigid-block rotation. There is a gradual eastward change in structural style from head-on thrusting in the Italian Alps to oblique and then to predominately strike-slip deformation in the Dinaric and Pannonian regions of Slovenia. Distribution of recent seismicity and first results of GPS measurements suggest that this, or a similar, mode of deformation is still active.

INTRODUCTION

Late Tertiary motion of the Adriatic microplate was characterised by continuous northward motion (Dewey et al., 1989). Paleomagnetic data indicate that this motion was associated with ~30° counterclockwise (CCW) rotation (Márton et al., 2003) since the late Miocene or Pliocene. This motion largely post-dates continental collision between the converging Eurasian and Nubian plates. The post-collisional shortening was accommodated within the Alpine and Dinaridic mountain chains. During the latest Oligocene to mid-Miocene period, strike-slip and minor reverse faulting was associated with lateral motion (escape) and considerable extension in parts of the orogen, which indirectly led to the formation of the Pannonian basin (Ratschbacher et al., 1991; Csontos, 1995). A major change in regional tectonics occurred at

N. Pinter et al. (eds.), The Adria Microplate: GPS Geodesy, Tectonics and Hazards, 151–168.

the beginning of the Pliocene, when termination of subduction in the Carpathians blocked further eastward escape in front of indenting Adria (Horváth and Cloetingh, 1996), causing widespread inversion of extensional structures in the Pannonian basin (Fodor et al., 1999), and predominately transpressional deformation in Slovenia.

Figure 1. Principal geographic features of the territory of Slovenia and surrounding regions.

Slovenia is located in the northeastern corner of the Adria-Europe collision zone, at the transition from the rigid, undeformed Adria microplate into the surrounding "soft deforming" Dinaric and South-Alpine orogenic systems (Figures 1, 2). Principal topographic and geographic features of the area are shown on Figure 1. The flat, low-lying Istria peninsula contains the only outcrop of rigid Adria in the northern Adriatic region. Undeformed Adria extends up to the Venetian-Friuli plain, where it is buried by Neogene foredeep sediments. The thrust belts of the Dinarides and the Southern Alps form a rim of high topography around the undeformed Adria. But areas with high relief and high altitude, like the Sava Folds region and the Karavanke-Kamnik Alps, extend far into the deforming zones that surround Adria and show a pronounced topographic grain, suggesting an important role of neotectonics in the formation of the modern topography. Major strike-slip faults such as the Periadriatic fault, the Sava fault and the Labot fault have spectacular topographic expression. Large Quaternary basins are located at or

between such faults, for example the Gorenjska basin, the Barje basin and the Savinja basin.

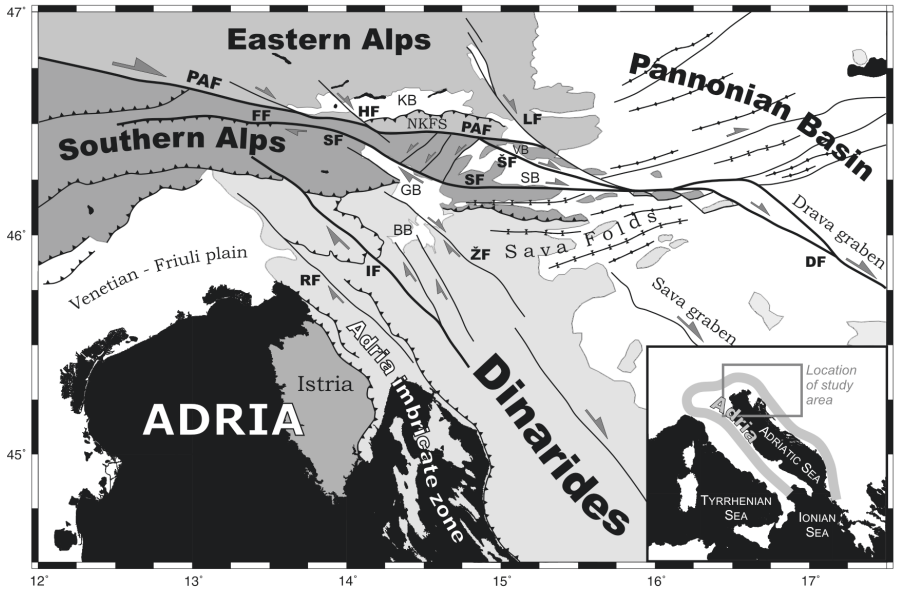

Figure 2. Simplified tectonic map of the northeastern corner of the Adria-Europe collision zone. Areas covered by Neogene sediments are shown in white. Letters denote major structures discussed in the text: BB - Barje basin, DF - Drava fault, KB - Klagenfurt basin, FF - Fella fault, GB - Gorenjska basin, HF - Hochstuhl fault, IF - Idrija fault, LF - Labot fault, NKFS - Northern Karavanke flower structure, PAF - Periadriatic fault, RF - Raša fault, SB - Savinja basin, SF - Sava fault, ŠF - Šoštanj fault, VB - Velenje basin, ŽF - Žužemberk fault. Note that the eastern extent of the Southern Alps unit is controversial; here the classical interpretation is shown (see text for discussion).

This complex and neotectonically active region is of particular interest not only because it offers insight into the structure of Adria-Europe contact, but also because understanding its tectonic history can help unravel the past kinematics of the Adria microplate, which are not directly observable with techniques like GPS, and can contribute to understanding of processes in continental collision zones in general. Due to considerable seismicity in the region (Figure 3), with earthquakes regularly causing loss of property and lives, understanding neotectonic processes and identification of active or potentially active structural systems is also of great importance to society.

In this paper, we briefly describe the structures that formed or were active in the territory of Slovenia during Miocene to recent times. We then discuss the style and timing of deformation, and how this deformation varied in space and time along the margin of the rigid Adriatic microplate.

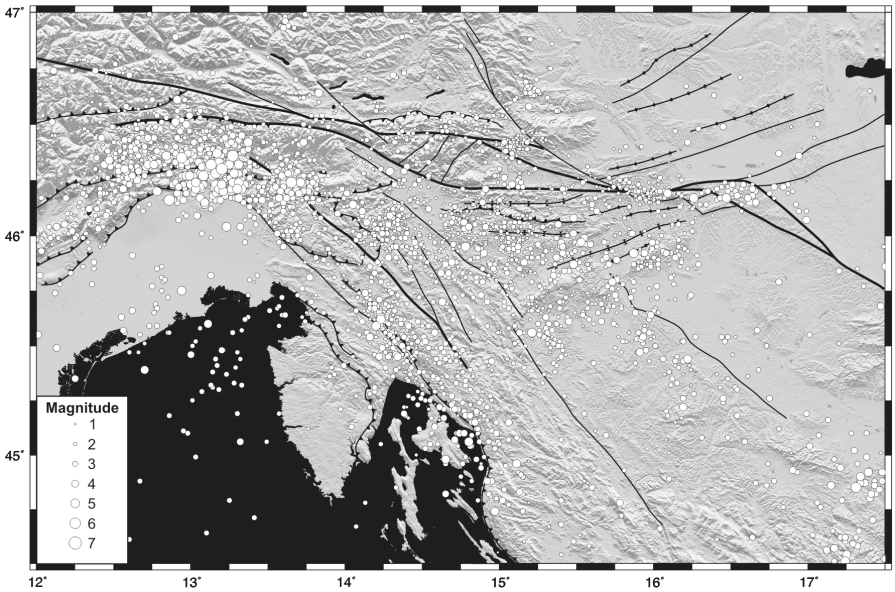

Figure 3. Seismicity from 1975 to 2003 (data source: NEIC catalog). Size of circles is proportional to earthquake magnitude.

THRUST BELTS ALONG THE RIGID ADRIA MARGIN

Dinaric thrust systems

The NW-SE-striking fold-and-thrust belt that runs from the Istria hinterland to central Slovenia belongs to the External Dinarides thrust system. This system is believed to have formed in response to Adria underthrusting the Dinaric carbonate platform domain in the later stages of late Jurassic-Recent evolution of the Dinarides (Tari, 2002). Total SW-NE shortening across the Slovenian External Dinarides is estimated to ~50 km in the kinematic reconstrucions of Placer (1981, 1999a). The age of thrusting is post-Eocene based on the age of flysch sediments involved in deformation (Placer, 1999a). A tighter, Oligocene-early Miocene time frame for deformation is implied by westward migration of the Friuli basin depocenter in the foreland (Mellere et al., 2000).

Continued post-early Miocene underthrusting of Adria formed a narrow SW-verging imbricate belt in front of the External Dinarides, extending from the northeastern rim of the Istria peninsula southward across the coastal islands (Placer, 1999a; Placer et al., 2001; Tari, 2002). Unlike the

predominately low-angle thrusts of the Slovenian External Dinarides with cumulative slip distances up to 20 kilometres, thrusts and reverse faults in the imbricate zone are steeper and have only minor horizontal displacements (Placer, 1999a; Tari, 2002).

South-Alpine thrust system

The S- to SE-verging fold-and-thrust belt of the Southern Alps formed in the Miocene as a late-stage retro-wedge of the Alpine collision, probably due to indentation of Adriatic lower crust into European lithosphere (Schmid et al., 1996). In the Dinarides-Southern Alps transition zone, the South-Alpine thrusts overthrust and refolded Dinaric thrust structures (Doglioni, 1987; Placer and Čar, 1998).

South-Alpine thrusts of the Julian Alps in western Slovenia continue into Valsugana thrust system in Italy of mid- to late Miocene age (e.g., Castellarin and Cantelli, 2000). In central Slovenia, sedimentation of predominately marine character occurred in the hinterland of Dinaric thrusts up to the end of the mid-Miocene in the western Sava Folds region (Kuščer, 1969) and until the end of Miocene in the eastern Sava Folds and eastwards (e.g., Buser, 1979). Facies and fossil assemblages of the topmost, Sarmatian (late-mid Miocene, 13-12 Ma) strata in the western Sava Folds region indicate a transition from marine to brackish conditions and eventually to continental sedimentation (Kuščer, 1969), but further east, the Sarmatian sediments are of marine origin and uncomformably overlie lower-mid Miocene strata (Buser, 1979). A brief Sarmatian NNW-SSE shortening episode was also recognised from seismic sections in Croatian part of the Sava Folds triangle (Tomljenović and Csontos, 2001). This event and the pattern of sedimentation might reflect thrusting and uplift of South-Alpine thrusts in northwestern Slovenia, which matches closely the 15-7 Ma time bracket established for the South-Alpine Valsugana thrust system in Italy (Castellarin and Cantelli, 2000).

The eastward extent of the South-Alpine thrust belt is controversial. Thrust sheets exposed in the Sava Folds region are regarded as South-Alpine due to the paleogeographic affinites of the thrust units (e.g., Placer, 1999a), but Oligocene sediments apparently cover the thrusts (Placer, 1999b). This implies that thrusting in the Sava Folds region pre-dates the Miocene South-Alpine episode. Post-Oligocene thrusts of the Kamnik Alps in north-central Slovenia probably are South-Alpine, however the entire unit was probably subsequently displaced eastward several tens of kilometres along the dextral Sava fault (see the Sava fault sub-chapter below). Therefore the eastern boundary of South-Alpine thrusting originally could have been at the present-day longitude of the Julian Alps in western Slovenia.

Dinaric faults

Southern and southwestern Slovenia is extensively faulted by NW-SE-trending dextral faults, which form conspicuous topographic lineaments, particularly in karstic areas (Figure 4). Since the faults are parallel to the strike of Dinaric folds and thrusts, they are classically called Dinaric faults, but no structural connection with Dinaric thrusting is known.

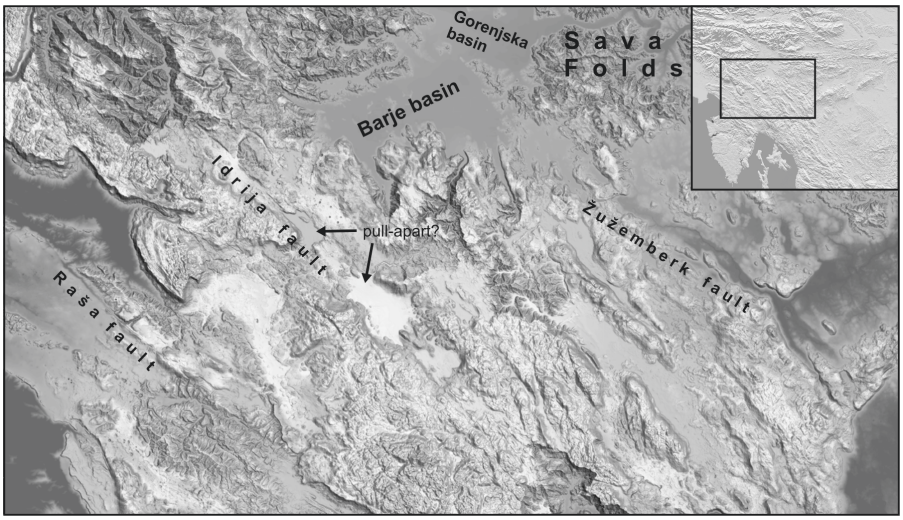

Figure 4. Topographic expression of NW-SE-trending Dinaric faults in southwestern Slovenia.

These faults cut and displace both Dinaric and South-Alpine fold-and-thrust structures. The average displacement is in the range of several kilometers and seems to become progressively smaller on the faults lying toward the southwest. The largest dextral offset known is about 12 km, and was inferred for Idrija fault on the base of displaced geological and geomorphological markers (Šušteršič, 1996). Fault-slip data and map relationships indicate that many of the faults, including Idrija fault, formed as dip-slip normal faults and were only later dextrally reactivated.

On the grounds of recent and historic seismicity it is believed that at least some of the Dinaric faults are active today (e.g., Poljak et al., 2000; Placer et al., 2001). Probable offsets of topographical features and flat karst poljes filled with thin Quaternary sediment cover, interpreted to be pull-apart basins in Dinaric fault zones (Vrabec, 1994), also support this idea.

Earthquake focal mechanisms imply dextral to oblique dextral motions (Poljak et al., 2000), but these determinations are not very reliable because of the predominately low magnitude of events in the region.

DEFORMATION AND ACTIVE STRUCTURES ALONG THE PERIADRIATIC FAULT ZONE (PAF)

Periadriatic Fault Zone

The Periadriatic fault zone (PAF) represents a major topographic and structural boundary in northern Slovenia (Figures 1, 2, 5). The PAF has accommodated at least 100 km of dextral motion during northward indentation of the Adria microplate and associated eastward displacement of the Eastern Alps during the Miocene (Ratschbacher et al., 1991; Frisch et al., 1998), indicated by displaced paleogeographic markers (Kázmér and Kovács, 1985). The Eastern Alps moved due to extrusion, a combined process of orogenic collapse, extension, and tectonic escape (Ratschbacher et al., 1991). In the generally convergent context of the Adria-Europe collision zone, extrusion was possible because of the retreating subduction arc in the Carpathian region, which formed a free boundary toward the east. The dextral PAF borders the southern edge of the extruding wedge.

A study of PAF exposures in Slovenia revealed several dextral reactivations since the initial formation of the fault in Oligocene (Fodor et al., 1998). The principal displacement zone shifted from the northern, main branch southward to other shear zones. The northern branch is covered by 17 Ma-old sediments, proving pre-early-Miocene dextral slip. Pre-17 Ma and post-13 Ma dextral slip can be inferred in the southern Karavanke shear zone on the basis of differently tilted Eocene and mid-Miocene sediments, but the Pliocene sedimentary cover (where present) is not disrupted. Both the main fault branch and southern shear zones are cut by the NW-SE-trending Labot fault, and features are offset by about 10-14 km (Kázmér et al., 1996) (Figures 2, 5, 6). Displaced mid-Miocene sediments and pre-Pliocene fault zones of the PAF suggest Pliocene-Quaternary dextral slip along the Labot fault.

Up to 1000 m of Plio-Quaternary sediments accumulated in the synsedimentary transtensional Velenje basin along the Šoštanj fault, which is the southernmost branch of the PAF (Figures 2, 6). Post-depositional dextral strike-slip movements suggest Quaternary activity on the fault (Vrabec, 1999). Ongoing eastward extrusion of the Eastern Alps and dextral activity of the PAF and the Šoštanj fault were recently observed using GPS (Grenerczy et al., 2000; Vrabec et al., 2003; Weber et al., this volume).

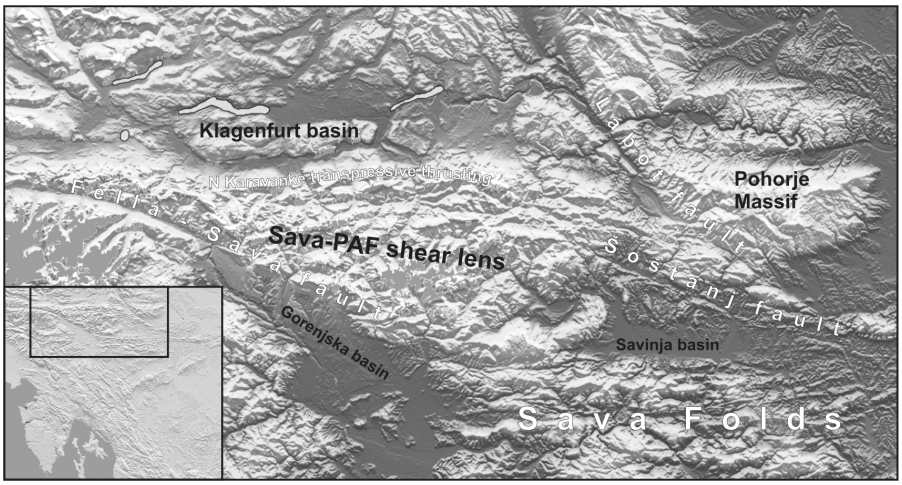

Figure 5. Topographic expression of the transpressional "shear lens" between the Sava fault and the Periadriatic fault.

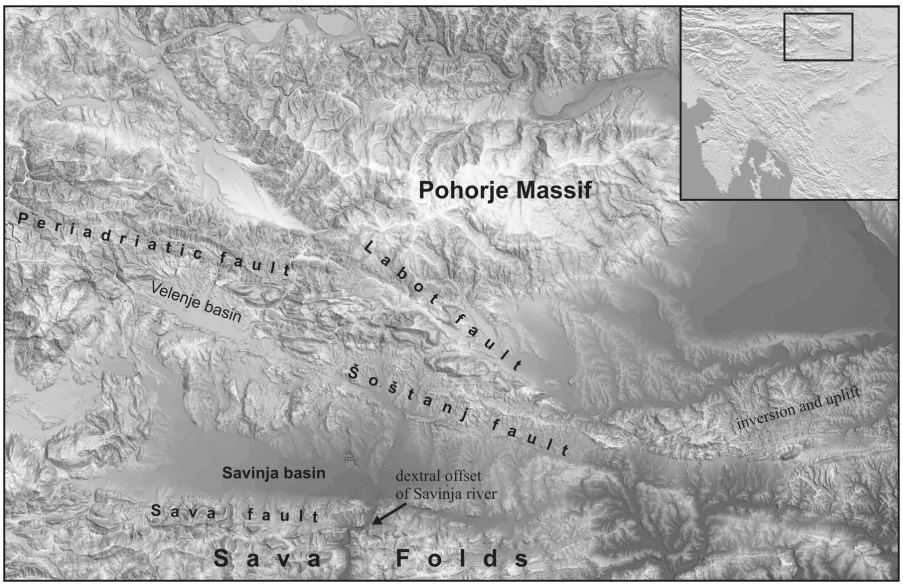

Figure 6. Junction of the Šoštanj, Labot and Sava faults, northeastern Slovenia.

The PAF can be traced eastward into a series of transtensional graben structures (e.g., the Drava fault) in Croatia (Fodor et al., 1998; Prelogović et al., 1998). This connection was established in late Miocene after major rotations and amalgamation of tectonic blocks in the Pannonian domain prevented slip on the former PAF continuation, now probably running in NE-SW direction across central Hungary (Fodor et al., 1998).

Sava fault

The E-W- to NW-SE-trending, gently curved dextral Sava fault south of the PAF has impressive topographic expression (Figures 1, 2, 5). Dextral slip of 30-60 km was inferred from the separation of a distinctive Oligocene volcanogenic formation (e.g., Fodor et al., 1998). Eastward, the Sava fault merges with the Šoštanj fault and the Labot fault, together forming the continuation of the PAF zone towards the Drava graben. Towards the west in Italy, where the Sava fault is known as the Fella Line, the slip sense gradually changes to reverse dextral, and the fault merges with the South- Alpine thrusts discussed above. Folding of late-mid-Miocene (Sarmatian, 13-12 Ma) strata in front of the restraining bend of the Sava fault north of Ljubljana constrains its timing as post-mid-Miocene. A main slip episode may have preceded bending and transpressive reorganization of the fault zone, but regional geological relationships and detailed structural mapping (Vrabec, 2001) suggest significant displacement of South-Alpine thrust units across the fault. Major movements on the Sava fault therefore post-date South-Alpine thrusting, which is presumed to have been active until the latest Miocene (see the Southern Alps subchapter above).

Sava-PAF shear lens

The lenticular area of the southern Karavanke and Kamnik Alps, situated between the Sava fault and the PAF, is strongly deformed and uplifted (Figure 5). Clockwise domino-like rotation of blocks inside the shear lens is indicated by paleomagnetic declinations from Oligocene to Neogene sediments (Fodor et al., 1998). On the northern side of the PAF zone, the northern Karavanke Mts. are interpreted as a dextral transpressive flower structure, which overthrusts the Sarmatian-Quaternary sediments of the Klagenfurt basin (e.g., Nemes et al., 1997). The eastern part of this shear lens, between the Šoštanj fault and the Sava fault, has much lower relief and is mainly covered by Pliocene-Quaternary sediments, deposited in fault-bounded basins such as the Savinja basin (Figures 5, 6). This area could be

deformed transtensionally, as suggested by the map-scale relationships of the faults and basins and by fault slip data (Fodor et al., 1998).

CENTRAL SLOVENIA

Sava Folds

The triangular region in central Slovenia and northeast Croatia, known as the Sava Folds (Figures 1, 2, 7), is dominated by E-W- to ENE-WSW-trending synclines of Neogene strata. Synclines formed between pop-ups of pre-Tertiary basement, uplifted along moderately dipping reverse faults (Placer, 1999b; Tomljenović and Csontos, 2001). Seismic sections show that most of these reverse faults are inverted early- and mid-Miocene normal faults (Tomljenović and Csontos, 2001). Folds and reverse faults are either cut by, or linked by, short obliquely-trending dextral tear faults. Such a geometrical arrangement is typical of transpressive deformation with a large component of shear-perpendicular shortening (Schreurs and Coletta, 1998).

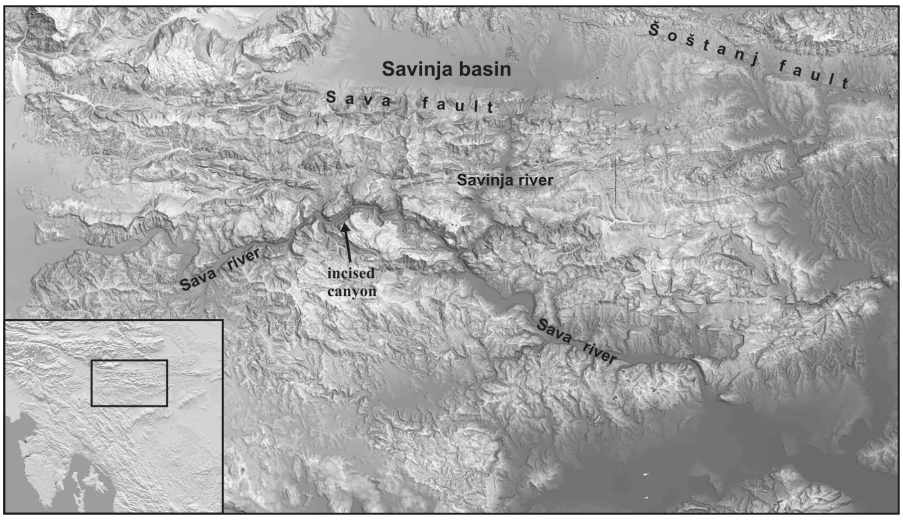

Figure 7. Topography of the west-central Sava Folds. Note the clearly visible E-W-trending folds, dissected by an antecedent, predominately N-S-trending fluvial network.

Folding and uplift in the Sava Folds region started at the end of the Miocene and lasted throughout Pliocene (Tomljenović and Csontos, 2001), and this deformation could still be locally active as indicated by considerable seismicity (Figure 3) and relationships inferred from seismic-reflection profiles in the southernmost syncline (Accaino et al., 2003). Despite the Sava Folds uplift, an antecedent fluvial network maintained its original course, in many areas perpendicular to the fold axes (Placer, 1999b; Vrabec, 2001; see also Figure 7). Moderately folded late Miocene sediments suggest that inversion structures of the same age and of similar architecture extend into easternmost Slovenia (Márton et al, 2002) and into Hungary, where their existence is well documented in petroleum industry seismic-reflection profiles (e.g., Horváth, 1995; see also Bada et al., this volume).

Quaternary basins

The Gorenjska basin in central Slovenia is a remarkably rectangular topographic feature (Figure 8), located between the Sava fault and the westernmost segment of the Dinaric Žužemberk fault (Figure 2). The basin is filled with Quaternary alluvium (Žlebnik, 1971). An early Quaternary age for the oldest terrace surfaces was established using Be^{10} dating (Vidic, 1994). Boreholes indicate that the thickness of Quaternary sediments reaches 150 m in asymmetric depressions, which probably represent half-grabens that subsided along NNE-SSW trending master faults.

The eastern Gorenjska basin margin bounds the Sava Folds. E-W-trending folds occur in Neogene beds in the NE corner of the basin. These structures are separated from the Sava Folds proper by mapped N-S- to NNW-SSE-trending faults with normal separation and are structurally lower than their eastern counterparts.

Post-depositional tectonic activity in the Gorenjska basin is indicated by tilted alluvial terrace surfaces, a displaced alluvial fan of the Kokra river in the NW corner of the basin, and observations of folds and probable fault scarps in Quaternary deposits (Vrabec, 2001; Figure 8). Some of these features imply a change from transtensional subsidence to pure strike-slip or even transpressional deformation. Throughout the basin, the rivers are deeply incised into the basin fill, locally to the level of pre-Quaternary bedrock.

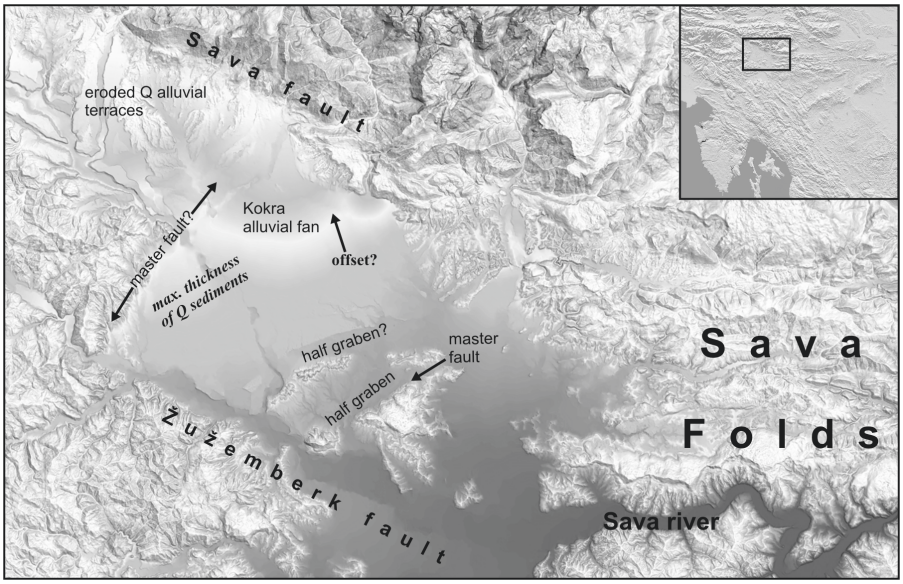

Figure 8. Quaternary Gorenjska basin, central Slovenia. Quaternary sediments cover the low-relief regions.

The smaller Barje basin (Figures 2, 4) is separated from Gorenjska basin by the Žužemberk fault and a pre-Quaternary basement ridge. Subsidence in Barje basin did not start before mid-Quaternary (Šifrer, 1984) and probably remains active today as suggested by its flat topography, absence of river incision and burial of roads from the Roman era. Data from boreholes and seismic- reflection profiles (Mencej, 1988) show that Barje basin consists of several half-grabens with maximum known depths of 200 m. Some of the intervening basement highs crop out as small inselbergs. NE-SW-oriented normal faults appear to be linked to terminations of (N)NW-(S)SE-trending Dinaric dextral faults. The presence of Dinaric faults at the southeastern basin margin is clear both from topography and from existing geological maps, but they apparently do not cross to the northwestern side of the basin.

TOWARDS A TECTONIC MODEL OF POST-MIOCENE DEFORMATION

Many workers have recognized that a major change in regional tectonics occurred around 6 Ma, around the time of the Miocene-Pliocene transition. This is likely related to termination of subduction in the

Carpathians that blocked further eastward escape in front of indenting Adria (Horváth and Cloetingh, 1996). This change ended subsidence and sedimentation in most of the Pannonian basin and started widespread inversion of the earlier extensional structures (Fodor et al., 1999; Bada et al., this volume). Additionally, paleomagnetic investigations indicate that, at about the same time, the Adria microplate might have had started its CCW rotation (Márton et al., 2002; Márton, this voume). The onset of major strike-slip and contractional deformation in central and eastern Slovenia, discussed in detail above, corresponds quite well with this major change. In Figure 9 we present a simplified tectonic map, emphasizing our inferred mechanisms for post-Miocene deformation.

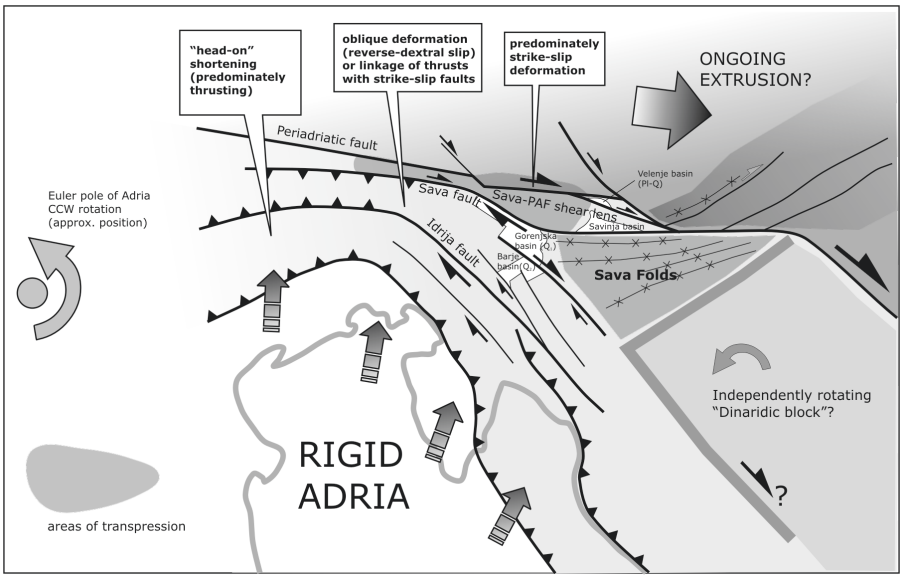

Figure 9. A model of post-Miocene tectonics at the northeastern corner of the rigid Adria microplate. CCW rotation of Adria is assumed to be the main mechanism driving deformation. See text for detailed discussion.

In the Southern Alps, Miocene-to-recent deformation was predominately absorbed by shortening across S- to S(S)E-directed thrusts and backthrusts (Castellarin and Cantelli, 2000). This is reflected in the straight trace of the PAF. Concurrent Miocene to recent dextral slip on the PAF during extrusion suggests strain partitioning in this region. Focal mechanisms of large earthquakes in the Friuli region (Slovenian-Italian border) indicate ongoing southward thrusting along a part of the Miocene thrust zone, very

close to the Dinarides-Southern Alps transition (e.g., Peruzza et al., 2002; see also Anderson and Jackson, 1987).

From central Slovenia eastward, strike-slip tectonics become the dominant mode of deformation. The spatial transition between thrusting and strike-slip faulting seems to be gradual. In the case of the Fella-Sava fault, a smooth eastward steepening of the fault plane and change in kinematics from dextral transpression to pure dextral slip is observed. This change is more abrupt to the south, where E-W trending thrusts are probably directly linked to NW-SE-oriented, steep Dinaric dextral faults like the Idrija fault.

From the Julian Alps eastward to the Pohorje Massif, the PAF becomes increasingly more segmented and is offset by oblique dextral faults of Pliocene (Labot fault) to Quaternary age (Hochstuhl fault). The eastward increase in age and amount of displacement of the PAF may be related to CCW rotation of Adria around the pole located in the western Southern Alps in Italy (Anderson and Jackson, 1987; Weber et al., this volume). After the Miocene, the sub-parallel Sava fault probably has pirated most of dextral displacement from the PAF, which was blocked in the east by the Labot fault. Some of the "missing" deformation could also be taken up by transpressional shortening and block rotation inside the Sava-PAF shear lens. To a first approximation, the inferred 30-60 km of dextral displacement on the NW-SE-oriented Sava fault could easily match the magnitude of post-Miocene N-S shortening along the S- to SE-verging South-Alpine thrusts to the west.

The tectonics of the Sava Folds are not completely understood. Their position just south of the Sava fault and east of the fault's bend from WNW-ESE to an E-W orientation implies the folds could have formed by deformation partitioning between dextral slip on the fault and N-S shortening to the south. The structure and even the exact location of the Sava fault zone along the NW portion of the Sava Folds is unclear (e.g., Fodor et al., 1998), which could mean that, at some stage, folding overprinted the structure and no further eastward slip was possible.

To explain the conspicuous eastward tightening of the Sava Folds region into its triangular shape, Tomljenović and Csontos (2001) devised a regional deformation model in which several relatively rigid blocks rotated independently in a CCW sense and slid along dextral faults. In their model, the Sava Folds formed in front of the so-called "Dinaridic block", which is bounded to the east by the Drava fault (Figure 9). Interestingly, the apparent seismicity void located SE of the Sava Folds triangle (Figure 3) implies a rigid block there that agrees with such an idea. This concept was also used by Márton et al. (2002), who noted that their observed CCW rotations and local transpression and transtension in Slovenia could be explained by the presence of a number of rigid blocks rotating between Dinaric NW-SE-trending dextral faults.

Structural relationships and age constraints suggest that the Gorenjska basin post-dates the main period of folding in the Sava Folds. We interpret the basin as a pull-apart that formed in a releasing step-over between the Sava fault and Žužemberk fault during the early Quaternary. Such a southward transfer of dextral slip could have been caused by termination of the eastern continuation of Sava fault due to transpressive deformation of the fault zone. The curved geometry of the Žužemberk fault and its questionable SE continuation does not allow significant strike-slip on the fault. Formation of the Barje basin in the mid-Quaternary implies a further transfer of deformation onto the NW-SE-trending Dinaric faults in SW Slovenia, where a considerable part of present-day seismicity is concentrated.

Our model proposes that east of the South-Alpine thrust system, most of the Pliocene-recent Adria movement was accommodated by strike-slip deformation. The age of Pliocene-Quaternary basins in central Slovenia that formed at or between the dextral strike-slip faults seems to decrease to the SW towards the interior of the Adria microplate. Does this mean that strike-slip deformation in the Adria collision zone is limited to a relatively narrow active deformation zone which is gradually shifting southwards? Such a southward shift could, for example, be forced by progressive tightening, abandonment, and cross-cutting of older structures by younger faults. A southward shift of the principal strike-slip deformation zone could have also followed a forward-breaking propagation of the South-Alpine thrust system, to which these strike-slip structures are connected. This interpretation would imply that the next deformation corridor will move south of the Barje basin into SW Slovenia. Or is the deformation in Slovenia more widely distributed and tied to large-scale, long-lived fault structures like the PAF system? Other structures could then accommodate differential deformation, for example the possible formation of the Sava Folds triangle due to the CCW rotating "Dinaridic block" of Tomljenović and Csontos (2001).

Measurements of ongoing deformation with GPS provide important new insights into active tectonic processes. The wide-aperture study of Grenerczy et al. (2000), observations in the Slovenian PAF zone (Vrabec et al., 2003), and the recent PIVO experiment which included more than 40 points from Istria to easternmost Slovenia (see Weber et al., this volume) indicate that the largest displacement gradients occur across faults of the PAF zone. It seems that a large part of regional deformation is still concentrated on this important long-lived structural system, whereas the younger structures south of it, such as Dinaric faults, have a comparatively minor role. However, many questions remain open and require improvements in our knowledge of structural relationships, the chronology of deformation, and paleoseismological and quantitative geomorphological aspects before this complex but fascinating region is more fully understood.

ACKNOWLEDGEMENTS

We thank John Weber for many helpful comments and suggestions during writing the early versions of the manuscript. The final paper was improved by a constructive review by Nicholas Pinter.

REFERENCES

Accaino F., Gosar A., Millahn K., Niccolich R., Poljak M., Rossi G., Zgur F. Regional and high-resolution seismic reflection investigations in the Krško basin (SE Slovenia). Annales Universitatis Scientarium Budapestinensis, Sectio. Geologica 2003; 35: 116-117.

Anderson H.A., Jackson J.A. Active tectonics of the Adriatic region. Geophys. J. R. Astr. Soc. 1987; 91: 937-983.

Buser S. *Basic geological map of SFR Yugoslavia 1: 100.000. Explanatory notes for sheet Celje* (In Slovenian with English abstract). Zvezni geološki zavod, Beograd 1979.

Castellarin A., Cantelli L. Neo-Alpine evolution of the Southern Eastern Alps. J. Geodynamics 2000; 30: 251-274.

Csontos L. Tertiary tectonic evolution of the Intra-Carpathian area: a review. Acta Vulcanologica 1995; 7: 1-13.

Dewey J.F., Helman L., Turco E., Hutton D.H.W., Knott S.D. "Kinematics of the Western Mediterranean." In *Alpine Tectonics*, M.P. Coward, D. Dietrich, R.G. Park, eds., London: Geol. Soc. London Spec. Publ. 1989; 45: 265-283.

Doglioni C. Tectonics of the Dolomites. J. Structural Geology 1987; 9: 181-193.

Fodor L., Jelen B., Márton E., Skaberne D., Čar J., Vrabec M. Miocene-Pliocene tectonic evolution of the Slovenian Periadriatic Line and surrounding area - implication for Alpine-Carpathian extrusion models. Tectonics 1998; 17: 690-709.

Fodor L., Csontos L., Bada G., Györfi I., Benkovics L. "Tertiary tectonic evolution of the Pannonian basin system and neighbouring orogens: a new synthesis of paleostress data." In *The Mediterranean Basins: Tertiary extension within the Alpine Orogen*, B. Durand, L. Jolivet, F. Horváth, M. Séranne, eds., Geol. Soc. Spec. Publ. 1999; 156: 295-334.

Frisch W., Kuhlemann J., Dunkl I., Brügel A. Palinspastic reconstruction and topographic evolution of the Eastern Alps during late Tertiary tectonic extrusion. Tectonophysics 1998; 297: 1-15.

Grenerczy G., Kenyeres A., Fejes I. Present crustal movement and strain distribution in Central Europe inferred from GPS measurements. J. Geophys. Res. 2000; 105(B9): 21835-21846.

Horváth F. Phases of compression during the evolution of the Pannonian basin and its bearing on hydrocarbon exploration. Marine and Petroleum Geology 1995; 12: 837-844.

Horváth F., Cloething S. Stress-induced late-stage subsidence anomalies in the Pannonian Basin. Tectonophysics 1996; 266: 287-300.

Kázmér M., Kovács S. Permian-Paleogene paleogeography along the Eastern part of the Insubric-Periadriatic Lineament system: Evidence for continental escape of the Bakony-Drauzug unit. Acta Geologica Hungarica 1985; 28: 71-84.

Kázmér M., Fodor L., Józsa S., Jelen B., Herlec U., Kuhlemann J. Late Miocene paleogeography of Slovenia and the Southern Alps: a palinspastic approach. 6th Symposium on Tektonik, Strukturgeologie, Kristalingeologie, Salzburg, Austria, 1996.

Kuščer D. Tertiary formations of Zagorje (in Slovenian with English abstract). Geologija 1969; 10: 5-85.

Márton E., Ćosović V., Drobne K., Moro A. Palaeomagnetic evidence for Tertiary counterclockwise rotation of Adria. Tectonophysics 2003; 377: 143-156.

Márton E., Fodor L., Jelen B., Márton P., Rifelj H., Kevrić R. Miocene to Quaternary deformation in NE Slovenia: complex paleomagnetic and structural study. J. Geodynamics 2002; 34: 627-651.

Mellere D., Stefani C., Angevine C. Polyphase tectonics through subsidence analysis: the Oligo-Miocene Venetian and Friuli Basin, north-east Italy. Basin Research 2000; 12: 159-182.

Mencej Z. The gravel fill beneath the lacustrine sediments of the Ljubljansko barje (in Slovenian with English abstract). Geologija 1988; 31-32: 517-553.

Nemes F., Neubauer F., Cloething S., Genser J. The Klagenfurt basin in the Eastern Alps: an intra-orogenic decoupled flexural basin? Tectonophysics 1997; 282: 189-203.

Placer L. Contribution to macrotectonic subdivision of the border region between Southern Alps and External Dinarides. Geologija 1999a; 41: 223-255.

Placer L. Structural meaning of the Sava folds. Geologija 1999b; 41: 191-221.

Placer L. Geological structure of Southwestern Slovenia (in Slovenian with English abstract). Geologija 1981; 24: 27-60.

Placer L., Živčić M., Vrabec M. "Recent deformation and seismic activity at the Adria microplate boundary in Western Slovenia and Croatia." In *Quantitative neotectonics and seismic hazard assessment: new integrated approaches for environmental management*, G. Bada eds., Malév Air Tours str. 2001; 74-75.

Placer L., Čar J. Structure of Mt. Blegoš between the Inner and Outer Dinarides. Geologija 1998; 40: 305-323.

Peruzza L., Poli E., Rebez A., Renner G., Rogledi S., Slejko D., Zanferrari A. The 1976-1977 seismic sequence in Friuli: new seismotectonic aspects. Mem. Soc. Geol. It. 2002; 57: 391-400.

Poljak M., Živčić M., Zupančič P. The seismotectonic characteristics of Slovenia. Pure and Applied Geophysics 2000; 157: 37-55.

Prelogović E., Saftić B., Kuk V., Velić J., Dragaš M., Lučić D. Tectonic activity in the Croatian part of the Pannonian basin. Tectonophysics 1998; 297: 283-293.

Ratschbacher L., Frisch W., Linzer H. G., Merle O. Lateral extrusion in the Eastern Alps, part 2.: structural analysis. Tectonics 1991; 10: 257-271.

Schreurs G., Coletta B. "Analogue modeling of faulting in zones of continetal transpression and transtension." In *Continetal transpressional and transtensional tectonics*, R.E. Holdsworth, R.A. Strachan, J.F. Dewey, eds., Geol. Soc. Spec. Publ. 1998; 59-79.

Schmid S.M., Pfiffner O.A., Froitzheim N., Schönborn G., Kissling E. Geophysical-geological transect and evolution of the Swiss-Italian Alps. Tectonics 1996; 15: 1036-1064.

Šifrer M. Nova dognanja o geomorfološkem razvoju Ljubljanskega Barja. Geografski zbornik 1984; 23: 8-48.

Šušteršič F. Poljes and caves of Notranjska. Acta Carsologica 1996; 25: 251-289.

Tari V. "Evolution of the northern and western Dinarides: a tectonostratigraphic approach." In *Continetal collision and the tectono-sedimentary evolution of* forelands, G. Bertotti, K. Schulmann, S.A.P.L Cloething, eds., EGU Stephan Mueller Publication Series 2002; 1: 223-236.

Tomljenović B., Csontos L. Neogene-Quaternary structures in the border zone between Alps, Dinarides and Pannonian basin (Hrvatsko zagorje and Karlovac basin, Croatia). Int. J. Earth Sciences 2001; 90: 560-578.

Vidic N. *Pedogenesis and soil-age relationships of soils on glacial outwash terraces in the Ljubljana basin*, PhD thesis, Boulder: University of Colorado, 1994.

Vrabec M. *Structural analysis of the Sava fault zone between Trstenik and Stahovica (in Slovenian with English abstract),* PhD thesis, University of Ljubljana, 2001.

Vrabec M. Style of postsedimentary deformation in the Plio-Quaternary Velenje basin, Slovenia. Neues Jahrbuch für Geologie und Paläontologie Monatshefte 1999; 8: 449-463.

Vrabec M. Some thoughts on the pull-apart origin of karst poljes along the Idrija strike-slip fault zone in Slovenia. Acta Carsologica 1994; 23: 158-168.

Vrabec M., Pavlovčič Prešeren P., Stopar B. Active movements along the faults of the Periadriatic line system in NE Slovenia: first results of GPS measurments. Annales Universitatis Scientarium Budapestinensis, Sectio Geologica 2003; 35: 114-115.

Žlebnik L. Pleistocene Deposits of the Kranj, Sora and Ljubljana Fields (in Slovenian with English abstract). Geologija 1971; 14: 5-51.

RECENT MONITORING OF CRUSTAL MOVEMENTS IN THE EASTERN MEDITERRANEAN

The Use of GPS Measurements

Günter Stangl[1] and Carine Bruyninx[2]
1: Federal Office of Metrology and Surveying, Graz, Austria
guenter.stangl@oeaw.ac.at
2: Royal Observatory of Belgium, Brussels, Belgium

ABSTRACT

The main goal of this paper is to show the different influences that affect the estimation of site velocities using GPS. Coordinate time series can be disturbed by jumps of up to several centimeters. The velocities derived from GPS permanent stations have accuracies better than 1 mm/yr. Unfortunately the current station distribution does not allow description of the movements of all tectonic plates in the Adriatic region.

INTRODUCTION

The tectonics of the Eastern Mediterranean are influenced by three large plates (African, Arabian, Eurasian) and several minor ones (one or more Anatolian blocks, Sinai, and others). While the larger boundaries have been well known for several decades from seismicity, gravity measurements and geology, the other boundaries and the potential behavior of additional small plates are not. Along with other methods, GPS measurements can help to monitor crustal movements in that region over the past decade or longer. It is obvious that GPS measurements are a direct measure of surface movement, which can reflect both local influences and tectonic motion. In many cases there is a good coincidence between GPS-derived movements and long-term movements estimated from geology. Because of the vast area, large damages caused by earthquakes and future danger for big cities like Istanbul, several political authorities and research groups have already undertaken extensive investigations. This paper can only pick out some details with aspects of the international GPS services. The focus lies on the usage of GPS permanent sites that contribute to these services and how these services provide us with a stable reference that helps to separate the prime geophysical signal of station velocities from other effects.

N. Pinter et al. (eds.), The Adria Microplate: GPS Geodesy, Tectonics and Hazards, 169–181.

GENERAL METHODS

GPS delivers position accuracies down to the sub-centimeter level, and the choice of a reference system is therefore crucial. This reference is defined by the precise ephemeris of the satellites, a set of precise coordinates and velocities for the reference stations and consistent and well-defined model parameters, like the direction of the pole, earth tides and the structure of the atmosphere. The most accurate and most consistent reference system is provided by the International GPS Service, (IGS; http://igscb.jpl.nasa.gov/) together with station coordinates from ITRS (International Terrestrial Reference System) computed by the International Earth Rotation and Reference Systems Service (IERS). The last ITRS realization, ITRF2000 (Altamimi et al., 2001; Boucher et al., 2004; or http://lareg.ensg.ign.fr/ITRF/ITRF2000/) contains station coordinates from several hundred stations computed at a global scale. It is a cumulative solution that combines the coordinates and velocities from different space geodetic techniques. Only observations up to January, 2000 were used. It is updated by the IGS with the use of the European Reference Frame (EUREF) through the EUREF Permanent Network (EPN; http://www.euref-iag.net/). The weekly results also provide actual coordinates for new stations after Jan., 2000. All those stations are well monitored and have to fulfill special quality criteria. Provided there are no physical displacements of the antenna, the coordinates refer to the same marker.

In theory, one can use all coordinates of a station dating back to the first measurements at that site to produce a time series from which station velocities may be derived. Provided there are no other influences, those velocities represent the movements of the underlying geological structure. Unfortunately there are several components which disturb this geophysical signal. A partial list is given in Table 1. Fortunately all errors are not combined at any station, and the largest errors primarily influence the height component. For time series covering several years, the seasonal effects are smoothed out when computing station velocities. Unfortunately, jumps caused by changes in reference system do not disappear in the same way (see station ANKR = Ankara, Figure 1). These jumps can be partly eliminated by choosing a stable station and relating all networks to that site. The historical effects, caused for example by model updates and processing changes, can be eliminated by reprocessing old data. Reliable reprocessing is possible from the early 1990s until the start of IGS. All observations completed earlier lack continuity and represent campaign measurements. Also, precise orbits that are consistent with the later IGS orbits are not available before that date.

Table 1. Effects on station coordinates from a range of possible sources.

COMPONENT	PROBABLE BIAS
Reference System:	
Improvements in realization 1992-2000	About 20 mm
Changes in antenna definitions (satellites+receivers)	About 10 mm
Modeling errors	About 5 mm
Seasonal variations (earth center, atmosphere, ocean loadings)	Up to 10 mm
Site problems:	
Displacements (antenna change)	Up to 10 mm
Configuration (Radom, height)	Up to 60 mm
Receiver malfunction	Up to 30 mm
Seasonal variations (snow, ice)	Up to 60 mm
Seasonal variations (water content)	Up to 10 mm
Adjustment problems:	
Improved orbits 1992-2004	Up to 30 mm
Improved models (clocks, ionosphere, troposphere)	Up to 20 mm
Changing strategies (ambiguity/station fixing, cut-off angle)	Up to 20 mm
Network effects (configuration, weighting of results)	Up to 10 mm

The earlier results are definitely less accurate when compared to the newer ones (Reilinger et al. 1997). The incomplete satellite constellation, short observation periods, and adjustment problems considerably reduced the accuracy of those earlier results. Station coordinates which in 1987 had a typical error of 30 mm (an excellent value at that time) still introduce a bias of 3 mm/year into the velocities when estimated using a decade of observations. As a consequence, the earliest observations of 1988-1992 in the region of the Eastern Mediterranean, for example by (McClusky et al. 2000), were omitted here. It is also questionable which improvements might give orbital relaxation (Reilinger et al. 1997; McClusky et al. 2000) for a combination of campaigns since 1992. Provided there is no new information for the stations, all information is already stored in the IGS orbits and the ITRF coordinates of the different solutions. To remove the jumps due to reference frame changes, it would be more efficient to use transformation formulae, which are available for all ITRF solutions back to ITRF88 (Boucher and Altamimi 2001;

ftp://lareg.ensg.ign.fr/pub/itrf/ITRF.TP), or to stack the reprocessed campaigns together at the normal equation level. In any case, the positioning accuracies of the older campaigns remain at the level of several centimeters, with uncertainties in the height components being much greater.

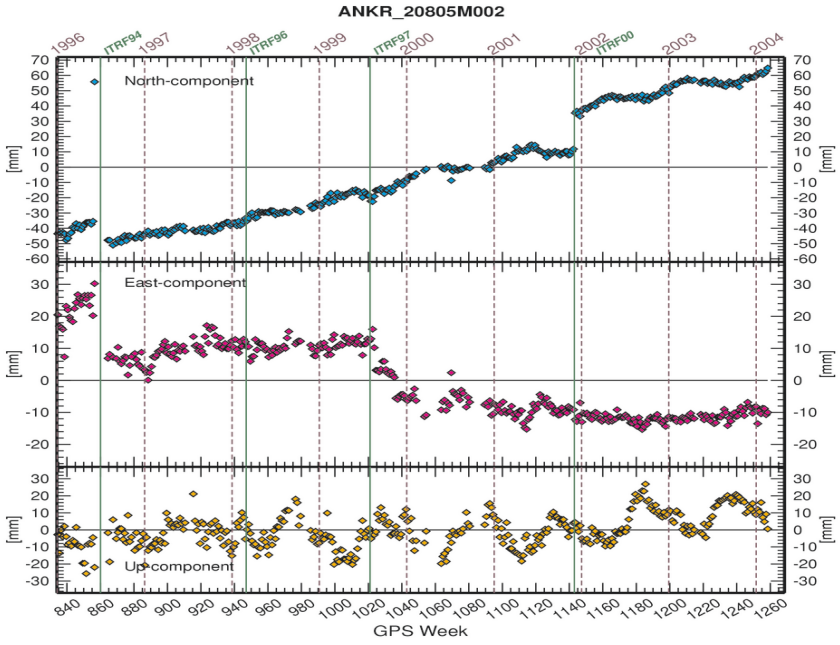

Figure 1. Example of jumps in time series due to changes in the ITRF reference system.

The usual way to calculate station velocities is to stack all daily or weekly solutions from both permanent and campaign observations together and to estimate the velocities from the change in station coordinates. There are several numerical methods to do this. A very simple method is to construct a regression line assuming constant velocities. However, the jumps mentioned above would strongly bias the estimation. It is therefore necessary to correct the jumps with known values before velocity estimation. The jumps caused by changes in reference frames might also be considered as jumps to be estimated and to be eliminated. However, this disregards, for example, frame rotations and scale biases. A better way of estimating velocities is to transform the solutions (daily, weekly, even monthly) to a common reference frame using, for example, a Helmert transformation and estimate the velocities by a Kalman filter (McClusky et al. 2000). However, we should note that the Helmert transformation has the disadvantage of being strongly dependent on the choice of reference points. The Helmert transformation also

may cause an unwanted elimination of a common geophysical signal. Figure 2 shows the transformation to the "stable" part of Eurasia, in which the ETRS89 system is defined. The transformation uses the formulae of (Boucher and Altamimi, 2001) between the different ITRF realizations. One can see minor jumps at the 5-10 mm level with the introduction of ITRF2000. In the east component, the strong signal shows the differential velocity of ANKR, which does not belong to the Eurasian plate. Figure 3 shows a refined time series in which the known jumps, and the general trend have been removed. Because the differential velocity is a trend, it is also removed, including the differential station velocity. The remaining residuals can be interpreted in different ways, including seasonal variations, variations due to the equipment, adjustment biases, but also geophysical signals (see Table 1).

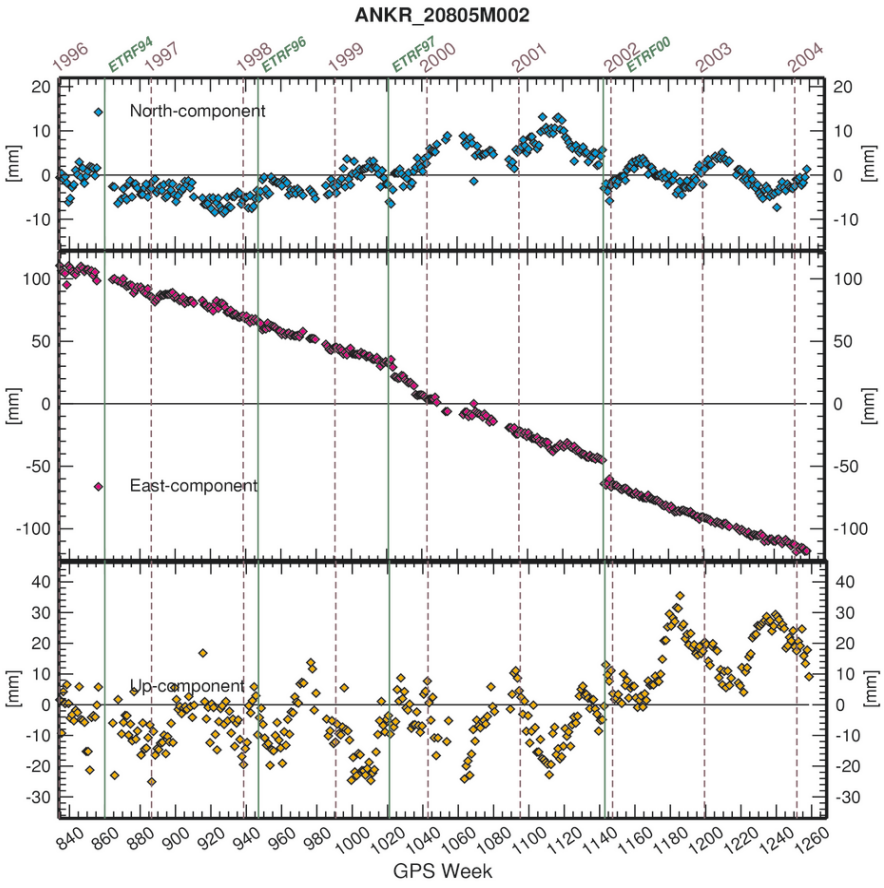

Figure 2. Example of small jumps in time series of ANKR after transformation from ITRF to ETRS89 (realized by ETRFYY), superimposed on a strong tectonic signal.

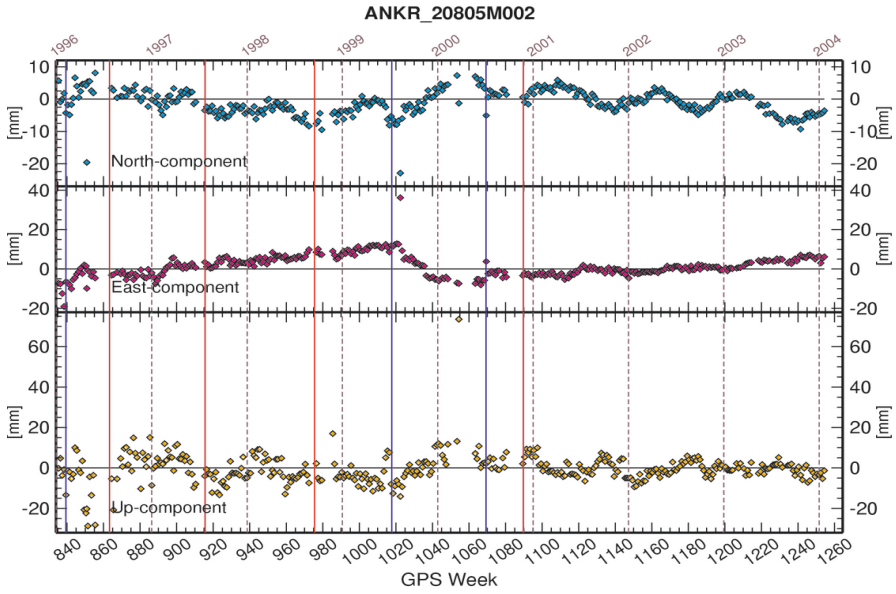

Figure 3. "Raw" time series at the same station (ANKR) as shown in Figure 2 with reference frame jumps and the overall trend removed. Cumulated EPN solutions, ITRF2000, central epoch.

Stacking normal equations of single solutions or estimations using coordinates and their covariance matrices are equivalent provided that the biases have been filtered or smoothed away. In every case, a sufficient time span and session distribution (for campaigns) are required. It is obvious that a velocity estimation using data covering a time span less than one year or with only two observation periods becomes very unreliable. If there are more data and a longer time span, one can even try to estimate changes in velocities over time. As Figure 3 suggests, there might be a change in the movement of ANKR in 1999 which might be connected to the Izmit earthquake. Estimating two different velocity sets and neglecting the transition in 1999, both eastern components differ significantly by more than 3 mm/year. Such interpretations should be corroborated by additional stations. GPS campaigns have the advantage of giving a more representative picture by proving that this change in movement is representative of the region and not of one station. Therefore both observation types, permanent and epoch, can be combined for geophysical interpretation.

DATA SETS

The Eastern Mediterranean region does not contain many permanent stations and even campaign measurements are irregularly distributed. The African Plate is very poorly covered. Even concentrating only on the boundary zones, not all major faults can be observed. The permanent stations in the region may be divided into three groups according to their standards and availability:

- public stations following international standards (IGS and EPN),
- public stations, probably following international standards,
- non-public stations.

Many of the more than 20 stations in Table 2 are located in Turkey, but the distribution over the different tectonic units is very uneven. In most cases, the locations were not chosen to monitor fault zones, but rather for other purposes. Unfortunately, a large number (one third) of the stations are not yet or no longer operating. The spacing of stations is also quite uneven and varies between 100 km up to 1,000 km and more.

Since the late 1980s, efforts have been made to observe some regions by GPS campaigns. Western Turkey and Greece have been observed several times as well as the Caucasus. There are few observations at the African (Fernandes et al., 2003) and Arabian plate boundaries, but they will be much better covered in the future. Outside the Aegean Sea, only Cyprus can be observed by GPS due to lack of islands and oil platforms in the Eastern Mediterranean. As can be seen easily from Table 2, no public station exists in Greece or in large parts of Turkey. A handful of non-public stations is known from oral communication, but these may or may not currently be operating.

Table 2. Public IGS/EPN and other GPS permanent stations around the Eastern Mediterranean.

STATION	NET	ACRONYM	PLATE
Amman (Jordan)	IGS	AMMN	Arabian
Ankara (Turkey)	IGS	ANKR	Anatolian
Manama (Bahrain)	IGS	BAHR	Arabian
Bucuresti (Romania)	IGS	BUCU	Eurasian
Simeiz (Ukraine)	UNAVCO	CRAO	Eurasian
Metzoki Dragot (Israel)	IGS	DRAG	Sinai?
Diyarbakir (Turkey)	IGS	DYR2	Anatolian
Halat Ammar (Saudiarabia)	UNAVCO	HALY	Arabian
Istanbul (Turkey)	IGS	ISTA	Eurasian
Jbeil (Lebanon)	UNAVCO	LAUG	Arabian?
Mersin (Turkey)	UNAVCO	MERS	Anatolian
Namas (Saudiarabia)	UNAVCO	NAMA	Arabian
Nicosia (Cyprus)	IGS	NICO	?
Yerevan (Armenia)	IGS	NSSP	?
Helwan (Egypt)	UNAVCO	PHLW	African
Mitzpe Ramon (Israel)	IGS	RAMO	Sinai?
Sofia (Bulgaria)	IGS	SOFI	Eurasian
Solar Village (Saudiarabia)	UNAVCO	SOLA	Arabian
Trabzon (Turkey)	IGS	TRAB	Eurasian
Gebze (Turkey)	IGS	TUBI	Eurasian
Damascus (Syria)	UNAVCO	UDMC	Arabian
Yibal (Oman)	IGS	YIBL	Arabian
Zelenchukskaya (Russia)	IGS	ZECK	Eurasian

STATION MONITORING EXAMPLES AND VELOCITIES DERIVED FROM GPS

As an example of possible coordinate changes without any tectonic meaning, the site RAMO (Israel) can be mentioned. Figure 4 has been detrended in order to highlight the residuals. Leaving the height problems aside, one can see a sudden offset in the North and East components of 10-20 mm in the summer of 2000, followed by a change in the remaining trend and a yearly oscillation with the amplitudes damped over time. At RAMO, an antenna change caused a lateral coordinate oscillation of about one year with an amplitude of up to 20 mm. Each geophysical signal and even the station velocity are biased by this effect.

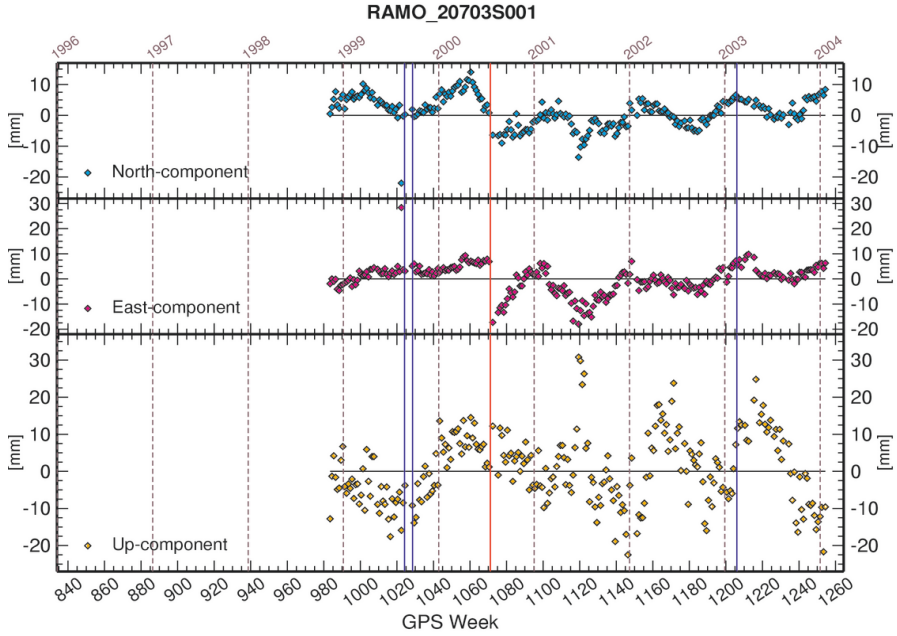

Figure 4. Example of "raw" time series with equipment problems. System as in Figure 3.

The potential tectonic effect at ANKR was already discussed. This effect is much stronger at TUBI near Izmit, where the co-seismic displacement was -33 cm to the North, +53 cm to the East, and +6 cm in the Vertical. A post-seismic creep of up to 3 cm can be seen in Figure 5. It should also be mentioned that the station is stable since at least the beginning of 2001. No significant signal can be seen at ANKR at the time of the Bingöl earthquake of May 1, 2003. In most cases, the permanent stations seem to be too far away from the epicenters for the displacements to show up in their time series.

The ITRF velocities and, more recently, the EPN velocities are estimated either by removing the known jumps from the time series or by subdividing the time span. Within the EPN, OLG Observatory Lustbuehel Graz (OLG) has the responsibility to monitor stations in the zone around the Eastern Mediterranean and to compute the size of jumps (Cristea and Stangl, 2003). Table 3 gives the recent estimations of velocities for several stations and compares it to the NUVEL-1A values derived from geology. All stations north of the North Anatolian Fault have very similar velocities, close to NUVEL-1A values for the Eurasian Plate, but with a significant bias (Altamimi and Boucher, 2002). It should be mentioned again that TUBI near the fault also behaves in the same way. This is not the case for ANKR, where the eastern component differs by more than 20 mm/year. This motion is well known, the values at the same (epoch) site are –2/-27 mm/year (Reilinger et al., 1997, site ANKA) or –2/-21 mm/year (McClusky et al., 2000, ANKA and ANKR) for the North/East components with respect to a fixed Eurasian frame.

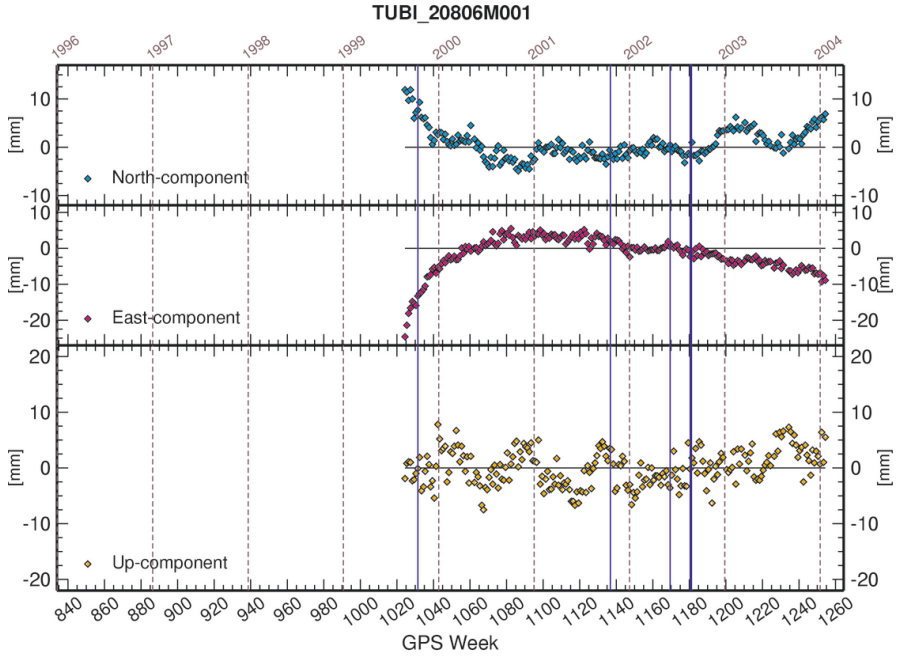

Figure 5. Post-seismic creep of TUBI after the Izmit earthquake of 1999. System of Figure 3.

Given the fact that only NSSP (Armenia) is available at the very complicated transition zone between several faults, only a few hints regarding the movements in this region can be given. It seems that movement of this site is straight to the North and not to the northwest as was indicated in Lundgren et al. (1998). The shortening across the Caucasus, expressed by the difference

NSSP-ZECK, can be estimated at 5 mm/year instead of the 12 mm/year previously proposed (Reilinger et al., 1997), provided that NSSP is representative. The differential values 8/4 mm/year for the North/East components (McClusky et al., 2000, same site NSSP) do not fit well.

Cyprus does not move with the "stable" part of Eurasia but seems to be pushed to the northwest by several mm/year, the EPN values of Table 3 should be better than those 4/-5 mm/year given in McClusky et al. (2000, same site NICO) because of the much longer time span (5 years versus 1.5).

Due to lack of stations within the Eastern part of the African Plate, no comparisons are available there. Both stations in Israel, DRAG and RAMO, show the same feature. Both are located on the Sinai block and suggest a strong connection to the African Plate or its eastern Somalia block (Fernandes et al., 2003). Also, a significant deviation from the NUVEL-1A values to the northwest can be seen, which seems to be characteristic for the Somalia block (McClusky et al., 2000, Fernandes et al., 2003).

The regions of western Turkey, the Aegean Sea, mainland Greece, and the East Anatolian Fault, are covered by extensive campaign data (McClusky et al., 2000; Reilinger et al., 1997). Unfortunately no public permanent GPS station can be used as a control in this regions.

Table3. EPN and NUVEL-1A velocity components of permanent stations (mm/year) EPN accuracy better than 1mm/year.

STATION	PLATE	NORTH		EAST		UP
		EPN	NU	EPN	NU	EPN
BUCU	Eurasian	12	11	23	23	-1
ISTA	Eurasian	8	10	26	24	1
SOFI	Eurasian	11	12	24	23	0
TRAB	Eurasian	13	8	24	25	0
TUBI	Eurasian	8	10	23	24	-4
ZECK	Eurasian	11	7	24	25	2
NSSP	???	16	7	26	25	5
NICO	???	16	9	17	24	-2
RAMO	African?	21	20	20	25	-2
DRAG	African?	20	19	22	25	2
ANKR before 1999	Anatolian	11	10	2	24	-1
ANKR after 1999	Anatolian	12	10	-2	24	1

CONCLUSIONS

The use of GPS permanent stations together with campaign data already gives a good picture of the movements of some parts of the Eastern Mediterranean region. Permanent stations provide the stability of the reference frame, allow high resolution in time, and usually have a multi-purpose role which reduces the financial maintenance costs. Campaigns are very useful for high resolution in space, so that several regions of interest can be covered without exorbitant costs. The combination of permanent and campaign GPS observations gives a stable, high-precision framework for long-term investigations of crustal movements with accuracies of better than 1 mm/year. This approach can be implemented by comparing the station velocities of permanent stations with those derived from previous GPS campaigns. The biggest improvement occurred during the early 1990s with the introduction of the International GPS Service. Older campaigns must be neglected in most cases due to their large uncertainties.

One should be aware that influences which might affect the geophysical signal of crustal movements must be considered. All reference-frame changes can be taken into account by any one of several numerical methods. Assuming that crustal movements of larger tectonic blocks do not vary much in time, influences of higher frequencies, for example seasonal effects, can be separated. Station effects should be controlled by comparison with neighboring sites and by inspection of each time series. Unfortunately, in many cases there are only few or no controls due to the sparse density of stations.

Some tectonic regions of the Eastern Mediterranean are well covered with campaign measurements, for example Greece and Turkey south of the North Anatolian Fault, but not with permanent stations. The eastern part of the African Plate presently contains no permanent station at all. The boundaries between the African, Arabian, and Anatolian plates are very sparsely covered and need much more attention, even where seismic activity is low. The collision zone of eastern Turkey, western Iran, and the Caucasus region would require much more than the existing one permanent station to yield insight into the recent movements along theseveral faults meeting there.

REFERENCES

Altamimi Z., Angermann D., Argus D., Blewitt G., Boucher C., Chao B., Drewes H., Eanes R., Feissel M., Ferland R., Herring T., Holt B., Johannson J., Larson K., Ma C., Manning J., Meertens C., Nothnagel A., Pavlis E., Petit G., Ray J., Ries J., Scherneck H.-G., Sillard P., Watkins M. The Terrestrial Reference Frame and the Dynamic Earth. EOS Trans AGU 2001; 82(25): 273-279.

Altamimi Z., Boucher C. The ITRS and ETRS89 Relationship: New Results from ITRF2000, EUREF Publication No. 10, Mitteilungen des Bundesamtes für Kartographie und Geodäsie Band 23, Frankfurt am Main 2002; 49-52.

Boucher C., Altamimi Z. 2001, Specifications for reference frame fixing in the analysis of a EUREF GPS-campaign, available from http://lareg.ensg.ign.fr/EUREF/memo.pdf.

Boucher C., Altamimi Z., Sillard P., Feissel-Vernier M. The ITRF2000, Technical Note No. 31, 2004 (In print, available online).

Cristea E., Stangl G. OLG Monitoring of the Balkan Mountains and the Eastern Mediterranean area – Report 2002, EUREF Publication No. 12, Mitteilungen des Bundesamtes für Kartographie und Geodäsie Band 29, Frankfurt am Main 2003; 73-75.

Fernandes R.M.S., Ambrosius B.A.C., Noomen R., Bastos L., Wortel M.J.R., Spakman W., Govers R. The relative motion between Africa and Eurasia as derived from ITRF2000 and GPS data. Geophys. Res. Lett. 2003; 30(16): 1828, doi:10.1029/2003GL017089.

Lundgren P., Giardini D., Russo R. M. A geodynamic framework for eastern Mediterranean kinematics. Geophys. Res. Lett. 1998; 25(21): 4007-4010.

McClusky S., Balassanian S., Barka A., Demir C., Ergintav S., Georgiev I., Gurkan O., Hamburger M., Hurst K., Kahle H., Kastens K., Kekelidze G., King R., Koetzev V., Lenk O., Mahmoud S., Mishin A., Nadariya M., Ouzounis A., Paradissis D., Peter Y., Prilepin M., Reilinger R., Sanli I., Seeger H., Tealeb A., Toksöz M. N., Veis G. Global Positioning System constraints on plate kinematics and dynamics in the eastern Mediterranean and Caucasus. J. Geophys. Res. 2000; 105 (B3): 5695-5719.

Reilinger R. E., McClusky S. C., Oral M. B., King R. W., Toksöz M. N., Barka A. A., Kinik I., Lenk O., Sanli I. Global Positioning System measurements of present-day crustal movements in the Arabia-Africa-Eurasia plate collision zone. J. Geophys. Res. 1997; 102 (B5): 9983-9999.

CONSORTIUM FOR CENTRAL EUROPEAN GPS GEODYNAMIC REFERENCE NETWORK (CEGRN CONSORTIUM)

István Fejes
Satellite Geodetic Observatory, FÖMI, Budapest, Hungary
fejesi@sgo.fomi.hu

ABSTRACT

Application of GPS measurement for monitoring tectonic processes in Central Europe on a regional scale was initiated in 1993 in the framework of the "Central Europe Regional Geodynamics Project", or CERGOP. The initial basic reference network (CEGRN) consisted of 31 sites, established in 1994 and monitored regularly ever since. These sites already have spanned7 epochs of monitoring results over 9 years. CEGRN was extended in 1998 and presently consists of 62 official sites of which about 50% are permanently operating stations. The additional 31 sites monitored since 1999 span 3 epochs of monitoring results over 4 years. Densification of CEGRN up to about 100 sites is foreseen in the framework of the CERGOP-2/Environment project, supported within the EU 5th FP in the years 2003-2006. The CEGRN network meets the highest quality standards and is outstanding in the areas of homogeneity and long time series of measurements. A consortium of institutes was formally established in 2001 for securing the long-term operation of CEGRN.

INTRODUCTION

The Consortium for Central European GPS Geodynamic Reference Network of 14 institutes from 13 Central European countries was formally established in 2001. The consortium members are committed to long-term monitoring and maintenance of CEGRN. The consortium concept emphasizes long-term *binding institutional commitments*. This opens the way to a broader and more efficient collaboration and a better division of responsibilities among participants. Another aspect of this collaboration is the clear division between "*maintaining and operating a facility*" and "*using a facility*". CEGRN should be considered as *a facility,* a well-established research infrastructure in Central Europe for earth sciences. This infrastructure is used as a research and educational tool in the region by a large number of users outside the consortium.

N. Pinter et al. (eds.), The Adria Microplate: GPS Geodesy, Tectonics and Hazards, 183–193.

THE OBJECTIVES

The CEGRN Consortium is a non-profit organization of institutes that supports and promotes:

- coordinated establishment, maintenance and upgrades of CEGRN sites,
- monitoring CEGRN by permanent and epoch type-measurements and
- the establishment, maintenance and development of the CEGRN Data Centre and Processing Centres.

MEMBERSHIP

The "Memorandum of Agreement" of the consortium was signed on 5 September, 2001 in Budapest, Hungary. The agreement shall remain in force for a period of five years.

The following 14 institutes have joined the Consortium so far:

1. Space Research Institute, Austrian Academy of Sciences, Graz, Austria, represented by Dr. P. Pesec;
2. Department of Geodesy, Faculty of Civil Engineering, University of Sarajevo, Bosnia- Herzegovina, represented by Ms. M. Mulic
3. Central Laboratory for Geodesy, Bulgarian Academy of Sciences, Sofia, Bulgaria, represented by Prof. G. Milev;
4. Research Institute of Geodesy, Topography and Cartography, Zdiby, Czech Republic, represented by Dr. J. Simek;
5. Faculty of Geodesy, University of Zagreb, Zagreb, Croatia, represented by Dr. D. Medak
6. Faculty of Civil Engineering and Geodesy, University of Bundeswehr, Munich, Germany, represented by Prof. M. Becker;
7. Institute of Geodesy Cartography and Remote Sensing (FÖMI), Budapest, Hungary, represented by Prof. I. Fejes;
8. Centro di Geodesia, Agencia Spaciale Italiana, Matera, Italy, represented by Dr. F. Vespe;
9. Institute of Geodesy and Geodetic Astronomy, Warsaw University of Technology, Warsaw, Poland, represented by Prof. J. Sledzinski;
10. The Institute of Cadastre, Geodesy, Photogrammetry and Cartography, Bucharest, Romania, represented by Mr. F. Ciobanu;
11. Department of Theoretical Geodesy, Slovak University of Technology, Bratislava, Slovakia, represented by Prof. M. Mojzes;
12. Faculty of Civil and Geodetic Engineering, University of Ljubljana, Slovenia, represented by Prof. F. Vodopivec;

13. Chair of Geodesy and Astronomy, Lviv Polytechnic National University, Lviv, Ukraine, represented by Prof. F. Zablotskij;
14. Dipartimento di Geologia, Paleontologia e Geofisica, University of Padova, Padova, Italy, represented by Prof. A. Caporali

THE CEGRN

The initial basic reference network of CEGRN, consisting of 31 sites, was established in 1994 (Fejes and Kenyeres, 1994) and monitored regularly ever since. These sites now span 7 epochs of monitoring results over 9 years. CEGRN was extended in 1998 and presently consists of 62 functioning official sites, of which about 50% are permanently operating stations. The additional 31 sites monitored since 1999 span 3 epochs of monitoring results over 4 years. Figure 1 shows the geographic distribution of the CEGRN sites as of 2004, and the list of the sites is given in Table 1. Some of the earlier CEGRN sites are no longer functioning for various reasons such as displacements, mechanical damage, etc. These defunct sites are listed in Table 2. In the framework of the CERGOP-2/Environment project (Fejes and Pesec, 2003), further extension of CEGRN is planned up to about 100 sites. Each monitoring campaign to date took 5 days of continuous observations, generally in the same period of the year in order to reduce seasonal effects. The participation of the sites in the monitoring campaigns is given in Table 3 (based on Stangl, 2003). Note that in a few cases, a new site was established near the old one due to site destruction (e.g. GILA – GIL2, and VATR – VAT1), and monitoring continued at the new site. In some other cases, the new site is a newly established permanent station near the old epoch site (e.g. BUCA – BUCU, and UZHD – UZHL). At these sites, parallel occupations ensure good quality ties between the old and new sites. As a general policy, however, the site displacements were minimized. The high quality of results is illustrated in Figure 2, where the sums of daily repeatabilities are shown for the series of monitoring campaigns. We can safely state that the horizontal accuracies (1 sigma) are equal to or better than 3.1 mm and the vertical accuracies (1 sigma) are equal to or better than 7.3 mm.

THE COMMITMENTS

Member institutes contribute to CEGRN with their own established and accepted sites, with site maintenance and with coordinated observations on these sites. These institutes are committed to the highest quality standards and a minimum of 5*24 hours observations at least every second year. They

supply observational data to the common Data Centre. Additional contributions by designated institutes consist of operation of the Data Centre and/or Processing Centres.

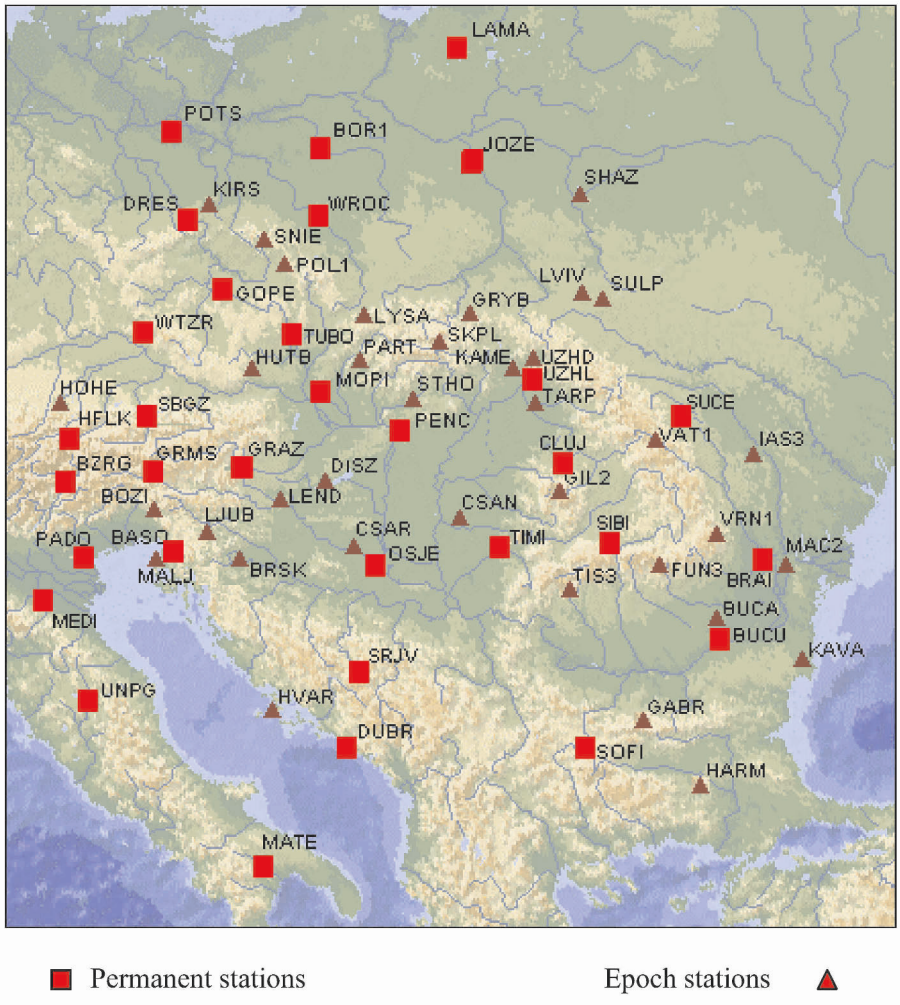

Figure 1. The Central European GPS Geodynamic Reference Network (CEGRN) in 2004.

Table 1. The Central European GPS Geodynamic Reference Network

Country	Site	Code	P/E	Lat.	Long.
AUT	Graz	GRAZ	P	47° 04′	15° 30′
	Reisseck	GRMS	P	46° 55′	13° 22′
	Innsbruck	HFLK	P	47° 19′	11° 23′
	Hutbiegl	HUTB	E	48° 39′	15° 36′
	Salzburg	SBGZ	P	47° 48′	13° 07′
BIH	Sarajevo	SRJV	P	43° 52′	18° 24′
BUL	Gabrovo	GABR	E	42° 58′	25° 16′
	Harmanli	HARM	E	41° 53′	25° 51′
	Kavarna	KAVA	E	43° 25′	28° 22′
	Sofia	SOFI	P	42° 33′	23° 24′
CRO	Brusnik	BRSK	E	45° 35′	15° 34′
	Dubrovnik	DUBR	P	42° 38′	18° 07′
	Hvar	HVAR	E	43° 11′	16° 27′
	Osijek	OSJE	P	45° 34′	18° 41′
CZE	Pecny	GOPE	P	49° 55′	14° 47′
	Lysa Hora	LYSA	E	49° 33′	18° 27′
	Polom	POL1	E	50° 21′	16° 19′
	Brno	TUBO	P	49° 12′	16° 36′
GER	Dresden	DRES	P	51° 02′	13° 44′
	Hohenpeissenberg	HOHE	E	47° 48′	11° 01′
	Potsdam	POTS	P	52° 23′	13° 04′
	Wettzell	WTZR	P	49° 09′	12° 53
HUN	Csanádalberti	CSAN	E	46° 19′	20° 40′
	Csarnóta	CSAR	E	45° 53′	18° 13′
	Diszel	DISZ	E	46° 53′	17° 29′
	Penc	PENC	P	47° 47′	19° 17′
	Tarpa	TARP	E	48° 08′	22° 33′
ITA	Trieste	BASO	P	45° 39′	13° 53′
	Bolzano	BZRG	P	46° 29′	11° 22′
	Matera	MATE	P	40° 39′	16° 42′
	Medicina	MEDI	P	44° 31′	11° 39′
	Padova	PADO	P	45° 24′	11°53′
	Perugia	UNPG	P	43° 07′	12° 21′

Table 1. (cont.)

POL	Borowiec	BOR1	P	52° 17′	17° 04′
	Grybow	GRYB	E	49° 38′	20° 57′
	Jozefoslaw	JOZE	P	52° 06′	21° 02′
	Lamkowko	LAMA	P	53° 54′	20° 40′
	Sniezka	SNIE	E	50° 44′	15° 44′
	Wroclaw	WROC	P	51° 07′	17° 04′
ROM	Braila	BRAI	P	45° 16′	27° 58′
	Bucharest	BUCA	E	44° 21′	26° 03′
	Bucharest	BUCU	P	44° 28′	26° 08′
	Cluj	CLUJ	P	46° 46′	23° 35′
	Fundata	FUN3	E	45° 25′	25° 15′
	Macin	MAC2	E	45° 15′	28° 11′
	Sibiu	SIBI	P	45° 47′	24° 08′
	Suceava	SUCE	P	47° 39′	26° 14′
	Timisoara	TIMI	P	45° 45′	21° 14′
	Tismana	TIS3	E	45° 08′	23° 08′
	Vrancea	VRN1	E	45° 51′	26° 39′
SVK	Kamenica nad Cirochou	KAME	E	48° 56′	22° 01′
	Modra-Piesky	MOPI	P	48° 22′	17° 16′
	Partizánske	PART	E	48° 36′	18° 20′
	Skalnate Pleso	SKPL	E	49° 11′	20° 14′
	Strazna Hora	STHO	E	48° 13′	19° 32′
SLO	Bozica	BOZI	E	46° 16′	13° 29′
	Lendavske gorice	LEND	E	46° 34′	16° 29′
	Ljubljana	LJUB	E	46° 03′	14° 30′
	Malija	MALJ	E	45° 30′	13° 39′
UKR	Lviv	LVIV	E	49° 55′	23° 57
	Shazk	SHAZ	E	51° 28′	23° 51′
	Sulp	SULP	E	49° 50′	24° 01′
	Uzhgorod	UZHD	E	48° 34′	22° 27′
	Uzhgorod	UZHL	P	48° 38′	22° 18′

Table 2. CEGRN defunct sites

Country	Site	Code	P/E	Lat.	Long.
ALB	Tirana	TIRA	P	41° 19′	19° 46′
GER	Kirschberg	KIRS	E	51° 13′	14° 17′
ITA	Padova	UPAD	P	45° 24′	11°53′
ROM	Gilau	GIL2	E	46° 41′	23° 03′
	Iasi-Repedea	IAS3	E	47° 05′	27° 39′
	Vatra Dornei	VAT1	E	47° 27′	25° 21′
SLO	Tosko Celo	TOSK	P	46° 05′	14° 25′

ORGANIZATION

The governing body of the consortium consists of the representatives of the member institutes as appointed by each institute's director. The governing body is called the CEGRN Consortium Governing Board (CCGB). CCGB appoints a chair and a co-chair from its members who will remain in office for a 3-year period. The chair, the co-chair and 2 additional members selected by the CCGB together form the CEGRN Steering Committee for facilitating operation and prompt decision-making. CCGB convenes users meetings at least once every second year for the purpose of obtaining feedback from the user community on the performance of CEGRN and on directions for future developments.

The Space Research Institute, of the Austrian Academy of Sciences in Graz, acts as CEGRN Data Centre.

The following 5 institutes maintain and operate CEGRN Processing Centres:

- FÖMI, Satellite Geodetic Observatory, Penc, Hungary,
- Institute of Geodesy and Geodetic Astronomy of the Warsaw University of Technology, Warsaw, Poland,
- Agenzia Spaziale Italiana Centro di Geodesia Spaziale, Matera, Italy,
- Space Research Institute of the Austrian Academy of Sciences, Austria,
- Department of Theoretical Geodesy of the Faculty of Civil Engineering of the Slovak University of Technology, Bratislava, Slovakia.

Table 3. Participation in monitoring campaigns

Country	Marker Name	SITE OCCUPATION						
		1994	1995	1996	1997	1999	2001	2003
AUT	GRAZ	x	x	x	x	x	x	x
	GRMS		x	x	x	(x)		x
	HFLK		x	x	x	x	x	
	HUTB	x	x	x	x	x	x	x
	SBGZ					x	x	x
BIH	SRJV					x	x	x
BUL	GABR							x
	HARM			x	x			x
	KAVA							x
	SOFI			x	x	x	x	x
CRO	BRSK	x	x	x	x	x	x	x
	CAOP						x	x
	DUBR						x	x
	HVAR				x	x	x	x
	OSJE					(x)	x	x
CZE	GOPE	x	x	x	x	x	x	x
	LYSA					x	x	x
	POLO	x	x	x				
	POL1					x	x	x
	SNEZ							x
	TUBO		x			x	x	x
GER	DRES					x	x	x
	HOHE	x	x	x	x	x		x
	KIRS	x	x	x	x	x		
	POTS		x	x	x	x	x	x
	WTZR			x	x	x	x	x
HUN	CSAN					x	x	x
	CSAR	x	x	x	x	x	x	x
	DISZ	x	x	x	x	x	x	x
	PENC	x	x	x	x	x	x	x
	TARP					x	x	x
ITA	BASO	x	x	x	x			
	BZRG					x	x	x
	CAME							x
	MATE	x	x	x	x	x	x	x
	MEDI					x	x	x
	UPAD	(x)	x	x	x	x	x	
	PADO							x
	UNPG						x	x

Table 3. (Cont.)

Country	Marker Name	OCCUPATION						
		1994	1995	1996	1997	1999	2001	2003
POL	BOR1	x	x	x	x	x	x	x
	GRYB	x	x	x	x	x	x	x
	JOZE	x	x	x	x	x	x	x
	LAMA	x	x	x	x	x	x	x
	SNIE	x	x	x	x	x	x	x
	WROC					x	x	x
ROM	BRAI							x
	BUCA		x	x	x	x		x
	BUCU					x	x	x
	CLUJ							x
	FUND		x	x				
	FUN3					x	x	x
	GILA		x	x				
	GIL2				x	x		
	IAS3			x	x	x		
	MACI		x	x	x			
	MAC2							x
	SIBI							x
	SUCE							x
	TIMI							x
	TIS3			x	x	x		x
	VATR		x	x				
	VAT1				x	x		
	VRAN		x	x				
	VRN1				x	x	x	x
SVK	KAME					x	x	x
	MOPI	x	x	x	x	x	x	x
	PART					x	x	x
	SKPL	x	x	x	x	x	x	x
	STHO	x	x	x	x	x	x	x
SLO	BOZI					x	x	x
	LEND					x	x	
	LJUB	x	x	x	x	x	x	x
	MALJ					x	x	x
	MRZL							x
	SNEK							x
UKR	IVAN							x
	LVIV		x	x	x	x	x	x
	SHAZ					x		
	SULP				x	x	x	x
	UZHD	x	x	x	x	x	x	x
	UZHL						x	x

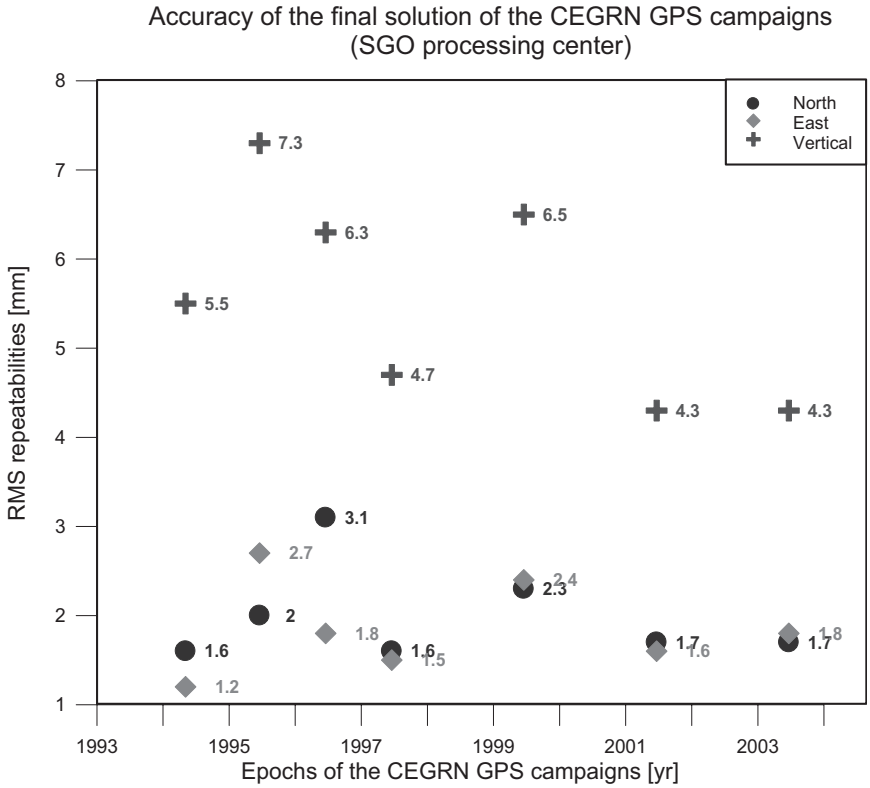

Figure 2. Overall daily root mean square (RMS) repeatability of CEGRN site positions in the epoch campaigns

DATA ACCESS POLICY

The data access is regulated the following ways: (1) CEGRN data from the permanent stations are freely available for all users; (2) epoch CEGRN data are freely available for CEGRN consortium member institutes; (3) member institutes are free to decide on the transfer of their own data to external parties; (4) CEGRN epoch data availability, however, is restricted for users outside of the consortium until the end of the EU project (in 2006); (5) requests for CEGRN data export for outside users should be approved by the Steering Committee on case-by-case basis; and (6) any publication of results based on CEGRN data should contain a note of acknowledgement to the consortium.

MEMBERSHIP POLICY

The consortium is open to institutes in the Central European region. New membership applications should be addressed to the Chairman and should contain the scientific justification for the request, proved performance of the institute in the field of geodynamic investigations and commitments to the objectives and rules of the consortium, as described in the Memorandum of Agreement. Acceptance is subject to the approval of the CCGB or, in urgent cases, by the Steering Committee.

CONCLUSION

The CEGRN consortium serves as the institutional foundation for the CERGOP-2/Environment project. International cooperation among the institutes of the consortium ensures the long-term maintenance of CEGRN and high-quality data products. CEGRN serves as a virtual large-scale facility in Central Europe for a large number of studies in earth sciences (e.g., Becker et al., 2002; Grenerczy et al. 2000; Grenerczy, 2000). Further details can be found at the consortium's website (**www.fomi.hu/cegrn**).

ACKNOWLEDGEMENTS

The author thanks the valuable contributions of Dr. Gyula Grenerczy and Mr. Gábor Virág. This work was supported financially by the OTKA T042900 and by the EU EVK2-CT-2002-00140 grants.

REFERENCES

Becker M., Cristea E., Figurski M. et al. Central European Intraplate Velocities from CEGRN Campaigns. Reports on Geodesy 2002; 1(61): 83.

Fejes I., Kenyeres A. The Central Europe Regional Geodynamic Project (CERGOP). Proc. 1st Turkish Int. Symp. on Deformations. Sept. 5-9, 1994, Istanbul, Turkey. p.991.

Fejes I., Pesec P. CERGOP-2/Environment – a challenge for the next 3 years. Reports on Geodesy 2003; 1(64): 23.

Grenerczy Gy., Kenyeres A., Fejes I. Present crustal movement and strain distribution in Central Europe inferred from GPS measurements. J. Geophys. Res. 2000; 105 (B9): 21,835.

Grenerczy Gy. A decade of space geodetic monitoring of crustal deformation from the Mediterranean to Fennoscandia. Proc. of the 10th General Assembly of the WEGENER Project, San Fernando, Spain 18-22 Sept., Boletin ROA, No. 3/2000, 100, 2000.

Stangl G. CEGRN'03 Status and Availability – Proposed Processing Rules. Geodesy 2003; 3(66): 139.

GEODYNAMIC INVESTIGATION IN BOSNIA AND HERZEGOVINA

Medžida Mulić, Mirza Bašagić, and Safet Čičić,
University of Sarajevo, Civil Engineering Faculty, Sarajevo, Bosnia and Herzegovina
mmulic@yahoo.com

ABSTRACT

This paper is an overview of the geological and tectonic framework of Bosnia and Herzegovina, recent geodetic monitoring within the country, and plans for future geodynamic investigations using GPS. The geology, tectonics, and crustal structure underlying Bosnia and Herzegovina are outlined. Geodynamic investigation in Bosnia and Herzegovina using GPS started in 1998. In the summer of 2000, a GPS campaign for the densification of the reference-frame network for Bosnia was carried out, and 23 points were observed. The data of the 2000 campaign have not yet been processed, but this processing is planned for the near future, and Bosnian velocities will be available for geodynamical research into motion of the Adriatic microplate or other regional problems. The complexity and richness of the geology and geodynamics of the region in and around Bosnia and Herzegovina merits further densification of the GPS network, which would have benefits for geodynamical research as well as hazard assessment and regional environmental protection.

INTRODUCTION

This paper is an overview of geodetic, geological, and tectonic investigations in Bosnia and Herzegovina and plans for future geodynamic investigations using GPS. Bosnia and Herzegovina is composed of three geomorphologic units: the Pannonian Plain, the Dinaric mountain range, and the Adriatic zone. Climatic conditions in this region range from continental to temperate-continental to sub-Mediterranean and Mediterranean climate. In most, winters are long and cold.

Bosnia and Herzegovina is composed of a complex assemblage of geological units, including sedimentary, igneous and metamorphic rocks that range in age from Paleozoic to Cenozoic. This geologic framework comprises three geotectonic zones: the Outer, Central and Inner Dinarides. The detailed lithology and stratigraphy of these regions have been described by Čičić (2002) and on the 1:300,000 geological map of Bosnia and Herzegovina, published in 2003.

Geodynamic investigation within Bosnia and Herzegovina using GPS techniques started 1998. One point near Sarajevo (SARA) was observed in the

N. Pinter et al. (eds.), The Adria Microplate: GPS Geodesy, Tectonics and Hazards, 195–207.

frame of the EXTAGED 98 GPS campaign. The data were process by the Institute for Geodesy and Geodetic Astronomy of Warsaw University of Technology. In the next year (1999), Bosnia and Herzegovina was officially involved in the CERGOP geodynamical project.. Since 1999, SRJV was officially accepted as a EUREF permanent station and has been part of the regional CEGRN network.

GEOLOGY OF BOSNIA AND HERZEGOVINA

In 2003, the geological map of Bosnia and Herzegovina was printed at a scale of 1:300,000. The map synthesized all important data and results obtained during previous 1:100,000 mapping, by different special studies, and in many doctoral dissertations and theses. In Bosnia and Herzegovina, igneous, metamorphic and sediment rock masses date from Silurian to Quaternary in age and are related to the deformational events of the Hercynian and Alpine orogenies. A review of the litho-stratigraphy and tectonics of Bosnia and Herzegovina as well as applications and implications of the region's geologic framework are presented in this paper.

Geological History of Bosnia and Herzegovina

Palaeozoic Era

Lithological units of Palaeozoic age underlie about 9% of Bosnia and Herzegovina. These units range in age from Silurian to Permian. The existence of rocks of Cambrian to Orovician age near the village of Crvice, but these units have not been rigorously studied, mapped, or dated.

Outcrops of the rocks of Silurian age are found near the Drina River near Ustikolina. They are represented by horizontally stratified cherty shale, phylltic shale, and limestone. The Silurian sequence is between 100 m and 300 m thick. Rocks of Upper Silurian to Devonian age include shale, rhyolite, quartzite, and limestone, with a total thickness of up to 800 m. These units crop out across central Bosnia (Vranica, Bitovnja) over an area of about 1,000 km^2. Ages are assigned based on conodont stratigraphy, which does not allow more detailed age determinations within this sequence.

Rocks of Devonian age are found in southeastern and central Bosnia around Prača and Goražde and in the vicinity of Jajce. Sedimentary material from the Lower to Middle Devonian is composed of limestone containing corals and conodonts (G. Vakuf, pers. comm.), as well as dolomite, meta-sandstone, and shale (near Prača and Šipovo). Thickness of this formation ranges from 100 to 700 m. Different clastic and carbonate sediments of the Upper Devonian have been mapped in southeastern Bosnia and in the Pliva

river basin. Significant portions of central Bosnia and the area surrounding Jajce are underlain by rhyolite; spilite and diabase are found in southeastern Bosnia, central Bosnia and the Sana region. Dolomitic marble is found in the area surrounding Gornji Vakuf and Begova Brezovača, and this material is widely used as building stone.

Material of Carboniferous age is found in four areas: a) eastern Bosnia, between Šekovići, Vlasenica and Srebrenica; b) southeastern Bosnia, between Foča, Goražde and Trnovi; c) central Bosnia and in the centre of Bitovnja and Vranica, from Konjic and Prozor to Donji Vakuf; d) western Bosnia, between Sanski Most, Prijedor, and Bosanska Krupa. Thickness of the Carboniferous clastic complex varies from 100 to 1000 m. Previously, presence of Upper Carboniferous was not recognized in Bosnia and Herzegovina, but the Paleozoic sequence in the vicinity of Ljubija appears to contain a complete Carboniferous section, in fact continuing up to the Middle Permian (Grubi_ et al., 2000). Figure 1 shows the stratigraphic column for Bosnia and Herzegovina (Čičić, 2003).

Mesozoic Era

Rocks of Triassic, Jurassic, and Cretaceous age crop out across roughly 70% of Bosnia and Herzegovina and cross the full range of lithologies from igneous to sedimentary to metamorphic. Carbonate materials, however, are the most common and record littoral to neritic depositional conditions in the Mesozoic Tethys Sea.

Sedimentary and igneous rocks of the Triassic are among most important formations in Bosnia and Herzegovina. The thickness of the lower Triassic section ranges from 200 to 700 m. The lower Triassic sequence is composed of terrigenous and lagoonal sediments, with lesser amounts of limestone in parts of the section. The Middle Triassic contains material of the Anisian and Ladinian stages. In the Anisian, limestone and dolomites predominate. Thickness varies generally from 200-500 m, and up to 1,000 m near Zvijezda and Tara. Ladinian-stage deposits include slate, sandstone, chert, marl and limestone, as well as volcanic material. An additional 400-800 m of sedimentary and volcanic lacks fossils, but this material is estimated to date to the middle to upper Triassic. In the upper Triassic, carbonates are found across much of Bosnia and Herzegovina, with a total thickness of roughly 200-800 m. Dolomites are most common in northwest Bosnia, dolomites and limestone in central Bosnia, whereas limestone predominates in the southeast parts of the country. In addition, due to regression at this time, bauxite was formed in parts of eastern Bosnia, near Milići and Srebrenica, and near Grmeč.

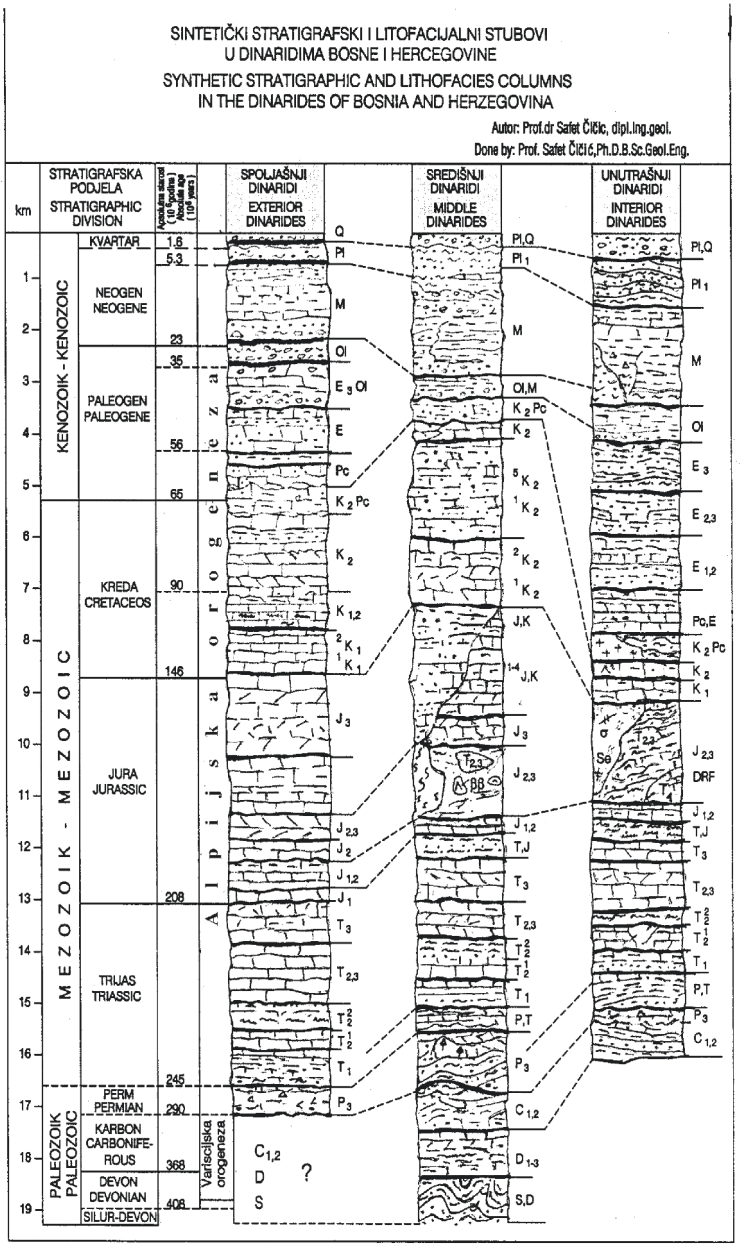

Figure 1. Stratigraphic column of the Dinarides of Bosnia and Hercegovina.

Around the Triassic-Jurassic boundary, chert and radiolarite are found in the western parts of Kozara to Nemila and Vranduk in the Bosna River valley. The chert is finely stratified and intensely folded, with intercalated slate and limestone. Finely stratified limestone was mapped in Triassic-Jurassic sediments, including nodules of chert. Conodonts and foraminifera are found in these deposits, but these provide very limited age constraints on the deposits.

Rocks of Jurassic age (200-140 Ma) underlie about 24 % of Bosnia and Herzegovina. They appear in all parts of our country but with great differences in lithofacies characteristics and origins. It has been shown that all three members of this system are represented.

During the Cretaceous, about 5000 m of flysch and carbonate rocks were deposited in littoral, shelf and open-sea environments of the Tethys Sea. These carbonates represent the best preserved carbonate platform in the Dinarides.

Cenozoic Era

Very little rock material formed in the area of Bosnia and Herzegovina during the entire Paleogene. Only 80-100 m of limestone may be of Palaeocene age, but loose age determinations using foraminifera also allow a Cretaceous age for this material.

Much more voluminous deposits formed in the region during the Neogene, during which time lake, lagoon, marine, brackish facies have been identified, including coal deposits. The oldest lake sediments with brown coal date to the Lower Miocene and are best developed in Sarajevo – Zenica, Banovići and Ugljevik basin. Also in the lower Miocene, volcanic activity in the region produced the dacitic-andesitic Srebrenica massif, which covers an area of about 100 km^2, as well as tuffs of the eastern Majevica and Tuzla basins. In northern Bosnia, Cenozoic marine facies are widespread. These materials represent deposition in the southern part of the Pannonian basin, and include marine, brackish environments of deposition. Lacustrine-lagoonal facies have been identified in the lower and middle Miocene in the Tuzla and Lopare basins.

During the Pliocene, clay, marl, lignite, and quartz sand were deposited in Bosnia and Herzegovina. Pliocene deposits of Kreka and Dubrave are characterized by rhythmic sequences of lignite interbedded with clay and quartz sand. Four cycles have been identified; with a total thickness of 1000-1200 m. Plio-Quaternary sediments were deposited in pre-existing topographic lows, from Prijedor to Semberija. These materials include clays, gravel (often cemented into thick beds of conglomerate), and sand and siltstone. Thickness of these deposits is generally less than 100 m, although

up to 500 m have been mapped in some local depressions (Vitanovići, Spreča field, between Živinice and Tuzla). Quaternary deposits represent three groups of facies: glacial, non-marine aquatic, and colluvial (hillslope) settings. Glacial deposits occur in high parts of Bjelašnica, Treskavica and Prenj. Aquatic sediments include fluvial, lacustrine, and swamp facies. Lastly, various slope deposits and other terrestrial materials are also found.

TECTONICS OF BOSNIA AND HERZEGOVINA

General notes

Most of the territory of Bosnia and Herzegovina is part of the Dinaride chain, located between the Adriatic Sea to the southwest and the Pannonian basin to the southeast. Tectonic style and deformation correspond to the regional pattern seen elsewhere in the Dinarides. The Dinarides are oriented northwest-southeast, running between the peri-Adriatic and the Peć dislocation zone. The range is bounded by the Serbian-Macedonian massif to the east and the Adriatic Sea to the west. The Dinarides represent a very broad geotectonic unit that, for the most part, records a local history different from the regional Hercynian folding cycles. The Dinarides evolved from the upper Permian to the Quaternary, including episodes of subduction and folding, rifting, and reverse faulting. The original cause of these activities was disintegration of Gondwana and later subduction of Africa beneath the Dinarides. Long-term regional motion has been from the south to the north, with increased intensity of deformation from east towards west. That was, according to many opinions, the main reason for the change in the Dinarides trend from primarily east-west to its present northwest-southeast orientation. That orientation appears to be a consequence of Africa or Adria's subduction beneath the Eurasian Plate (Figure 2).

Deep crustal structure

Based on deep seismic profiling, the thickness of earth's crust in Dinarides ranges up to about 50 km near the Albania border down to about 27 km in southeast part of Adriatic Sea (Daragačević,1980). The greatest depth of the Mohorovčić discontinuity in Bosnia and Herzegovina is between Livno and Kotor Varoš (40-42 km), and the shallowest is from Prnjavor to Derventa and Sava (25-30 km). Thicknesses of sedimentary deposits are greatest in the triangle Livno - Čitluk - Jajce (8 - 10 km), and thinnest in the area of Bijeljina and Foča (2-4 km). Regionally, crustal thicknesses are greatest in the central Dinarides and thin both towards the Adriatic and towards the Pannonian basin

(Jeli_, 1982). Crustal thicknesses, gravity, and regional crustal structure do not appear to support the existence of Benioff zone in the region. Convergence between Africa and Eurasia in this region therefore must be accommodated either by horizontal motions or crustal-scale internal deformation (Dragičevic,1974).

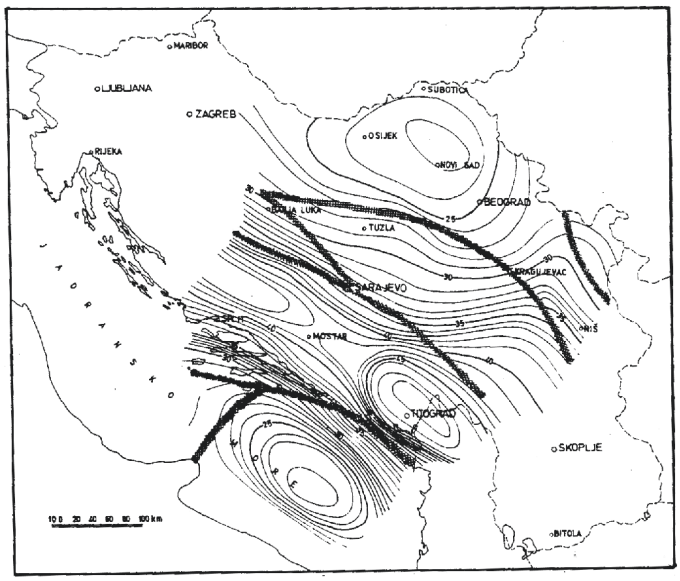

Figure 2. Map of crustal thickness of the Dinarides (Dragačević, 1974).

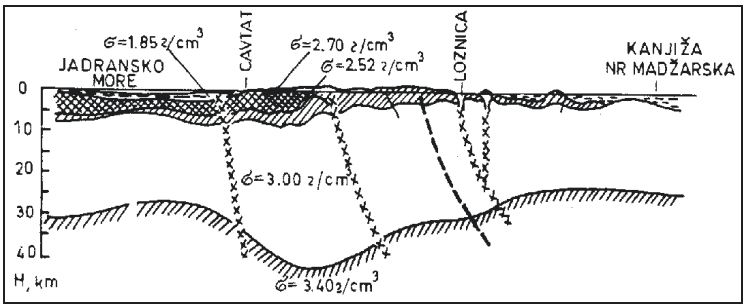

Figure 3. Cross section of the crust along a line of section: Adriatic Sea - Cavtat - Loznica - Kanjiža (Dragačević, 1974).

Across Bosnia and Herzegovina, three tectonic units can be distinguished: the Outer (or "External"), Central, and Inner Dinarides (Fig. 4). These units are subdivided by two crustal-scale reverse faults: the High Karst and the Durmitor faults. The High Karst reverse fault represents the boundary between the Outer and Central Dinarides, and the Durmitor fault is the boundary between the Central and Inner Dinarides.

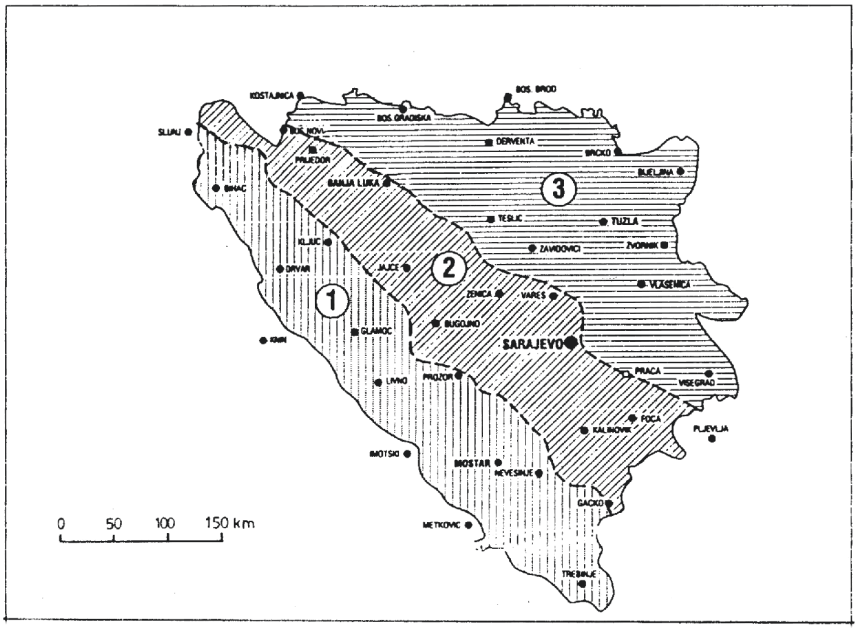

Figure 4. Geotectonic subdivision of the Dinarides in Bosnia and Herzegovina. 1. OUTER DINARIDES: Mesozoic carbonate, Tertiary flysch and molasse. 2. CENTRAL DINARIDES: Palaeozoic clastics and extrusive volcanic rocks, Mesozoic carbonates, Jurassic-Cretaceous flysch and Neogene molasse. 3. INNER DINARIDES: Palaeozoic and Mesozoic clastic rocks and carbonate, Jurassic ophiolitic rock and melange, Cretaceous and Palaeogene flysch and granite, Neogene andesite dacite, and lacustrine, lacustrine-lagoonal and marine molasse.

Formation of the large-scale geotectonic structure of the Dinarides through Bosnia and Herzegovina, and of the Dinarides as a whole, is largely a result of three major events:

a) Formation of the Tethys Sea at the end of the Ordovician and into the Silurian, about 450 Ma, when the area of Bosnia and Herzegovina became part of that ocean;

b) Three orogenic events that affected south-central Europe: the Caledonian, Hercynian and Alpine orogenies;

c) The impingement of the African Plate and/or the Adriatic microplate from the Triassic until the present.

Convergence between the Dinarides and the African Plate and the inferred subduction of Africa beneath south-central Europe result in large-scale folding, generally oriented southwest-northeast, throughout the Dinarides. Three orogen-scale structures can be described:

- Syncline of the Outer Dinarides,
- Anticline of the Central Dinarides,
- Monocline of the Inner Dinarides.

During the Mesozoic and Tertiary, especially from the end of Cretaceous to the Miocene, deformation was widespread through the Dinarides. Regional folding was followed by crustal-scale faulting (B. Grahovo-Livno-Trsteno; Vrbaski, Busovački, Sprečko-Kozarački, Modrički, and Sava faults). Uplift of the central Dinarides fractured the earlier carbonate platform and initiated erosion of this material. Other large faults through Bosnia and Herzegovina include: the Split-Bihać- Karlovac, Banja Luka, Sarajevsko, Drina, and Neretva faults. These faults reflect Neogene compression. These faults contributed, among other things, to the occurrence of Palaeozoic rocks deformed by Hercynian folding in eastern and southeastern Bosnia, central Bosnia and Bosanska Krajina. Different deformation episodes in the region are not sharply divided, but rather they are largely overlapping, and form parts of a continuous tectonic evolution.

GEODYNAMIC INVESTIGATIONS USING GPS TECHNOLOGY

Geodynamical investigation in Bosnia and Herzegovina using GPS started in 1998. One point of old national trigonometric network, in Ilidža, which is near Sarajevo, was observed as part of the EXTAGED-98 European Satellite Geodynamical Traverses project. The data were processed at the Institute for Geodesy and Geodetic Astronomy of Warsaw University of Technology. The next year, 1999, Bosnia and Herzegovina became officially involved in the CERGOP (Central European Regional Geodynamical Project) project. The SRJV site in Sarajevo was established as a permanent station on the roof of the building of Geodesy Department of Civil Engineering Faculty of Sarajevo University. That point has been part of the European Permanent

Network since November 1999 and included in EUREF weekly solution. It was the first permanent station within the territory of the former Yugoslavia.

The Sarajevo permanent station (SRJV) was part of the CEGRN 99, CEGRN 01, CEGRN 03 GPS campaigns. In 1999, one epoch station was observed in northern of Bosnia, in Gradačac (observed in CROREF 96, BIHREF98). The point was not officially accepted as an epoch CEGRN station, but the observation data were available for processing.

In addition to the geodynamical GPS activities above, GPS campaigns were carried out for establishing a local reference frame. These campaigns included CROREF 96 (5 points over the Bosnian area observed in the frame of Croatian EUREF 96), Balkan EUREF 98- BIHREF 98 (13 points of the old national trigonometric points observed for the 5 days; Mulić, 1999). In the summer of 2000, a GPS campaign for the densification of the reference-frame network for Bosnia was carried out, and 23 points were observed (Fig. 5). The data of the 2000 campaign have not yet been processed, but this processing is planned for the near future. Thus some points from the Bosnian reference frame velocities will be available for geodynamical research into motion of the Adriatic microplate or other regional problems.

Figure 5. Points observed in the BIHREF 98 and BIHREF 2000 GPS campaigns.

PLANS FOR FUTURE ACTIVITIES

There are several objectives for future geodetic work in Bosnia and Herzegovina:

1. Upgrade the Sarajevo permanent station
2. Install additional permanent stations
3. Process GPS observation data from the BIHREF 2000 campaign using Bernese software.
4. Investigate deformation near the town of Tuzla in northern Bosnia.
5. Establish a network of national (or international) permanent stations, which also could be useful for geodynamic investigations.

Some known deformation is the result of subsidence associated with the Tušanj salt mine. Damage in the town of Tuzla and in the surrounding area has been severe. The old downtown disappeared, and many buildings have been damaged. Local geodetic measurements have been undertaken in this region during the past 50 years with main task of characterizing this deformation using ground-based geodetic methods. New investigations utilizing GPS have been proposed. Support would be welcome for this interesting local geodetic project.

For the continuation of geodynamic research in Bosnia and Herzegovina within the framework of the CERGOP and WP 4 (Becker et al., 2003) projects, three new permanent stations would be optimal to cover the Dinarides and detect how far deformation extends into the continent. Proposed new stations are indicated by white circles in Figure 6: in Tuzla, Bihać and Mostar. The complexity and richness of the geology and geodynamics of the region in and around Bosnia and Herzegovina merit further densification of the GPS network, which would have benefits for geodynamical research as well as hazard assessment and regional environmental protection.

Plans for future GPS investigation in Bosnia and elsewhere in south-central Europe should also seriously consider the importance of this work for assessing seismic hazard in the region. In April and May of 2004, three earthquakes (magnitude ~4) occurred within Bosnia and Herzegovina. Historically the Bosnian region has seen regular earthquakes of this magnitude or greater, including events that have threatened human life and property. The 1996 earthquake in Banja Luka (M 5.2) caused significant loss of life. The Sarajevo seismological observatory has collected data since 1901, including local to regional seismicity, thus representing one of the oldest and

most complete instrumental seismic archives in Europe. Continued geodynamic GPS research in the region, including densification of the GPS network, is vital for assessing the nature and distribution of the seismic hazard that threatens Bosnia and Herzegovina.

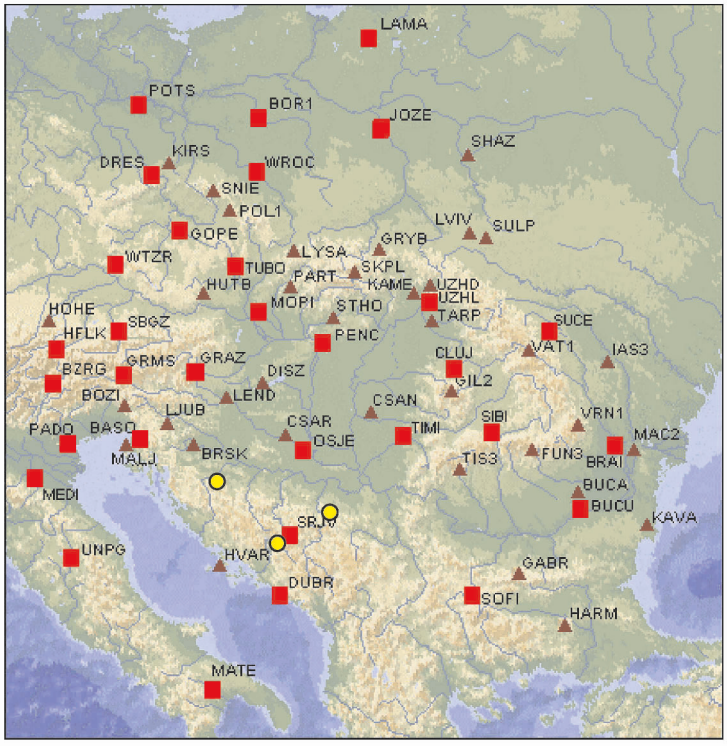

Figure 6. Present and proposed new permanent stations (circles).

REFERENCES

Becker M., Kirchner M., Grenerczy G. Creation of new permanent observation facilities in CEI country- Network design and permanent station configuration. Report on Geodesy, Proceedings of the 22. CERGOP – Working Conference and CEGRN Consortium Steering Committee and User Meetings , Warsaw, Poland, 29-30 September, 2003.

Behlilović S. Geology of mountain Čabulja in Hercegovina. Geological Herald, Special edition, book IV, Sarajevo 1964.

Čelebić Đ. Geological composition and tectonic structure of terrain of Palaeozoic and Mesozoic between Konjic and Prozor, with special consideration of deposits of Fe-Mn ore. Geological Herald, Special edition, book X, Sarajevo 1967.

Čičić S., Atanacković M., Jovanović Č., Soklić I., Stevanović P., Eremija M., Bušatlija I. Geology of BH. book 3, Cainozoic periods, Geoinženjering, Sarajevo 1977.

Čičić, S., Mojićević M., Papeš J. Geology of BH. book 2, Mesozoic periods, Geoinženjerin, Sarajevo 1984.
Čiči S. Comparative analysis of folding of Dinarides and Great Kavkaz. Geological Herald, Geoinženjering, Sarajevo 1985.
Čičić S., Miošić N. Geothermal energy of BH. Geoinženjering, Sarajevo 1986.
Čiči, S. Geological composition and tectonics of BH. Monograph. Earth Science Institute, Sarajevo, 2002; 1-350.
Čičić S. Geological map of Bosnia and Herzegovina 1: 300.000. Institute of Geology of Civil Engineering Faculty, Sarajevo 2003.
Gaković M. Stratigraphy of lias of Zalomka and Gacko in Herzegovina as grounds of biostratigraphic classification of lower Jurassic in Dinarides. Geological Herald, special edition, book XXI, Sarajevo 1986.
Katzer F. Geology of Bosnia and Herzegovina, Palaeozoic, Sarajevo 1926.
Kober L. Leitlinien der Tektonik Jugoslaviens. SANU, Special edition, book CLXXXIX, Belgrade 1952.
Kulenović E. *Palaeozoic of SE Bosnia*. Doctorate dissertation. Fakultet za naravoslovlje in tehnologijo, Ljubljana 1986.
Milojević R. Geological composition and tectonic structure of Central Bosnia basin with special consideration of development and economic values of coal facies. Geological Herald, Special edition, bookVII, Sarajevo 1964.
Miljuš P. Geological – tectonic structure and history of Outer Dinarides. Geological Annals of Balkan Peninsula, Beograd 1972.
Mojićević M. et al. Deep geological profiles through Dinarides, from Cavtav to Fruška Gora. Geological Herald, book 17, Sarajevo 1973.
Mojićević M. Geological content and tectonic relations of terrain between Sarajevo and Nevesinje. Geological herald, book XIV, Sarajevo 1978.
Mulić M., Muminagić A. National report of Bosnia and Herzegovina, Euref symposium in Prag , Chek Republic 1999.
Papeš J. Geology of southwest Bosnia. Geological Herald. Special edition, book XIX, Sarajevo 1985.
Pamić J. Igneous formation of Dinarides, Vardar zone and south parts of Pannonian basin. "Nafta", Zagreb 1986.
Pamić - Sunarić O., Pamić J.: Vein magnezite of ophiolitic zone of Dinarides in Bosnia and their genesis. Geological Herald. Special edition, book XXII, Sarajevo 1988.
Petković K.: Tectonic map of FNR of Yugoslavia. Glas SANU CCXLIX. Beograd 1961.
Radoičić R.: Palaeocene micro flora of Kamenjak limestone, SE Majevica (fourth note). Papers of GEOINSTITUT, book 26, Belgrade 1992.
Sikošek B. Interpretation of geological map of SFR Yugoslavia, Federal geology institute, Belgrade 1971.
Soklić I. Chronology of geotectonic movements in Dinarides during Mesozoic and Cainozoic. ANUBiH. Papers, book 12, department of technical sciences, Sarajevo 1988.
Stevanović P.: Lower Pliocene of Serbia and surrounding area. Special edition. SANU, Book CLXXXVI, Belgrade 1951.
Stevanović P., Eremija M. Miocene of Donja Tuzla. Geological Annals of Balkan Peninsula, book XXVII, Belgrade 1960.
Tjeerd H., Andel V. New views on old Planet. Cambridge University. ISBN 0-521-44243-5. Cambridge CB2, 1RP, 1995.
Tokić S. Genesis and main characteristics of Quaternary sediments of Bosnia and Herzegovina. Geological Herald 28, Sarajevo 1983.
Trubelja F. Palaeozoic igneous stones of Central Bosnia shale mountains. Geology BH, book IV, Magmatism and metalogenia, Geoinženjering, Sarajevo 1978.

INSTRUMENTATION FOR TERRESTRIAL MEASUREMENTS OF GEODYNAMICS AND THE MAIN SOURCES OF DISTURBANCE

Radovan Marjanović Kavanagh.
Faculty of Mining Geology & Petroleum engineering, University Zagreb, Zagreb, Croatia
ramaka@rudar.rgn.hr

ABSTRACT

Geodetic measurement of the Earth's strain is determined from measurements between several points on stabilised benchmarks in special networks. The final goal based on such measurements is the description of the deformation of the whole surface.

Unlike for other purposes, instruments for geodynamical research are in fixed connection with the rocks. The rock mounts are a part of these instruments, so for proper data interpretation, special care and analyses of site behaviour in time are necessary. Several disturbing influences such as temperature, ocean loading effects, Earth tides, water-table and humidity changes, air pressure and other factors influence the stability of the mounts. An analysis of these influences for proper data interpretation is necessary in order to separate movements of tectonic, seismic and other origins.

The changes in position, which we get from repeated measurements in different epochs, are calculated as differences of co-ordinates, vectors or speed of deformation. To get information about what happens between these epochs, instruments for continuous measurements must be utilized. Mostly these are mechanical or LASER extensometers, fluid or pendulum tiltmeters, and nowadays real-time GPS, or a combination of several such instruments.

Keywords: Extensometer, tiltmeter, continuated measurements, strain, temperature change, air pressure, water-table, humidity change, Earth tides.

INTRODUCTION

Long-term deformation of the Earth’s surface is mostly caused by large-scale tectonic forces. After the Plate tectonic model, it is accepted that the Earth's crust consists of rigid lithospheric plates that ride upon the underlying asthenosphere (Turcotte, 2002). The thickness of these plates differs, but on average, it is about 100 km. The lithosphere consists of relatively cool rocks above a hotasthenosphere which behaves like a plastic fluid. At the boundaries between plates, a continual process of plate consumption and creation is taking place. At these boundaries, mountain building, faulting, seismicity and volcanic eruptions are concentrated. Because of the rigidity of the plates, stress accumulation is transmitted long

N. Pinter et al. (eds.), The Adria Microplate: GPS Geodesy, Tectonics and Hazards, 209–221.

distances, which can cause also bending of the plates and changes the heights. Stress release results in faulting and earthquake occurrence.

Using space-based technology such as VLBI (Very Long Baseline Interferometry), SLR (Satellite Laser Ranging) and GPS (Global Positioning System), movements of the plates have been successfully measured. The estimated speed of these movements ranges from a few mm to >20 cm/year. Although VLBI gives excellent measurement accuracy, the information of these extremely expensive instruments does not describe true deformations but only gives the position change for discrete points on large plates. Due to different rock materials, different lithospheric densities and several other influences, stress accumulation is spread in a complicated way, and the lithosphere is deformed locally.

From several points of view, direct measurement of strain of the Earth's crust is a difficult task, especially based on measurements between stabilised benchmarks. For such determinations, a good model is necessary. For that purpose, the number of measured points generally is not sufficient. As we only presume the form, shape and the dimensions of the deformed surface, the positions of characteristic points and the configuration of such a net is extremely difficult to project.

Strain, and parameters which describe strain, are invariant and independent of the co-ordinate system and of the geodetic datum (Welsch, 1982). As a result, strain measurements on plates and between these plates are not measured on absolute fixed points because each point changes in height and its position in time. In most cases, these changes occur over geological time scales, but for example near plate boundaries, vertically or horizontally deformations of several mm/year are common. It also has been observed that stress-releasing processes preceding, during and after earthquakes can produce displacements up to several meters. These deformations are defined as linear deformations, plane deformations or as speed.

MEASUREMENT METHODS OF GEODYNAMICS

Geodynamics could generally be described as changes in position, height and gravity. Therefore we measure changes in distances, angles, tilting, heights, gravity, and other parameters. We determine these parameters from repeated or from continuous measurements of point co-ordinates of specially projected nets. For such measurements, several terrestrial and satellite methods and instruments are in use, including:

a) Triangulation and trilateration
b) Levelling and gravity measurements

c) Extenso- and strain-meter measurements
d) Tilt-meter measurements
e) VLBI (Very Long Baseline Interferometry)
f) SLR (Satellite LASER Ranging)
g) GPS (Global Positioning System) measurements

Classical geodetic angle and distance measurements and differential GPS measurements are used as repeated measurements for point-co-ordinate determinations. The positions of points from re-measurements of ground-based geodetic nets with angle measurements, as done earlier, included uncertainties at the same level as the strain. Thus such measurements yielded poor information about the deformation itself. Nowadays, GPS methods have almost completely replaced triangulation measurements due to lower time requirements and costs. The biggest advantage of GPS, however, is the possibility of point coordinate determination over large distances, with much greater accuracies than possible with other methods even at short distances.

CONTINUOUS MEASUREMENTS

Calculation of differences between measured coordinates from several epochs describes the deformation, but what happens between these epochs is only a matter of presumption. As a result, the use of even a few continuously measuring instruments can highly improve the results. For such purposes, different types of extensometers or strain meters, tilt meters and rotation meters as well as utilization of permanent GPS sites can be applied.

In general, the change of a distance in time between two points and tilting of the Earth's surface can be caused by several processes. For some of these processes, we presume they are quasi-linear with constant speed and sign, but others occur repeatedly or periodically over very different time intervals or occurrence frequencies.

When measuring strain as a result of released stress in the Earth's crust, we mostly measure the position change of benchmarks where our measuring instruments are mounted. These movements represent shifts, translations or other displacements caused by normal and tangential forces affecting rock masses on which our mountings are fixed. Unlike for other purposes, instruments for geodynamic research are in fixed connection with the rocks. As the rock sites are a part of these instruments, special care and analyses of the behaviour of these sites in time is necessary for proper data interpretation.

Determining strain with terrestrial methods from strain meters or repeated length measurements, we measure the change ΔL of the distance L in time between two points A and B*; e* = ΔL / L (Figure 1).

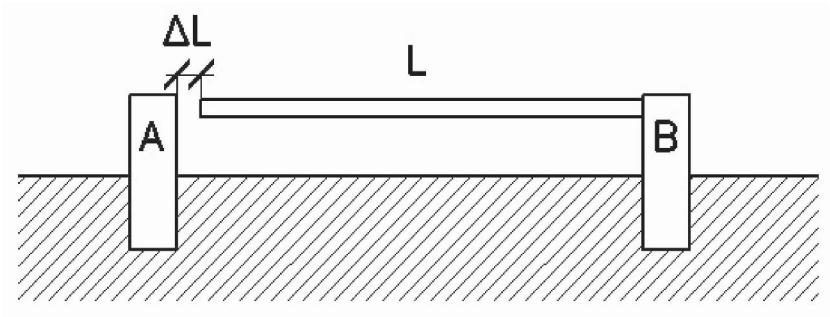

Figure 1. Schematic illustration of a linear strain meter; e = ΔL / L

After this definition the change of the distance ΔL is normalised, strain *e* is a dimensionless number that enables easy comparisons of different measurements. Strain measurements between two points and the interpretation of strain is simple, but the results are not sufficient for describing real surface deformations. Such measurements are just a part of specially prepared deformation nets, and a critical surface deformation analysis must be applied (Altiner, 1999).

A strain meter consists of two points provided with a length-changing detector. A commercially produced strain meter suitable for such purposes does not exist. Although precise electronic distance meters such as the MEKOMETER ME 5000 or others can be applied for many purposes, such instruments are not real-time strain meters. Most strain-meter constructions are different prototypes. In common use are:

a) Mechanical strain meters have normal lengths from several meters to several tens of meters and are made from fused silica, INVAR, carbon fibre or similar materials with low coefficients of expansion. Different sensing systems are used, including: capacitive, inductive and others.

b) LASER strain meters are generally several hundred meters long, and interferometric sensing is common.

Tilt meters are instruments for detection of tilt or tilt change. The principle of a tilt meter is shown in Figure 2.

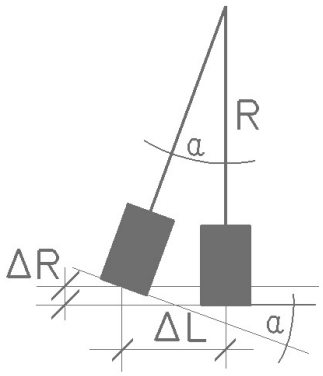

Figure 2. A vertical pendulum tilt meter.

Several different commercial constructions and many prototypes are in common use. These instruments could be divided in characteristic groups as follows:

a) Vertical pendulums (suitable for boreholes)
b) Horizontal pendulums
c) Different fluid tilt meters (suitable for large excavations)

Sensing systems for tilt meters are similar to those used for strain meters. Small changes in angle are generally measured as linear displacements. Data from analogue or digital sensors are transmitted to data storage, for on-line or later analysis or calculation. Excellent sensitivity and linearity of these instruments are possible, but problems with long-term stability caused by temperature, air-pressure and other disturbing influences may degrade the accuracy of these types of instruments. So when comparing such instruments, long term-drift is much more important than the maximal resolution (Marjanović Kavanagh, 1999; Valliant et al., 1987).

DISTURBING INFLUENCES ON TERRESTRIAL MEASUREMENTS

Geodynamic movement is, for the most part, a slow process that occurs over large time intervals with very small amplitudes of signals over short time intervals. So several disturbing influences directly affect geodynamical measurements. These influences are of the same order of magnitude or even bigger than the signal. In addition to instrumental error, it

is necessary to know the signs and magnitudes of of several other potential error souces, including:

1. Temperature changes of the Earth's crust, the surrounding of the instruments and of the instruments itself.
2. Water-table and humidity changes in the crust and the instrument surrounding
3. Earth tides and ocean loading effects.
4. Air pressure change and Earth tides of the atmosphere.
5. Cavity effect, topography effect, geologic effect.

Temperature changes

Temperature changes in the local surroundings strongly affect measurements of the Earth's crust. In first approach, temperature from the Sun penetrates the Earth's surface, and this process can be estimated as a daily or a yearly periodic function in the form of

$$T = T_0 \cos \omega t$$

For a homogeneous elastic half space, the temperature change from outside influences the interior in the form of damped waves:

$$T = T_0 e^{-ky} \cos(\omega t - ky)$$

Where: T = temperature at the depth y, $k = \sqrt{\omega / 2K}$,
K = thermal conductivity.

So the depth y as a function of wavelength λ could be expressed as:

$$\lambda = 2\pi / k$$

Below depths of y $= \lambda$, we can neglect the temperature influence from outside, and this can be taken as the limit of the temperature influence. For typical values, when K= 10^{-6} m^2/s, depth limits are approximately y = 20 m for yearly and y = 1 m for daily temperature change influences (Harrison and Herbst, 1977).

In a homogeneous isotropic material on a semi-infinite half space under influence of temperature, stress release is possible only in the direction of a normal to the plane surface. In all other directions parallel to the plane, the compression-stress alters without measurable strain (Figure 3).

On the real Earth, at a point T, the combined effects of temperature, topography, and stress are manifested as strain and tilting (Figure 4).

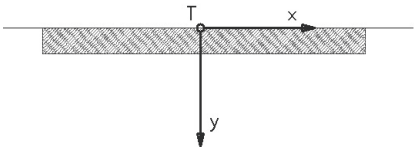

Figure 3. Point T on a horizontal semi-infinite half-space.

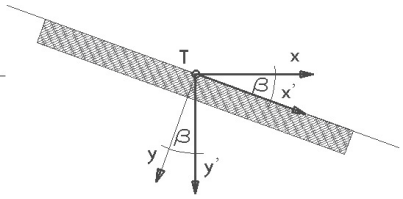

Figure 4 Tilting of the semi-infinite half space through an angle ß.

In a simplified model, these effects can be calculated as (after Harrison and Herbst, 1977):

$$e_{xx} = \frac{1+\nu}{1-\nu}\alpha T_0 e^{-ky}\cos(\omega t - ky)\sin^2\beta$$

$$e_{yy} = e_{xy} = 0$$

Where: $\nu = 0{,}33$ (Poisson's ratio),
$\alpha = 10^{-5}$ (linear expansion coefficient of the rocks),
$T_0 = 10\ ^0\text{C}$, $\beta =$ Angle of the slope

On a slope with $\sin\beta = 0.1$ (about 10°), the surface strain amounts to 2 x 10^{-6} and tilt to 20μ radians. This shows that temperature change can cause strain and tilt on slopes on the Earth's surface, which must be taken in account, especially when geodetic benchmarks or mounts are positioned on hills. Therefore deformation measurements must be very carefully interpreted, and a temperature correction model must be applied. At the same time, all instruments and mounts for geodynamic research must be well insulated from direct temperature influences.

When possible, a good method for instrument temperature insulation is installation in disused mines or boreholes. Installing instruments in boreholes at depths of >20 m achieves temperature insulation, but at these depths maintenance of the instruments presents a problem.

In general, temperature difference causes dimensional changes of all materials. So if we know the linear expanding coefficient α of the corresponding material and the length l_1 at temperature T_1, we can calculate the length l_n at the temperature T_n by the following formula:

$$l_{Tn} = l_{T1}(1 + \alpha/T_n - T_1)$$

Numerous investigations show that the realistic threshold of resolution for a capacitive sensing system (similar for others) is about:

$$R = 10^{-10}\ \text{cm}/\sqrt{Hz} = 0.001\ \text{nm}/\sqrt{Hz}$$

So if we presume our instrument could detect a linear dimension change of a 20 mm-long brass rod with a resolution of 10^{-10} mm, the environment temperature must be known and stable to 2×10^{-7} °C (Jones and Richards, 1973).

Temperature variation is time-dependent, and its influence on the measuring tool happens gradually. So even if our instruments could be produced from one material with equal and excellent thermal conductivity, the temperature distribution is time-dependent. Thus thinner parts of the instrument respond sooner than thicker parts to external temperature changes. Therefore, in addition to temperature insulation, we must provide a temperature accommodation time for our instruments. To minimise such error sources, it is necessary to build instruments from materials with uniform and extremely small temperature expansion coefficients or as temperature compensating constructions. For such purposes we can use INVAR, fused silica, or carbon fibre (with negative temperature expanding coefficients; Marjanović Kavanagh, 1982).

Water-table and humidity changes

Water-table and humidity changes in the Earth's crust and of the local surroundings can affect strain measurements. Water from outside causes local temperature transport to certain places in the interior and swelling of porous or hygroscope materials (like clay), directly producing stress and strain. The modeling of these disturbing influences is extremely complicated, especially where the geologic substrate is heterogeneous or unknown. From numerous observations, it has been shown that strain is coherent with rainfall and water-table change, but with phase lags. The signals differ but could reach about 10^{-7} or more. Therefore it is recommended to avoid humid surroundings for precise measurements. On the other hand, after strong rainfall, a dry environment is much more affected than a humid one.

Although boreholes are sealed and water-insulated, very often condensing water fills the bottom of the tubes after some time. So a water pump is necessary which might disturb the measurements. Vacuum tubing is a

better solution but raises the costs of the borehole installation and complicates the maintenance.

Earth tides

Caused by rotation of the Earth and attraction of the Moon, the Sun and other planets, gravitational forces are continuously generating periodic shape deformations of the Earth. These shape deformations are called Earth tides. There are tides of the sea, but also tides of the rigid Earth. These two dynamics are interconnected and influenced. So when registering ocean tides with tide gauges mounted on the coast, we neglect the fact that the continents are also affected by tides. Additional forces known as loading effect also affect the continents. However the Earth tides of the continents have much smaller magnitudes than those of the sea. The amplitudes of Earth-tide strain are in the range of 10^{-7}, but they are time-, azimuth- and latitude-dependent. In accordance to a chosen model, Earth tides can be calculated.

The partial tide analysis is based on Fourier transform algorithms that resolve amplitudes and phases. The frequency spectrum of the five main partial tides and the amplitude dependence of the latitude are shown in Figure 5.

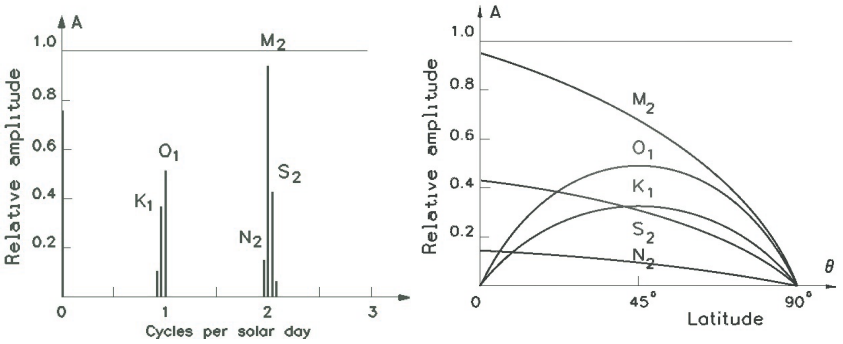

Figure 5. The frequency spectrum and the latitude dependence of the 5 main partial tides (after Vaníček, 1980).

When observing long-term deformation, the Earth-tide measurements are interpreted as noise, but by analysis of such Earth-tide observations with respect to theoretical tides, we get information about the Earth's interior and about local inhomogeneities. A measure of such disagreement in the form of a "strain factor"(S) based on the relation between disturbed e_{ij} and undisturbed $e_{ij}^{\inf}$ strain.

In an elastic homogeneous material, the strain tensor consists of three translational and three rotational components. On a free surface where Earth-tide strain measurements take place, the strain tensor is completely described by three of these components. By installing three strain meters in three different azimuths, the complete strain tensor can be calculated. It is seldom possibile to install strain meters exactly in orthogonal directions, so a correction must be calculated using the following equation (Love, 1926):

$$e_\alpha = e_{xx} \cos^2 \alpha + e_{yy} \sin^2 \alpha + e_{xy} \cos \alpha \sin \alpha$$

When measuring Earth strain from repeated distance measurements in precise geodetic nets with modern accurate distance meters, a typical accuracy is in the range of: ±(0.1 mm + 0.1 ppm). This means that the multiplication factor is 10^{-7}, which is in the magnitude range of Earth-tide strain. So for precise distance measurements, an azimuth-dependant correction must be applied. As Earth tides are time-dependent, the correction must be applied for the moment when the distance measurements took place.

In geodynamic research when monitoring secular strain, secular tilt or gravity changes, a good knowledge of the amplitudes and phases of the local Earth tides is important. However, the Earth-tide signals are considered as noise and are subtracted from the observed data. For Earth-tide registration measured as strain, tilt or gravity several instrument types are used. Most of them are of the same type as for long-term geodynamic deformation measurements, including:

a) Gravimeters,
b) Tilt meters
c) Strain meters.

Although all of these instruments measure Earth tides, their usage and the information obtained are very different. Generally it can be stated that:

a) Gravimeters measure periodic or secular gravity changes. The signals from relative gravimeters are clear, and a good signal-to-noise ratio is easy to achieve.

As geometric heights and gravity along the leveling lines are dependent, gravimeters must be used when repeated spirit leveling is used for secular height-change determination. Recently, several small and accurate absolute gravimeters hae become available, promising excellent results.

b) Tilt meters are used for measurement of the Earth's crustal tilting. The signal-to-noise ratio is low, and expensive precautions are required for achieving good results (insulation, installation in mines and boreholes).

c) Strain meters measure strain, but inhomogeneities of the surrounding rocks and local disturbing influences degrade this information. Using simple mechanical strain meters, a good signal-to-noise ratio is possible but is difficult to achieve. Modern expensive LASER technology, however, enables precise measurements even over large distances. The disadvantage of these instruments is the high cost of installation and maintenance.

Air-pressure changes

In the same way as on the rigid Earth and its oceans, the atmosphere also has tides. In comparison with the rigid Earth, these tides have different frequency spectra. The biggest partial tides are the half-day period (S_2), caused first by the absorption of the radiation through ozone. In the frequency spectrum of the half-day Moon-tides, atmospheric tides are produced in the same way as for the rigid Earth and are of much smaller magnitude. Several other influences can also strongly disturb the daily periodicity of atmospheric tides, but a significant coherence between strain and barometric pressure exists over periods of several days. Air-pressure changes cause sinking or uplift of the rigid Earth. Under the approximation that air-pressure act normal to the free Earth's surface, an air-pressure difference of 700 Pa ($1Pa = 1N/m^2$) will cause crustal uplift of 5×10^{-2} m (or more). This deformation is manifested as tilting or strain on order of 2×10^{-8}.

In general, air-pressure changes affect dimensional changes of all materials, and correction for this disturbing influence is extremely difficult. If we assume a cube of brass with sides of 10 mm, normal air pressure causes a contraction of about 3×10^{-6} m. Assuming that we can detect a dimensional change of 10^{-10} mm, we could use a brass block as a micro barometer (Jones and Richards, 1973). Thus, in some cases of instrumental calibration, we must also take into account the dimensional change of our measuring tools under the influence of air-pressure change.

Cavity, Topography and Geology Effects

By mounting our instruments for geodynamic research in excavations or in disused mines, we can try to minimise thermal and air-pressure influences on geodetic measurements (Wyatt and Berger, 1980). But the excavations itself, the topography and the geologic and mineral composition of the surrounding rocks change the stress pattern, and the measured strain or tilt can be affected. These phenomena are known as Cavity, Topography, and Geology effects. Local inhomogeneities, cavities and different elasticity

parameters of rocks under special circumstances can enhance or damp the expected strain. When measuring Earth tides, these site-dependent influences could enhance the amplitudes to amounts of several times the theoretical tide signal. Due to topography, the theoretical condition of a free surface in a homogeneous half-space is violated. So when the normal on a free plane is not in the radial direction, a rotation with angle difference ß of the normal takes place. Cavities are deformed which induce abnormal strain (Blair, 1977).

If sufficient parameters for describing the surrounding rocks are available, such disturbing effects can be modelled with finite-element methods (Harrison, 1976).

CONCLUSION

For many reasons, instruments for geodynamic research must be located at carefully chosen sites in accordance with geologic and topographic conditions. Whichever method, location and instrumentation we apply, special care for the sites of mounts must be considered. The pillar mountings must be in perfect contact with the bedrock with thermal insulation and a cover for protection. Continuous measurements of the pillar stability with built-in tilt meters or similar instruments would be important (Wyatt, 1982; Čolić and Marjanović Kavanagh, 1990). Knowledge of local geology, topography and thermal conductivity and temperature, air-pressure, humidity and water-table measurements must also be collected for a correction model.

Generally it is presumed that GPS measurements are much superior to classic geodetic methods. There is no doubt that when measuring over large (global) distances, GPS yields excellent results. But when all local disturbing influences such as instability of sites and monuments due to temperature, air pressure, humidity, topography and Earth tides are properly modelled, GPS measurements in small local nets would be strongly degraded.

For local purposes, carefully projected combined deformation nets with large redundancy, measured with modern instruments and with continuous strain- or tilt-meter measurements for mount stability estimation is still a good choice. Such measurements must be used for local Earth-tide model estimation, and the same for measurements of daily and yearly temperature, air pressure, humidity and water-table change. As the amplitudes of measured deformation signals generally fall within the range of uncertainty, this effort will be worth the trouble. Using GPS as a reference frame, local networks can be integrated in the global IGS and national permanent GPS networks (Beutler et al., 1998).

REFERENCES

Altiner Y. *Analytical Surface Deformation Theory for Detection of the Earth's Crust Movements.* Berlin, Springer, 1999.

Beutler G., Rothacher M., Springer T., Kouba J., Neilan R.E. The International GPS Service (IGS): An Interdisciplinary Service in Support of Earth Sciences In 32nd COSPAR Scientific Assembly, Nagoya, Japan, July 12 to 19, 1998; 27-50.

Blair D. Topographic, geologic and cavity effects on the harmonic content of tidal strain. Geophys. J. of the Royal Astronomical Society 1977; 48.

Čolić P.K., Marjanović Kavanagh R. An attempt of earthquake prognostic from tilt-extensometer-measurements in combination with GPS in the earthquake-hazardous region near Zagreb. Proceedings of the fifth international seminar and exhibition on earthquake prognostics, Lagos, 2-6 December, 1990.

Harrison J.C. Cavity and Topographic Effects in Tilt and Strain Measurement. J. Geophys. Res. 1976; 2: 81.

Harrison J.C., Herbst K. Thermoelastic strains and tilts revisited. J. Geophys. Res. 1977; 4: 11.

Jones R.V., Richards J.C.S. The design and some applications of sensitive capacitance micrometers. J.Physics E: Scientific Instruments 1973; 6.

Love A.E.H. *A treatise on the mathematical theory of elasticit.* Dover Publications, N.Y., 1926.

Marjanović Kavanagh, R. *Beiträge zur Deformationsmessung mit mechanischen Extensometern.* TU-Darmstadt, Darmstadt 1982.

Marjanović Kavanagh, R. Some experiences with a new digitally Tiltmeter. Proceedings of the second international symposium Geodynamics of the Alps-Adria area by means of terrestrial and satellite methods. Dubrovnik, September 28 - October 02, 1998, Zagreb and Graz 1999.

Turcotte D.L., Schubert G. *Geodynamics.* Cambridge University Press 2002.

Valliant H.D., Burris L.J., Levine J. Evaluation of a miniature horizontal pendulum tilt transducer. 13th. Biennial Test Symposium Holloman Air Force Base, New Mexico, 6-8 October, 1987.

Vaniček P. *Tidal Correction to Geodetic Quantities*. National Geodetic Survey, Rockville, Md. February, 1980.

Welsch W. Activities in the field of Recent Crustal Movements, Ground and Space Geodesy in Geodynamics and Earthquake Prediction Research. Meeting of the European Seismological Commission and the European Geophysical Society, Leeds, 23-28 August, 1982.

Wyatt F., Berger J. Investigations of Tilt Measurements Using Shallow Borehole Tiltmeters. J. Geophys. Res. 1980; B9:85.

Wyatt F. Displacement of Surface Mounts: Horizontal Motion. J. Geophys. Res. 1982; B2: 87.

VERTICAL MOVEMENTS IN SLOVENIA FROM LEVELING DATA

Božo Koler
University of Ljubljana, Faculty of Civil and Geodetic Engineering, Ljubljana, Slovenia
bkoler@fgg.uni-lj.si

ABSTRACT

The paper provides an overview of historical and modern measurements of leveling net in Slovenia and some local areas of interest in Slovenia (Ljubljana Marshlands-"Ljubljansko barje", and the Slovenian coast, Krško). Vertical movement rates and corresponding analysis of precision are defined.

Keywords: Slovenia, Krško, Slovenian coast, Ljubljana Marshland, benchmark, leveling net, vertical movement rate, precision of vertical movement rate

HISTORIC MEASUREMENTS OF LEVELING NETWORKS IN SLOVENIA

Historic and modern leveling data are useful data sets for determining vertical movements. Leveling networks in Slovenia are heterogeneous, as heights were defined in different vertical datums and with different accuracy. To compare data from such different measurements, in this study, I calculate vertical movement rates and determine their precisions.

Precise leveling measurement networks in Slovenia can be divided into four groups. Table 1 shows data on length of leveling lines, year of measurement and accuracy of leveling for each group. Figure 1 shows the locations of these leveling lines and loops.

The accuracy of precise leveling can be assessed using a variety of criteria. *A priori* assessment of accuracy can be made if high differences have been measured in a leveling line. In this case, the accuracy can be assessed based on discrepancies of leveling lines or based on the closure of leveling loops. On the other hand, *a posteri* assessment of accuracy is based on correction of measured height differences made after adjustment (Vodopivec, 1997).

N. Pinter et al. (eds.), The Adria Microplate: GPS Geodesy, Tectonics and Hazards, 223–236.

Table 1. Characteristics of historic leveling measurements in Slovenia

Measurement	Year	Length km	Precision mm/km
Austro-Hungarian leveling	1873-1895	734	± 4.1
1st Yugoslav leveling	1946-1957	1084	± 1.2
2nd Yugoslav leveling	1971	688	± 0.949
1st Order leveling after 1989	> 1989	678	About ± 1.0

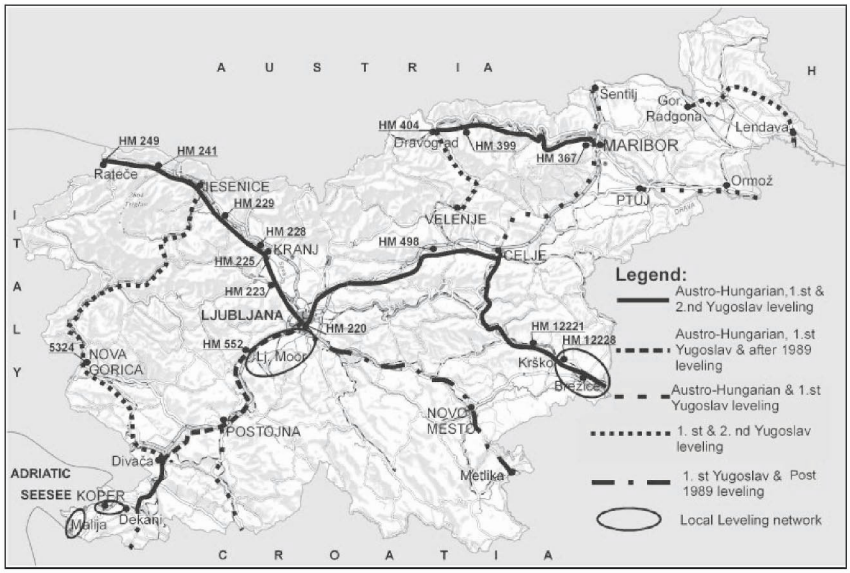

Figure 1. Precise leveling networks in Slovenia.

Connection of leveling networks to normal benchmarks

According to convention, the altitude of the median sea level is set as a uniform zero datum. The position of the reference-surface plane is defined by a vertical distance from so called normal benchmark which is stabilised in an area regarded as geologically stable (Stefanović, 1955).

The normal benchmark for connection to the 1873-1895 Austro-Hungarian leveling network to the reference-surface plane is the benchmark at Sartorio pier in Trieste, Italy. The altitude of the Sartorino normal benchmark was determined on the basis of one year of observations of oscillations of the level of the Adriatic Sea in 1875 to be 3.352 ± 0.01[1] m.

When surveying and adjusting the leveling network of the 1st leveling in the former Yugoslavia, there was no stabilised normal benchmark. The altitudes of this network was instead connected to the Sartorino normal benchmark of the Austro-Hungarian network (discussed above), giving the same vertical datum for these two networks.

The 2nd leveling was originally connected to the normal benchmark, which was stabilised in Maglaj (Bosnia and Herzegovina) in the former Yugoslavia. The vertical datum of the 2nd Yugoslav leveling – the median sea level – was defined on observations from six individual tide gauges located on the eastern coast of the Adriatic Sea.

VERTICAL MOVEMENTS IN SLOVENIA

Vertical movements and their precision in Slovenia were determined for the period from the Austro-Hungarian leveling to 1st and 2nd Yugoslav levelings. I also determined the vertical movements between 1st and 2nd Yugoslav levelings and a post-1989 leveling. The leveling networks in Slovenia are heterogeneous; individual height above sea level were defined by different measurements with different uncertainty levels. In addition, we have not measured height differences for the Austro-Hungarian and part of the 1st Yugoslav leveling.

In addition, different lengths of time exist between individual leveling measurement epochs in Slovenia. We calculated vertical movements as height change per year to eliminate this effect. For the historic measurements, no information on the precision of measurement of level heights and measured height differences between benchmarks are available. The vertical movement between benchmarks “a” and “b”, during a time period “t” can be calculated on the basis of the height difference between the two benchmarks. Vertical movement rate between the two points is obtained as the ratio between the difference in height and the time interval between the respective measurements.

[1] All precisions in this paper are defined with 1 σ.

Vertical movement rates from Austro-Hungarian, 1st and 2nd Yugoslav leveling

The heights of benchmarks in the Austro-Hungarian, and the 1st and 2nd Yugoslav leveling were not determined in the same vertical datum, so they are not directly comparable. To obtain comparable data, it was necessary to adjust the networks to the same vertical datum. Table 2 shows the heights of benchmarks after free network adjustment (Krueger, 1980), year of measurement and vertical movement rate for the benchmarks. The vertical movement rates determined between different measurement epochs are not the same. The high apparent vertical movement rates for benchmark HM12228 is not real; it is because the benchmark was moved during construction.

Table 2. Heights and vertical movement rates of Slovene leveling benchmarks

Benchmark	Height of benchmark			Vertical movement rate mm/yr		
	Austro-	Yugoslav leveling				
	Hung. level.	1st	2nd	1st-A.-H.	2nd-A.H.	2nd-1st
5324	100.5526	100.5688	100.5413	0.23 ±0.59	-0.12 ±0.44	-1.20 ±0.61
HM249	868.7686	868.8689	868.9510	1.43 ±0.47	1.96 ±0.35	3.57 ±0.49
HM241	712.0602	712.1660	712.2380	1.53 ±0.48	1.91 ±0.35	3.00 ±0.47
HM229	395.1693	395.1959	395.2477	0.39 ±0.36	0.84 ±0.27	2.16 ±0.35
HM228	451.8826	451.8633	451.9075	-0.28 ±0.36	0.27 ±0.27	1.84 ±0.35
HM225	359.3816	359.1341	359.1666	-3.59 ±0.24	-2.31 ±0.18	1.35 ±0.23
HM223	349.1590	349.1069	349.1452	-0.76 ±0.24	-0.15 ±0.18	1.60 ±0.23
HM404	348.6722	348.6852	348.6742	0.21 ±0.65	0.02 ±0.48	-0.50 ±0.64
HM220	320.6456	320.6702	320.7074	0.36 ±0.24	0.66 ±0.18	1.55 ±0.23
HM367	289.5066	289.5563	289.5428	0.79 ±0.52	0.43 ±0.39	-0.61 ±0.51
HM399	335.3416	335.3645	335.3485	0.36 ±0.65	0.08 ±0.48	-0.73 ±0.64
HM498	309.5668	309.6730	309.7206	1.69 ±0.39	1.81 ±0.29	2.16 ±0.38
HM552	298.9962	298.9667	298.9634	-0.42 ±0.35	-0.35 ±0.27	-0.15 ±0.38

HM12221	168.6677	168.6200	168.6616	-0.75 ±0.64	-0.07 ±0.48	1.98 ±0.67
HM12228	154.5730	154.5040	154.1279	-1.08 ±0.64	-5.24 ±0.48[2]	-17.91 ±0.67[2]

Vertical movements from 1st, 2nd Yugoslav leveling and post-1989 leveling

The results here show the smallest vertical movements rates in the area from Planina to Postojna to Hruševje (Figure 2). In the presumed stable area near Postojna, the vertical movement rates are from -0.06 ± 0.18 mm/yr up to 0.03 ± 0.18 mm/yr and are not significant.

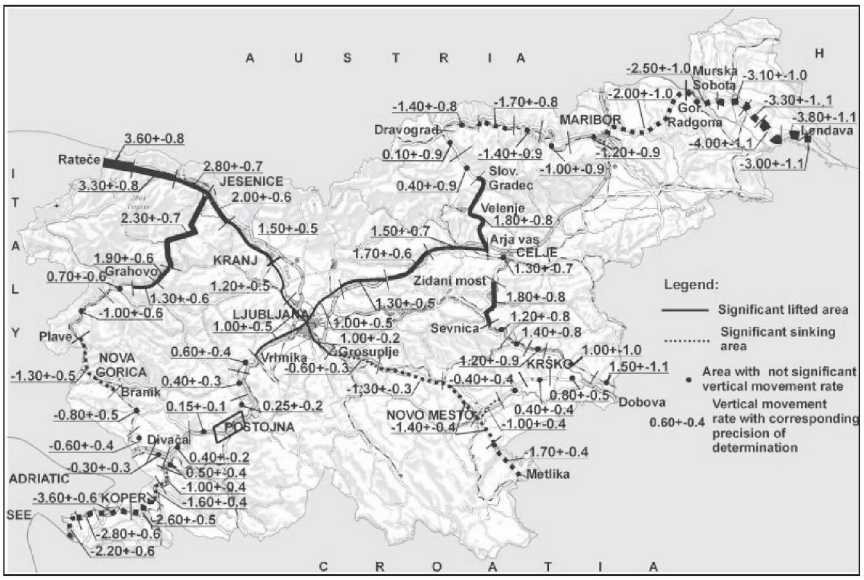

Figure 2. Vertical movement rate (mm/yr) in Slovenia determinate from 1st , 2nd Yugoslav leveling and post-1989 leveling.

MODERN VERTICAL MOVEMENTS OF LOCAL AREAS OF INTEREST IN SLOVENIA

In this section, I present data from modern leveling networks of local interest. These leveling networks are connected to fundamental benchmarks

established on solid bedrock, which serve as the base for the leveling network. These bedrock benchmarks are expected to provide the height stability necessary for determining possible settling of benchmarks established in materials others than solid bedrock, such as in sediment, on building, etc. Benchmark stabilization was established to eliminate local effects of sinking, etc.

High differences were measured with a Leica NA3000 digital leveling instrument. Measured height differences were then adjusted according to the method of adjustment of indirect observations (Mikhail et al., 1982). The precision of measurements is assessed based on the calculated standard deviation and are comparable with the accuracy stated by the manufacturer of the leveling instrument used for the measurements (±0.5 mm/km for the Leica NA3000, from Leica manual).

The vertical movement rate of a benchmark "i" is obtained as the ratio between the difference in height and the time interval between the respective measurements.

Ljubljansko barje (Ljubljana marshlands)

The Ljubljana marshlands (known in Slovenian as the "Ljubljansko barje"), which spread to the south and west of the city of Ljubljana and cover an area of 150 km^2 represent, in many ways, a unique natural environment. Many and diverse studies on the natural science of this area have been performed.

The Slovenian historian, J.V. Valvasor, wrote about the first known plan to drain the Ljubljana marshlands, prepared by Stefan de Grandi and Niklas Vendaholo in 1554. The most important period regarding the draining of the Ljubljana marshlands was between 1769 and 1890, when individual plans were prepared by Gruber, Lecchi, Schemerl, Francesconi, and Beyer (Uhlir, 1956).

In about 1881, the surveyor Podhayski carried out leveling works along the edge of the Ljubljana marshlands, along the River Ljubljanica and Gruber's Channel, and then finally on the area of the Ljubljana marshlands itself. Podhayski included 163 benchmarks in his network. In areas where it was not possible to find suitable structures which could be used as benchmarks (e.g., the edges of steps, windowsills on houses, bridges, milestones), Podhayski arranged for oak piles to be driven into the ground until a firm base was reached. He then knocked a nail into the top of each pile, which served as a benchmark. In this way, he established 62 benchmarks (Koler et al., 2000).

At the end of the First World War, it was decided that it was necessary to continue draining the Ljubljana marshlands according to Podhayski's plans, making changes only if the ground conditions had changed significantly. Geodetic survey measurements were begun on the Ljubljana marshlands in 1925, and were continued, with interruptions, until 1929. During this period, 69% of the total area of the Barje was surveyed. After the Second World War had ended, a leveling network was developed on the Ljubljana marshlands. In 1949, the benchmarks were stabilized, although many of them were later destroyed. Today there is a lot of interest in building in the Ljubljana marshlands, since the capital city of Ljubljana could naturally expand in this direction. On the other hand, many of Slovenia's and Ljubljana's citizens would like the Ljubljana marshlands remain undeveloped. Despite this controversy, it is an opportunity to obtain data about vertical settling and sinking.

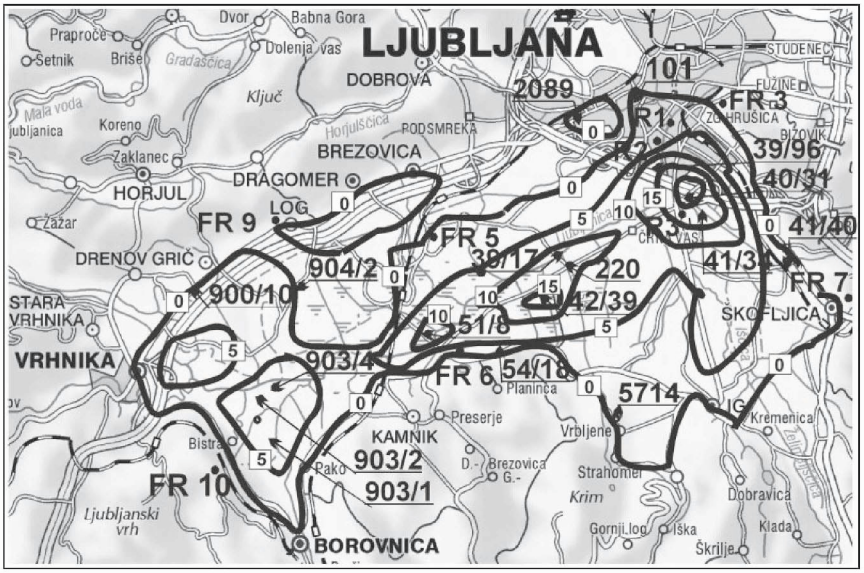

Figure 3. Map of contours of equal vertical movement rate across the Ljubljana marshland determined from measurements carried out in 1994 and 1996.

Over the period between 1976 and 1996, systematic surveys were carried out in the Ljubljana marshlands. Both stabilized fundamental benchmarks (designated FR) and temporary benchmarks were established. In the measurements done in 1996 and 2000, we included presumed high stability benchmarks built on piles. Great effort was made to assure that these benchmarks were stabilized to the bottom of the Barje, that is, on the firm

ground directly underlying the marshland sediments. Any vertical movement of such benchmarks could thus be attributed to tectonic movement and not to compaction of the Barje's sediments and organics. Piling depths are between 9 and 29 m. The general arrangement of the leveling network and the positions of the fundamental benchmarks and of the benchmarks on piles (designated R1 to R3) are shown in Figure 3. On the Figure 3, the benchmark mentioned in Table 3 and contours of equal settlement in mm/yr are also shown.

Table 3 shows the vertical movement rates for benchmarks which were stabilized and located in those areas where the greatest vertical movements rate (1994–1996) were determinate. The vertical–movement-rate signal is much greater than the uncertainty.

Table 3. Calculated vertical movements rate, with the corresponding precisions of determination

Unstable benchmark	Vertical movement rate mm/yr.	Stable benchmark	Vertical movement rate mm/yr.
903/1	- 9.0 ± 1.27	900/10	- 0.4 ± 1.15
903/2	- 8.8 ± 1.29	904/2	+ 0.3 ± 1.15
903/4	- 9.0 ± 1.31	54/18	- 0.3 ± 1.15
51/8	- 12.9 ± 0.85	2089	- 0.1 ± 0.71
39/17	- 10.8 ± 0.89	101	+ 0.1 ± 0.64
220	- 11.6 ± 0.85	41/40	- 0.2 ± 0.75
42/39	- 16.7 ± 0.89	5714	- 0.1 ± 0.85
39/96	- 14.6 ± 1.11		
40/31	- 24.1 ± 0.80		
41/34	- 17.4 ± 0.98		

In the western part of the marshlands, settling rates increase from the edge towards the middle, where they reach a rate of almost 10±1 mm/yr. The region of rapid settling also extends eastwards to the southern edge of the Barje. On the eastern side of the Barje, the general pattern of observed settling rates is less clear. Three possible centres of high settling rates are observed. Annual settling reaches as much as 25±1 mm/yr (see Figure 3). However, Table 3 shows the results for benchmarks 900/10, 904/2, 54/18, 2089, 101, 41/40 and 5714, which were stabilized on structures anchored into the solid substrate beneath the Barje. On these probably high-stability benchmarks, we observe that the vertical movement rate is smaller than the precision. In case of benchmark on pilings, it can be observed that the vertical movement rate is not significant (Table 4).

Table 4. Calculated vertical movements rate, with the corresponding precisions of determination, for presumed high stability benchmark on pilings

Benchmark	Height –1996 m	Height-2000 m	Vertical movement rate mm/yr.
R1	288.6976	288.6963	-0.33 ± 0.28
R2	287.7585	587.7562	-0.58 ± 0.30
R3	257.8764	287.8765	0.03± 0.30

Area around the Krško nuclear power station

Slovenian and international concerns about earthquake security at nuclear power stations was high in the beginning of 1990s. Slovenia has such a power plant near Krsko, in southeastern Slovenia. From 1992 to 1994, a seismo-tectonic model for the region was created from old geophysical and geological information (Gosar, 1999). This seismo-tectonic model was thought by many geoscientists to be unreliable because the old geophysical and geological information was incomplete (Gosar, 1999). To obtain a more complete and up-to-date picture of the seismo-tectonics of this region, extensive geophysical, geological and geodetic investigations were started in 1994 with support from the Administration for Nuclear Safety. As part of this effort, we re-measured a number of leveling lines, stabilised in the Krško and Krško polje area (Figure 4).

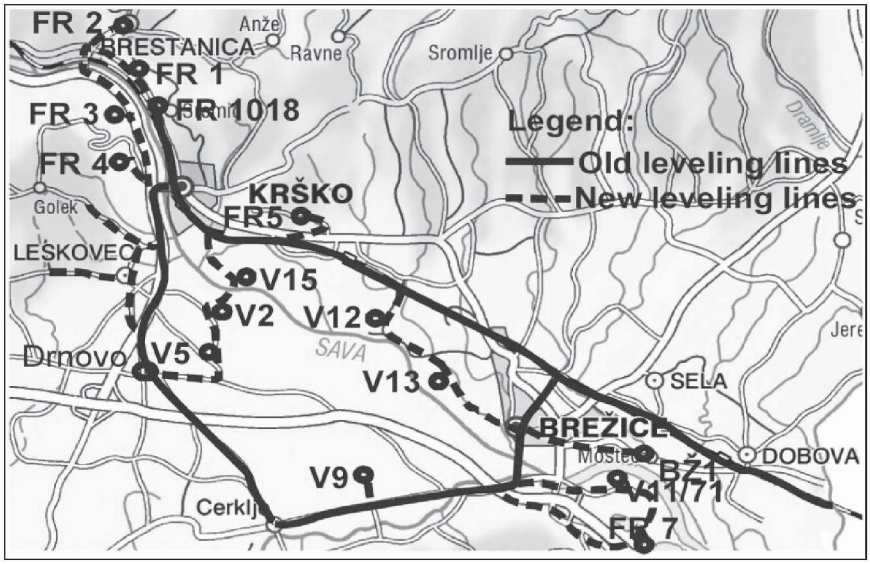

Figure 4. Leveling networks in Krško and Krško polje area.

After making initial measurements in 1995, we decided to include geologists in the study to assess the suitability of the benchmarks. An attempt was made to identify those benchmarks that were likely to be stable, so that the effects of geodynamics versus benchmark instability on vertical-movement measurements could be assessed. The suitability of the benchmarks were qualitatively; the geologists reported 48% of benchmarks were stabilised unsuitably or were moved from their original locations and cannot be connected with the geodynamics of the area.

In order to obtain as complete a picture as possible of vertical movements in the stated region, we added new leveling lines to the existing network in 1996 (Figure 4). The new benchmarks were stabilised in solid bedrock (marked FR to a depth of 1 m) or in abandoned bore holes that were used in earlier geological studies (marked V or B on Figure 4). The depths of these boreholes were between 10 and 390 m.

Vertical movements in the Krško polje

Table 5 shows vertical movement rates and uncertainties of individual benchmarks in this network.

Table 5. Vertical movement rate and uncertainties for benchmarks in leveling networks near the Krško nuclear power station, Slovenia. 1st refers to first epoch measurements, which vary for this data set from 1943 to 1992.

Benchmark	Vertical movement rate (1st-1997) mm/yr.	Vertical movement rate (1995-1997) mm/yr.
MLXI	0.07±0.13	/
HM 12223	-1.12±0.02	0.20±0.84
MXVII	-0.23±0.04	0.20±0.84
OP 903	-0.30±0.09	-0.16±0.95
OP647	-0.11±0.06	-0.41±1.18
MXC	-0.10±0.06	0.26±1.29
OP 541	-0.26±0.12	-0.38±1.38
OP610	-0.30±0.13	0.23±1.45
OP875	-0.06±0.15	0.94±1.56
MIV	-0.36±0.08	0.60±1.61
OP686	-0.22±0.17	0.43±1.85
OP857	-0.34±0.18	1.24±2.06

Benchmark	Vertical movement rate (1st-1997) mm/yr.	Vertical movement rate (1995-1997) mm/yr.
MN 15	-0.20±0.16	-0.18±1.66
5398c	-0.39±0.09	0.09±1.68
5398a	-0.49±0.10	-0.71±1.71
5398	-0.50±0.10	-0.84±1.72
A160	-0.62±1.03	-0.92±1.72
5397b	-0.81±0.10	-0.98±1.72
5397a	-0.90±0.33	-0.06±1.71
5397	-0.97±0.32	-0.36±1.69
402206	1st=1995	-0.81±1.66
402205	1st=1995	-1.35±1.65
402204	1st=1995	0.14±1.56
R38	-0.71±0.32	-3.47±1.42

MLXIII	-0.36±0.19	1.00±2.14
OP584	-0.13±0.20	1.94±2.21
R25	-0.65±0.25	0.27±1.62
A161	-0.16±1.46	0.28±1.63
R28	-0.32±0.15	0.07±1.65
R4	-0.44±0.27	0.20±1.65
5399a	-0.25±0.16	-0.10±1.66
MN16	-0.09±0.16	-0.35±1.67

R39	-0.51±0.29	-3.39±1.34
R40	-0.76±0.14	-3.56±1.23
R41	-0.31±0.13	-2.47±1.16
MN226	-0.63±0.16	-2.61±1.07
MN205	-0.01±0.04	0.29±0.70
MN201	-0.02±0.10	/
MN222	-0.08±0.32	/
MN221	-0.02±0.33	/

Statistically significant movements were obtained only in the area from Leskovec to Drnovo on benchmarks: R38, R39, R40 and R41 (Figure 4). The second centre of high vertical movement rates is between Cerklje and Brežice (Figure 4). So we have significant movements on benchmarks R25, R28, 5398c, 5398a, 5393, 5397b, 5397a, 5397, R38, R39, R40 R41 and MN226. We interpret, however, that these movements are not geodynamically significant. For example, significant movement was detected for benchmark HM12223, which was relocated during the construction work at the Krško railway station. This comparison was made between the 1997 and the Austro-Hungarian (1897) leveling measurements. However, we determine a substantially lower vertical movement rate for benchmark MXVII nearby, over a 47 year time period. A similar situation also exists for two additional pairs of benchmarks stabilised during railway station construction (MIV - Brežice and MLXIII - Dobova). It seems most probable that in all– cases, statistically significant vertical movement rates observed near Krško are due to causes other than geodynamics.

Vertical Movements on the Slovenian Coast near the Koper Tide Gauge station

We now discuss two leveling networks that we have built on the Slovenian coast (Figure 5). The first leveling loop was stabilised and measured again in 1997. Our objective for measuring these leveling networks was to define the height of EUREF (European Reference Frame) and EUVN (European Vertical GPS Reference Network) point SI03 (in national numbering, 180-Malija; Kuhar et al, 2000). This point is stabilised with a concrete pillar on the Malija hill. Additionally we are using these networks to determine possible vertical movements of additional benchmarks in this region.

Our second coastal leveling network is in the Koper area. Koper is on the Adriatic coast and has the only working tide gauge in Slovenia. This tide gauge was constructed in 1957 and was connected to the 2nd Yugoslav leveling network in 1971.

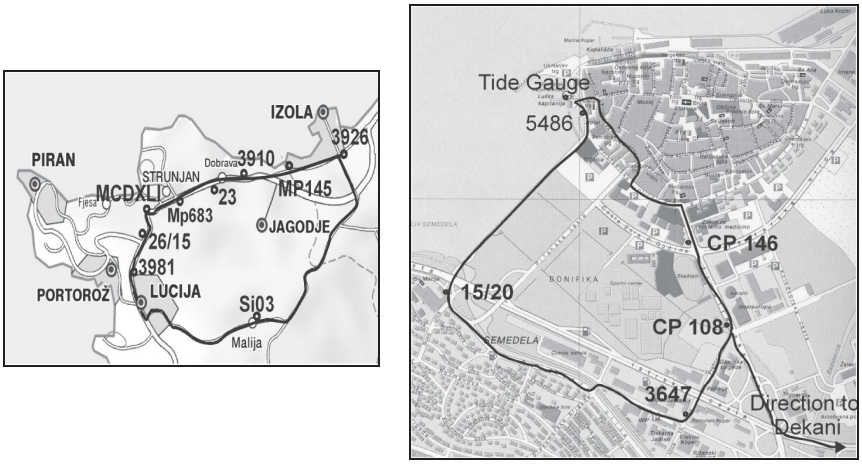

Figure 5 . Malija and Koper leveling networks in Slovenian coastal regions.

The vertical movement rates determined in the Malija leveling loop and the Koper leveling network are shown in Table 6.

Table 6. Vertical movement rates on the Slovenian coast

Malija leveling loop		Koper leveling network	
. Benchmark	Vertical movement rate (1971-1997) mm/yr.	Benchmark	Vertical movement rate (1971-2000) mm/yr.
MP145	-0,04 ± 0.06	3959	0.03 ± 0,04
3910	-0.13 ± 0.07	16/15	- 0.03 ± 0.05
23	-0.08 ± 0.07	OP743	0.02 ± 0.06
MP683	-1.90 ± 0.08	14/122A	0.06 ± 0.07
MCDXLI	-0.20 ± 0.08	3647	-1.32 ± 0.07
26/15	-0.08 ± 0.08	CP108	-2.84 ± 0.08
3981	-0.29 ± 0.08	CP146	-0.99 ± 0.08
		5486	-1.13 ± 0.08
		15/20	-1.83 ± 0.08

In the Malija leveling loop, we detected the biggest vertical movement rate at the MP683 benchmark. However, this benchmark is stabilised on a bridge that has been renovated. Therefore, we infer that the benchmark MP683 has moved during reconstruction. We also get a statistically significant movement rate for the 3981 benchmark, stabilized in Lucija, and the MCDXLI benchmark, which was stabilized using an old building near Strunjan.

Old city Koper lies on a former island which is surrounded by artificial fill and marshland. In the Koper network, we detected significant vertical movement rates on benchmarks 15/20, 3647, CP 108 and CP 146. These benchmarks were stabilized on buildings built on marshland. We also detected significant movement at tide gauge benchmark 5486, stabilized on a building constructed on artificial fill. We interpreted that this benchmark was not stable and not suitable as a tide-gauge benchmark. In 2000 a new fundamental benchmark was stabilised in solid rock on a former island which is presumably stable. Vertical movements of the benchmarks stabilised in suitable objects from Koper to Dekani (Figure 1. 14/122A,OP743 and 3959) were small and within the limits of measurement precision. In the future, we hope to connect the leveling loop at Malija with the leveling network at Koper.

CONCLUSIONS

Our results show that the area from Vrhnika to Divača is stable. The leveling results also suggest that the area near Postojna is stable. The second stable area is between Slovenj Gradec and Dravograd, where we see vertical movement rates of 0.10 ± 0.9 mm/yr. In the western part of Slovenia, vertical movement rates are not significant, in the Kras region from Divača to Branik and from Plave to Grahovo in Soča valley. Some stable areas are also in the northern part of Slovenia in the Drava valley between Dravograd and Maribor. According to the stable area near Postojna, we also did not get significant vertical movement rates on some areas in Sava region from Celje to Dobova. In this region, also lie the Krško and Krško polje areas (Figure 2).

Unstable areas in Slovenia include the area in Gorenjska from Kranj to Rateče and from Jesenice to Grahovo, where we see the greatest uplift rate (3.60 ± 0.8 mm/yr.). Our results also show uplift from Kranj to Ljubljana (Vrhnika, Grosuplje) to Celje to Velenje. The greatest subsidence area, we see in Prekmurje (near Lendava) and on the Slovenian coast (Figure 2).

In local areas such as Ljubljansko barje, maps showing subsidence and subsidence rates are helpful when planning any building or other works in

those particular areas. Areas of large subsidence are clearly visible on these maps. Planners should therefore take these results into account.

It will be possible to increase the reliability of results, as illustrated by the collaboration with geologists in the Krško case. It is necessary to study the suitability of benchmark sites. In this way, we can determine those benchmarks that were stabilized using suitable objects, with the result that any vertical movements thus detected are the result of geodynamics in the region and not due to movement of the points themselves.

REFERENCES

Gosar A. Geofizikalne raziskave v okolici jedrske elektrarne Krško (Geophysical researches around the Nuclear Power Station Krško). Proceedings of Geodetic and geophysical researches projects sponsored by Slovenian Geodetic and Geophysical Association during the 5th Meeting of the Slovenian Geodetic and Geophysical Association; December 15, 1999; Ljubljana: Slovenian Geodetic and Geophysical Association, 1999.

Kuhar M., Koler B. Poročilo o izvedbi gravimetričnih meritev z relativnim gravimetrom na točkah EUVN: SI01 Velika Pirešica, SI02 Lendavske gorice (388), SI03 Malija (180), (Technical report about relative gravimetric measurements on EUVN points: SI01 Velika Pirešica, SI02 Lendavske gorice (388), SI03 Malija (180)). University of Ljubljana, Faculty of Civil and Geodetic Engineering, 2000.

Koler B., Breznikar A. "Historical and recent measurements of the vertical movement of benchmarks on the Ljubljana marshlands." In *Faculty of Civil and Geodetic Engineering on the Doorstep of the Millennium-on the Occasion of its 80th Anniversary*, M. Fischinger, eds., Ljubljana: University of Ljubljana, Faculty of Civil and Geodetic Engineering, 2000.

Krueger J. "Numeriche Behandlung von Datums- und Konfigurationsdefekten." In *Geodaetische Netze in Landes- und Ingenieurvermessung*, H. Pelzer, eds., Stuttgart: Verlag Konrad Wittwer KG, 1980.

Edward M., Ackerman M., Friedrich E. *Observations and least squares*. Lanham, New York, London: University press of America, 1982.

Stefanović M. Normalni reper nivelmanske mreže (Normal benchmark of levelling net). Geodetski list 1955; 9(1-2): 3-14.

Uhlir H. A history of drying out works on the Ljubljana Marshlands - Books I and II, Water Economy Administration Center of the People's Republic of Slovenia, Ljubljana 1956.

Vodopivec F. Geodezija 2 - Višinomerstvo (Geodesy 2 - Leveling). Ljubljana: University of Ljubljana, Faculty of Civil and Geodetic Engineering, 1997.

Vodopivec F. et al. Določitev premikov zemeljske skorje v testnih mrežah Ljubljane. Ljubljana, Univerza v Ljubljani, Fakulteta za gradbeništvo in geodezijo, Katedra za geodezijo, 1993.

Vodopivec F. et al. Projekt stalnega odkrivanja tektonskih premikov v okolici JE Krško. Univerza v Ljubljani, Fakulteta za gradbeništvo in geodezijo, Katedra za geodezijo, 1996.

GEOID DETERMINATION IN SERBIA

Oleg Odalović
Faculty of Civil Engineering-Department of Geodesy, University of Belgrade, Serbia
odalovic@grf.bg.ac.yu

ABSTRACT

At the end of 2003, a preliminary geoid of Serbia was determined by fitting the gravimetric geoid into undulations determined by GPS and leveling (GPS/dh) techniques.

The gravimetric geoid was determined using data from regional gravimetric survey in Serbia (13,326 points) by applying collocation within the remove-restore method, and undulations GPS/dh (in total, 53 undulations) refer to ETRS89 as well as to the height datum defined by the second leveling network of height of high precision (NVT2).

Comparing the gravimetric geoid to the GPS/dh undulations shows that there are differences ranging from -20 cm to -90 cm that are relatively regularly distributed in an east-west direction. Of the total of 53 GPS/dh undulations, 18 were used for fitting the gravimetric geoid and 35 for external checking. This check shows that the remaining discrepancies range from -9 cm to 14 cm, with an average value of 1.3 cm and a standard deviation of 7.7 cm.

Keywords: Gravity, gravimetric, undulation, GPS, anomaly height

INTRODUCTION

All up-to-date geoid determinations in Serbia are for scientific research, and there is no official geoid for practical work. The first determinations were done in 1950 and in 1970 based on the method of astrogeodetic leveling (Bosković, 1952; Muminagić, 1971). Muminagic's geoid covered the whole territory of the former Socialistic Federal Republic of Yugoslavia (SFRJ), whereas Boskovic's solution, in accordance with data available at that time, determined the geoid for northeast Serbia.

In the second part of the last century, gravimetric measurements were done almost continuously over the former SFRJ, but those data were used only for the local geophysical research (Bilibajkić, 1979) as well as for establishing NVT2 (Bratuljević, 1995). In the 30 years up to 1980, more than 80,000 gravity points were measured within Serbia (Starcević, 1999). In 2000, these data were used for the first time for determinating the local gravimetric geoids in 2 areas in Serbia with an extent of 50 x 50 km (Odalović, 2000).

After the disintegration of the former SFRJ, these data were archived in different institutions in Serbia. In 2001, an organized gathering of data began in order to determine the preliminary geoid.

N. Pinter et al. (eds.), The Adria Microplate: GPS Geodesy, Tectonics and Hazards, 237–246.

DATA

Gravimetric survey

The gravity values mentioned earlier were referred to the Potsdam system. The position of points was defined by SFRJ trigonometric network of the first order (Bessel ellipsoid), and point heights referred to the first leveling network of high precision (NVT1)(Bratuljević, 1995)

Data from different institutions were gathered and, in mid-2003, transformation of these data was completed:

- Gravity values were transformed into ISGN71,
- Point heights from the NVT1 network were transformed into the system of orthometric and normal heights defined within NVT2, and
- Datum transformation between Bessel and ETRS89 was done (transformation procedure - Blagojević, 1998;, Odalović, 2000).

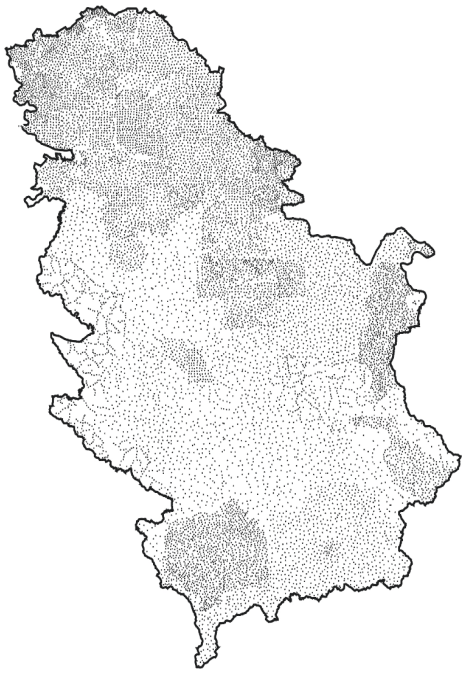

Figure 1: Distribution of regional gravimetric points.

A total of 13,326 points were assembled and used for determination of the preliminary geoid.

The regional gravimetric points were chosen in accordance with the needs of regional geology and geophysics research and with the needs of their origin, the available data and the requirements for accuracy and connection to the basic gravimetric networks). The accuracy of gravity measurements at regional measurement points and under the limits of ISGN71 is not less than 0.1 mgal (Starcevic, 2003). Gravity data from the neighboring countries were not available.

Deflection of verticals

During the data-gathering campaign, deflection–of-vertical values at 22 points obtained in the second half of the last century were provided. Their accuracy is better than 0.7 arc seconds, but considering the small number of determinations (Bratuljević, 1995) as well as their homogenous spatial distribution (Figure 2), these data were not used in the determination of preliminary geoid.

GPS/dh undulations

Undulations were determined by the GPS/dh method at points within the Serbia reference network that represents the densification of EUREF/ETRS89 in Serbia.

Determinations of heights by geometric leveling were done for 53 points that were close to benchmarks in NVT2. A total of 18 points were chosen for fitting the gravimetric geoid and the other 35 points for later external control. For the accuracy of such determined undulations, a value of 3 cm was adopted.

Digital terrain model

Along with GPS/dh undulations, a digital terrain model (DTM) was created especially for the geoid determination. A DTM of 5x5 arc seconds resolution (DTM 5) in both directions was formed using 80 million points gathered by the different methods (mainly by transformation of 1:50000-scale maps in digital form, as well as the orthophoto method for some urban settlements). Analysis of differences of "original" trigonometric points heights

that were relatively regularly distributed throughout Serbia and there a model height indicates that the model has maximum discrepancies of about 25 m.

DTM data outside the borders of Serbia were taken from the global digital terrain model GTOPO.

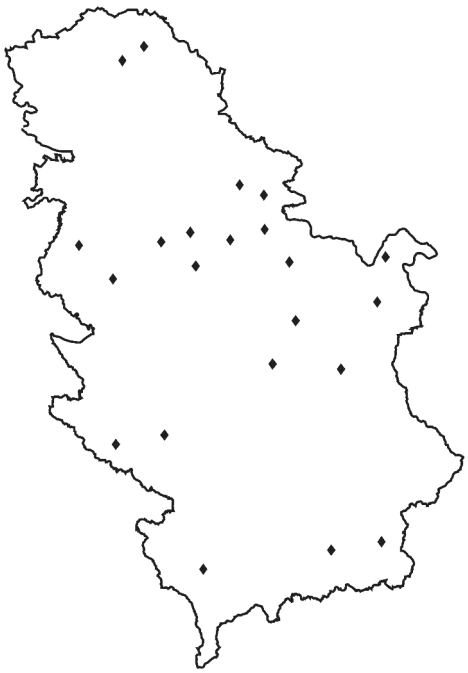

Figure 2. Distribution of the deflection–of-vertical measurement points.

PRELIMINARY GEOID DETERMINATION

Remove-Restore

Regional gravimetric measurement data, the newly created DTM, global geopotential model EGM96 and GPS/dh undulations represented the basic information for preliminary geoid determination. Undulations were determined by predetermination of the quasi-geoid by applying the remove-restore method, summarized below.

Free-air anomalies for all points were determined using the measured gravity value g', the normal heights of regional gravimetric points, and atmospheric corrections δ_A as follows:

$$\Delta g = g' + \delta_A - \gamma \tag{1}$$

where γ is the value of normal gravity on telluroid.

From the free-air anomalies, both the long-wavelength partial value Δg_{EGM96} determined by the global geopotential model EGM96, and the short-wavelength part Δg_{TOPO} determined by residual terrain model (RTM) (Forsberg, 1981) by which residual anomalies were formed, were removed:

$$\Delta g_R = \Delta g - \Delta g_{EGM96} - \Delta g_{TOPO}\,. \tag{2}$$

From residual anomalies applying collocation, corresponding values of anomaly heights were determined, and the total values of height anomalies were determined by the addition:

$$\zeta = \zeta_R + \zeta_{EGM96} + \zeta_{TOPO} \tag{3}$$

where ζ_{EGM96} is the long-wavelength part determined by EGM96 and ζ_{TOPO} is the short- wavelength part determined by DTM 5 and RTM.

On the basis of predetermined height anomalies to obtain geoid undulation, it was necessary to use (Heiskanen, 1967):

$$N = \zeta + \frac{\Delta g_B}{\bar{\gamma}} H^O \tag{4}$$

where Δg_B are Bouguer anomalies, H^O is the orthometric height, and $\bar{\gamma}$ is an average value of normal gravity.

Residual anomaly and covariance function

Residual anomalies were determined at all 13,326 points, and their basic statistics data are shown in Table 1.

Table 1. Basic statistical data of anomalies (mgal).

Statistic	Minimum	Maximum	Average	Standard deviation
Δg	-58.87	209.73	27.01	26.07
$\Delta g - \Delta g_{GGM}$	-115.43	125.55	-2.09	22.05
Δg_R	-57.85	81.144	1.17	11.97

To apply collocation, empiric covariance of residual anomalies were calculateeed, together with a covariance function formed by applying the Tscherning and Rapp (1974) model:

$$\sigma_n = \frac{A(n-1)}{(n-2)(n+B)} \tag{5}$$

where covariance function, with $\sigma_0 = (R_B / R)^2$, is:

$$C_{\Delta g_P \Delta g_Q} = \alpha \sum_{n=2}^{n_l} \varepsilon_n \left(\frac{R^2}{r_P r_Q} \right)^{n+2} P_n(t) + \sum \sigma_n \sigma_0^{n+2} \left(\frac{R^2}{r_P r_Q} \right)^{n+2} P_n(t) \tag{6}$$

where A and B are scale factors for degree variances, R is the radius of the Bjerhammar sphere, R_E is the average earth radius, r_P and r_Q are radial distances of points, and n_l order of local covariance function, α is a scale factor of error associated with the reference field, P_n is a Legendre polynomial of degree n, σ_n is the variance in degrees, and $t = \cos(\psi)$, where ψ is a spherical distance.

While fitting, 360 degrees was chosen for the covariance function degree and the value of 24 was adopted for B. After fitting for the unknowns, the following values were obtained: α = 0.326092, $R_B - R_E$ = -1871.03m, A/R^2=110.85 mgal^2, $C_{H=0}$=149.96 mgal^2, as well as C_0=134.86 mgal^2 and correlation length ζ = 6′ (arc minutes). The empirical covariance graph and covariance function are shown in Figure 3.

Height anomaly and geoid undulation

After covariance-function determination, the residual heights anomalies at all points of regional gravimetric survey were predicted. Next, the effect of referent field ζ_{EGM96}, topographic mass effect ζ_{TOPO}, and the total height anomaly were obtained in accordance with (3).

Finally, height anomaly geoid undulations were determined by applying (4). Differences between the geoid and quasigeoid for Serbia ranges from 1 cm to –30 cm.

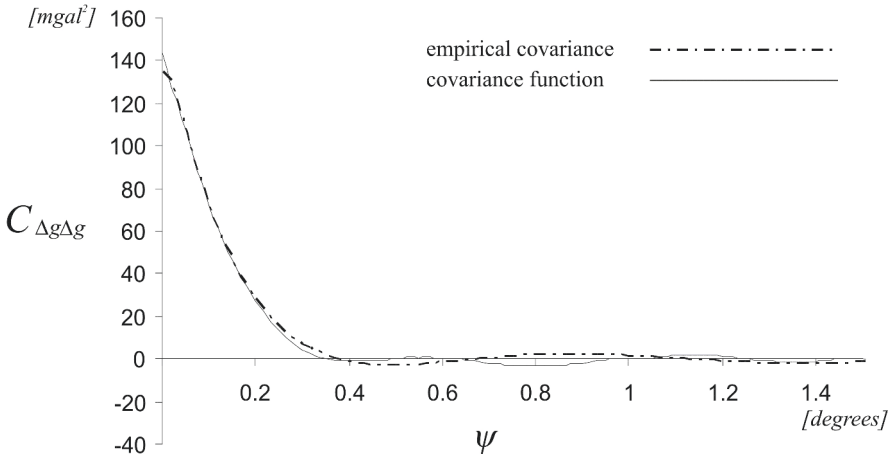

Figure 3. Empiric covariance and covariance function.

Geoid fitting

After undulation determination, the differences between gravimetric undulations and 53 GPS/dh undulations (Figure 4) were determined. From Figure 5, where the general shape of surface differences is shown, it is easy to notice a significant trend ranging from -0.2 m to -0.9 m in the east-west direction. Fitting of the gravimetric geoid, meaning the removal of trend, was done using GPS/dh undulations as follows: 1) at 18 points, the differences between gravimetric geoid undulations and GPS/dh undulations were determined (Figure 4, triangles); 2) obtained differences were modeled within the framework of a regular grid with 6x10-arc-minute resolution; 3) on the basis of this grid, the values of remaining residual values were estimated at all the regional gravimetric measurement points; and 4) the remaining values of the residual were added to the total undulations of gravimetric geoid (Figure 6). The remaining 35 GPS/dh undulations were used for external checking from which it is evident that, after fitting, the differences range from -9 cm to 14 cm, with the average value of 1.3 cm and a standard deviation of 7.7 cm. The general shape of surfaces of the residual differences after fitting is shown in Figure 7.

Figure 4. Distribution of undulation determined by the GPS/dh method (triangles for fitting, black marks for external checking).

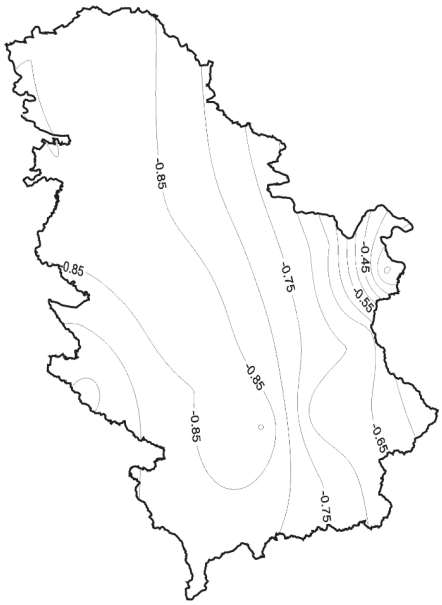

Figure 5. General shape of surface differences between gravimetric geoid and undulations determined by the GPS/dh method (contour interval 0.05 m).

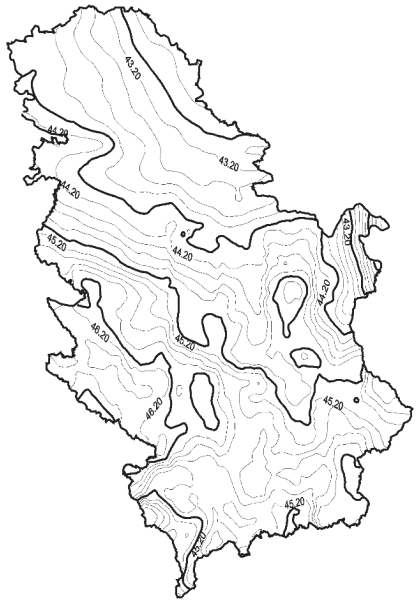

Figure 6. General shape of the Serbia preliminary geoid (contour interval 0.2 m).

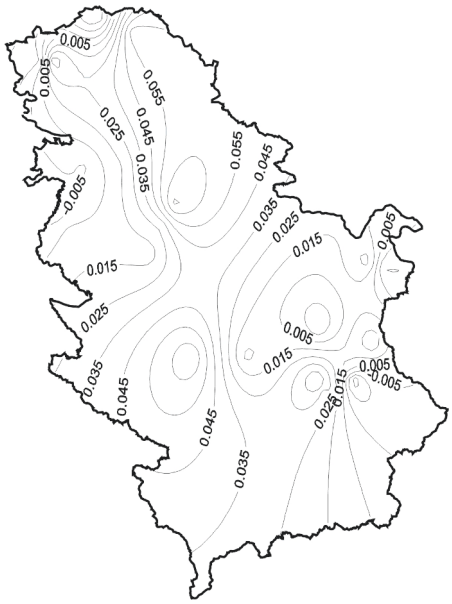

Figure 7. General shape of surfaces of the remaining residuals (contour interval 0.01 cm).

CONCLUSION AND FUTURE ACTIVITIES

This study shows that it is possible to determine the geoid in Serbia to an accuracy of about 10 cm with the available data. The average differences between the preliminary geoid and GPS/dh undulations averaged about 1.3 cm, with a standard deviation of 7.7 cm. In the remaining residuals, local distortion is evident, especially in eastern parts of Serbia.

These results use all available data, spanning 50 years from 1950 until 2003. However, documentation on some data is very unreliable and some data are out of date. Hence, to obtain a geoid of centimeter accuracy, it would be necessary to do new measurements in Serbia and to exchange data with neighboring countries.

REFERENCES

Bilibajkić P., Mladenović M., Mujagić S., Rimac i I. Tumač za gravimetrijsku kartu SFR – Jugoslavije Bouguerove anomalije 1:500000, Savezni geološki zavod, Beograd, 1979.

Blagojević D. Private communication, 1998.

Bošković S. Skretanje vertikala u Srbiji, Srpska akademija Nauka, 1952.

Bratuljević N. i dr. Geodetske referentne mreže, Institut za geodeziju. Beograd 1995.

Forsberg R.,.Tscherning C.C. The Use of Height Data in Gravity Field Approximation by Collocation. J. of Geophys. Research, 1981; 86 (B9): 7843-7845.

Heiskanen W. A., Moritz H. *Physical Geodesy*. W. H. Freeman and Co., San Francisco, 1967.

Muminagić A. Preliminary investigation in establishment of the Yugoslav first order triangulation network: orientation, isostatic corrections, astronomic leveling and the figure of the geoid. Beograd, 1967.

Odalović O. Odredivanje lokalnog geoida visoke rezolucije primenom modela integralne geodezije. Magistarska teza, Beograd 2000.

Starčević M. Private communication, 1999.

Tscherning C. C., Rapp R.H. Closed covariance expressions for gravity anomalies, geoid undulation, and deflections of the vertical implied by the anomaly degree variance models, Reports of the Department of Geodetic Science, Report No. 208, The Ohio State University, Ohio, 1974.

Weber G., Zomorrodian H. Regional geopotential model improvement for the Iranian geoid determination, Bulletin Géodésique 1988; 62:125-141.

PROCESSING OF GEODYNAMIC GPS NETWORKS IN CROATIA WITH GAMIT SOFTWARE

Damir Medak and Boško Pribičević
Department of Geomatics, Faculty of Geodesy, University of Zagreb, Zagreb, Croatia
dmedak@geof.hr

ABSTRACT

This paper presents geodetic results for the area around the city of Zagreb. After three series of GPS measurements, the analysis of the first results with scientific software GAMIT show significant geodynamic activity in the research area. Horizontal velocities of several millimeters per year were obtained, whereas the error budget of GPS observations was smaller by an order of magnitude. Comparison of geodetic results with geologic research show that the motions at the surface and under the ground have opposite directions. The velocity magnitudes are compatible with recent seismic activity in the Medvednica area. In order to get more reliable results, new measurements have been planned.

Keywords: geodynamics, tectonics, GPS, processing of geodetic measurements, GAMIT

INTRODUCTION

The Adriatic microplate area is seismically very active (Anderson and Jackson, 1987), (Mantovani et al. 1992), (Skoko and Mokrović, 1998), especially in the eastern part (Altiner, 1999), (Pribičević et al. 2003). During last ten years GPS technology plays a major role in providing geodetic contribution to the geodynamic investigation in central-european countries. Aside from GPS, very-long base interferometry (VLBI), satellite laser ranging (SLR) and satellite radar interferometry are used in geodynamic research (Keller and Pinter, 2002).

Geodetic investigation of the kinematics of the Croatian side of the Adriatic microplate at started in 1994 through the Croatian Geodynamical Project (CRODYN). A number of stations along the Slovenian and Croatian coasts were observed simultaneously. There were two more campaigns in 1996 and 1998. The results of the first two campaigns including the movements and the interpretation were published in Altiner (1999).

Outside the area studied by CRODYN, the second most seismically active area in Croatia is the area of the city of Zagreb (Prelogović et al. 1998). A strong earthquake in 1880 caused the beginning of research in seismology

N. Pinter et al. (eds.), The Adria Microplate: GPS Geodesy, Tectonics and Hazards, 247–256.

in Croatia, notably by Andrija Mohorovičić, who started regular seismological services in this region. Recent developments enabled the beginning of geodynamic geodetic research around the Croatian capitol. The main goal of the project is to provide accurate information for seismic zoning to be included in the construction code.

ZAGREB GEODYNAMIC GPS NETWORK

Through the realization of the project GPS network for Zagreb, a well-founded network of points was established (Medak and Pribičević, 2001). All 43 points in the base network had special stabilization that fulfilled all criteria for geodynamic research. The first measurements were carried out in 1997. The purpose of the network was twofold: to be used for the state survey and to monitor tectonic movements. The first goal was fulfilled in 1998, as the homogenous field with more than 4000 GPS points in Zagreb area was measured and adjusted. The second goal, geodynamic monitoring is a long-term project involving repeated observations every 3-4 years.

During the choice of point locations scientists from other disciplines were included: geologists, geophysicists, seismologists and civil engineers. The stability of points was the most important issue during the preparatory phase of the project. All pillars are equipped with forced centering screws. Since the area is mainly gravel, special stabilization is constructed and checked with precise leveling after a couple of years to determine if the pillars are vertically stable with respect to nearby leveling points. Locations are chosen with respect to fault zones to optimally describe motions. Several other criteria were important: nearby leveling points, durability with respect to landslides, engineering works, vehicle accessibility and, clear sky view at 10-15° elevation and above, especially in S, SW and SE direction. Sources of strong radio-emission, and reflective surfaces were avoided. Altogether, 33 points were stabilized with special pillars, while the rest of the points had other marks for forced centering of GPS antennas. The locations of all points are shown in Figure 1.

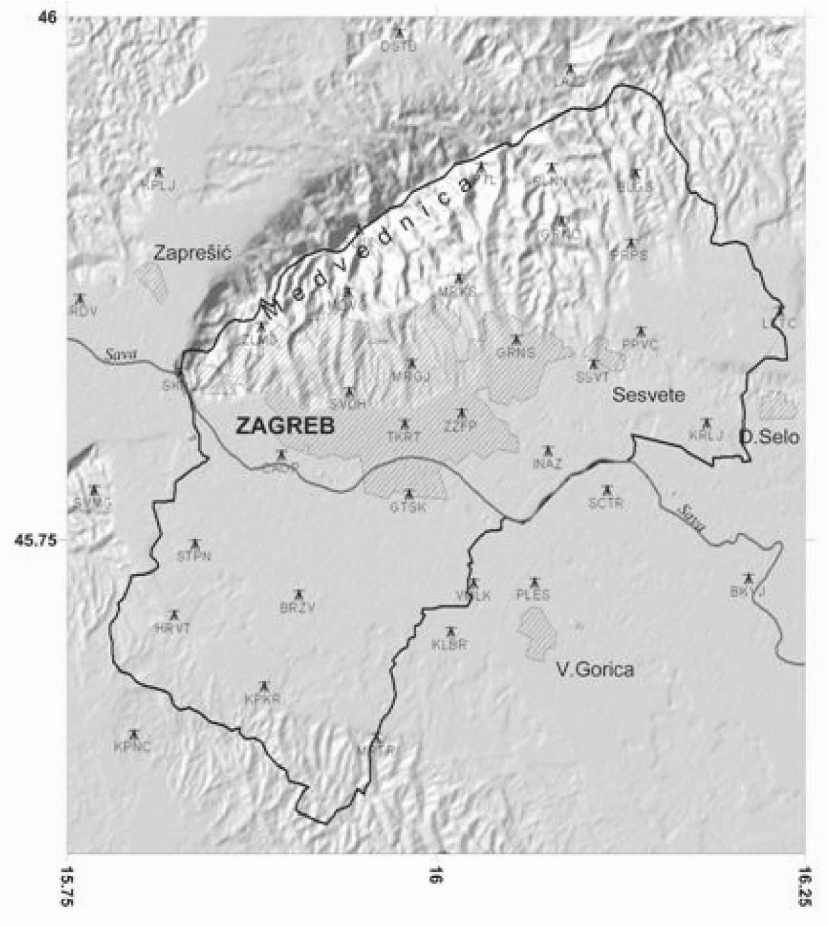

Figure 1. Distribution of points in the Zagreb Geodynamic Network.

GEOLOGIC STRUCTURE AND RECENT TECTONIC ACTIVITY

In the inland part of Croatia, the Medvednica area is the most active seismically and has the highest seismic potential, with an estimated maximum magnitude of 6.5. All epicenters are above the Moho. Several times during its history Zagreb has been shaken by large earthquakes, whose hypocenters are likely to have been under Mount Medvednica. The strongest known earthquake is thought to be that of 9th November 1880. This event had a

maximum intensity estimated at IXº of the Mercali-Cancani-Sieberg (MCS) scale and is thought to have had a focal depth of only 10 km (Skoko and Mokrović 1998). The magnitude of the earthquake was estimated as 6.3.

The geologic and seismotectonic setting of the research area is shown on figures 2 and 3.

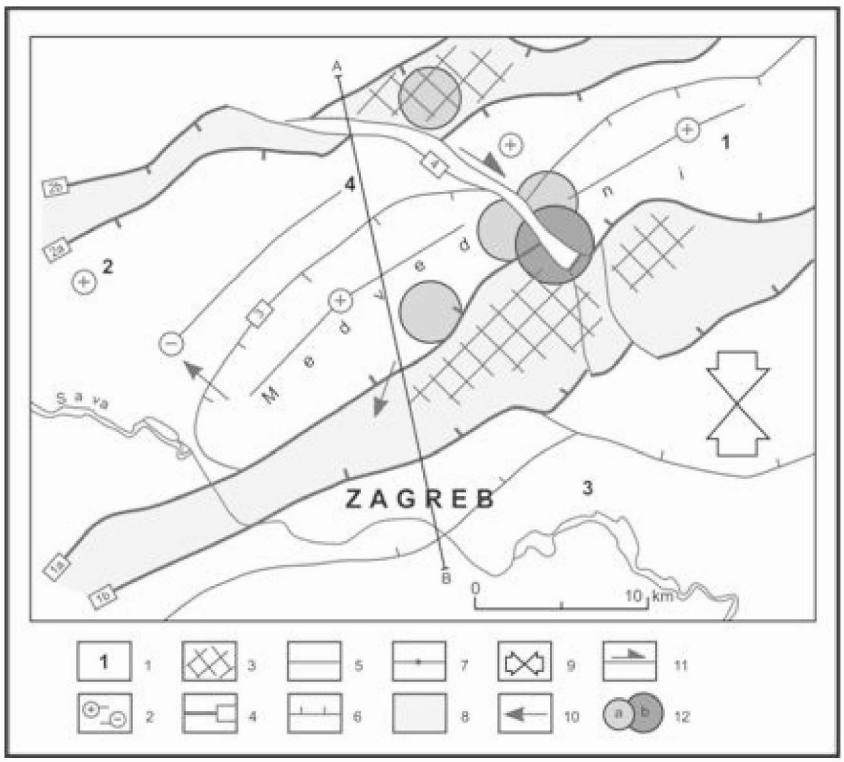

Figure 2. Geologic structure of Mount Medvednica: 1 – structures, 2 – axes of maximal and minimal Bouguer anomalies, 3 – zones of larger gravity gradients, 4 – Medvednica-Zumberak fault (1a – Zagreb fault), 5 – Medvednica faults, 6 – reverse faults, 7 – faults with unknown direction, 8 – fault zones, 9 – orientation of maximal compression stress, 10 – direction of subsurface motions of Medvednica, 11 – fault with horizontal motion, 12 – Epicentres of the strongest earthquakes.

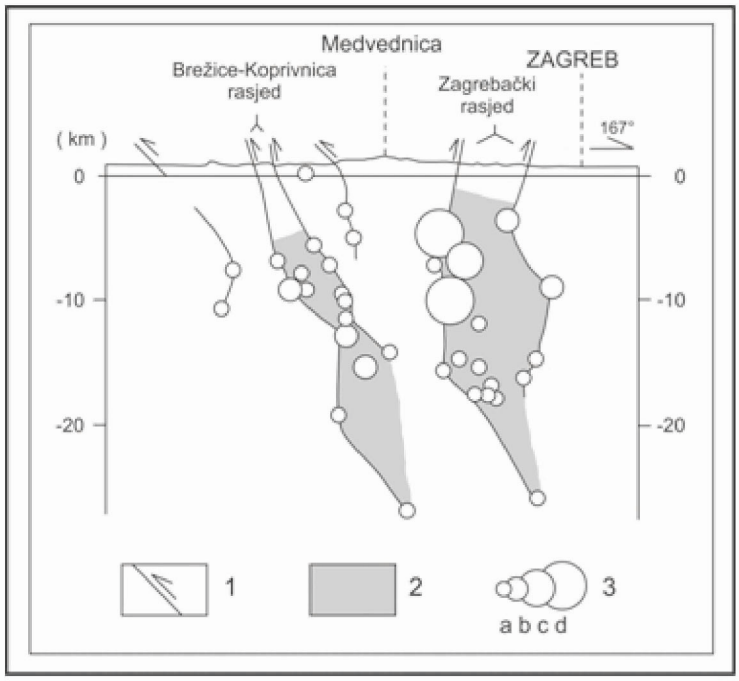

Figure 3. Seismotectonic profile of the research area. 1 – faults, 2 – seismically active zone, 3 – earthquake hypocenters, magnitudes a: $M \leq 4$, b: 4-5, c: $M = 5{,}6$, d: $M \geq 6$.

OBSERVATIONS AND PROCESSING WITH GAMIT

The Zagreb Geodynamic Network has been observed in three GPS campaigns. In 1997 and 2001 the whole network was observed (Medak and Pribičević, 2002), whereas in 2003 only 13 selected points were measured. For the purpose of this paper, only campaigns in 1997 and 2001 are taken into account.

The data were analyzed with GAMIT, a GPS analysis package developed by the Department of Earth, Atmospheric, and Planetary Sciences of the Massachusetts Institute of Technology, Scripps Institution of Oceanography and Harvard University primarily to study crustal deformation, (King and Bock, 1995), (Bock et al. 1986), (Schaffrin and Bock, 1988). GAMIT is capable of combining different kinds of observations to estimate station positions and velocities (Dong et al. 1998).

Table 1. Sites, locations, errors and velocities of horizontal components in the Zagreb Geodynamic Network

site	location		errors 1997		errors 2001		velocities 2001-1997	
	lon	lat	σE [mm]	σN [mm]	σE [mm]	σN [mm]	v(N-S) [mm/yr]	v(E-W) [mm/yr]
LKTC	16.233	45.86	±0.8	±1.0	±1.5	±1.7	4.0	-1.8
BKVJ	16.211	45.732	±1.0	±1.2	±1.3	±1.5	6.6	-4.6
KRLJ	16.183	45.807	±0.7	±0.8	±1.3	±1.5	4.8	-3.2
PPVC	16.139	45.85	±0.9	±1.1	±1.3	±1.6	2.3	-3.5
BLGS	16.135	45.926	±0.6	±0.8	±1.8	±2.1	1.9	-3.4
PRPS	16.132	45.893	±0.9	±1.1	±1.4	±1.6	2.4	-2.5
SCTR	16.116	45.774	±0.9	±1.1	±1.4	±1.6	3.1	-2.3
SSVT	16.107	45.835	±0.9	±1.1	±1.2	±1.5	-4.0	0.5
LAZZ	16.091	45.976	±0.9	±1.1	±1.5	±1.8	3.5	-2.6
GRNC	16.085	45.903	±0.7	±0.9	±1.3	±1.5	2.2	-2.4
PLNN	16.078	45.928	±0.7	±0.8	±1.4	±1.7	1.6	-3.2
INAZ	16.076	45.793	±0.9	±1.1	±1.2	±1.5	3.1	-3.0
PLES	16.066	45.731	±1.0	±1.3	±1.1	±1.4	3.9	-1.8
GRNS	16.054	45.847	±1.0	±1.2	±1.2	±1.5	-0.4	-0.4
KPTL	16.03	45.929	±1.0	±1.2	±1.5	±1.8	1.7	0.9
VMLK	16.025	45.73	±0.7	±0.8	±1.5	±1.9	3.6	-3.4
ZZFP	16.017	45.811	±0.8	±1.0	±0.9	±1.1	3.5	-2.9
MRKS	16.015	45.876	±1.4	±1.7	±1.5	±1.9	3.1	-2.8
KLBR	16.01	45.707	±0.8	±1.0	±1.0	±1.3	4.7	-0.8
MRGJ	15.983	45.835	±1.0	±1.3	±1.8	±2.2	10.0	3.6
GTSK	15.981	45.773	±1.4	±1.7	±1.7	±2.0	4.6	-2.4
TKRT	15.979	45.806	±1.0	±1.3	±1.3	±1.6	10.6	-0.2
DSTB	15.975	45.993	±0.8	±1.0	±1.8	±2.3	1.4	-3.6
MRTR	15.96	45.656	±0.8	±1.1	±1.1	±1.3	3.4	1.3
SVDH	15.941	45.822	±1.0	±1.3	±1.3	±1.6	4.4	-5.1
MDVG	15.94	45.869	±0.7	±0.9	±1.2	±1.4	3.4	-1.6
BRZV	15.907	45.725	±1.0	±1.3	±1.7	±2.0	5.7	-1.1
CAOP	15.895	45.791	±1.2	±1.4	±0.9	±1.1	4.0	-1.8
KPKR	15.883	45.681	±0.9	±1.1	±1.1	±1.3	5.3	-3.4
ZLMG	15.881	45.853	±0.9	±1.2	±1.4	±1.7	4.9	-2.6
STPN	15.836	45.749	±0.8	±1.0	±1.1	±1.3	3.6	-2.0
SKRL	15.826	45.831	±0.8	±1.1	±1.3	±1.5	3.3	-3.7
HRVT	15.822	45.715	±0.8	±1.0	±1.2	±1.4	4.0	-2.2
KPLJ	15.812	45.927	±0.8	±1.0	±1.3	±1.5	4.1	-2.1
KPNC	15.795	45.658	±0.9	±1.1	±1.1	±1.4	4.1	-4.0
SVMG	15.768	45.775	±1.0	±1.2	±1.2	±1.4	2.2	-1.6
BRDV	15.759	45.866	±1.0	±1.2	±1.3	±1.5	5.0	-2.5

RESULTS

Results of processing the GPS Network with GAMIT are summarized in tables 2, 3 and 4, where minimal, maximal and average RMS errors in millimeters are given for each campaign and each coordinate component (latitude, longitude, and ellipsoidal height). In 1997, we got slightly more accurate results due to the lesser Sun activity than in 2001. Another possible cause might be the number of sessions in these campaigns. The errors in the vertical component are significantly larger. Thus, we performed precise leveling measurements on the pillars to check if there are any local land-slides causing possible vertical aseismic movements.

Displacements and the most important geological structures are graphically shown in Figure 6. The movements are calculated relative to the point KZJC and given as yearly rates, i.e. averages between the campaigns performed in 1997 and 2001.

Table 2. Summary of latitude-accuracy in Zagreb Geodynamic Network – φ

Campaign	pts	m_φ [mm]		
		min	max	avg
Zagreb 1997	43	0,6	1,4	0,9
Zagreb 2001	40	0,9	1,8	1,3
Zagreb 2003	13	1,6	3,1	2,0

Table 3. Summary of longitude-accuracy in Zagreb Geodynamic Network – λ

Campaign	pts	m_λ [mm]		
		min	max	avg
Zagreb 1997	43	0,8	1,7	1,1
Zagreb 2001	40	1,1	2,4	1,6
Zagreb 2003	13	2,0	3,8	2,4

Table 4. Summary of height-accuracy in Zagreb Geodynamic Network – h

Campaign	pts	m_h [mm]		
		min	max	avg
Zagreb 1997	43	2,9	9,3	4,6
Zagreb 2001	40	4,0	11,5	6,3
Zagreb 2003	13	8,0	19,9	10,3

Figure 4. Horizontal displacements (movements 1997-2001) and structural fabric near Zagreb.

CONCLUSIONS

Special stabilization of GPS points in the geodynamic network of the City of Zagreb, unique in Croatia, was confirmed as extremely important for success of repeated GPS measurements of local crustal movements. Without special pillars, it would not have been possible to setup the antenna at the same place, since there is no suitable bedrock in the area.

Forced centering of GPS antennae resulted in excellent accuracy of measurements in both campaigns yielding significant displacements of local geological structures. The obtained results have been already interpreted in

multidiscipline cooperation. First results show that the magnitude of the movement is larger than measurement noise. The Zagreb geodynamic network was the first project yielding numerical data about movements of geologic units in this area. Obtained results are compatible with previous geologic research.

Geodetic points are located in the foot wall block of the reverse fault, while the main direction of compression in Medvednica area is NW-SE. Medvednica is being pushed by the collision of Eastern Alps from the north and Dinnarides from the south-west, with subsurface resistence of Pannonian structures, producing the compression. The main direction is related to the hanging wall block of the fault, observed and mapped by geologists. Geodetic measurements are compatible with opposite movements of the foot wall block. Additional geodetic points in the hanging wall block should reveal more information about the activity of the reverse fault. Largest velocities indicate locations or zones of tectonic movements between the measurement campaigns. These zones include Zagreb fault (1a) and Stubica fault (4). This is compatible with stronger seismic activity in the western part of Medvednica during the same period.

Repeating the campaign every three years would give better insight into geological processes in the area. Application of GAMIT software GLORG module to calculate origin shift instead of displacements should reveal new information about relative movements of points. Current method of fixing only single station (KZJC) has the drawback that the magnitudes and directions of horizontal movements are related to the station at the boundary of the area, which is on the other side of the fault.

Further research includes the third complete GPS observation campaign to be performed in 2004 which will give reliable information about movements of the area. Two approaches are going to be tested: fixed point and fixed set of points which defines the reference frame of the local network. GAMIT software will also be tested in a wider, regional setup: reprocessing of CRODYN data or CEGRN campaigns would be an excellent and independent control on analyses already performed.

REFERENCES

Altiner Y. *Analytical Surface Deformation Theory for Detection of the Earth's Crust Movements*, Springer Verlag, 1999.

Anderson H. A., Jackson J.A. Active tectonics of the Adriatic region. Geophys. J.R. Astr. Soc. 1987; 91: 937-983.

Bock Y., Gourevitch S.A., Counselman C.C., King R.W., Abbot R. I. Interferometric Analysis of GPS phase observation. Manuscripta Geodaetica 1986;11: 282-288.

Dong D.N., Herring T.A., King R.W. Estimating regional deformation from a combination of space and terrestrial geodetic data. J. Geodesy 1998; 72: 200–214.

Keller E.A., Pinter N. *Active Tectonics, Earthquakes, Uplift and Landscape*. Second Edition. Prentice Hall, Upper Saddle River, New Jersey, 2002.

King R.W., Bock Y. Documentation for the MIT GPS analysis software: GAMIT. Massachusetts Institute of Technology, 1987.

Mantovani E., Albarello D., Babbucci D.R., Tamburelli C. Recent Geodynamic Evolution of the Central Mediterranean Region. Tipografia Senese 1992; 1-88, Siena.

Medak D., Pribičević B. Geodynamic GPS-Network of the City of Zagreb – First Results. The Stephan Mueller topical conference of the European Geophysical Society: Quantitative neotectonic and seismic hazard assessment: new integrated approaches for environmental management. Balatonfüred, Hungary, 2001.

Medak D., Pribičević B. Geodynamic Network of the City of Zagreb (in Croatian: Geodinamička mreža Grada Zagreba). Proceedings of the Faculty of Geodesy, University of Zagreb 1962-2002, Zagreb 2002; 145-156.

Medak D., Pribičević B. Processing of Geodynamic GPS-Networks with GAMIT Software. Reports on Geodesy, Warsaw University of Technology 2003; 1 (64): 75-84.

Prelogović E., Saftić B., Kuk V., Velić J., Dragaš M., Lučić D. Tectonic activity in the Croatian part of the Panonian basin. Tectonophysics 1998; 297: 283-293.

Pribičević B., Medak D., Prelogović E. Investigation of geodynamics of Adriatic micro-plate by means of geodetic, geophysical and geologic methods. Reports on Geodesy, Warsaw University of Technology 2003; 1(64): 85-92.

Schaffrin B., Bock Y. A unified scheme for processing GPS phase observations, Bulletin Geodesique 1988; 62: 142-160.

Skoko D., Mokrović J. *Andrija Mohorovičić*, Skolska knjiga, Zagreb 1998.

ACTIVE DEFORMATION OF THE NORTHERN ADRIATIC REGION:

Results from the CRODYN geodynamical experiment

Yüksel Altiner[1], Marijan Marjanović[2], Matija Medved[3], Ljerka Rasić[2]
1: Bundesamt für Kartographie und Geodäsie, Frankfurt am Main, Germany
altiner@ifag.de
2: State Geodetic Administration of the Republic of Croatia, Zagreb, Croatia
3: State Geodetic Administration of the Republic of Slovenia, Ljubljana, Slovenia

ABSTRACT

The accuracy of a position determined using Global Positioning System (GPS) technology depends in the first place on the evaluation of so-called station- and distance-dependent errors. For precise determination of small crustal movements, additional error sources must be taken into account. In this paper, the advantages of an analytical surface deformation theory for describing movements of the earth's crust are briefly presented, and the results of deformation analysis based on the annual velocities derived from the GPS data acquired in the region of the Adriatic Sea are discussed.

Keywords: Adria, analytical surface deformation theory, Earth's crust deformation, GPS, strain

INTRODUCTION

If we assume that the earth is a body consisting of points, all points on this body are subject to permanent and temporary displacements due to tidal effects of the sun and the moon, plate tectonic motions, atmospheric, hydrological, ocean loading, and local geological processes. The measurement of small movements of the points over the plate boundaries and faults has been made possible by the development of the space-based techniques, including Very Long Baseline Interferometry (VLBI), Satellite Laser Ranging (SLR), and the Global Positioning System (GPS). In the last 15 years, GPS has become the most used technique for the determination of crustal movements. Generally, GPS observations are subject to errors arising from the environments of the measurement stations, such as multipath effect, receiver noise, and missed or incorrect values of antenna calibration (variations of the antenna phase-center depending upon elevation and azimuth from the transmitting direction of satellite signals), and to errors of atmospheric influences resulting in transit-time delay of the satellite signals in the ionosphere and troposphere (Figure 1). A large part of the influences of the multipath effect and the effect of phase-center variations of antennas can

N. Pinter et al. (eds.), The Adria Microplate: GPS Geodesy, Tectonics and Hazards, 257–267.

be reduced by choosing a suitable antenna location and by calibrating the antennas, whereas for the reduction of the transit-time delay in the troposphere and stratosphere, the modelling of atmospheric data (dry and wet temperature and pressure) as well as a suitable mapping function depending upon height and latitude of station position will have to be applied. The reduction of the effect of the transit-time delay of the satellite signals in the ionosphere is performed by means of the ionosphere free solution.

Additional GPS error sources that constrain the accuracy of a position include eccentricity error for non-permanent stations and the application of different strategies for data processing from each individual GPS campaign. These remaining errors propagate according to the following equation:

$$\sigma_p^2 = \sigma_e^2 + \sigma_o^2 + \sigma_c^2 + \sigma_m^2, \qquad 1.1$$

where σ_p is position error, σ_e is eccentricity error of the station marker, σ_o is error of transformation of satellite coordinates from an old realisation to an up-to-date realisation of the International Terrestrial Reference Frame (ITRF), σ_c is antenna calibration error, and σ_m is error created from the application of the different mapping functions and/or from elevation-dependent weighting of observations for the determination of transmissions delays of satellite signals in the troposphere and stratosphere (tropospheric delay). The magnitude of these remaining errors, extracted from a study undertaken in Germany (no error for eccentricity has been considered) can reach up to 8 mm in the horizontal components and up to a few cm in the vertical component of motion (Altiner, 2004). The accuracy of the vertical movements derived by GPS is 2-4 times worse than the accuracy of the horizontal component of velocities. However, this fact does not change the face that crustal deformation is three-dimensional. For a realistic derivation of 3D deformation, the results must be referenced to the physical surface of the Earth, namely to topography.

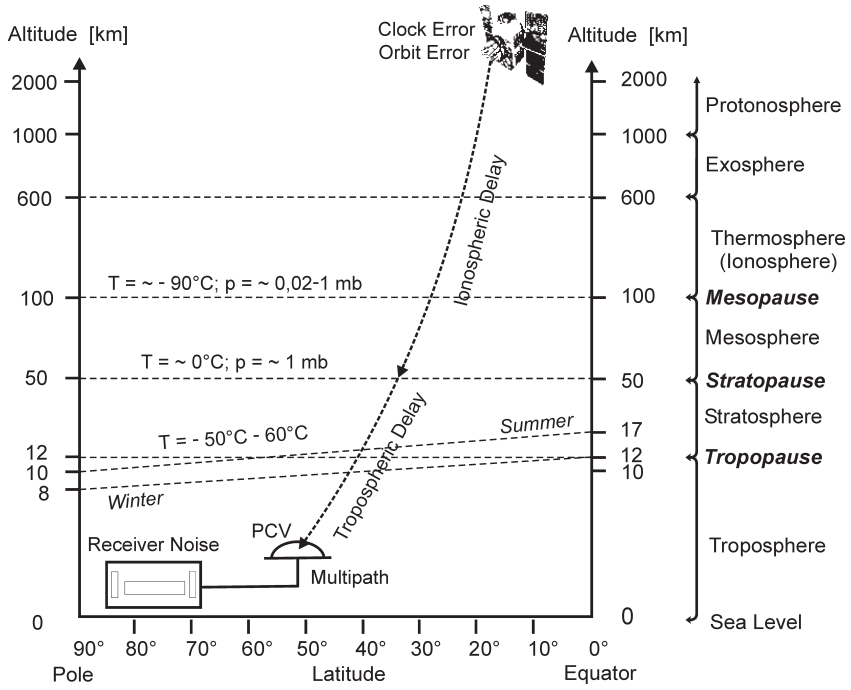

Figure 1. Layers of the atmosphere and error sources as determined by the GPS technique.

TECTONICAL BACKGROUND

Geological and seismological studies indicate that the tectonic framework of the Adriatic Sea is dominated by the collision of the African Plate with the Eurasian Plate. Anderson & Jackson (1987) described this area as a relatively rigid block the motion of which relative to Eurasia occurs as a rotation about a pole located in NW Italy. Jackson & McKenzie (1988) supported this idea and stated that Adria is not behaving as a promontory of Africa but may have done so in the past. Oldow et al. (2002) examined GPS site velocities and seismicity and asserted that Adria is divided into northwestern and southeastern tectonic blocks, whereas Kuk et al. (2000) subdivided the area with respect to the magnitude and rate of movements of the microplate into three different seismic zones (northern, central and southern parts) with differential movement of the microplate explained by the resistance of the Dinarides and the existence of the active faults along the Adriatic margin. Udias (1982) noted that seismic stresses in the Alpine region are predominatly horizontal compressions oriented normal to the trend of the mountain chain (Figure 2).

According to Prelogović et al. (1999) and Dragičević et al. (1999) the southern part of the Adriatic microplate moves in a NNW direction. In this area, the compression is the dominant factor, whereas the NE part shows characteristics of an extension zone. Generally, the frequencies of earthquakes in the Adriatic region indicate that seismic activity is concentrated in the onshore areas, especially to the NW and SE of the Adriatic Sea (Skoko & Mokrović, 1998). The recent earthquakes of 1996 and 1998 in Ston and Bovec also support this suggestion (Altiner, 2001). Studies focused on the detection of crustal deformation using GPS data in the Adriatic region and its surroundings include Mantovani et al. (2001), Caporali et al. (2003), Grenerczy (2002), Hefty & Draciova (2002), and McClusky et al. (2000).

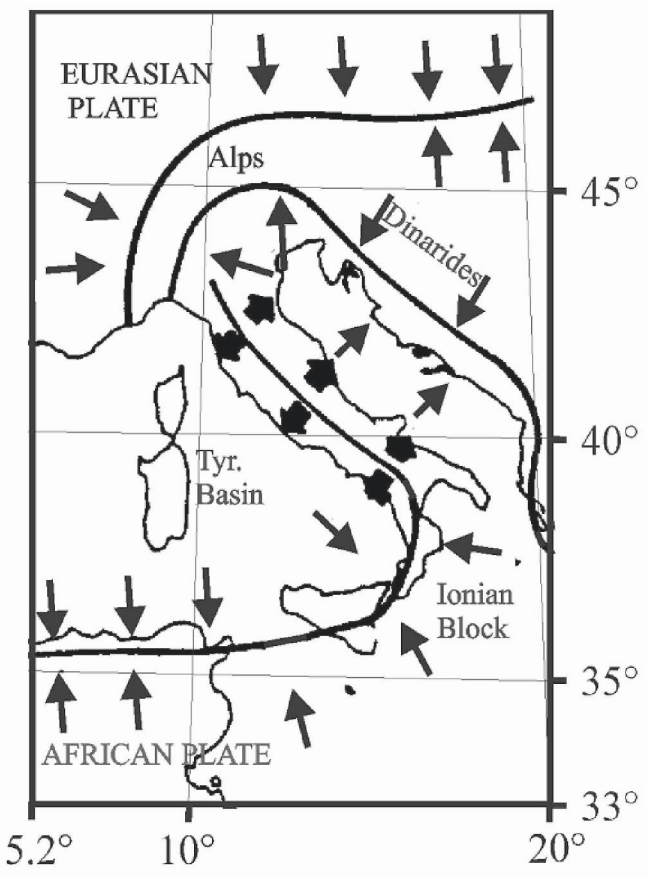

Figure 2. Tectonic features in the Alpine region (modified from Udias, 1982).

PROCESSING OF GPS DATA

For the study of present-day tectonics in the Adriatic region, a GPS network of 20 stations located in Croatia, Italy and Slovenia was established in 1994. In 1996 and 1998, the network was extended with new stations in Albania, Bosnia and Herzegovina and Italy, bringing the total number of stations to 34. The first GPS campaign within this network was conducted in 1994, from June 7 to June 10, in three sessions each with a session length of 24 hours. Observations were repeated in 1996, from September 9 to September 12, and in 1998, from September 4 to September 7, using the same observation strategy and the identical set of Trimble receivers (Čolić et al., 1996, Mišković & Altiner, 1997). The acquisition of this GPS data was realized in cooperation between the Bundesamt für Kartographie und Geodäsie in Frankfurt am Main (BKG), the State Geodetic Administration in Zagreb (SGAZ), and the State Geodetic Administration in Ljubljana (SGAL). With contributions from Ljerka Rasić and Marijan Marjanović of the SGAZ, the first two GPS campaigns were processed using the GPS software (v. 4.0) of the University of Bern (Switzerland) at the BKG (Hugentobler et al., 2001). The final orbits of the Center for Orbit Determination in Europe (CODE), which referred to the International Terrestrial Reference Frame 1994 (ITRF94), were introduced in the processing (Boucher et al., 1996). The evaluation of data for the last campaign from 1998 to estimate velocities for stations observed within the three GPS campaigns in a improved realization of the ITRF (e.g., ITRF96, ITRF97, and ITRF2000) is still on-going.

In order to reduce the dependence of the results on the datum of fixed station coordinates, annual velocities of stations within the GPS network were estimated to the coordinates of the station GRAZ, the closest IGS station to the network. The final coordinates and annual velocities of stations estimated are defined in ITRF94 and illustrated in Figs. 3 and 4 for the horizontal and vertical components of velocities, respectively. The velocity uncertainties computed within the CRODYN-Network average ± 3 mm/yr. According to the Fisher test for the normally distributed observations with a probability of 95 % (the confidence level $1-\alpha = 0.95$), the horizontal and vertical movements are significant. The magnitudes of the horizontal velocities relative to GRAZ vary between 0.5 and 1.5 cm/yr, increasing from north to south (Figure 3). The movements of the stations in the southern part of the study area show a NNW direction, whereas those in the northern part are more westerly. The vertical velocities are within the range of 0.5 and 2.0 cm/yr (Figure 4).

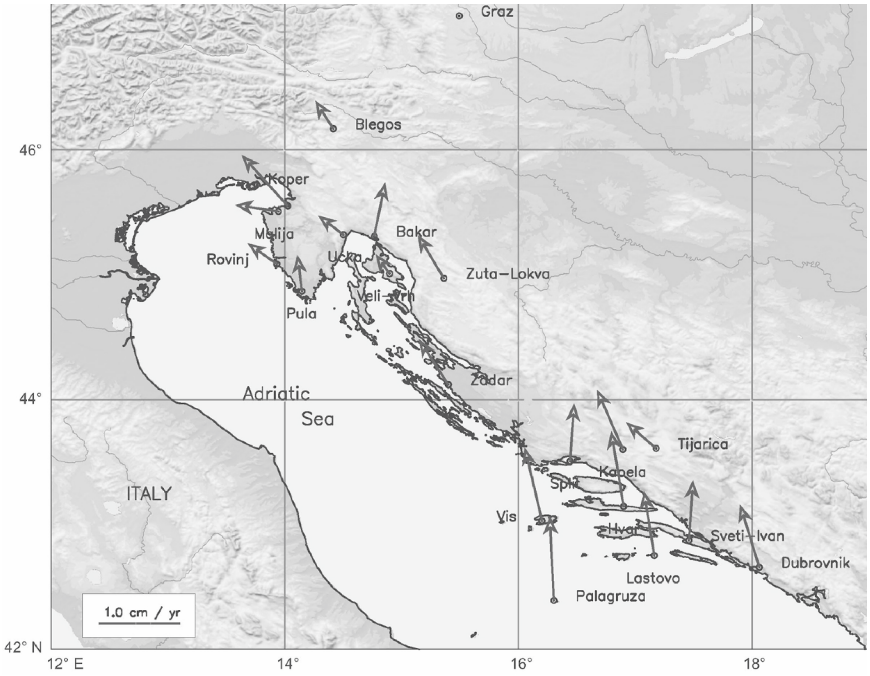

Figure 3. Annual horizontal velocities relative to the station GRAZ in cm/yr.

ANALYTICAL SURFACE DEFORMATION THEORY

Analytical surface deformation theory allows the derivation of 3D deformation measurements relative to the topography, which is defined as a curved surface embedded in a three-dimensional Euclidian space (Heitz, 1988). Derivation of internal (surface elongation [stretch] and surface dilatation) and external (changes of the mean and principal curvatures) surface deformation measurements using Cartesian and ellipsoidal coordinates are given in Altiner (1996, 1999, and 2001) and are applied to observations on different VLBI and GPS networks (Haas et al., 2000; Hefty & Duraciova, 2002; Klek et al., 2003; Şalk et al., 1999). Here, we limit our explanations to a brief presentation of some advantages of analytical surface deformation theory (see also Voosoghi, 2000) for strain analysis based on Cartesian coordinate differences to a mean horizontal plane (McClusky et al., 2000; Ayhan et al., 2002). With application of analytical surface deformation theory:

- the effects of rigid body motions, such as shifting and rotation, on station velocities are eliminated,
- ellipsoidal height variations in the study area are taken into account,
- three-dimensional deformations become detectable on the physical surface of the Earth,
- not only internal, but also external surface deformations are determined, and
- stress changes can be locally focused.

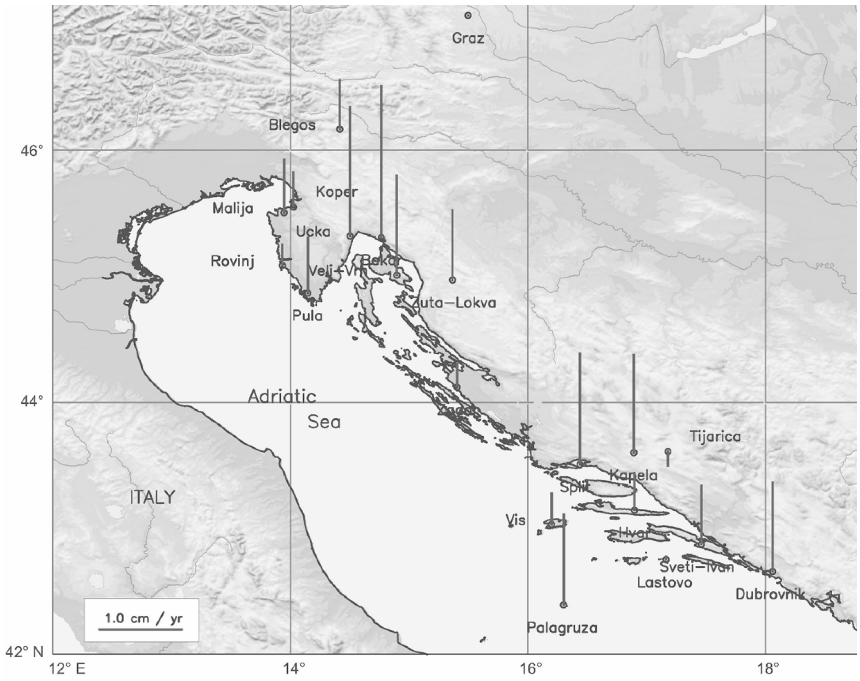

Figure 4. Annual vertical velocities relative to the station GRAZ in cm/yr.

INTERNAL AND EXTERNAL DEFORMATIONS

Evaluation of internal and external deformation measurements for the Adriatic region was realised using analytical surface deformation theory for a regular area-wide grid spanning 42.4° to 46.4° latitude and 13.6° to 17.6° longitude with a grid increment of 0.1°. At each grid point, the ellipsoidal heights (reference ellipsoid: GRS80), horizontal, and vertical movements were interpolated using splines based on the point distribution within the GPS network (DeBoor, 1978).

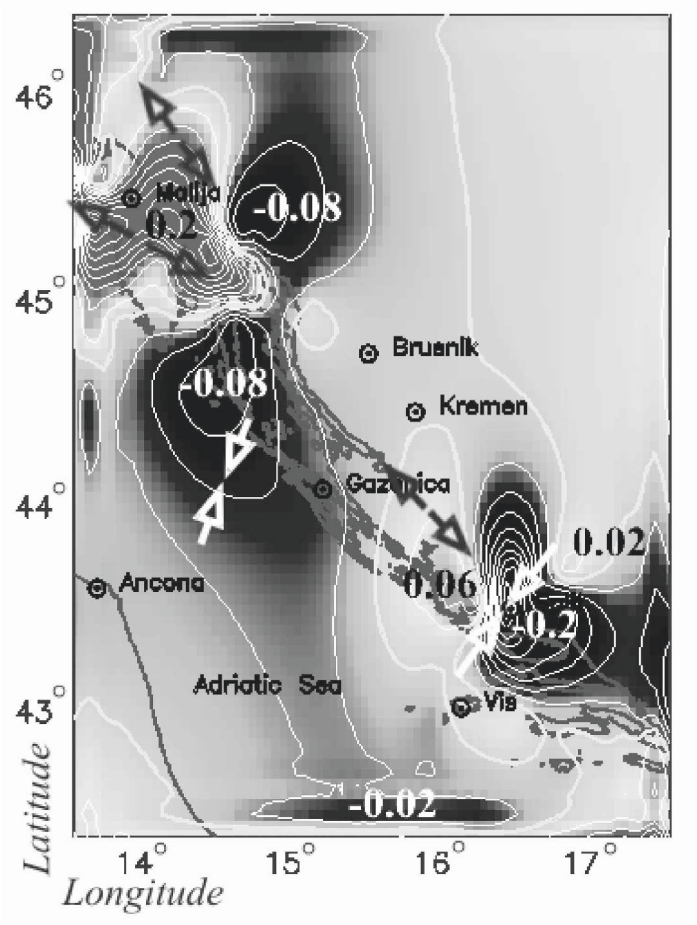

Figure 5. Surface dilatation determined by analytical surface deformation theory. The numbers in white show the area of compression, and the numbers in black the area of extension as ppm/yr. The arrows in white show the directions of compression, and the arrows in black the direction of extension (no scale).

The results of the deformation analysis suggest three different deformation zones within the study area (Figure 5). The NW part of the area exhibits predominant extension, with a magnitude of 0.2 ppm/yr, whereas the SE part of the study area exhibits compression (0.2 ppm/yr). The extension in the NW part is generally oriented NW-SE. The compression in the SE part indicates a NE-SW direction.

According to the changes in the mean curvatures of the points, the NW part of the study area between Koper and Pula, and Split area exhibit subsidence, whereas the southern part of the study area and the Dubrovnik

area exhibit uplift (Altiner, 2001). Most external changes have been observed in NW and SE (near Split and Ston).

NEW RESULTS

Just before publication of this paper, evaluation of data for stations observed during the third CRODYN campaigns in 1998 was completed. During processing, the elevation-dependent phase-center variations of antennas were considered.

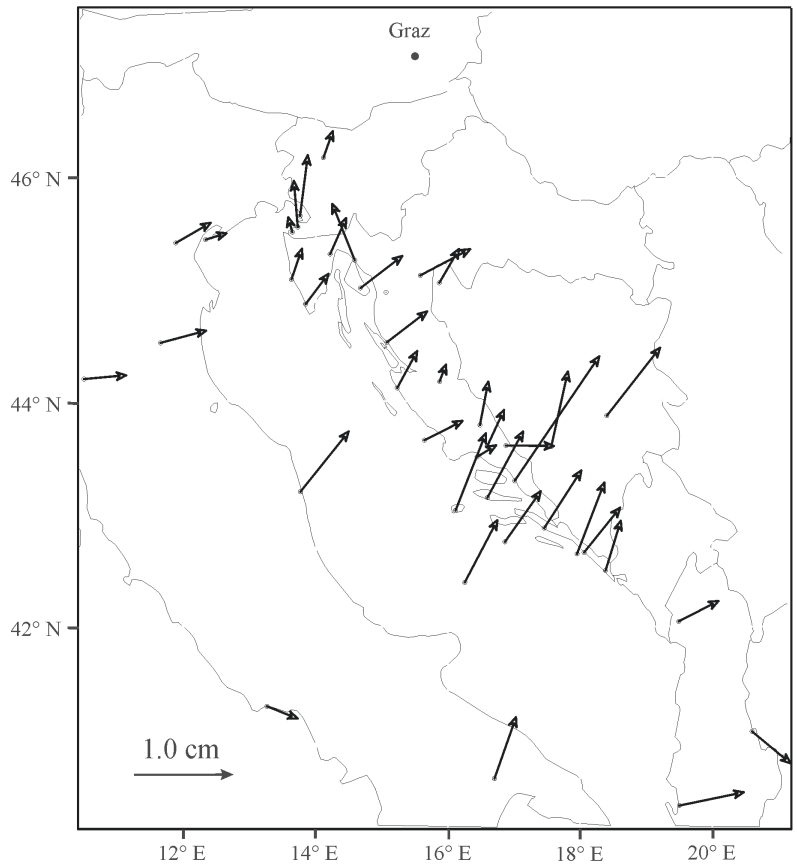

Figure 6. Annual horizontal velocities relative to the station GRAZ in cm/yr estimated from data acquired during the CRODYN GPS campaigns in 1994, 1996, and 1998.

This potential error source was unknown during the earlier processing of the 1994 and 1996 CRODYN campaigns (the offsets for L1 and L2 were known, but not the variations of the phase center). An additional important

difference to the earlier data processing is the consideration of an improved realization of the ITRF (here ITRF96). Velocity uncertainties estimated with respect to the IGS station GRAZ varied from ± 0.5 to ±1.5 mm (Figure 6). Based on the Fisher test for normally distributed observations with a probability of 95 %, the horizontal and vertical movements were significant.

REFERENCES

Altiner Y. *Geometrische Modellierung innerer und äusserer Deformationen der Erdoberfläche*, Deutsche Geodätische Kommission, Reihe C, Heft Nr. 462, 1996.

Altiner Y. *Analytical Surface Deformation Theory for Detection of the Earth's Crust Movements,* Springer-Verlag, Berlin Heidelberg New York, 1999.

Altiner Y. The contribution of GPS data to the detection of the Earth's crust deformations illustrated by GPS campaigns in the Adria region. Geophysic. J. Int. 2001; 145(2): 550-559.

Altiner Y. Diagnoseausgleichung SAPOS®: Integration von SAPOS®-Stationen in Internationale Netze, ZfV, 2004. In press.

Anderson H.A., Jackson J.A. 1987. Active tectonics of the Adriatic Region. Geophys. J. R. Astr. Soc. 1987; 91: 937-983.

Ayhan M. E., Demir C., Lenk O., Kilicoglu A., Altiner Y., Barka A. A., Ergintav S., Özener H. Interseismic Strain Accumulation in the Marmara Sea Region, Bull. Seismo. Soci. of America 2002; 92(1): 216-229.

Boucher C., Altamimi Z., Feissel M., Sillard P. Results and Analysis of the ITRF94, IERS Technical Note 20, 1996, Observatoire de Paris, Paris.

Caporali A., Martin S., Massironi M. Average strain rate in the Italian crust inferred from a permanent GPS-network - II. Strain rate versus seismicity and structural geology. Geophysic. J. Int. 2003; 155: 254-268.

Čolić K., Bašić T., Seeger H., Gojčeta B., Altiner Y., Rašić L., Medić Z., Pribičević B., Medak D., Marjanović M., Prelogović E. 1996. Croatia in EUREF'94 and the Project CRODYN (in Croatian), Geodetski List 1996*;* 50(73): 331-351, Zagreb.

DeBoor C. *A Practical Guide to Splines,* Springer-Verlag (Series: Applied Mathematical Sciences, Vol. 27), Berlin Heidelberg New York, 1978.

Dragičević I., Prelogović E., Kuk V., Buljan R. Recent Tectonik Activity in the Imotsko Polje Area, Geol., Croat. 1999; 53(2): 191-196, Zagreb.

Grenerczy G. Towards a dense interplate velocity map for central Europe, Reports on Geodesy; 2002; 1(61): 27-36.

Haas R., Gueguen E., Scherneck H.-G., Nothnagel A., Campbell H. Crustal motion results derived from observations in the European geodetic VLBI network, Rarth Planets Space 2000; 52: 759-764.

Hefty J., Duraciova R. Stochastic properties of deformation characteristics obtained from GPS site velocities, Slovak University of Technology, Department of Theoretical Geodesy, Bratislava, Slovakia; (http://www.fomi.hu/cegrn/public/Hefty_03.pdf), 2002.

Heitz S. *Coordinates in Geodesy*, Springer-Verlag, Berlin Heidelberg New York, 1998.

Hugentobler U., Schaer S., Fridez P. *Bernese GPS Software Version 4.2*. Astronomical Institute of the University of Berne, Switzerland, 2001.

Jackson J., McKenzie D. The relationship between plate motions and seismic moment tensors, and the rates of active deformation in the Mediterranean and Middle East. Geophys. J. 1998; 93: 45-73.

Klek M., Ragowski J. B., Jarosinski M. Study on deformation parameters in Poland obtained from techtonophysics and GPS data analysis. Proceedings of the 11th FIG symposium on deformation measurements, Santorini, Greece; (http://www.fig.net/commission6/santorini/A-TECTONOPHYSICS%20&%20SEISMOLOGY/ A9.pdf), 2003.

Kuk V., Prelogović E., Dragičevič I. Sesimotectonically Active Zones in the Dinarides. Geol. Croat 2000; 53(2): 295-303.

Mantovani E., Viti M., Cenni N., Albarello D., Babbucci D. Short and long term deformation patterns in the Aegean-Anatolian systems: insights from space geodetic data (GPS). Geophys. Res. Lett. 2001; 28: 2325-2328.

McClusk S. et al. Global Positioning System constraints on plate kinematics and dynamics in the eastern Mediterranean and Caucaus, Geophys. Res. Lett. 2000; 105(B3): 5695-5719.

Mišković D., Altiner Y. National Report of the Republic of Slovenia, Report on the Symposium of the IAG Subcommision for EUROPE, Astronomisch-Geodaetische Arbeiten 1997; 58: 202-208, eds., Gubler, E. and Hornik H., Verlag der Bayerischen Akademie der Wissenschaften, München.

Oldow J. S., Ferranti L., Lewis D. S., Campbell J. K., D'Argenio B., Catalano R., Rappone G., Carmignani L., Conti P., Aiken C. L. V. Active fragmentation of Adria, the North African promontori, central Mediterranean orogon, Geology (Geological Society of Amerika) 2002; 30 (9): 779-782.

Prelogović E., Kuk V., Buljan R., Tomijenović B., Skoko D. Recent tectonic movements and earthquakes in Croatia. Proceedings of the Geodynamics of the Alps-Adria Area by Means of Terrestrial and Satellite Methods 1999; 255-262, Zagreb and Graz.

Şalk M., Altiner Y., Ergün M. Geodynamics of Western Turkey. Proceedings of the International Conference on Earthquake Hazard and Risk in the Mediterranean Region 1999; 1: 179-189, Near East University, Nicosia.

Skoko D., Mokrović J. Development of Seismology - a review, in Andrija Mohorovičić 1998; 9-41, eds., Skoko, D., Mokrović, J., Državni Hidrometeorološki Zavod, Zagreb.

Udias A. Seismicity and Seismotectonic Field in the Alpine-Mediterranean Region. In *Alpine Mediterranean Geodynamic*, eds., H. Berckhemer, K. Hsü, Geodynamic Series 1982; 7: 75-82, Washington.

Voosoghi B., *Intrinsic Deformation Analysis of the Earth's Surface Based on 3-Dimensional Displacement Fields Derived from Space Geodetic Measurements*. Geodätisches Institut der Universität Stuttgart, 2000.

FRAGMENTATION OF ADRIA AND ACTIVE DECOLLEMENT TECTONICS WITHIN THE SOUTHERN PERI-TYRRHENIAN OROGEN, ITALY

John. S. Oldow[1] and Luigi. Ferranti[2]
1: Department of Geological Sciences, University of Idaho, Moscow, Idaho 83844-3022 USA
oldow@uidaho.edu
2: Dipartimento di Scienze della Terra, Universitá di Napoli Federico II, 80138 Napoli, Italy

ABSTRACT

Seismicity and GPS velocities in the southern peri-Tyrrhenian orogen record complex differential motion amongst crustal blocks constituting the tectonically fragmented paleotectonic domain, Adria. Coeval transpressional and transtensional belts within the orogen are kinematically coordinated and are consistent with displacement above a through-going basal decollement system that separates the heterogeneously deforming upper and middle crust from a presumed pattern of regular displacement within the underlying lithosphere. Seismicity and GPS velocities within the orogen reflect only indirectly the relative convergence between Africa and Eurasia.

INTRODUCTION

Although mountain-building is regarded as the dominant process in most ancient and active collisional orogens, in the western and central Mediterranean, convergence between Africa and western Eurasia is accompanied by the formation of deep extensional basins locally floored by oceanic crust (Figure 1). The extensional basins are ringed by fold-thrust belts that carry sedimentary rocks and crystalline basement away from the extended hinterland regions toward continental interiors (Jolivet and Faccenna, 2000). During the Cenozoic, the north and northwest convergence of Africa with respect to Europe is poorly reflected in the progression of basin development, which migrated easterly from the Alboran Sea to the Tyrrhenian basin at rates four to five times faster than the convergence between the continental plates (Gueguen et al., 1998). Displacements within the orogenic belts are not directly related to the trajectory of relative plate motion, and the complexity of the circum-Mediterranean orogen is attributable, in large part, to the original geometry of the opposing plate margins and to the existence of

N. Pinter et al. (eds.), The Adria Microplate: GPS Geodesy, Tectonics and Hazards, 269–286.

continental blocks within the western Tethys (Dewey et al., 1989; Ziegler, 1988; Wortmann et al., 2001).

In the central Mediterranean, the structural complexity and tectonic evolution of the region was profoundly influenced by Adria, a tectonic domain composed of Mesozoic carbonate platform and basin deposits and Cenozoic synorogenic rocks deposited on and adjacent to continental crust with African affinity (Argand, 1924). Adria has been viewed both as a promontory of North Africa (Channell et al., 1979; D'Argenio and Horvath, 1984) and as an independent microplate lying between Europe and Africa (Dercourt et al., 1986). In either case, Adria served as a tectonic indentor of the southern European margin during Alpine tectonism (Laubscher, 1991).

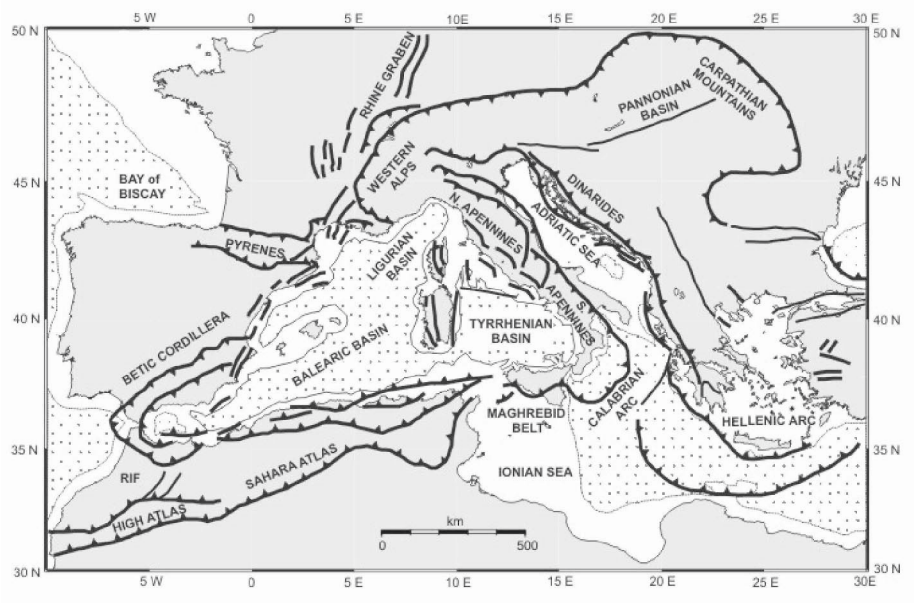

Figure 1. Generalized tectonic map of the western and central Mediterranean.

At a more restricted scale, deformation belts surrounding the margins of Adria exhibit substantial spatial variability in deformation style attributable, at least in part, to the interaction of crustal blocks that were detached from their lithospheric basement during tectonic transfer to the European continental margin. Although contraction dominates Mesozoic and Cenozoic deformation histories, coupled extension and contraction have resulted in large-scale shortening and stretching along the western margin of Adria. The peri-Tyrrhenian orogen forms an arcuate belt of contraction ringing the eastern and southern margins of the extensional basin underlying the Tyrrhenian Sea. In northern Italy, peri-Tyrrhenian deformation is expressed as northeasterly-directed foreland contraction and southwesterly

hinterland extension, ongoing since the Miocene. Today the pattern of deformation in this part of the orogen is reflected by seismicity and a regular pattern of small (<5 mm/yr) GPS site velocities. In contrast, within the southern peri-Tyrrhenian belt, Miocene to Recent foreland contraction and hinterland extension are much more complex. Formation of the curved part of the orogenic belt involved progressive changes in tectonic transport direction by as much as 90º, large-scale (up to 130º) vertical-axis rotation of tectonic blocks, and nonplane extensional stain within the orogenic hinterland. Today, deformation is recorded by contractional, extensional, and transcurrent earthquake focal mechanisms in kinematically related but spatially segregated tectonic belts (Figure 2) and by relatively rapid (up to 12 mm/yr) GPS site velocities exhibiting spatially heterogeneous patterns of displacement (Anzidei et al., 2001; Oldow et al., 2002).

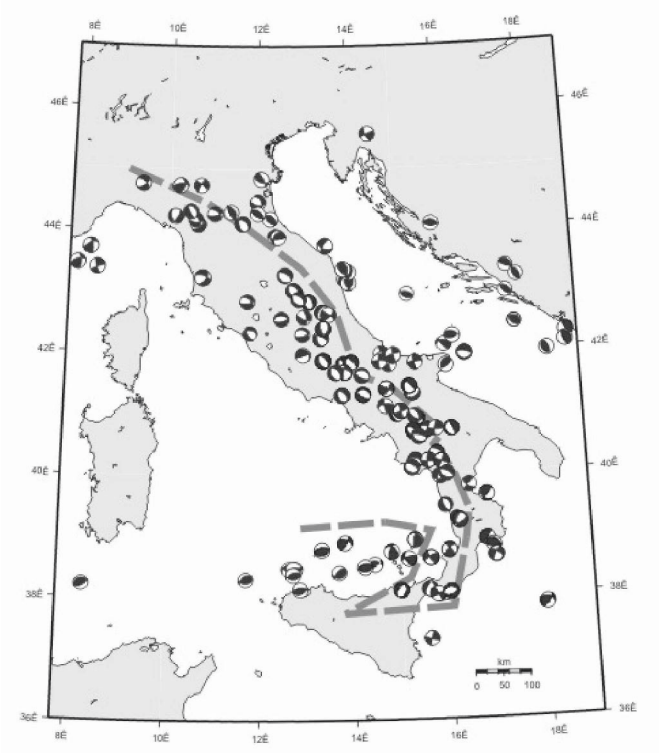

Figure 2. Earthquake focal mechanisms M>4.5 (CMT, RCMT, Gasparini et al., 1985). Dashed gray line marks boundary between contractional and extensional deformation.

As we develop below, active deformation within parts of Adria reflect continuation of deformational patterns initiated in the late Mesozoic and Tertiary. Seismicity and geodetically determined surface motions provide a

record of the differential displacement of crustal blocks within active segments of the tectonic belt. The pattern of crustal displacements is consistent with motion above a decollement system underlying the orogen. The decollement separates the heterogeneously deforming upper and middle crust from a regular pattern of motion presumed for the underlying, lithosphere. Although broadly driven by the relative convergence between Europe and Africa, the complex pattern of displacement within much of the Adriatic orogen is strongly influenced by intra-plate anisotropy and deformation processes. In this context, earthquakes and GPS site velocities reflect lithospheric plate motions only indirectly.

FRAGMENTATION OF ADRIA

The dimensions of Adria have been strongly modified by belts of late Mesozoic and Cenozoic contraction developed along the eastern, northern, and western margins of the paleotectonic domain. For the region centered on the Adriatic Sea, the existence of Adria as a paleotectonic domain is well established (Wortmann et al., 2001) but the lateral extent prior to collision with Europe, the displacement history in the context of the motions of Europe and Africa, and the degree of structural integrity retained by Adria are still open questions.

The eastern margin of Adria clearly includes Cenozoic and Mesozoic carbonate and siliciclastic rocks in the west-facing Dinaride belt that were detached from continental basement and imbricated during the late Mesozoic and Tertiary (Sengor, 1987). The lateral continuity of Dinaric units and those exposed in the northern Calcareous Alps (Channell et al., 1990; Wortmann et al., 2001) and within and adjacent to the Pannonian basin (Channell and Horvath, 1976; Bada and Horvath, 2001) is less certain, however. The coeval units may represent parts of a continuous Adriatic domain fragmented during collision with Europe, or alternatively, may be parts of discrete paleotectonic domains transferred to the European margin during closure of the Tethys (Channell, 1996; Wortmann et al., 2001). Although questions surround the degree of initial continuity shared by Mesozoic units in the northeastern Dinarides, Calcareous Alps, and Pannonian basin, coeval units exposed in the Carpathian foreland, stretching from northern Europe to the southern Balkans, are of clear European origin (Sengor, 1987) and set a firm eastern extent for Adria.

Mesozoic and Cenozoic rocks exposed within the eastern and southern Alps mark the northern extent of Adria and were thrust to the north over the continental margin in the European Alps during the late Mesozoic and early Tertiary (Laubscher, 1989). The Adriatic continental rocks were detached from their lithospheric basement and transferred to the European

borderland as tectonic sheets. The mass transfer from Adria to Europe was accompanied by widespread crustal delamination where mantle and possibly lower crust were separated from their cover and subducted beneath the orogen (Laubscher, 1991; Schmid et al., 1996). Detachment of the lithospheric roots of Adria allowed the crustal sheets to be imbricated over the European margin on a regionally extensive basal decollement system of the so-called orogenic float (Oldow et al., 1990a). The crustal sheets were stranded as the deformation front migrated into the Southern Alps (Doglioni and Bosellini, 1987) and are clearly separated from the northern margin of present-day Adria by the active deformation front along the northern margin of the Po Plain (Roeder, 1989).

Farther west, the boundary of Adria is more difficult to resolve because of severe Miocene to Recent extensional and contractional deformation. Based on paleogeographic reconstructions, the original boundary extended south across the Ligurian Sea east of the present-day location of Corsica and Sardinia (Dewey et al., 1989). Both Corsica and Sardinia are composed of European sedimentary and metamorphic units that rotated away from southern France in the Early Miocene (Alvarez, 1972) and collided with western Adria in the mid-Miocene (Patacca et al., 1990). Today, much of western Adria is underlain by highly extended continental crust and in the southern Tyrrhenian basin by Late Miocene to Pleistocene oceanic seafloor (Kastens et al., 1988). Crustal extension and local formation of oceanic seafloor followed the eastward and southward migration of the Apenninic and Maghrebid contractional belts of mainland Italy and Sicily, respectively (Malinverno and Ryan, 1986). The greatest extension was concentrated in the southern Tyrrhenian Sea, and the locus of extension migrated to the southeast behind the Calabrian arc (Figure 1). Estimates of the magnitude of shortening in the Apenninic chain (Bally et al., 1986; Lavecchia et al., 1994) and structural and paleomagnetic investigations in Sicily (Channell et al., 1990; Oldow et al., 1990b) and in Southern Italy (Scheepers and Langeries, 1994; Gattaceca and Speranza, 2002) indicate that the present-day Tyrrhenian basin was originally occupied by Mesozoic carbonate platform and basin units deposited upon and adjacent to continental crust.

Today, seismicity places limits on the spatial continuity of the remaining parts of contiguous Adria. Well defined belts of seismicity run along the northern coast of Sicily, along the axis of the Apennines in Italy, to the Alps in the north, and along the Dinarides in the east (McKenzie 1972). The absence of a well organized belt of seismicity in the south supports the promontory model for the origin of Adria (McKenzie, 1972) but using selected earthquake focal mechanisms, Anderson and Jackson (1987) proposed that Adria is an independent microplate with a pole of rotation in the Alps. More recently, Westaway (1992) viewed the Adriatic area to be a

deforming tectonic domain caught between Africa and Eurasia, and the seismicity (M>4.5) in and around the northern Adriatic Sea support this interpretation. A plot (Figure 3) of the intersections of normals to earthquake slip directions, where the angle of intersection is 15° or greater, clearly does not support the single rotation pole proposed by Anderson and Jackson (1987). Rather the scatter in individual pole positions indicates that Adria is deforming heterogeneously and that strain is accommodated by differential motion between crustal blocks at various scales.

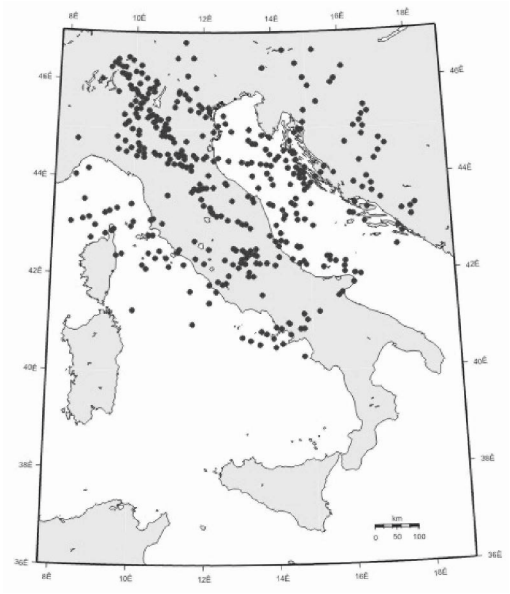

Figure 3. Intersections (angle > 15°) of the normals to earthquake slip vectors (black dots) for M>4.5 showing the lack of a single rotation pole defined by earthquake focal mechanisms.

The expanded record of seismicity shows a lack of coherent motion within deforming Adria and helps explain the ambiguous picture of lithospheric motion provided by the sparse coverage of earlier space-geodetic measurements in the central Mediterranean (Kahle et al., 1993; Noomen, et al., 1996). As we show below for the southern peri-Tyrrhenian belt of western Adria, increased spatial resolution of the GPS velocity field illuminates the complexity of the regional kinematics and supports the interpretation that surface motions document differential displacement between crustal blocks or sheets and only indirectly reflect the movement of lithospheric plates.

PERI-TYRRHENIAN GEODETIC ARRAY

The Peri-Tyrrhenian Geodetic Array (PTGA) was deployed to characterize active differential motion within the curved peri-Tyrrhenian orogenic belt. The GPS network is composed of 49 campaign sites, consisting of stainless steel pins drilled and cemented into bedrock, located around the southern Tyrrhenian Sea in southern Italy, Sicily and Sardinia. Twenty-four of the PTGA sites were occupied three times and used to determine a regional velocity field for the southern peri-Tyrrhenian orogen. Campaign sites were occupied in 1995, 1997, and 2000, with GPS receivers at four to six sites running simultaneously. Baselines between simultaneously occupied sites were short, not exceeding 150 km, and typically were much less than 100 km. In 1995, each site was occupied for at least two 10- to 12-hour sessions on consecutive days, and in 1997 and 2000 each site was occupied continuously for 24 to 48 hours.

Data processing with BERNESE 4.2 (Hugentobler et al., 2001) used precise satellite ephemerides and earth rotation parameters available from the IGS, transformed into the ITRF00 (Lewis, 2001). Carrier-phase ambiguity was resolved and cycle slips detected and repaired. Alignment of the PTGA coordinate solutions with the ITRF00 coordinate realization was accomplished by processing PTGA observations with continuously monitored IGS sites: MATE, NOTO, and CAGL that bound the southern Tyrrhenian basin (Figure 4). Coordinate solutions were calculated in 8-hour sessions to improve statistical measures of repeatability. Sessions with less than 6 hours of observation substantially increase coordinate uncertainty and were excluded from velocity-field determination.

Velocity uncertainties were estimated using a propagation of coordinate uncertainty, where formal errors are scaled root mean square values from each session solution. To accommodate improvement in velocity estimation by the time span between campaigns, we included a gain factor calculated using the formulation of Brockmann (1996).

Using weekly coordinate solutions from EUREF, we determined a combined velocity field for the PTGA and the local IGS sites in three reference frames to illustrate different aspects of deformation in the peri-Tyrrhenian orogen (Lewis, 2001). Coordinate solutions of IGS and PTGA sites were combined to produce a regional velocity field to illustrate differential motion within the peri-Tyrrhenian orogen in a fixed European frame. The European frame was defined by fixing EUREF sites BOR1, GRAZ, JOZE, PENC, POTS, and WTZR, which were determined to have <0.5 mm/yr differential velocity residual with respect to one another (Nocquet et al., 2001). Local velocity fields also were computed for fixed sites in southern Italy (MATE) and Sicily (NOTO) to highlight differential motions

within specific segments of the orogenic belt and facilitate comparison with active seismicity.

DEFORMATION WITHIN THE SOUTHERN PERI-TYRRHENIAN OROGEN

Neogene Deformation

The crustal architecture of the southern peri-Tyrrhenian orogen formed during large-scale delamination of lower crust and mantle (Royden et al., 1987; Channell and Mareschal, 1989). Continental crust beneath the Apennines and Adriatic Sea is between 30 and 40 km thick but abruptly thins beneath the Tyrrhenian Sea to between 20 and 10 km where crustal stretching and local emplacement of oceanic sea floor accompanied a rise of the asthenosphere. A Moho discontinuity underlies the axis of the Apennines and reflects the location of delaminated lower crust and upper mantle (Lavecchia, 1988; Cassinis et al., 2003). The west-dipping slab is imaged to depths of 90 and possibly 160 km by seismicity and to 250 km by seismic tomography (Di Stefano et al., 1999). In the Calabria region, the delaminated slab dips northwest and is imaged to depths of ~600 km beneath the adjacent Tyrrhenian Sea by earthquakes and seismic tomography (Cimini, 1999).

Neogene contraction in the peri-Tyrrhenian belt resulted in hundreds of kilometers of shortening above a basal decollement that extends from the foreland west (Southern Apennines) and north (Maghrebid) to depths of 10 to 15 kilometers beneath the internal parts of the orogenic system (D'Argenio et al., 1975; Bally et al., 1986; Catalano et al., 2000). Thrusting involved a history of changing tectonic transport direction accompanied by large-scale rotation and arcuation of the orogenic belt (D'Argenio et al., 1980; Channell et al., 1990). In western Sicily, Miocene to Pliocene tectonic transport for the contractional front was easterly and changed to southerly during the Pliocene-Pleistocene (Catalano, 1987; Oldow et al., 1990b). Similarly in mainland Italy, the Southern Apennines underwent east-directed transport changing to north-northeast (D'Argenio et al., 1980; Patacca et al., 1990). Large, coherent-body rotations of thrust sheets (up to 130°) occurred in western Sicily during progressive deformation (Channell et al., 1990; Oldow et al., 1990b), and there were smaller clockwise rotations (up to 90°) in the Apennines (D'Argenio et al., 1980; Scheepers and Langereis, 1994).

Extension in the orogenic hinterland kept pace with the migration of the foreland thrust fronts (Patacca et al., 1990; Oldow et al., 1990b; Ferranti and Oldow, this volume) and culminated in the local formation of oceanic sea floor in parts of the southern Tyrrhenian basin (Kastens et al., 1988). The submergence of older segments of the extensional belt beneath the Tyrrhenian

Sea precludes assessment of the extension direction as a function of time for most of the deformation history, but during the Pliocene and Pleistocene, extension along the Tyrrhenian margins of the Southern Apennines and Sicily are essentially parallel to the contractional axis recorded in the foreland thrust belt. Extensional half-grabens define the physiography of the Tyrrhenian margin of southern Italy and extensional faults are active today along the axis of the Apenninic chain. Similarly, the mountains of northern Sicily are formed by a complex array of faults bounding half-grabens containing Messinian to Early Pleistocene sediments. Unlike southern Italy, however, the extensional half-grabens in the Sardinia Strait and northwestern Sicily experienced tectonic inversion in the Late Pleistocene (Catalano et al., 1996, 2000).

Active Deformation

Today, deformation in the Southern Apennines and Sicily is dominated by belts of seismicity variably recording transpression, transtension, and contraction. In the Southern Apennines, seismologically active high-angle faults are concentrated along the axis of the mountain chain and overlie the tip of crustal delamination (Di Stefano et al., 1999). The earthquakes have hypocenter depths of 10 to 15 km and have strike-slip and extensional focal mechanisms (Figure 2), consistent with right-transtensional displacement observed in fault-slip inversion investigations (Hippolyte et al., 1994). From north to south, the belt of transtensional earthquakes is localized between the Apenninic carbonate massif on the west and the frontal thrust belt to the east. Just north of the Calabrian arc, the belt of seismicity steps toward the Tyrrhenian coast and continues south along western Calabria; swinging westerly to a termination in northeastern Sicily.

E-W-striking, dextral transpressional faults are exposed along the margins of the Gargano Peninsula and are traced offshore into the Adriatic in seismic-reflection profiles (de Alteriis, 1995). Seismicity in the region defines a broad belt of earthquakes with NW, N, and NE shortening axes and focal depths of 15 to 30 km that extends across the central Adriatic Sea (Favali et al., 1993). The onland projection of the fault system west of Gargano is marked by a system of E-W-striking faults and earthquakes with right-lateral focal mechanisms. South of Gargano, along the Murge platform and Apulian foreland, seismicity wanes until the eastern Calabrian arc, where thrust and strike-slip earthquakes occur at depths of 10 to 20 km along the continental margin and into the Ionian Sea (Figure 2). The transpressional deformation front is mapped on the seafloor by seismic-reflection profiles (Finetti, 1982) and turns westerly and crosses southern Sicily, north of the Hyblean foreland. In southern Sicily, no focal mechanisms are recorded, but

the transpressional front is marked by small earthquakes, borehole break-outs with NW-SE shortening axes (Ragg et al., 1999), and active structures observed offshore in seismic-reflection profiles (Catalano et al., 2000). The transpressional front extends southwest to the north coast of Tunisia.

Along the northern shore of Sicily, a belt of contractional earthquakes with hypocenters of between 10 and 20 km and NW-SE shortening axes stretches from 50 km west of central Calabria west-southwest into the Sardinia Strait (Figure 2). The belt of contractional earthquakes lies seaward of transtensional faults in northeasterly Sicily but track onland in northwest Sicily where the belt merges with the transpressional frontal belt of southern Sicily.

In a fixed European reference frame, displacements in the southern peri-Tyrrhenian belt are dominated by N to NE GPS velocities ranging from 5 to 12 mm/yr (Figure 4). The velocity field defined by PTGA and IGS sites varies around the southern Tyrrhenian Sea, with greatest magnitude displacements localized in Sicily and southern Italy. IGS sites in Corsica (AJAC) and Sardinia (CAGL) have small to statistically insignificant E velocities with respect to stable Europe, but the PTGA network in southern Sardinia records velocities with variable orientations up to 5 mm/yr. In northwestern Sicily, velocities are N to NE, with magnitudes reaching 10 mm/yr. To the southeast, near the Hyblean foreland, velocities of sites straddling the contractional front are N and vary between 3 to 8 mm/yr. In southern Italy, GPS site velocities show large spatial variability and range from near zero along the Tyrrhenian coast to magnitudes up to 12 mm/yr with NE, with locally NW azimuths in the Apennines and near the Adriatic coast.

Comparison between the GPS velocity field fixed on stable Europe and deformation recorded by the belts of seismicity is difficult. Incremental strain axes associated with earthquakes record differential motion between fault blocks and are not easily reconciled with velocities referenced to the external European frame. To aid comparison of earthquake focal mechanisms and the GPS displacements, we recomputed the GPS velocities in local reference frames. For southern Italy, we depict the GPS velocities fixed on the IGS site MATE and for Sicily develop a velocity field fixed on NOTO.

When viewed in a fixed MATE frame, the PTGA velocity field for southern Italy depicts a complex pattern of motion (Figure 5). Along the Tyrrhenian coast, sites move SW at rates up to 5 mm/yr and decrease to 3 mm/yr along the axis of the Apenninic chain. NW motion of one site at 2 mm/yr is consistent with active right-transtension in the coastal deformation belt recorded by earthquake focal mechanisms. To the south in Calabria, SW displacement of a site near the Tyrrhenian coast at 2 mm/yr is compatible with extensional earthquake focal mechanisms.

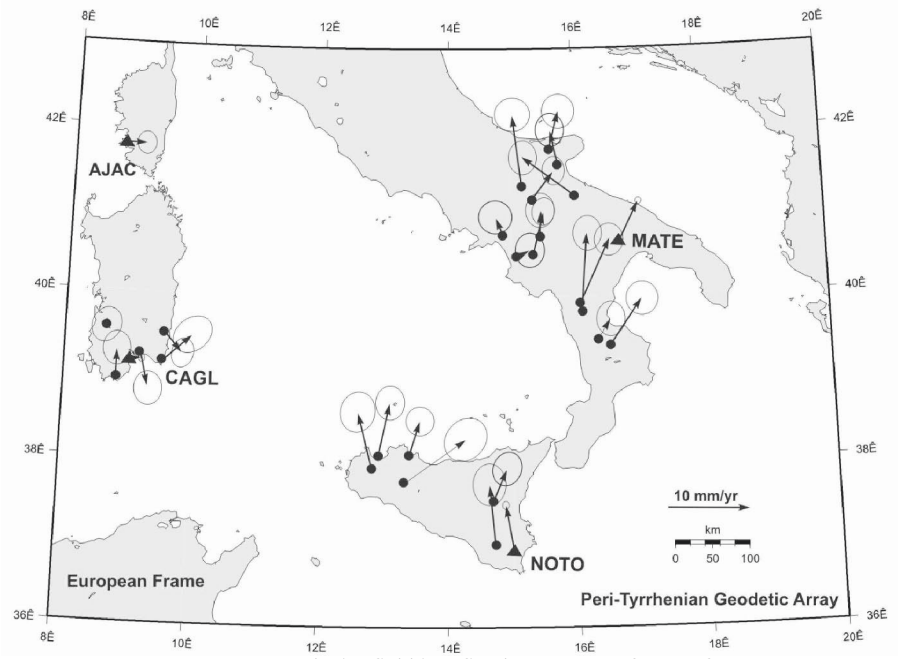

Figure 4. PTGA velocity field in a fixed European reference frame.

Farther east, in central Calabria, N displacement at 2 mm/yr coincides with contractional and strike-slip earthquake focal mechanisms in the area and marks the transition between extension and transpression in Calabria. The transition between SW and N site velocities is traced north from Calabria along the Tyrrhenian coast, where two sites straddling an active extensional fault are moving toward the foreland with N displacements at rates of 5 and 6 mm/yr. Continuing northwest along strike, site velocities record SE and NW motions of 3 to 5 mm/yr and indicate longitudinal extension, consistent with earthquake focal mechanisms and mapped active faults. Sites along the Adriatic coast have NE displacements of only 2 to 5 mm/yr or large NW to N motions of 8 to 10 mm/yr. Here, differential motions demonstrate dextral transpression across the Southern Apennine foreland and western Adriatic Sea (Figure 5).

Site velocities in Sicily, when viewed in a frame fixed on NOTO located in the Hyblean foreland, also show substantial spatial variability. In the Hyblean foreland, a site separated from NOTO by a northerly striking right- lateral fault system (Ghisetti and Vezzani, 1980) moves N at nearly 2 mm/yr. Across the frontal thrust of the Maghrebid belt, the PTGA site in eastern Sicily moves SE at about 3 mm/yr indicating active contraction. Central western Sicily is characterized by active E-W-striking transcurrent faults (Ghisetti and Vezzani, 1984), and the PTGA site in this area has an E velocity of nearly 10 mm/yr, consistent with active right-lateral displacement.

Taken together with the SE motion of the PTGA site north of the frontal thrust, displacements suggest active dextral transpression.

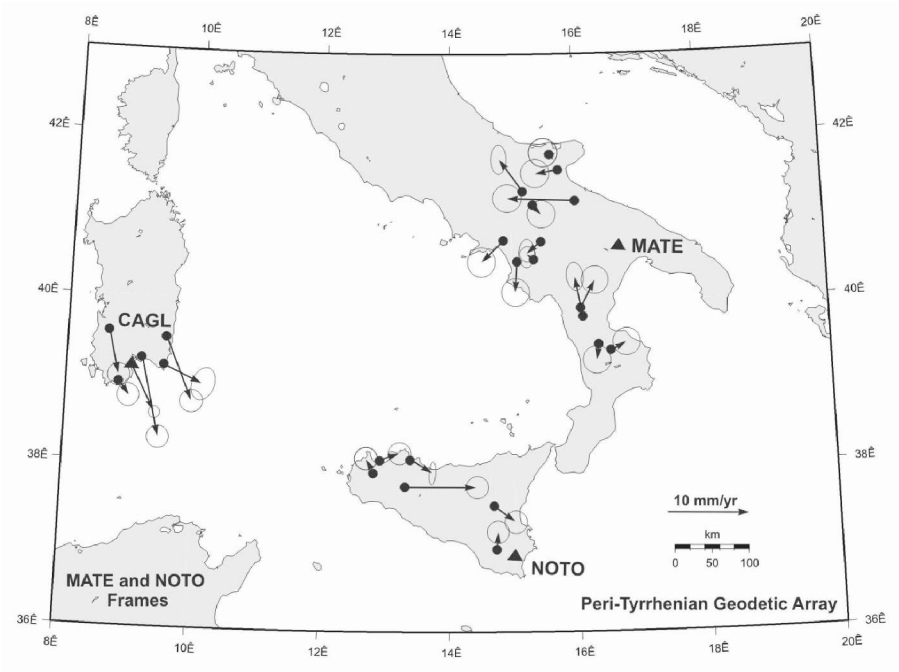

Figure 5. PTGA velocity field in local reference frames. Southern Italy in MATE-fixed frame. Sicily and Sardinia in NOTO-fixed frame.

Three sites along the northwestern shore of Sicily have velocities of 2 to 4 mm/yr that systematically change in azimuth from west to east along the coast from NW, to ENE, to SE. These sites lie west of the transtensional deformation front defined by seismicity and are located on fault blocks bound by a system of WNW- and NE-striking active faults. The pattern of displacement indicates clockwise vertical-axis rotation of northwestern Sicily and lies in the area where paleomagnetic and structural data document up to 130° of clockwise rotation since the Late Miocene (Channell et al., 1990; Oldow et al., 1990b). Block rotation appears to occur all along northern Sicily and also is recognized in the GPS velocity field for the Aeolian Islands northeast of Sicily (Hollenstein et al., 2003).

Finally, displacements of the PTGA and IGS site CAGL in southern Sardinia, when viewed in a fixed NOTO frame, provide insight into the origin of the contractional belt along the northern margin of Sicily and in the Sardinia Straits. Although experiencing substantial differential motion, southern Sardinia sites are moving primarily SSE at rates up to 10 mm/yr. The displacement is compatible with the axis of shortening recorded by the

thrust earthquakes forming the northern contractional belt in Sicily and support the interpretation that the shortening is a direct response to the differential motion between Europe (Sardinia) and Africa (Hyblean foreland of Sicily).

DISCUSSION AND CONCLUSIONS

The spatial complexity of the active kinematics of the peri-Tyrrhenian belt is clearly reflected in the distribution of earthquakes and GPS velocities. In mainland Italy, deformation is expressed by belts of extension and contraction that are traced northwest to southeast along the length of Apennine chain. Along the Tyrrhenian margin of the Northern and Central Apennines, extension dominates, but in the Southern Apennines and Calabria, both extensional and strike-slip focal mechanisms are prevalent, and the belt is right-transtensional. Similarly, contraction dominates the frontal belt in northern and central Italy, but in southern Italy and Calabria, the transpressional character of the deformation increases. In Calabria, the two belts form concentric arcs around the southeastern margin of the Tyrrhenian basin and extend westward into Sicily. The boundary between the extensional and contractional belts is sharp and marked by a narrow zone of seismogenic normal faults that follows the axis of the mountain chain (Figs. 2 and 6). The eastern flank of the extensional belt has a relatively smooth trajectory along the Tyrrhenian margin of mainland Italy and follows the major morphologic-tectonic arcs viewed as the characteristic expression of this orogen (Doglioni, 1991). The front of the contractional belt also expresses the local arcuate nature of the orogen and underlies the Adriatic margin of mainland Italy and locally steps offshore to lie beneath the western Adriatic Sea in northern Italy. At Gargano, the relatively smooth geometry of the frontal belt is disrupted by an E-W trending tectonic link with the southern Dinarides and Albanides of the eastern Adriatic margin. The E-W-trending belt crosses the central Adriatic and is expressed by seismically active E-W-striking transpressional structures. To the south from Gargano, the location of the transpressional front is poorly defined by seismicity, but based on the GPS velocity field, ostensibly lies between the Murge Plateau and Mesozoic rocks near MATE. We suspect that the boundary corresponds with the physiographic separation between Murge and Salento Plateaus in southeastern Italy and extends south into the Ionian Sea, where the transpressional front forms the broad arc east of Calabria. West from Calabria, the transtensional and transpressional belts continue into eastern Sicily, where the transtensional structures terminate. Unlike southern Italy and Calabria, the Maghrebid belt of Sicily is bound on the north by a belt of contractional structures defined by thrust earthquakes and partially inverted Miocene-Pliocene extensional half-grabens. To the

west, the transpressional foreland belt merges with the northern belt of contraction and continues into Tunisia and the Sardinia Strait.

Spatial heterogeneity within the southern peri-Tyrrhenian deformed belt is attributed in large part to the interplay between crustal blocks above a basal decollement system dipping from the fontal thrust belt to depths of 10 to 15 km in the hinterland. Existence of the decollement is well established for the Southern Apennines and Maghrebid belts (Bally et al., 1986; Lavecchia et al., 1994; Catalano et al., 2000), but the relationship between hinterland extensional structures and the decollement has not been confirmed. Seismic-reflection profiles do not provide sufficient resolution to document whether normal faults sole into or truncate the regional decollement. The PTGA velocity field provides critical insight into this longstanding question and supports the existence of a through-going basal decollement shared both by contractional and extensional structures.

In southwestern Italy, two PTGA sites have 5 to 6 mm/yr displacement toward the foreland (MATE) bordering the Adriatic coast (Figure 5). The two sites are situated on footwall and hanging wall blocks of an active normal fault system with down-to-the-Tyrrhenian displacement. The active fault system marks the transition between extensional and contractional domains within this segment of the Southern Apennines. To the east, regional shortening continues and is documented by involvement of Pleistocene and Quaternary rocks of the San Arcangelo basin in contractional structures (Casciello et al., 2000). The displacement toward the Adriatic foreland by both hanging wall and footwall blocks of an active extensional fault system provides direct evidence that the extensional structures of the hinterland sole into and do not truncate the orogen decollement system.

Similarly, right-transpressional deformation in central and southern Sicily recorded by PTGA site velocities is consistent with geologic studies of the frontal Maghrebid belt. More importantly, however, is recognition that structures of northwestern Sicily accommodate a broad region of clockwise vertical-axis rotation apparent in the PTGA velocity field (Figure 5). Paleomagnetic and structural analysis of western Sicily have documented clockwise rotation of large coherent domains by up to 130° during the Late Miocene and to Early Pleistocene (Channell et al., 1990) and were inferred to indicate that the rotating structural sheets rode above the basal decollement of the orogen (Oldow et al., 1990b).

The PTGA velocity field and published results showing similar, active vertical-axis rotation in the near offshore of northeastern Sicily (Hollenstein et al., 2003) north of the western extent of extensional deformation, pointing to a shared basal decollement system underlying the entire orogen.

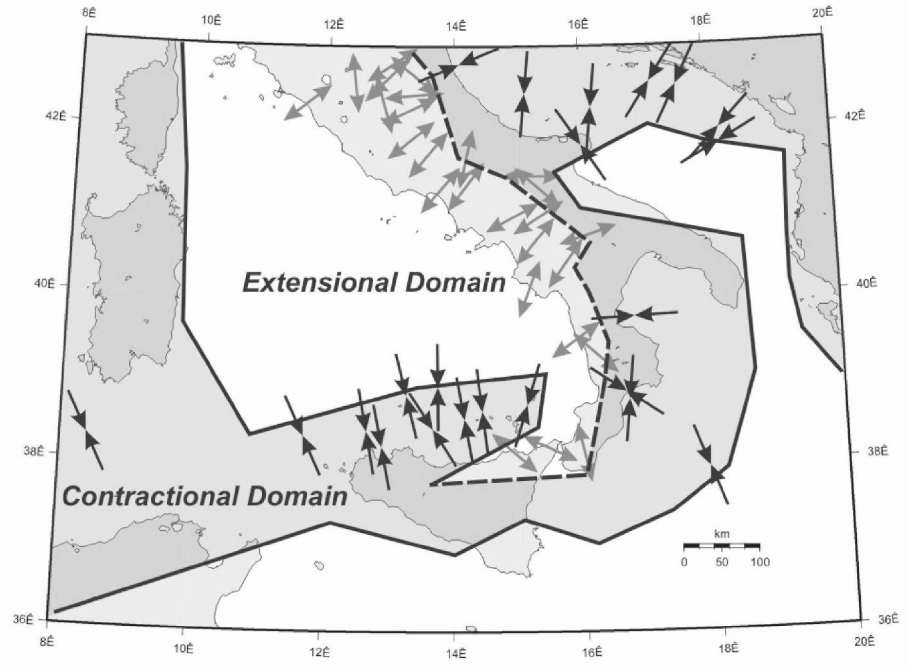

Figure 6. Tectonic map showing contractional belt (shaded gray) around the southern Tyrrhenian basin and extending east into the Dinarides and Albanides. Extensional domain is localized along the western margin of Italy and in northeastern Sicily. Contractional and extensional incremental strain axes (black and gray arrows, respectively) are determined from earthquake focal mechanisms.

A through-going basal decollement system linking contractional and extensional structures within the peri-Tyrrhenian orogen has important implications for the interpretation of geodetically determined surface motions in tectonic belts. Decoupling of the deformed crustal section and underlying lower crust and mantle is well established by geometric models and seismic-reflection profiles in the Alps (Laubscher, 1991; Schmid et al., 1996) and is recognized in orogenic belts around the world (Oldow et al., 1990a). Only recently, however, have surface displacements in active deformed belts been viewed in this context (Mazzotti and Hyndman, 2002). Detachment of the deformed crustal section from the underlying lower crust and/or mantle carries the implication that surface motions determined from earthquake focal mechanisms and GPS site velocities record differential displacements within the upper plate of deforming orogens, the orogenic float, and do not directly reflect lithospheric plate motion.

REFERENCES

Alvarez W. Rotation of the Corsica-Sardinia microplate. Nature 1972; 235: 103-105.

Anderson H.A., Jackson J.A. Active tectonics of the Adriatic region. Geophys. J. of the Royal Astronomical Society 1987; 91: 937-983.

Anzidei M., Baldi P., Casula G., Galvani A., Mantovani E., Pesci A., Riguzzi F., Serpelloni E. Insights into present-day crustal motion in the central Mediterranean area from GPS surveys. Geophys. J. Int. 2001; 146: 98-110.

Argand E. La Tectonique de l'Asie. Proceeding International Geologic Congress 1924; 13:171-374.

Bally A.W., Burbi L., Cooper C., Ghelardoni R. Balanced sections and seismic profiles across the Central Apennines. Memoirs of the Geological Society of Italy 1986; 35: 257-310.

Bada G., Horvath F. On the structure and tectonic evolution of the Pannonian basin and surrounding orogens. Acta Geologica Hungarica 2001; 44: 301-327.

Brockman E. Combination of solutions for geodetic and geodynamic applications of the Global Positioning System (GPS), Ph.D. Thesis, Switzerland: Universitat Bern, 1996.

Casciello E., Cesarano M., Ferranti L., Oldow J. S., Pappone G. Pleistocene non-coaxial fold development in the northern portion of the S. Arcangelo Basin (Southern Apennines). Memorie della Societa Geologica Italiana 2000; 55: 133-140.

Cassinis R., Scarascia S., Lozej A. The deep crustal structure of Italy and surrounding areas from seismic refraction data. A new synthesis. Bollettino della Societa Geologica Italiana 2003; 122: 365-376.

Catalano R. Northeastern Sicily Straits. Stratigraphy and structures from seismic reflection profiles. Rendiconti della Societa Geologica Italiana 1987; 9: 103-112.

Catalano R., Di Stefano P., Sulli A., Vitale F. P. Paleogeography and structure of the central Mediterranean; Sicily and its offshore area. Tectonophysics 1996; 260: 291-323.

Catalano R., Franchino A., Merlini S., Sulli A. Central western Sicily structural setting interpreted from seismic reflection profiles. Memorie della Societa Geologica Italiana 2000; 55: 5-16.

Channell J.E.T. Palaeomagnetism and palaeogeography of Adria. Geol. Soc. Spe. Publ. 1996; 105: 119-132.

Channell J.E.T., Horvath F. The African-Adriatic promontory as a paleogeographical premise for Alpine orogeny and plate movements in the Carpatho-Balkan region. Tectonophysics 1976; 35: 71-110.

Channell J.E.T., D'Argenio B., Horvath F. Adria, the African Promontory, in Mesozoic Mediterranean paleogeography. Earth Science Reviews 1979; 15: 213-292.

Channell J.E.T., Mareschal J.C. Delamination and asymmetric lithospheric thickening in the development of the Tyrrhenian Rift. Geol. Soc. London Spec. Publ. 1989; 45: 285-302.

Channell J.E.T., Oldow J.S., Catalano R., D'Argenio B. Paleomagnetically determined rotations in the western Sicilian fold and thrust belt. Tectonics 1990; 9: 641-660.

Cimini G.B. P-wave deep velocity structure of the Southern Tyrrhenian subduction zone from non-linear teleseismic travel time tomography. Geophys. Res. Lett. 1999; 26: 3709-3712.

D'Argenio B., Pescatore T., Scandone P. Structural pattern of the Campania-Lucania Apennines. Quaderni de 'La ricerca scientifica, CNR 1975; 90: 312-327.

D'Argenio B., Channell J.C., Horvath F. Palaeotectonic evolution of Adria, the African Promontory. Bureau de Recherches Geologiques et Minieres, Memoire 1980; 115: 331-351.

D'Argenio B., Horvath F. Some remarks on the deformation history of Adria, from the Mesozoic to the Tertiary. Annales Geophysicae 1984; 2: 143-146.

de Alteriis G. Different foreland basins in Italy: examples from the central and western Adriatic sea. Tectonophysics 1995; 252: 349-373.

Dercourt J., Zonenshain L.P., Ricou L.E., Kazmin V.G., Le Pichon X., Knipper A.L., Grandjacquet C., Sbortshikov I.M., Geyssant J., Lepvrier C., Pechersky D.H., Boulin J., Sibuet J.C., Savostin L.A., Sorokhtin O., Westphal M., Bazhenov M.L., Lauer J.P., Biju-Duval B. Geological evolution of the Tethys Belt from the Atlantic to the Pamirs since the Liassic. Tectonophysics 1986; 123: 241-315.

Dewey J.F., Helman M.L., Turco E., Hutton D.H.W., Knott S.D. Kinematics of the Western Mediterranean. Geol. Soc. London Spec. Publ. 1989; 45: 265-284.

Di Stefano P., Vitale F. Sedimentazione e tettonica nel Plio-Pleistocene della valle del Belice (sicilia sud occidentale). Congresso Nazionale Societa Geologica Italiana 1988; 74: A-271 - A-272.

Doglioni C. A proposal for the kinematic modelling of W-dipping subductions - possible applications to the Tyrrhenian-Apennines system. Terra Nova 1991; 3: 423-434.

Doglioni C., Bosselini A. Eoalpine and mesoalpine tectonics in the Southern Alps. Geologische Rundschau 1987; 76: 735-754.

Favali P., Funiciello F., Pieri P. An active margin across the Adriatic Sea (central Mediterranean Sea). Tectonophysics 1993; 219: 109-117.

Finetti I. Structure, stratigraphy and evolution of central Mediterranean. Bollettino di Geofisica Teorica ed Applicata 1982; 24: 247-315.

Gasparini G., Iannaccone G. Scarpa R. Fault-plane solutions and seismicity of the Italian peninsula. Tectonophysics 1985; 117: 59-78.

Gattacceca J., Speranza F. Paleomagnetism of Jurassic to Miocene sediments from the Apennine carbonate platform (Southern Apennines, Italy): evidence for a 60° counterclockwise Miocene rotation. Earth Planetary Science Letters 2002; 201:19-34.

Ghisetti F., Vezzani L. The structural features of the Hyblean plateau and of the Monte Judica area (South-Eastern Sicily): a microtectonic contribution to the deformation history of the Calabrian Arc. Bollettino della Societa Geologica Italiana 1980; 99: 57-102.

Ghisetti F., Vezzani L. Thin-skinned deformations of the western Sicily thrust belt and relationships with crustal shortening; mesostructural data on the Mt. Kumeta-Alcantara fault zone and related structures. Bollettino della Societa Geologica Italiana 1984; 103: 129-157.

Gueguen E., Doglioni C., Fernandez M. On the post-25 Ma geodynamic evolution of the western Mediterranean. Tectonophysics 1998; 298: 259-269.

Hippolyte J.C., Angelier J., Roure F. A major geodynamic change revealed by Quaternary stress patterns in the Southern Apennines (Italy): Tectonophysics 1994(b); 230: 199-210.

Hollenstein C., Kahle H.G., Geiger A., Jenny S., Goes S., Giardini D. New GPS constraints on the Africa-Eurasia plate boundary in southern Italy: Geophys. Res. Lett. 2003; 30: 1935.

Hugentobler U., Schaer S., Fridez P. editors, *Bernese GPS software version 4.2*, Astronomical Institute, University of Berne, Switzerland, 2001.

Jolivet L., Faccenna C. Mediterranean extension and the Africa-Eurasia collision. Tectonics 2000; 19: 1095-1106.

Kahle H-G., Muller M., Muller S., Veis G. The Kephalonia transform fault and the rotation of the Apulian platform: Evidence from satellite geodesy. Geophys. Res. Lett. 1993; 20: 651-654.

Kastens K., Mascle J., ODP 107 Scientific Staff. ODP leg 107 in the Tyrrhenian Sea: Insights into passive margin and back-arc basin evolution. Geol. Soc. Amer. Bull. 1988; 100: 1140-1156.

Laubscher H.P. The tectonics of the Southern Alps and the Austro-Alpine nappes: a comparison. Geol. Soc. London Spec. Publ. 1989; 45: 229-241.

Laubscher H. The arc of the Western Alps today. Eclogae Geologicae Helvetiae 1991; 84: 631-659.

Lavecchia G. The Tyrrhenian-Apennines system: Structural setting and seismotectogenesis. Tectonophysics 1988; 147: 263-296.

Lavecchia G., Brozzetti F., Barchi M., Menichetti M., Keller J.V.A. Seismotectonic zoning in east-central Italy deduced from an analysis of the Neogene to present deformations and related stress fields. Geol. Soc. Amer. Bull. 1994; 106: 1107-1120.

Lewis D.S. *Kinematic constraints on coeval extension and contraction in the Southern Apennines (Italy) from space geodesy*, Ph.D. diss., Moscow, Idaho: University of Idaho, 2001.

Malinverno A., Ryan W.B.F. Extension in the Tyrrhenian Sea and shortening in the Apennines as a result of arc migration driven by sinking of the lithosphere. Tectonics 1986; 5: 227-245.

Mazzotti S., Hyndman R.D. Yakutat collision and strain transfer across the Canadian Cordillera. Geology 2002; 30: 495-498.

McKenzie D. Active tectonics of the Mediterranean Region. Geophys. J. of the Royal Astronomical Society 1972; 30:109-185.

Nocquet J.-M., Calais E., Altamimi Z., Sillard P., Boucher C. Intraplate deformation in western Europe deduced from an analysis of the International Terrestrial Reference Frame 1997 (ITRF97) velocity field. J. Geophys. Research 2001; 106: 11,239-11,257.

Noomen R., Springer T., Ambrosius B., Herzberger K., Kuijper D., Mets G-J., Overgaauw B., Wakker K. Crustal deformation in the Mediterranean area computed from SLR and GPS observations. J. Geodynamics 1996; 21: 73-96.

Oldow J.S., Bally A.W., Ave Lallemant H.G. Transpression, orogenic float, and lithospheric balance. Geology 1990(a); 18: 991-994.

Oldow J.S., Channell J., Catalano R., D'Argenio B. Contemporaneous thrusting and large-scale rotations in the western Sicilian fold and thrust belt. Tectonics 1990(b); 9: 661-681.

Oldow J.S., Ferranti L., Lewis D.S., Campbell J.K., D'Argenio B., Catalano R. Pappone G., Carmignani L., Conti P., Aiken C.L.V. Active fragmentation of Adria, the north African promontory, central Mediterranean orogen. Geology 2002; 30: 779-782.

Patacca E., Sartori R., Scandone P. Tyrrhenian Basin and Apenninic arcs: kinematic relations since late Tortonian times. Memorie della Societa Geologica Italiana 1990; 45: 425-451.

Ragg S., Grasso M., Mueller B. Patterns of tectonic stress in Sicily from borehole breakout observations and finite element modeling. Tectonics 1999; 18: 669-685.

Roeder D. South-Alpine thrusting and trans-Alpine convergence. Geol. Soc. London Spec. Publ. 1989; 45: 211-227.

Royden L., Patacca E., Scandone P. Segmentation and configuration of subducted lithosphere in Italy: An important control on thrust-belt and foredeep-basin evolution. Geology 1987; 15: 714-717.

Scheepers P.J.J., Langereis C.G. Paleomagnetic evidence for counter-clockwise rotations in the Southern Apennines fold-and-thrust belt during the late Pliocene and middle Pleistocene. Tectonophysics 1994; 239: 43-59.

Schmid S.M., Pfiffner O.A., Froitzheim N., Schoenborn G., Kissling E. Geophysical-geological transect and tectonic evolution of the Swiss-Italian Alps. Tectonics 1996; 15: 1036-1067.

Sengor A.M. Tectonics of the Tethysides; orogenic collage development in a collisional setting: Annual Review of Earth and Planetary Sciences 1987; 15: 213-244.

Westaway R. Seismic moment summation for historical earthquakes in Italy: tectonic implications. J. Geophys. Res. 1992; 97: 15,437-15,464.

Wortmann U.G., Weissert H., Funk H., Hauck J. Alpine plate kinematics revisited; the Adrian problem. Tectonics 2001; 20: 134-147.

Ziegler P.A. Evolution of the Arctic-North-Atlantic and the western Tethys. American Association of Petroleum Geologists Memoir 43, 1988.

GEODETIC MEASUREMENTS IN THE AEGEAN SEA REGION FOR THE DETECTION OF CRUSTAL DEFORMATION

Demitris Delikaraoglou[1], Harilaos Billiris[1], Demitris Paradissis[1], Philip C. England[2], Barry Parsons[2], Peter J. Clarke[3]
1: National Technical University of Athens, Faculty of Surveying Engineering, Greece
ddeli@mail.ntua.gr
2:Department of Earth Sciences, University of Oxford, Parks Road, Oxford, U.K.
3: Department of Geomatics, University of Newcastle, Newcastle upon Tyne, U.K.

ABSTRACT

Greece and the Aegean Sea form part of one of the most rapidly deforming areas of the Earth's surface and are characterized by a high level of intra-plate seismicity in comparison to neighboring regions. AEGEANET is a geodetic network that we have established in order to consistently measure the geodetic strain in the broader Aegean Sea region, including parts of the Greek mainland and spanning several areas of known fault systems. Our measurements so far span approximately 4- and 42-year periods up to 1997 using a combination of old triangulation/trilateration-derived coordinates and repeated GPS observations at various subsets of the stations of this network. The observed displacements reflect the present-day tectonic deformation of the region, showing more than one meter of north-south extension across the network. The crust in this region appears to contain a few relatively rigid blocks separated by more rapidly deforming zones. This conclusion is supported by the velocity and strain fields that we have estimated for six sub-regions, which provide a more detailed view of the crustal deformation in this region.

Keywords: GPS, GPS networks, Aegean Sea, strain accumulation, strain ellipses, crustal deformation, Greece

INTRODUCTION - GEODYNAMIC SETTING

The Aegean Sea and the surrounding area lie within the convergence zone between the African and Eurasian plates, and for that reason the tectonic activity in the region is very intense, accounting for the highest seismicity among the Mediterranean countries and indeed of the whole West Eurasia (Papazachos and Kiratzi, 1996; Koravos et al., 2003).

The most prominent tectonic features in the Aegean Sea and the surrounding area are (from south to north): the Mediterranean Ridge, the Hellenic Arc and its associated Hellenic Trench, and the Northern Aegean Trough. The Mediterranean Ridge is the submarine chain that runs from the

N. Pinter et al. (eds.), The Adria Microplate: GPS Geodesy, Tectonics and Hazards, 287–304.

Ionian Sea to Cyprus in parallel to the Hellenic Trench, which in turn runs parallel to the Hellenic Arc and consists of submarine depressions roughly 5 km deep and smaller linear trenches south of Crete and in the Ionian Sea. The Hellenic Arc consists of an outer sedimentary arc and the inner Hellenic Volcanic Arc (**Le Pichon and Angelier, 1979**). The former links the Dinaric Alps (through the Greek mountain ranges, the Ionian Islands, Crete and the island of Rhodes) to the Turkish Taurides. The latter parallels the sedimentary arc and trench, and consists of volcanic islands stretching from Methana in the east, to Milos and Santorini in the Cyclades islands and to Nisyros and Kos in the west.

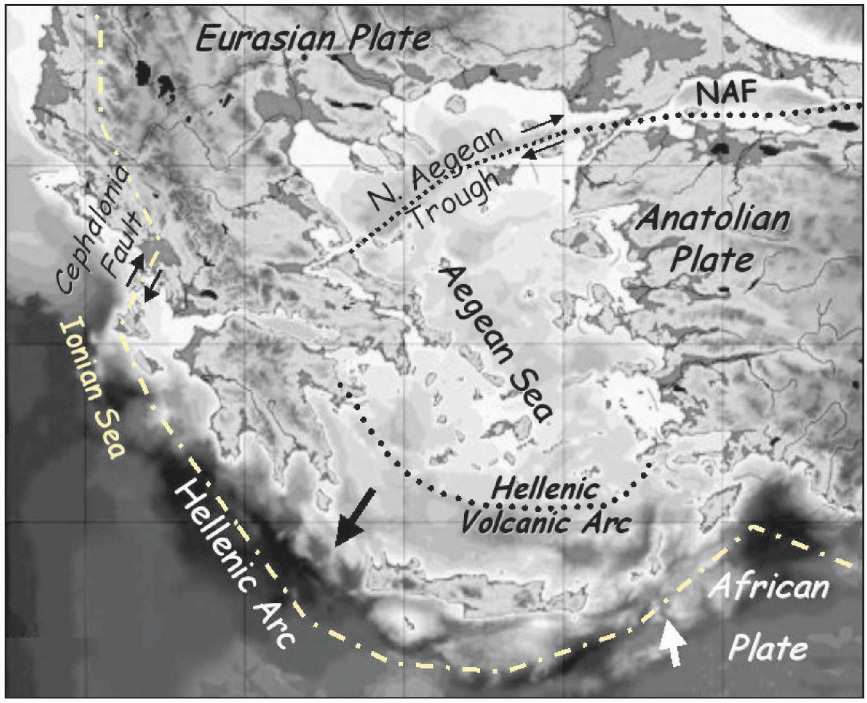

Figure 1 The geodynamic setting of the broader Aegean Sea region.

Between the sedimentary and the volcanic arc is the *Cretan Trough* with a depth of about 2000 m and, in the far end of the northern Aegean, the *Northern Aegean Trough* has a depth of about 1500 m. The northeast extension of the Northern Aegean Trough may form the small depressions of the Marmara Sea.

EARLIER GEODETIC WORK

Since the late 1980s, several GPS campaigns have been carried out in order to estimate strain accumulation throughout Greece and to support interdisciplinary projects aiming to identify areas of high seismic hazard. These activities have contributed towards developing new and more efficient operational and computational techniques and helped to improve our understanding of the relationships between geodetic strain, seismic and geological data, etc. As a direct outcome of these activities, a region-wide network has been established which now spans the entire Aegean Sea. *AEGEANET* provides a consistent geodetic framework for current and future repeat GPS observations and facilitates detailed studies of this highly active tectonic area.

The SLR Fundamental Network

Previous geodetic work in the Aegean Sea region was conducted in the early 1980s on large spatial scales or over long time scales. Satellite Laser Ranging (*SLR*) measurements were made at six sites which formed part of the WEGENER/MEDLAS network and have also been re-occupied with mobile SLR equipment at various times since 1986 (Robbins *et al*. 1993). This fundamental network consists of the sites DION (Dionysos Satellite Tracking Station, near Athens), KATV (*Katavia,* in the island of Rhodes), XRIS (*Xrisokellaria*, in Peloponnese), ROUM (*Roumeli*, in Crete), ASKT (*Askites*, in Thrace) and KRTS (*Karitsa*, in Epirus; see Figure 2b).

Subsequent analyses, for example by Jackson et al. (1994), have compared the estimated velocities from these SLR sites with those expected from seismic strain release in the period 1911-1992 and concluded that seismicity can account for at most 50 per cent of the deformation in the Aegean, although additional uncatalogued smaller earthquakes may account for some of the discrepancy. To date, this SLR network provides the fabric for the fundamental reference frame connections of the various geodynamic networks that have been established since then, including the AEGEANET network.

Earlier Aegean Sea Networks

GPS measurements in the broader Aegean region were initiated in the early 1980s in the form of two regional networks in the north and south Aegean, which were subsequently expanded and parts of them were re-

observed on various occasions between 1988 and 2000 (e.g., Cruddace et al., 1999).

The first thorough comparisons between GPS results and conventional geodetic measurements in the area were made as part of the Southeast Aegean Project (SEA 93) which took place in 1993 and included GPS observations at 16 sites of the national geodetic triangulation/ trilateration network and five new GPS sites, as well as at two SLR sites within the area (Zacharis, 1994). The estimated velocity fields from this network were further augmented with the fields computed within two prior similar projects: the South Aegean GPS project (SAE 88/92), with two GPS campaigns in 1988 and 1992, and the 1992 Sea Level Fluctuations (SELF) project. These first major efforts to compare historical geodetic data and newer GPS results revealed horizontal movements typically up to 30 cm over the nearly 16-year period between these data sets. However, the overall results for these observed displacements and the corresponding site velocities were difficult to assess without some ambiguity, mainly because of the conceivably lower precision of the coordinates derived from the historical geodetic data (roughly 3 ppm vs. < 1 ppm for the GPS-derived results).

The AEGEAN 88/96 Project

The AEGEAN 88/96 project involved the realization of a regional geodetic network consisting of 30 stations that spanned the entire Aegean Sea region (Ouzounis, 1998). This network was first observed in 1988 and was re-occupied on three subsequent epochs: in 1989, 1992 and 1996. These campaigns allowed the first GPS-GPS velocity fields determinations that demonstrated the obvious advantages over the previous methods based on triangulation-GPS comparisons, including: (i) there is no need to make scale and orientation assumptions in order to estimate unique velocity fields; (ii) the network stations can be chosen to optimize geometry for geodynamic requirements, rather than the mutual station indivisibility of conventional networks; and (iii) baselines can be chosen to vary over short, medium and long lengths in order to improve the quality of the GPS solutions.

The AEGEANET Network

Rationale

The earlier geodetic works in the broader Aegean Sea region and several more recent studies (e.g., Goldsworthy et al., 2000) based on evidence

from geomorphology, the spatial distribution of large earthquakes, and additional geodetic measurements have suggested that active faulting in mainland Greece and the Aegean Sea is concentrated on a small number of discrete, linear zones that bound relatively rigid blocks. These zones are not always well defined even on land, and are clearest where the faulting produces large topographic offsets. This makes it difficult to provide an adequate description of the tectonics of the region, since it would require both the knowledge of the overall velocity field (i.e., the motions) and how this is achieved by faulting. However, the notion of Greece as a mosaic of rigid blocks the boundaries of which change with time is still a useful framework for seismic hazard evaluation and monitoring. From the geodetic viewpoint, this would ideally require establishing a large-scale geodetic network and re-observing it regularly with modern space geodetic measurements. In turn, these measurements, in combination with longer-term conventional geodetic data, could provide an essential and complementary method for quantifying deformation over many known faults and probably many unmapped ones, which encompass a wide variety of orientations, geometries and faulting types. The AEGEANET project constitutes a major attempt to establish a geodetic network spanning a large area that includes many of the Aegean islands and parts of Macedonia and Thrace, as well as spanning many known faults on which large earthquakes have occurred.

The overall approach in establishing AEGEANET has been to observe approximately 100 stations (and possibly more in the future) at regular time intervals using geodetic-quality GPS receivers. The choice of stations and the scheme for repeat occupation intervals follows a three-tiered approach:

- Small station spacing in areas of identified high seismic risk.
- Large spacing region-wide (to fill in gaps from previous networks).
- A number of permanent (e.g., International GPS Service [IGS] sites) and semi-permanent stations occupied for relatively short time periods (three or more days).

This allows the fiducial stations in the network to be linked to the International Terrestrial Reference Frame (ITRF). Furthermore, this makes it possible to apply efficient observation strategies whereby local stations can be observed with respect to “local” permanent (during the observations) stations, thus reducing baseline lengths and observation periods during the observation campaigns. The ultimate goal of this network is to obtain an integrated kinematic model that will accurately describe (spatially and quantitatively) the geodetic strain distribution throughout the Aegean Sea and the northern part of the Greek mainland. This may then be integrated with the seismic, geologic and other data to serve as a basic tool for seismic-hazard assessment and monitoring.

GPS Observations

The first AEGEANET GPS campaign took place in September, 1997 (days 254-269) and included GPS observations at a total of 94 sites, which included:

- 2 permanent reference platforms at the Dionysos Satellite Tracking Station (DION), near Athens.
- 66 concrete pillars from the national triangulation/trilateration geodetic network with available coordinates in the Hellenic Geodetic Reference System 1987 (denoted in the subsequent discussion as *EGSA 87*).
- 4 platforms from the SLR network (DION, ASKT, ROUM, KATV).
- 22 previously established GPS markers, which had been observed during the SEA 93 campaign.

The distribution of these stations is shown in Figure 2. The majority of the previously established GPS geodetic markers are in the form of brass pins glued into (usually limestone) bedrock. In addition to the primary marker, two or three auxiliary markers were installed at each site, in order to permit reconstruction of the primary in the event of damage. Local site ties were determined by conventional high precision surveying techniques.

For collecting the GPS data in this campaign, two main observing strategies were followed: some key sites were observed during at least one 5- to 7-hour session during one single day; whereas the remaining sites were observed in a quasi-continuous manner (i.e., while other receivers were moved between islands) for two to three sessions of at least 2-hours duration each and taken over two or more days. Furthermore, all the observed baselines were chosen so as to minimize their length, to maximize common observations between stations, and to avoid receiver- and antenna-type mixing. Generally, the collected GPS data were processed on a daily basis and were cleaned for cycle slips automatically in most cases and manually whenever it was necessary in order to ensure the reliability of the results (Tomae and Tsagannidou, 1998).

The entire campaign was referenced to two main points among the SLR pads at Dionysos Tracking Station: the main GPS/SLR pad designated as DIONG and the SLR pad designated as DIONC at a distance of some 15 m from DIONG. DIONG is a permanent site, which operates a TRIMBLE 4000SSI receiver, whereas the observations at DIONC were collected using an ASHTECH-ZXII receiver. For the other stations, a mixture of dual-frequency ASHTECH and TRIMBLE GPS receivers was used. The coordinates of DIONG were estimated in the ITRF reference frame at epoch 1997.72 (i.e., the mean epoch of the GPS observations for this project) by utilizing available GPS data from the ITRF sites GRAZ (Austria), MATERA

(Italy) and WETTZEL (Germany). From these coordinates of DIONG, the coordinates of DIONC were subsequently determined using two full days of common data between these two nearby stations.

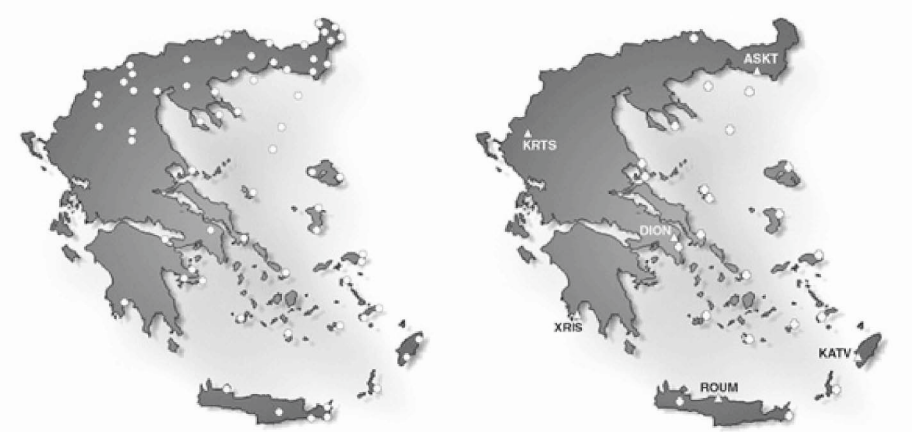

Figure 2. Parts of the AEGEANET network consisting of 66 pillars of the national geodetic network (left) and 4 SLR pads and 22 previously established GPS markers (right).

The solutions for the remaining stations of the AEGEANET network were carried out in two sub-networks, termed respectively as AEGEANET-I and -II. The AEGEANET-I sub-network consisted of 42 sites from which the observations were analyzed in two parts so that single-receiver-type daily networks could be formed in each case; specifically:

- All observations collected at sites utilizing ASHTECH receivers and in a radial baseline pattern using the DIONC site as reference station.
- All observations collected at sites utilizing TRIMBLE receivers and in a radial baseline pattern using the DIONG site as reference station.

The baselines lengths ranged from 15 to 450 km, and daily observing sessions were designed to include a range of processed baseline lengths for better integer ambiguity resolution. All the solutions were carried out using the Bernese v.4.0 software suite (Rothacher et al., 1996). Generally, the solutions were based on the L_3 frequencies combination for the longer baselines (> 20 km) and solutions based on the L_1 frequency data for the short baselines (< 15 km). The decision for this observing strategy was justified later by the small rms values (typically at the sub-millimeter range, up to 1-1.5 mm) that were obtained from this solution for the coordinates of these 42 stations. Another indication of the quality of the results was the percentage of successful resolution of the integer ambiguity parameters during the final processing of the GPS data, which was typically larger than 75% for the baselines greater than 100 km and larger than 85% for the baselines less than 100 km in length.

The AEGEANET-II sub-network consisted of the remaining 50 sites. Their coordinates were estimated from multi-baseline solutions, which used as reference stations the nearest sites whose coordinates were available from the AEGEANET-I solution. For a small number (15) of stations in this subset, the solutions for the final coordinates were obtained by averaging the coordinate values from individual session solutions for various baselines. For these baselines, a single solution was not possible (via the summation of normal equations resulting from all available observations) because for the various observing periods at the stations involved, the height of the antennas varied from occupation to occupation.

Comparison with other geodetic data

In order to further analyze these GPS results from a geodynamic viewpoint, we have estimated the horizontal displacement field, the corresponding crustal velocities and the strain ellipses inferred from these measurements and from prior coordinates of the sites (e.g., derived from terrestrial geodetic data or from previous GPS campaigns, like SEA 93). The accuracy of these prior coordinates had been assessed from previous analyses. All relative coordinates derived from conventional terrestrial geodetic data were estimated to be accurate to better than 3 ppm, determined from the re-adjustment of the national geodetic networks leading to the Hellenic Geodetic Reference System 1987 (EGSA 87). All GPS-derived coordinates from the SEA 93 campaign were estimated to be accurate to the 1-ppm level or better, as determined from the consistency of the entire network provided by the rms of the residuals. The quality of this processing was also evident from the day-to-day repeatability of baselines between stations with at least three observing sessions in this campaign, which were generally less than 10 mm per horizontal coordinate, while for the vertical component were 1-2 times higher (Ouzounis, 1998).

For that purpose, the coordinate differences (GPS minus EGSA 87) for 64 (out of the 66) pillars of the AEGEANET which were also part of the national triangulation/trilateration geodetic network, were computed relative to the fixed DIONG station and expressed in the North, East and Up components, after the whole-subnetwork rotations and translations were eliminated. Two additional sites (SAMO and SAMB on the island of Samos) showed values that were unreasonably large, possibly due to pillar instabilities, and hence these sites were excluded from any subsequent analyses.

In order to estimate the crustal velocities, it was necessary to carefully define the reference epoch of the EGSA 87 coordinates of the relevant sites, so that their transformation to ITRF epoch 1997.72 could be done without

ambiguity or any assumptions. This was done separately for each of the following sub-groups of stations, each having EGSA 87 coordinates derived from triangulation/trilateration measurements considered as collected at different epochs indicated in parentheses:

- pillars in the Northeast part of the AEGEANET, in the Prefecture Evros, in eastern Trace (with data epoch 1962).
- pillars in the Dodecanesse islands (with data epoch 1955).
- the remaining pillars (with data epoch 1972).

The velocities so derived from time-separated geodetic observations can be considered as interseismic velocities at each site; that is, the velocities that would be measured in the absence of any earthquakes. This is because, over timescales that are large compared with the repeat times of large earthquakes, upper-crustal strain is accommodated for the most part discontinuously by slip on the existing surface faults (Bourne et al., 1998; England, 2002). Because of the short timescale of our space-geodetic observations, we are not able to measure directly this long-term upper-crustal strain. Therefore, under this premise, what is measured geodetically at the surface will reflect the long-term deformation (i.e., distributed shear) of the underlying lithosphere, irrespective of whether that deformation is continuous or discontinuous.

At first we computed the velocities for each of these groups of stations, relative to the fixed DIONG station and averaged over the corresponding time intervals. Subsequently, as we wished to determine velocities with respect to a stable Eurasia, we subtracted the rigid-body rotation of Eurasia from the ITRF transformed velocities solution from Graz, Matera and Wettzell (evaluated at DIONG). The combined velocity field illustrating these velocities from these groups of stations relative to a non-rotating stable Eurasia is shown in Figure 3.

In the northern part of AEGEANET, the coordinate differences results for the sites in the Prefecture of Evros (i.e., between latitude 40.8 to 41.6 and longitude 25.7 to 26.6) imply unusually strong motions up to 49 mm/yr in the same southwestward direction, which however are not supported by other studies. This may be due to one of the following reasons: (a) undetected network adjustment discrepancies (i.e., scale and datum defects) in the historical data which may have affected the conventional geodetic coordinates of the sites; (b) use of inconsistent or incorrect information concerning the temporal distribution of the old geodetic data, which could have affected the transformation of the sites' geodetic coordinates to the specific ITRF epoch; or (c) the presence of small faults in this area. To resolve the first two possibilities, it would require another closer inspection of the relevant data. The second premise cannot be tested until repeat GPS observations are carried out in order to study the area in greater detail. Hence,

this aspect will be carefully looked into in any future GPS surveys in the area. For a further analysis of the problem, we plan to examine the possibility whether the changes in the horizontal kinematic pattern in this area correlate with changes in the vertical movements and seismicity.

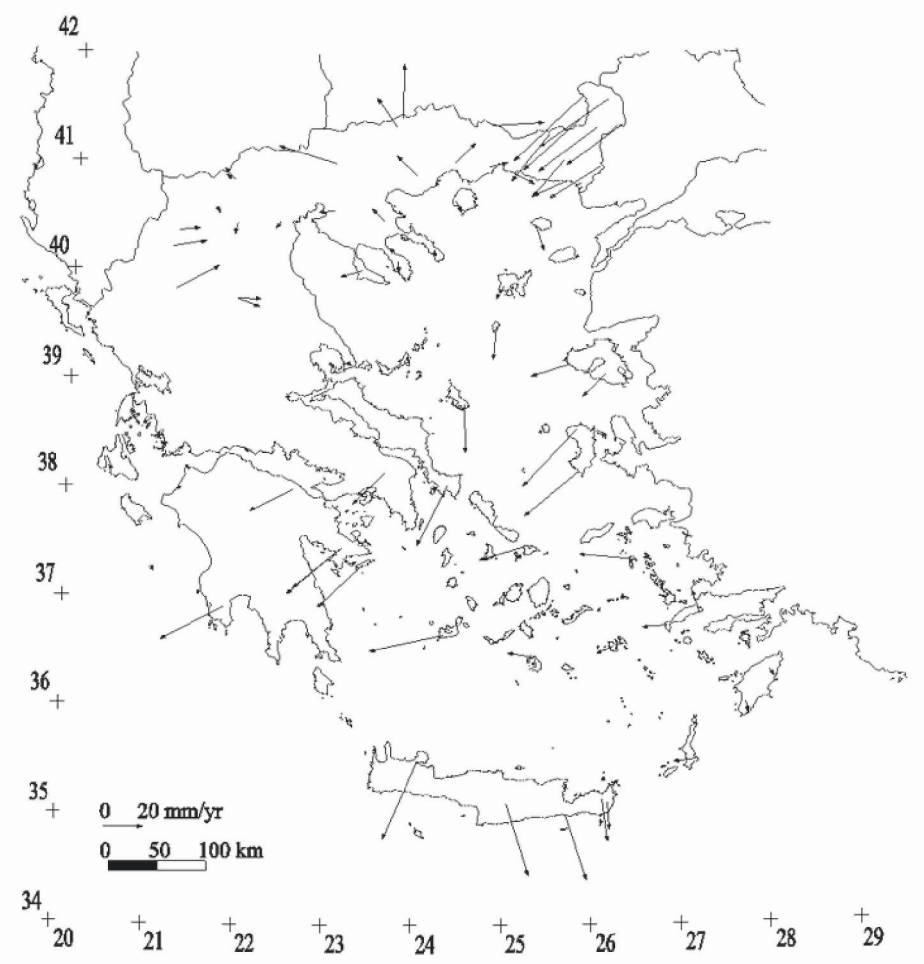

Figure 3 Mean velocities at the AEGEANET sites, determined over time intervals from 25 to 42 years, after effects of the whole-network rotations and translations were eliminated. The scale bar equals 20 mm/yr.

In the remaining northern part of the AEGEANET network (i.e., the western part of Macedonia), the eastward displacements (0.15 to 0.75 m) and velocities (5.8 to 29 mm/yr) are generally much smaller than those observed for the southern part. The sites in the Dodecanesse islands exhibit a slightly

different pattern with motions in the westward direction exceeding 1.2 m, over the 42-year period.

Variation of Strain

Apart from studying the displacements and the velocities fields, it is useful to examine the resultant strain field that is inferred from the available observations and is due to the tectonic strain that is accumulated within the area of interest. In this connection we consider the strain to be a tensor quantity that varies in time and space. In two dimensions, this can be expressed by a strain ellipse for each area, which is defined by the homogeneous transformation of a unit circle into an ellipse. Assuming homogeneous deformation throughout the area of a network (i.e., no discontinuities), the 2-dimensional change in length, shape or angle relative to the original orientation can be expressed by a unit circle transformed into an ellipse depicting the respective extension and contraction along the principal axes of strain.

Initially the whole AEGEANET area was treated as a single block. In other cases, the area was assumed as consisting of blocks each with distinct sets of strain ellipse parameters. For example, a north-south division of the Aegean Sea was considered. Finally, in order to better illustrate the deformation in the Aegean Sea region and its motion relative to the surrounding areas, we computed strain ellipses for six representative sub-regions spanned by the AEGEANET, in order to examine the more local strain accumulation patterns over different spatial scales. A brief discussion on these results is presented immediately below, while detailed results can be found in Tomae and Tsagiannidou (1998). An independent comprehensive account of the active deformation field inferred from both GPS and seismological data in this broader Aegean Sea region can be found in a recent detailed study by Papazachos (2002), in which results from the combination of these two different data sources are jointly interpreted assuming that the seismic deformation represents a part of the total deformation in the area.

Figure 4 shows the strain ellipses obtained when the area of the AEGEANET network is subdivided into the following six sub-regions (from top to bottom and from left to right), with the data period in each sub-region indicated in parentheses:

1—Central-Western Macedonia and Central Greece (1972 to 1997.72);
2—Prefecture of Evros and the islands of Samothraki, Thasos, and Limnos (1962 to 1997.72);
3—Evia, Attica and Peloponnese (1972 to 1997.72);
4—Northern Aegean islands Chios, Skyros, Lesvos, and Samos (1972 to 1997.72);

5─Cyclades and Crete (1972 to 1997.72);
6─Dodecanesse islands (1955 to 1997.72).

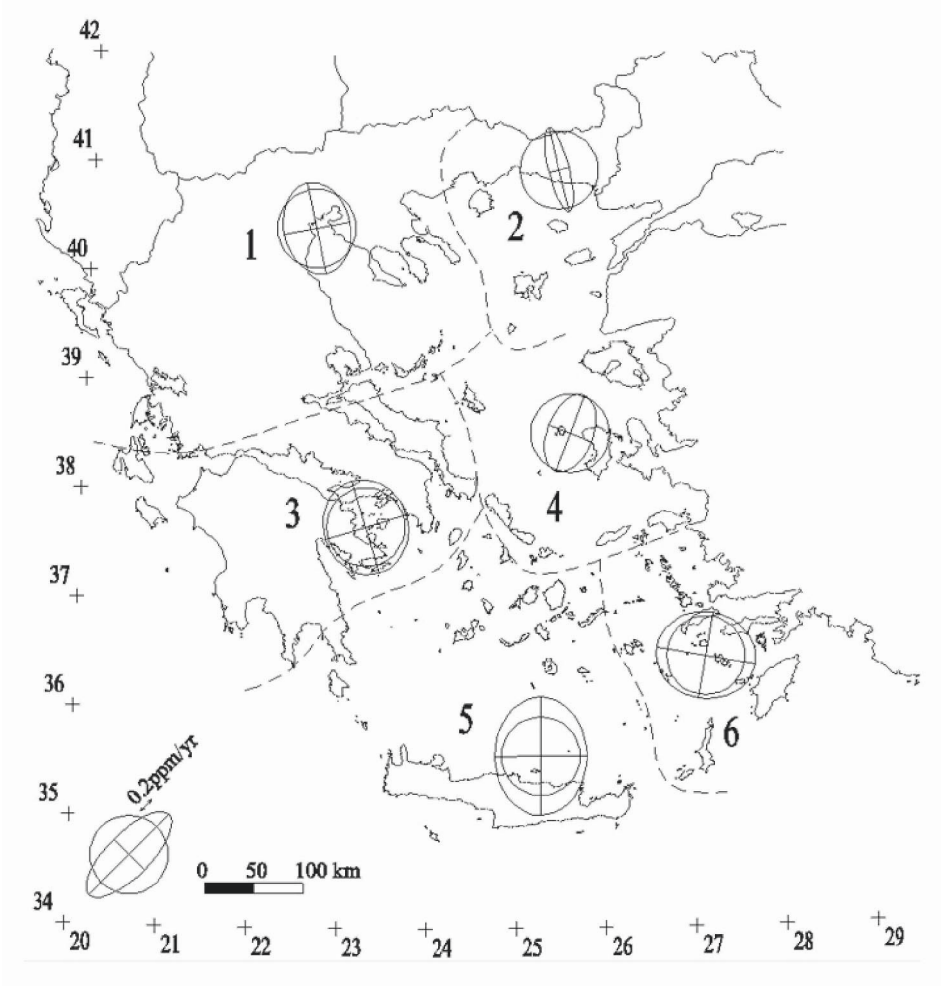

Figure 4 Strain ellipses for six sub-regions of the AEGEANET network, determined from the EGSA 87-GPS velocities fields for the sub-group of 66 pillar stations. The strain ellipse's scale bar equals 0.2 ppm/yr.

These sub-regions are considered to be representative of the different orientation and different geodynamic regimes (extensional, compression and transform) of the Aegean. The defining parameters of the strain ellipse for each sub-region are given in Table 1, where K_{max} and K_{min} are the respective extension and contraction along the principal axes of strain, Az is the orientation of the axes of the strain ellipse and the shear strain can be computed as $\gamma = K_{max} - K_{min.}$ The coordinates of the origin of the ellipse in

each case coincide with the planar coordinates of the centroid of each group of points in the area under consideration.

Table 1 Defining parameters of the corresponding strain ellipses shown in Figures 4 and 5 (columns 3 and 4) and their differences (column 5) reflecting changes in the strain patterns depicted by these two data sets

	Strain Ellipse Parameters	From Long-term (terrestrial-GPS) velocity field	From Short-term (GPS-GPS) velocity field	Differences in the parameters
Sub-region 1	**K_{max} (ppm)**	0.082	0.116	0.034
	K_{min} (ppm)	-0.069	0.011	0.080
	Az (deg)	-11.570	76.895	88.465
	γ (ppm)	0.151	0.105	-0.046
Sub-region 2	**K_{max} (ppm)**	0.043	0.142	0.099
	K_{min} (ppm)	-0.333	-0.066	0.267
	Az (deg)	-13.855	22.540	36.395
	γ (ppm)	0.376	0.209	-0.167
Sub-region 3	**K_{max} (ppm)**	0.102	0.041	-0.061
	K_{min} (ppm)	0.033	-0.024	-0.057
	Az (deg)	-16.500	90.680	107.180
	γ (ppm)	0.069	0.065	-0.004
Sub-region 4	**K_{max} (ppm)**	0.014	0.056	0.042
	K_{min} (ppm)	-0.187	-0.058	0.129
	Az (deg)	20.946	6.807	-14.139
	γ (ppm)	0.201	0.114	-0.087
Sub-region 5	**K_{max} (ppm)**	0.228	0.009	-0.219
	K_{min} (ppm)	0.078	-0.007	-0.085
	Az (deg)	-0.330	-28.160	-27.830
	γ (ppm)	0.149	0.015	-0.134
Sub-region 5	**K_{max} (ppm)**	0.123	0.093	-0.030
	K_{min} (ppm)	0.046	0.025	-0.021
	Az (deg)	99.637	77.630	-22.007
	γ (ppm)	0.077	0.069	-0.008

From the first column of Table 1 and the graphical representation in Figure 4, the following useful conclusions can be drawn regarding the observed strain regime for each sub-region. For sub-region 1, small deformations (<0.1 ppm/yr) are noted, whereas in sub-region 2, the strain ellipse exhibits an E-NE contraction on the order of ~0.3 ppm/yr and a smaller N-NW extension (~ 0.04 ppm/yr) that can be attributed to the presence of a known fault between the islands of Samothaki and Limnos. Sub-region 3 exhibits mainly N-NW extensional deformation on the order of ~ 0.1

ppm/yr, which agrees with earlier estimates by Ouzounis (1998) and can be explained by the presence of known faults in the Gulf of Korinth. Sub-region 4 shows a E-SE contraction (~ 0.2 ppm/yr) and almost negligible extension (~ 0.01 ppm/yr), whereas the remaining two sub-regions exhibit extensional deformations in all directions up to ~0.23 ppm/yr in the N-S direction in sub-region 5 and ~0.1 ppm/yr in the N-NE direction for sub-region 6.

Comparison with the Aegean 93 GPS results

A similar analysis was done for the additional 26 points of AEGEANET (i.e., 4 SLR pads and 22 GPS markers) that had been previously observed with GPS in 1993 (SEA 93 campaign). The GPS coordinates for this campaign were referenced to the mean ITRF epoch 1993.5, using the primary point of Dionysos (DIONG) which was held fixed to its ITRF93 position (i.e., the so-called Dionysos Datum 1993 or DD93 solution). The comparison of AEGEANET 97 to SEA 93 GPS coordinates for this common set of points allowed calculation of the purely GPS-GPS velocity field, which in spite of its shorter time span (1993.5 to 1997.72) provided a useful insight into the relation of the present-day deformation pattern with the previous longer-term deformation implied by the velocities inferred from the combination of terrestrial geodetic data and GPS measurements.

In a similar manner, the velocities derived from the repeated GPS surveys in the aforementioned 26 additional markers were determined relative to the fixed DIONG station and averaged over the corresponding time interval, after the whole-subnetwork translations and rotations were eliminated. The corresponding strain ellipses derived from these data for the six sub-regions are shown in Figure 5, with the corresponding strain-ellipse parameters for each sub-region shown in the second column of Table 1.

A direct quantitative comparison of these short-term deformations vis-à-vis the longer-term deformations depicted by the strain ellipses in Figure 4 is not straightforward, and any comparison should consider that for the short-term deformations, there were a smaller number of points in each area that contributed to the relevant computations. However, useful remarks can still be made, regarding some consistent trends that can be seen from the two comparisons, such as the similarities in the strain patterns along the eastern coastline of the Aegean Sea (sub-regions 4 and 6) and the sub-region of Evia, Attica and eastern Peloponnese (sub-region 3).

Sub-region 1 shows mainly an extensional deformation in the E-NE direction on the order of ~0.12 ppm/yr. In sub-region 2, the strain ellipse exhibits a N-NE extension on the order of ~0.14 ppm/yr and a smaller E-SE contraction on the order of ~0.07 ppm/yr. For sub-region 3, a small extensional deformation is noted in the E-W direction (~0.04 ppm/yr) and an

even smaller contraction (~0.02 ppm/yr) in the N-S direction. Sub-region 4 shows a small extensional deformation in the N-NE direction (~0.06 ppm/yr) and a similar contraction in the E-SE direction. Sub-region 5 shows almost negligible deformation in all directions, while sub-region 6 shows a small (~0.1 ppm/yr) extensional deformation in the E-SE direction.

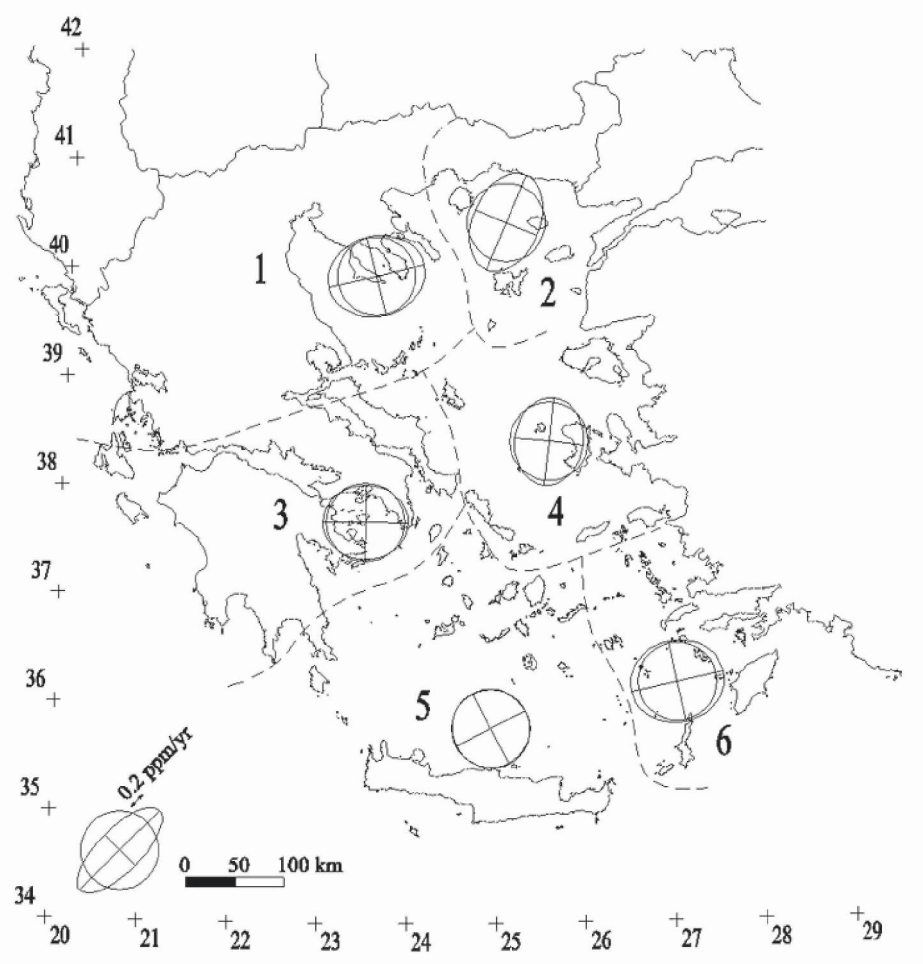

Figure 5 Strain ellipses for six sub-regions of the AEGEANET network, determined from the GPS-GPS velocities field spanning the period 1993.5 to 1997.72 for the sub-group of stations including 4 SLR pads and 22 GPS markers. The strain ellipse's scale bar equals 0.2 ppm/yr.

Overall, for sub-regions 1, 3, 4, and 6, the differences noted in the strain patterns between the short-term deformations derived from the GPS-GPS velocity field and the deformations derived from the "terrestrial-GPS" velocity field are of the order of 0.1 ppm/yr or less. Larger differences are

observed in the contraction exhibited in sub-region 2 (~0.07 vs. 0.33 ppm/yr) and in the extension exhibited in sub-region 5 (~0.01 vs 0.23 ppm/yr). For sub-region 2, the small magnitude of the short-term deformations derived from the GPS-GPS velocity field, in connection with the discussion made in section 3.3 regarding the likely reasons for the unusually large velocities in the Prefecture of Evros as computed from the respective terrestrial-GPS data, supports the notion that some discrepancies may exist in the conventional geodetic coordinates of the AEGEANET sites (pillars) in this sub-region. This also emphasizes the priority of collecting another set of GPS data at these sites during one of our future GPS campaigns to completely resolve the issues concerning the strain pattern in this particular sub-region. A similar explanation seems plausible for the large differences noted in sub-region 5, although in this case, one needs to consider the possibility that the differences may indicate a change in the kinematic and strain patterns after 1993. This premise, although difficult to explain without additional evidence, cannot be discounted at this point considering the complicated tectonic fabric and the high seismic activity in the Cyclades islands and Crete over the past several years.

CONCLUSIONS

A coordinated set of GPS campaigns has resulted in the establishment of an Aegean Sea regional geodetic network, termed AEGEANET. GPS and other geodetic measurements on this network have been adopted as the geodetic background for the most recent geodynamic interpretations related to the Aegean Sea region. Velocity fields spanning a 40 yr time interval, determined from comparisons of GPS with conventional geodetic measurements, have provided measures of relatively long-term crustal deformation, while shorter span GPS-GPS velocity fields have demonstrated that measurements of strain can be made for present-day deformations of local regions spanning a few tens of kilometers.

AEGEANET has been augmented with the Central Greece Network (CGN), a similar network of some 70 stations spanning Central Greece and the northern part of Peloponnese, which has provided similar results for crustal strain in central Greece from repeated GPS measurements during 1989-1997 (Clarke et al., 1998). Together with the new Continuous Ionian Network (CION), a 46-station GPS network in western Greece, the Ionian Sea and Crete (Peter at al., 1998; Kahle et al., 1995, 1996), these three major geodetic networks cover the entire Greek territory and provide a consistent integrated framework to study the kinematics and dynamics of plate interactions across this region.

Future work will include additional repeat GPS measurements on these networks which will further quantify the localized strain fields in the various sub-regions of the Aegean extensional basin and of the north-western and central Greece, in order to continue monitoring likely seismic hazards in this highly active tectonic region.

REFERENCES

Bourne S., England P., Parsons P. The motion of crustal blocks driven by flow of the lower lithosphere and implications for slip rates of continental strike-slip faults. Nature 1998; 391: 655-659.

Clarke P.J., Davies R.R., England P.C., Parsons B., Billiris H., Paradissis D., Veis G., Cross P.A., Denys P.H., Ashkenazi V., Bingley R., Kahle H.-G., Muller M.-V., Briole P. Crustal strain in central Greece from repeated GPS measurements in the interval 1989-1997. Geoph. J. Int. 1998; 135: 195-214.

Cruddace P.R., Cross P.A., Veis G., Billiris H., Paradissis D., Galanis J., Lyon-Caen H., Briole P., Ambrosius B.A.C., Simons W.J.F., Roegies E., Parsons B., England P., Kahle H.-G., Cocard M., Yannick P., Stavrakakis G., Clarke P., Lilje M. An Interdisciplinary Approach to Studying Seismic Hazard Throughout Greece. In *Geodesy Beyond 2000. The challenges of the first decade*, K.P. Schwarz, eds., Springer 1999; 279-284.

England P. The interpretation of geodetic data relevant to continental deformation. CD-Proceedings of the 11th General Assembly of the WEGENER Project, June 12-14, Athens, Greece, 2002.

Goldsworthy M., Jackson J. Active normal fault evolution in Greece revealed by geomorphology and drainage patterns. Geol. Soc. London Spec. Publ. 2000; 157: 967-981.

Jackson J.A., Haines J., Holt W. The horizontal velocity field in the deforming Aegean Sea region determined from the moment tensors of earthquakes. J. Geophys. Res. 1994; 135 (B12): 17,657-17,684.

Kahle H.-G., Cocard M., Peter Y., Geiger A., Reilinger R., McClusky S., King R., Barka A., Veis G. The GPS strain rate field in the Aegean Sea and western Anatolia. Geoph. Res. Let. 1999; 26 (16): 2513-2516.

Kahle H.-G., Mueller M.V., Geiger A., Danuser G., Mueller S., Veis G., Billiris H., Paradissis D. The strain field in northwestern Greece and the Ionian Islands: results inferred from GPS measurements. Tectonophysics 1995; 249: 41-52.

Kahle H.-G., Mueller M.V., Veis G. Trajectories of crustal deformation of western Greece from GPS observations 1989-1994. J. Geophys. Res. 1996; 23: 677-680.

Koravos G. Ch., Main I. G., Tsapanos T. M., Musson R.M.W. Maximum earthquake magnitudes in the Aegean area constrained by tectonic moment release rates. Geophys. J. Int. 2003; 152: 94–112.

Le Pichon X., Angelier J. The Hellenic arc and trench system: a key to the neotectonic evolution of the Eastern Meditteranean area. Tectonophysics 1979; 60: 1–42.

Ouzounis A. *Tectonic motions in the Aegean Sea region determined from GPS observations*, Dipl. Thesis (in Greek), Dept. Surveying Eng., Nat. Tech. Univ. Athens, 1998.

Papadimitriou E., Sykes L. Evolution of the stress field in the northern Aegean Sea (Greece), Geophys. J. Int. 2001; 146: 747–759.

Papazachos C.B., Kiratzi A.A. A detailed study of active crustal deformation in the Aegean and surrounding area. Tectonophysics 1996; 253: 129–153.

Papazachos C.B. The active crustal deformation field in the Aegean area inferred from seismicity and GPS data. CD-Proceedings of the 11th General Assembly of the WEGENER Project, June 12-14, Athens, Greece, 2002.

Peter Y., Kahle H.-G., Cocard M., Veis G., Felekis S., Paradissis D. Establishment of a permanent GPS network across the Kephalonia fault zone, Ionian Islands, Greece. Tectonophysics 1998; 294: 253-260.

Robbins J.W., Smith D.E., Ma C. Horizontal crustal deformation and large-scale plate motions inferred from space geodetic techniques. In *Contributions of Space Geodesy to Geodynamics*, D.E. Smith, D.L. Turcotte, eds., Crustal Dynamics, 23: 21-36. Washington, DC: AGU Geodynamics Series, 1993.

Rothacher M., Beutler G., Gurtner W., Brockmann E., Mervart L. 1996, in Bernese GPS Software Version 4.0., Rothacher M., Mervart L. (Eds.), University of Bern, Switzerland.

Tomae E., Tsaganidou Z. *Geodetic Determination of tectonic displacements in the broader Aegean Sea region,* Dipl. Thesis (in Greek), Department of Surveying Engineering, National Technical University of Athens, 1998.

Zacharis E. *Position determinations with GPS in the southern Aegean region*, Dipl. Thesis (in Greek), Dept. Surveying Eng., Nat. Tech. Univ. Athens, 1994.

THE PIVO-2003 EXPERIMENT: A GPS STUDY OF ISTRIA PENINSULA AND ADRIA MICROPLATE MOTION, AND ACTIVE TECTONICS IN SLOVENIA

John Weber[1], Marko Vrabec[2], Bojan Stopar[3], Polona Pavlovčič-Prešeren[3], and Tim Dixon[4]

1: Grand Valley State University, Department of Geology, Allendale, MI 49401, USA
weberj@gvsu.edu
2: University of Ljubljana, Faculty of Geology, Ljubljana, Slovenia
3: University of Ljubljana, Faculty of Geodesy, Ljubljana, Slovenia
4: University of Miami, RSMAS-MGG, Geodesy Lab, Miami, FL 33149, USA

ABSTRACT

This contribution introduces our PIVO-2003 (Periadriatic-Istria Velocity Observations) GPS (Global Positioning System) experiment, designed to measure the motion of the Adria microplate and to study active deformation in Slovenia, along the NE corner of the microplate. To measure Adria's motion, we used decade-scale episodic GPS data from seven sites in the Istria peninsula of Slovenia and Croatia, which is Adria's major aseismic onshore unit, together with continuous GPS data from two permanent GPS sites on the Po Plain. We processed all of the GPS data using GIPSY (release 2.5) software and precise satellite ephemeris and clock files. We used data from 15 permanent GPS sites to define a stable European ITRF-2000 reference frame. We formally inverted subsets of the Istria and Po Plain Europe-referenced GPS velocities for a series of trial Adria-Europe rotation poles. Our average pole locates near that of Anderson and Jackson (1987), which was derived from the inversion of a broadly distributed, circum-Adriatic set of earthquake slip vectors; this coincidence brings into question the recent hypothesis that Adria is fragmenting into two major sub-blocks. To quantify and study active deformation in Slovenia, we used the same analysis strategy and data from 35 episodic GPS sites in Slovenia and northern Croatia and tens of permanent GPS sites located in the surrounding region. We observed a significant and sharp (few mm/yr) dextral (to transpressive) gradient in the velocity field along the Sava Fault (Periadriatic zone), suggesting that lateral extrusion in the Alps may still be active today.

INTRODUCTION

Precisely quantifying the current motion of the Adria microplate, more simply termed Adria, remains a major challenge in Alpine geodynamics. Knowing how Adria moves is critical for understanding the kinematic boundary conditions that drive circum-Adria active deformation in the

N. Pinter et al. (eds.), The Adria Microplate: GPS Geodesy, Tectonics and Hazards, 305–320.

Apennines (Italy); the western, central, eastern, and southern Alps (France, Switzerland, Italy, Slovenia, Austria); and in the Dinaric Alps (Slovenia, Croatia, and Bosnia-Herzegovina, Serbia-Montenegro, and Albania; Figure 1). More broadly, knowing how Adria moves should also give some important basic constraints still required for developing a clearer understanding of the geodynamic evolution of the complex Nubia (West Africa)-Europe collision zone (e.g., see Stein and Sella, this volume).

Measuring Adria's motion is challenging for a number of reasons. This microplate is mostly submerged beneath the Adriatic Sea; a thick cover of young, unconsolidated sediment in the Po Plain also blankets much of its exposed portion (Figure 1). Adria also is surrounded by high-topography, high-seismicity, diffuse deforming zones. These factors make it difficult to establish a broad-aperture set of geodetic sites on stable Adria.

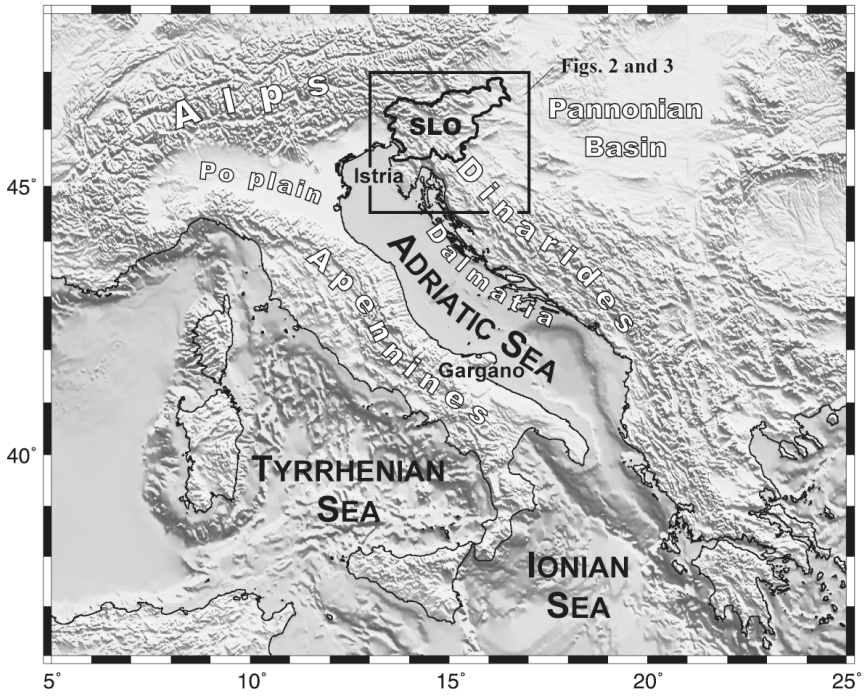

Figure 1. Topography of south-central Europe and bathymetry of surrounding sea floor. The Adriatic Sea and Po Plain are underlain by the Adria microplate (Adria), which is surrounded by the Alps, Dinarides, and Apennines. The Istria peninsula forms Adria's major outcrop. Slovenia (SLO) sits at NE corner of Adria at the junction between the Alps, Dinarides, Po Plain, and Pannonian Basin.

Geologic, seismic and seismic tomographic data all suggest that Adria is made up of a trapped block of continental lithosphere that is underthrusting its eastern, western, and northern margins (Anderson and Jackson, 1987; Royden et al., 1987; Selvaggi and Amato, 1992; Italiano et al., 2000; Wortel and Spakman, 2000). Adria thus forms the foreland to all of these surrounding deforming zones. Adria may be internally fragmented or fragmenting (e.g., Oldow et al., 2002), for example along the NE-SW-trending active fault zone that cuts the Italian peninsula and Adriatic Sea from Gargano to Dubrovnik; this zone was seismically active during an earthquake swarm in 1986-1990 (Favali et al., 1993; Console et al.,1993; Figure 1). But the magnitude of motion across this and possibly additional intra-Adria active faults is not yet quantified. Similarly, the southern boundaries between Adria and Nubia (western Africa) and between Adria and the Hellenic extensional province (McClusky et al., 2000) in northern Greece are not clearly marked by seismicity or bathymetry and are not fully understood (but see Hollenstein et al., this volume). Finally, Adria appears to be moving slowly relative to the neighboring European Plate, so precise and accurate measurements will be needed to quantify its motion.

NUVEL-1A predicts 9 mm/yr of 348°-directed African-Eurasian motion in the circum-Adriatic (DeMets et al., 1990, 1994). If Adria-Europe motion is related to Adria-Africa motion, then Adria may move at < 1 cm/yr relative to Europe (see also Sella et al., 2002).

Slovenia sits at the NE corner of the Adria microplate, where the Alps, Dinarides, and Pannonian Basin meet (Figures 1, 2). Several hypotheses have been proposed concerning neotectonics and the accommodation of late-stage convergence in the Alps. Testing and resolution of these hypotheses is important for assessing seismic hazard in Slovenia, which has not been thoroughly studied geomorphically and is not well quantified geodetically.

This contribution lays out the scientific rationale behind our PIVO-2003 (Periadriatic-Istria Velocity Observations) GPS (Global Positioning System) experiment, which was designed to measure the motion of Adria and to study active deformation in Slovenia. We review the background literature and preliminary data sets used to design our experiment, give some details of experiment logistics, present preliminary results, and suggest some avenues for future studies.

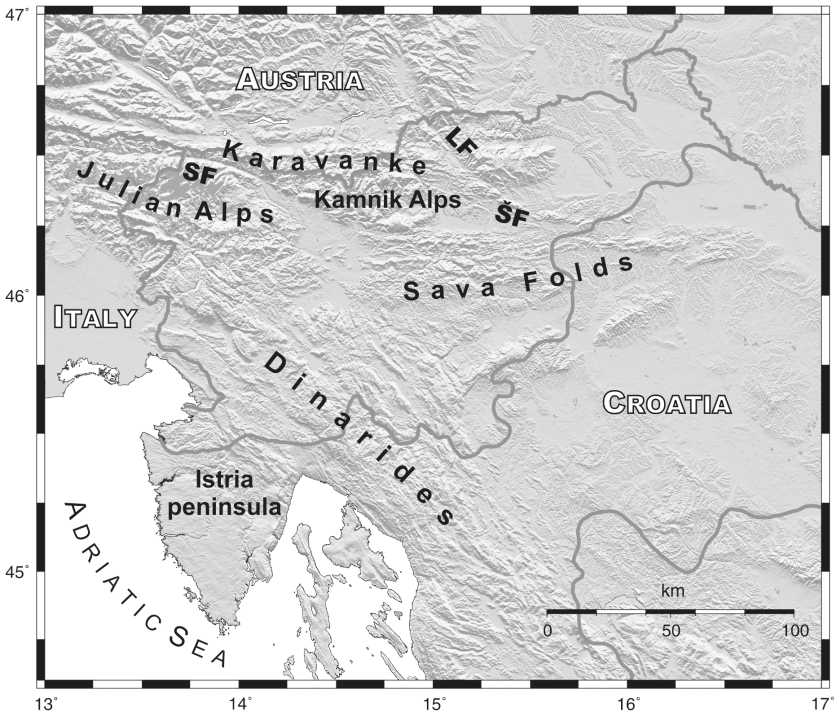

Figure 2. Topography of Slovenia and surroundings illustrating the Sava Folds region and selected active or potentially active faults: SF-Sava Fault, ŠF-Šoštanj Fault, Lf-Labot Fault. See Figure 1 for location.

GEODYNAMICS BACKGROUND

Adria microplate and Istria peninsula

The great tectonist, Argand, suggested early on that Adria forms a northern promontory of the African continent that is pushing into Europe and forming the arcuate Alpine mountain chain (Argand, 1924). Many subsequent workers, noting that the general low level of seismicity in the Adriatic Sea contrasts sharply with high seismicity in the surrounding mountain belts, have suggested that Adria moves as a separate microcontinent or microplate. Modern analyses of the active tectonics in the circum-Adria region began with McKenzie (1972) and Anderson and Jackson (1987). Anderson and Jackson (1987) postulated that the Adriatic aseismic zone marks the rigid interior of an Adria microplate, and they studied its motion based upon the seismicity along its boundaries (see below). In this light, the

Istria peninsula which is the focus of the GPS study presented here forms the major onshore portion of stable Adria within the interior aseismic zone (Figures 1, 3).

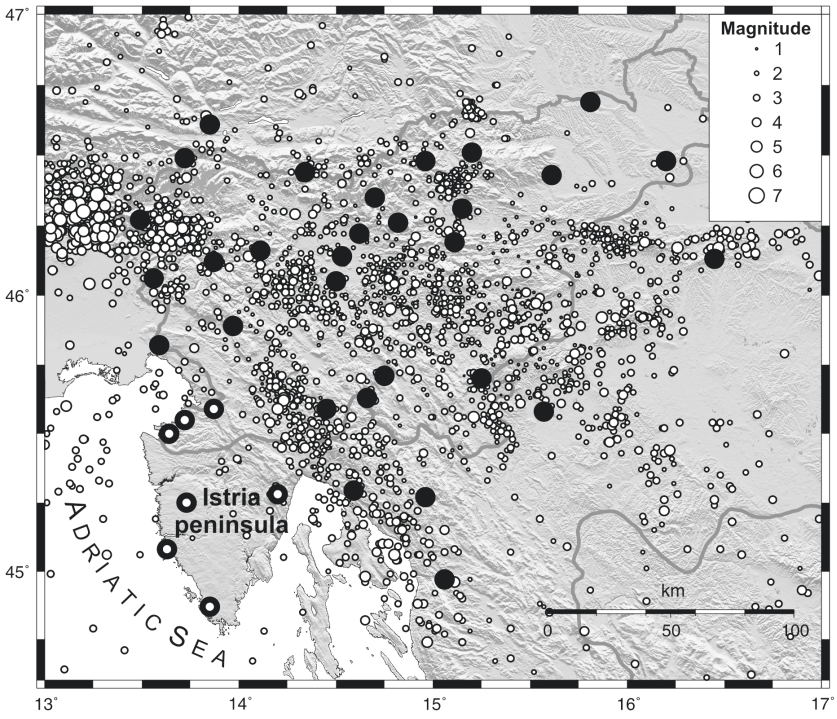

Figure 3. PIVO-2003 GPS network of Slovenia and northern Croatia shown by large dark dots and earthquake epicentres shown by small white dots. National borders shown by heavy lines. We derived decade-scale velocities at all 35 of these sites, 23 of which were re-occupied in September-October 2003 in the PIVO-2003 GPS campaign. Note that the Istria peninsula is largely aseismic. Seven Istria peninsula sites used in our Istria (Adria)-Europe Euler pole inversion are shown as large dark open dots; two permanent GPS sites UPAD and VENI on the Po Plain (not shown) were also used.

Adria's border zones

Anderson and Jackson (1987) studied 51 >5 M_b teleseismic earthquakes that occurred along the borders of the aseismic Adria microplate. The focal mechanisms they derived from these events gave systematic results, and showed NE-SW extension in the Apennines, N-S shortening in northern Italy, and NE-SW shortening in Yugoslavia (present-day Croatia) and Albania. Anderson and Jackson used the slip vectors from these events to determine a pole of rotation located at 45.8° N by 10.2°E that showed CCW

motion of Adria relative to Europe, but they were unable to determine a rotation rate because earthquake slip vectors give only directional plate motion data.

When designing our GPS experiment, we were suspicious that NE-SW extension in the Apennines, which is oriented sub-perpendicular to the trend of the young, contractional accretionary prism making up the Italian peninsula, could be related simply to orogenic collapse and unrelated to Adria-Europe motion (e.g., see Stein and Sella, this volume). In Anderson and Jackson's (1987) analysis, normal faulting events in the Apennines were thought to mark and, therefore were used to track, the movement of the western edge of the CCW-rotating Adria microplate. The Pliocene-Quaternary age, asymmetry, and great thickness of foreland basin sediments east of the Apennine accretionary prism (Royden et al., 1987), intermediate depth seismicity observed beneath the northern Apennines (Selvaggi and Amato, 1992), and arc volcanism, however, suggest recent west-dipping subduction of Adria beneath the Apennines. NE-SW Apennine extension thus could simply be related to upper-plate gravitational collapse of the NW-SE-trending Apennine prism (e.g., see Platt, 1986), and the normal fault focal mechanisms that Anderson and Jackson (1987) studied there could, in principal, be unrelated to Adria motion. We wanted to test this possibility by deriving an Adria-Europe rotation pole independent of Apennine slip vectors, and to compare such an independent result to that of Anderson and Jackson (1987).

Previous circum-Adria and Adria studies using space geodesy

Early in the application of space geodesy to Mediterranean tectonic studies, Ward (1994) used VLBI data from just two sites in Italy, MATE (Matera) and MEDI (Medicina), to solve for a Europe-Adria pole of rotation. 2D (N and E) velocity data from two sites on a plate is the bare minimum needed to solve for the three parameters that define a rotation pole (latitude, longitude, and rotation rate, or equivalently ω_x, ω_y, ω_z). Ward's VLBI-derived pole located near that of Anderson and Jackson (1987), at 46.8±2.5°N by 6.3±3.8°E, and also gave a CCW rotation, at a rate of –0.29±0.06 °/Myr.

More recent Adria kinematic studies that used GPS highlighted some still unresolved problems and indicated to us that we could make a significant contribution by collecting and analyzing some new strategically located data. Altiner (1999, 2001) published the first GPS velocities reported from Croatia and Slovenia. Altiner's network spans the eastern edge of the Adriatic Sea from Slovenia southward along the Dalmatian coast to Dubrovnik in Croatia. The Altiner papers focused mainly on developing a general deformation analysis technique using the eastern Adriatic velocities as an example data set.

The velocities published for these sites showed NNW motions of ≤ 1 cm/yr relative to GRAZ (Austria), a global tracking station (implicitly) presumed to be within stable Europe. The velocities were published without specific horizontal velocity uncertainties (but were reported to be generally precise to ± 1.5 mm/yr, possibly an average formal error that underestimates true uncertainty), and the original data set spanned only a two-year time period, 1994-1996. Despite these potential shortcomings, the published motions are above the reported general noise level, and suggest possibly significant dextral shear along the eastern edge of the Adria microplate or an Adria African promontory (see also more recent results in Altiner, et al., this volume).

Grenerczy et al. (2000) presented a high-precision analysis of GPS data (~2 mm horizontal RMS position repeatabilities) from a broad-aperture central European network spanning 10 countries, including Slovenia. Like that of Altiner, this work also resolved site motions along the eastern edge of the Adriatic Sea (~3-4 mm/yr) and, additionally, resolved ~2 mm/yr of N-S shortening across Slovenia and ~2 mm/yr of dextral shear across the Periadriatic fault zone, suggesting for the first time that eastward extrusion, driven by active movement of Adria and collision of Nubia with Eurasia, is an on-going rather than fossil process.

Calais et al. (2002) inverted GPS velocities from the two permanent sites UPAD and TORI together with the original (non-updated) earthquake slip vector data set of Anderson and Jackson (1987) and derived a rotation pole located at 45.36°N by 9.10°E, with CCW motion at a rate of 0.52°/Myr. Calais et al. chose not to use the GPS data from MATE and MEDI and many other publicly available permanent sites in their inversion. Their choice and use of data from only 2 GPS sites, UPAD and TORI, illustrates the paucity of GPS sites clearly on stable Adria, suggesting the potential importance of obtaining new data from additional stable sites.

In Italy, D'Agostino et al. (2001) used GPS to quantify that NE-SW extension across the central Apennines occurs at relatively high rates of 6 ± 2 mm/yr. Oldow et al. (2002) combined GPS velocities from their Italian Peri-Tyrrhenian Geodetic Array (PTGA) with those of Altiner (2001) from Croatia and Slovenia. Using the combined velocities, Oldow et al. (2002) suggested that Adria is currently in the process of fragmenting into northern and southern sub-blocks about a NE-SW-trending active fault zone that cuts the Italian peninsula and Adriatic Sea from Gargano to Dubrovnik. Many of the earthquakes used to define the possibly active central Adriatic fault zone may have occurred during a single protracted 1986-1990 swarm (Console et al., 1993), and Oldow et al. (2002) did not reprocess Altiner's (2001) raw GPS data, so the two velocity fields combined were in different "European" reference frames.

We sought to overcome some of the problems illustrated above by processing all of the GPS data used in our analysis with the same software and in the same and most up-to-date reference frame, and then relating them all to the same, robustly defined European reference frame.

Active tectonics in Slovenia

Slovenia sits along the NE corner of the Adria microplate, where long-term deformation involved NE-SW directed shortening in the Dinaric fold-and-thrust belt (Placer, 1982), southward thrusting of the Southern Alps, and large-scale lateral (strike-slip) movement accommodating eastward tectonic escape or extrusion of the Eastern Alps (Ratschbacher et al., 1991) during development of the Pannonian Basin and Carpathian Mountains (Royden et al., 1982; Fodor et al., 1998); Slovenia's neotectonics reflect late-stage deformation processes in this now highly evolved system. Both geologic and geodetic time-scale deformation rates on Slovenia's potentially active structures are currently poorly known. Vrabec and Fodor (this volume) provide some additional details.

Figure 2 shows the sharp topography of Slovenia, which illuminates its young and potentially active structures. In SW Slovenia, along the eastern edge of the Adria microplate, a moderately elevated, carbonate-rich, karstic region with a strong NW-SE topographic grain that coincides with mapped geologic faults, is generally referred to as the Slovene Dinarides. Some Dinaric faults have seismic expressions (Poljak et al., 2000). Our research was undertaken, in part, to address whether these Dinaric faults are dextral strike-slip faults consistent with NW-ward translation of Adria (e.g., Picha, 2002; Altiner, 1999, 2001) about a distant Euler pole, or reverse faults consistent with CCW rotation of Adria about a pole located nearby (Anderson and Jackson, 1989; Ward, 1993).

A sharp WNW-trending lineament (the Sava Fault) separates the Julian and Kamnik Alps; additional sharp topographic lineaments are present along mapped geologic faults in NE Slovenia. Together these lineaments reflect a network of faults related to the Periadriatic fault zone, an orogen-scale Alpine structure separating terrains with very different structural, sedimentary, metamorphic, and magmatic histories (Fodor et al., 1998; Schmidt et al., 1989). Faults in the Slovene portion of the Periadriatic zone include the Sava and Šoštanj Faults. The Sava Fault has an impressive topographic signature, suggesting that this structure is probably active (Figure 2). The Šoštanj Fault is also sharply expressed in Slovenia's landscape further east, and may cut Quaternary sediments (Vrabec, 1999). Faults in the Periadriatic zone, including those in Slovenia, have known or inferred dextral strike-slip motions based on fault kinematic analysis (Vrabec, 2001), regional

geologic and tectonic considerations (Laubscher, 1971, 1983; Schmidt et al., 1989; Fodor et al., 1998) and paleomagnetic evidence (Fodor et al., 1998).

The Sava Folds form an isolated, topographically high, and seismically active zone east of the Dinaric Alps and south of the Periadriatic fault zone and Kamnik Alps. The high topography and seismicity there probably indicate active shortening. This zone was named about a century ago for its location along the Sava River (Placer, 1999), but its relation to the regional neotectonic framework is still not well understood. The zone of folding has gradational southern, eastern, and western boundaries and is bounded sharply to the north by the Sava Fault. Individual macrofolds in the belt have predominantly E-W-trending axes and wavelengths ranging from hundreds of meters to kilometers. Some synclines are well mapped and thoroughly studied because of the coal beds in Tertiary rocks preserved in the synclinal cores. Principal strain-rate axes inferred from fault kinematics (Vrabec, 2001, and unpublished data) are oriented relatively uniformly across northern Slovenia in general and indicate N-S shortening and E-W stretching, which are consistent with active N-S shortening across the Sava Folds. The dendritic pattern of the Sava River and its tributaries, despite the strong E-W corrugations in the topography, is impressive. The Sava fluvial system thus probably is antecedent and predates active uplift (Placer, 1999); that it maintains a dendritic pattern probably indicates that shortening across this zone, and associated uplift, are both slow (a few mm/yr or less).

One hypothesis put forth to explain the late-stage tectonics in the Alps suggests that eastward extrusion of the Eastern Alps ceased in the Pliocene, about 5 m.y. ago, probably due to termination of slab pull and subduction along the eastern (leading) edge of the Carpathians (Horváth and Cloetingh, 1996). Indeed, deep subduction-related seismicity is now limited to the southeastern corner of the Carpathian arc (Oncescu, 1984). Grenerczy et al.'s (2000) recent broad-aperture GPS study, however, detected ~2 mm/yr of eastward differential motion of several widely spaced sites across the Periadriatic zone, suggesting that eastward extrusion is on-going, albeit slowly. We test whether active eastward extrusion is still occurring and whether any of this motion is taken up in Slovenia. In alternative late-stage tectonic models, the Sava Folds and active faults could simply accommodate differential motion between independent blocks (e.g., Vrabec et al., 2001; Tomljenović and Csontos, 2001; Vrabec and Fodor, this volume). Our new GPS data provide data to test whether such blocks exist, and if so, to begin mapping block boundaries, and determining poles of rotation for each block (e.g., Dixon et al., 2000).

PIVO-2003 STUDY

GPS Data Analysis Methods

To measure Adria's motion, we used decade-scale episodic GPS data from seven broadly distributed sites mounted in bedrock in Adria's major aseismic outcrop, the Istria peninsula of Slovenia and Croatia, together with continuous GPS data from two permanent GPS sites on the Po Plain. We processed all of the GPS data at the University of Miami using GIPSY (release 2.5) software and precise satellite ephemeris and clock files produced at the Jet Propulsion Lab (JPL). Details of the analysis strategy are given in Zumberge et al. (1997) and Weber et al. (2001). Initially, we derived point positions precise at the sub-centimeter level, and then ultimately we derived site velocities with < ±1-2 mm/yr level scaled uncertainties that account for both white and colored noise (Mao et al., 1999) in ITRF-2000 (Boucher et al., 1999). We also processed data from 15 permanent GPS sites to define a stable European ITRF-2000 reference frame (Sella et al., 2002) and then formally inverted subsets of the Istria and Po Plain Europe-referenced GPS velocities for a series of Adria-Europe rotation poles.

To quantify deformation within Slovenia, we used the same data analysis strategy together with data from 35 episodic GPS sites in northern Croatia and Slovenia, tens of surrounding regional permanent (and episodic) GPS sites, and the 15 continuous GPS stable European Plate reference stations discussed above.

PIVO-2003 and circum-Adria permanent GPS networks

The 35 Slovenian and northern Croatian sites in our PIVO-2003 GPS network are shown in Figure 2. All of these sites were initially established and measured in earlier GPS campaigns, including the EUREF campaigns of 1994, 1995, and 1996; a geodynamic campaign to study a large earthquake in NE Slovenia (Mišković et al., 1998); a Slovene national campaign conducted in 1996; the 1997 European Unification of Vertical Networks campaign; 1996, 1997, 1999, 2002 campaigns for a local geodynamic study done around the Velenje coal mine; a 2002 campaign connecting four tide gauges in the northern Adriatic; and the Central European Regional Geodynamics project campaigns of 2001 and 2003. We included data from all of these campaigns into our analysis; we also re-measured 23 of these 35 sites in the fall of 2003. In all the campaigns, sites were typically observed for at least 12 hours per day, and for at least several days per campaign. In addition to the 35 PIVO-2003 sites and 15 European reference sites discussed above, we also processed data from tens of publicly available circum-Adria permanent and episodic GPS stations in our analysis.

Preliminary velocity field and Istria (Adria)-Europe Euler pole and implications

We present only a partial set of our velocities here (Figure 4); the complete set and full details will be published in several papers currently in progress. In general, the decade-scale motions we derived are small (~a few mm/yr), but statistically significant at 1σ; the velocity field also shows a smooth and consistent change from northeasterly motions in southern Istria and to northerly motions in central and northern Slovenia (Figure 4).

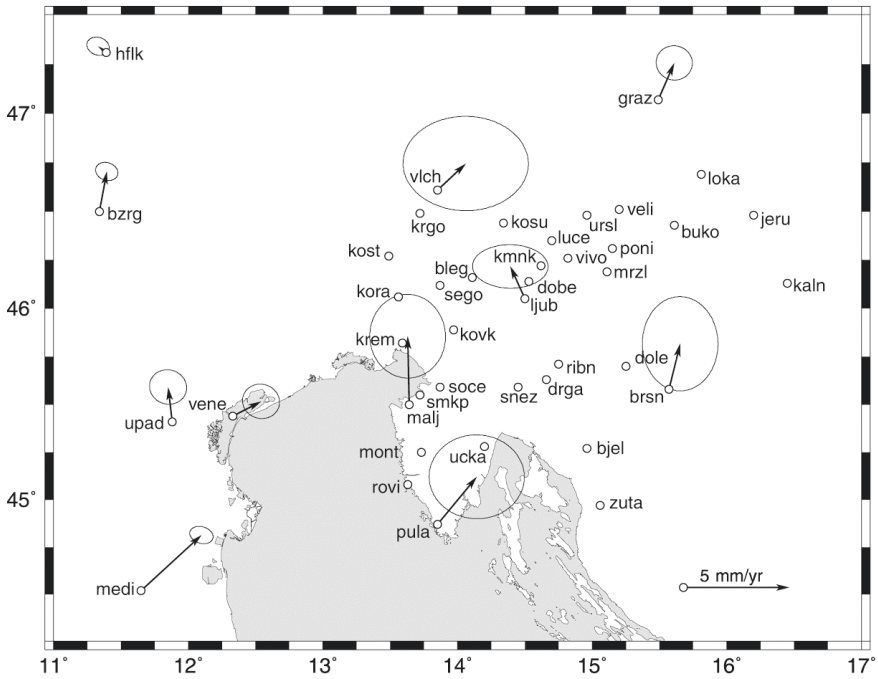

Figure 4. GPS-derived velocities relative to stable Europe for some selected PIVO-2003 and regional sites.

We tested the robustness of Ward's (1994) VLBI-derived Adria-Europe Euler pole using the long time series of GPS data now available for the 2 permanent stations, MATE and MEDI. We were unable to reproduce this result. The position of the new GPS-derived pole shifted significantly. The difference is mainly because the GPS velocity of MATE has a much larger north component of motion relative to stable Europe than the early MATE VLBI velocity used by Ward (1994).

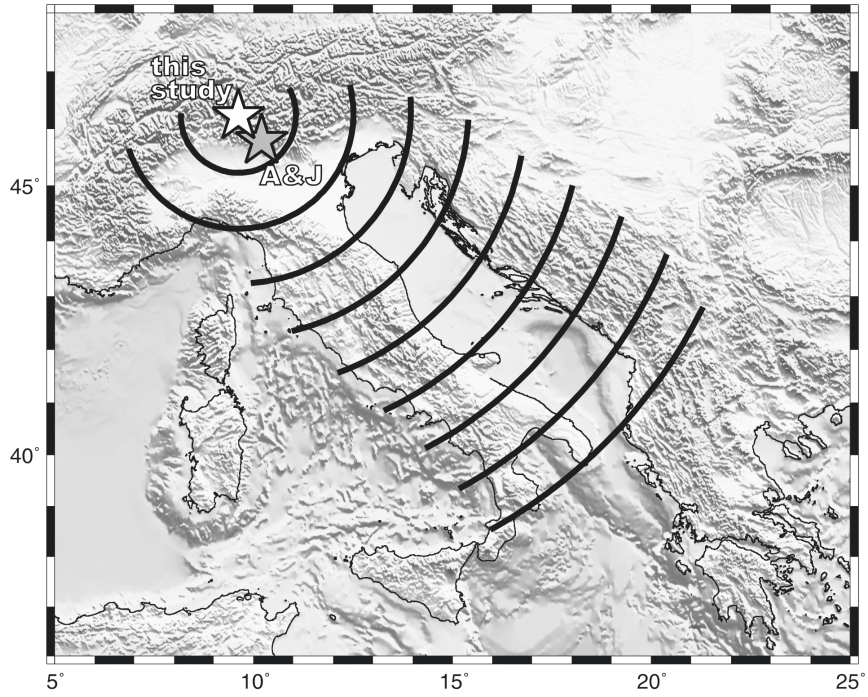

Figure 5. Istria (Adria)-Eurasia Euler pole derived in this study shown at center of small circles that describe trajectories of Adria site motions relative to Eurasia. The small circles represent the direction component of the precise and testable predictions made from the pole (which predicts rates as well), which can be compare with independent data such as earthquake slip vectors, geodetic principal strain rates, additional GPS velocities, etc. Anderson and Jackson's (1987) pole location (A&J) is shown for comparison.

We formally inverted data from subsets of our seven Istria peninsula and two Po Plain sites for an Istria (Adria)-Europe Euler pole, and this analysis yielded a robust result. The pole position changes by only a few degrees using various subsets of the data. Our average PIVO-2003 Adria-Europe Euler pole locates at 46.7°N by 9.7°W (with a rotation rate of 0.4°/Myr), which is very near the pole identified by Anderson and Jackson (1987) derived from inversion of broadly distributed earthquake slip vectors (Figure 5). This coincidence brings into question Oldow et al.'s (2002) hypothesis that Adria is fragmenting into two major sub-blocks and suggests that the Apennine events are indeed related to Adria-Europe motion, and not simply related to extensional collapse of the Apennines. Our rate residuals (scalar differences between model and observed values) show that the Istria peninsula (i.e., the northern Adria microplate) is rigid, on average, to ~1 mm/yr.

Preliminary neotectonic findings in Slovenia

Slovenia is located close to the Adria-Europe Euler pole, so stable-Europe-referenced motions are small and its seismic hazard is low relative to that further from the pole along Adria's boundary (e.g., in the central and southern Apennines, and along the Dalmatian coast). The sharpest gradient we observe in the Slovenia velocity field is a few mm/yr of dextral (to transpressive) shear along the Sava Fault (Periadriatic zone), suggesting that eastward tectonic escape (extrusion) of the Eastern Alps is still on-going and has not been supplanted by other later-stage deformation processes such as block rotation. The sharp Sava Fault gradient becomes diffuse to the east, and may be taken up across the Sava Folds, but data from additional Sava Folds sites are needed to resolve this issue.

REMAINING QUESTIONS, RECOMMENDATIONS, SPECULATIONS, ETC.

To better constrain Adria's motion, more stable interior sites are needed in eastern Italy and on the Po Plain in Italy, along the Dalmatian coat of Croatia, and in Albania. Having some GPS sites on the Italian and Croatian islands in the Adriatic Sea would help to better quantify the motion across possibly significant intra-Adria sub-blocks and faults and to more completely quantify the level of Adria rigidity. In addition, the earthquake slip vector data set used by Anderson and Jackson (1987) should be updated and re-inverted to derive an up-to-date seismically derived Adria-Europe Euler pole; research should continue to better define Adria's enigmatic southern boundary with Nubia.

An important unanswered question is why the entire Dalmatian coast is submergent (Figures 1, 6). Is this related to long-term sinking driven by deep processes or short-term elastic locking? Precise vertical deformation rates will be needed to solve this mystery. What drives the motion of Adria (Figure 6)? Is this motion related to Nubia (Africa)-Eurasia collision or slab pull? Is the westward subduction of Adria beneath the Apennines active; if so, does Adria simultaneously subduct westward and rotate eastward (CCW)? Is Apennine slab break-off driving normal faulting in the Apennines and Adria's CCW motion (e.g., Stein and Sella, this volume)? Is there really no slab beneath the Dinarides (Stein and Sella, this volume) pulling Adria eastward? Finally, the application of tectonic geomorphology and paleoseismology to study the active faults and landscapes bordering Adria could help better define long-term fault-slip and uplift rates.

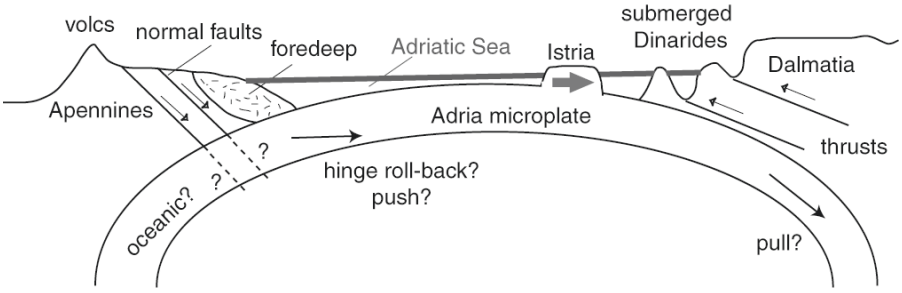

Figure 6. Cartoon cross section showing the Adria microplate, bounding normal faults in the Apennines to the west and thrust faults in the Dinarides to the east, some major geologic and mega-geomorphic features, and possible plate-driving forces.

ACKNOWLEDGEMENTS

This research was supported by the Slovene Ministry of Science and American Chemical Society-Petroleum Research Fund grant 40225-B8.

REFERENCES

Anderson H.A., Jackson J.A. Active tectonics of the Adriatic region. Geophys. J. R. Astr. Soc. 1987; 91: 937-983.

Altiner Y. *Analytical Surface Deformation Theory*. BerlIn Springer, 1999.

Altiner Y. The contribution of GPS to the detection of the Earth's crust deformations illustrated by GPS campaigns in the Adria region. Geophys. J. Int. 2001; 145: 550-559.

Argand E. La Tectonique de l'Asie. Proceedings of the International Geological Congress, XIII, 1924.

Boucher C., Altamimi Z., Sillard P. The 1997 International Terrestrial Reference Frame (ITRF-97). Paris: Observatoire de Paris, IERS Technical Note 27, 1999.

Calais E., Nocquet J.M., Jouanne F., Tardy M. Current strain regime in the Western Alps from continuous Global Positioning System measurements, 1996-2001. Geology 2002; 30: 651-654.

Console R., Di Giovambattista R., Favali P., Presgrave B.W., Smriglio G. Seismicity of the Adriatic microplate. Tectonophysics 1993; 218: 343-354.

D'Agostino N., Giuliani R., Mattone M., Bonci L. Active crustal extension in the central Apennines (Italy) inferred from GPS measurements in the interval 1994-1999. Geophys. Res. Lett. 2001; 28: 2121-2124.

DeMets C., Gordon R., Argus D., Stein S. Current plate motions. Geophys. J. Int. 1990; 101: 425-478.

DeMets C., Gordon R., Argus D., Stein S. Effect of recent revisions to the geomagnetic time scale on estimates of current plate motion. Geophys. Res. Lett. 1994; 21: 2191-2194.

Dixon T.H., Miller M., Farina F., Wang H., Johnson D. Present-day motion of the Sierra Nevada block and some tectonic implications for the Basin and Range province, North American Cordillera. Tectonics 2000; 19: 1-24.

Favali P., Funiciello R., Mattietti G., Mele G., Salvini F. An active margin across the Adriatic Sea (central Mediterranean Sea). Tectonophysics 1993; 219: 109-117.

Fodor L., Jelen B., Márton E., Skaberne D., Čar J., Vrabec M. Miocene-Pliocene tectonic evolution of the Slovenian Periadriatic fault: Implications for Alpine-Carpathian extrusion models. Tectonics 1998; 17: 690-709.

Grenerczy G., Kenyeres A., Fejes I. Present crustal movement and strain distribution in Central Europe inferred from GPS measurements. J. Geophys. Res. 2000; 105(B9): 21835-21846.

Horváth F., Cloething S. Stress–induced late–stage subsidence anomalies in the Pannonian Basin. Tectonophysics 1996; 266: 287–300.

Italiano F., Martelli M., Martelli G., Nuccio P.M. Geochemical evidence of melt intrusions along lithospheric faults of the Southern Apennines, Italy: Geodynamic and seismogenic implications. J. Geophys. Res. 2000; 105: 13,569-13,578.

Laubscher H. The large-scale kinematics of the western Alps and the northern Apennines and its palinspastic implications. Am. J. Sci. 1971; 271: 193-226.

Laubscher H. The late Alpine (Periadriatic) intrusions and the Insubric Line. Mem. Soc. Geol. It. 1983; 26: 21-30.

Mao A., Harrison C.G.A., Dixon T. H. Noise in GPS coordinate time series: J. Geophys. Res. 1999; 104: 2797-2816.

McClusky S., Balassanian S., Barka A., Demir C., Ergintav S., Georgiev I., Gurkan O., Hamburger M., Hurst K., Kahle H., Kastens K., Kekelidze G., King R., Kotzev V., Lenk O., Mahmoud S., Mishin A., Nadariya M., Ouzounis A., Paradissis D., Peter Y., Prilepin M., Reilinger R., Sanli I., Seeger H., Tealeb A., Toksoz M. N., Veis G. Global positioning system constraints on plate kinematics and dynamics in the eastern Mediterranean and Caucasus. J. Geophy. Res. 2000; 105: 5695-5719.

McKenzie D.P. Active tectonics of the Mediterranean region. Geophys. J. R. Astr. Soc. 1972; 30: 109-185.

Miškovič D., Pesec P, Stangl G. GPS re-measurments in the Bovec-Tolmin earthquake region. Proceedings Second International Symposium "Geodynamics of the Alps-Adria area by means of terrestrial and satellite methods", Dubrovnik, 1998.

Oldow J., Ferranti L., Lewis D., Campbell J., D'Argenio B., Catalano R., Pappone G., Carmignani L., Conyi P., Aiken C. Active fragmentation of Adria, the north African promontory, central Mediterranean orogen. Geology 2002; 30: 779-782.

Oncescu M.C. Three-dimensional P-wave velocity image under the Carpathian arc. Tectonophysics 1984; 106: 305-319.

Picha F.J. Late orogenic strike-slip faulting and escape tectonics in frontal Dinarides-Hellenides, Croatia, Yugoslavia, Albania, and Greece. AAPG Bull 2002; 86: 1659-1671.

Placer L. Geologic structure of southwestern Slovenia. Geologija 1982; 24: 27-60.

Placer L. Structural meaning of the Sava Folds. Geologija 1999; 41: 191-221.

Platt J. Dynamics of orogenic wedges and the uplift of high-pressure metamorphic rocks. GSA Bull.1986; 97: 1937-1053.

Poljak M., Živčič M., Zupančič P. The seismotectonic characteristics of Slovenia. Pure and Applied Geophysics 2000; 157: 37-55.

Ratschbacher L., Frisch W., Linzer H.G., Merle O. Lateral extrusion in the Eastern Alps, part 2: Structural analysis. Tectonics 1991; 10: 257-271.

Royden L., Horvath F., Burchfiel B.C. Transform faulting, extension, and subduction in the Carpathain Pannonian region. GSA Bull. 1982; 93: 717-725.

Royden L., Patacca E., Scandone P. Segmentation and configuration of subducted lithosphere in Italy: an important control on thrust-belt and foredeep-basin evolution. Geology 1987; 15: 714-717.

Schmidt S., Aebli H. R., Heller F., Zingg A. The role of the Periadriatic Line in the tectonic evolution of the Alps. In: *Alpine Tectonics*, M.P. Coward, D. Dietrich, R.G. Parks, eds., London: Geol. Soc. London Spec. Publ. 1989; 45.

Sella G., Dixon T., Mao A. REVEL: A model for recent plate velocities from space geodesy. J. Geophys. Res. 2002; 1029:2000JB000033.

Selvaggi G., Amato A. Subcrustal earthquakes in the northern Apennines (Italy): evidence for a still active subduction? Geophys. Res. Lett. 1992; 19: 2127-2130.

Tomljenović B., Csontos L. Neogene-Quaternary structures in the border zone between Alps, Dinarides and Pannonian Basin (Hrvatsko zagorje and Karlovac Basins, Croatia). Int. Geol. J. 2001; 90: 560-578.

Vrabec M. Style of postsedimentary deformation in the Plio–Quaternary Velenje basin, Slovenia. Neues Jahrbuch für Geologie und Paläontologie Monatshefte 1999; 8: 449–463.

Vrabec M. *Structural analysis of the Sava fault zone between Trstenik and Stahovic,* PhD thesis., University of Ljubljana, 2001.

Vrabec M., Fodor L., Márton E. Pliocene to recent structural evolution at the junction of the Alps, Dinarides and the Pannonian basin. In: *Quantitative neotectonics and seismic hazard assessment: new integrated approaches for environmental management*, G. Báda, eds., 2001.

Ward S. Constraints on the seismotectonics of the central Mediterranean from Very Long Baseline Interferometry. Geophys. J. Int. 1994; 11: 441-452.

Weber J., Dixon T., DeMets C., Ambeh W., Jansma P., Mattioli G., Bilham R., Saleh J., Perez O. A GPS Estimate of the Relative Motion between the Caribbean and South American Plates, and Geologic Implications for Trinidad and Venezuela. Geology 2001; 29: 75-78.

Wortel M., Spakman W. Subduction and slab detachment in the Mediterranean-Carpathian region. Science 2000; 290: 1910-1917.

Zumberge J., Heflin M., Jefferson D., Watkins M., Webb F. Precise point positioning for efficient and robust analysis of GPS data from large networks. J. Geophys. Res. 1997; 102: 5005-5017.

CRUSTAL DEFORMATION BETWEEN ADRIA AND THE EUROPEAN PLATFORM FROM SPACE GEODESY

Gyula Grenerczy[1, 2] and Ambrus Kenyeres[2]
1: Department of Geology, Southern Illinois University, Carbondale, IL, 62901-4324, USA
grener@elte.hu
2: Satellite Geodetic Observatory, Institute of Geodesy Cartography and Remote Sensing, Penc, Hungary

ABSTRACT

From the Adria microplate, the main engine of the Central European tectonics, in the southwest to the rigid, aseismic European Platform in the northeast, 14 countries have been jointly operating a regional Global Positioning System- (GPS-) based geodynamic network since 1994. Many of these countries also established national networks in the 1990s. A continental-scale, continuously observing GPS network has also been providing data for about a decade now, and there are several stations of the global network in the region. Within these networks, site density is generally inversely proportional to the covered area, thus an adequately dense velocity field at a regional level, required by the complex crustal structure and highly interconnected tectonic processes, can only be achieved by the integration of smaller-scale networks. We provide a preliminary GPS intraplate velocity solution for this region by combining GPS networks from continental to local scales. The independent and overlapping networks also provide independent confirmation of velocities at common sites. Furthermore, the combined velocity map thus obtained makes possible a more effective identification of problematic sites and allows more critical evaluation of data quality and accuracy. The compiled GPS intraplate velocity field is analyzed in order to provide quantitative constraints for the motion of Adria, for the deformation along its northern and eastern boundaries, and by studying station baseline-length time series, for the evaluation of far-field effects from the Pannonian-Carpathian region to the European Platform.

INTRODUCTION

The collision between the Eurasia and the Africa/Nubia Plate and the motion of smaller blocks trapped in the wide boundary zone controlled the Neogene evolution of the Mediterranean region, including the southern part of Central Europe. The formation of the Alps, Dinarides, Pannonian basin, and the Carpathian belt are all related to the ongoing Alpine orogeny that started in the Late Cretaceous. The convergence between the two major plates and also the motion of the Adria block in the central part of the plate boundary changed over time in both rate and direction (Dewey et al., 1989; Mantovani et al., and Stein and Sella, this volume). Recent space geodetic studies show

N. Pinter et al. (eds.), The Adria Microplate: GPS Geodesy, Tectonics and Hazards, 321–334.

5-6 mm/yr NW-oriented Nubia motion relative to Eurasia (Sella et al., 2002; McClusky et al., 2003). A major Neogene event in the region was the formation of the Alpine-Carpathian-Pannonian system. The disintegration and extensional collapse of the former East Alpine thrust-fold belt took place along major transcurrent fault zones driven by collisional escape, gravitational sliding and slab-pull effect along the Carpathian arc (Csontos et al., 1992; Fodor et al., 1999). Due to the ongoing plate convergence, the Magura oceanic crust was consumed, the subduction stopped, and the accretionary wedge reached the rigid European Platform. The formation of the Pannonian region ended recently, and a compressional tectonic regime prevails (Horváth and Cloething, 1996) with mostly strike-slip and thrust seismicity (Tóth et al., this volume; Bada et al., 1999). In the modern compressional tectonic environment, the motion of the Adria block became a primary driving mechanism. Space geodetic data show that Adria still converges and collides with the Eastern Alps and the Dinarides. It squeezes out the western part of Alpine-North Pannonian unit and compresses the entire western and southern margin of the Pannonian basin through the Alps and Dinarides. Meanwhile the eastern parts of the Pannonian crust and the Carpathian orogen are encircled and blocked by the rigid European Platform. Several local-scale space geodetic studies have been undertaken in the circum-Adriatic region (Altiner et al.; Hollenstein et al.; Oldow and Ferranti; Weber et al.; this volume); nonetheless, issues regarding the motion, independence, fragmentation, and boundaries of the Adria crustal unit remain controversial. There is little quantitative knowledge about how the deformation is absorbed at its collisional boundary zones in the Eastern Alps and Dinarides and further into the plate interior, and whether the large strike-slip fault zones are active and what present-day slip-rate and characteristics they have, what the present amount of deformation the basin experiences, and whether there is any more contraction along the Carpathians. This paper attempts to provide a dense GPS velocity field and quantitative constraints to better our understanding of the present-day deformation from the Adriatic to the Eurasian plate interior.

GPS NETWORKS

Several local geodetic networks have been established and monitored through the study area (Figure 1). The Austrian AGREF was the first national GPS network, but it has not yet been completely re-measured. The Hungarian GPS Geodynamic Reference Network (HGRN) was established between 1990 and 1991 with 13 sites on outcropping solid bedrock and has been measured in every second year since 1991 with 3 times 24-hour sessions (Fejes et al., 1993). The Polish SAGET is an open network since 1992; it includes the data of all simultaneously measured European GPS sites (Sledzinski, 1991). The SLOVGERENET (Priam, 1995) and the Ukrainian GEODUC (Baran et al.,

1994) were established in 1993, but while SLOVGERENET is still active, GEODUC has not been resurveyed since 1994. The CRODYN network was operated by a German-Croatian cooperation investigating the eastern boundary of the Adria microplate, but after three observational campaigns the project ended (Altiner 2001). The Bohemian Massif is represented by the Czech GEODYN (Simek, 1999) network since 1995. There are a couple of more-or-less independent GPS networks covering the Vrancea seismic zone and its surrounding areas since 1997 and 2002 (Dinter et al., 2001; Van der Hoeven et al., 2003). At the northern tip of Adria, an area with special importance to Adria motion, the PIVO experiment (Weber et al., this volume) re-measured the Slovene and northern Croatian GPS networks after 1994-1995. The PTGA network (Oldow et al., 2002) has a major role in investigating the southeastern boundary of Adria.

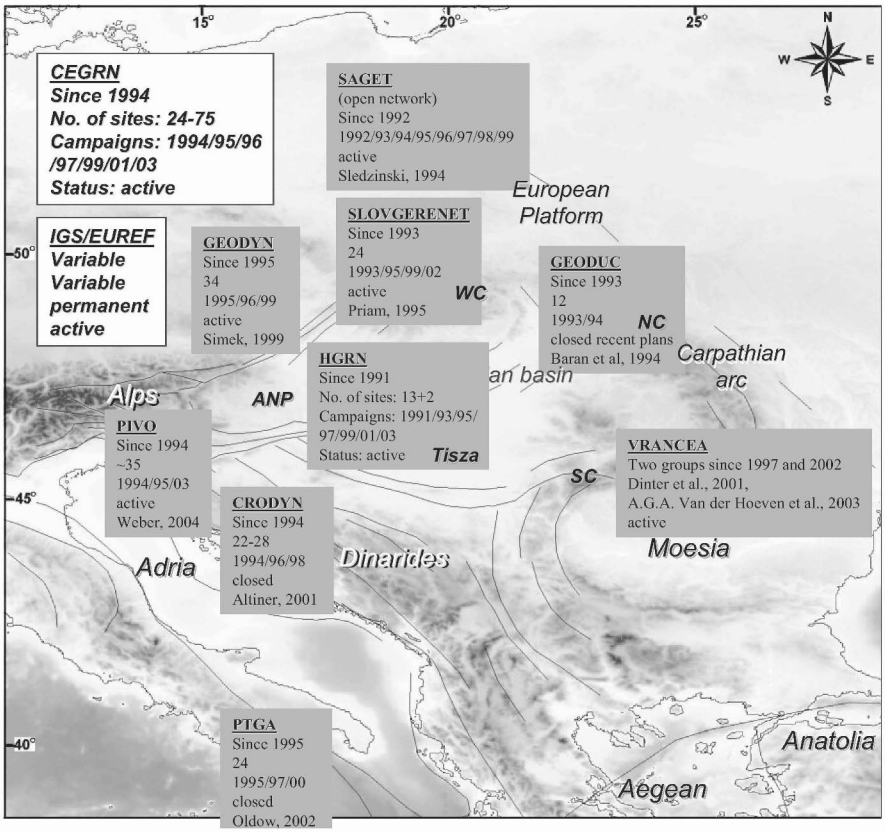

Figure 1. Summary of the GPS geodynamic networks from Adria to the Eurasian plate interior. Inserted tables show the first measurements, number of sites, campaigns, and current status. ANP: Alpine-North Pannonian unit, WC, NC, SC; Western, Northern, and Southern Carpathians.

The regional-scale Central European GPS Geodynamic Reference Network (CEGRN) is the product of the joint effort of all Central European countries (Pesec, 2003; Fejes, this volume). The network covers the whole region with homogeneous site density providing precise GPS data (Becker et al., 2001; Grenerczy, 2000, 2002; Hefty, 2001). The CEGRN was established in 1994 and to date it has been measured seven times with each campaign consisting of 5 day 24-hour simultaneous observations. There are also several IGS (Mueller and Beutler, 1992) and EUREF (Bruyninx et al., 2003) permanent GPS sites in the region. Although their number and distribution are not optimized for detailed tectonic study, they provide reliable continuous data that enable detection of coordinate outliers, offsets and periodicities. The goal of this work is to combine these velocities and unify the data sets to generate an adequately dense velocity field to better understand the interconnected tectonic processes of the region.

DATA

We processed data from global, continental, continuous sites and regional and national epoch campaigns from the IGS, EUREF, CEGRN, and HGRN networks. The first observation of HGRN dates back to 1991, and to 1994 for the CEGRN network. For the permanent sites, the dates are variable depending upon when each permanent station started operation. All data were processed using the Bernese GPS Software, version 4.2 [Beutler et al, 2001] with pole information, satellite maneuvers, and precise orbits determined by the International GPS Service. Two ambiguity resolution strategies were applied: the SIGMA-dependent and quasi-ionosphere-free [Beutler et al, 2001], depending on the length of the baselines. The network was tied to ITRF2000, and daily coordinate sets and covariance files were calculated based on L3 linear combination, using double differences, the Saastamoinen troposphere model, elevation-dependent weighting, and hourly troposphere parameter estimation using all observations above 10 degrees. In general we obtained daily repeatabilities in the range of 1.5 – 2.5 mm in the horizontal and 4.5-6 mm in the vertical components. The EUREF and the CEGRN data were processed by several individual processing centers and a combined solution was also calculated.

RESULTS

For the velocity solution, stable Eurasia was defined based on all 11 sites located on the stable European Platform for the CEGRN network, and 9 sites for the continuous network. The remaining random orientation and the 0.3 mm/yr mean residual velocity magnitudes in both cases indicate the accuracy and the rigidity of the frame. All ITRF2000 velocities are referenced

to this stable European frame. In the case of the continuous observations, velocities were calculated after detection and removal of jumps in the time series due to equipment changes, antenna and monumentation problems, and periodicities. Errors were derived and scaled to account for both white and colored noise [Mao et al. 1999]. Figure 2 shows the calculated intraplate velocities with reference to stable Eurasia and the confidence ellipses, together with three estimates for the relative motion of Nubia relative to Eurasia.

Figure 2. Velocities of GPS stations in Central Europe from continuous and epoch-type observations together with their 95% confidence ellipses relative to stable Eurasia. Plate motion of Nubia with reference to Eurasia 1: NUVEL-1A Africa-Eurasia (geophysical data over 3 Myr), after DeMets et al., 1994; 2: Nubia-Eurasia (recent space geodetic data) after McClusky et al., 2003; 3: REVEL IT97-2000 Nubia-Eurasia (recent space geodetic data); after Sella et al., 2002. Figures 3 and 4 show interpolated velocity fields derived from the velocities shown here.

The Adria Microplate

The obtained GPS intraplate velocity map shows that, at the southern part of the Adria region, GPS sites have 3.5-5 mm/yr north-northeastward-oriented velocity with respect to Eurasia. The velocities decrease to 3-4 mm/yr in the central, and to 2.5-3.5 mm/yr at the northern part of Adria with more northerly velocity vector orientations (Figure 2). This region does not appear to be part of Nubia since these velocity values are all significantly lower in magnitude and differ in orientation from all three estimates of Nubia-Eurasia motion (Figure 2). The data indicate a uniformly moving block (Figure 2 and 3) and appear to show a counterclockwise rotation with respect to Eurasia. For the whole Adria the formal inversion of velocities gives a rotation around a pole located at 47.6° latitude, -20.7° longitude with an angular velocity of -0.09 deg/Myr. The Euler motion calculated from only the northern Adria sites suggests rotation around 46.1° latitude and 7.7° longitude with an angular velocity of -0.35 deg/Myr. These values are similar to those of Battaglia et al., (2004) and Weber et al., (this volume) for the whole and northern Adria respectively. The residuals support a high level of rigidity across the northern Adria since they are around 0.5 mm/yr. However, according to the latter, northern Adria Euler motion prediction, sites in the south should move at a significantly higher rate (> 2 mm/yr) than the actual observed values. This indicates that although sites across the complete Adriatic region have similar motion, the rigid core Adria may not extend farther south than Gargano-Dubrovnik zone. Besides, since Adria is mostly covered by the Adriatic Sea, some of the southern GPS sites are very close to actively deforming zones that may affect their velocities, and they may not represent the rigid core of the block. Although recent space geodetic studies (Nocquet and Calais, 2004; Battaglia et al., 2004, and also papers in this volume) have improved our understanding of the region, establishment of sites on islands within the Adriatic Sea could help to better resolve the rigidity and possible fragmentation of Adria.

Eastern Alps

We have compiled contour maps of velocity magnitudes for the collisional boundaries of Adria. Because of the counterclockwise rotation of the Adria block, the convergence with the Eastern Alps, within a few degrees of uncertainty, has a N-S direction. As a result, the E-W oriented mountain chain experiences perpendicular velocities from the northward motion of Adria. The magnitude of this component of velocities is shown by the contour map. The GPS data indicate a 2.3 ± 0.3 mm/yr convergence, and the contour map shows how this N-S motion is absorbed in the collisional zone (Figure

3). The Adria block appears as a wedge intruding into the southern part of the Eastern Alps. The velocity magnitudes abruptly drop below 0.5 mm/yr in the Southern Alps, leaving the majority of the Alps free of significant present-day contraction. The average contraction rate in this narrow collisional is zone is around 18 ppb/yr, reaching 30 ppb/yr in the central part of the cross-section. The GPS data suggest that extrusion of the Alpine-North Pannonian unit from the Adria-Eurasia collisional zone to the east is still occurring at a rate of 1-1.5 mm/yr. The interpolated velocity field also suggests that this process has a major role in releasing the compression caused by the Adria convergence. North of the narrow and intense contraction zone, a major dextral transpressional fault system and, further to the north, a sinistral strike-slip zone exist that contribute to the extrusion and stress release. This is also supported by the seismicity pattern (Figure 3b) and the earthquake focal mechanism solutions (Bada et al., 1999).

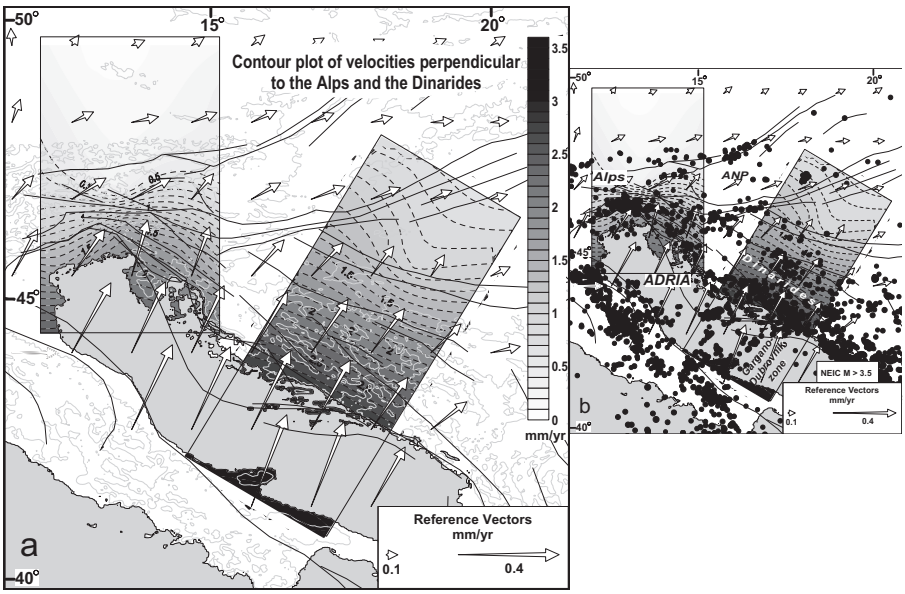

Figure 3. Contour map of crustal velocities for two collisional boundaries of the Adria block. Grayscale shows the magnitudes of perpendicular velocity components to the Alps and the Dinarides. Interpolated velocity vector field from data on Figure 2 is also shown. The 'b' insert indicates the seismicity of the region based on the NEIC catalogue with M > 3.5 threshold.

Central Dinarides

A similar contour plot has been also compiled for our observed velocity magnitudes in the Adria-Central Dinarides collisional boundary as for the Eastern Alps (Figure 3). The relative motion between Adria and the

Dinarides is NE-oriented, and therefore the magnitude of this component of the interpolated velocities is shown by the contour map. This northeastward velocity is perpendicular to the chain of the Dinarides, similarly to the northward motion of Adria in case of the chain of the Alps. At the southern part of Adria, we observe 4.1 ± 0.3 mm/yr northeastward motion oriented towards the Central Dinarides. According to the contour map, the velocity magnitudes decrease quickly along the eastern Adriatic coastal zone to 2.5-3 mm/yr due to the Adria-Dinarides collision. However, further into the interior of the Dinarides, the contraction becomes rather homogeneous. The interpolated velocity magnitudes decrease slowly and gradually across a far wider zone than in the case of the Eastern Alps. The uniform contraction rate from the Adriatic coast to the Pannonian basin is 6-7 ppb/yr, which is equivalent with around 2 mm/yr shortening within approximately 360 km. There is still detectable motion along the southern margin of the Pannonian basin in the range of 1 ± 0.5 mm/yr. Across the Central Dinarides, the observation shows that the contraction occurs within a much wider zone than in case of the Eastern Alps and the contraction is not completely taken up with the Dinarides mountain. This is a major difference between the two collisional boundaries. At the northern boundary, Adria collides with Alps and the 100-200 km thick and rigid lithosphere of the European Platform is behind the collisional zone, and there is a weak ~60 km thin Pannonian Basin sideways. Therefore an extrusion occurs from the collisional zone into the basin, and this process significantly contributes to the absorption of the compression. However, in the case of the Central Dinarides, the weak, deformable Pannonian lithosphere is behind the collisional zone and the rigid European Platform is several hundreds kilometers away. Therefore no extrusion takes up the compression here but the resulting contraction therefore occurs in a much wider area. It is detectable over the mountains in the basin as well. Further to the south (Figure 2) however, between Adria and the rigid Moesia the data suggest that extrusion may again pick up towards the extending Aegean block.

Pannonian Basin

We have studied the changes in distances between GPS sites and performed their baseline length variation analysis for many different vectors crossing the Pannonian basin (Figure 4). Since the interpolated GPS velocity field and its variation are both oriented N-E in the northern part of the basin and NE-SW in the southern part, the baselines were selected to be parallel to these orientations.

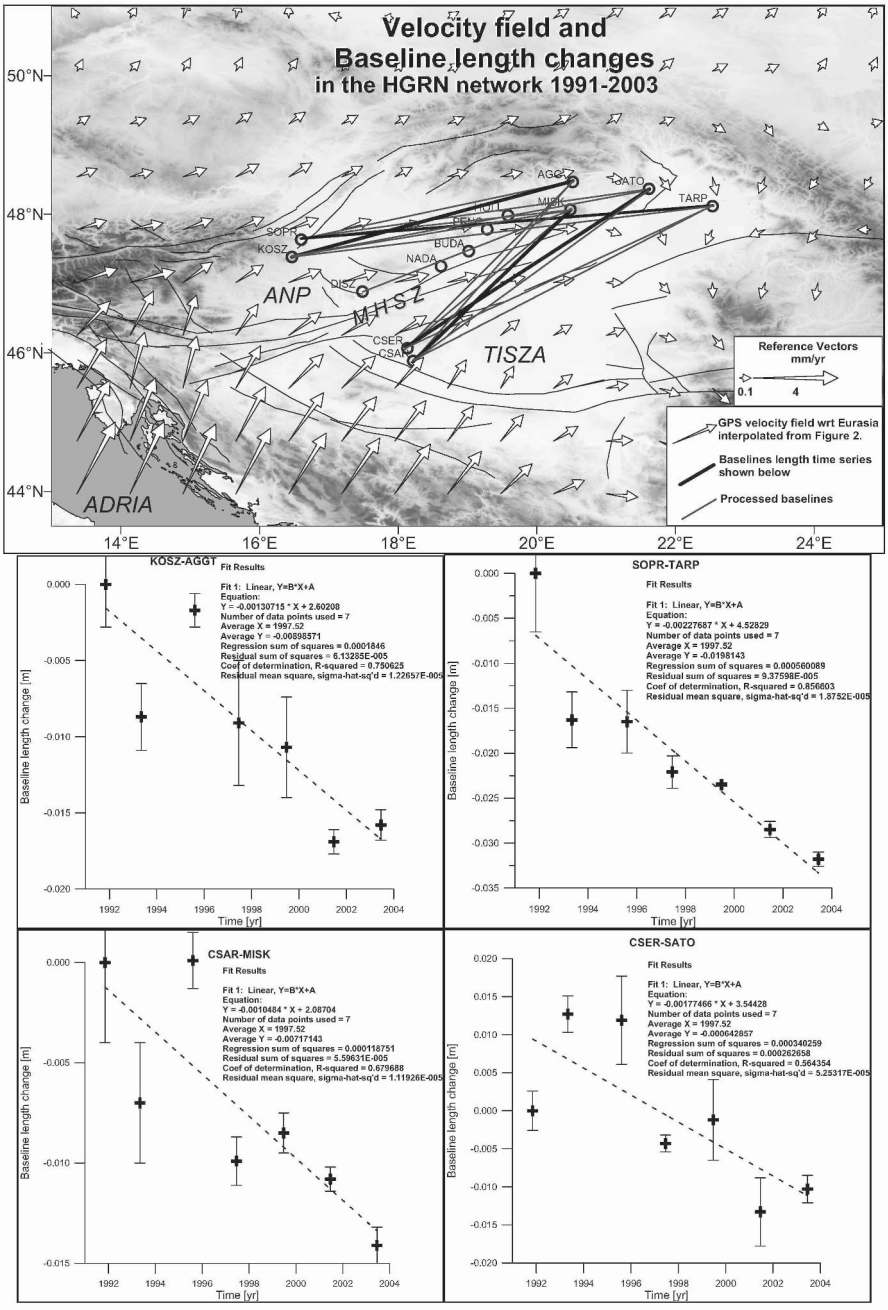

Figure 4. The Alpine-Pannonian-Carpathian system. White arrows indicate the intraplate crustal velocity field interpolated from the velocity data shown in Figure 2. Baseline-length time series for four independent station pairs and the results of linear regression. The error bars represent daily repeatability of the length of the particular baseline during campaigns.

This method provides a simple one-dimensional determination of strain rates and is relatively independent of reference system effects. There is no scale change between ITRF97 '96 '94, and compared to these only 0.3-0.4 ppb/yr in case of ITRF92 and ITRF91. Furthermore the scale rate difference between the ITRF97 and ITRF2000 is 0.01 ppb/yr ± 0.05 ppb/yr (Altamimi, 2001). An additional advantage of the time series is that each campaign result is visible and not averaged out as in a velocity or strain-rate representation. Linear regression and error calculation have been carried out on several HGRN baselines, statistical tests have been performed, and the confidence limits of the linear regression have been determined along with the values, correlation, and standard errors of the estimated parameters. This work is still in progress; Figure 4 shows the baselines that have already been processed and four examples of baseline-length time series based on eight different GPS sites with the graphical results of the linear regression and error estimation.

Data show that the entire Pannonian Basin, including both the Alpine-North Pannonian and the Tisza unit, undergo a ~1.5 mm/yr shortening. Shortening is E-W oriented in the north due to the extrusion of the Alpine-North Pannonian unit into the basin, and NE-SW in the south, as a result of the Adria compression that "leaks out" over the Dinarides. The observed ~1.5 mm/yr shortening over the entire basin implies 3-4 pbb/yr of uniform contraction rate. The contraction in the north between the moving western part of the Alpine-North Pannonian unit and the eastern, stable, trapped part of the basin (E-W oriented baselines on Figure 4) appears to be similar to what we observe between the western part of the Tisza unit and the same eastern sites (NE oriented baselines on Figure 4). The average shortening in the north from eight baselines (western sites of the ANP) is 1.54 ± 0.42 mm/yr versus 1.39 ± 0.58 mm/yr in the south (western sites of Tisza). Relative motion between these two units cannot yet be resolved over the confidence level. The compressional component along the Mid-Hungarian Shear Zone (Figure 4) is detectable from the data and is around 0.8 ± 0.65 mm/yr, but the strike-slip character is not yet detectable. Our space geodetic data already revealed that the Alpine North Pannonian unit is not moving and deforming uniformly. The eastward motion of the extruded western part of the unit is absorbed in the central part of the basin. The eastern part of the unit shows no detectable uniform motion with reference to the European Platform. In contrast to this, the internal deformation of the Tisza unit is still mostly unknown because of the poor representation by GPS sites both within the basin and further to the east.

Carpathian Arc

During Miocene times, subduction and volcanism were gradually extinguished along the Carpathian arc from west to east and then to south. The migration of the young Carpathian orogenic belt was limited by the edge of the European Platform (Horváth, 1993). A slab can now only be detected at the southeastern bend of the Carpathian arc at the Vrancea zone (Oncescu 1984; Wenzel et al., 2002) where the present-day deformation is being investigated by dense local GPS surveys. (Dinter et al., 2001, Van der Hoeven et al., 2003). As subduction and related tectonic processes has ended along the arc the only source of compression could be the result of the ongoing large-scale plate convergence in the southwest. The GPS data show that compression and associated contraction due to the Adria collision with the Alps and the Dinarides are not taken up in the mountain belts and the contraction can be detected far over the collisional boundaries. At the Eastern Alps, the eastward extrusion, at the Dinarides, the remaining NE compression cause significant shortening in the Pannonian basin. However, the GPS velocities and strain calculation show that both sources of shortening are taken up by the Pannonian Basin. As a result of this, we found no present-day deformation above the 1 mm/yr level further to the north-northeast in the Western and Northern Carpathians. Although the eastern part of the Tisza unit is poorly represented and there is no GPS site in the southern part of the Northern Carpathians, uplift suggested by leveling [Joó, 1992] is probably not due to present-day contraction since the Carpathians are free from major present-day contraction.

European Platform

The European Platform in our present-day kinematic definition consists of all tectonic domains located north of the Alps and the Carpathian arc regardless whether the domain is Precambrian, affected by the Caledonian orogeny, or the later Hercynian orogeny. Our data show that the majority of active contraction is taken up either in the Alps, the Dinarides, and the Pannonian Basin, and the deformation is not detectable even at the Carpathian arc. The reference frame for the intraplate velocity solution was determined using data from 11 sites across the European Platform. After the calculation of the Euler motion from these data, the random orientations of the residual velocities indicate no uniform motion. The 0.3 mm/yr value of the mean residual of velocities shows the rigidity of the European Platform or rather the current significance level of the data set. At present, neither the site density of the networks nor the current significance level allows us to make additional conclusions than the upper level of rigidity.

SUMMARY

We combined GPS data from continental to local level to better understand the highly complex and interconnected tectonic processes within the Eurasia-Nubia continental collision zone, from the Adria block to the European Platform. A summary was given about several GPS networks operated in the region that provide high quality data at sub-regional level. This contribution is intended to provide a regional coverage of the present-day tectonic processes from the Adria block through its collisional boundaries to the stable plate interior. The data show that the whole Adria block is independent from both neighboring plates, but its fragmentation and southern extent requires further detailed local data. The collision of Adria with the Eastern Alps and Central Dinarides results in different deformation pattern due to the boundary conditions. In the case of the Alps, contraction occurs in a narrow zone solely in the southern part. In addition, eastward extrusion along dextral transpressional and sinistral strike-slip fault zones significantly contributes to the stress release. In contrast, across the Central Dinarides, the contraction zone is several hundred kilometers wide and the mountain cannot absorb the compression completely. The Pannonian basin experiences compressional deformation both from the Dinarides and from the extrusion, but the basin seem to isolate both the western and northern Carpathians from the present-day contraction. Over the Alps, the Carpathians, and the European Platform appear to be rigid above a few tens of millimeters per year level.

ACKNOWLEDGEMENTS

We thank the support of the European Union under EVK2-CT-2002-00140 grant and the OTKA projects: T042900, and T034929, and the North Atlantic Treaty Organization under a grant awarded in 2003 in co-operation with the National Science Foundation of the United States, and the NATO Science Fellowship Programme of Hungary. The support of the Hungarian Academy of Sciences is appreciated, and special thanks go to Giovanni Sella at the Northwestern University, USA and the IGNS, New Zealand as well.

REFERENCES

Altamimi Z. Transformation parameters between ITRF solutions. http://lareg.ensg.ign.fr/pub/itrf/ITRF.TP, 2001.

Altiner Y. The contribution of GPS data to the detection of the Earth's crust deformations illustrated by GPS campaigns in the Adria region. Geophys. J. Int. 2001; 145: 550-559.

Bada G., Horváth F., Gerner P., Fejes I. Review of the present-day geodynamics of the Pannonian basIn Progress and problems. J. Geodynamics 1999; 27: 501-527.

Baran L.W., Busics I., Cacon S., Dobrzycka M., Zablotsky F. Status of subregional GPS geodynamics project GEODUC. Proceedings of the 1st Turkish International Symposium on Deformations; Istambul, 1994.

Becker M., Cristea E., Figurski M., Gerhatova L., Grenerczy G., Hefty J., Kenyeres A., Liwosz T., Stangl G. Central European intraplate velocities from CEGRN campaigns. Reports on Geodesy 2002; l(61): 83-91.

Bruyninx C., Carpentier G., Roosbeek F. Today's EPN and its network coordination. Proceedings of EUREF Symposium, June 4-6; Toledo, Spain, 2003, In press.

Csontos L., Nagymarosy A., Horváth F., Kovác M. Tertiary evolution of the Intra-Carpathian area: A model. Tectonophysics 1992; 208: 221-241.

Czarnecki K., Mojzes M., Papco J., Walo J. First results of GPS measurement campaigns in Tatra Mountains. Geophys. Res. Abstracts 2003; 5: 06592.

Dinter G., Nutto M., Schmitt G., Schmidt U., Ghitau D., Marcu C. Three dimensional deformation analysis with respect to plate kinematics in Romania. Reports on Geodesy, Warsaw University of Technology 2001; 2(57): 29–42.

Fejes I., Borza T., Busics I., Kenyeres A. Realization of the Hungarian Geodynamic GPS Reference Network. J. Geodynamics 1993; 18: 145-152.

Fodor L., Csontos L., Bada G., Györfi I., Benkovics L. Tertiary tectonic evolution of the Pannonian basin system and neighbouring orogens: a new synthesis of paleostress data. In *The Mediterranean Basins: Tertiary extension within the Alpine Orogen*, B. Durand, L. Jolivet, F. Horváth, M. Séranne, eds., Geol. Soc. Spec. Publ. 1999; 156: 295-334.

Grenerczy Gy., Kenyeres A., Fejes I. Present crustal movement and strain distribution in Central Europe inferred from GPS measurements. J. Geophys. Research 2000; 105(B9): 21,835-21,847.

Grenerczy Gy. "Tectonic processes in the Eurasian-African plate boundary zone revealed by space geodesy." In *Plate Boundary Zones* AGU Monograph, S. Stein, J. T. Freymueller, eds., Geodynamics Series 2002; 30: 67-86, *ISBN# 0-87590-532-3.*

Hefty J. 2001 Possibilities of improving the velocity estimates from CERGOP campaigns. Reports on Geodesy 2001; 2(57): 71-81.

Hoeven van der A.G.A., Ambrosius B.A.C., Spakman W., Mocanu V. Crustal motions in the Eastern Carpathians (Vrancea) measured by GPS. Geophy. Res. Abstracts 2003; 5: 03918.

Horváth F., Cloething S. Stress-induced late-stage subsidence anomalies in the Pannonian Basin. Tectonophysics 1996; 266: 287-300.

Horváth F. Towards a mechanical model for the formation of the Pannonian basin. Tectonophysics 1993; 226: 333-357.

Joó I. Recent vertical surface movements in the Carpathian Basin. Tectonophysics 1992; 202: 129-134.

McClusky S., Reilinger R., Mahmoud S., Ben Sari D., Tealeb A. GPS constraints on Africa (Nubia) and Arabia plate motions. Geophys. J. Int. 2003; 155: 126-138.

Mueller I., Beutler G. The International GPS Service for Geodynamics –Development and Current Structure. Proceedings of 6th lnt. Symp. on Satellite Positioning, OSU, Columbus, Ohio, 1992.

Oldow J.S., Ferranti L., Lewis D.S., Campbell J.K., D'Argenio B., Catalano R. Pappone G., Carmignani L., Conti P., Aiken C.L.V. Active fragmentation of Adria, the north African promontory, central Mediterranean orogen. Geology 2002; 30: 779-782.

Oncescu M.C. Deep structure of the Vrancea region, Romania, inferred from simultaneous inversion for hypocenters and 3-D velocity structure. Annales Geophysicae 1984; 2: 23-28.

Pesec P. CERGOP-2, a multipurpose and interdisciplinary sensor array for environmental research in central Europe. Geophys. Research Abstracts 2002; 4; 01650.

Priam S. National Report of Slovakia. Report on Geodesy 1995; 1(14).

Schenk V., Caco´n S., Kontny B., Schenková Z., Bosy J., Kottnauer P. GPS geodynamic movements of the East Sudeten area in connection to regional geological structures. Geophys. Research Abstracts 2003; 5: 12365.

Sella G. F., Dixon T. H., Mao A. REVEL, A model for recent plate velocities from space geodesy. J. Geophys. Res. 2002; 107(B4): 10.1029.

Simek J. Geodynamical Network of the Czech Republic and National Densification of EUVN. Paper presented at the 5th International Seminar on GPS in Central Europe, Penc, Hungary 5-7 May 1999.

Sledzinski J. Satellite Geodetic Traverses (SAGET) in Central and Southern Poland. Reports on Geodesy 1991; 1(3): 7.

Wenzel F., Sperner B., Lorenz F., Mocanu V. "Geodynamics, tomographic images and seismicity of the Vrancea region (SE-Carpathians, Romania)". In *Neotectonics and Surface processes: the Pannonian basin and the Alpine/Carpathian system*, S.A.P.L. Cloetingh, F. Horváth, G. Bada, A.C. Lankreijer, eds., EGU St. Mueller Special Publications Series, 2002; 3: 95-104.

SEISMICITY ALONG THE NORTHWESTERN EDGE OF THE ADRIA MICROPLATE

François Thouvenot[1] and Julien Fréchet[2]
1: Laboratoire de Géophysique Interne et Tectonophysique (UJF/CNRS), Observatoire des Sciences de l'Univers de Grenoble, France
thouve@ujf-grenoble.fr
2: Institut de Physique du Globe de Strasbourg (ULP/CNRS), École et Observatoire des Sciences de la Terre, Strasbourg, France

ABSTRACT

This contribution is an overview of the seismic activity observed along the northwestern edge of the Adria microplate over the last 15 years. The study area stretches from Lyons to Turin, and from Geneva to Nice. The discussion focuses on several key zones where significant earthquakes occurred during this period, or where the connection between seismicity and tectonics provides clear-cut results. Our main conclusions are: E–W to NW–SE compression in the Ligurian Sea and at depth beneath the southwestern Po plain; in the core of the western Alps, widespread extension radial to the chain, with a component of right-lateral strike slip along faults longitudinal to the chain; in the European foreland, almost exclusively strike slip, either right-lateral along faults longitudinal to the chain or left-lateral in a conjugate direction. The observed right-lateral strike slip is consistent with an anticlockwise rotation of Adria about a pole in the Po plain, but the extension observed in the root zone cannot be explained with a simple rigid-plate model. This extension probably also involves gravitational collapse and/or slab roll-back or break-off.

Keywords: Seismicity, stress, extension, rotation pole, western Alps, Adria

INTRODUCTION

Curved in a smooth arc from the Mediterranean coast to Geneva, the Western Alps form a 400-km-long, 200-km-wide segment of the great Alpine chain. Their geodynamic evolution, though complex, can be minimally summarized as follows: a long pre-rifting period during the Triassic and Lower Jurassic (225–165 Ma) eventually gave birth (165–100 Ma) to the Piedmont and Valais oceans, which formed contemporaneously with opening in the central Atlantic Ocean. This extension process stopped and inverted when the North Atlantic Ocean opened, the two newly-born pre-Alpine oceans progressively closed (100–65 Ma), culminating with the continental collision between Adria and stable Europe from 65 Ma onwards (Tapponnier, 1977; Platt et al., 1989; Lemoine et al., 2000).

N. Pinter et al. (eds.), The Adria Microplate: GPS Geodesy, Tectonics and Hazards, 335–349.

Although their frequency has long been underestimated, felt earthquakes are reported in the Western Alps on the order of several tens each year. Only a few of these felt events have had sufficient impact to leave a written trace in newspapers, scientific articles or reports. Rothé (1941) was the first to identify two active seismic zones in the French and Italian Western Alps: the Briançonnais and Piedmont seismic arcs. Since the middle of the 20th century, when instrumental data have become progressively more available, many studies have detailed the seismic activity in several additional seismic zones in Switzerland, Italy, and France. Relatively few studies of the overall seismicity of the Western Alps exist. They include Fréchet (1978), Guyoton (1991), Thouvenot (1996), Béthoux et al. (1998), and Nicolas et al. (1998).

Since the inception of plate-tectonic theory, earthquakes have been used to delineate major plate boundaries, while focal mechanisms provide constraints on relative plate motions. In the case of the Western Alps, such an exercise is subtler. First, regarding Adria as a microplate is still considered controversial. Second, the limits of a possible Adria microplate are not as clearly defined as are boundaries between major plates. Third, the seismicity level in the Western Alps is much lower than elsewhere in the circum-Adria orogenic belts, including the southern Apennines and Dinarides. The last two points are closely linked, but can be overcome by an increase in earthquake location accuracy and a decrease in detection threshold. Both involve developing more robust monitoring networks in the region.

SEISMIC MONITORING

In the mid 1980s, the Swiss and Italian short-period seismic networks monitored the seismicity to the north and to the east down to very low levels. However there were very few seismic stations in the French Alps, and these proved insufficient to monitor the seismicity there stretching over an 80,000-km^2 area. The aim of the Sismalp project was to fill this gap. Since that time, 44 seismic stations fitted with 1-Hz sensors now cover the area from Geneva to the south of Corsica and from the French Massif Central to the Italian border (Thouvenot et al., 1990; Thouvenot, 1996). They complement the 9 stations that LDG (Laboratoire de Détection et de Géophysique) runs in southeast France, the 12 stations of IRSN (Institut de Radioprotection et de Sûreté Nucléaire), as well as the 15-station Provence–Nice network operated by RéNaSS (Réseau National de Surveillance Sismique) close to the Mediterranean coast. Solarino et al. (1997) compiled data from these different networks in France and elsewhere along the Alpine belt to produce 3D tomography of the greater Alpine region.

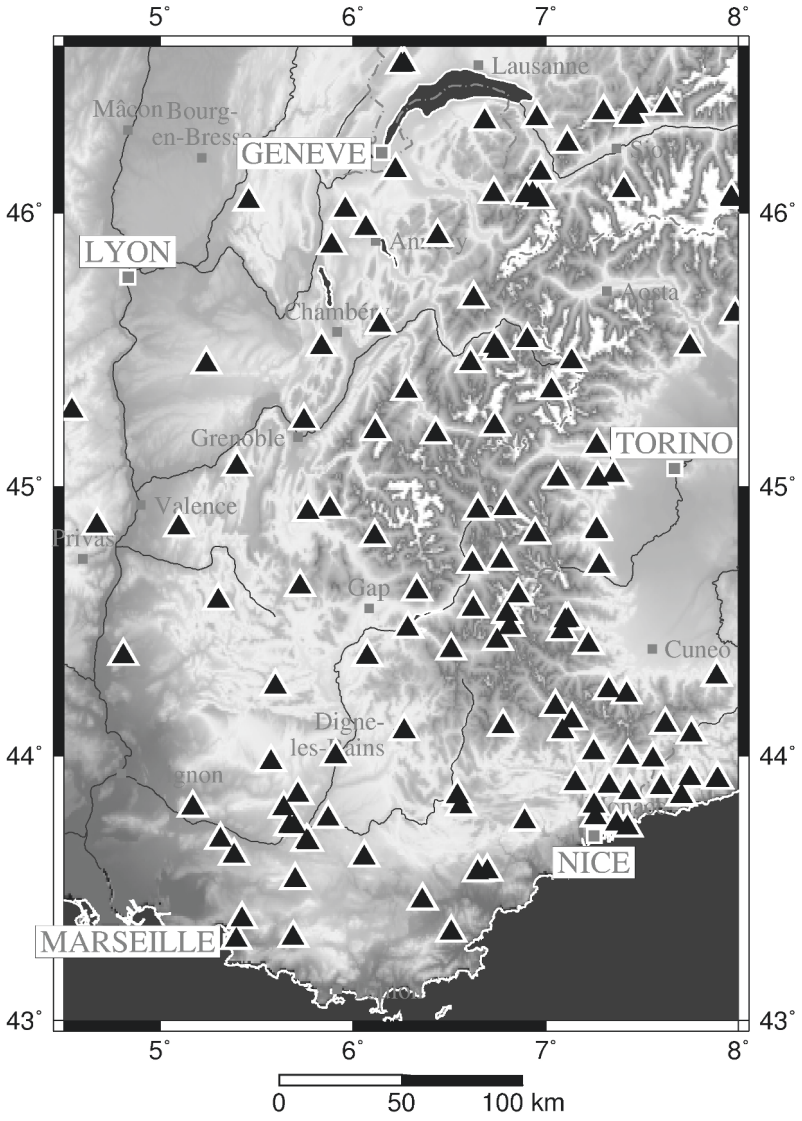

Figure 1. Permanent seismic velocimetric stations in the study area (short-period and broadband instruments).

Since the mid 1990s, the instrumental effort has focused more on broadband velocimetry and accelerometry. The 28 stations of the Swiss Seismic Network are now fitted with 0.02–120-s sensors, Rosalp and TGRS (Très Grande Résolution Sismique) installed 11 broadband instruments in southeast France, while, in northwest Italy, out of the 29 stations operated by IGG (Istituto Geofisico e Geodetico, Genoa), 7 stations are now equipped

with broadband velocimeters. In addition, the Swiss National Strong Motion Network and Rap (French Réseau Accélérométrique Permanent) have installed several tens of accelerometers over the region.

A total of about 120 seismic velocimetric stations are available in the study area as shown in Figure 1. Although seismic monitoring cannot yet make real-time use of all these networks because of efficiency reasons, arrival times are merged after events. Epicentral uncertainties are smaller than 1 km for most epicentres. All events with magnitudes over about 1.5 can be located. Focal mechanisms can be obtained for events as small as magnitude 2, although their reliability depends on focal depth, rupture process, and the epicentre being located in the core of the monitoring network rather than on its periphery.

DESCRIPTION OF INSTRUMENTAL SEISMICITY

Briançonnais, Piedmont, and Padan seismic arcs

Fourteen years of dense monitoring now allow us to identify reliably several seismically active zones (Fig. 2). Most activity concentrates along the two seismic arcs discovered 60 years ago (as mentioned above in the introduction), which are now sharply defined.

The Briançonnais seismic arc (Fig. 2, label 1) coincides with the Penninic Front, a major boundary between the external autochthonous domain and the internal Alpine nappes. Most foci there are shallower than 10 km. The Piedmont seismic arc (Fig. 2, label 2) is active mostly within the 10–15 km depth range and follows the western limit of the Po plain, precisely where the upper mantle of Adria comes into contact with the European crust through complex lithospheric flaking (Paul et al., 2001).

Most of the focal mechanisms in these two seismic arcs reveal a general extension radial to both arcs (Sue et al., 1999), a phenomenon previously described by Fréchet and Pavoni (1979), but which was then considered local and not as widespread as is now recognized. Where strike-slip motion is observed, it involves right-lateral displacement along faults longitudinal to the Alpine chain (Thouvenot et al., 1991). In southern Switzerland, between the upper Rhone valley and the Swiss–Italian border, Maurer et al. (1997) also presented evidence for extension in a N–S direction, i.e. more or less perpendicular to the local strike of the belt.

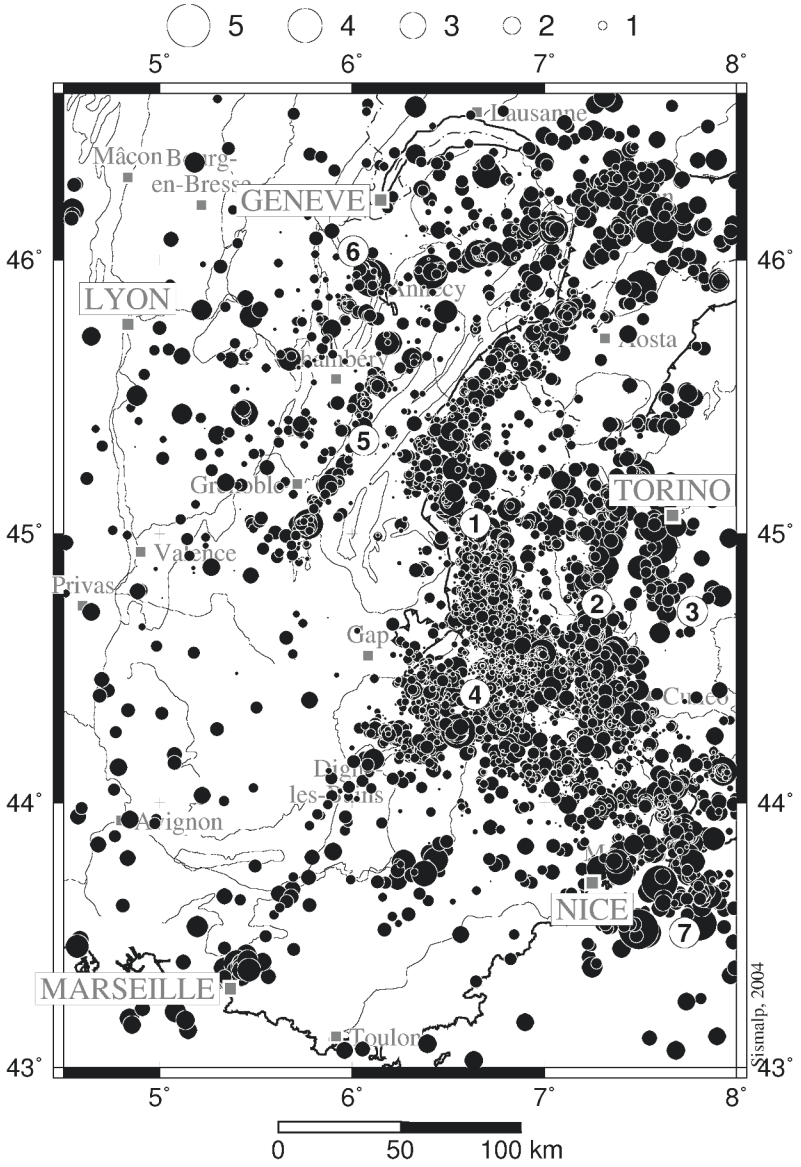

Figure 2. 1989–2002 instrumental seismicity. Background shows the main geological units (see Figure 3 caption for details). Arrival times used for locating earthquakes: Sismalp, RéNaSS, LDG, and IGG. Only events with RMS smaller than 1 s are plotted. Labels refer to seismic alignments or zones discussed in the text: 1 = Briançonnais arc; 2 = Piedmont arc; 3 = Padan arc; 4 = Embrunais-Ubaye; 5 = Subalpine arc; 6 = Vuache Fault; 7 = Ligurian Sea.

South of Turin, the Padan arc (Fig. 2, label 3) is yet another seismic arc in the NW Alps. It is characterized by deep earthquakes, down to 112 km according to Cattaneo et al. (1999). The Padan arc seems much less active than the Briançonnais and Piedmont arcs, although the difficulty in monitoring deep, low-magnitude seismic events beneath the densely-populated Po plain might partly explain this difference. It is tempting to relate the Padan arc to steep (80°?) subduction of the European Plate beneath Adria; however no reliable tomographic image has ever been produced for such a slab. More clearly, while the Piedmont arc mimics the western side of the Ivrea gravity high, the Padan arc follows its eastern side, making clear the relation of both of these seismic arcs with anomalous mantle structures beneath. Eva et al. (1997) report E–W compression for focal mechanisms computed along the Padan arc.

Embrunais-Ubaye nappes

In the study area, the internal Penninic nappes overlap the external domain in several places. This is the case in the Embrunais-Ubaye region (Fig. 2, label 4), which corresponds to a basement depression between the Pelvoux and Argentera crystalline massifs. The seismic activity in this zone is the highest in the French Western Alps. This is also where the most significant event of the second half of the 20th century (Saint-Paul-sur-Ubaye, $M_L = 5.5$) took place in 1959. Connecting seismicity to faults mapped at the surface is difficult, partly because the nappes are made up of flysch which lacks clear marker beds.

The main characteristic of the seismicity in this zone is that swarms of variable durations occur frequently (Guyoton et al., 1991). The latest, and one of the longest swarms ever observed in France, the La Condamine swarm, begun in January 2003, with more than 15,000 events (maximal magnitude 2.7) and lasted for more than 20 months. The fault zone that corresponds to the seismogenic source is nearly vertical, 8-km long, 2 to 8-km deep, and in the crystalline basement; it trends NW–SE, i.e. along the local strike of the Alps. About two-thirds of fault-plane solutions show right-lateral strike slip in the NW–SE direction, the remaining one third corresponding to normal faulting with E–W extension. This result is in agreement with that obtained earlier by Sue et al. (1999) in this region, where E–W extension was derived from the inversion of the focal mechanisms available prior to the La Condamine swarm.

Alpine foreland

The domain to the west of the Penninic Front is much less active than the internal zones to the east. In this part of the Alpine foreland, a further difference is observed south of latitude 45°N where the seismicity—at least the *instrumental* seismicity—is negligible. North of latitude 45°N, seismicity is more active, with earthquakes in the upper 15 km of the crust.

In this zone, which encompasses the densely-populated Annecy, Chambéry, Geneva, Grenoble, and Lyons regions, no clear seismicity pattern can be recognized. A major exception to this apparent mess is the recently discovered Subalpine seismic arc (Fig. 2, label 5). This rather straight epicentral alignment can be followed from the south of Grenoble toward Annecy to the northeast, where it veers to the ENE. It eventually joins the seismic zone situated north of the upper Rhone valley in the Valais (southern Switzerland), which also trends WSW–ENE. Earthquakes along this arc occur in the 5–10-km depth range, and a corresponding basement fault zone is not known at the surface. The alignment intersects several different geological units, as if seismotectonics at depth have no relation with the surface geologic features.

The proximity to the front of the Belledonne crystalline massif earned the southwestern section of this fault zone its name the Belledonne Border Fault (BBF; Thouvenot et al., 2003). This ~50-km-long epicentre alignment runs in a N30°E direction and includes ~150 earthquakes with magnitudes between 0 and 3.5. Available focal solutions are consistent with the N30°E orientation of the BBF; all but one involve strike slip with right-lateral displacement. The BBF can thus be interpreted as the reactivation of a Hercynian basement fault with almost pure right-lateral strike slip, with an E–W-trending P axis and a N–S-trending T axis.

To the northeast, along the other section of the Subalpine arc with a WSW–ENE orientation, the focal mechanisms are more varied. They often imply strike slip with right-lateral displacement, although transpression exists locally (Fréchet et al., 1996). As for the continuation of the Subalpine arc in Switzerland, on the northern bank of the Rhone river, Maurer et al. (1997) mainly report strike slip, either with a right-lateral displacement along faults longitudinal to the Alpine belt, or with a left-lateral displacement in the conjugate direction.

Farther to the northwest in the Lyons–Geneva–Annecy–Grenoble area, seismicity in the Alpine foreland is very scattered. This seismicity seems to reflect the presence of active NW–SE-trending faults. One such fault, the Vuache Fault (Fig. 2, label 6), has been identified as seismically active. It connects the Jura to the Alps, and is responsible for the Épagny-Annecy M_L-5.3 earthquake in 1996 (Thouvenot et al., 1998). In the field, impressive slickenlines reflecting fossil slip are observed along this ~30-km-long fault.

The focal mechanism of the main 1996 shock, as well as aftershock monitoring indicate left-lateral strike-slip motion on a N130–135°E-striking fault; this orientation is perpendicular to the local trend of the Alpine belt. The P axis trends E–W and the T axis N–S, in agreement with what we observed along the BBF.

Ligurian Sea

Seismicity observed offshore in the Ligurian Sea (Fig. 2, label 7) is restricted to the northern margin of the oceanic domain created by the rotation of the Corsica-Sardinia block (Béthoux et al., 1992). Reactivation of faults formed during this early tectonic phase, due to E–W to NW–SE compression in this region, is recorded by several reliable focal mechanisms. This leads to a speculation that this aborted oceanic domain is now being closed by northward motion of Corsica-Sardinia. However, GPS measurements such as those processed by Calais et al. (2002) or Hollenstein et al. (2003), suggesting that Corsica-Sardinia is practically immobile relative to stable Europe, do not corroborate this speculation. Another possibility to explain the compression along the Ligurian margin is that it is due to lateral expulsion of the southwestern Alps as Adria collides with Europe.

Provence

The southwestern part of the study area is not discussed here for two reasons. First, this zone, at least the Marseilles area and the lower Rhone valley, lies a fair distance from Adria, and discussing its seismicity is beyond the scope of this paper. Second, much of it (Figure 2) appears seismically inactive. However, we know from historical seismicity records that several destructive earthquakes have occurred there, the most damaging event being the Lambesc earthquake, north of Marseilles (1909, maximum MSK intensity IX). In contrast to what happens elsewhere in the study area, a 14-year monitoring is not long enough to provide us with a reliable seismotectonic map of Provence. Clearly, such a map should take into account historical seismicity, no matter how imprecise the corresponding epicentre locations. Suffice it to say that Provence is not as inactive as it might seem at first glance, as indicated by the SW–NE seismic alignment extending from Marseilles to Digne along the Durance valley. This alignment is parallel to the BBF, and suggests a possible similarly reactivated fault, which would also be of Hercynian origin.

ADRIA ROTATION

Although scrutiny of McKenzie's (1972) paper reveals that he sketched an almost imperceptibly curved velocity arrow on what he named 'the Adriatic', Gidon (1974) can be considered the first to have proposed anticlockwise rotation of Adria about a pole in the western Po plain. This hypothesis was based on the observation of many longitudinal displacements along right-lateral strike-slip faults in the Western Alps. Ingenious and innovative at that time, it has been substantiated in the following decades first by paleomagnetic results, then by GPS measurements. Geometric criteria were also used by Ménard (1988), Vialon et al. (1989), Laubscher (1996), Stampfli and Marchant (1997), Schmid and Kissling (2000), and Collombet (2001) when they discussed the importance of successive rotations in the Alpine orogeny. However, there is a consensus that few tectonic, morphological or stratigraphic markers exist with which to identify and quantify these rotations.

Our description of the stress field along the northwestern edge of Adria is summarized in Figure 3. This summary makes clear that the current tectonics in the Western Alps is by no means dominated by collision-related radial crustal shortening as expected in a collision belt. Since the late 1980s, several authors have computed an anticlockwise rotation of Adria about an Euler pole in the Po plain, close to 46°N/10°E (Fig. 4). Anderson and Jackson's (1987) pole position remains a good starting model to describe the overall kinematics of Adria. It fits well with the observations of extension in the Apennines and convergence in the Dinarides. It also explains the right-lateral strike-slip faults that we observed in the Western Alps from many focal mechanisms derived from events along faults longitudinal to the belt and along-strike alignments of epicentres detected either through aftershock studies or long-term monitoring. However, Anderson and Jackson's (1987) pole falls right in the middle of the fairly active Milan-Trient seismic zone, which marks the northern limit of Adria. This is an unlikely position for an Euler pole, since the distance from the pole to the boundary is the shortest, and differential motion between Europe and Adria probably very faint.

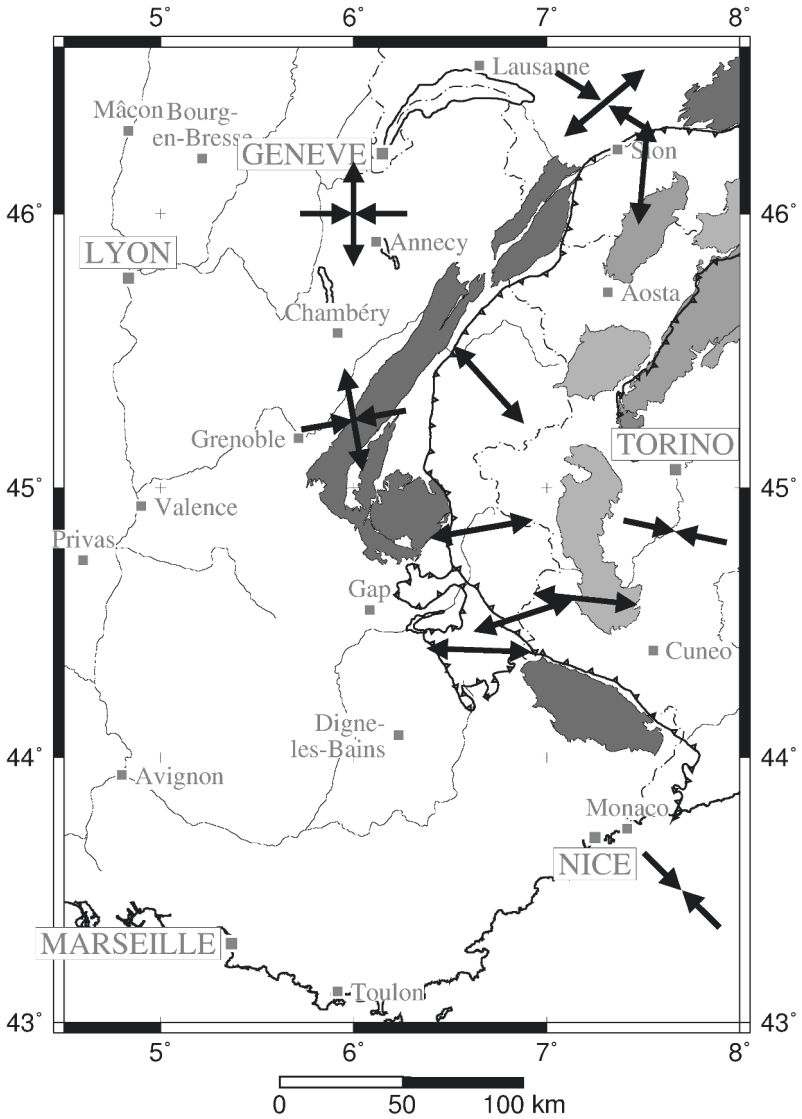

Figure 3. Stress tensors in the study area showing directions of horizontal compression and extension. Crystalline massifs form two arcs separated by the Frontal Penninic Thrust (barbed line). Most results are from stress tensor inversions by Eva et al. (1997), Maurer et al. (1997), and Sue et al. (1999), except in 3 places: east of Grenoble, south of Geneva, and southeast of Nice (*P* and *T* axes from focal mechanisms). Note: extension in the internal zones; strike slip in the foreland; compression restricted to the Po plain and Ligurian Sea.

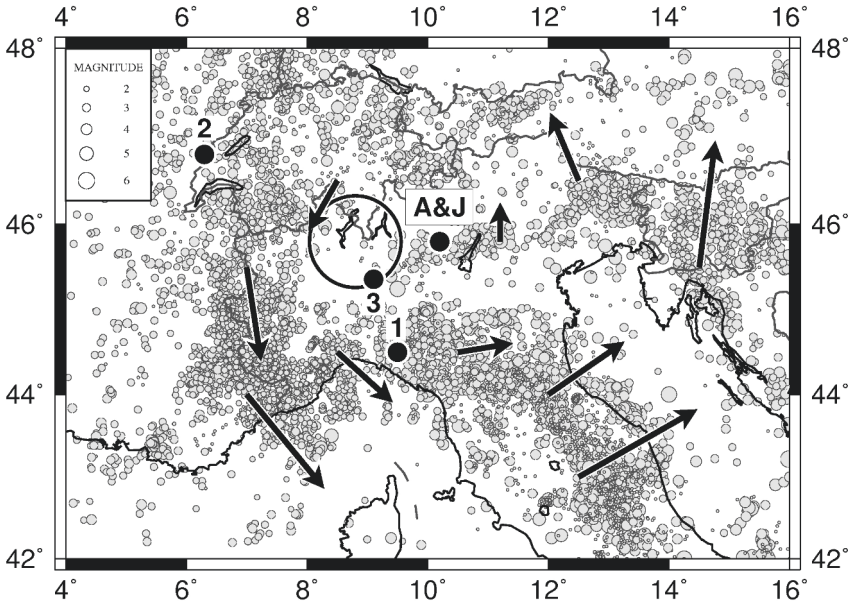

Figure 4. Anticlockwise rotation of Adria about different Euler poles. A&J = Anderson and Jackson (1987), with corresponding relative velocity vectors computed along the Adria-Europe boundary (velocity magnitude is arbitrary); 1 = Westaway (1990); 2 = Ward (1994); 3 = Calais et al. (2002); circle = Lake Maggiore region where the seismicity at the Adria-Europe boundary is almost nonexistent. Seismicity data from USGS (1900–1995).

Other Euler poles fit seismotectonic data more or less correctly. Westaway's (1990) pole located east of Genoa (Fig. 4, label 1) implies compression in the French-Italian Alps and strike slip in the Swiss-Italian Alps; neither phenomena is observed. Ward's (1994) pole north of Geneva (Fig. 4, label 2) explains extension in the French-Italian Alps, but infers compression in the Swiss-Italian Alps, which is not observed. Calais et al.'s (2002) pole (Fig. 4, label 3) is not basically different from Anderson and Jackson's (1987) pole as concerns relative velocity vectors computed along the Adria-Europe boundary. But its position at the western tip of the Milan-Trient seismic zone discussed above makes it more likely for us. In the Lake Maggiore region (Fig. 4, circle), seismicity of the northern boundary of Adria is almost nonexistent. This is another zone where the Euler pole could be searched for.

EXTENSION: GRAVITATIONAL COLLAPSE OR BUOYANCY FORCES?

The Adria rotation pole position computed by Calais et al. (2002) integrates two continuous GPS stations on Adria with Anderson and Jackson's (1987) earthquake slip vectors. Although this pole position is consistent with the extension observed in southern Switzerland, it fits neither the azimuths nor values of velocities observed in the Western Alps with respect to stable Europe, as Calais et al. (2002) themselves recognized. The reason invoked by Calais et al. (2002) is the extension revealed by their strain rate analysis in the internal French Alps.

We show that stress tensor inversion yields widespread extension radial to the belt from south Switzerland to the southwestern Alps (Fig. 3). It is difficult to conceive how such extension over such a wide area results from the Adria-Europe rotation discussed above. Moving the Adria rotation pole farther to the west—that is, closer to the Adria-Europe plate boundary—would favour extension in the French-Italian Alps but would also induce convergence in southern Switzerland, which is contrary to observations. One way to explain such extension is to allow deformable plate margins.

Several mechanisms can be invoked for explaining extension in mountain belts, as reviewed for instance by Sue et al. (1999) or Calais et al. (2002). The models of tensional strain within a crustal-scale ramp anticline or an upward extrusion of a rigid mantle indenter can be excluded in the Western Alps because both models require active convergence, which is not observed. Gravitational collapse is a more likely candidate. Orogenic collapse normally affects high-elevation plateaus where the crust has been overthickened. The altitudes of the Briançonnais and Piedmont zones are certainly not comparable with that of Tibet or the Basin-and-Range province. Sue et al. (1999) therefore also discarded this model and invoked buoyancy forces such as those produced by a slab retreat or break-off to produce the observed extension in the Western Alps. However such a lithospheric-instability model is also difficult to defend. Many lithospheric-scale models of this belt include a European Plate subducted under Adria, and the anomalously deep earthquakes located by Cattaneo et al. (1999) beneath the Po plain might be related to subduction of Europe beneath Adria. But there is still no clear evidence of a European slab beneath the Western Alps. Although neither the lithospheric-instability model nor gravitational collapse are satisfactory for explaining the observed extension, they appear less unlikely than the other models. Further investigations are necessary to decide if either of these two models, or a combination thereof, represents the actual cause of widespread extension observed in the core of the Western Alps.

CONCLUSIONS

This brief description of the stress field along the northwestern edge of Adria makes clear that current tectonics in the Western Alps are in no way dominated by collision-related radial crustal shortening as could be expected in a collision belt. Instead, extension and right-lateral strike slip along faults longitudinal to the chain are most prominent. Convergence is eventually restricted to very specific zones, not within the belt, but at its periphery (e.g. Ligurian Sea, southwestern Po plain, Jura). The anticlockwise rotation of Adria about a pole in the central Po plain remains a good starting model for describing the overall kinematics of the circum-Adria orogens, especially the right-lateral strike slip we observe in the Western Alps; but this model fails to explain the synorogenic extension we observe there. Among several mechanisms offered to explain the observed extension, gravitational collapse and buoyancy forces, such as produced by slab retreat or break-off, may complement the rigid-plate motion.

REFERENCES

Anderson H.A., Jackson J.A. Active tectonics in the Adriatic Region. Geophys. J. R. Astr. Soc. 1987; 91: 937–983.

Béthoux N., Fréchet J., Guyoton F., Thouvenot F., Cattaneo M., Eva C., Nicolas M., Feignier B., Granet M. A closing Ligurian Sea? Pure Appl. Geophys. 1992; 139: 179–194.

Béthoux N., Ouillon G., Nicolas M. The instrumental seismicity of the Western Alps : spatio-temporal patterns analysed with the wavelet transform. Geophys. J. Int. 1998; 135: 177–194.

Calais É., Nocquet J.-M., Jouanne F., Tardy M. Current strain regime in the Western Alps from continuous Global Positioning System measurements, 1996–200. Geology 2002; 30: 651–654.

Cattaneo M., Augliera P., Parolai S., Spallarossa D. Anomalously deep earthquakes in northwestern Italy. J. Seismol. 1999; 3: 421–435.

Collombet M. *Cinématique et rotation des Alpes occidentales. Approche paléomagnétique et modélisation analogique*, Thèse, 222 pp., Univ. J.-Fourier, Grenoble, 2001.

Eva E., Solarino S., Eva C., Neri G. Stress tensor orientation derived from fault plane solution in the southwestern Alps. J. Geophys. Res. 1997 ; 102 : 8171–8185.

Fréchet J. *Sismicité du Sud-Est de la France, et une nouvelle méthode de zonage sismique,* Thèse, 159 pp., Univ. Sci. Méd. Grenoble, 1978.

Fréchet J., Pavoni N. Étude de la sismicité de la zone briançonnaise entre Pelvoux et Argentera (Alpes occidentales) à l'aide d'un réseau de stations portables. Eclogae Geol. Helv. 1979 ; 72 : 763–779.

Fréchet J., Thouvenot F., Jenatton L., Hoang-Trong P., Frogneux M. Le séisme du Grand-Bornand (Haute-Savoie) du 14 décembre 1994 : un coulissage dextre dans le socle subalpin. C. R. Acad. Sci., Paris 1996 ; 323 : 517–524.

Gidon M. L'arc alpin a-t-il une origine tourbillonnaire? C. R. Acad. Sci., Paris 1974; 278: 21–24.

Guyoton F. *Sismicité et structure lithosphérique des Alpes occidentales,* Thèse, 290 pp., Univ. Grenoble, 1991.

Guyoton F., Fréchet J., Thouvenot F. La crise sismique de janvier 1989 en Haute-Ubaye (Alpes-de-Haute-Provence, France) : étude fine de la sismicité par le nouveau réseau SISMALP. C. R. Acad. Sci., Paris 1990 ; 311 : 985–991.

Hollenstein C., Kahle H.-G., Geiger A., Jenny S., Goes S., Giardini D. New GPS constraints on the Africa-Eurasia plate boundary zone in southern Italy. Geophys. Res. Lett. 2003; 30: 1935.

Laubscher H. Shallow and deep rotations in the Miocene Alps. Tectonics 1996; 15: 1022–1035.

Lemoine M., de Graciansky P.-C., Tricart P. *De l'océan à la chaîne de montagne. Tectonique des plaques dans les Alpes,* 207 pp., Gordon and Breach, Paris, 2000.

Maurer H., Burkhard M., Deichmann N., Green G. Active tectonism in the central Alps: Contrasting stress regimes north and south of the Rhone Valley. Terra Nova 1997; 9: 91–94.

McKenzie D. Active tectonics of the Mediterranean region. Geophys. J. R. Astr. Soc. 1972 ; 30 : 109–185.

Ménard G. *Structure et cinématique d'une chaîne de collision. Les Alpes occidentales et centrales,* Thèse d'État, 268 pp., Univ. J.-Fourier, Grenoble, 1988.

Nicolas M., Béthoux N., Madeddu B. Instrumental Seismicity of the Western Alps: A Revised Catalogue. Pure Appl. Geophys. 1998; 152: 707–731.

Paul A., Cattaneo M., Thouvenot F., Spallarossa D., Béthoux N., Fréchet J. A three-dimensional crustal structure velocity model of the south-western Alps from local earthquake tomography. J. Geophys. Res. 2001; 106: 19,367–19,389.

Platt J. P., Behrmann J. H., Cunningham P. C., Dewey J. F., Helman M., Parish M., Shepley M. G., Wallis S., Weston P.J. Kinematics of the Alpine arc and the motion of Adria. Nature 1989; 337: 158–161.

Rothé J.-P. Les séismes des Alpes Françaises en 1938 et la séismicité des Alpes Occidentales, Annales Inst. Phys. Globe Strasbourg 1941; 3 (3): 1–105.

Schmid S., Kissling E. The arc of the Western Alps in the light of geophysical data on deep crustal structure. Tectonics 2000; 19: 62–85.

Solarino S., Kissling E., Sellami S., Smriglio G., Thouvenot F., Granet M., Bonjer K.P., Sleijko D. Compilation of a recent seismicity data base of the greater Alpine region from several seismological networks and preliminary 3D tomographic results. Annali di Geof. 1997; XL: 161–174.

Stampfli G., Marchant R. Geodynamics of the Tethyan margins of the Western Alps. In *Deep Structure of the Swiss Alps*, O.A. Pfiffner et.al, eds., Birkhäuser Boston, Cambridge,1997; 223–239.

Sue C., Thouvenot F., Fréchet J., Tricart P. Widespread extension in the core of the Western Alps revealed by earthquake analysis. J. Geophys. Res. 1999 ; 104 : 25,611–25,622.

Tapponnier P. Évolution tectonique du système alpin en Méditerranée : poinçonnement et écrasement rigide–plastique. Bull. Soc. Geol. Fr. 1977 ; 7 : 437–460.

Thouvenot F. *Aspects géophysiques et structuraux des Alpes occidentales et de trois autres orogènes (Atlas, Pyrénées, Oural)*, Thèse d'État, 378 pp., Univ. J.-Fourier, Grenoble, 1996.

Thouvenot F., Fréchet J., Guyoton F., Guiguet R., Jenatton L. SISMALP: an automatic phone-interrogated seismic network for the Western Alps. Cahiers Centre europ. Géodyn. Séism. 1990 ; 1 : 1–10.

Thouvenot F., Fréchet J., Vialon P., Guyoton F., Cattaneo M. Les séismes de Cervières (Hautes-Alpes) des 11 et 13 février 1991 : un coulissage dextre entre zones piémontaise et briançonnaise. C. R. Acad. Sci., Paris 1991 ; 312 : 1617–1623.

Thouvenot F., Fréchet J., Tapponnier P., Thomas J.-C., Le Brun B., Ménard G., Lacassin R., Jenatton L., Grasso J.-R., Coutant O., Paul A., Hatzfeld D. The M_L 5.3 Épagny (French Alps) earthquake of 1996 July 15: a long-awaited event on the Vuache Fault. Geophys. J. Int. 1998; 135: 876–892.

Thouvenot F., Fréchet J., Jenatton L., Gamond J.-F. The Belledonne Border Fault: identification of an active seismic strike-slip fault in the Western Alps. Geophys. J. Int. 2003; 155: 174–192.

Vialon P., Rochette P., Ménard G. Indentations and rotations in the western Alpine arc. In *Alpine Tectonics*, M.P. Coward et.al, eds., Geol. Soc. Spec. Publ. 1989; 45: 329–339.

Ward S.N. Constraints on the seismotectonics of the central Mediterranean from very long baseline interferometry. Geophys. J. Int. 1994; 117: 441–452.

Westaway R. The Tripoli, Libya, earthquake of September 4, 1974: Implications for the active tectonics of the central Mediterranean. Tectonics 1990; 9: 231–248.

SEISMICITY OF THE ADRIATIC MICROPLATE AND A POSSILE TRIGGERING: GEODYNAMIC IMPLICATION

Betim Muço
Seismological Institute, Tirana, Albania
Betmuco@cs.com

ABSTRACT

The aim of this work is to show the distribution in time and space of seismic activity exhibited in the area of Adriatic Sea or the Adria microplate searching for any possible inter-correlation between different parts of circum Adriatic region. Based on the generalized tectonic setting of the contact between Adriatic block and surrounded mountain chains, we subdivided 6 zones in our study area and constructed two working catalogues of earthquakes. Some characteristics of seismic activity as number of earthquakes, maximal magnitude, mean depth, b coefficient, and seismic energy release are investigated for each zone. From the statistical analysis a strong correlation is also revealed for some of the zones of peri-Adriatic region.

INTRODUCTION

The Mediterranean region forms part of the second most important earthquake belt of the world, which extends from Java through the Himalayas, Asia Minor and to the Atlantic. This belt accounts for about 17 percent of the world's largest earthquakes.

The area surrounding the Adriatic Sea represents one of the most seismically active regions of the Mediterranean basin. In this area, earthquakes have been observed since the earliest recorded history. The Adriatic microplate has played a major role in the tectonic history of central Mediterranean region and the development of Alpine system.

The aim of this work is to show the distribution in time and space of seismic activity in this area and to search for any possible inter-correlation between seismicity in different parts of circum-Adriatic region.

N. Pinter et al. (eds.), The Adria Microplate: GPS Geodesy, Tectonics and Hazards, 351–367.

TECTONIC ENVIRONMENT

It is widely believed that Mesozoic development of western Tethys Sea has been governed by the opening of north and south Atlantic oceans. The general feature of all the models proposed for describing the way the African Plate converges with Eurasia, is that Africa moves slowly relative to Eurasian Plate with a counterclockwise rotation. Its direction changed slowly from NE to N-S and later to NNW (Dewey et al., 1989; Dercourt et al., 1993). In the convergence between these two plates, the basement of Adriatic Sea, being trapped between east Apennines Peninsula, west Balkan and southern Alps, shaped the rising of these surrounding mountain chains. Given the high level of seismicity of the peri-Adriatic region and, in contrast, only rare seismic events within the basin itself, many authors have defined the peri-Adriatic as a microplate that extends north to south from the Po plain to Apulia (Anderson and Jackson, 1987). The hypothesis of Adriatic block as a promontory of the African Plate pushing into the Eurasian Plate (McKenzie, 1972; Channell et al., 1979) is still very popular. A continuous zone of earthquakes surrounds the Adriatic plate. The general characteristic is that the coastal earthquakes of Croatia, Montenegro, Albania and northwestern Greece indicate mostly a belt of thrust faults generally striking NW-SE in response to NE-SW-directed compression, and in the Apennines of central Italy, normal faulting earthquakes show NE-SW extension perpendicular to the mountain chain (Costandinescu et al., 1966; McKenzie, 1972; Udias, 1982; Anderson & Jackson, 1987; Gasparini et al. 1985; Muço, 1994 a, 1995; Frepoli and Amato, 1997; Louvari et al., 2001; Pondrelli et al., 2002). Transverse faults that cut the orogenic belt both to the east and west of the Adriatic basin are connected with zones of extension of almost N-S direction on the back of collision front of the western Balkans (Cvijanovic et al., 1976; Muço, 1994a, 1998; Aliaj, 2001; Sulstarova et al., 2001; Goldsworthy et al., 2002) and with strike-strip earthquakes in the Apennines peninsula (Frepoli and Amato, 1997).

The hypothesis of counterclockwise rotation of Adria matches well with all of the tectonic implications described above. It agrees well with the compressive tectonics along the southern Alps, Dinarides and Albanides as well as with tectonics along the Apennine chain.

This rotation is confirmed by geophysical and GPS data. What is still a matter of debate is the current connection between Adria and the African Plate: is Adria a part of the African Plate or does it behave as an independent unit? Anderson and Jackson (1987) proposed that the Adriatic region is currently behaving as a rigid and independent block detached from the African Plate. The drift between Africa and Adria and the oceanic nature of Ionian basin are other arguments that support the idea (Dercourt et al., 1993). Some geodetic research also indicate that motion of the Adriatic region is independent from motion of the African Plate (Battaglia et al., 2003). Other

authors, based on geological, geophysical and seismological data, suggest that Adria is still a promontory of the African Plate (McKenzie, 1972; Channell and Horvath, 1976; Lowrie, 1986; Channell, 1996; Mele, 2001). Furthermore, where is the southern margin of this unit if it is already detached? Some authors consider weak seismicity near the Otranto strait as evidence that this strip forms the southern margin of the Adria block (Anderson and Jackson, 1987). Others instead argue that the southern margin of Adria could be located somewhere between continental collision to the north and oceanic subduction to the south, in the areas of the central Ionian islands, where a dextral strike-slip faulting is observed firstly by Scordilis et al. (1985; Babbuci et al., 2003). Another opinion is that the southern margin of Adria forms a line north to the Gargano and Tremiti islands (Westaway, 1990; Favali et al., 1993). The epicenters of earthquakes located in the Gargano area have suggested another hypothesis – that of two separate zones, including a northern Adriatic plate and a southern one (Console et al., 1993; Louvari and Kiratzi, 2000, Panza et al., 2003).

The integration of all the data from monitoring of ancient and recent seismicity, geology, seismotectonic modeling, geophysics and geodesy might in the near future be able to solve the puzzle of the Adria microplate and its geodynamic relations with the surrounding area.

SEISMIC HAZARD

Although a complete regional analysis of the seismicity of the entire peri-Adriatic region has not yet been produced, a study on probabilistic seismic hazard of Adria has been carried out into the framework of the Global Seismic Hazard Assessment Program (GSHAP; Slejko et al., 1999).

The maximum expected hazard is found to be around the Ionian islands, which is the highest seismic hazard spot throughout the peri-Adriatic region (about 5.0 m/s^2). The values of PGA larger than 4.0 m/s^2 are calculated from southern Albania to Cephalonia through northwestern Greece. Going north, along eastern coast, the PGA values drop to PGA values a little bit more than 2.0 m/s^2 and a gap with a weaker acceleration values is shown in northern Dalmatia. Most of the Italian peninsula shows values that are larger than 1.6 m/s^2, with local spots of about 3 m/s^2 in central and southern Italy and 3.2 m/s^2 in northeastern Italy (Slejko et al., 1999).

Having comparable hazard values with eastern Turkey and southern and southeastern Greece, the peri-Adriatic region has the highest PGA and SA values in the whole Mediterranean, around 0.5 g and around 1.0 g, respectively (Jimenez et al., 2001).

DATA USED

Two working catalogues were constructed. ADRIA-1 is a composite catalogue for the period 1501-2003 and earthquakes with M≥5.5. The 372 strongest earthquakes of the Apennine peninsula, Liguria and the Western Alps, the Italian Southern Alps and Slovenia, the Croatian coast, Montenegro, Albania and northwestern Greece are included in this catalogue. The following sources were used: Shebalin et al. (1974); Macropoulos and Burton (1981); Karnik, (1996); Papazachos & Papazachou (1997); Boschi et al. (1997); Shebalin et al. (1998); Sulstarova et al. (2001); Ambraseys, (2001). Duplicate solutions for the same events are removed. The type of magnitude used is M_S.

ADRIA-2 is constructed on the seismological data of last decades of 20th century. There are about 20,000 earthquakes with magnitude M≥2.0 for the period 1963-2003. Creating this catalogue, we used the catalogue of ANSS (Advanced National Seismic System) of the Northern California Earthquake Data Center, which is a composite worldwide earthquake catalogue created by merging master catalogues from contributing ANSS institutions (see *http://quake.geo.berkeley.edu/anss*).

SEISMOLOGICAL ANALYSIS

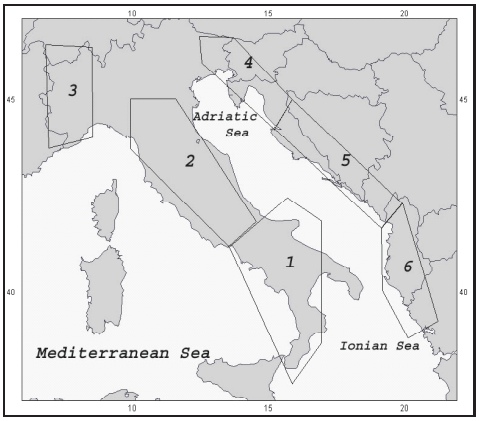

Figure 1. Based on the generalized tectonic setting of the contact between Adriatic block and surrounded mountain chains, we subdivided the study area into 6 zones (Figure 1). Characteristics of seismic activity were investigated for both ADRIA-1 and ADRIA-2, including the number of earthquakes, maximum magnitude, mean depth, b coefficient.. The results are given in Tables 1 and 2.

The seismic energy release during more then five centuries was also studied. The earthquake magnitudes of the ADRIA-1 catalogue were converted into seismic energy release by using the Gutenberg-Richter equation: $\log E = 1.5\ M_S + 11.8$. The square root of energy is plotted as a strain factor for each zone (Figure 2).

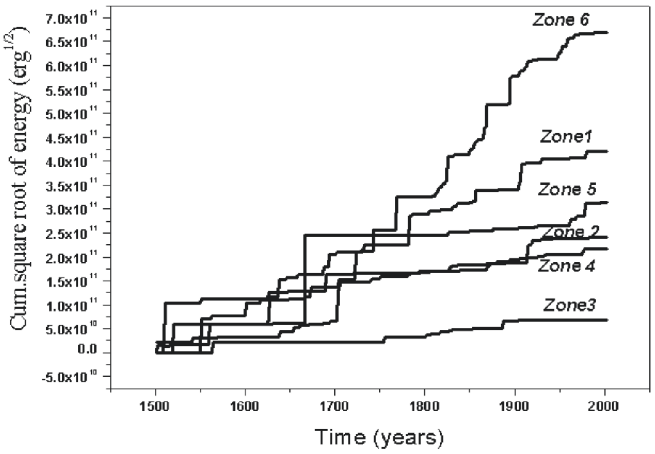

Figure 2. Cumulative square root of energy released in each of the six zones in the study area (see Figure 1)

Table 1. Seismological analysis for ADRIA-1. West side comprises zones 1,2 and 3, and east side zones 4,5 and 6. Adria contact comprises all zones.

Zn	*Area (km^2)*	*Span time years*	*Num. of earthq*	*Min. mag*	*Max. mag*	*Coeff. b*	*∑E (erg)*	*Density of energy ($erg/km^2.yr$)*
1	91.229	488	67	5.5	7.4	0.91	$1.772x10^{23}$	$3.98x10^{15}$
2	89.110	496	65	5.5	6.9	1.29	$5.771x10^{22}$	$1.366x10^{15}$
3	42.588	433	12	5.5	6.3	-	$4.72x10^{21}$	$2.56x10^{14}$
4	38.439	495	37	5.5	6.8	1.09	$4.661x10^{22}$	$2.46x10^{15}$
5	51.370	477	48	5.5	7.3	0.93	$9.852x10^{23}$	$4.02x10^{15}$
6	51.377	446	153	5.5	7.3	1.05	$4.475x10^{23}$	$1.756x10^{16}$
West wing	222.927	496	144	5.5	7.4	1.13	$2.396x10^{23}$	$2.167x10^{15}$
East wing	102.785	495	228	5.5	7.3	1.10	$5.926x10^{23}$	$1.165x10^{16}$
All	325.712	502	372	5.5	7.4	1.18	$8.332x10^{23}$	$5.09x10^{15}$

Table 2. The results of seismological analysis for ADRIA-2

Zone	*Area (km^2)*	Span *time years*	*Num. of earthq*	*Min. magn.*	*Max. magn.*	Mean *depth (km)*	*Coeff. b*
1	91.229	40	1826	2.0	6.9	14	0.69
2	89.110	40	1601	2.0	6.0	11	0.90
3	42.588	40	5467	2.0	5.5	10	1.05
4	38.439	40	1344	2.0	6.1	12	0.64
5	51.370	40	2392	2.0	6.9	11	0.76
6	51.377	40	2851	2.0	6.3	13	0.82
West side	222.927	40	13394	2.0	6.9	11	0.89
East side	102.785	40	6587	2.0	6.9	12	0.79
Adria all	325.712	40	19981	2.0	6.9	11	0.86

The seismic energy released in the east side of the Adria microplate is more then two times the seismic energy release on the west side, and the density of energy for the east side is almost five times larger then for the west side. The total energy released on the whole Adriatic periphery for the last 500 years is 8.32×10^{23} erg, which is equivalent to the energy of about two earthquakes with M=7.5 and one with M=8.0.

CROSS-CORRELATION ANALYSIS

The seismic activity of any region is a function of complex geodynamical processes and, at first sight, may present no statistical trends. But if we consider that this seismic activity is also produced by a tectonic unit and also that the seismic disturbances might be transmitted across this area, then in a larger extent, the earthquakes of these zones may show a certain degree of interdependence.

From the ADRIA-1 and ADRIA-2 catalogues, we constructed time series for each zone . For the time series from ADRIA-2, only the earthquakes $M \geq 4.0$ were taken into consideration. We filtered out the earthquakes with hypocentral depth greater than 50 km, considering only crustal earthquake generation (see Figures 3 and 4). The time series were constructed by

calculating the number of earthquakes in each interval, which was set at three months for Adria 2 time series and at six months for Adria 1.

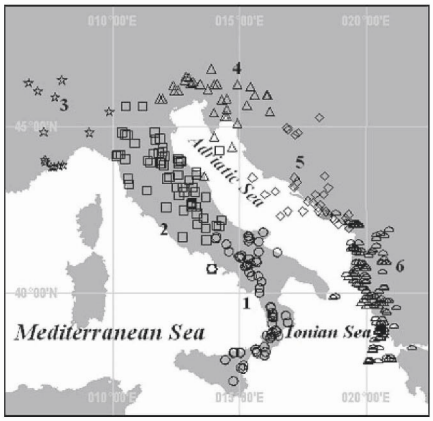

Figure 3. Epicenters of earthquakes from ADRIA-1 for each zone.

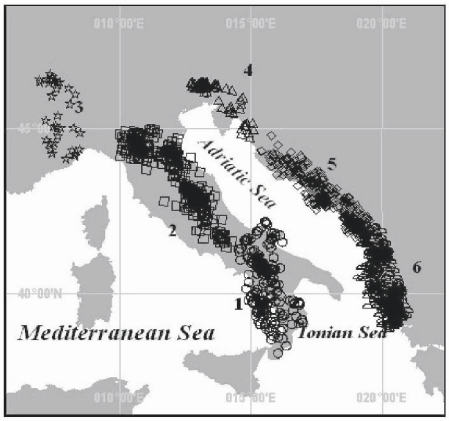

Figure 4. Epicenters of earthquakes from ADRIA 2 for each zone

Temporal relationships between time series were explored using cross-correlation time-series analysis. This is a standard method for estimating the degree to which two series are correlated and has been used extensively for seismological studies (e.g., McGinnis, 1963; Huang et al., 1979; Bath, 1984; Mantovani et al., 1986; Mantovani et al., 1987; Mantovani et al., 1991; Kafri and Shapira, 1990; Buckthought and Polimenakos, 1993; Muço, 1995, 1999; Pandey and Chadha, 2003; etc.). First we standardized the time series converting linearly the segment between the minimum and maximum of the original data, into the segments 0-10. The standardized time series for each zone are shown in Figures 5 and 6.

Then we obtained the cross-correlation function (CCF) by evaluating the cross-correlation coefficients between the elements of each pair of time series, $x(t)$ and $y(t)$. That is, for each lag k (positive or negative), the cross-correlation function estimates the correlation between $y(t+k)$ and $x(t)$. The lags are the time periods separating data in one time series from the data in the other time series when calculating the cross-correlation coefficients. A high correlation with a positive lag means that the 2nd variable can be used to predict the 1st variable, while a correlation with a negative lag means that the 1st variable can be used to predict the 2nd variable. Figure 7 shows some CCFs of the time-series combinations.

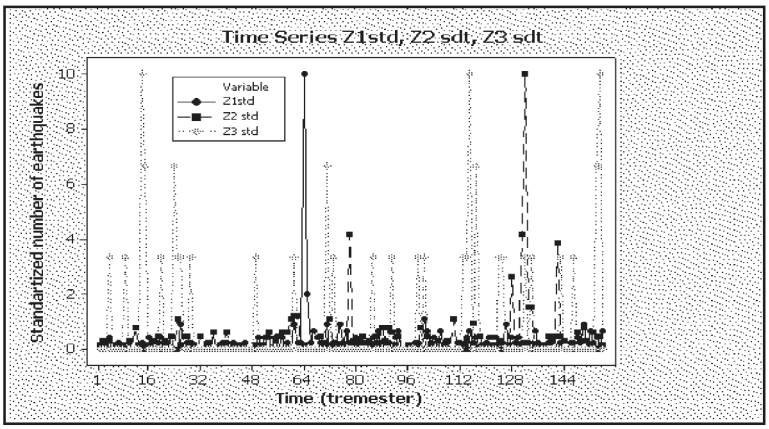

Figure 5. Standardized time series for zones 1,2 and 3

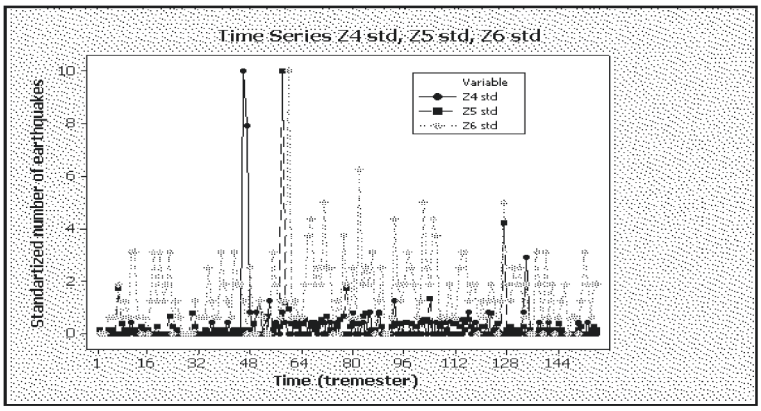

Figure 6. Standardized time series for zones 4,5 and 6

The second step involved checking the CCF results by cross-correlating the time series obtained from ADRIA-1 catalogue. Because this catalogue is not complete for M≥5.5 for the entire time period, the construction of the time series for all the period 1501-2003 doesn't help much. We limited this check of our first cross-correlating results to the time series of ADRIA-2, with the time series of ADRIA-1 for the period 1900-2003 and 1800-2003.

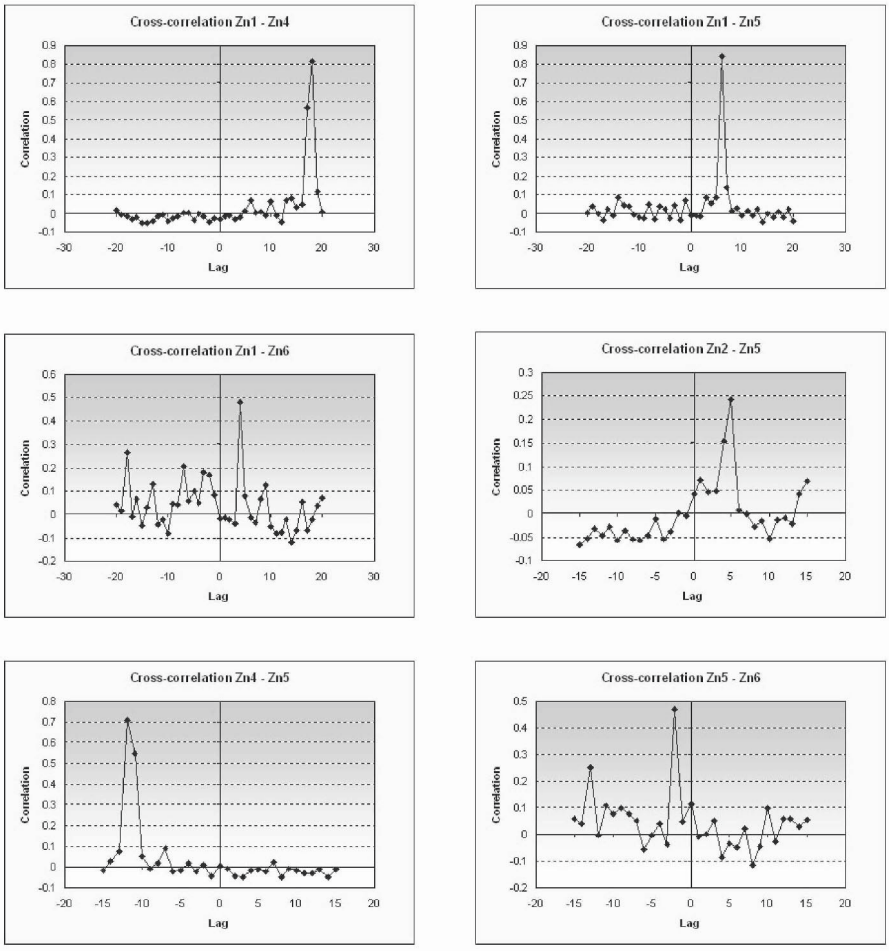

Figure 7. Graphs of cross-correlation between some of the time series.

When the distribution of time series is not normal (the case here) the degree of association between time series can be calculated using rank correlation. Instead of using the precise values of the time series, the data are ranked in order of size and calculations are based on the ranks of corresponding values of z_i and z_j. For testing the significance of correlations, we used Kendall rank correlation for the lags of the best cross-correlation results. From the results of the Kendall rank correlation tests, we accepted only the cases where the associated probability values were less than 5%.

The results of cross-correlation analysis and testing of Kendall rank correlation are comprised in Tables 3 and 4.

Table 3. The results of Kendall's tau rank correlation analysis. The arrows in the first column show the direction of relationships.

Zone relations	Kendall's τ rank correlation		
	τ	Probab.	Interval
Zone 1→ Zone 2	0.043	0.449	-0.09 – 0.203
Zone 1 → Zone 3	0.044	0.432	-0.174 – 0.11
Zone 1 ← Zone 4	0.114	0.041	-0.041 – 0.284
Zone 1 ← Zone 5	0.279	0.0015	0.044 – 0.307
Zone 1 ← Zone 6	0.114	0.041	-0.024 – 0.239
Zone 2 ← Zone 3	0.024	0.475	-0.086 – 0.187
Zone 2 → Zone 4	0.080	0.148	-0.193 – 0.045
Zone 2 ← Zone 5	0.117	0.036	-0.014 – 0.237
Zone 2 ← Zone 6	0.031	0.578	-0.101 – 0.177
Zone 3 - Zone 4	-	-	-
Zone 3 ← Zone 5	0.150	0.009	0.0 – 0.288
Zone 3 - Zone 6	-	-	-
Zone 4 → Zone 5	0.146	0.011	0.0 – 0.314
Zone 4 → Zone 6	0.148	0.034	-0.047 – 0.255
Zone 5 → Zone 6	0.196	0.0427	-0.029 – 0.230

DISCUSSION AND CONCLUSIONS

Generally earthquakes in a sequence are not independent (Scholz, 1990). Their time of generation is a function of tectonic loading of the seismogenic faults but is also affected by stress changes caused by prior events occurring nearby (Voisin, 2002). Modeling of earthquake interactions pointed out that even small stress changes of the order of 1 bar (0.1 MPa), a fraction of the stress drop during an earthquake, can influence the time and location of other earthquakes in the region. Even cumulative stress changes much smaller than 0.1 bar (0.01 MPa) can have a significant triggering effect (Ziv and Rubin, 2000).

Table 4. Results of cross-correlation analysis and Kendall's tau rank correlation. CCF is cross-correlation coefficient, the column "months" shows the time lag for which the best CCF is reached. Last column shows if the hypothesis of interdependence is true or false after Kendall's tau rank correlation whose detailed results are given on Table 3.

Zone relations	1963-2003		1901-1003		1801-2003		Kendall's τ rank correlation
	CCF	mon.	CCF	mon.	CCF	mon.	
Zone 1→ Zone 2	0.275	42	0.163	39	-	-	not accepted
Zone 1 → Zone 3	0.198	21	-	-	-	-	not accepted
Zone 1 ← Zone 4	0.815	54	-	-	-	-	accepted
Zone 1 ← Zone 5	0.837	18	0.161	18	0.165	18	accepted
Zone 1 ← Zone 6	0.479	12	0.115	15	-	-	accepted
Zone 2 ← Zone 3	0.454	51	-	-	-	-	not accepted
Zone 2 → Zone 4	0.149	6	-	-	0.157	48	not accepted
Zone 2 ← Zone 5	0.242	15	-	-	-	-	accepted
Zone 2 ← Zone 6	0.218	15	-	-	0.116	12	not accepted
Zone 3 - Zone 4	-	-	-	-	-	-	no correlation
Zone 3 ← Zone 5	0.246	39	-	-	-	-	accepted
Zone 3 - Zone 6	-	-	-	-	-	-	no correlation
Zone 4 → Zone 5	0.706	36	0.250	33	0.124	30	accepted
Zone 4 → Zone 6	0.339	42	0.203	6	0.130	6 →	accepted
Zone 5 → Zone 6	0.467	6	0.193	3	-	-	accepted

Numerous studies have emphasized the role of static Coulomb stress transfer (Harris, 1998 and references therein). Dynamic stresses also have been considered responsible for triggering earthquake aftershocks (King et al., 1994; Kilb et al., 2000, 2002) or of temporal doublets of strong earthquakes (Tao et al., 2002). The triggering of subsequent seismic events along the same fault also has been suggested for small earthquakes and short periods (Muço, 1994a, 1994b) as well as for large earthquakes and long periods (Roth, 1988; Stein et al., 1997; Wan et al., 2003). More impressively, one earthquake may change the failure stress of a different fault (Stein et al., 1992; Papadimitriu, 2002). Some authors have modeled dynamic triggering on different faults (Harris et al., 1991; Yamashita, 1995). It has been suggested, for example, that the Landers earthquake of 1992 triggered successive rupture on four other faults (Wald and Heaton, 1994).

There are authors who have studied triggering of small events for relatively short time periods (Harris and Simpson, 1992; King et al., 1994; Muço, 1994b; Harris et al., 1995). Other authors have focused instead on the

interaction of large earthquakes and large time scales (Harris and Simpson, 1997; Deng and Sykes, 1997; Nalbant et al., 1998; Pollitz et al., 2003), and others have pointed out that earthquakes might produce long-term physical changes over large areas (Gao et al., 2000).

Coming back to Adria microplate we can say that the faults along its convergent margin with both the Balkans and the Apennine peninsula, to a large extent, belong to the same fault system or at least to systems that are connected with each other. On the other hand, considering the microplate as a rigid and homogenous tectonic unit, we suggest that the interaction between earthquakes at different parts of this unit might be realized through stress transfer and post-seismic relaxation more easily than where interrupted by various heterogeneities and randomly oriented faults. Arguing this way, one the interdependence between earthquakes in different parts of the peri-Adriatic region is a plausible phenomenon.

The pioneering papers for this region (Mantovani et al., 1986, 1987, 1991) presented the first evidence of this interrelation. The results of cross-correlation analysis depend on the earthquake data used, from the zones delineated and from the time series constructed and compared. Some of the results from previous analyses include the following. 1) One earthquake with $M \geq 6.0$ in the southern Dinarides is expected to precede another one in the southern Apennines with $M \geq 5.5$ within less than 5 years (Mantovani et al., 1987). 2) The time lag between earthquakes of northern Aegean region and Calabrian earthquakes is less than 5 years, with a dominant value of 2 years (Mantovani et al., 1986). 3) Post-seismic relaxation induced in the Adriatic plate by Dinaric earthquakes might be responsible for the occurrence of seismic events in southern Italy within a few years of the triggering event. In this way, the Montenegro earthquake of 1979 may have induced the Irpinia earthquake of 1980 with a time lag of 1.6 years (Viti et al., 2003). 4) A strong correlation exists between the earthquakes in Apennine chain with a delay of some years (Troise et al., 1998).

As a result of our cross-correlation analysis, the pairs of zones most correlated are: zone 1 and zone 4 with a time lag of 54 months, zone 1 and zone 5 with a time lag of 18 months, zone 1 and zone 6 with a time lag of 12 months, zone 2 and zone 5 with a time lag of 15 months, zone 3 and zone 5 with a time lag of 39 months, zone 5 and zone 4 with a time lag of 36 months, zone 6 and zone 4 with a time lag of 42 months and zone 6 and zone 5 with a time lag of 6 months. One can see that the presumed triggering of earthquakes is coming from the east side of the Adriatic region to the west side; thus there are the earthquakes of the western Balkan coast that influence the timing of seismic events in the Italian peninsula. On the other hand, it is the most northern part of the Dinarides and Italian part of the Southern Alps (zone 4) that influence southern zones 5 and 6. Further detailed analysis and seismic stress modeling is needed to clarify if this statistical correlation is due to focal

mechanisms of earthquakes of the eastern zones (mostly thrust) or because of some other geodynamic processes.

As for seismological analysis of the area, it is clear that the most part of seismic energy during the last 500 years has been released in zones 5 and 6 (Dinarides, Albanides, and northwestern Helenides). This is evident even from the seismic hazard of the region. The seismic energy released on the east side of the Adriatic is almost 5 times greater than the energy released on the west side. If the Adriatic plate would have an independent movement, it would be hard to explain such a difference in seismic energy release. The kinetic energy produced by motion of an independent Adria microplate for 500 years and the gravitational energy of its mass under Apennine Peninsula, are far lower than the seismic energy release we have calculated as $E= 8.32 \times 10^{23}$ erg. This suggests that the Adria microplate probably is still attached to the African Plate.

ACKNOWLEDGEMENTS

The author thanks D. Simpson for valuable comments and S. Hardy for generously providing the facilities of the Carnegie Institution of Washington, USA. SPSS, MedCalc and WinSTAT were used for statistical data analysis. A part of seismological analysis was made with Wizmap 2.05, with the help of its author, R. Musson, which is deeply appreciated. AGIS 1.73 was used for mapping epicenters.

REFERENCES

Aliaj Sh. Transverse faults in Albanian Orogen front. Alb.J. Nat.Techn. Sci. 1999; 6.

Ambraseys N.N. Reassessment of earthquakes, 1900-1999, in the Eastern Mediterranean and the Middle East. Geophys. J. Int. 2001;145: 471-485.

Anderson H., Jackson, J.A. Active tectonics of the Adriatic region. Geoph. J. R. A. Soc. 1987; 91: 937-983.

Babucci D., Tamburelli C., Mantovani E., Viti M., D'Onza F., Albarello D. Geophys. Res. Abstracts, European Geophysical Society 2003; 5: 11,333.

Bath M. Correlation between regional and global seismic activity. Tectonophysics 1984; 104: 187-194.

Battaglia M., Murray M.H., Serpelloni E., Burgman R., The Adriatic region: an independent microplate within the Africa-Eurasia collision zone. Eos Trans., AGU, 2003, 84 (46), Fall Meeting, Suppl. Abstracts.

Boschi E., Guidoboni E., Ferrari G., Valensise G., Gasperini P. Catalogo dei forti terremoti in Italia dal 461 a.c. al 1990. Istituto Nazionale di Geofisica e SGA editori, Bologna, 644 pp.(available also at web page: http://www.ingv.it/~roma, maintained by National Institute of Geophysics, Roma, Italy).

Buckthought K., Polimenakos L.C. Earthquake seasonality in the area of Greece. Proceeding of the 2nd Congress of the Helenic Geophys. Union, Florina, Greece, 5-7 May, 1993; 366-377.

Channell J.E.T., Horvath F. The African/Adriatic Promontory as a Paleogeographical Premise for Alpine Orogeny and Plate Movements in the Carpatho-Balkan Region. Tectonophysics 1976; 35: 71-101.

Channell J.E.T., D'Argenio B., Horvath F. Adria, the African Promontory, in Mesozoic Mediterranean paleogeography. Earth Science Reviews 1979; 15: 213-292.

Channell J.E.T. Paleomagnetism and Paleogeography of Adria. In *Paleomagnetism and tectonics of the Mediterranean region*, A. Morris, D.H. Tarling, eds., Geol. Soc. Spec. Publ. 1996; 105: 119-132.

Console R., Giovambattista R., Favali P., Presgrave B.W., Smriglio, G. Seismicity of the Adriatic microplate. Tectonophysics 1993; 218: 343-354.

Constandinescu L., Ruprechtova L., Enescu D. Mediterranean-Alpine earthquake mechanism and their seismotectonic implication. Geophys. J. 1966; 10: 147-168.

Cvijanovic D., Prelogovic E. Skoko D. Seismotektonska karta SR Hrvatske. Acta Seismologica Iugoslavica 1976; 4, Beograd, 19-23.

Deng J., Sykes L.R. Evolution of the stress field in southern California and triggering of moderate-size earthquakes: a 200-year perspective. J. Geophys. Res. 1997; 102: 9859-9886.

Dercourt J., Zonenshain L.P., Ricou L.-E., Kazmin V.G., Le Pichon X., Knipper A.L. Grandjacquet C., Sbortshikov I.M., Geyssant J., Lepvrier C., Perchersky D.H., Boulin J., Sibuet J.-C., Savostin L.A., Sorokhtin O., Westphal M., Bazhenov M.L., Lauer J.P., Duval B. Geological evolution of the Tethys from the Atlantic to the Pamirs since the Lias. In *"Evolution of the Tethys",* J. Auboin, X. Le Pichon, A.S. Monin, eds., Tectonophysics 1986; *123:* 241-315.

Dewey J.F., Helman M.L., Turco E., Hutton D.H.W., Knott S.D. Kinematics of western Mediterranean. In *Alpine Tectonics*, M.P. Coward, D. Dietrich, R.G. Park, eds., London: Geol. Soc. Spec. Publ. 1989; 45: 265-283.

Favali P., Funicello R., Mattietti G., Mele G., Salvini F. An active margin across the Adriatic Sea (central Mediterranean Sea). Tectonophysics 1993; 219: 109-117.

Frepoli A., Amato A. Contemporaneous extension and compression in the Nothern Apennines from earthquake fault plane solutions. Geophys. J. Int. 1997; 129: 368-388.

Gao S.S., Silver P.G., Linde A.T., Sacks I.S. Annual modulation of triggered seismicity following the 1992 Landers earthquake in California. Nature 2000; 406: 500-504.

Gasparini G., Iannaccone G., Scarpa R. Fault-plane solutions and seismicity of the Italian peninsula. Tectonophysics 1985; 117: 59-78.

Goldsworthy M., Jackson J., Haines J. The continuity of active fault systems in Greece. Geophys. J. Int. 2002; 148(3): 596-618.

Harris R.A., Archuleta R.J., Day S.M. Fault steps and the dynamic rupture process: 2-d numerical simulation of a spontaneously propagating shear fracture. Geophys. Res. Lett. 1991; 18: 893-896.

Harris R.A., Simpson R.W. Changes in static stress on southern California faults after the 1992 Landers earthquake. Nature 1992; 360: 251-254.

Harris R.A., Simpson R.W., Reasenberg P.A. Influence of static stress changes on earthquake location in southern California. Nature 1995; 375: 221-224.

Harris R.A. Introduction to special section: Stress triggers, stress shadows, and implication for seismic hazard. J. Geophys. Res. 1998; 103: 24,347-24358.

Huang L.Sh., McRaney J., Teng T.L., Prebish M. A preleminary study on the relationship between precipitation and large earthquakes in Southern California. Pure Appl. Geophys. 1979; 117: 1286-1300.

Jimenez M.J., Giardini D., Grunthal G., SEZAME Working Group (Erdik, M., Garcia-Fernandez, M., Lapajne, J., Makropoulos, K., Musson, R., Papaioannou, Ch., Rebez, A., Riad, S., Sellami, Sh., Shapira, A., Slejko, D., van Eck, T., el Sayed, A.). Unified Seismic hazard modeling throughout the Mediterranean region. Boll. Geofis. Teor. Appl. 2001; 42 (1-2): 3-18.

Kafri U., Shapira A. A Correlation Between Earthquake Occurrence, Rainfall And Water Level In Lake Kinnereth, Israel. Phys. Earth Plan. Int. 1990; 62: 277-283.

Karnik V. Seismicity of Europe and the Mediterranean, Klima, K., eds., Geophys. Inst. of the Academy of Sciences of the Czech Republic and StudiaGeo, Praha, 1996.

Kilb D., Gomberg J., Bodin M. Triggering of earthquake aftershocks by dynamic stresses. Nature 2000; 408: 570-574.

Kilb D., Gomberg J., Bodin P. Aftershock triggering by complete Coulomb stress changes, J. Geophys. Res. 2002; 107, 10.1029/2001JB000202.

King G. C. P., Stein R., Lin J. Static stress changes and the triggering of earthquakes. Bull. Seism. Soc. Am. 1994; 84: 935-953.

Lowrie W. Paleomagnetism and the Adriatic promontory: A reappraisal. Tectonics 1986; 5: 797-807.

Louvari E., Kiratzi A. Pattern of deformation in a broader Adriatic area. In *Proc. of 3rd Int.Conf. on the Geology of Eastern Mediterranean,* I. X. Panayides, J. Malpas, eds., 2000; 147-158.

Louvari E., Kiratzi A., Papzachos B., Hatzidimitriou P. Fault-plane solutions determined by waveform modeling confirm tectonic collision in the Eastern Adriatic. Pure Appl. Geoph. 2001; 158: 1613-1637.

Macropoulos K., Burton P.W. A catalogue of seismicity of Greece and adjacent areas. Geophys. J. R. Astron. Soc. 1981; 65: 741-762 (and Microfische GJ 65/1).

Mantovani E., Albarello D., Mucciarelli M. Seismic activity in North Aegean region as middle term precursor of Calabrian earthquakes. Phys.Earth Planet.Inter.1986; 44: 264-273.

Mantovani E., Mucciarelli M., Albarello D. Evidence of interrelation between the seismicity of Southern Apennines and Southern Dinarides. Phys. Earth Planet. Inter. 1987; 49: 259-263.

Mantovani E., Boschi E., Albarello D., Babbucci D., Mucciarelli M. Regularities of time-space distribution of seismicity in the periadriatic regions: tectonic implications. Tectonophysics 1991; 188: 349-356.

McGinnis L. Earthquakes and crustal movement related to water load in the Missisipi Valley, Il. State Geol. Surv. Circ. 1963; 344: 20.

McKenzie D.P. Active Tectonics of the Mediterranean region. Geoph. J. R. Astr. Soc. 1972; 30: 109-185.

Mele G. The Adriatic lithosphere is a promontory of the African plate: Evidence of a continuous mantle lid in the Ionian Sea from efficient Sn propagation. Geophys. Res. Lett. 2001; 28 (3): 431-434.

Muço B. A. Focal Mechanism solutions of Albanian earthquakes for the period 1964 – 1988. Tectonophysics 1994; 231: 311-323.

Muço B.B. Fault Detection by Lineaments of Consecutive Epicenters. Bull. Geol. Soc. of Greece 1994; Vol.XXX/5: 285-294.

Muço B. The Seasonality of Albanian Earthquakes and Cross-Correlation with Rainfall. Phys. Earth Planet. Int. 1995; 88: 285 - 291.

Muço B. The collision between Adria and Albanian orogen on the light of focal mechanism solutions, 10th European Conference on Earthquake Engineering, Viena, Austria, Duma (ed.), Balkema, Roterdam 1995; 37-41.

Muço B. The Shkoder-Peja (Northern Albania) transcurrent fault and its seismic activity, 1976-1995. Bulletin of Geological Society of Greece 1998; XXXI/1: 165-171.

Muço B. Statistical investigation on possible seasonality of seismic activity and rainfall - induced earthquakes in Balkan area. Phys. Earth Planet. Int. 1999; 114: 119-127.

Nalbant S. S., Hubert A., King G. C. P. Stress coupling between earthquakes in northwest Turkey and the north Aegean Sea. J. Geophys. Res. 1998; 103: 24,469-24,486.

Pandey A.P., Chadha R.K. Surface loading and triggered earthquakes in the Koyna-Warna region, western India, Phys. Earth Planet. Int. 2003; 139: 207-223.

Panza G.F., Pontevivo A., Chimera G., Raykova R., Aoudia A. The lithosphere-asthenosphere: Italy and surroundings. Episodes, Contents and Abstracts 2003; 26 (3).

Papadimitriou E. Mode of strong earthquake recurrence in the Central Ionian Islands (Greece): Possible triggering due to Coulomb stress changes generated by the occurrence of previous strong shock. Bull. Seism. Soc. Am. 2002; 92 (8): 3293-3308.

Papazachos B., Papazachou C. *The earthquakes of Greece*, Ziti editions, 1997, Thessaloniki, 304 pp.

Pondrelli S., Morelli A., Ekström G., Mazza S., Boschi E., Dziewonski A.M. European-Mediterranean regional centroid-moment tensors: 1997-2000. Phys. Earth Planet. Int. 2002; 130: 71-101.

Pollitz F., Vergnolle M., Calais E. Fault interaction and stress triggering of twentieth century earthquakes in Mongolia. J. Geophys. Res. 2003; 108 (B10): 2503.

Roth F. Modelling of stress patterns along the western part of the North Anatolian fault zone. Tectonphysics 1988; 152: 215-226.

Scholz C. *The mechanics of earthquakes and faulting*. Cambridge Univ. Press, Cambridge, 1990, 439 pp.

Scordilis E.M., Karakaisis G.F., Karakostas B.G., Panagiotopoulos D.G., Comninakis P.E., Papazachos C. Evidence for transfrom faulting in the Ionian Sea: the Cephalonia Island earthquake sequence. Pure Appl. Geophys. 1985; 123: 388-397.

Shebalin N.V., Leydecker G., Mokrushina N.G., Tatevossian R.E., Erteleva O.O., Vassiliev V.Ju. Earthquake Catalogue for Central and Southwestern Europe (342 B.C – 1990 A.D.). European Commission , Rep.No.ETNU CT 93-0087, Brussels, 1998 (available also at web page: http://www.bgr.de/quakecat/eng/catalogs.htm, maintained by Günter Leydecker, Bundesanstalt für Geowissenschaften und Rohstoffe, Hannover, Germany).

Slejko D., Camassi R., Cecic I., Herak D., Herak M., Kociu S., Kouskouna V., Lapajne J., Makropoulos K., Meletti C., Muco B., Papaioannou C., Peruzza L., Rebez L., Scandone P., Sulstarova E., Voulgaris N. GSHAP seismic hazard assessment for the Adria region. Ann. Geofis. 1999; 42(1): 1085-1107.

Stein R. S., King G. C. P., Lin J. Change in failure stress on the southern San Andreas fault system caused by the 1992 magnitude = 7.4 Landers earthquake. Science 1992; 258: 1328-1332.

Stein R., Barka A., Dieterich J. Progressive failure on the North Anatolian fault since 1939 by earthquake stress triggering. Geophys. J. Int. 1997; 128: 594-604.

Sulstarova E., Peci V., Shuteriqi P. Vlora-Elbasani-Dibra (Albania) transversal fault zone and its seismic activity. J. Seismol. 2000; 4: 117-131.

Tao P., Cheng-hu Zh., Quan-lin L., Jin-biao C. Statistical analysis on temporal-spatial correlativity within temporal doublets of strong earthquakes in North China and its vicinity. Acta Seismol. Sinica 2002; 15, 1: 56-62.

Troise C., De Natale G., Pingue F., Petrazzuoli S.M. Evidence for static stress interactionamong earthquakes in the south-central Apennines (Italy). Geophys. J. Int. 1998; 134: 809-817.

Udias A. Seismicity and seismotectonic stress field in the Alpine-Mediterranean region. Am. Geophys. Union, Geodynamics series 1982; 7: 75-82.

Udias A., Buforn E., Ruiz de Gama J. Catalogue of focal mechanism of European earthquakes. Dept. of Geophysics, Universidad Complutense, Madrid, 1989.

Viti M., D'Onza F., Mantovani E., Albarello D., Cenni N. Post seismic relaxation and earthquake triggering in the Southern Adriatic region. Gephys. J. Int. 2003; 153: 645-657.

Voisin C. Dynamic triggering of earthquakes: The nonlinear slip-dependent friction case. J. Geophys. Res. 2002; 107: 1029/2001JB001121.

Wald D.J., Heaton T.H. Spatial and temporal distribution of slip for the 1992 Landers, California, earthquake. Bull. Seismol. Soc. Am. 1994; 84: 668-691.

Wan Y.-G., Wu Zh.-L., Zhou G.-W., Huang J. "Stress triggering" between different rupture events in several earthquakes, Acta Seismol. Sinica 2000; 13, 6: 607-615.

Westaway R. Present-day kinematics of the plate boundary zone between Africa and Europe, from Azores to the Aegean, Earth Plan. Sci. Lett. 1990; 96: 393-406.

Yamashita T. Simulation of seismicity due to ruptures on noncoplanar interactive faults. J. Geophys. Res. 1995; 100: 8339-8350.

Ziv A., Rubin A.M. Static Stress Transfer and Earthquake Triggering: No Lower Threshold in Sight? J. Geophys. Res. 2000; 105: 13,631-13,642.

SEISMIC HAZARD IN THE PANNONIAN REGION

László Tóth[1,3], Erzsébet Győri[2], Péter Mónus[1,3], Tibor Zsíros[1,3]
1: Seismological Observatory, Hungarian Academy of Sciences, Budapest, Hungary
toth@georisk.hu
2: Research Group of Geophysics and Environmental Physics of HAS , Budapest, Hungary
3: GeoRisk Earthquake Research Institute, Budapest, Hungary

ABSTRACT

Seismic hazard for single sites and hazard maps for the whole Pannonian region (44.0-50.0N; 13.0-28.0E) have been calculated. The hazard assessment was carried out using a probabilistic approach by incorporating a wide range of parameter values and viable interpretations that were consistent with the data. Alternative interpretations were described by branches of a logic tree. Each branch was weighted according to the ability of that interpretation to explain the available data. The resulting seismic hazard map describes expected shaking with a 475-year return period in terms of peak ground acceleration. Furthermore, some important contributors to seismic risk are highlighted, and a liquefaction hazard map is presented for the territory of Hungary.

Keywords: seismicity, seismic hazard, Pannonian Basin

INTRODUCTION

The Pannonian region is situated between the Mediterranean area, which is one of the most seismically active regions in the world, and the East European platform, which can be treated as nearly aseismic. Deformation in the Pannonian basin system is ongoing (Bada et al. 1998, Horváth and Cloetingh 1996). One of the most direct pieces of evidence for the continuing deformation, in addition to GPS geodetic data (Grenerczy et al. 2002), is current seismic activity (Bada et al. 1999, Gerner et al. 1999).

In the following paper, we give a brief review of seismic hazard methodology, present the latest seismic hazard map of the region and highlight some chief factors (e.g., site effect, liquefaction) contributing to seismic risk.

N. Pinter et al. (eds.), The Adria Microplate: GPS Geodesy, Tectonics and Hazards, 369–384.

SEISMICITY SUMMARY

Seismic activity in the Pannonian region can be characterized as moderate, with significant variations in different tectonic domains. The highest seismicity rate is observed in the Vrancea region in the southeast Carpathians, where strong earthquakes occur quite frequently. Within the last decades, three events were detected with magnitudes larger than 6.5 (1977: M7.2; 1986: M7.0; 1990: M6.7), while magnitude 5.0 earthquakes occur on an almost yearly basis.

In the less active Pannonian basin area (about 200,000 km^2), the return period of magnitude 6 earthquakes is about 100 years while magnitude 5 events occur every 20 years on average. Based on the results of high sensitivity monitoring in the last decade (Tóth et al. 2004), the average number of magnitude 3 earthquakes is 4 per yearwhile that of magnitude 2 events is about 30 per year.

Distribution of focal depths suggests three depth domains. Shallow focal depths within the top 20 km of the earth's crust occur almost exclusively through the whole Pannonian region except the Vrancea zone. In the Pannonian basin, the majority of events occur between 6 and 15 km below ground level. Earthquakes of the Vrancea region are characterized by intermediate depths. Strong earthquakes occur between either 70-110 km or 125-160 km depth domains within an almost vertical column. Deeper and shallower events also have been recorded but only with small magnitudes.

Inferred from focal mechanism solutions (Tóth et al., 2002), strike-slip and thrust faulting occurs almost exclusively through the Southern Alps and the Dinarides. The maximum horizontal stress direction clearly shows N-S and NNE-SSW compression that can be explained by the collision of Adria with Europe.

Moderately active seismicity is observed in the Eastern Alps and the western Carpathians. Focal mechanism solutions are available mostly from the Vienna Basin area, documenting exclusively strike-slip mechanisms. NNW-SSE and N-S directions of the largest horizontal stresses are the most frequent, but NE-SW directions are occasionally encountered.

In the Pannonian Basin, the picture shown by the focal mechanism solutions is more diverse, however thrust and strike-slip faulting seems to be dominant. NNE-SSW and NE-SW directions of maximum horizontal stresses prevail, highlighting significant differences from Western Europe, where the dominant stress direction is perpendicular to that. The very few fault-plane solutions available from the area of eastern and southern Carpathians indicate thrust faulting and E-W dominant stresses. Most events in the Vrancea area are compressional and occur at intermediate depths. Fault-plane solutions of instrumentally recorded large earthquakes show remarkably similar

characteristics. They typically strike SW-NE and dip to the NW. The maximum horizontal stress characteristically trends NW-SE and in fewer cases E-W.

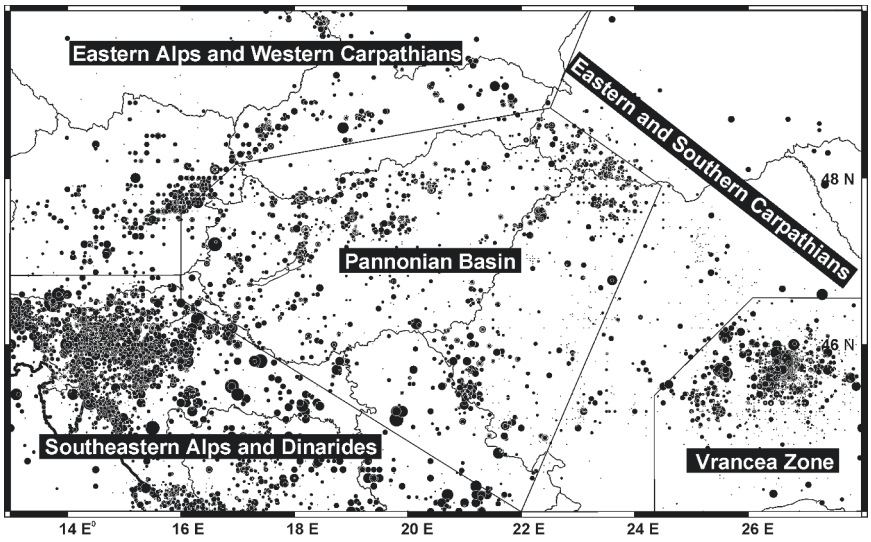

Figure 1. Seismicity of the Pannonian region (44.0-50.0N; 13.0-28.0E). The earthquake database contains more than 20,000 historical and instrumentally recorded events from 456 AD until 2002.

SEISMIC HAZARD METHODOLOGY APPLIED

Seismic hazard is the probabilistic measure of ground shaking associated with the recurrence of earthquakes as originally defined by Cornell (1968). Seismic hazard shows the level of chosen ground motion that likely will not be exceeded during a specified time interval. Hazard assessment for civil use commonly specifies a 90% probability of non-exceedance of some ground motion parameter (most often ground acceleration) for an exposure time of 50 years, corresponding to a return period of 475 years. For nuclear power plants and other installations posing higher environmental risk, it is common practice to use much lower probability events on the order of 10^{-4} to 10^{-6}/year.

The methodology used to assess seismic hazard and the associated uncertainty at nuclear and non-nuclear fields must provide technically sound results and should: be experience-based, be data-driven, incorporate proper treatment of uncertainties, be flexible and facilitate sensitivity analysis.

Six essential steps are involved in the assessment of seismic hazard:

Step 1: Evaluation of seismic sources.

Estimate the geometries and spatial distribution of potential sources of future seismic activity in the region. Characterize the assumed uncertainty in the spatial description of each source.

Step 2: Characterization of seismic sources.

For each seismic source, describe the distribution of occurrence rates of future earthquakes as a function of magnitude. Estimate the maximum magnitude for each source. Characterize the uncertainty in recurrence relations and in maximum magnitude.

Step 3: Ground motion attenuation.

Evaluate or estimate relations that express how the amplitudes of selected ground-motion parameters vary with earthquake magnitude and distance for the region. Characterize the uncertainty in these ground-motion attenuation relations.

Step 4: Mathematical model to calculate seismic hazard.

Calculate the seismic hazard for each combination of inputs (determined in steps 1-3) and integrate the results. Plot a curve expressing the annual probability that a given value of ground motion will be exceeded. Carry out the integration for all combinations of inputs to incorporate the variability of input estimates.

Step 5: Presentation of the hazard results.

Express the results of step 4 as a distribution of seismic hazard curves that can be represented by a mean curve and curves representing particular percentiles of the distribution.

Step 6: Site effect, secondary seismic effects

Calculate the influence of the local geological setting on the ground motion.

DATABASE

The first and most important component of a probabilistic seismic hazard study is the compilation of the geological, geophysical and geotechnical data on regional (1:500,000), near-regional (1:50,000), site vicinity (1:5,000) and site area (1:500) scales. Seismological databases are developed on different time scale zooming on different event recurrence rates such as paleo-earthquakes ($<10^{-3}$/yr), historical earthquakes (10^{-3}-10^{-2}/yr), instrumental earthquake data (10^{-2}-10^{-1}/yr) and site-specific instrumental data or local seismic monitoring ($>10^{-1}$/yr).

The geology and tectonic evolution of the Pannonian region has been studied intensively over recent decades. The development of the Carpathian mountain belt and the Pannonian basin has been attributed to the collision between the Eurasian Plate and the African Plate between the Paleocene and Middle-Late Miocene (e.g., Horváth, 1988; Csontos et al., 2002; Fodor et al., 1999).

The comprehensive earthquake catalogue of the Pannonian region (44.0-50.0 N latitude and 13.0-28.0 E longitude) contains more than 20,000 events ranging from 456 A.D. to the present. The preparation of the earthquake catalogue is documented in detail in Zsíros (2000), Tóth et al. (2002) and Zsíros (2003a and 2003b).

Magnitude

The earthquake catalogue of the Pannonian region goes far back to pre-instrumental time. However, for historical earthquakes the only source of information is macro seismic observation. It seems rational to suppose that there is some relation between magnitude, epicentral intensity and depth. Many authors (eg. Csomor and Kiss, 1959; Karnik, 1968) suppose that magnitude depends on epicentral intensity and focal depth according to the relation:

$M_M = a\, I_0 + b\, \log h + c$

where M_M is the macroseismic magnitude, I_0 the epicentral intensity, h the focal depth in km; and a, b, c are constant parameters.

Table 1 shows the best-fit constants in the above equation for shallow Pannonian-region earthquakes, and for intermediate-depth events in the Vrancea region.

Table 1. Value and uncertainty of a, b and c in $M_M = a\, I_0 + b\, \log h + c$, as well as the magnitude and intensity intervals and the number of events N.

Area	a	b	c
for the Pannonian region $1 \le h \le 65$ $III \le I_0 \le X$ $0.6 \le M_M \le 6.2$ N = 514	0.68 ± 0.02	0.96 ± 0.07	- 0.91 ± 0.10
for the Vrancea region $1 \le h \le 200$ $II \le I_0 \le IX$ $2.4 \le M_M \le 7.3$ N = 130	0.52 ± 0.02	0.55 ± 0.11	1.18 ± 0.20

The best-fit relation for shallow Pannonian-region earthquakes using 12.6 km average focal depth gives: $M_M = 0.68\ I_0 + 0.15$.
For intermediate-depth seismicity in the Vrancea region, using 92.5 km average focal depth: $M_M = 0.52\ I_0 + 2.27$.

A simple linear regression between measured surface-wave magnitude (M_S) and epicentral intensity (I_0) for the whole catalogue of events where both M_S and I_0 exist, gives: $M_S = 0.74\ I_0 - 0.28$. The macroseismic and surface-wave magnitude values estimated from intensity are generally quite similar (Tóth et al., 2002). Table 2 shows the empirical relations between different magnitude scales used in the earthquake catalogue.

Table 2. Value and uncertainty of a and b in the equation of $M_X = a\ M_Y + b$ as well as the magnitude intervals and the number of events N.

	M_M	M_B	M_L	M_D
M_S =	a = 1.03 ± 0.02 b = - 0.20 ± 0.10 2.0 ≤ M_S ≤ 7.0 2.0 ≤ M_M ≤ 6.8 N = 186	a = 0.97 ± 0.05 b = 0.04 ± 0.24 2.5 ≤ M_S ≤ 7.0 2.1 ≤ M_B ≤ 6.4 N = 127	a = 0.86 ± 0.06 b = 0.57 ± 0.27 2.0 ≤ M_S ≤ 7.0 2.0 ≤ M_L ≤ 6.6 N = 97	a = 1.21 ± 0.11 b = - 1.23 ± 0.52 2.3 ≤ M_S ≤ 6.9 2.8 ≤ M_D ≤ 6.5 N = 27
M_B =			a = 0.59 ± 0.55 b = 1.75 ± 0.22 2.6 ≤ M_B ≤ 6.4 2.1 ≤ M_L ≤ 6.6 N = 259	a = 0.90 ± 0.08 b = 0.20 ± 0.32 2.6 ≤ M_B ≤ 6.3 3.2 ≤ M_D ≤ 6.5 N = 160
M_L =				a = 1.14 ± 0.02 b = - 0.69 ± 0.06 0.8 ≤ M_L ≤ 5.5 1.4 ≤ M_D ≤ 5.6 N = 894

Earthquake recurrence

Seismicity in the Pannonian area is a typical example of distributed seismicity. Due to inaccurate seismic and geological information, most earthquakes cannot be assigned to specific tectonic structures: i.e., the present seismotectonic knowledge of the area does not allow us to ascertain which fault produced which earthquake. This is particularly true for events below magnitude 4. For large historical earthquakes, the difficulty mostly comes from inaccurate hypocenter information. In areas where underlying faults are unknown, the current practice is to represent the temporal occurrence of earthquakes as a Poisson process. For this purpose, all foreshocks and aftershocks should be removed from the earthquake catalogue, and the

completeness of the catalogue should be assessed. In a complete catalogue, all earthquakes above a lower bound magnitude – the threshold magnitude M_0 – are assumed to be included.

For identifying main shocks, space and time filters should be applied. Dieterich (1994) proposed that the aftershock duration T generally increases with the inferred recurrence time of the main shock T_r such that $T \approx T_r/20$. Stein and Newman (2004) put forward the possibility of much longer aftershock duration for low seismicity intraplate settings, especially for the New Madrid area. This possibility could be explained by higher earthquake stress drops and larger normal stresses on intraplate faults and would have major consequences for seismic hazard of low seismicity areas.

Based on empirical considerations and on our professional judgment to some extent, we used a magnitude-dependent space and time filter to identify main shocks in the catalogue as detailed by Table 3.

Table 3. Space and time windows used for filtering out the aftershocks and foreshocks from the catalogue. In the vicinity of radius R of the magnitude M main earthquake, all shocks with M'< M are regarded as aftershocks or foreshocks if their origin time difference is less than T or T' respectively

Magnitude	R (km)	T (day)	T' (day)
$M_M \leq 1.8$	5	1	1
$1.9 \leq M_M \leq 2.7$	10	2	1
$2.8 \leq M_M \leq 3.3$	15	5	1
$3.4 \leq M_M \leq 4.0$	20	30	2
$4.1 \leq M_M \leq 4.7$	25	130	4
$4.8 \leq M_M \leq 5.4$	30	260	10
$5.5 \leq M_M \leq 6.1$	35	650	15
$6.2 \leq M_M$	40	850	30

A simple comprehensiveness test based on "magnitude recurrence fit" shows that our catalogue is complete since 1500 for magnitude $M_0 \geq 6.4$, since 1600 for magnitude $M_0 \geq 5.8$, since 1700 for magnitude $M_0 \geq 5.3$, since 1800 for magnitude $M_0 \geq 4.7$, since 1850 for magnitude $M_0 \geq 4.2$, and since 1880 for magnitude $M_0 \geq 3.5$ for the whole Pannonian region (Table 4).

The probability of earthquake occurrence as a function of magnitude is generally represented by an exponential distribution, as proposed by Gutenberg and Richter (1944): $\log N = a - bM$, where N is the annual number of earthquakes with magnitude equal or greater than M. From the whole Pannonian region dataset, we find that $a = 5.27 \pm 0.11$ and $b = 1.04 \pm 0.02$ in the $3.5 \leq M_M \leq 7.3$ magnitude range.

Table 4. Completeness test results for the Pannonian region earthquake catalogue

The catalogue is complete	for magnitude
since 1500	$M_0 \geq 6.4$
since 1600	$M_0 \geq 5.8$
since 1700	$M_0 \geq 5.3$
since 1800	$M_0 \geq 4.7$
since 1850	$M_0 \geq 4.2$
since 1880	$M_0 \geq 3.5$

EVALUATION AND CHARACTERIZATION OF SEISMIC SOURCES

In seismic source modeling, a thorough analysis of the main tectonic structures and their correlation with seismicity is the basis for the definition of the source zones. Three source zone models (M1, M2 and M3) were defined with 20, 25, and 15 zones, respectively.

Due to the diffuse seismicity of the whole region, specific faults cannot be identified. We deal here with polygons within which future earthquakes may occur (Figure 2).

An important parameter for source zone characterization is the maximum magnitude value. M_{max} values were assigned only on a seismological basis; seismotectonic or geological evidences were not considered in this respect. The one-step-beyond technique (Slejko et al., 1998) was applied where the number of earthquakes was large enough: the rates were fitted by the Gutenberg-Richter relationship, and the extrapolated rate for a magnitude greater than the maximum observed value by 0.5 magnitude value. In addition, variations were added to handle epistemic uncertainty (Table 5).

The present-day crustal velocity field derived from GPS measurements (Grenerczy et al., 2002) shows that the largest velocities (1.5-2 mm/yr northward) in the Pannonian region can be found in the SW, located in the Alpine-Adriatic collision zone. Inside the Pannonian basin, the typical velocity is about 1.0-1.5 mm/yr eastward.

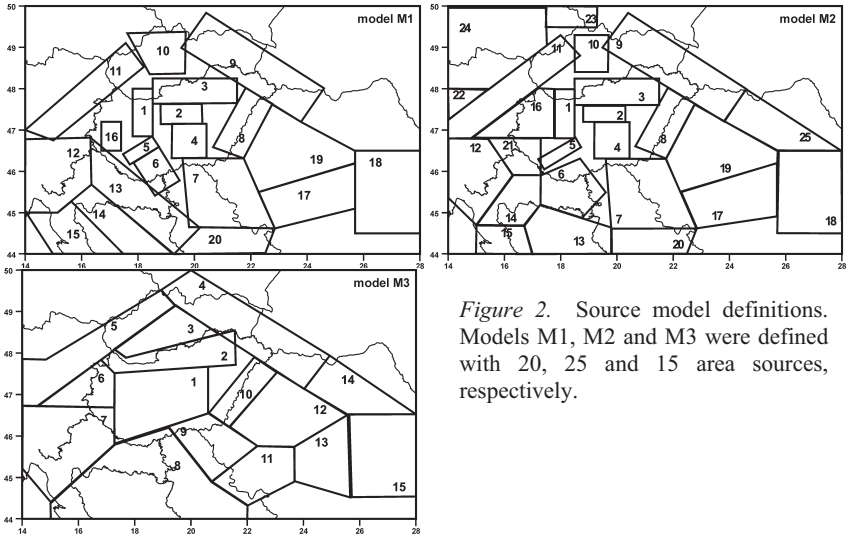

Figure 2. Source model definitions. Models M1, M2 and M3 were defined with 20, 25 and 15 area sources, respectively.

Table 5. Source models M1, M2, M3 and different M_{max} values used in the hazard computations for source zones (see Figure 2 for the definition of the polygons)

Zone #	Source model *M1*			Source model *M2*			Source model *M3*		
	M_{max}^{1}	M_{max}^{2}	M_{max}^{3}	M_{max}^{1}	M_{max}^{2}	M_{max}^{3}	M_{max}^{1}	M_{max}^{2}	M_{max}^{3}
1	6.2	6.4	6.0	6.2	6.4	6.0	6.0	6.2	5.8
2	6.0	6.2	5.8	6.0	6.2	5.8	6.2	6.4	5.8
3	5.8	6.0	5.5	5.8	6.0	5.5	5.8	6.0	5.6
4	6.0	6.2	5.8	6.0	6.2	5.8	5.8	6.0	5.6
5	5.4	5.8	5.0	5.4	5.8	5.0	6.2	6.4	6.0
6	5.8	6.0	5.6	6.0	6.2	5.8	5.4	5.6	5.2
7	6.0	6.2	5.8	6.0	6.2	5.8	6.5	6.7	6.3
8	6.2	6.4	6.0	6.2	6.4	6.0	6.2	6.5	6.0
9	5.8	6.0	5.4	5.8	6.0	5.4	6.0	6.2	5.8
10	5.8	6.0	5.6	5.8	6.0	5.6	6.2	6.4	6.0
11	6.2	6.4	6.0	6.2	6.4	6.0	6.0	6.2	5.8
12	6.5	6.7	6.3	6.5	6.7	6.3	5.6	6.0	5.2
13	6.2	6.4	6.0	6.2	6.4	6.0	6.5	6.7	6.4
14	6.2	6.4	6.0	6.2	6.4	6.0	5.8	6.0	5.6
15s	6.2	6.4	6.0	6.0	6.2	5.8	6.0	6.2	5.8
15d							7.5	7.7	7.3
16	5.4	5.6	5.2	5.4	5.6	5.2			
17	6.5	6.7	6.4	6.5	6.7	6.4			
18s	6.0	6.2	5.8	6.0	6.2	5.8			
18d	7.5	7.7	7.3	7.5	7.7	7.3			
19	5.6	6.0	5.2	5.6	6.0	5.2			
20	6.2	6.4	6.0	6.2	6.4	6.0			
21				6.0	6.2	5.8			
22				5.8	6.0	5.6			
23				5.6	5.8	5.4			
24				5.8	5.8	5.2			
25				5.8	6.0	5.6			

These values seem to be in accordance with earthquake recurrence estimated from historical and instrumental seismicity. However, Lenkey et al. (2002) suggested that seismicity in the region is mainly controlled by the different thermal conditions of the lithosphere.

GROUND MOTION ATTENUATION

Attenuation relations for the Pannonian region based on the strong motion data are practically non-existent. Based on the analysis of macroseismic effects and intensity attenuation, Zsíros (1996) concluded that the attenuation of ground motion with distance in the Pannonian basin is greater than in many similar areas with low to moderate seismicity.

For the hazard computations in this study, attenuation relations developed by Ambraseys et al. (1996), Boore et al. (1997) and Sadigh et al. (1997) were adopted with 1/2, 1/4, and 1/4 weights respectively.

MATHEMATICAL MODEL TO CALCULATE SEISMIC HAZARD

We established a logic tree including all uncertainties involved (Figure 3). Uncertainty in seismic source evaluation was represented by weighted alternative seismotectonic models; uncertainty in recurrence was characterized by probability distributions on the recurrence parameters; and uncertainty in ground motion evaluations was characterized by a set of alternative ground-motion relationships and their associated weights.

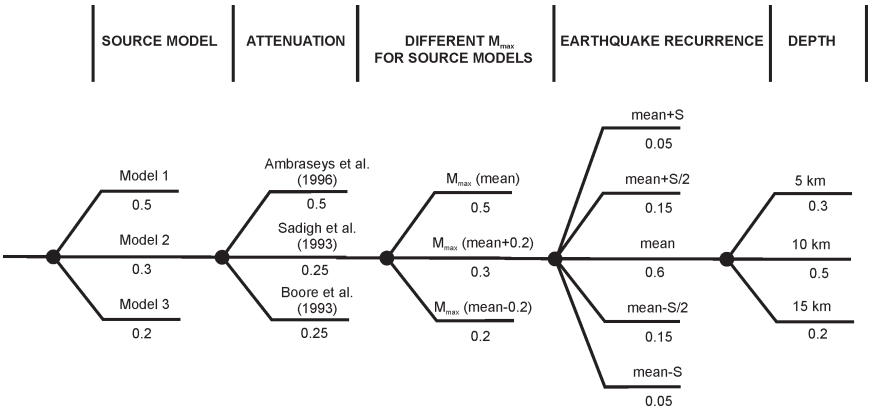

Figure 3. Simplified logic tree for the probabilistic seismic hazard computation.

SEISMIC HAZARD RESULTS

Using the methodology described above, seismic hazard curves for single sites were calculated even for very low probabilities, for example for the Paks NPP site (Figure 4). Furthermore, hazard maps for the whole Pannonian region were calculated.

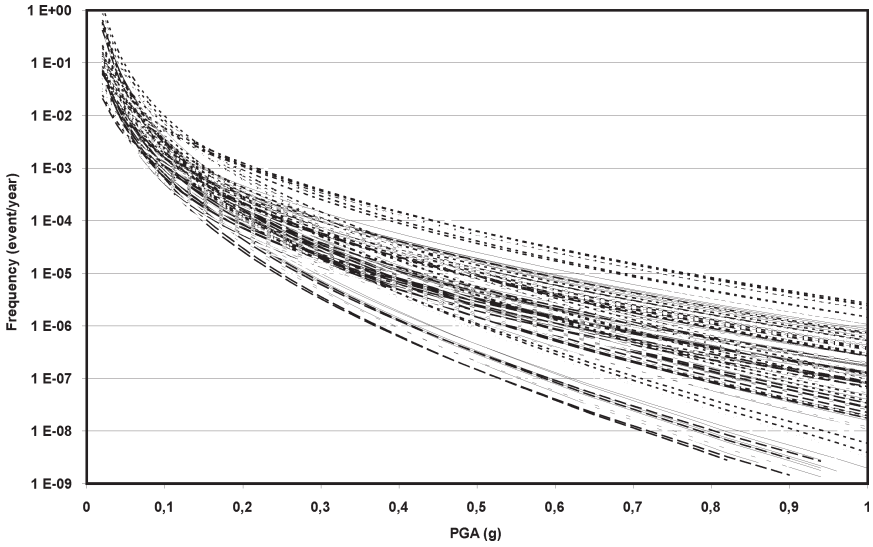

Figure 4. Seismic hazard curves for Paks NPP site along logic tree branches.

The seismic hazard map of the Pannonian region shown in Figure 5 depicts the mean PGA with a 90% probability of non-exceedance in 50 years. Not surprisingly, the highest seismic hazard values (more than 4-5 m/s^2) are expected in the Vrancea region, corresponding to high levels of seismicity. The second highest hazard in the region is found in the Slovenia-Croatia border region (Trieste-Ljubljana-Zagreb area) with 2.0-2.5 m/s^2 PGA. In addition, areas of relatively high seismic hazard include some other areas of moderate seismicity, such as in the Dinarides and in the Mur-Mürz valley. Most of the Pannonian basin has a relatively low seismic hazard, with less than 1 m/s^2 expected PGA, however there are some patches with greater hazard, in the range of 1-2 m/s^2, at Komárom and northeast of Lake Balaton, east of Budapest, and the southwest portion of Hungary.

Two similoar sets of maps have been released in the framework of the Global Seismic Hazard Assessment Program (GSHAP) in 1999 (Grünthal et al., 1999; Musson, 1999). It goes beyond the possibilities of the present study

to compare these maps in detail, but some fundamental similarities and a few major differences should be mentioned.

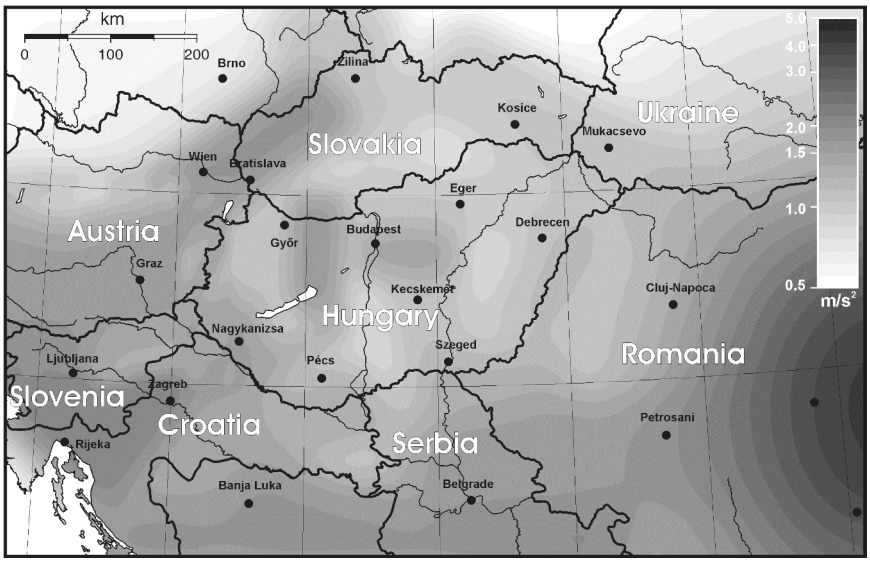

Figure 5. Seismic hazard in the Pannonian region. Expected peak ground acceleration in m/s^2 (10% probability of exceedance in 50 years, 475 year return period).

Each of the three studies employed a fairly similar method and used more-or-less identical earthquake catalogs. The largest differences are the different philosophies in evaluation and characterization of the seismic sources and the selection of suitable attenuation relationships.

Although there are similarities in general hazard levels between the different maps, hazard contours and patches of enhanced hazard are not necessarily equivalent. Obviously enough, the Vrancea region results the highest hazard values on each map. Southwest of the investigated area, the GSHAP hazard values are generally higher than our values. Our model, as well as that of Musson, spreads the historical seismicity in the Zagreb-Ljubljana-Rijeka area, whereas the GSAP map concentrates the hazard in a smaller area around Zagreb. The same outcome can be seen in some other regions, for example in the historically active Komárom region.

SITE EFFECT AND SECONDARY SEISMIC EFFECTS

Soft surface layers, strong lateral discontinuities in the immediate vicinity, or abrupt changes in topography can result in considerable amplification or alteration of earthquake-induced ground motion. These effects have to be accounted for by a calculation of the dynamic response of each site's geological setting to incoming seismic waves. The importance of this effect generally varies with frequency.

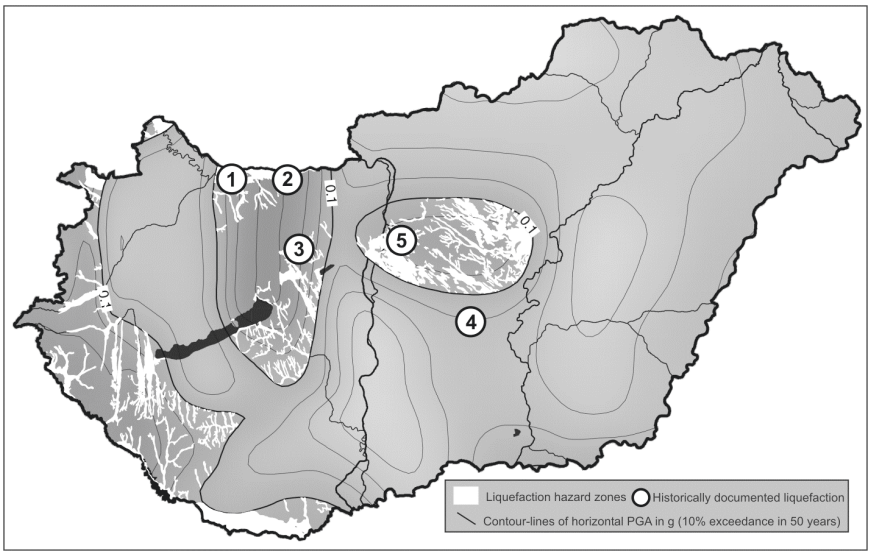

Figure 6. Liquefaction-prone areas in Hungary with 10% probability of exceedance in 50 years, 475 year return period. White dots show area of documented liquefactions after the 1 – Komárom (1763), 2 – Komárom (1783), 3 – Mór (1810), 4 – Kecskemét (1911) and 5 – Dunaharaszti (1956) earthquakes.

Large areas of the Pannonian basin are covered by young, loose sediments. One of the most serious secondary seismic effects is liquefaction ground failure. Liquefaction is defined as the temporary loss of load-bearing strength of a saturated, loose granular soil during, and for some time after an earthquake due to cyclic loading and the build-up of pore-water pressure. The likelihood of liquefaction depends primarily on the presence of water, the particle size distribution of the material, the density of the material, and the effective confining stress. Examples show that sands tend to liquefy very easily, whereas clays and gravels do not. Following the recommendations of Lew (2001) to develop liquefaction hazard maps, we have convolved the seismic hazard map shown in Figure 5 with maps of surface geology (Jámbor, 1989) and maximum ground water levels (Deseő, 1989). The map in Figure 6

shows the zones in Hungary generally prone to liquefaction. The predicted liquefaction hazard zones match fairly well with historically documented liquefaction cases, for example after the Komárom (1763, 1783), Mór (1810), Kecskemét (1911) and Dunaharaszti (1956) earthquakes.

The user communities in Hungary have responded very positively to the current seismic hazard map. The *Hungarian National Committee on Earthquake Engineering* has accepted these hazard estimates and made recommendations to their use in developing national annexes to the EUROCODE-8.

ACKNOWLEDGEMENTS

The research presented in this contribution has been supported by Paks NPP and GeoRisk Ltd. We thank Seth Stein and Francois Thouvenot for their constructive reviews and editorial assistance.

REFERENCES

Ambraseys N., Simpson K., Boomer J. Prediction of Horizontal Response Spectra in Europe. Earthquake Engineering and Structural Dynamics 1996; 25: 371-400.

Bada G., Gerner P., Cloetingh S., Horváth F. Sources of recent tectonic stress in the Pannonian region: inferences from finite element modelling. Geophys. J. Int. 1998; 134: 87-102.

Bada G., Horváth F., Gerner P., Fejes I. Review of the present-day geodynamics of the Pannonian basIn progress and problems. J. Geodynamics 1999; 27: 501-527.

Boore D.M., Joyner W.B., Fumal T.E. Equations for Estimating Horizontal Response Spectra and Peak Acceleration from Western North American Earthquakes: A Summary of Recent Work. Seism. Res. Let. 1997; 68(1): 128–153.

Cornell C.A. Engineering seismic risk analysis. BSSA 1968; 58: 1583-1606.

Csomor D., Kiss Z. Geofizikai Közlemények 1959; 7: 169-180 (in Hungarian)

Csontos L., Márton E., Wórum G., Benkovics L. Geodynamics of SW-Pannonian inselbergs (Mecsek and Villány Mts, SW Hungary): Inferences from a complex structural analysis. In *Neotectonics and surface processes: the Pannonian basin and Alpine/Carpathian system*, S. Cloetingh, F. Horváth, G. Bada, A. Lankreijer, eds., EGU St. Mueller Special Publication Series 2002; 3: 9-28.

Deseő É., Maximális talajvízállás (1961-1980) (térkép), 1:2 000 000, Magyarország Nemzeti Atlasza, MÁFI, Budapest, 1989.

Dieterich J.H. A constitutive law for rate of earthquake production and its application of earthquake clustering. J. Geophys. Res. 1994; 99(2): 2601-2618.

Fodor L., Csontos L., Bada G., Benkovics L., Győrfi I. Tertiary tectonic evolution of the Carpatho-Pannonian region: a new synthesis of paleostress data. Geol. Soc. Lond. Spec. Publ. 1999; 156: 295-334.

Gerner P., Bada G., Dövényi P., Müller B., Oncescu M.C., Cloetingh S., Horváth F. Recent tectonic stress and crustal deformation in and around the Pannonian basIn data and

models. In *The Mediterranean basins: Tertiary extension within the Alpine orogen,* B. Durand, L. Jolivet, F. Horváth, M. Séranne, eds., Geol. Soc. London Spec. Publ. 1999; 156: 269-294.

Grenerczy G., Fejes I., Kenyeres A. Present crustal deformation pattern in the Pancardi Region: Constraints from Space Geodesy. In *Neotectonics and surface processes: the Pannonian basin and Alpine/Carpathian system*, S. Cloetingh, F. Horváth, G. Bada, A. Lankreijer, eds., EGU St. Mueller Special Publication Series 2002; 3: 65-77.

Grünthal G., Bosse C., Sellami S., Mayer-Rosa D., Giardini D. Compilation of the GSHAP regional seismic hazard for Europe, Africa and the Middle East. Annali di Geofisica 1999; 42(6): 1215-1223.

Gutenberg J., Richter C.F. Frequency of earthquakes in California. BSSA 1944; 34: 185-188.

Horváth F. Neotectonic behaviour of the Alpine-Mediterranean region. In *The Pannonian Basin - A study in basin evolution*, L.H. Royden, F. Horváth, eds., AAPG Memoir 1988; 45: 49-51.

Horváth F., Cloetingh S. Stress-induced late-stage subsidence anomalies in the Pannonian basin. Tectonophysics 1996; 266: 287-300.

Jámbor Á. Földtan (térkép), 1: 1 000 000, Magyarország Nemzeti Atlasza, MÁFI, Budapest, 1989.

Karnik V. Seismicity of the European Area I. Praha, 1968.

Lapajne J., Motnikar B.S., Zupancic P. Probabilistic Seismic Hazard Assessment Methodology for Distributed Seismicity. BSSA 2003; 93(6): 2502-2515.

Lenkey L., Dövényi P., Horváth F., Cloetingh S.A.P.L. Geothermics of the Pannonian basin and its bearing on the neotectonics. In *Neotectonics and surface processes: the Pannonian basin and Alpine/Carpathian system*, S. Cloetingh, F. Horváth, G. Bada, A. Lankreijer, eds., EGU St. Mueller Special Publication Series 2002; 3: 29-40.

Lew M. 2001. Liquefaction Evaluation Guidelines for Practicing Engineering and Geological Professionals and Regulators. Environmental & Engineering Geoscience 2001; VII(4): 301–320.

Musson R. Probabilistic seismic hazard maps for the North Balkan region. Annali di Geofisica, 1999; 42(6): 1109-1124.

Sadigh K., Chang C.-Y., Egan J.A., Makdisi F., Youngs R.R. Attenuation Relationships for Shallow Crustal Earthquakes Based on California Strong Motion Data. Seism. Res. Let. 1997; 68(1): 180–189.

Slejko D., Peruzza L, Rebez A. Seismic hazard maps of Italy. Ann. Geophys. 1998; 41: 183-214.

Stein S., Newman A. Characteristic and Uncharacteristic Earthquakes as Possible Artifacts: Applications to the New Madrid and Wabash Seismic Zones. Seismological Research Letters 2004; 75(2): 173-187.

Tóth L., Mónus, P., Zsíros, T. and Kiszely, M., Seismicity in the Pannonian Region – earthquake data. In *Neotectonics and surface processes: the Pannonian basin and Alpine/Carpathian system*, S. Cloetingh, F. Horváth, G. Bada, A. Lankreijer, eds., EGU St. Mueller Special Publication Series 2002; 3: 9-28.

Tóth L., Mónus P., Zsíros T., Kiszely M. Micro-seismic monitoring of seismoactive areas in Hungary. Studi Geologici Camerti, Special Issue: Proceedings of the workshop COST Action 625 "Active faults: analysis, processes and monitoring" 2004.

Zsíros T. Macroseismic focal depth and intensity attenuation in the Carpathian region. Acta Geod. Geoph. Hung. 1996; 31:115-125.

Zsíros T. A Kárpát-medence szeizmicitása és földrengés veszélyessége: Magyar földrengés katalógus (456-1995). MTA GGKI, Budapest 2000, ISBN 9638381159. p. 495 (in Hungarian).

Zsíros T. Earthquake activity and hazard in the Carpathian basin I. Acta Geod. Geoph. Hung. 2003a; 38(3): 345-362.

Zsíros T. Earthquake activity and hazard in the Carpathian basin II. Acta Geod. Geoph. Hung. 2003b; 38(4): 445-465.

SOCIETAL ASPECTS OF ONGOING DEFORMATION IN THE PANNONIAN REGION

Gábor Bada[1], Frank Horváth[2], László Tóth[3], László Fodor[4], Gábor Timár[2], Sierd Cloetingh[1]
1: Vrije Universiteit Amsterdam, the Netherlands
gabor.bada@falw.vu.nl
2: Eötvös L. University, Budapest, Hungary
3: Seismological Observatory, Hungarian Academy of Sciences, Budapest, Hungary
4: Hungarian Geological Institute, Budapest, Hungary

ABSTRACT

This contribution presents an overview on the societal aspects of active tectonic processes in the Pannonian region. Progress and problems are reported from the field of flood hazard related to ongoing vertical land motions and related surface development. The potential of late-stage reactivation of the Pannonian basin system for the petroleum industry is discussed through the processes of hydrocarbon maturation, migration and trapping. The seismic hazard of nuclear power plants, a topic of major societal concern worldwide, is discussed in the context of seismicity and seismoactive faulting in Central Europe.

INTRODUCTION

On-going deformation in the Pannonian region, mainly driven by the motion of Adria, has generated great scientific interest and attention in recent years. Research activities, on national as well as international level, have led to the growing recognition of the increasing societal importance of neotectonic and landscape-forming processes. Understanding and quantifying related natural hazards, such as earthquakes, slope instability, and flooding in the vulnerable environment of Central Europe is a serious challenge for the geoscience community. Besides hazards, however, active deformation and basin inversion can result in better prospects for the petroleum industry. The diversity of neotectonic processes in the Pannonian basin and the evaluation of their societal impact require sensible and careful analysis. Geoprediction in this actively inverting sedimentary basin requires a multidisciplinary approach and, therefore, the interaction and collaboration of researchers from a significantly broader field of geo-expertise than hitherto considered. One of

N. Pinter et al. (eds.), The Adria Microplate: GPS Geodesy, Tectonics and Hazards, 385–402.

the main challenges is to understand the solid Earth as a dynamic system by improving the quantification of recent lithospheric deformation and the controls and feedback mechanisms of neotectonic processes. This is a prerequisite for a proper response to the needs and safety of humanity in this vulnerable environment.

In this paper, we review several societal implications of on-going deformation in the Pannonian region. Our objective is to provide an overview of:

- how society is influenced by natural hazards of neotectonic origin,
- how society can handle such hazards,
- how society can benefit from the consequences of active deformation.

For a neotectonic framework, first we briefly outline the main characteristics of on-going deformation in the Pannonian region. Then we present snapshots of a few selected case studies and highlight problems and progress in the field of landscape evolution and related flood-hazard evaluation, hydrocarbon exploration, and seismic-hazard assessment. All these aspects give an essential context for future research into neotectonic processes.

ONGOING DEFORMATION IN THE PANNONIAN BASIN

The Pannonian basin is an excellent natural laboratory for environmental studies due to the availability of multidisciplinary data sets and because of its peculiar tectonic setting. Extensional basin formation within the Alpine orogenic belt started in the early Miocene, whereas structural inversion has been taking place since late Pliocene-Quaternary times (Horváth et al., 2004). Inversion is related to changes in the regional stress field, from a state of tension that controlled basin formation and subsidence, to a state of compression resulting in active faulting, seismicity, and contraction that led, eventually, to folding of the lithosphere (Horváth and Cloetingh, 1996; Bada et al., 1999; Gerner et al. 1999). Earthquake data indicate that current deformation is mainly concentrated in the vicinity of the contact zone between Adria and the Alpine-Dinarides orogen (Tóth et al., 2002). Some of the stresses and deformation are, however, transferred well into the Pannonian basin, resulting in a complex stress and strain pattern (Figure 1).

Due to intra-plate compression, the Pannonian lithosphere exhibits large-scale bending manifested in Quaternary subsidence and uplift (Horváth and Cloetingh, 1996). Extensional basin formation led to significant weakening of the deforming medium, allowing subsequent deformation to be localized at crustal discontinuities. Thus, the extended, hot, and hence weak lithosphere underlying sedimentary basins is prone to reactivation under relatively low compressional stresses. The Pannonian basin has been

interpreted as a well documented case of irregular lithospheric folding (Cloetingh et al., 1999), with a wavelength spectum ranging from a few kilometres (local basin inversion) to hundreds of kilometres (whole lithospheric folding). Folding of the Pannonian lithosphere is often manifested as differential vertical motion (Horváth and Cloetingh, 1996; Fodor et al., 2003; Ruszkiczay et al., 2004), which in turn has a number of important consequences for environmental issues such as flooding, slope stability, soil erosion, water management (Timár et al., 2002, 2004) and for hydrocarbon habitat, maturation history, hydrodynamic regime, overpressures zones, sealing of fault systems, and reservoir integrity (e.g., Horváth, 1995; Horváth and Tari, 1999).

The importance of late-stage compression in the Pannonian basin for explaining its anomalous topography and intraplate seismicity has been recognised, and a novel model for the structural reactivation of back-arc basins has been developed (Horváth et al., 2004). Understanding the Quaternary 3D deformation pattern is a key for the reconstruction of related landscape evolution processes (Horváth and Cloetingh, 1996; Bada et al., 1999). Paleostress data (Fodor et al., 1999) indicate a characteristic temporal as well as spatial variation of both the stress and the strain fields. Accordingly, the structural styles of inversion vary both in time and space, resulting in a complex pattern of recent tectonic activity (Bada et al., 1999).

Possible sources of compression in the context of basin inversion were investigated by means of numerical modelling (Bada et al., 1998, 2001). Results suggest that the state of recent stress in the Pannonian-Carpathian system, particularly in its western and southern part, is controlled by the complex interaction of plate boundary and intraplate forces. These are the counterclockwise rotation and northward indentation of the Adriatic microplate ("Adria-push") combined with buoyancy forces associated with the elevated topography and crustal thickness variation along the Alpine, Carpathian and Dinaric orogens. Model predictions indicate that significant compressional stresses are concentrated in the elastic-brittle core of the lithosphere that approach the integrated strength of the system. Such stress concentration may lead to large-scale lithospheric buckling manifested in differential vertical motions, and brittle faulting associated with the recorded seismicity. The spatial distribution of subsiding and uplifting areas inside the Pannonian basin (Figures 1, 2) appears to be the result of intraplate compressional stresses as demonstrated by neotectonic structural analysis, seismological studies and contemporaneous stress data (Horváth and Cloetingh, 1996; Gerner et al., 1999).

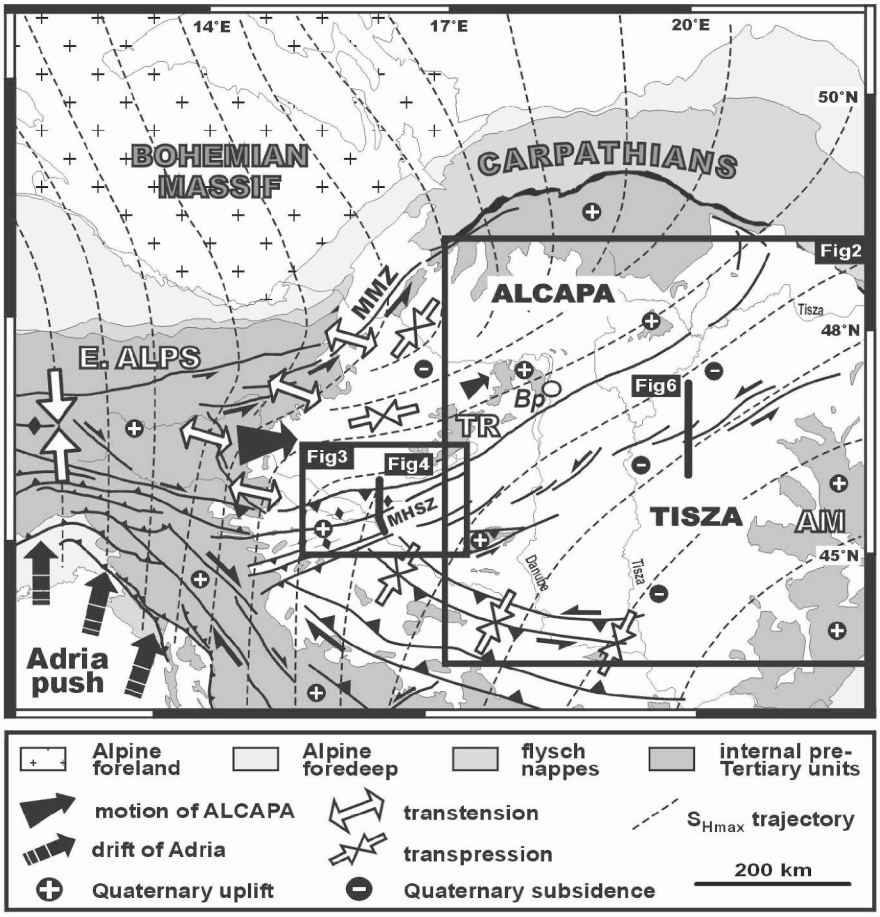

Figure 1 Neotectonic stress and strain pattern in the Pannonian basin and surrounding orogens (modified from Bada et al., 2001). Due to the CCW rotation and resulting northward indentation of the Adriatic microplate ("Adria push"), crustal wedges are currently squeezed out from the axial zone of Alpine collision towards the interior of the weak and thinned Pannonian lithosphere. The E-NE motion of the extruding ALCAPA block has a strong effect on the kinematics and spatial distribution of seismotectonic faults and the contemporary stress pattern indicated by S_{Hmax} trajectories. AM: Apuseni Mts., Bp: Budapest, MHSZ: mid-Hungarian shear zone, MMZ: Mur-Murz-Žilina fault, TR: Transdanubian Range.

Several flat-lying, low-altitude areas (e.g., Great Hungarian Plain, Sava and Drava troughs) have been continuously subsiding since the onset of basin formation in the early Miocene and were completely filled with a Pliocene-Quaternary alluvial-lacustrine sequence 500-2500 m in thickness during the last stages of basin evolution. In contrast, the periphery of the basin system, as well as some internal mountain ranges have been uplifted and

significantly eroded since late Miocene-Pliocene times. Results of fission-track studies, exposure dating, and morphotectonic analysis suggest that this process was not entirely simultaneous with basin subsidence but started earliest in the Carpathians and Apuseni Mts. during the Miocene (Sanders et al., 1999). This was followed by an early phase of uplift in southern Transdanubia from the Pliocene and then the uplift of northern Transdanubia during the Pleistocene (Fodor et al., 2003; Ruszkiczay et al., 2004).

TECTONIC TOPOGRAPHY AND FLOOD HAZARD

Processes controlling continental topography and related natural hazards include climatic forcing as well as the dynamic behaviour of the deforming medium. The recognition of the impact of neotectonic processes on landscape evolution has led to the concept of tectonic topography in the Pannonian region (Cloetingh et al., 2003). Current research efforts concentrate on the interplay among active tectonics, topography evolution, and drainage pattern development. The aim is to understand and quantify neotectonic processes controlling landscape formation and deformation and related natural hazards during the late-stage (late Pliocene-Quaternary, i.e., the last 5 My) evolution of the Pannonian basin-Carpathian system.

In essence, when the surface is subsiding, the risk of flooding increases and can seriously affect local ecosystems and the human habitat. On the other hand, uplift can lead to a higher risk of land destruction in the form of erosion. These environmental changes are governed mainly by natural processes but can be triggered by human activities as well. However, the absolute and relative contributions of the various processes are still poorly understood.

The large-scale bending of the Pannonian lithosphere represents a major driving force behind differential vertical land motions in the region (Horváth and Cloetingh, 1996). Topography development is strongly influenced by the tectonic reactivation of pre-existing structures. The broad up-warping of Transdanubia, and a general uplift of the north Hungarian mountain range (Mátra, Bükk) and the Apuseni Mts. in Romania are characteristic positive topographic expressions of neotectonic processes (Figure 2). On the other hand, subsidence has continued in the centre of the Great Hungarian Plain, giving rise to considerable topographic relief along the periphery of the plain. This relief has changed through time and space, as indicated by the evolution of the drainage network, a sensitive recorder of active deformation. It follows that the rate and pattern of on-going vertical motions are reflected in the drainage-pattern development and related flood hazard. In particular, changes in river bed morphology and rapid lateral shifts

or avulsions of river channels (Figure 2) indicate differential vertical motions of recent as well as paleo-surfaces.

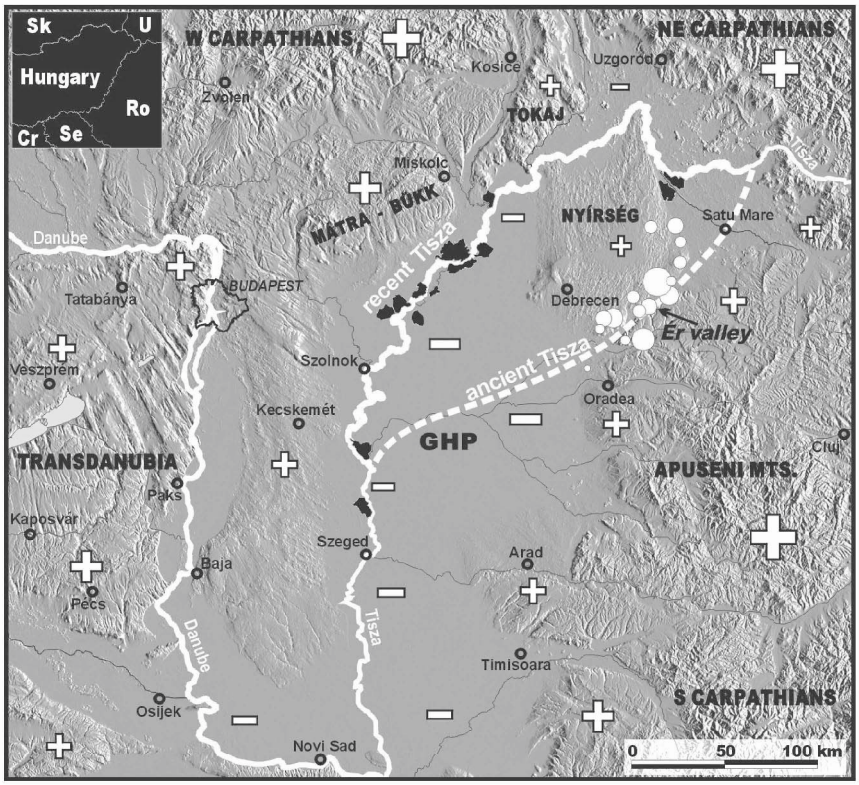

Figure 2. Shaded topography relief, drainage network, and location of the Danube and Tisza rivers in the uplifting (marked by + sign) and subsiding (marked by – sign) parts of the Pannonian basin. Elevation data are from the SRTM database (Rabus et al., 2003). Black shaded areas upstream from Szeged and Szolnok indicate planned emergency reservoirs. Upper left insert shows political boundaries (Cr: Croatia, Ro: Romania, Se: Serbia, Sk: Slovakia, U: Ukraine, GHP: Great Hungarian Plain). For location see Figure 1.

Morphological data and reconstructed river channel geometries suggest that the Tisza river and its tributaries in the Great Hungarian Plain underwent remarkable lateral shifts during late Pleistocene-Holocene time (Mike, 1975; Timár et al., 2004). This has been driven by the interplay of climatic changes and westward tilt of the lithosphere due to the uplift of the western and northern flanks of the neighbouring Apuseni Mts. Rivers tend to follow the areas of maximum subsidence governed by sediment compaction and vertical tectonic motions (Horváth and Cloetingh, 1996). The channel of ancient Tisza could have been controlled by seismogenic faulting in the Ér

valley of NE Hungary and NW Romania, as indicated by an earthquake epicentre concentration (Figure 2). Current estimates suggest maximum basin subsidence of a few mm/year, substantial enough to influence flood hazard on a human time scale (Joó, 1992; Timár and Rácz, 2002). On the other hand, the vast lands of the Tisza floodplain, an area of about 1.5 million inhabitants where the river is fully regulated by dykes and dams, offer open space that the river could partially reoccupy during maximum floods as it once did naturally. Such measures could considerably reduce the highest flood stages and are now being seriously considered as a flood-defence option in planning the framework for a major river re-engineering project, the New Vásárhelyi Plan, named after the legendary engineer who first regulated the Tisza in the 19th century (Figure 2). Another case is illustrated by the Danube, particularly near Budapest, where the river cuts through the uplifting Transdanubian Range. Active incision results in a confined river valley, narrower upstream and wider downstream from Budapest. In contrast to the Tisza river, the Danube valley offers few, if any, suitable sites for flood-control reservoirs. Unlike the Tisza case, thus, flood defence is feasible only with the aid of a trustworthy dyke system all along the Danube. These remarkable differences between the Danube and the Tisza have had a major impact on the costs and strategies for flood defence as well as other aspects of water management.

BASIN INVERSION AND HYDROCARBON PROSPECTS

Basin inversion tectonics and related surface processes have received considerable attention in the hydrocarbon industry because of their significance in hydrocarbon generation, migration, and trapping. Rapid basin subsidence, for instance, can increase seal integrity and facilitate hydrocarbon expulsion. In contrast, subsequent uplift and related cooling of hydrocarbon-prone areas generally reduces the maturation potential of organic-rich sediments. Uplift and erosion can decrease seal quality, remove prospective reservoirs and, eventually, lead to the leakage of geofluids. On the other hand, structural traps resulting from late-stage basin inversion may form large petroleum reservoirs. Anisotropic tectonic stress fields can result in pressure gradients that may drive deep fluid migration through a porous rock matrix. Moreover, active faults and shear zones can maintain high pressure gradients that facilitate fluid flow in their vicinity. Rapid uplift of the substratum can strongly influence the pressure system and, hence, both exploration and exploitation potential. In essence, the last phases of deformation shape and fine-tune the structure and pressure system of the rock masses containing petroleum reserves. In the following section, two examples are presented from the Pannonian basin to highlight the economical importance of basin

inversion in hydrocarbon prospecting (e.g., Kőrössy, 1988; Horváth, 1995; Jósvai, 1996; Horváth and Tari, 1999).

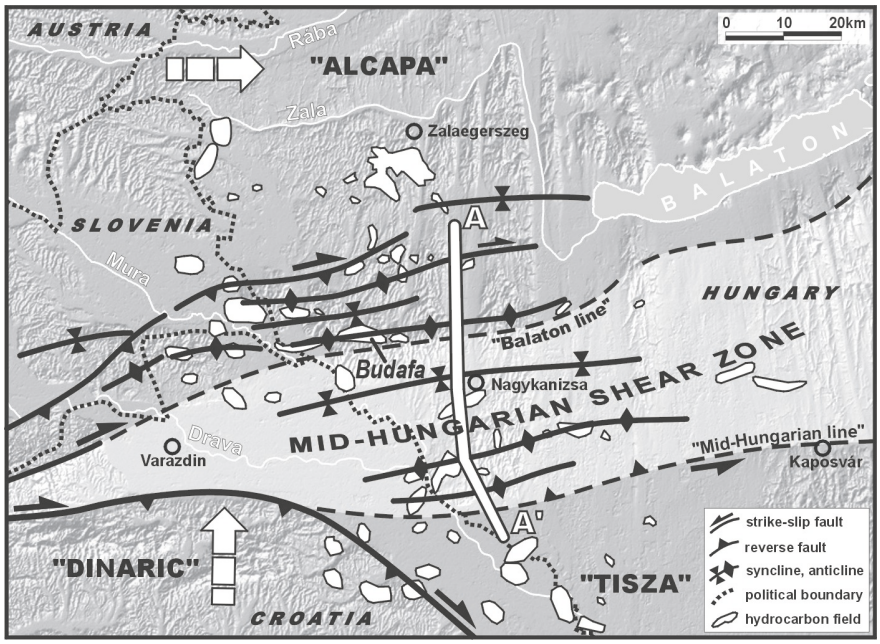

Figure 3 Neotectonic structural pattern (partly after Fodor et al., 2002) and distribution of hydrocarbon fields (Dank, 1988) in the Zala-Mura depression, located along the Zala and Mura rivers, SW Pannonian basin. Note the dominance of contractional structures along the southwestern segment of the mid-Hungarian shear zone (light shading) between the Balaton and the mid-Hungarian lines. Large white arrows (not to scale) indicate generalised direction of present-day motion of crustal blocks from GPS data (Grenerczy, 2000; Weber et al., 2004). Profile A-A' is presented in Figure 4. For location see Figure 1.

The Zala-Mura depression in SW Pannonia (Figure 3) is part of the Sava fold belt of the Alpine-Dinaric-Pannonian junction zone. The depression is characterised by Pliocene through Quaternary folding of the Neogene sedimentary cover (Pávai Vajna, 1917). This area, sandwiched in the contact zone of the converging ALCAPA, Tisza and Dinaric units, represents one of the most deformed parts of the Pannonian basin. Numerous structures of intense, roughly N-S directed horizontal shortening have been inferred mainly on the basis of geophysical data sets (Figure 3). The close proximity of the Zala-Mura basin to the active Adria/Dinarides collisional interface explains the high level of strain localisation along the SW segment of the mid-Hungarian shear zone (MHSZ). The MHSZ has been the subject of repeated tectonic reactivation throughout Tertiary times (Csontos and Nagymarosy,

1998) and has acted as an active structural contact between the ALCAPA and Tisza terranes, constituting the basement of the Pannonian basin (Figure 1).

A roughly N-S oriented structural cross section through the MHSZ (Figure 4) reveals that intense contraction inverted several deep Miocene half grabens. Reactivation of major mid-Miocene normal faults, separating different tectonic units while rooted deep in the basement, has formed several sets of roughly east-west trending, sub-parallel synclines and anticlines (Figure 3). The section shows that reactivated faults rarely reach the surface, but uplift of fault-bounded basement blocks warp the overlying strata. Therefore, these faults are blind thrusts and are covered by deformed Pannonian (upper Miocene) sediments, often forming fault propagation folds above the thrusts. This structural geometry is favorable for reservoir formation, as no major fracture zones break up the integrity ofcut the structural traps or their seals at higher stratigraphic levels. In addition, these blind thrusts offer efficient migration pathways for the overpressured fluids from the hydrocarbon kitchen below to migrate to the hinge zone of the folds above. If porous lithologies are present, which is often the case, for example where lower Pannonian sandstones are present, the unbroken folds then form excellent structural traps for petroleum (Kőrössy, 1988). Due to folding and related uplift, however, considerable portions of the inverted structures have been eroded, a process that is an important but still poorly constrained factor in reserve estimates.

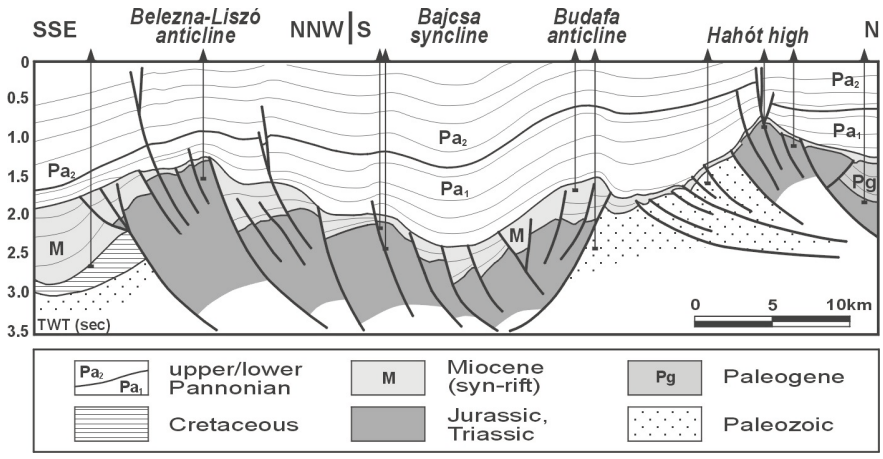

Figure 4 Interpretation of seismic reflection profile A-A' which cross-cuts the mid-Hungarian shear zone in SW Hungary. Pre-existing basement structures, mostly Cretaceous through early Miocene thrusts and strike-slip faults reactivated during Miocene rifting, have been again reactivated during subsequent basin inversion during the Pliocene through Quaternary. For location see Figures 1 and 3.

A schematic history of hydrocarbon generation, migration and trapping in the Zala basin can be outlined in three major steps (Figure 5):

- **Early through late Miocene**: deposition of organic-rich sediments as source rocks, rapid burial and maturation, start of oil and gas generation at a depth of 3-5 km.
- **Latest Miocene through early Pliocene**: onset of folding and reactivation of former normal faults, onset of uplift and erosion of higher stratigraphic levels, oil and gas generation taking place at ~3 km depth, start of hydrocarbon migration.
- **Pliocene through Quaternary**: intense folding and shortening, total uplift and erosion of about 1-2 km, hydrocarbons expelled by tectonic compression, secondary migration along reactivated normal faults, trapping in higher, mainly lower Pannonian strata.

In summary, inversion of the Pannonian basin has led to the formation of a number of antiformal structures that are, if sealed properly, suitable for hydrocarbon accumulation. Several of these structural traps indeed contain oil and/or gas (Figure 3). The Budafa field in the Zala depression is a textbook example of complete basin inversion and related folding (Figure 4). It is probably the best known field in the Pannonian basin, as it was the first major discovery in Hungary after World War I (Dank, 1988; Kőrössy, 1988; Jósvai, 1996).

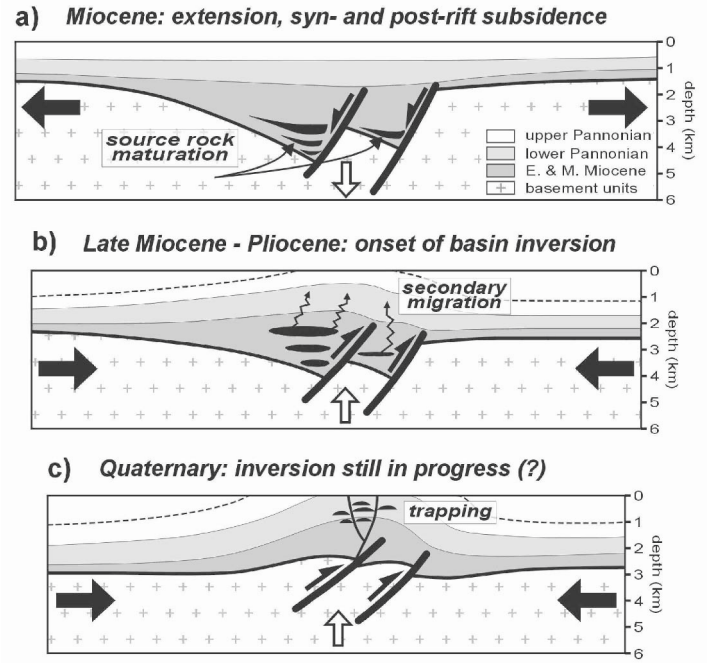

Figure 5 Conceptual model for hydrocarbon generation, migration and trapping in the context of basin formation and subsequent inversion of the Zala-Mura basin, SW Pannonia.

Reactivation of pre-existing fault zones also can offer good exploration targets even when they reach close to the surface. Several such examples are known from the so-called Szolnok flysch belt in centre of the Great Hungarian Plain. The neotectonic structural style of this area is characterised by a large-scale positive flower structure rooted deep in the Paleozoic crystalline basement of the basin system (Figure 6). The current fabric of this deformation zone is the result of multiple episodes of tectonic reactivation involving Late Cretaceous through Oligocene marine basin formation followed by latest Oligocene through early Miocene transpression related to the juxtaposition of the ALCAPA and Tisza terranes (Figure 1). Next, Middle Miocene rifting of the Pannonian basin occurred and was terminated by a transient inversion event marked by regional uplift and erosion at the turn of the middle to late Miocene. Subsequently, late Miocene through Pliocene thermal subsidence took place and was followed by a final phase of Quaternary wrench faulting (e.g., Csontos and Nagymarosy, 1998; Fodor et al., 1999; Horváth and Tari, 1999; Lőrincz et al., 2002).

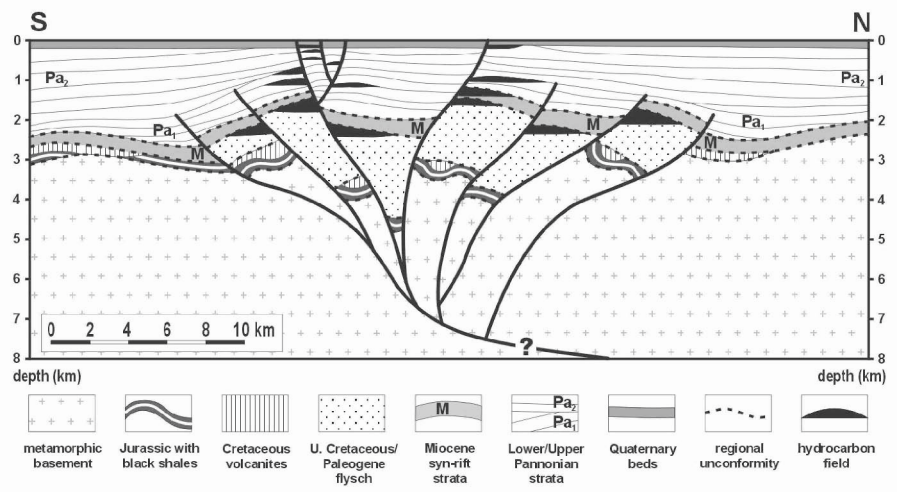

Figure 6 Structural cross section and hydrocarbon habitat of the Szolnok flysch belt in the central Great Hungarian Plain. Most of the hydrocarbon fields are located in structural traps associated with Quaternary tectonic reactivation of pre-existing fault zones. The large-scale positive flower structure is rooted deep in the Paleozoic basement of the basin fill. At depth, the structure probably dies out along a mid-crustal detachment level. 2x vertical exaggeration. For location see Figure 1.

In this structural setting, prospective plays are connected to positive flower structures and stratigraphic traps within the Cretaceous-Paleogene flysch sequence and overlying gently folded sedimentary cover of the

Pannonian basin. Most hydrocarbon pools are located in anticlines within the Neogene basin fill that are often arranged in *en echelon* patterns related to local transpression. These anticlines form structural closures in and above uplifted basement blocks, roll-over anticlines and drape folds, partly due to differential compaction. Individual fields are often bounded by Quaternary strike-slip faults, where fault compartments (reservoirs) are fed from below along structures of neotectonic origin. Although largely disregarded to date, this play type offers one of the most promising prospects in the Pannonian basin. At depth, the folded Szolnok flysch contains large porous and permeable sandstone bodies that contain gas that was probably sourced from a mature lower Jurassic black shale. Large amount of hydrocarbon can be accumulated in these gentle antiformal structures, as evidenced by a number of important gas accumulations along the Szolnok belt (Dank, 1988).

SEISMIC HAZARD AND SOCIETY

Seismicity alone does not necessarily result in a threat to human life and welfare. It is always the combination of seismic activity together with the presence of a social and industrial infrastructure that causes seismicity to pose a certain level of risk in a particular region. Accordingly, seismic hazard is a required but by far not the only contributor to seismic risk, which is obtained by convolving the seismic hazard with local site effects and vulnerability factors. The following section provides a brief description of the seismicity of the Pannonian region and a summary of recent progress in seismic-hazard assessment of the nuclear power plants in the Pannonian region.

Seismicity in the Pannonian region

A major consequence of on-going deformation in the Pannonian lithosphere is brittle faulting manifested in earthquake activity. The region is characterised by low- to medium-level seismicity (Tóth et al., 2002). Earthquake epicentre distribution (Figure 7) suggests that the most actively deforming parts of the system are the Alpine-Dinaric belt and the Vrancea region in the southeast Carpathians. Plate convergence is still taking place in these orogens as a result of the indentation of the Adriatic microplate against the Alps-Dinarides (Anderson and Jackson, 1987) and the final phases of subduction along the SE Carpathians (Spakman and Wortel, 2000; Cloetingh et al., 2003). Seismicity inside the Pannonian basin is more moderate; epicentres exhibit a rather scattered lateral as well as depth distribution.

Earthquakes are concentrated predominantly in the uppermost, brittle part of the crust, mainly along pre-existing faults inherited from earlier (Miocene, Cretaceous) tectonic events. The focal-depth distribution suggests three depth provinces where most events are concentrated (Tóth et al., 2002). Shallow earthquakes, within the uppermost 15-20 km of the crust, occur almost exclusively through the whole region except the Vrancea zone. In the Vrancea zone, severe earthquakes with magnitudes up to M7.7 occur at intermediate depths, mostly 70-110 km or 125-160 km. Inside the Pannonian basin, the vast majority of events occurs at very shallow depth, primarily between 6 and 15 km. Focal mechanism solutions (Gerner et al., 1999; Tóth et al., 2002) indicate the dominance of strike-slip to thrust faulting in the area, supporting models of ongoing structural inversion (Horváth, 1995).

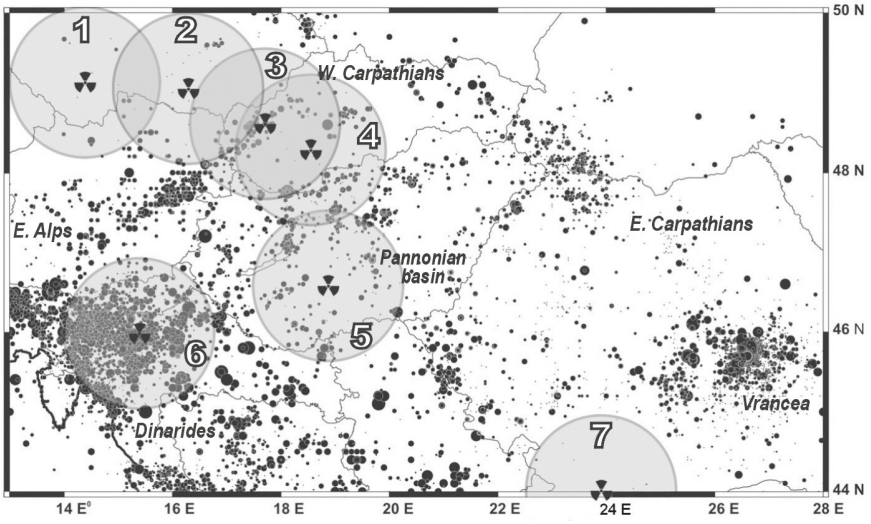

Figure 7. Seismicity of the Pannonian basin and its surroundings (Tóth et al., 2002), and the locations of nuclear power plants (NPPs) with 100 km radii shown. Numbers of NPPs refer to numbers in Table 1. Sizes of epicentre circles are proportional to earthquake magnitudes.

Given the relatively low level of seismic activity and the lack of long-term micro-seismic monitoring, assessment of seismotectonics and seismic hazard is very difficult. Nevertheless, several seismically active structures have been identified in the system (Gerner et al., 1999; Tóth et al., 2002) that may pose considerable threat to social welfare, human life and economical interests. These regions include several large urban areas situated close to active fault segments (Vienna and Bratislava, at the active Vienna Basin fault; Budapest, at the northern branch of a central Hungarian fault zone; Ljubljana

and Trieste, close to the Idrija-Friuli fault; and Zagreb, at the Medvednica fault). These urban areas constitute densely populated industrial centres where a significant proportion of several countries' gross domestic product (GDP) is produced, and contain vulnerable infrastructure of international importance including motorways, energy transmission lines, and high-risk facilities such as power plants, dams, waste disposal sites.

Seismic safety of nuclear power plants

The 1977 Vrancea earthquake, with a magnitude of M_w7.4, hit the Kozloduy nuclear power plant in Bulgaria. The plant's reactors survived the earthquake without major damage of vital structures. However, this event reminded the public and the power plant industry that external events, especially earthquakes, may be important safety issues for many of the nuclear power plants (NPPs) operating in the region (Katona and Kostov, 1997; Figure 7). Insufficient seismic safety of NPPs arose from underestimating seismic hazard of those sites, from earlier design practice and from inadequate safety requirements. Significant progress was achieved during the 1990's, when projects were launched worldwide for seismic-hazard re-evaluation of plant sites, seismic resistance evaluation and upgrading. This was particularly important as the life span of existing NPPs is expected to be extended considerably in most Central and Eastern European countries. Practice shows, however, that the seismic risk of NPPs is not only a design issue, but is also related to factors such as earthquake loads that were often not considered in the design, earthquake hazard that was underestimated during site selection, and changes in safety requirements.

There are numerous cases worldwide when the re-evaluation of seismic hazard resulted in the need for upgrading an older design at an operating NPP (e.g., Budnitz, 1998). This applies to 75% of U.S. plants, and practically all of the NPPs in Central and Eastern Europe. Considering the seismic resistance of NPPs, at present there are very strict safety regulations enforced by the International Atomic Energy Agency (IAEA, 1993) as well as at national levels. These regulations define different levels of seismic loads, mostly in terms of peak ground acceleration (PGA in m/s^2), to be taken into account in design and during operation. The highest load is the safe shutdown earthquake (SSE) that is a design base limiting event. In this case, the reactor should be safely shut down and cooled, no radioactive releases should occur above a certain limit. SSE can be defined either in a deterministic way or by probabilistic seismic-hazard assessment (PSHA). If it is estimated deterministically, SSE will be the maximum historically credible earthquake increased by one level of intensity. When PSHA is carried out, 10^{-4}-10^{-5}

probability levels are generally used (IAEA, 2002). The operational base earthquake (OBE) is the level of seismicity below which safe operation continues. Once OBE is reached, operators must decide if the plant is operational without interaction or if safety measures are needed. A very up-to-date approach for hazard assessment is the complex Probabilistic Safety Assessment (PSA) for a range of external hazards, including seismic hazard, when hazard curves across a wide range of probabilities are produced and analysed. In Table 1, the list of NPPs in the Pannonian region and their design and review level earthquake loads are summarised.

Besides the assessment of seismic hazard, it is crucial to ensure foundation stability, meaning the load-bearing capacity of the immediate subsurface of NPPs. Particularly, liquefaction potential should be assessed. Last but not least, a most important site acceptance criterion is the absence of capable faults at the site, defined here as active faults reaching to the surface. To date, there are no proven design techniques against surface fault movements beneath the reactor buildings of NPPs.

Table 1. Nuclear power plants in the Pannonian region, with their original seismic design base and review level earthquake loads in terms of peak ground acceleration (PGA). Numbers of NPPs refer to their locations in Figure 7.

No	Nuclear Power Plant	Design Base PGA	Review Level PGA	Methods for Seismic Hazard Assessment
1	**Temelin NPP**, Czech Rep. 2 units, WWER-1000	0.6 m/s^2	1.0 m/s^2	Deterministic
2	**Dukovany NPP**, Czech Rep.	0.6 m/s^2	1.0 m/s^2	Deterministic
3	**Bochunice NPP V1**, Slovakia	not designed	3.4 m/s^2	earlier deterministic; later PSHA
3	**Bochunice NPP V2**, Slovakia	not designed	3.4 m/s^2	earlier deterministic; later PSHA
4	**Mochovce NPP**, Slovakia 4 units, WWER-440/V213	0.6 m/s^2	1.0 m/s^2	earlier deterministic; later PSHA
5	**Paks NPP**, Hungary 4 units, WWER-440/V213	not designed	2.5 m/s^2	PSHA; recently extended for PSA
6	**Krsko NPP**, Slovenia Westinghouse	3.0 m/s^2	6.0 m/s^2	earlier deterministic; later PSHA
7	**Kozloduy NPP**, Bulgaria 1-4 units, WWER-440/V230	not designed	2.0 m/s^2	earlier deterministic; later PSHA; recently extended for PSA
7	**Kozloduy NPP**, Bulgaria 5-6 units, WWER-1000	2.0 m/s^2	2.0 m/s^2	earlier deterministic; later PSHA; recently extended for PSA

As a primary aim, the societal risk imposed by NPPs should be kept as low as possible by adopting appropriate design and construction technologies. Research programs for assessing seismic safety issues at NPPs should include several fundamental tasks analysing various aspects of seismic risk, which is normally quantified as the probability of an accident multiplied by the magnitude of its consequences (e.g., casualties). These tasks include:

- re-evaluation of seismic hazard at the site, including geotechnical surveys, analyses of ground and foundation stability, liquefaction potential, dynamic settlement, sliding;
- establishing techniques for safe shutdown and heat removal, elaborating the list of sensitive structures, systems and components relevant for ensuring seismic safety;
- installation of seismic instrumentation (strong motion and site monitoring), elaboration of pre-earthquake preparedness and post-earthquake actions (mitigation);
- evaluation of the seismic capacity of tectonic systems and fault structures relevant for seismic safety;
- performing the necessary upgrades, prioritisation of these measures, and performing the urgent and simple fixes as soon as possible even if only a preliminary seismic-hazard data are available.

ACKNOWLEDGEMENTS

The research presented in this paper has been supported by the Netherlands Research Centre for Integrated Solid Earth Science (ISES) and the Hungarian Research Fund (OTKA projects no. F043715 and T034928). We also thank L. Ferranti, N. Pinter and J. Weber for their constructive reviews and valuable editorial assistance.

REFERENCES

Anderson H.A., Jackson J.A. Active tectonics of the Adriatic region. Geophys. J. R. Astron. Soc. 1987; 91: 937-983.

Bada G., Gerner P., Cloetingh S., Horváth F. Sources of recent tectonic stress in the Pannonian region: inferences from finite element modelling. Geophys. J. Int. 1998; 134: 87-102.

Bada G., Horváth F., Fejes I., Gerner P. Review of the present-day geodynamics of the Pannonian basIn progress and problems. J. Geodynamics 1999; 27: 501-527.

Bada G., Horváth F., Cloetingh S., Coblentz D.D., Tóth T. The role of topography induced gravitational stresses in basin inversion: The case study of the Pannonian basin. Tectonics 2001; 20: 343-363.

Budnitz R.J. State-of-the-art report on the current status of methodologies for seismic PSA. NEA/CSNI/R (97)22, OECD Nuclear Energy Agency, Paris, 1998.

Cloetingh S., Burov E., Poliakov A. Lithosphere folding: Primary response to compression? (from central Asia to Paris basin). Tectonics 1999; 18: 1064-1083.

Cloetingh S., Horváth F., Dinu C., Stephenson R.A., Bertotti G., Bada G., Matenco L., Garcia-Castellanos D. and the TECTOP Working Group. Probing tectonic topography in the aftermath of continental convergence in Central Europe. EOS Trans. AGU 2003; 84(10): 89-93.

Csontos L., Nagymarosy A. The Mid-Hungarian line: a zone of repeated tectonic inversions. Tectonophysics 1998; 297: 51-71.

Dank V. Petroleum geology of the Pannonian basin, Hungary: An overview. In *The Pannonian BasIn A case study in basin evolution*, L.H. Royden, F. Horváth, eds., AAPG Memoir 1988; 45: 319-331.

Fodor L., Csontos L., Bada G., Benkovics L., Györfi I. Tertiary tectonic evolution of the Carpatho-Pannonian region: a new synthesis of paleostress data. In *The Mediterranean basins: Tertiary extension within the Alpine orogen*, B. Durand, L. Jolivet, F. Horváth M. Séranne, eds., Geol. Soc. London Spec. Publ. 1999; 156: 295-334.

Fodor L., Jelen B., Márton E., Rifelj H., Kraljic M., Kevric R., Márton P., Koroknai B., Báldi-Beke M. Miocene to Quaternary deformation, stratigraphy and paleogeography in NE Slovenia and SW Hungary. Geologija 2002; 45: 103-114.

Fodor L., Bada G., Csillag G., Dunai T., Horváth E., Ruszkiczay-Rüdiger Zs., Síkhegyi F., Leél-Össy Sz., Cloething S., Horváth F. Neotectonics of the Pannonian basin II: Interplay between deformation and landscape evolution. Geophys. Research Abstracts 2003 (Nice, France); 5: 09671.

Gerner P., Bada G., Dövényi P., Müller B., Oncescu M.C., Cloetingh S., Horváth F. Recent tectonic stress and crustal deformation in and around the Pannonian basIn data and models. In *The Mediterranean basins: Tertiary extension within the Alpine orogen*, B. Durand, L. Jolivet, F. Horváth M. Séranne, eds., Geol. Soc. London Spec. Publ. 1999; 156: 269-294.

Grenerczy Gy., Kenyeres A., Fejes I. Present crustal movement and strain distribution in Central Europe inferred from GPS measurements. J. Geophys. Res. 2000; 105: 21,835-21,846.

Horváth F. Phases of compression during the evolution of the Pannonian Basin and its bearing on hydrocarbon exploration. Mar. Petr. Geology 1995; 12: 837-844.

Horváth F., Cloetingh S. Stress-induced late-stage subsidence anomalies in the Pannonian basin. Tectonophysics 1996; 266: 287-300.

Horváth F., Tari G. IBS Pannonian Basin project: a review of the main results and their bearings on hydrocarbon exploration. In *The Mediterranean basins: Tertiary extension within the Alpine orogen*, B. Durand, L. Jolivet, F. Horváth M. Séranne, eds., Geol. Soc. London Spec. Publ. 1999; 156: 195-213.

Horváth F., Bada G., Szafián P., Tari G., Ádám A., Cloetingh S. Formation and deformation of the Pannonian basIn constraints from observational data. In *European Lithosphere Dynamics*, D.G. Gee, R. Stephenson, eds.,. Geol. Soc. London Spec. Publ. 2004; submitted.

IAEA TECDOC-724, Probabilistic Safety Assessment for seismic events. IAEA, Vienna, Austria, 1993.

IAEA Safety Standard Series, Evaluation of seismic hazard for nuclear power plants. IAEA Safety Guide No. NS-G-3-3, IAEA, Vienna, Austria, 2002.

Joó I. Recent vertical surface movements in the Carpathian Basin. Tectonophysics 1992; 202: 129-134.

Jósvai J. *Hydrocarbon prospect and exploration potential of the Budafa-Oltárc-Magyarszentmiklós anticline*. MSc. Thesis, Hungary: Eötvös University Budapest, 1996.

Katona T., Kostov M. Seismic assessment and upgrading of nuclear power plants in Eastern Europe. International Symposium on Seismic Safety Relating to Nuclear Power Plants, Kobe, Japan, 1997.

Kőrössy L. Hydrocarbon geology of the Zala Basin in Hungary. Ált. Földt. Szemle 1988; 23: 3-162.

Lőrincz D.K., Horváth F., Detzky G. Neotectonics and its relation to the Mid-Hungarian Mobile Belt. In *Neotectonics and surface processes: the Pannonian basin and Alpine/Carpathian system*, S. Cloetingh, F. Horváth, G. Bada, A. Lankreijer, eds., EGU St. Mueller Spec. Publ. Series 2002; 3: 247-266.

Mike K. Utilization of the analysis of ancient river beds for the detection of Holocene crustal movements. Tectonophysics 1975; 29: 359-368.

Pávai Vajna F. On the youngest movements of the Earth's crust. Földtani Közlöny 1917; 47: 249-253.

Rabus B., Eineder M., Roth A., Bamler R. The shuttle radar topography mission - a new class of digital elevation models acquired by spaceborne radar. Photogr. Rem. Sensing 2003; 57: 241-262.

Ruszkiczay-Rüdiger Zs., Fodor L., Bada G., Leél-Össy Sz., Horváth E., Dunai T. Quantification of Quaternary vertical movements in the central Pannonian BasIn review of chronological data, Danube river, Hungary. Tectonophysics 2004; submitted.

Sanders C., Andriessen P., Cloetingh S. Life cycle of the East Carpathian orogen: Erosion history of a doubly vergent critical wedge assessed by fission track thermochronology. J. Geophys. Res. 1999; 104, 29,095-29,112.

Timár G., Rácz T. The effects of neotectonic and hydrological processes on the flood hazard of the Tisza Region (East Hungary). In *Neotectonics and surface processes: the Pannonian basin and Alpine/Carpathian system*, S. Cloetingh, F. Horváth, G. Bada, A. Lankreijer, eds., EGU St. Mueller Spec. Publ. Series 2002; 3: 267-275.

Timár G., Sümegi P., Horváth F. Late Quaternary dynamics of the Tisza River: evidence of climatic and tectonic controls. Tectonophysics 2004; submitted.

Tóth L., Mónus P., Zsíros T., Kiszely M. Seismicity in the Pannonian Region - earthquake data. In *Neotectonics and surface processes: the Pannonian basin and Alpine/Carpathian system*, S. Cloetingh, F. Horváth, G. Bada, A. Lankreijer, eds., EGU St. Mueller Spec. Publ. Series 2002; 3: 9-28.

Weber J., Stopar B., Vrabec M., Schmalzle G., Dixon T. The Adria microplate, Istria peninsula, GPS, and neotectonics in the NE Slovene corner of the Alps. In *The Adria microplate: GPS Geodesy, Tectonics, and Hazards*, N. Pinter, Gy. Grenerczy, eds., NATO ARW, Veszprém, Hungary, Abstract book, 2004; 134-135.

Wortel M.J.R., Spakman W. Subduction and slab detachment in the Mediterranean-Carpathian region. Science 2000; 209: 1910-1917.

AUTHOR LIST

Dario Albarello
Dipartimento di Scienze della Terra
Università di Siena
Via Laterina 8
53100 Siena
Italy

Shyqyri Aliaj
Seismological Institute
Academy of Sciences of Albania
Tirana
Albania

Yüksel Altiner
Bundesamt für Kartographie und Geodésie
Richard-Strauss-Allee 11
60598 Frankfurt am Main
Germany

Daniele Babbucci
Dipartimento di Scienze della Terra
Università di Siena
Via Laterina 8
53100 Siena
Italy

Gábor Bada
Dept. of Geophysics
Eötvös Loránd University
Pázmány P. sétány 1/C
1117 Budapest
Hungary

Mirza Basagic
Civil Engineering Faculty
University of Sarajevo
Patriotske lige 30
Sarajevo 71000
Bosnia and Hercegovina

Harilaos Billiris
Department of Surveying Engineering
National Technical University of Athens
Iroon Polytechneiou 9
15780 Zografou
Athens
Greece

Carine Bruyninx
Royal Observatory of Belgium
Avenue Circulaire 3
B-1180 Bruxelles
Belgium

Giuseppe Casula
Istituto Nazionale di Geofisica e Vulcanologia
INGV – Bologna
Via Donato Creti n. 12
40128, Bologna
Italy

Giuseppe Cello
Department of Earth Sciences
University of Camerino
Via Gentile IIII da Varano
62032 Camerino (MC)

Nicola Cenni
Departimetno di Fisica
Universita degli studi di Bologna
Viale C. Berti Pichat, 6/2
40127 Bologna
Italy

Safet Cicic
Grbavicka 127a
Sarajevo 71000
Bosnia and Herzegovina

Peter J. Clarke
Dept. of Geomatics
University of Newcastle
Newcastle upon Tyne
U.K.

Sierd Cloetingh
Dept. of Tectonics
Vrije University
De Boelelaan 1085
1081 HV Amsterdam
The Netherlands

Demitris Delikaraoglou
Department of Surveying Engineering
National Technical University of Athens
Iroon Polytechneiou 9, 15780 Zografou
Athens
Greece

Tim Dixon
Geodesy Lab
RSMAS-MGG
University of Miami
Miami, FL 33149
USA

Philip C. England
Dept. of Earth Science
Oxford University
Parks Road
Oxford
U.K.

István Fejes
FOMI Satellite Geodetic Observatory
PO Box 585
H-1592 Budapest
Hungary

Luigi Ferranti
Dipartimento di Scienze della Terra
Università di Napoli Federico II
Largo S. Marcellino 10
80138 Napoli
Italy

László Fodor
Hungarian Geological Institute
Stefánia út 14
H-1143 Budapest
Hungary

Julien Fréchet
Institut de Physique du globe de Strasbourg
5, rue René-Descartes
67084 Strasbourg Cedex
France

Alain Geiger
Geodesy and Geodynamics Lab
Inst. of Geodesy and Photogrammetry
ETH Hoenggerberg
CH- 8093 Zurich
Switzerland

Gyula Grenerczy
FOMI Satellite Geodetic Observatory
PO Box 585
H-1592 Budapest
Hungary

Erzsebet Györi
Research Group of Geophysics and Environmental Physics
Hungarian Academy of Sciences
Pázmány sétány 1/C
Budapest, H-1117
Hungary

Christine Hollenstein
Geodesy and Geodynamics Lab
Inst. of Geodesy and Photogrammetry
ETH Hoenggerberg
CH- 8093 Zurich
Switzerland

Frank Horvath
Geophysical Department
Eötvös Loránd Technical University
Pázmány P. sétány 1/C
H-1117 Budapest
Hungary

Hans-Gert Kahle
Geodesy and Geodynamics Lab
Inst. of Geodesy and Photogrammetry
ETH Hoenggerberg
CH- 8093 Zurich
Switzerland

Ambrus Kenyeres
FOMI Satellite Geodetic Observatory
PO Box 585
H-1592 Budapest
Hungary

Enzo Mantovani
Dipartimento di Scienze della Terra
Università degli Studi di Siena
Via Laterina, 8
53100 Siena
Italy

Marijan Marjanovic
State Geodetic Administration
Gruska 20
10000 Zagreb
Croatia

Radovan Marjanovic-Kavanagh
University of Zagreb
Faculty of Mining, Geology and Petroleum Engineering
Pierrotijeva 6
HR-10000 Zagreb
Croatia

Emö Márton
Paleomágneses Laboratórium
Columbus u 17-23
1145 Budapest
Hungary

Damir Medak
University of Zagreb, Faculty of Geodesy
Institute of Geomatics
Kaciceva 26
HR-10000 Zagreb
Croatia

Matija Medved
State Geodetic Administration
Gruska 20
10000 Zagreb
Croatia

Péter Mónus
Seismological Observatory
Meredek u. 18
Budapest
Hungary

Betim Muco
Seismological Institute, Academy of Sciences of Albania
4 Maryland Avenue
Rockville, MD 20850
USA

Enrico Mugnaioli
Dipartimento di Scienze della Terra
Università di Siena
Via Laterina 8
53100 Siena
Italy

Medzida Mulic
Civil Engineering Faculty
Patriotske lige 30
Sarajevo 71000
Bosnia and Hercegovina

Oleg Odalovic
Republic Geodetic Authority
Bul. vojvode Mi.i.a 39
11000 Belgrade
Serbia

John Oldow
Dept. of Geological Sciences
University of Idaho
Moscow, Idaho 83844-3022
USA

Demitris Paradissis
Department of Surveying Engineering
National Technical University of Athens
Iroon Polytechneiou 9
15780 Zografou
Athens
Greece

Barry Parsons
Dept. of Earth Science
Oxford University
Parks Road
Oxford
U.K.

Polona Pavlovcic-Preseren
University of Ljubljana
Faculty of Civil and Geodetic Engineering
Department of Geodesy
Jamova 2
SI-1000 Ljubljana
Slovenia

Luigi Piccardi
C.N.R. - Istituto di Geoscienze e Georisorse
Via G. La Pira, 4
50121 Firenze
Italy

Nicholas Pinter
Dept. of Geology
Southern Illinois University
Carbondale, IL 62918-4324
USA

Bosko Pribicevic
University of Zagreb, Faculty of Geodesy
Institute of Geomatics
Kaciceva 26
HR-10000 Zagreb
Croatia

Ljerka Rasic
State Geodetic Administration
Gruska 20
10000 Zagreb
Croatia

Leonardo Sagnotti
Istituto Nazionale di Geofisica e Vulcanologia
Via di Vigna Murata 605
00143 - Roma
Italy

Giovanni F. Sella
Department of Geological Sciences
Northwestern University
Evanston, IL 60208
USA

Günter Stangl
Institut für Weltraumforschung
Österreichische Akademie der Wissenschaften
Schmiedlstrasse 6
A-8042 Graz,
Austria

Seth Stein
Department of Geological Sciences
Northwestern University
Evanston, IL 60208
USA

Bojan Stopar
University of Ljubljana
Faculty of Civil and Geodetic Engineering
Department of Geodesy
Jamova 2
SI-1000 Ljubljana
Slovenia

François Thouvenot
LGIT (UJF/CNRS)
Observatoire de Grenoble
Maison des geosciences
BP 53
38041 Grenoble Cedex 9
France

Gábor Timár
Geophysical Department
Eötvös Loránd Technical University
Pázmány P. sétány 1/C
H-1117 Budapest
Hungary

Emanuele Tondi
Department of Earth Sciences
University of Camerino
Via Gentile IIII da Varano
62032 Camerino (MC)
Italy

László Tóth
Seismological Observatory
Meredek u. 18
Budapest
Hungary

Marcello Viti
Dipartimento di Scienze della Terra
Università di Siena
Via Laterina 8
53100 Siena
Italy

Marko Vrabec
Department of Geology,
NTF, University of Ljubljana
p.p. 312
SI-1001 Ljubljana
Slovenia

John Weber
Department of Geology
Grand Valley State University
Allendale, MI 49401
USA

Tibor Zsíros
Seismological Observatory
Meredek u. 18
Budapest
Hungary